This is to certify that the
dissertation entitled

Exploring the Underlying Chemical Basis for Color Vision:
Designing a Protein Mimic of Rhodopsin

presented by

Rachael M. Crist

has been accepted towards fulfillment
of the requirements for the

Ph.D. degree in Chemistry

Major Professor's Signature

May 14, 2004

Date

EXPLORING THE UNDERLYING CHEMICAL BASIS FOR COLOR VISION: DESIGNING A PROTEIN MIMIC OF RHODOPSIN

Volume I

By

Rachael M. Crist

A DISSERTATION

Submitted to
Michigan State University
in partial fulfillment of the requirements
for the degree of

DOCTOR OF PHILOSOPHY

Department of Chemistry

2004

ABSTRACT

EXPLORING THE UNDERLYING CHEMICAL BASIS FOR COLOR VISION: DESIGNING A PROTEIN MIMIC OF RHODOPSIN

By

Rachael M. Crist

The mechanism by which we see colors has been long studied, but still not fully understood. The research performed in our group during the past few years, and presented here, has been directed to understand the underlying chemical reasons that enable color vision. In brief, there are four proteins in the eye which allow us to see, rod rhodopsin and three cone rhodopsins, red, blue, and green. Each of the four proteins bind the same compound, 11-*cis*-retinal, as a protonated Schiff base with an active site lysine residue. This chromophore is the compound responsible for vision. 11-*cis*-Retinal absorbs at 380 nm, and as the Schiff base with *n*-butylamine, absorbs at 365 nm. The key to color vision is that when this Schiff base is protonated, it red shifts 75 nm, to 440 nm. This is the manner in which the chromophore, 11-*cis*-retinal, binds to each of the four opsin proteins. This protonated Schiff base has a different maximal absorbance in each of the four proteins ranging from ~400 nm to ~600 nm (species dependent). It is the unique interactions of the protonated Schiff base of 11-*cis*-retinal with each of the four proteins that result in the opsin shift and ultimately allows us to see the entire visible spectrum from approximately 400 nm to 700 nm.

Determining the mechanisms by which color vision is mediated, i.e., the protein / substrate interactions responsible for the difference in retinal absorbance between the four opsin pigments, is what I have begun to address and present here within the text of

this thesis. D

membrane-bo

mimic, i.e., a

dimensional s

of Human Ce

that will in fa

In addition,

derivatives th

proteins, and

wavelength r

this thesis. Due to the difficulties in expressing, handling, and studying mammalian, membrane-bound proteins, such as rhodopsin, I have sought out to engineer a protein mimic, i.e., a protein that will bind retinal as a protonated Schiff base, yet has its three dimensional structure solved, and is much easier to manipulate and modify. Mutagenesis of Human Cellular Retinoic Acid Binding Protein II (CRABPII) has afforded a protein that will in fact bind retinal as a protonated Schiff base via an engineered lysine residue. In addition, synthetic efforts have resulted in the production of both retinal and model derivatives that may be used with both the aforementioned rhodopsin mimics, CRABPII proteins, and the native mammalian rhodopsin proteins to aid in uncovering the modes of wavelength regulation.

Dedicated to my parents

for their continuous support of all my dreams.

Gre

research ar

physically.

For

dictated in

uncharted t

both mana

mentoring

when he le

encountere

mentor. bu

experience

I w

countless c

indebted tc

of this rese

all the His-

insight. B

from the i

molecular

time spent

ACKNOWLEDGMENTS

Great appreciation goes out to all of people who helped me accomplish the research and educational goals I have achieved throughout my career, whether it was physically, emotionally, or spiritually.

Foremost I would like to thank Babak, without whom none of the research dictated in this manuscript would have been possible. We began an adventure previously uncharted to either of us, and although there were many obstacles along the way, we have both managed to learn and grow through this experience. I am very appreciative for the mentoring he has provided me over the last six years, but more grateful for the times when he let me make my own decisions and mistakes, and work through the dilemmas encountered by way of my own persistence and dedication . Not only has he been a great mentor, but also an exceptional friend. This friendship has helped to make my time and experience at MSU extremely memorable.

I would also like to extend my gratitude to all the members of the lab for countless days and nights of entertainment and newly found friendships. I am especially indebted to several colleagues who put forth tremendous efforts, aiding in various aspects of this research. Chrysoula Vasileiou, who not only supplied the MALDI-TOF data for all the His-tagged CRABPII proteins, but has also been a constant source of wisdom and insight. Both the progress and level of understanding for this research have benefited from the intellectual foresight of Chrysoula. Courtney Olmsted performed all of the molecular modeling and supplied all of the pictures presented in this manuscript. Her time spent on protein minimizations has provided invaluable information in helping to

analyze the re
synthesis of I
available for
one of th
diphenylbutac
help in the fi
Katie Kahl an
all aspects of
of all these in

Sincer
efforts. Profe
and students
Honggao Yar
gift of the C
Dr. Karen Fr
skills necess
equipment a

The
University
mass spectra
sequencing
Biochemistry

analyze the results of the retinal binding assays. Montserrat Rabago-Smith performed the synthesis of 11-*cis*-retinal for binding analysis with the CRABPII proteins, and was also available for helpful discussions. Dr. Pulgam Veera Reddy performed the synthesis of one of the model butadiene compounds, (*E*,*E*)-2-ethoxycarbonyl-1,4-[$^{13}C]_2$-diphenylbutadiene, and 15-^{3}H-retinal. Dr. Meenaksi Ramarathnam provided valuable help in the final steps of the synthesis of 15-^{13}C-*trans*-retinal. Undergraduate students Katie Kahl and Sarah Goins offered extraordinary efforts and enthusiasm both in learning all aspects of the project helping out wherever possible. Without the collaborative efforts of all these individuals, the progress of this research would have been severely hampered.

Sincere thanks also goes out to our collaborators on the protein crystallography efforts, Professor James Geiger (Department of Chemistry, Michigan State University) and students Erika Mathes and Soheila Vaezeslami. I also wish to thank Professor Honggao Yan (Department of Biochemisty, Michigan State University) for the generous gift of the CRABPII clone. A special gratitude is extended to Professor John Frost and Dr. Karen Frost. They invited me into their lab, taught me the basic molecular biology skills necessary to start this project, and offered me full access to both their laboratory equipment and their vast biology knowledge base.

The mass spectrometry facility (Department of Biochemistry, Michigan State University) provided both the instrumentation and a helpful staff for acquiring and all mass spectral data. The genomics facility (Michigan State University) provided all DNA sequencing analysis and the Macromolecular Structure Facility (Department of Biochemistry, Michigan State University) provided all the primers. I also wish to thank

the National I

(GM67311).

I mu

stream of su

it as far as I h

their power t

their love an

supported m

and would g

Janell. Paco.

hours of fun

important in

memorable b

always sarca

how proud t

support to m

out of their

kitchen was

I wou

my life grow

always prov

her youth. N

to share con

the National Institutes of Health for funding the research presented within this manuscript (GM67311).

I must also thank all of the friends and family who have provided a constant stream of support throughout my academic career, without which I might not have made it as far as I have. My Mom and Dad have always been there for me, doing everything in their power to be sure I received everything I ever wanted or needed. I owe so much to their love and dedication to me and my dreams. My sisters Robbie and Randa have also supported me in everything I set out to do. They would not stop at anything to help me, and would go so far as to give me the shirt off their back or the shoes off their feet. Janell, Paco, and Angie have given me a lightened spirit, a youthful attitude, countless hours of fun and entertainment, and have helped me to keep sight on what is really important in life. My Grandma G. has given me everything I ever asked for, most memorable being a barrel of laughs from her incredibly hilarious, brutally honest, and always sarcastic sense of humor. Grandma and Grandpa C. have never been shy about how proud they are of my hard work and accomplishments, and have always offered support to me in any way I needed. My Aunt Becky and Uncle Greg have always gone out of their way to support me as well, and among other things, always made sure my kitchen was well-stocked.

I would also like to remember the grandmothers I was fortunate enough to have in my life growing up, but have sadly lost in the past few years. My Great-Grandma B. always provided a surplus of love and hours of amusement with the outrageous stories of her youth. My Great-Grandma C. was so full of life and energy, and always had the time to share conversation over a drink or two. My Great-Grandma W. never had a shortage

of compli e

missed de ly

Fu l

everything sh

we have c ed

has kept r

my diffic tic

love and e

thankfuln s

her preser e.

of compliments and admiration for the desire I had to pursue my goals. You are all missed dearly and will never be forgotten.

Finally, I would like to express my heartfelt thanks and gratitude to Connie for everything she has done over the course of the last six years. We have laughed together, we have cried together, and we have shared every emotion between. Her sense of humor has kept my spirits high, her patience and understanding have helped me overcome all of my difficulties, her sense of adventure has kept me young and lively, and her devoted love and friendship has made me complete. Although words cannot begin to express the thankfulness and appreciation I have for her sense of humor, her friendship, her love, and her presence, thank you. I love you all.

TABLE C

TABLE OF CONTENTS

APPEND

SUMMA
SUMMA
MUTANT
SUMMA
MUTANT

Data Colle

WILD TY
R132K..
R132K::
R132K::
R132K::
R132K::
R132K::
R132K::
R132K::
R132K::
Y134F::R
R132L::Y
R132K::Y
R132K::Y
R132K::Y
R132K::Y
R132K::Y
R132K::Y
R132K::Y
R132K::Y
R132K::Y
R132K::Y
R132K::Y
Y134K....
Y134K::R
Y134K::R
Y134K::R
Y134K::R
Y134K::R
Y134K::R
Y134K::R
Y134K::R
Y134K::R
F15W.....
R132K::Y
L19W.....
R132K::Y

Data Collected for:

LIST OF T

LIST OF TABLES

LIST OF FI

Note:

LIST OF FIGURES

Note: Select figures in this manuscript are presented in color.

Figure I 31

Figure I 32

Figure I 33

Figure I 34

Figure I 35

Figure I 36

Figure I 37

Figure I 38

Figure I 39

Figure I .

Figure I .

Figure I .

Figure I .

LIST O S

LIST OF SCHEMES

KEY TO S

Å

ε

λ_{max}

Abs. A

Amino Aci

Ala, A

Arg, R

Asn, N

Asp, D

Cys, C

Gln, Q

Glu, E

His, H

Leu, L

Lys, K

Phe, F

Pro, P

Thr, T

Trp, W

Tyr, Y

Val, V

KEY TO SYMBOLS AND ABBREVIATIONS

Å	Angstrom
ε	Extinction coefficient
λ_{max}	Maximal wavelength
Abs, A	Absorbance

Amino Acids:

Ala, A	Alanine
Arg, R	Arginine
Asn, N	Asparagine
Asp, D	Aspartic acid
Cys, C	Cysteine
Gln, Q	Glutamine
Glu, E	Glutamic acid
His, H	Histidine
Leu, L	Leucine
Lys, K	Lysine
Phe, F	Phenylalanine
Pro, P	Proline
Thr, T	Threonine
Trp, W	Tryptophan
Tyr, Y	Tyrosine
Val, V	Valine

Amp

BCA

BSA

bp

CD

cfu

cGMP

Clm

CRABPII

DABCO

DBU

DCC

DEAE

den

DNA

GDP

GMP

GTP

GPCR

HWE

IPTG

IUPAC

Amp	Ampicillin
BCA	Bicinchoninic acid
BSA	Bovine Serum Albumin
bp	Base pairs
CD	Circular Dichroism
cfu	Colony forming units
cGMP	Cyclic-Guanidine Monophosphate
Clm	Chloramphenicol
CRABPII	Human Cellular Retinoic Acid Binding Protein II
DABCO	1,4-Diazabicyclo[2.2.2]octane
DBU	1,8-Diazabicyclo[5.4.0]undec-7-ene
DCC	Dicyclohexylcarbodiimide
DEAE	Diethylaminoethyl-resin
den	Denatured
DNA	Deoxyribonucleic acid
GDP	Guanidine Diphosphate
GMP	Guanidine Monophosphate
GTP	Guanidine Triphosphate
GPCR	G-Protein Coupled Receptor
HWE	Horner-Wadsworth-Emmons
IPTG	Isopropylthiogalactoside
IUPAC	International Union of Pure and Applied Chemists

Kb

LB

MALDI-TO

nat

nm

nM

NMR

PBS

PCR

PDE

PSB

RA

Rt

SB

SDS-PAGE

TBDPS

THP

TIPS

Mutant pr

acid follo

for the new

Kb	Kilo-Base pairs
LB	Luria bertani
MALDI-TOF	Matrix assisted laser desorption ionization – Time of flight
nat	Natured
nm	Nanometer
nM	Nanomolar
NMR	Nuclear Magnetic Resonance
PBS	Phosphate buffered saline
PCR	Polymerase chain reaction
PDE	Phosphodiesterase
PSB	Protonated Schiff base
RA	Retinoic acid
Rt	Retinal
SB	Schiff base
SDS-PAGE	Sodium dodecyl sulfate – Polyacrylamide Gel Electrophoresis
TBDPS	tert-Butyldiphenylsilyl
THP	Tetrahydropyran
TIPS	Triisopropylsilyl

Mutant proteins are designated by the one letter abbreviation for the wild type amino acid, followed by the amino acid position number, followed by the one letter abbreviation for the new mutant amino acid.

I.

A. In rodu

Me

availa ility

20-50' of

has be n w

compa ies

Howe er, c

in sol' ng

memb ane

directe l m

explor ng t

interac ion

model or

i.e., th e n

conseq ten

Wa

remark ble

four di fer

rhodop in

Chapter 1

I. The Principles of Vision and the Need to Engineer a Rhodopsin Mimic

A. Introduction

Membrane bound proteins are the next frontier in structural biology. Through the availability of whole genome sequences it has become clear that they comprise between 20-50% of known proteins. Their importance in pharmaceutical science and biomedicine has been well documented. This is evident by the simple fact that most pharmaceutical companies have geared drug development to target different membrane proteins.[1,2] However, difficulties in crystallizing them have limited the use of X-ray crystallography in solving their structures. As a result, most of the structural information gathered on membrane bound proteins are through theoretical analysis coupled with results of site directed mutagenesis, and low resolution structural data. We are very interested in exploring the nature of protein / substrate interactions at the molecular level since these interactions are at the heart of biochemical events that regulate biological systems. As a model for such studies we have chosen the case of wavelength regulation in rhodopsin, i.e., the mechanism by which we can see colors as a powerful example of the consequences of protein / substrate interactions.

Wavelength regulation exhibited by various rhodopsin pigments in the eye is a remarkable example of the power of protein-substrate interactions. Human eyes contain four different types of rhodopsin; however, the chromophore bound to different types of rhodopsin is the same. In fact, all vertebrate pigments employ the same 11-*cis*-retinal (**I**-

a) chro nop
Schiff ase
cis-reti ial.
for the per
differe it rh
examp e o
proper ies
interac ion
mecha ism
Thi
study rote
stereo lect
invest gati
with s udy
retinal co
labele ret
techni ues
demor stra
In
differe it a
Schiff base
same I SB
from t heir

a) chromophore for vision, bound to the protein as a protonated Schiff base (PSB) via a lysine residue.[3,4] This chromophore, 11-*cis*-retinal, is tuned to absorb at various wavelengths allowing for the perception of color. Absorption maxima associated with different rhodopsin pigments range from ~400 nm to ~600 nm.[5] This is a remarkable example of protein / substrate interaction in which different proteins elicit different properties from the same substrate. A better understanding of protein / substrate interactions is central to rational drug development and new insights into enzymatic mechanisms.

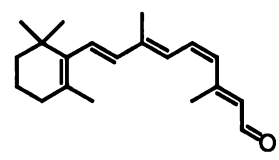

I-a

This system, i.e., how we see colors, can provide a simple and elegant platform to study protein / substrate interactions. It has been suggested that conformational and/or stereoelectronic effects control wavelength regulation of rhodopsin, however investigations into these theories have been hampered due to the difficulties associated with studying membrane bound rhodopsins. We propose to study the possibility of retinal conformational differences in different pigments by the synthesis of bis-^{13}C-labeled retinal, which will be bound to various rhodopsins. The use of solid state NMR techniques will probe the degree of single bond twisting within the polyene, and hence demonstrate the possibility of this as a mode of wavelength regulation.

In order to investigate the stereoelectronic factors, we will probe the effect of different amino acid residues at varying locations with respect to the retinal protonated Schiff base. For this, we plan to use protein mimics of rhodopsin that bind retinal in the same PSB manner, but yet are not membrane bound proteins, and therefore, do not suffer from their limitations in structural analysis. In essence, we will modify a well-

charact

advanta

the 3-di

mutager

respect t

N

derivativ

for meas

optimal c

model co

isolation

M

Retinoic A

Through v

have demo

engineered

mimic furt

pH is attai

acids with

covalently

characterized protein to bind retinal as a protonated Schiff base, but with the added advantage of being small, soluble, and easily manipulated. In addition, having at hand the 3-dimensional structure of the protein will allow us to propose rational site directed mutagenesis to position different functional groups at precisely the desired locations with respect to the bound chromophore to probe their roles in wavelength regulation.

My efforts on this project include the synthesis of 1,4-$[^{13}C]_2$-butadiene model derivatives which will be used in optimizing the solid state NMR techniques necessary for measurement of bis-labeled 11-*cis*-retinal bound to different opsin proteins. Provided optimal conditions are attained for determining the dihedral angle differences with these model compounds, synthesis of the labeled retinal will need to be completed, along with isolation of the desired rhodopsin proteins.

My primary focus however, has been on the engineering of Human Cellular Retinoic Acid Binding Protein II (CRABPII) to bind retinal as a protonated Schiff base. Through various spectroscopic techniques, coupled with site directed mutagenesis, we have demonstrated the formation of a protonated Schiff base between retinal and the engineered protein. While these efforts have brought us close to the ideal rhodopsin mimic further tuning of the PSB's pK_a is still needed. Once a stable PSB at physiological pH is attained, this engineered CRABPII mutant can be used to rationally place amino acids with different charges, dipoles, and sterics at various locations with respect to the covalently bound retinal, and the effects on wavelength regulation will be characterized.

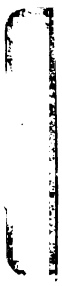

B. T e Vis

Vis

transi ittal

Withi n the

comp nent

lining the

captu ing t

The

the c nes.

cone ells.

are re pon

envir nme

cells t ke

times nor

The

more abu

functi n o

extrap late

with t o u

brain t or p

disks t nad

The m ake

B. The Visual Process

Vision, the act or sense of sight, involves the capture of light waves by the eye, transmittal of electrical impulses to the brain, and the recognition of images and colors.[6] Within the eye it is the cornea, lens, and the vitreous fluid that are the primary components responsible for focusing light waves onto the retina.[7] The retina, the tissue lining the inner part of the eye, contains the photoreceptors and is responsible for capturing the image and sending the signal to the brain via the optic nerve.

The retina is layered with the photoreceptors responsible for vision, the rods and the cones.[8] An eye contains approximately 100 million rod cells and about 6 million cone cells.[9] The cone cells are responsible for color (photopic) vision and the rod cells are responsible for dim (scotopic) vision. Cone cells are both quicker to adapt to dark environments (~10 min) and sensitive to a broader range of wavelengths. While rods cells take longer to adapt to dark environments (20 – 30 min), once adapted they are 500 times more as sensitive than cone cells.

The structure and function of rods and cones are very similar. Rod cells, being more abundant, have been more thoroughly investigated. While the structure and function of rod cells will be briefly introduced here, this information may also be extrapolated to include cone cells. The rod cell is a typical nucleus containing cell, but with two unique parts: the synaptic ending, where the neural signals pass through to the brain for processing, and the outer segment (Figure I-1). The outer segment is filled with disks made of a phospholipid bilayer and the protein opsin, which spans the bilayer disk. The make-up of rod and cone cells is very similar, but where the disks in rod cells are

disconnect

membrane

Op

coupled r

protonated

that chrom

to as opsi

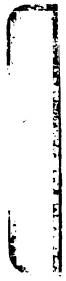

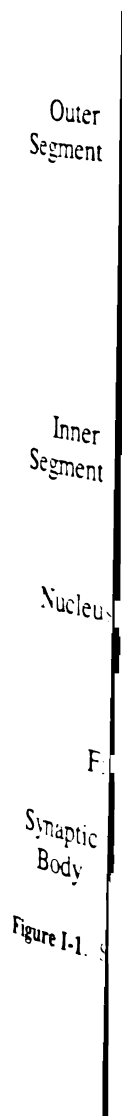

Figure 1-1. S

disconnected from their plasma membrane, the disks in cone cells form the plasma membrane.[10]

Opsin is a *trans*-membrane 7-α-helical protein from the family of G-protein coupled receptors (GPCR). Opsin binds the aldehydic chromophore retinal as a protonated Schiff base via a lysine residue (Figure I-2).[11] In humans and most animals, that chromophore is the 11-*cis* isomer of retinal. In the apo form, the protein is referred to as opsin; in the holo (retinal bound) form, the protein is known as rhodopsin.

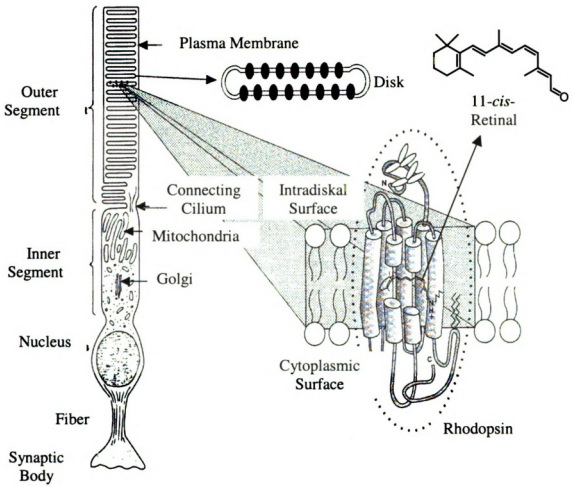

Figure I-1. Schematic representation of a vertebrate rod cell.

Although

each disk

one uses a

continuou

GH

which, rh

biological

others, vis

Th

is bound

protein)

photon o

Although variable in different species, each rod cell can contain up to 1700 disks and each disk can contain up to 1.5 million molecules of rhodopsin.[12] At one time, however, one uses about 10% of the rhodopsin complexes, which is what allows for vision to be a continuous process.

GPCRs are the predominant proteins in the class of membrane-bound proteins, of which, rhodopsin constitutes ~90%. GPCR's are responsible for a variety of important biological functions including signal transduction, gene regulatory control, and among others, vision.[13]

The visual process begins in the dark state where the chromophore, 11-*cis*-retinal, is bound as a protonated Schiff base via Lys 296, and visual participants transducin (G-protein) and phosphodiesterase (PDE) are in an inactive state. The absorption of a photon of light starts the conformational change of 11-*cis*-retinal to all-*trans*-retinal,

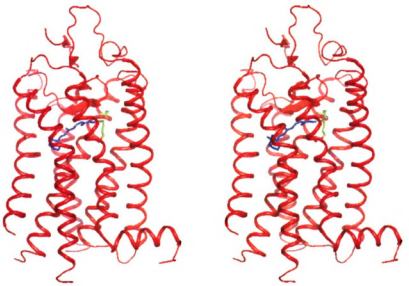

Figure I-2. Stereoview of the *trans*-mambrane 7-α-helical G-protein coupled receptor, rhodopsin. Rhodopsin binds the visual receptor 11-*cis*-retinal as a protonated Schiff base via Lys 296. Glu 113 serves as the counter anion for the PSB.

which be

T

can be m

(Figure I

including

meta I. m

Th

while the

up to and

Schiff ba

intermed

Phot

all-trans

Figure I-3

retinal to a

which begins a series of enzymatic events culminating in vision.[14]

The isomerization of the 11-*cis* isomer of the chromophore to the all-*trans* form can be monitored by various low temperature spectroscopic techniques including UV-vis (Figure I-3).[15-21] The chromophore goes through a series of discrete intermediates including photo rhodopsin, batho rhodopsin (a "distorted" *trans* PSB), lumi rhodopsin, meta I, meta II (all-*trans* unprotonated Schiff base), and meta III states.[22,23]

The initial stages of the transduction pathway are controlled by steric factors,[24,25] while the latter stages primarily involve proton transfer processes.[26,27] All intermediates up to and including meta I maintain a protonated Schiff base. The deprotonation of the Schiff base and protonation of the counter anion (Glu 113) occur in the meta II intermediate, and the visual transduction pathway is initiated from. Following meta II,

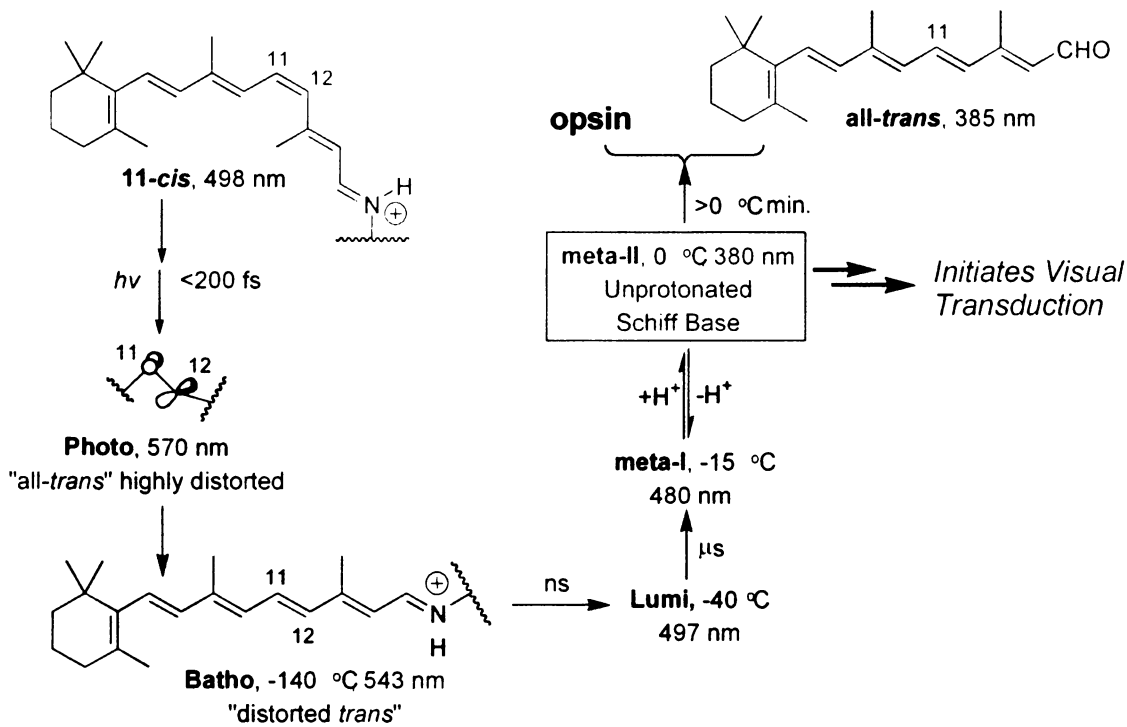

Figure I-3. Schematic representation of the intermediates involved in the isomerization of 11-*cis*-retinal to all-*trans* retinal as it is excited with a photon of light.

the SB

trans-re

retinal t

which a

Trans-du

compone

undergo

G_t-subu

subgroup

a

b

Figure 1-4

the C11-C

rhodopsin

the SB is reprotonated in the meta III stage, and finally eliminated from the protein. All-*trans*-retinal is transported to another site for re-isomerization to the 11-*cis* isomer.

Vision is initiated as light is absorbed by rhodopsin. The isomerization of 11-*cis*-retinal to the all-*trans* form leads to a conformational change in the protein (Figure I-4), which allows for binding and activation of the G-protein transducin (Figure I-5).[15] Transducin is composed of α, β and γ subunits, as well as a GDP subunit bound to the α component. When bound to activated rhodopsin, the G-protein, transducin, also undergoes a conformational transition, which leads to displacement of the GDP unit in G_α-subunit by a GTP. This substitution, in turn, results in the release of the G_α-GTP subgroup from the remainder of the transducin complex. In the free state, the G_α-GTP

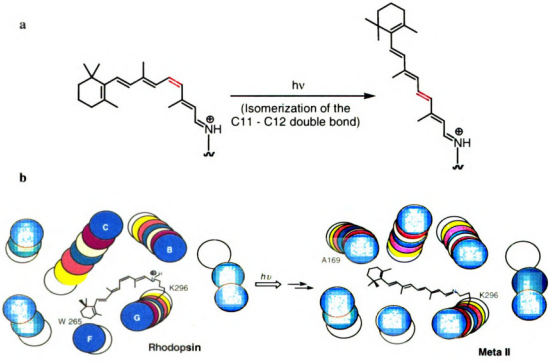

Figure I-4. **a**) Depiction of the movement of the chromophore as it undergoes an isomerization of the C11-C12 double bond. **b**) Representation of the resultant change in orientation of the helices of rhodopsin when hit with a photon of light.

unit can

consists

released

units init

cGMP to

cC

cyclic-GM

halts the f

μM to 0.1

being sent

Th

photon of

isomerizat

and transm

retains a

initiates

hydrolysis

Th

harnesses

even a sin

molecules

conversio

visual tra

unit can now initiate the activation of the phosphodiesterase enzyme (PDE). PDE consists of an α, β and two γ subunits in the unactivated state. As the G_α-GTP unit is released from transducin, it then binds the γ subunit of PDE. Cleavage of both PDE-γ units initiates activation of the PDE enzyme, which then catalyzes the hydrolysis of cGMP to GMP (Figure I-5).

cGMP is responsible for the regulation of ion channels in the cell. Hydrolysis of cyclic-GMP to GMP forces the Ca^{2+} ion channel in the rod outer segment to close and halts the flow of Ca^{2+} into the cell. This forces a concentration change in Ca^{2+} from 0.5 μM to 0.1 μM.[28,29] These ion concentration changes are what initiate the electric signal being sent to the brain and results in a visual image.[30,31]

The overall visual transduction process is summarized in Figure I-6.[32] As a photon of light hits the photoreceptor, the simple action of a single double bond isomerization begins the cascade of events culminating in the hydrolysis of cyclic GMP and transmission of a neural signal to the brain, resulting in vision.[33,34] The chromophore retains approximately 27 kcal/mole of the photon's energy in the meta II state, which initiates the rhodopsin conformational change, activation of transducin, PDE, and hydrolysis of cGMP.[19,35,36]

The magnitude of the visual process is demonstrated by the means in which it harnesses the energy of a single photon. Rhodopsin has the ability to be activated by even a single photon. An activated rhodopsin can catalyze conversion of 100 transducin molecules to the activated G_α-GTP state. These 100 molecules of G_α-GTP can catalyze conversion of 100,000 molecules of PDE to the activated γ-PDE cleaved form.[37,38] The visual transduction cascade is one of the most efficient and sensitive processes known,

with

sensi

darks

with a quantum efficiency of ~0.67,[39-42] allowing detection of a single photon.[43] It is this sensitivity coupled with the energetic enhancement that allows vision to still occur in the darkest of environments.

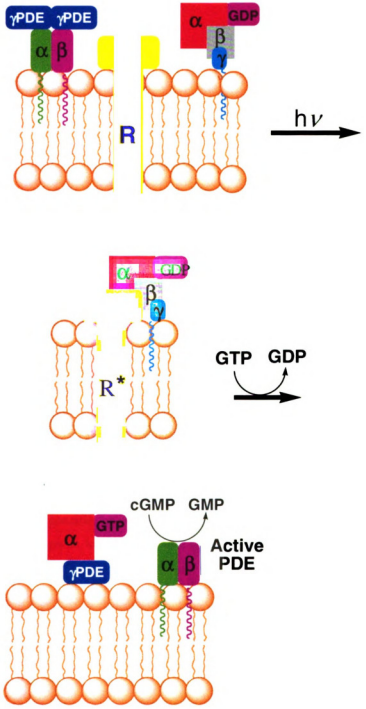

Figure I-5. The visual pathway involves the activation of the G-protein coupled receptor rhodopsin. The comformational change in rhodopsin allows for binding and acitivation of the G-protein transducin. Once activated, the α subunit of transducin activates the enzyme phosphodiesterase (PDE) by binding and cleaving the γ subunit. Active PDE catalyzes the hydrolysis of cGMP to GMP, which causes changes in ion concentrations in the cell and results in an electrical signal being sent to the brain.

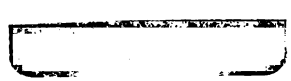

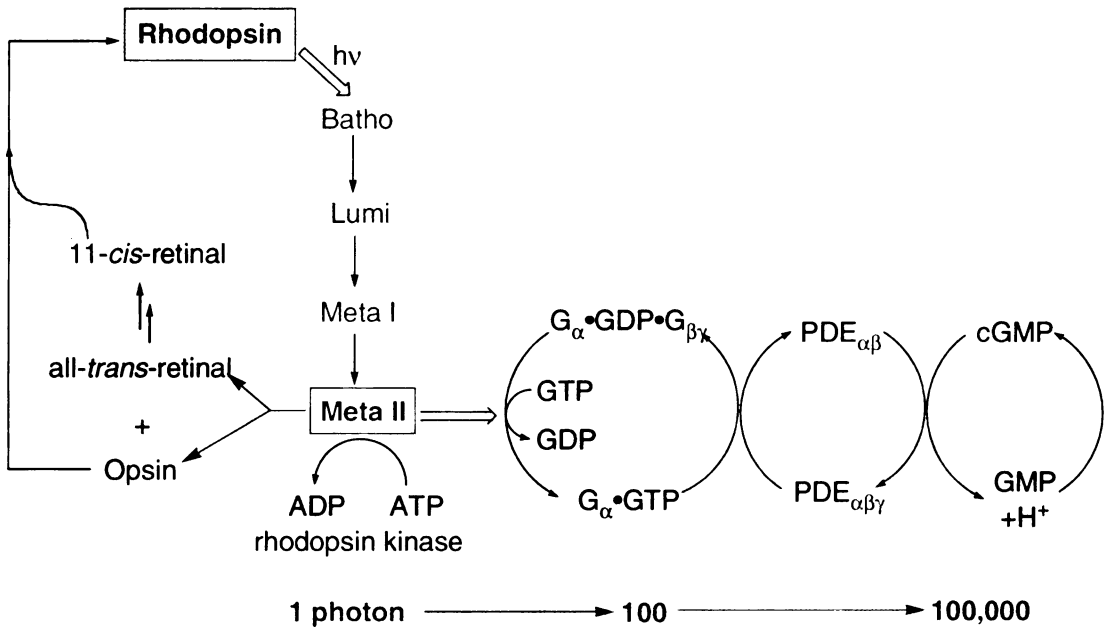

Figure I-6. Schematic representation of the visual transduction process. Opsin binds 11-*cis*-retinal to form rhodopsin. When rhodpsin absorbs a photon of light, it initiates the isomerization of retinal, observable through several discrete intermediates and culminating in meta II. The conformational change in retinal produces a conformational change in the protein, which in turn allows for activation and binding of the G-protein transducin. Activation of transducin in turn activates the enzyme phosphodiesterase, which is responsible for the hydrolysis of cGMP to GMP. cGMP regulates the ion channels in the cell, and changes in ion concentration, as a result of conversion to GMP, forces an electrical signal to be sent to the brain and results in vision.

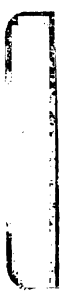

C. C

Diff

and

thre

chro

prop

Schr

n-bo

shift

How

prot

shift

to

conc

may

of th

not s

as 4

regio

spec

C. Color vision: Modes of wavelength regulation

Vision not only involves the act of detecting objects, but also colors. Differentiating colors means that within the process of vision there must also be detection and regulation of the multitude of light wavelengths. To accomplish this, the eye utilizes three colored proteins: red, green, and blue. Each of these opsins bind the same chromophore, 11-*cis*-retinal. It is the unique ability of these proteins to elicit different properties from the same substrate that allow us to see the whole visible spectrum.

As the free aldehyde, 11-*cis*-retinal absorbs at 380 nm (Figure I-7). When the Schiff base is formed with *n*-butylamine, there is a slight blue shift in absorbance, 365 nm. However, when the Schiff base is protonated, there is a significant red shift of the chromophore's absorbance to 440 nm.[44,45] With controlled concentration and solvent, this value may shift up to 500 nm.[46] Protonation of the Schiff base alone, however, is not solely responsible for color vision, as 440 nm is just the beginning of the region of the electromagnetic spectrum that we can actually see

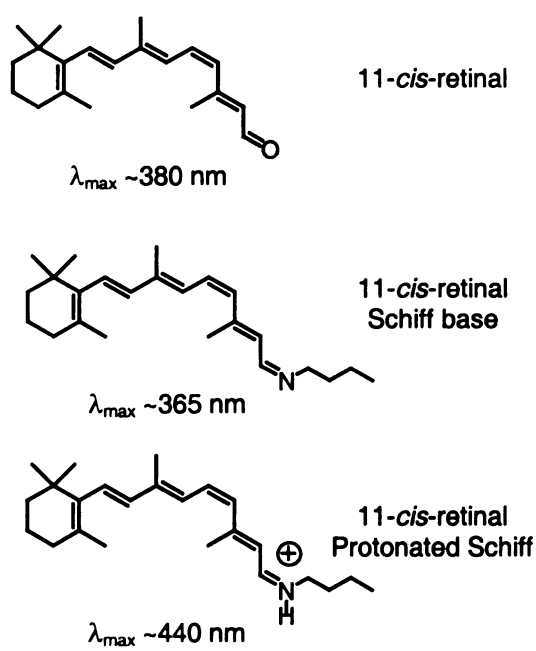

Figure I-7. 11-*cis*-Retinal absorbs at 380 nm. As the Schiff base with *n*-butylamine, there is not much change in the maximal absorbance, 365 nm. Protonation of the Schiff base leads to a large bathochromic shift to 440 nm.

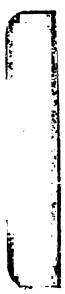

(~400 – 700 nm).

Each of the four opsin proteins binds 11-*cis*-retinal in the same manner, as a protonated Schiff base through a Lys residue. Interestingly however, they each produce a dramatically different maximal absorbance for the chromophore. The absorption values of each of the human pigments has been investigated for more than a hundred years,[47] utilizing techniques such as psychophysical color matching,[48] reflection densitometry,[49] electroretinography,[50] single-cell action spectra,[51] and microspectrophotometry.[52,53] Human rod rhodopsin absorbs at 500 nm and the cone rhodopsins, red, green, and blue absorb at 570 nm, 530 nm, and 420 nm, respectively.[3,4] The difference in the absorbance value observed for the visual pigments as compared to the PSB of 11-*cis*-retinal in solution is known as the *opsin shift* and must be due to the interaction of the protein with the retinylidene chromophore.[54,55] It is the unique interactions of the individual proteins with the chromophore, and the coexistence of the four complexes that allow us to see the entire visible spectrum (Figure I-8).

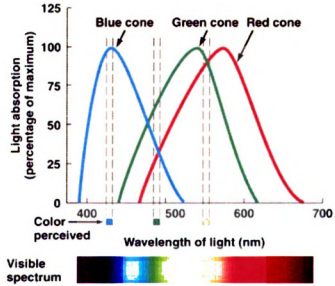

Figure I-8. The visible spectrum ranges from approximately 400 – 700 nm. Although each of the rhodopsin complexes absorb only at a specific wavelength, it is the combination of the absorbance patterns of all rhodopsins that allow us see the entire visible range.

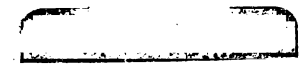

Due to the fact that rhodopsins are membrane-bound proteins, they are difficult to work with and particularly difficult to crystallize. In 2000, Palczewski, et al, published the first crystal structure of a rhodopsin protein, diffracting to 2.8 Å resolution.[56] Until then, there were only models of the three dimensional protein structure as a result of site-directed mutagenesis, photoaffinity labeling, NMR, cryoelectron microscopy, and theoretical calculations.[14,57-63] As of yet, there are still no crystal structures of any of the cone rhodopsins, hampering efforts to fully understand the underlying mechanisms responsible for wavelength regulation.

Although there are no crystal structures available for the cone opsins, there have been several hypotheses presented to explain the factors responsible for wavelength regulation, most inferring a change in the degree of conjugation within the chromophore.[64-66] An early hypothesis suggested the possible twisting of the planes about the single bonds in the molecule to achieve different levels of conjugation. Although retinal would prefer to adopt a planar conformation to maximize p-orbital overlap, it is known that 11-*cis*-retinal is not a planar molecule. The chromophore exists in a nonplanar 6-s-*cis*-, 12-s-*trans* conformation, where steric interactions at the C5-Me and C8-H as well as the C10-H and C13-Me force twisting of the C6 – C7 and C12 – C13 single bonds, respectively (Figure I-9).[67,68] Differing steric requirements within the various rhodopsin protein binding cavities may force more or less twisting in each case.[69] Red rhodopsin would be expected to have steric constraints forcing retinal into a more planar conformation, resulting in more orbital overlap. More twisting of the single bonds and less orbital overlap would be expected in the blue pigment. Different degrees of

twisting can result in different degrees of overall conjugation, which in turn would lead to different maximal absorbances.

Other postulated theories on possible modes of wavelength regulation involve the charge delocalization on the protonated Schiff base of the chromophore in response to the different charged or polar species in the binding pocket (Figure I-10).[70] More specifically, it has been suggested that the distance of the counter anion to the PSB may aid in modulating the maximal wavelength of retinal. A shorter counter anion distance would lead to a more blue shifted retinal, and conversely, a larger counter anion distance, or removal of the counter anion, would result in a more red shifted retinal absorbance.[71] In addition, localization of charges or dipoles at different positions along the polyene backbone may also effectively shorten or elongate the polyene's conjugation resulting in different maximal absorbances and a possible mode of wavelength regulation.[72]

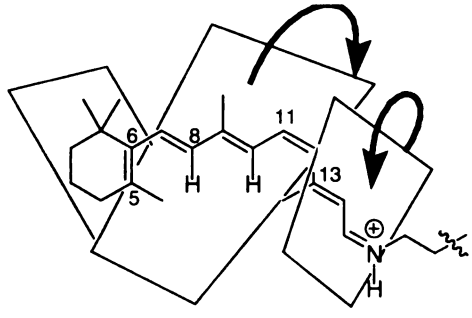

Figure I-9. Twisting of the single bonds will reduce the degree of π orbital overlap, and thus will lead to different maximal wavelengths. Individual rhodopsin proteins may modulate this by altering the steric restrictions placed on the chromophore, resulting in different degrees of conjugation and ultimately different maximal wavelengths.

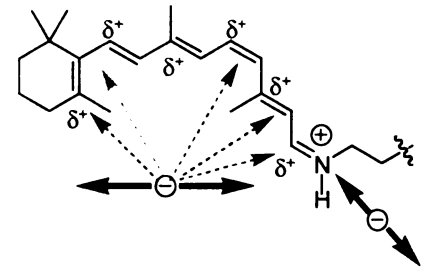

Figure I-10. Distance of the counter anion to the protonated Schiff base and positioning of charges or dipoles along the backbone of the polyene may modulate the maximal wavelength of the chromophore.

Without crystallographic information on all four rhodopsin proteins and a means to correlate protein structure to retinal maximal absorbance, determination or validation of the mechanisms responsible for wavelength regulation will remain unconfirmed.

The studies into the chemistry of vision and the specific protein / substrate interactions responsible for color vision has been enthusiastically researched for more than 50 years. Retinal was first isolated in 1933 by George Wald[73] (then called 'retinene'), but it was not until 1944 that Morton and Goodwin suggested that this compound was actually the aldehydic form of vitamin A.[74] The terms 'retinaldehyde' and 'retinene' were used for the photoreceptors' substrate until 1960 when the IUPAC coined the term retinal.

Rhodopsin is a large, hydrophobic, membrane-bound protein consisting of 348 amino acids and two oligosaccharide chains (~39,000 Da). Although countless efforts were put into solving the structure of rhodopsin,[75,76] it was not until 2000 that the first crystal structure of a rod rhodopsin was published.[56] The structures of the cone opsins have yet to be solved.

Collins and Morton first suggested that retinal is covalently linked to opsin via a Schiff base in 1953 and 1955, respectively.[77,78] Firm evidence of this Schiff base linkage, via a lysine residue with the protein was not provided for another ten years by Bownds in 1965[79] and Akhtar in 1968.[80] It took approximately another ten years of research before the exact attachment site for retinal in rhodopsin was known. Many proteolytic digestions of the protein / substrate complex had failed to generate a retinal containing fragment, presumably due to the hydrophobic nature of opsin, making the binding cavity inaccessible to the enzyme. A nonspecifc enzyme mixture from *Streptomyces griseus*,

known

contai

sequer

interac

polyer

1974 t

11-*cis*

regula

acids

acid,

charge

NMR

and th

achiev

Sakm

490 n

forced

nm (S

the S

uncon

known as Pronase, however was able to generate small amounts of retinylidene containing fragment, which were purified by HPLC, sequenced, and compared to known sequence data.[79]

In 1958 that Hubbard suggested this Schiff base had to be protonated, and interactions with the protein force a delocalization of the positive charge throughout the polyene backbone.[81] Confirmation of the protonation of this Schiff base was unveiled in 1974 through Raman studies.[82] Wald was also the first to show that the isomerization of 11-*cis*-retinal to all-*trans*-retinal was the primary step in the transduction process.[83]

Kropf and Hubbard had originally suggested in 1958 the theory that wavelength regulation may result from electrostatic interactions between the SB and charged amino acids within the binding pocket.[70] Honig suggested that both a negatively charged amino acid, suitably placed, could serve as a counter anion, and that a second negatively charged amino acid could be placed at another position along the polyene backbone.[84] NMR studies did in fact conclude that there was a second negative charge in the cavity, and that it resides near carbon 12 of retinal.[85-87]

Identification of Glu 113 as the counter anion in bovine rhodopsin was not achieved until 1989 by Sakmar[88] and Oprian[89] independently, and 1990 by Nathans. Sakmar discovered that mutation of Glu 113 to Gln produced a mixture of two species, 490 nm and 380 nm, that existed as a pH-dependent equilibrium. Lowering the pH forced the mixture to 490 nm (PSB), while increasing the pH forced the mixture to 380 nm (SB).[88] Removal of the counter anion does not allow for significant protonation of the Schiff base to occur, presumably due to unfavorable energetics of having an uncompensated positively charged residue within a hydrophobic cavity. Similarly,

Nathans generated the E113Q mutation that portrayed a 380 nm absorbing protein / retinal complex.[65] Increasing the halide ion concentration in the sample, i.e., addition of another counter anion source, forced a shift back to 500 nm. An increase in halide ion concentration in the wild type rhodopsin protein did not change the chromophore's maximal absorbance. Additionally, mutation of any of the other 19 Asp or Glu residues in the protein does not generate a significant change in absorbance value, leading to the belief that Glu 113 serves as the PSBs counter anion. Incidentally, Glu 113 has been highly conserved among all vertebrate opsins.[90]

The hypothesis of varying counter anion distances in the different rhodopsin proteins was proposed by Blatz in 1972.[71] If the counter anion was further removed from the positively charged iminium ion, a red shift of retinal's absorbance would be expected, and vice versa. Mutation of Glu 113 in bovine rhodopsin to Asp (one methylene unit shorter) does produce a small red shift to 505 nm. Sheves and co-workers have probed the effect of varying the counter anion distance by utilizing differing ring size compounds containing both an amino group and a carboxylate.[91] They have found that by altering the angle between the PSB and the counter anion, the pK_a of the retinal PSB can be significantly perturbed. An optimal angle is desired such that effective bridging with one or more water molecules takes place.

In 1976 Honig suggested that as an alternative or supplement to the counter anion, the positive charge on the nitrogen could be solvated by polar groups within the proteins' binding cavity.[72] Nathans also suggested negatively charged amino acids could be distributed at varying locations to account for the wavelength regulation observed in cone pigments.[90]

The theory of possible excitonic interactions between the bound chromophore and Trp residues positioned in close proximity was first suggested in 1979 by Rafferty.[91] Although calculations of opsin shifts utilizing these interactions suggests they may be involved and partially responsible, the degree of shifting calculated does not support this as being a primary mode of wavelength regulation.[66]

Blatz proposed the possibility of the chromophore's single bonds being twisted as a mode of wavelength regulation.[69] Solution analysis of the conformation of retinal in the absence of protein has not offered much insight into this theory, as theoretical and experimental studies have shown that there are a multitude of torsional angles possible for the C6-C7 single bond alone.[92] Theoretical analysis suggests that twisting of the chromophore's bond cannot be the sole mechanism responsible for the large observed opsin shifts.[66]

Human green and red cone proteins are 96% sequence identical and differ by only 15 amino acids.[90] Given the high similarity of these two proteins, yet their different maximal absorbances when bound with retinal, most of the wavelength regulations studies have been done with these two cone proteins. Green rhodopsin absorbs at 530 nm while red rhodopsin absorbs at 570 nm. Mutation of only 7 of the 15 amino acids in the red pigment is required to shift the absorbance from 570 nm to 530 nm (S116Y::S180A::I230T::A233S::Y277F::T285A::Y309F).[93] However mutation of only three of these residues in the green pigment will account for the majority of the red shift.[50,94] All substitutions involve the conversion of a hydrophobic amino acid to a polar residue near the ionone region, F277Y, A285T, and A180S. Hydrophobic to polar mutations at analogous positions in rod rhodopsin also will produce a red shift in the

retinal absorbance. The rod mutant F261Y::A269T::A164S red shifts to 700 nm from 500 nm.[95]

Blue opsin is both less abundant and more difficult to express and obtain ample quantities of. In addition, blue rhodopsin is only ~46% sequence similar to the other opsins,[90,96] resulting in only limited work being done with blue opsin. Rather, the route more commonly approached is mutagenesis of another opsin to promote absorption at the blue wavelengths. Sakmar has found that by mutating nine positions simultaneously, an hypsochromic shift can be observed to 438 nm.[64] These substitutions include M86L::G90S::A117G::E122L::A124T::W265Y::A292S::A295S::A299C. Similar work was done by Farrens, and found that mutation of T118A::E122D::A292S in rod rhodopsin, produced a protein that maintains structure stability and normal photoactivation and transducin activity, and absorbs at 453 nm, 47 nm blue shifted.[97]

While mutagenesis of this nature may serve to help predict the amino acids necessary for blue shifting the retinal absorbance as compared to rod rhodopsin, mutagenesis of the actual blue opsin indicates that this may only be true for predicting amino acids near the β-ionone ring and not near the Schiff base region.[98] As shown previously, mutation of W265Y, G90S and A292S in the rod opsin individually produce 15 nm, 11 nm, and 10 nm blue shifts, respectively. Mutation of corresponding amino acids in the blue pigment thus should force red shifting. Blue opsin mutant Y262W (β-ionone ring vicinity) generates a 10 nm red shift, whereas S289A (SB vicinity) results in no change, and S87G (SB vicinity) actually blue shifts 10 nm.

The extensive investigations into the structures of opsin proteins has lead to an increased understanding of the factors responsible for color vision deficiencies. These

deficiencies are a result of mutagenesis of one or more of the opsin proteins, or more rarely, lack of one of the opsin proteins. Color blindness has been known since the 18th century, and is often referred to as Daltonism in honor of John Dalton, one of the first reported color deficient people.[9] Although color vision deficiencies are often termed 'color blindness', more generally it is simply a reduced ability to differentiate between colors.

Red and green cones are highly conserved, and have 96% sequence identity. Blue cones, which constitute only 10% of all cones in a human eye, are only 46% identical based on sequence similarity. Knowing this, it is not surprising that the most common color vision deficiencies involve the red and/or green cones. The red / green color vision deficiencies are known as protanope ("red blind"), deuteranope ("green blind"), protanomalous ("red weak"), and deuteranomalous ("green weak"). The latter of these conditions accounts for approximately 50% of the red / green color blind cases (~1/25 males and 1/625 females), while the remaining contribute in approximate equal proportions (~1/100 males and 1/10,000 females).[99,100] There is one mutation in the red cone pigment that is fairly common, but does not result in color vision defects. In a recent survey, it was found that 62% of males have a serine in position 180, while 38% have an alanine residue.[101]

Blue cone deficiencies are more rare. Tritanopia is a weakened discrimination of the blue, short wavelengths (~1/500 males and 1/65,000 females). The rarest of the color deficiencies is blue cone monochromacy, which results from lack of both the red and green cone opsins, and exists in only 1/100,000 males. Finally, the severest form of color

deficiency is rod monochromacy (~1/20,000 males and 1/50,000 females). This condition produces total color blindness from the lack of all three cone pigments.[102]

While much work in the past several decades has generated a significant database of information regarding the visual transduction process, the structure of opsin proteins, and even the amino acids required to be in close proximity to the bound chromophore to obtain the observed opsin shifts, the precise mechanisms for color vision remain unknown. It is not known which of the possible theories is most predominant in forcing the opsin shift, nor how many different factors are involved in the shift of each cone pigment. This research project, through use of an engineered rhodopsin mimic, will attempt to answer these questions.

D. The need for a surrogate

Membrane-bound proteins comprise between 20-50% of all known proteins and are of tremendous importance in pharmaceutical sciences and drug development.[103] An important class of membrane-bound proteins is the G-protein coupled receptors (GPCRs), of which rhodopsin is a member. GPCRs are involved in numerous biological functions including gene regulation, signal transduction and color vision. Also of significance are the specific protein-substrate interactions that are involved in regulating many of these biochemical events. The mechanism by which we see colors is a remarkable example of protein / substrate interaction in which different proteins elicit different properties from the same substrate. Our approach at investigating the protein / substrate interactions that lead to color vision may provide useful insight that may be extrapolated to offer insights into rational drug development and unknown enzymatic mechanisms.

Only limited information is known about membrane-bound proteins, including rhodopsin, due to difficulties in handling and manipulating them. Most of the current information known is a result of theoretical analysis coupled with site directed mutagenesis studies and low resolution structural data. The membrane bound nature of cone rhodopsins has made purification, manipulation, and biophysical studies tedious. Until recently, there was no concrete crystallographic information available on the rhodopsin pigments. In 2000, Palczewski, et al published the first high resolution crystal structure of bovine rhodopsin.[56] Still however, there are no crystal structures of the cone opsins for comparison, and only theoretical models exist. Because of this, the studies necessary for a complete understanding of the mechanisms responsible for wavelength

regulation have not been completed, and prompted us to engineer of rhodopsin protein mimic. By designing a protein to mimic the PSB formation with retinal we will systematically introduce charges, sterics, and dipoles at varying locations with respect to the bound chromophore with hopes of deciphering the possible reasons for the altering opsin shifts.

A suitable protein mimic of rhodopsin must fulfill certain criteria. Foremost, it should be tolerant and structurally robust to withstand multiple mutations. Not only will many amino acid substitutions be necessary for probing wavelength regulation, but also in engineering the protein to bind retinal as a protonated Schiff base. Also of significant importance, it should have its three dimensional structure solved so that mutagenesis of the protein could be planned rationally. In addition, the chromophore in the binding pocket should optimally be protected from the solvent to ensure the results we see are only a result of the direct interactions of the protein with the substrate. Most importantly, it must bind retinal as a protonated Schiff base, just as in rhodopsin.

In choosing the protein we would transform into the rhodopsin surrogate, several other factors were considered as well. Besides having a three-dimensional crystal structure already solved, the ability of the surrogate protein to produce high resolution crystal structures in an efficient manner would be advantageous for our progress. Ultimately, we will want to determine precise orientations and distances of amino acids with respect to the substrate, retinal. A quick turn-around time in crystallography will be the most effective means of determining the consequences of the mutagenesis performed and in helping to decide which mutations to pursue next.

Additionally, we desired a protein cloned into a system that was much easier to work with than mammalian cultures, ideally an *E. coli* expression system. The surrogate protein should also be non-membrane bound, small, and cytosolic. Preference for binding retinoid structures will also be advantageous to the engineering process. Several proteins were of initial interest including RXR's and cellular retinoid binding proteins. The cellular retinoid binding proteins have been more thoroughly studied, in particular Cellular Retinoic Acid Binding Protein II. Professor Honggao Yan (Department of Biochemistry, Michigan State University) has done extensive studies with Human Cellular Retinoic Acid Binding Protein II (CRABPII) including mutagenesis and solution NMR.[104,105] It was cloned into a pET-17b plasmid (an *E. coli* expression system) and had a published crystal structure.[106,107] Additionally, CRABPII is a small protein (137 amino acids) that has high expression levels. It belongs to the lipocalin family of proteins in which all members have a very robust structure, and CRABPII natively binds a retinoid, retinoic acid. For these reasons, we believed that CRABPII would be a suitable target for re-engineering into the rhodopsin surrogate, and Professor Yan graciously gifted a pET-17b CRABPII containing clone to us.

E. References

1. Beeley, N. R. A.; Sage, C. "GPCRs: An update on structural approaches to drug discovery." *Targets* **2003**, *2*, 19-25.
2. Klabunde, T.; Gerhard, H. "Drug design strategies for targeting G-protein coupled receptors." *Chembiochem.* **2002**, *3*, 928-944.
3. Oprian, D. D.; Asenjo, A. B.; Lee, N.; Pelletier, S. L. "Design, chemical synthesis, and expression of genes for the 3 human color vision pigments." *Biochemistry* **1991**, *30*, 11367-11372.
4. Merbs, S. L.; Nathans, J. "Absorption spectra of human cone pigments." *Nature* **1992**, *356*, 433-435.
5. Lythgoe, J. N., Handbook of sensory physiology. In *Handbook of sensory physiology*, ed.; Dartnall, H. J. A., Springer: New York, 1972; Vol. 7/1, pp 604-624.
6. Shichi, H., *Biochemistry of vision*. ed.; Academic Press, Inc.: New York, NY, 1983; Vol. p.
7. Tiffany, J. M.; Noorjahan, P.; Abdel-Latif, A. A.; Harding, J. J.; Mayne, R.; Brewton, R. G.; Ren, Z. X., *Biochemistry of the Eye*. ed.; Chapman and Hall: London, UK, 1997; Vol. p.
8. Crescitelli, F., The visual cells and visual pigments of the vertebrate eye. In *Handbook of Sensory Physiology*, ed.; Dartnell, H. J. A., Springer-Verlag: New York , NY, 1972; Vol. VII, pp 245-363.
9. Wissinger, B.; Sharpe, L. T. "New aspects of an old theme: The genetic basis of human color vision." *Am. J. Hum. Genet.* **1998**, *63*, 1257-1262.

10. Pugh, E. N. "Rods are rods and cones are cones, and (never) the twain shall meet." *Neuron* **2001**, *32*, 375-380.

11. Dixon, R. A.; Kobilka, B. K.; Strader, D. J.; Benovic, J. L.; Dohlman, H. G.; Frielle, T.; Bolanowski, M. A.; Bennett, C. D.; Rands, E.; Diehl, R. E.; Mumford, R. A.; Slater, E. E.; Sigal, I. S.; Caron, M. G.; Lefkowitz, R. J.; Strader, C. D. "Structural and thermodynamic consequences of burying a charged residue within the hydrophobic core of T4 lysozyme." *Nature* **1986**, *321*, 75-79.

12. Fein, A.; Szuts, E. Z., *Photoreceptors: Their role in vision*. ed.; Cambridge University Press: Cambridge, 1982; Vol. p.

13. Hoffmann, R., *The Same and Not the Same*. ed.; Columbia University Press: New York, NY, 1995; Vol. p.

14. Sakmar, T. P. "Rhodopsin: a prototypical G-protein coupled receptor." *Prog. Nucleic Acid Res. Mol. Biol.* **1998**, *59*, 1-34.

15. DeGrip, W. J.; Gray, D.; Gillespie, J.; Bovee, P. H.; Van den Berg, E. M.; Lugtenburg, J.; Rothschild, K. J. "Photoexcitation of rhodopsin: conformation changes in the chromophore, protein and associated lipids as determined by FTIR difference spectroscopy." *Photochem. Photobiol.* **1988**, *48*, 497-504.

16. Konig, B.; Welte, W.; Hofmann, K. P. "Photoactivation of rhodopsin and interaction with transducin in detergent micelles. Effect of 'doping' with steroid molecules." *FEBS Lett.* **1989**, *257*, 163-166.

17. Birge, R. R. "Photophysics of light transduction in rhodopsin and bacteriorhodopsin." *Annu. Rev. Biophys. Bioeng.* **1981**, *10*, 315-354.

18. Mathies, R., Resonance Raman spectroscopy of rhodopsin and bacteriorhodopsin isotopic analogs. In *Methods Enzymol.*, ed.; 1982; Vol. 88, pp 633-643.

19. Cooper, A. "Energy uptake in the first step of visual excitation." *Nature* **1979**, *282*, 531-533.

20. Emeis, D.; Kuhn, H.; Reichert, J.; Hofmann, K. P. "Complex formation between metarhodopsin II and GTP-binding protein in bovine photoreceptor membranes leads to a shift of the photoproduct equilibrium." *FEBS Lett.* **1982**, *143*, 29-34.

21. Bennett, N.; Michel-Villaz, M.; Kuhn, H. "Light-induced interactivation between rhodopsin and the GTP-binding protein. Metarhodopsin II is the major photoproduct involved." *Eur. J. Biochem.* **1982**, *127*, 97-103.

22. Kliger, D.; Lewis, J. "Spectral and kinetic characterization of visual pigment photointermediates." *Isr. J. Chem.* **1995**, *35*, 289-307.

23. Souto, M. L.; Borhan, B.; Nakanishi, K., Low-temperature photoaffinity labeling of rhodopsin and intermediates along transduction path. In *Methods Enzymol.*, ed.; 2000; Vol. 316, pp 425-345.

24. Shieh, T.; Han, M.; Sakmar, T. P.; Smith, S. O. "The steric trigger in rhodopsin activation." *J. Mol. Biol.* **1997**, *269*, 373-384.

25. Yan, B.; Nakanishi, K.; Spudich, J. L. "Mechanism of activation of sensory rhodopsin I: Evidence for a steric trigger." *Proc. Natl. Acad. Sci. U. S. A.* **1991**, *88*, 9412-9416.

26. Arnis, S.; Hofmann, K. P. "Two different forms of metarhodopsin II: Schiff base deprotonation recedes proton uptake and signaling state." *Proc. Natl. Acad. Sci. U. S. A.* **1993**, *90*, 7849-7853.

27. Szundi, I.; Mah, T. L.; Lewis, J. W.; Jaeger, S.; Ernst, O. P.; Hofmann, K. P.; Kliger, D. S. "Proton transfer reactions linked to rhodopsin activation." *Biochemistry* **1998**, *37*, 14237-14244.

28. Gray-Keller, M. P.; Detwiler, P. B. "The calcium feedback signal in the phototransduction cascade of vertebrate rods." *Neuron* **1994**, *13*, 849-861.

29. Schnetkamp, P. P. M. "How does the retinal rod Na-Ca + K exchanger regulate cytosolic free Ca^{2+}?" *J. Biol. Chem.* **1995**, *270*, 13231-13239.

30. Rando, R. R. "The chemistry of vitamin A and vision." *Angew. Chem. Intl. Ed. Engl.* **1990**, *29*, 461-480.

31. Rando, R. R. "Polyenes and vision." *Chem. Biol.* **1996**, *3*, 255-262.

32. Pepe, I. M. "Rhodopsin and phototransduction." *J. Photochem. Photobiol. B-Biol.* **1999**, *48*, 1-10.

33. Wheeler, G. L.; Bitensky, M. W. "A light-activated GTPase in vertebrate photoreceptors: regulation of light-activated cyclic GMP phosphodiesterase." *Proc. Natl. Acad. Sci., USA* **1977**, *74*, 4238-4242.

34. Fung, B. K.; Hurley, J. B.; Stryer, L. "Flow of information in the light-triggered cyclic nucleotide cascade of vision." *Proc. Natl. Acad. Sci., USA* **1981**, *78*, 152-156.

35. Cooper, A.; Converse, C. A. "Energetics of primary processes in visual excitation: Photocalorimetry of rhodopsin in rod outer segment membranes." *Biochemistry* **1976**, *15*, 2970-2978.

36. Schnick, G. A.; Cooper, T. M.; Holloway, R. A.; Murray, L. P.; Birge, R. R. "Energy storage in the primary photochemical events of rhodopsin and isorhodopsin." *Biochemistry* **1987**, *26*, 2556-2562.

37. Miki, N.; Keirns, J. J.; Marcus, F. R.; Freeman, J.; Bitensky, M. W. "Regulation of cyclic nucleotide concentrations in photoreceptors: An ATP-dependent stimulation of cyclic nucleotide phosphodiesterase by light." *Proc. Natl. Acad. Sci. U. S. A.* **1973**, *70*, 3820-3824.

38. Lamb, T. D. "Gain and kinetics of activation in the G-protein cascade of phototransduction." *Proc. Natl. Acad. Sci. U. S. A.* **1996**, *93*, 566-570.

39. Dartnall, H. J. A. "The photosensitivities of visual pigments in the presence of hydroxylamine." *Vision Res.* **1968**, *8*, 339-358.

40. Dartnall, H. J. A.; Goodeve, C. F.; Lythgoe, R. J. "The quantitative analysis of the photochemical bleaching of visual purple solutions in monochromatic light." *Proc. Roy. Soc. A* **1936**, *156*, 158-170.

41. Kim, J. E.; Tauber, M. J.; Mathies, R. A. "Wavelength dependent cis-trans isomerization in vision." *Biochemistry* **2001**, *40*, 13774-13778.

42. Schneider "Spectral variation in the photosensitivity of visual purple." *Proc. Roy. Soc. A* **1939**, *170*, 102-112.

43. Hecht, S.; Shlaer, S.; Pirenne, M. H. "Energy, quanta, and vision." *J. Gen. Physiol.* **1942**, *25*, 819-840.

44. Pitt, G. A. J.; Collins, F. D.; Morton, R. A.; Stok, P. "Rhodopsin. VIII. N-Retinylidenemethylamine, an indicator yellow analog." *Biochem. J.* **1955**, *59*, 122-128.

45. Blatz, P. E.; Baumgartner, N.; Balasubramaniyan, B.; Balasubramaniyan, P.; Stedman, F. "Wavelength regulation in visual pigment chromophore. Large induced bathochromic shifts in retinol and related polyenes." *Photochem. Photobiol.* **1971**, *14*, 531-549.

46. Erickson, J. O.; Blatz, P. E. "N-retinylidene-1-amino-2-propanol: a Schiff base analog for rhodopsin." *Vision Res.* **1968**, *8*, 1367-1375.

47. Maxwell, J. C. *Phil. Trans. Roy. Soc.* **1860**, *150*, 57-84.

48. Smith, V. C.; Pokorny, J. "Spectral sensitivity of color-blind observers and the human cone photopigments." *Vision Res.* **1972**, *12*, 2059-2071.

49. Rushton, W. A. H., *Handbook of sensory physiology*. ed.; Springer: New York, NY, 1972; Vol. 7, p 364-394.

50. Neitz, M.; Neitz, J.; Jacobs, G. H. "Spectral tuning of pigments underlying red-green color vision." *Science* **1991**, *252*, 971-974.

51. Schnapf, J. L.; Kraft, T. W.; Baylor, D. A. "Spectral sensitivity of human cone photoreceptors." *Nature* **1987**, *325*, 439-441.

52. Brown, P. K.; Wald, G. "Visual pigments in single rods and cones of the human retina. Direct measurements reveal mechanisms of human night and color vision." *Science* **1964**, *144*, 45-52.

53. Dartnall, H. J. A.; Bowmaker, J. K.; Mollon, J. D. "Human visual pigments:microspectrophotometric results from the eyes of seven persons." *Proc. R. Soc. B* **1983**, *220*, 115-130.

54. Nakanishi, K.; Balogh-Nair, V.; Arnaboldi, M.; Tsujimoto, K.; Honig, B. "An external point charge model for bacteriorhodopsin to account for its purple color." *J. Am. Chem. Soc.* **1980**, *102*, 7945-7947.

55. Motto, M. G.; Sheves, M.; Tsujimoto, K.; Balogh-Nair, V.; Nakanishi, K. "Opsin shifts in bovine rhodopsin and bacteriorhodopsin. Comparison of two external point-charge models." *J. Am. Chem. Soc.* **1980**, *102*, 7947-7949.

56. Palczewski, K.; Kumasaka, T.; Hori, T.; Behnke, C. A.; Motoshima, H.; Fox, B. A.; Le Trong, I.; Teller, D. C.; Okada, T.; Stenkamp, R. E.; Yamamoto, M.; Miyano, M. "Crystal structure of rhodopsin: A G protein-coupled receptor." *Science* **2000**, *289*, 739-745.

57. Schertler, G. F. X.; Hargrave, P. A. "Projection structure of frog rhodopsin in two crystal forms." *Proc. Natl. Acad. Sci. U. S. A.* **1995**, *92*, 11578-11582.

58. Unger, V. M.; Hargrave, P. A.; Baldwin, J. M.; Schertler, G. F. X. "Arrangement of rhodopsin transmembrane α-helices." *Nature* **1997**, *389*, 203-206.

59. Baldwin, J. M.; Schertler, G. F. X.; Unger, V. M. "An α-carbon template for the transmembrane helices in the rhodopsin family of G-protein coupled receptors." *J. Mol. Biol.* **1997**, *272*, 144-164.

60. Pogozheva, I. D.; Lomzie, A. L.; Mosberg, H. I. "The transmembrane 7-α-bundle of rhodopsin: Distance geometry calculations with hydrogen bonding constraints." *Biophys. J.* **1997**, *72*, 1963-1985.

61. Herzyk, P.; Hubbard, R. E. "Combined biophysical and biochemical information confirms arrangement of transmembrane helices visible from three-dimensional map of frog rhodopsin." *J. Mol. Biol.* **1998**, *281*, 741-754.

62.

63.

64.

65.

66.

67.

68.

69.

62. Schertler, G. F. X.; Villa, C.; Henderson, R. "Projection structure of rhodopsin." *Nature* **1993**, *362*, 770-772.

63. Unger, V. M.; Schertler, G. F. "Low resolution structure of bovine rhodopsin determined by electron microscopy." *Biophys. J.* **1995**, *68*, 1776-1786.

64. Lin, S. W.; Kochendoerfer, G. G.; Carool, K. S.; Wang, D.; Mathies, R. A.; Sakmar, T. P. "Mechanisms of spectral tuning in blue cone visual pigments." *J. Biol. Chem.* **1998**, *273*, 24583-24591.

65. Nathans, J. "Determinants of visual pigment absorbance: Role of charged amino acids in the putative transmembrane segments." *Biochemistry* **1990**, *29*, 937-942.

66. Kakitani, H.; Kakitani, T.; Rodman, H.; Honig, B. "On the mechanism of wavelength regulation in visual pigments." *Photochem. Photobiol.* **1985**, *41*, 471-479.

67. Tan, Q.; Lou, J.; Borhan, B.; Karnaukhova, E.; Berova, N.; Nakanishi, K. "Absolute sense of twist of the C12-C13 bond of the retinal chromophore in bovine rhodopsin based on exciton-coupled CD spectra of 11,12-dihydroretinal analogues." *Angew. Chem. Intl. Ed. Engl.* **1997**, *36*, 2089-2093.

68. Verdegem, P. J. E.; Bovee-Geurts, P. H. M.; de Grip, W. J.; Lugtenburg, J.; de Groot, H. J. M. "Retinylidene ligand structure in bovine rhodopsin, metarhodopsin-I, and 10-methylrhodopsin from internuclear distance measurements using ^{13}C-labeling and 1-D rotational resonance MAS NMR." *Biochemistry* **1999**, *38*, 11316-11324.

69. Blatz, P. E.; Liebman, P. A. "Wavelength regulation in visual pigments." *Exp. Eye Res.* **1973**, *17*, 573-580.

70.

71.

72.

73.

74.

75.

76.

77.

78.

79.

80.

70. Kropf, A.; Hubbard, R. "The mechanism of bleaching rhodopsin." *Ann. N.Y. Acad. Sci.* **1958**, *74*, 266-280.

71. Blatz, P. E.; Mohler, J.; Navangul, H. "Anion induced wavelength regulation of absorption maxima of Schiff bases of retinal." *Biochemistry* **1972**, *11*, 848-855.

72. Honig, B.; Greenberg, A.; Dinur, U.; Ebrey, T. "Visual pigment spectra: Implications of the protonation of the retinal Schiff base." *Biochemistry* **1976**, *15*, 4593-4499.

73. Wald, G. "Vitamin A in the retina." *Nature* **1933**, *132*, 316-317.

74. Morton, R. A.; Goodwin, T. W. "Preparation of retinene *in vitro*." *Nature* **1944**, *153*, 405-406.

75. Hargrave, P. A. "The amino-terminal tryptic peptide of bovine rhodopsin. A glycopeptide containing two sites of oligosaccharide attachment." *Biochim. Biophys. Acta* **1977**, *492*, 83-94.

76. Hargrave, P. A.; McDowell, J. H.; Curtis, D. R.; Wang, J. K.; Juszczak, E.; Fong, S. L.; Mohanna Rao, J. K.; Argos, P. "The structure of bovine rhodopsin." *Biophys. Struct. Mech.* **1983**, *9*, 235-244.

77. Collins, F. D. "Rhodopsin and indicator yellow." *Nature* **1953**, *171*, 469-472.

78. Morton, R. A.; Pitt, G. A. J. "Rhodopsin. IX. pH and the hydrolysis of indicator yellow." *Biochem. J.* **1955**, *59*, 128-134.

79. Bownds, D. "Site of attachment of retinal in rhodopsin." *Nature* **1967**, *216*, 1178-1181.

80. Akhtar, M.; Blosse, D.; Dewhurst, P. "Studies on vision. The nature of the retinal-opsin linkage." *Biochem. J.* **1968**, *110*, 693-702.

81

82

83

84

85.

86.

87.

88.

89.

81. Hubbard, R. E. In *Paper 4*, Proc. Nat. Phys. Lab. Symp. No. 8, London, 1958; 'Ed.'^'Eds.' London, 1958; p^pp.

82. Oseroff, A.; Callender, R. "Resonance Raman spectroscopy of rhodopsin in retinal disk membranes." *Biochemistry* **1974**, *13*, 4243-4248.

83. Wald, G. "The molecular basis of visual excitation." *Science* **1968**, *162*, 230-239.

84. Honig, B.; Dinur, U.; Nakanishi, K.; Balogh-Nair, V.; Gawinowicz, M. A.; Arnaboldi, M.; Motto, M. "An external point-charge model for wavelength regulation in visual pigments." *J. Am. Chem. Soc.* **1979**, *101*, 7084-7086.

85. Nakanishi, K. *Pure Appl. Chem.* **1985**, *57*, 769-776.

86. Mollevanger, L. C. P. J.; Kentgens, A. P. M.; Pardoen, J. A.; Courtin, J. M. L.; Veeman, W. S.; Lugtenburg, J.; de Grip, W. J. "High-resolution solid-state carbon-13 NMR study of carbons C5 and C12 of the chromophore of bovine rhodopsin. Evidence for a 6-s-*cis* conformation with negative charge perturbation near C12." *Eur. J. Biochem.* **1987**, *163*, 9-14.

87. Arnaboldi, M.; Motto, M. G.; Tsujimotto, K.; Balogh-Nair, V.; Nakanishi, K. "Hydroretinals and hydrorhodopsins." *J. Am. Chem. Soc.* **1979**, *101*, 7082-7084.

88. Sakmar, T. P.; Franke, R. R.; Khorana, H. G. "Glutamic acid-113 serves as the retinylidene Schiff base counterion in bovine rhodopsin." *Proc. Natl. Acad. Sci., USA* **1989**, *86*, 8309-8313.

89. Zhukovsky, E. A.; Oprian, D. D. "Effect of carboxylic side chains on the absorption maximum of visual pigments." *Science* **1989**, *246*, 928-930.

90.

91.

92.

93.

94.

95.

96.

97.

98.

90. Nathans, J.; Thomas, D.; Hogness, D. S. "Molecular genetics of human color vision: The genes encoding blue, green, and red pigments." *Science* **1986**, *232*, 193-232.

91. Gat, Y.; Sheves, M. "A mechanism for controlling the pK_a of the retinal protonated Schiff base in retinal proteins. A study with model compounds." *J. Am. Chem. Soc.* **1993**, *115*, 3772-3773.

92. Rafferty, C. N. "Light-induced perturbation of aromatic residues in bovine rhodopsin and bacteriorhodopsin." *Photochem. Photobiol.* **1979**, *29*, 109-120.

93. Honig, B.; Hudson, B.; Sykes, B. D.; Karplus, M. "Ring orientation in β-ionone and retinals." *Proc. Natl. Acad. Sci. U. S. A.* **1971**, *68*, 1289-1293.

94. Asenjo, A. B.; Rim, J.; Oprian, D. D. "Molecular determinants of human red/green color discrimination." *Neuron* **1994**, *12*, 1131-1138.

95. Yokoyama, R.; Yokoyama, S. "Convergent evolution of the red- and green- like visual pigment genes in fish, astyanax fasciatus, and human." *Proc. Natl. Acad. Sci. U. S. A.* **1990**, *87*, 9315-9318.

96. Chan, T.; Lee, M. L.; Sakmar, T. P. "Introduction of hydroxyl-bearing amino acids causes bathochromic spectral shifts in rhodopsin. Amino acid substitutions responsible for red-green color pigment spectral tuning." *J. Biol. Chem.* **1992**, *267*, 9478-9480.

97. Yoshizawa, T. "The road to color vision: structure, evolution and function of chicken and gecko visual pigments." *Photochem. Photobiol.* **1992**, *56*, 859-867.

98. Janz, J. M.; Farrens, D. L. "Engineering a functional blue-wavelength-shifted rhodopsin mutant." *Biochemistry* **2001**, *40*, 7219-7227.

99.

100.

101.

102.

103.

104.

105.

106.

107.

99. Fasick, J. I.; Lee, N.; Oprian, D. D. "Spectral tuning in the human blue cone pigment." *Biochemistry* **1999**, *38*, 11593-11596.

100. Francois, J., *Heredity in ophthalmology.* ed.; Mosby: St. Louis, 1961; Vol. p.

101. Jager, W., Genetics of congenital colour deficiencies. In *Handbook of sensory physiology.*, ed.; Autrum, V. H.; Jung, R.; Loewenstein, D., Springer: Heidelberg, 1972; Vol. pp 625-669.

102. Winderickx, J. "Polymorphism in red photopigment underlies variation in colour matching." *Nature* **1992**, *356*, 431-433.

103. Hess, R. F.; Sharpe, L. T.; Nordby, K., *Night vision: Basic clinical and applied aspects.* ed.; Cambridge University Press: Cambridge, 1990; Vol. p.

104. Arkin, I. T.; Brunger, A. T.; Engelman, D. M. "Are there dominant membrane protein families with a given number of helices?" *Proteins Struct. Func. Genet.* **1997**, *28*, 465-466.

105. Wang, L.; Yan, H. "NMR study suggests a major role for Arg111 in maintaining the structure and dynamical properties of type II Human Cellular Retinoic Acid Binding Protein." *Biochemistry* **1998**, *37*, 13021-13032.

106. Wang, L.; Li, Y.; Abildgaard, F.; Markley, J. L.; Yan, H. "NMR solution structure of type II Human Cellular Retinoic Acid Binding Protein: Implications for ligand binding." *Biochemistry* **1998**, *37*, 12727-12736.

107. Kleywegt, G. J.; Bergfors, T.; Senn, H.; Le Motte, P.; Gsell, B.; Shudo, K.; Jones, T. A. "Crystal structures of cellular retinoic acid binding proteins I and II in complex with all-*trans* retinoic acid and a synthetic retinoid." *Structure* **1994**, *2*, 1241-1258.

108. Chen, X.; Tordova, M.; Gilliland, G. L.; Wang, L.; Li, Y.; Yan, H.; Ji, X. "Crystal structure of apo cellular retinoic acid bind protein type II (R111M) suggests a mechanism of ligand entry." *J. Mol. Biol.* **1998**, *278*, 641-653.

Chapter 2

II. Engineering a Rhodopsin Protein Surrogate

A. Human Cellular Retinoic Acid Binding Protein II (CRABPII)

Human cellular retinoic acid binding protein II (CRABPII) is a member of the lipocalin family of proteins, all of which have a well conserved β-barrel as the central part of their secondary structure.[1-3] The volume of work done with this family of proteins has demonstrated the stability of the structural scaffold with regards to sequence modifications.[2,4] The high tolerance of the protein structure to changes in its sequence is of utmost importance for this project since many mutations are envisioned in order to accomplish our goals.[5]

Lipocalin proteins are typically small, but have a large binding cavity defined by the β-barrel motif, and principally bind hydrophobic molecules. This will be ideal for introduction of the hydrophobic visual receptor, retinal. Additionally, the large binding cavity (~600 $Å^3$) may allow for some flexibility with regards to the structure of the chromophore, i.e., 11-*cis*-retinal versus all-*trans*-retinal.

CRABPII is a small, soluble protein with only 137 amino acids, and is easily prone to site directed mutagenesis.[6] It natively binds retinoic acid via a salt bridge with Arg 132 and through the intermediacy of a water molecule to Arg 111, and is believed to protect cells from the detrimental effects of free retinoic acid.[5] The secondary structure of CRABPII is consistent with the lipocalin family, and is made up of two five-stranded β-sheets and a helix-turn-helix motif with a large binding cavity (Figure II-1).

Although the native human chromophore for rhodopsin is the 11-*cis* isomer of retinal, we have initially performed all of the binding assays utilizing the all-*trans* isomer. All-*trans*-retinal will be much easier to work with, since 11-*cis*-retinal isomerizes to all-*trans* very readily in the presence of minimal natural light. Once the binding assays have been perfected, select proteins will be used with 11-*cis*-retinal, however should this not bind as well as the all-*trans* it should not hinder the ultimate goals of this project. All-*trans* retinal exhibits the same red shifting ability as the 11-*cis* isomer when transformed into the protonated Schiff base moiety. Bacteriorhodopsin, a light driven proton pump, binds the all-*trans*- and 13-*cis* isomers of retinal as PSB, and both exhibit a red shifted retinal λ_{max} (all-*trans*, 570 nm and 13-*cis*, 412 nm).[7] Although the degree of wavelength regulation seen in all-*trans*-retinal versus 11-*cis*-retinal may be different, the mechanism which guides their spectral shifts should be very similar. All data presented utilize all-*trans*-retinal with the exception of section II-I that specifically addresses our attempts at utilizing 11-*cis*-retinal.

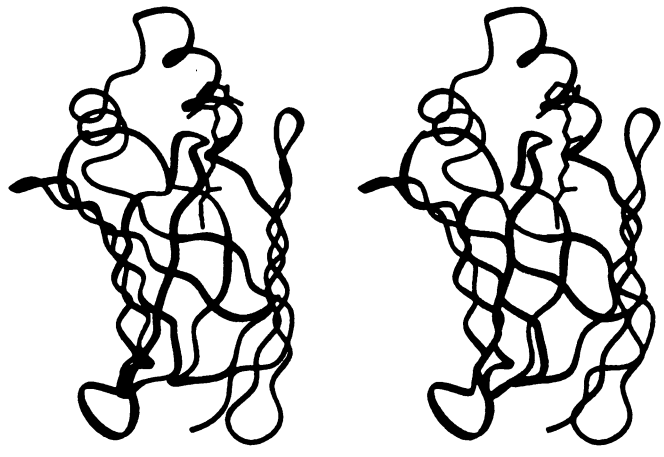

Figure II-1. Stereo view of CRABPII with bound retinoic acid. The β-barrel motif provides a large interior cavity utilizing a small number of amino acid residues.

As cloned into the pET-17b vector (between the NdeI and EcoRI cleavage sites), CRABPII (434 base pairs) would be expressed as the native protein with only 137 amino acids. Since this project will require production of a significant number of protein mutants, we opted to add an affinity purification tag to reduce the amount of time spent on the purification process. Because of ease and availability, we chose to use a 6x-His tag. This tag consists of a chain of six histidine residues that will bind to a Ni^{2+} bound resin (Ni-NTA, Novagen) allowing clean and rapid purification of the desired His-tagged protein from other protein impurities (Figure II-2).[8]

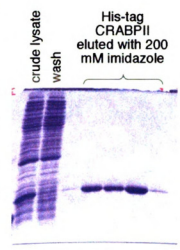

Figure II-2. Gel of a His-tagged CRABPII protein. The first lane shows over-expression of the desired CRABPII band. The second lane shows a separation of all undesired proteins away from the desired CRABPII, shown in > 90% purity in the last five lanes.

In brief, proteins are expressed from the Tuner(DE3)pLacI *E. coli* strain (BL21(DE3)pLysS is used to express from the pET-17b plasmid), following typical IPTG induced protocols.[9] The crude lysate, which contains the soluble CRABPII protein was poured through the Ni-NTA column, binding the histidine tag. Undesired proteins can be washed away from the column and the desired protein can be eluted with an imidazole containing buffer, affording the CRABPII protein in very high purity. Typical expressions yield 10 – 50 mg of protein per liter of culture. Excess imidazole must be washed away before proceeding any further with the protein, as imidazole absorbs in the same region as proteins (~280 nm), which will interfere with determination of protein concentration.

In choosing to incorporate this tag there were several factors to consider, the first being, whether to add the tag to the N-terminus or the C-terminus of the protein. In CRABPII, both termini are on the opposite side of the protein as the opening to the binding cavity (Figure II-3), and addition of several new amino acids should not cause any interference with retinal binding. For this reason, we concluded that choice of either terminus, in our case, would not make a difference.

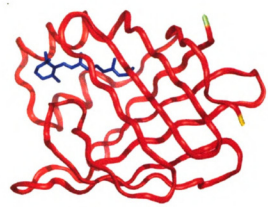

Figure II-3. CRABPII with retinal bound, showing the relationship of the N- and C-terminus being on the opposite of the protein as compared to the entrance of the binding pocket.

Secondly, one must decide whether or not to install a cleavage site for the tag so that it may be removed after purification. Along the same lines, one must also decide which plasmid to use for incorporation of the gene and expression of the protein. We had initially looked into, and actually completed, the cloning of CRABPII into the pET-30a plasmid (Novagen). This clone incorporated the CRABPII gene through the BamHI restriction site and placed a cleavable His tag on the N-terminus of the protein. Through this cloning however, 47 extra amino acids were added onto the N-terminus of the protein. Although after purification, the His tag could be cleaved enzymatically with thrombin, it would still leave 33 additional amino acids. Since this project requires extensive protein / substrate analysis, and confidence in the structure of the protein to assure the mutations we make are at the locations, relative to the chromophore, as desired, the large number of new amino acids was of concern. Without being certain of

the proteins' three-dimensional structure, and whether or not these additional amino acids would affect the overall established structure, we opted to abandon this clone for one that would add fewer extra amino acids.

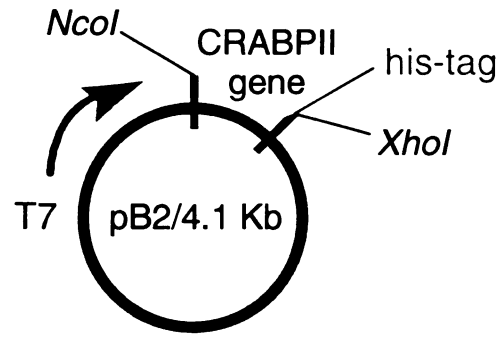

Figure II-4. CRABPII is cloned into the pET-Blue2 plasmid via NcoI and XhoI restriction sites, incorporating a six residue Histidine tag on the gene. The plasmid operates under the lac operon and T7 promoter and is ampicillin resistant.

The second plasmid utilized was pET-Blue2 (3653 bp, Novagen).[10] CRABPII was cloned into the NcoI and XhoI restriction sites (Figure II-4), which lead to two additional residues being added to the N-terminus of the protein. The initial methionine residue (the start codon) is not retained in the native system, pET-17b. In many cases the starting Met residue is subject to post-translational elimination, and is not retained. However, expression of the CRABPII gene in pET-Blue2 allows for retention of the initial Met. An alanine residue was also added in the second position as a result of using the NcoI restriction site. This is because the NcoI site incorporation adds the Met start codon, but not in frame with the remainder of the proteins' codons, therefore, two additional base pairs had to be added in order to keep the expression in frame. We chose an alanine residue solely because of the small size, and felt that this small residue would have minimal, if any, effect on the protein structure and folding.

In addition to the two extra residues added onto the N-terminus, eight amino acids had to be added to the C-terminus; six of those consist of the histidine purification tag, and two result from the XhoI restriction site incorporation necessary for the cloning. We

assumed that by adding these extra amino acids, we would not alter the overall structure of the protein, which we could probe through CD spectroscopic analysis of the resultant proteins and crystallographic comparison with the wild type protein.

As an alternative, the His tag could be incorporated into our gene by PCRing six His residues onto either terminus with the original pET-17b plasmid. We in fact did attempt to do this while at the same time pursuing the pET-Blue2 clone. We later abandoned this idea for two reasons. First, the cloning into pET-Blue2 proceeded with greater ease and produced the desired product faster. Secondly, we found that pET-17b is a low copy plasmid providing only minimal DNA, whereas pET-Blue2 is a high copy plasmid regularly providing more than 400 μg of pure plasmid DNA upon purification of a 500 mL culture. Our choice between the 6x-His incorporated pET-17b or the cloned pET-Blue2 CRABPII, as we would later establish, would not make a difference. As the PCR mutagenesis protocol was established and optimized, even the low copy pET-17b plasmid would have provided us with ample DNA for our purposes. Additionally, comparison of fluorescence, UV-vis, and MALDI-TOF data of the slightly longer pET-Blue2 protein to the identical protein derived from pET-17b (no His tag) proved the additional 10 amino acid residues have no effect on the retinal binding properties.

The pET-Blue2 CRABPII containing clone has added a minimal number of residues to the protein while still incorporating a purification tag for a more rapid production of a protein library. However, by only adding the minimal number of residues, we have removed the cleavage site for the His tag making it a permanent addition to the protein. As mentioned above though, the additional residues do not interfere in retinal binding.

Though the lengthy purification procedure of the unaltered CRABPII protein expressed from the pET-17b clone initially forced us into the use of pET-Blue2 His-tagged CRABPII clones, we eventually had to go back to the native clone. As our collaborators have found, incorporation of the additional residues as acquired from pET-Blue2 (2 on the N-terminus and 8 on the C-terminus) have a detrimental effect on crystallization. There are known cases where the addition of a His tag has no effect on production of well-diffracting crystals,[11] as well as cases where addition of the His tag has hindered the crystallization progress.[12] Reasons why it may or may not effect crystallography are not known to any degree of certainty. Because of the inability to crystallize His-tagged CRABPII proteins, we had to go back to producing the native pET-17b derived CRABPII proteins without the His tag.

Crystallographic efforts (collaboration with Professor James Geiger, Department of Chemistry, Michigan State University) will be an important part of the structural information gathering. Through crystallography of the CRABPII mutants, not only will we be able to tell if the mutations are causing a change in the overall structure of the protein, but we will be able to determine the orientation of those amino acids within the binding pocket. The most crucial piece of information we hope to gain from crystallography is the direct amino acid relations to the bound chromophore retinal.

Since production and purification of the pET-Blue2 proteins occurred at a more rapid pace, as compared to the pET-17b clone, we first made all proteins with the His tag, performed all binding assays, and then determined which proteins were most interesting to pursue crystallographic analysis. These proteins were remade with the pET-17b plasmid (no His tag). By having the same protein mutants from both pET-17b and the

His tag containing pET-Blue2, we could verify that the existence of the extra amino acids has no effect on the retinal binding properties. All duplicate proteins (His tag vs. no His tag with the same mutations) demonstrated the same results in binding affinity, retinal absorbance, and covalent bond formation as monitored by MALDI-TOF. Production of the pET-17b proteins was taken over by Chrysoula Vasileiou (Michigan State University) and more details of the data can be found in her thesis. All of the data I present here are from His-tagged CRABPII proteins arising from the pET-Blue2 plasmid.

B. Spectroscopic Techniques Utilized for Characterization of Proteins and Protein / Substrate Complexes

Once proteins have been expressed and purified, they will be analyzed through CD for structural features, and UV-vis for determination of extinction coefficients which will be used for preparation of protein solutions with high concentration accuracy. In addition to methods for protein characterization, several assays will be used for determination of the retinal binding properties of each protein, including fluorescence, UV-vis, and MALDI-TOF. Each binding assay is equally, yet uniquely important in the complete analysis of the retinal binding properties with the CRABPII proteins as they each provide us with different informative insight into the protein / substrate interactions taking place.

Fluorescence titrations of the protein with retinal (or retinoic acid) will give us a binding affinity by providing dissociation constants. UV-vis experiments will demonstrate the existence of a retinal protonated Schiff base as visible through the expected bathochromic shift for this species. Finally, MALDI-TOF will be utilized to investigate the existence of any covalent complex between retinal and the protein.

These spectroscopic techniques will be introduced here, explaining why each procedure is necessary, what information we can and cannot gain from it, and giving a brief description of the technique involved and how it was optimized. More descriptive details of the procedures involved in each method can be found in the materials and methods section at the end of this chapter. Detailed results of these experiments will be

discussed with the introduction of each new protein, or can be found in the Appendix, but the general trends to make note of will be addressed here as well.

B.1. Extinction Coefficients

The first measurement made on a protein was the extinction coefficient determination, utilizing the method as described by Gill and von Hippel.[13] Briefly, protein solutions of identical concentration were prepared in both a native and a denaturing buffer and the A_{280} was measured by UV-vis. The theoretical extinction coefficient for the denatured sample can be calculated as a function of the number of Trp, Tyr, and Cys residues in the protein. Utilizing this calculated value and the two absorbance measurements for the natured and denatured samples, the extinction coefficient for the protein in the native state can be calculated by Beer's Law. Care must be taken in this measurement, and repetition must be done to ensure accuracy, as this calculated extinction coefficient will be used for protein concentration determinations. Accuracy in the concentration is a very important issue in many of the binding assays used, particularly the fluorescence and UV-vis experiments where precise concentrations of protein relative to chromophore must be known for accurate conclusions to be drawn.

Proteins demonstrate a signature 280 nm peak in the UV-vis primarily due to Trp absorbance, although Phe contributes a little as well.[14] Provided an accurate extinction coefficient is found, protein concentrations can simply be measured by using the A_{280}. There are alternative ways to obtain protein concentration values by utilizing standardized methods such BioRad or the BCA reagent.[15] Both techniques involve preparing various concentration samples of another protein, BSA, in order to create a standardized curve to which measurement of our protein samples can be compared to. Initially I had ensured the accuracy of the CRABPII extinction coefficients by comparing

the concentrations obtained from UV-vis (utilizing the experimentally determined extinction coefficient) with the concentrations determined from the BioRad assay. Reproducible values confirmed accurate extinction coefficients, hence future concentration measurements were simply made with the UV-vis measurement alone.

The wild type CRABPII has a reported extinction coefficient of 19,480 $M^{-1}cm^{-1}$.[6] Our experimentation with the His-tagged CRABPII provided an extinction coefficient of 20,215 $M^{-1}cm^{-1}$, which closely agrees with the published result. All CRABPII mutants made, with the exception of four proteins that incorporate an additional Trp residue whose extinction coefficients are in the range of 25,000 – 30,000 $M^{-1}cm^{-1}$, produce extinction coefficients in the range of approximately 16,700 – 22,800 $M^{-1}cm^{-1}$. All values were reproduced several times and found to be within an acceptable range as compared to the published data. Exact values for the extinction coefficient of all proteins can be found in the Appendix.

B.2. Circular Dichroism

The second mode of protein characterization was via CD spectroscopy. Proteins have unique characteristics in the CD spectrum.[16] The use of CD spectroscopy for protein characterization depends mostly on empirical rules. In particular, proteins with α-helical regions show two negative peaks at 222 nm and 210 nm, and a positive peak near 200 nm, while β-sheet structures show a characteristic negative peak near 220 nm and a positive peak near 200 nm. Also present in some CD spectra is a 230 nm peak that arises from the absorbance and interaction of Trp and other aromatic residues in the protein.[17] This peak may or may not be present in a protein's spectrum depending on the nature and orientation of these residues. The CD curve for the wild type CRABPII as shown in Figure II-5, cleanly depicts all three peaks, 200 nm α-helical and β-sheet peak, 220 nm β-sheet peak, and the 230 nm peak due to the aromatic amino acid absorbances, and compares very well to CD spectra published for the structurally related proteins CRABPI, CRBPII, and CRALBP proteins.[18,19]

All CRABPII mutant proteins expressed do show the characteristic β-sheet peak at approximately 220 nm. The CD curves for all these proteins can be found in the Appendix. However, with some proteins, it was difficult to

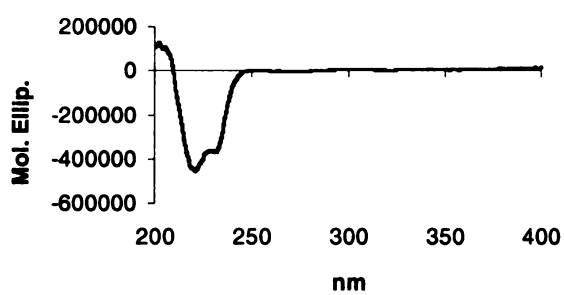

Figure II-5. CD spectra of the wild type CRABPII protein clearly shows a β-sheet folding pattern as evident through the negative 221 nm negative peak and the 200 nm positive peak.

positively identify the α-helical region. The amount of helicity in CRABPII is masked by the dominant β-sheet formation, thus the 210 nm peak expected is not clearly depicted.

The 230 nm peak that was clearly visible in the wild type protein was not always visible in the spectra of the mutant proteins. In most cases, the two peaks (220 nm and 230 nm) are hardly distinguishable from one another. The variation in the appearance of the 230 nm peak is probably due to small changes in structure that lead to changes in extinction. This is not completely unexpected as variations in the extinction coefficients, which are also a measure of the absorbances of aromatic amino acids, changes from one protein to the next as well.

Instrument settings and sample concentrations were very important in acquiring reproducible CD spectra, as they are for most all of the analytical techniques used in this project. The protein concentrations used had to be in the range of 1 – 5 μM. Lower concentrations gave very noisy spectra, while higher concentrations produced spectra where the amino acid absorbance overshadowed the structural features and the only peak visible was the 230 nm peak. The bandwidth of the instrument, which defines how much light is allowed to enter the sample chamber, also played a role in this as well. The reported data was obtained while using a bandwidth of 1 nm, a bandwidth any higher than this produced similar results where the 230 nm peak was dominant and overbearing.

The CD data gathered thus far has only been used as a crude analysis of the protein structure, primarily to ensure the presence of the characteristic β-sheet peak. Analysis of this nature does not tell us exactly what percent of the protein in the sample actually maintains all of either the β-sheet or α-helical properties. A more thorough

analysis of the CD data, and possible calculation of the percent of secondary structure relative to protein concentration may prove to be a beneficial tool in future protein analyses.

Retinal itself does not portray a CD curve, however when bound to rhodopsin, it can be observed via CD.[20] Retinal demonstrates an induced chirality as a result of covalently binding to a chiral molecule in a chiral environment. There are also published spectra which exhibit induced CD in retinoic acid when bound to CRABPI, although the peaks are not very pronounced.[19] The difference between these two is that retinal is covalently bound to rhodopsin, while retinoic acid with CRABPI is not. The CD curve observed is a result of induced chirality as a consequence of the strong H-bonding with the protein and rigid structure the chromophore adopts.

We will also use CD to probe retinal binding with the CRABPII mutants, where it may be possible to see both bound aldehyde and covalently linked SB, albeit the SB peak is expected to be more prominent. These attempts will be addressed in Section II-G.

B.3. Crystallography

Crystallographic analysis of CRABPII will be a crucial part of obtaining direct protein / retinal interaction information, and in fact, CRABPII was selected as the protein of choice for conversion into the rhodopsin mimic because it is highly amenable to crystallography. The crystallographic efforts on this project are being performed in collaboration with Professor Jim Geiger (Department of Chemistry, Michigan State University), and precise details on crystallization procedures can be found in the thesis of Soheila Vaezeslami.

We have been able to reproduce the previously published crystal structure of the retinoic acid bound wild type protein, as well as obtain a crystal structure of the apo wild type protein.[5] Previously, an apo crystal structure was only obtainable for the R111M mutant protein.[21] We have also obtained crystal structures for a retinoic acid bound F15W mutant, in addition to both an apo- and a retinoic acid bound R132K::Y134F double mutant CRABPII.

Of course, we ultimately desire a high resolution crystal structure of a retinal bound protein. Unfortunately, this has been hampered due to the low solubility of retinal in water and instability of retinal over the extended periods of time required for protein crystallization. Crystallizing conditions require a high concentration protein sample in an aqueous environment, which is not very suitable for the hydrophobic chromophore. In order to address this, a couple of techniques are being applied. One involves using pre-formed crystals of the apo-protein, and soaking them in a high concentration retinal solution. The other method requires the use of a co-solvent in the protein buffer solution

that will help to solubilize the retinal. The difficulty in this is that different solvents and concentrations must be applied so as to maximize retinal solubility, yet not harm the protein folding and crystallization. In addition to co-solvents, some detergents may have the same effect, but again extreme caution must be used to find a concentration that will not disrupt the protein structure or crystallization. Additionally, to increase the life of the chromophore and its binding to the protein, crystallization is now being performed at 4°C as opposed to room temperature.

Besides the trouble in acquiring a retinal bound crystal structure, the other major setback in the crystallography is the acquisition of well diffracting crystals of the CRABPII proteins that have multiple mutations. Efforts have included the tetra mutant R132K::Y134F::R111L::L121E and the penta mutant R132K::Y134F::R111L::L121E::T54V. Experimentation with these mutants is still ongoing, and very hopeful. We believe to be close to acquiring crystallographic data on the penta mutant, R132K::Y134F::R111L::L121E::T54V.

B.4. Fluorescence

Fluorescence quenching is used for determination of the dissociation constants for binding of both retinal and retinoic acid for each CRABPII protein.[6,22] The fluorescence of Trp residues in the protein is monitored as a function of the added chromophore (Figure II-6). As the chromophore is titrated into the protein solution, some amount of the Trp fluorescence will be quenched. Addition of chromophore continues until the pocket is fully saturated and there is no longer a change detected in the Trp fluorescence. These measurements will be plotted against chromophore concentration and used to determine the dissociation constant (see Materials and Methods for a more detailed description).

The fluorescence titration experiment took a lot of work in optimizing the proper

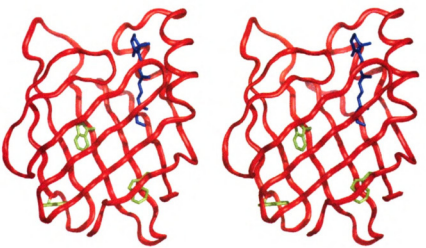

Figure II-6. Stereoview of CRABPII with retinal bound. Binding affinity of chromophores to the CRABPII mutant proteins is monitored by fluorescence quenching of Trp residues. CRABPII contains three Trp residues, 109 (9.4 Å), 7 (10.7 Å), and 87 (17.8 Å).

conditions for adequate, reproducible data. Initially we made several mutants incorporating an additional Trp residue closer to the binding cavity in hopes of solving this problem. An extra Trp residue would not only increase the overall fluorescence of the protein, but by moving it closer to the binding pocket, and closer to retinal, the quenching effect would be dramatically more visible. Tryptophan residues were added at positions 19 (3.7 Å from the nearest point to retinal) and 15 (4.5 Å from the nearest point to retinal) in the wild type protein and the double mutant R132K::Y134F to give the four proteins F15W, L19W, R132K::Y134F::F15W, and R132K::Y134F::L19W. These proteins were later found to be unnecessary for this purpose, but nonetheless still provided us with some valuable insight. The two single mutants, F15W and L19W, demonstrate similar retinal binding properties as compared to the wild type protein. However, the mutations at either position 15 or 19 were ineffective in producing a protein that bound retinal as a PSB. This data will be introduced and discussed in more detail later, but in brief, R132K::Y134F does demonstrate a red shift in retinal's absorbance, which is lost with either R132K::Y134F::F15W or R132K::Y134F::L19W.

The F15W and L19W mutations may have also provided some insight into the structure of the protein. Crystallographic analysis of the F15W protein by Professor Geiger's laboratory has revealed two crystal forms, one in tact and resembling the previously published crystal structure of the wild type CRABPII, and another where the α-helical region near the opening of the binding pocket has been disrupted. Position 15 may be one of the key residues for maintaining the structural integrity of the protein. It is believed that there are only a few specific amino acids in the Lipocalin family of proteins that are responsible for the overall structure of the protein.[23] Another protein was made

to look into this possibility of structural collapse near the entrance to the binding cavity, R132K::Y134F::R111L::L121E::F15A, however, we have yet to obtain crystallographic data on this protein. Binding analysis of this mutant, which will be introduced later, will be used to help in determining the possibility of any structural deviances due to mutation of residue 15.

Optimization of the fluorescence titration experiments was the most tedious of all the assays, as the instrument and the spectra are sensitive to many common, yet potentially detrimental problems. Air bubbles and small particles will cause noisy spectra, therefore buffers should be de-gassed and samples filtered before using them.[24] Fingerprints actually demonstrate quite a bit of fluorescence, so care has to be taken not to touch the quartz cuvettes.[25] When handling the cuvettes lint free gloves should always be worn, as lint on the outside of a cuvette will interfere with a reading just the same. All samples should be stored in glass containers.[25] In the case of protein samples, use silanized glassware, as many plastic containers will leach fluorescent materials into the sample.

Sample concentrations are also very important. Although most of the published work has utilized concentrations in the 10^{-6} M range, I used 10^{-7} M protein solutions. For the most accurate result, you should use a concentration in the range of the expected K_d. Besides, a 10^{-6} M solution could not be used in most cases since retinal binding affinity was very low and a large excess of the substrate had to be added. The low solubility of retinal would produce a cloudy sample and give erroneous results. The amount of EtOH added to the measurement sample was also of concern. Retinal is titrated into the protein from a stock in EtOH (spectral grade). The final EtOH concentration must be kept below

2%. It has been shown that EtOH concentrations between 2-8% can red shift the maximum wavelength up to 40 nm.[26] Additionally, an optimum salt concentration must be used for protein analysis in buffer. Polar solvents, including water have been shown to quench some amount of Trp fluorescence.[27] A high salt concentration (150 mM) potentially helps to shield the protein and reduce the amount of unwanted quenching. All salts used in the buffer must be of the highest grade available to ensure minimal background fluorescence.

Temperature and pH of the measurement samples are also critical to maintain. If the temperature is raised above ambient, the wavelength of the Trp emission will red shift and the intensity of the peak will decrease. At higher temperatures, the excited state can return to the ground state via other means such as phosphorescence.[24,28] Likewise, an optimal pH is required for the protein sample, if it is either too acidic or too basic, the protein sample may denature.[29] Typical protein samples have a Trp emission in the range of 330 – 350 nm, but this varies with the protein, the number of Trp residues, and whether or not they are solvent exposed.[30-32] Free Trp emits at 365 nm. A denatured protein will red shift towards 365 nm and provide a false saturation point for the titration.

Proteins like to stick to the surface of glass. When storing the samples, silanized glassware should be used to avoid loss of protein and a change in protein concentration. When performing the actual fluorescence titration with low concentration protein samples a dummy protein, such as gelatin, should be used to stabilize the protein and avoid loss due to binding with the surface of the cuvette. The cuvettes were incubated for approximately thirty min with a 1% gelatin (w/v) buffer solution. Gelatin is a protein that

does not contain Trp residues, therefore it will not interfere with the fluorescence measurements.

A final note to mention is the fact that retinal alone actually interferes some with the Trp fluorescence detection. The free chromophore will quench some of the Trp emission. To correct for this, one must perform a blank titration with *N*-acetyltryptophanamide, and add back this lost fluorescence.[33] Details of this process are given in the Materials and Methods section. Interestingly however, retinoic acid, which has a closer λ_{max} value to the Trp emission wavelength, does not have the same effect.

In comparing the fluorescence titration curves for retinoic acid binding to retinal binding, the retinoic acid curves generally give a lower relative intensity (~0.2) upon saturation than retinal (~0.5). The drop in intensity is the amount of Trp fluorescence quenched by the chromophore. The closer the chromophore's absorbance is to the Trp emission wavelength, the more it may quench. Retinoic acid absorbs at a similar wavelength to where most of the CRABPII proteins emit fluorescence. Retinoic acid's absorbance is concentration dependent and varies from 350 nm at 10^{-4} M to 338 nm at 10^{-6} M. Trp emission wavelength also varies with the protein and concentration, but typically is at 345 nm for CRABPII protein at 10^{-7}M. Retinal, whose maximal absorbance also varies slightly with concentration, absorbs near 370 nm in a protein solution, that is if it exists as the aldehyde. The Schiff base will absorb near 365 nm and the PSB will absorb anywhere from 420 nm – 465 nm. The lower relative saturation point observed in the retinal titrations may just be due to the fact that retinal cannot quench the Trp absorbance as efficiently as retinoic acid.

We cannot dispute the fact that different forms of retinal may not quench as efficiently, but we also cannot say with certainty that this is the only reason for the observed lower saturation point. Another theory for this could be that two or more isoforms of the mutant proteins exists, and only a percentage of the protein binds retinal. If for example only 50% of the protein binds retinal, that would produce a fluorescence quenched curve with similar characteristics as if 100% of the protein were to bind retinal. The only difference being that the protein that exhibits 100% binding should have a lower relative intensity. This is one instance where a more thorough analysis of the CD curves may help in providing useful insight into degrees of protein secondary structure.

B.5. UV-vis

UV-vis will be the primary means of distinguishing whether or not the formation of a protonated Schiff base has occurred, (diagnostic through a large red shift of the retinal absorbance, Figure II-7). Free retinal absorbs near 380 nm in phosphate buffered saline. As the retinal migrates to the binding cavity of the protein we did not expect a significant difference in absorbance. However, we do in fact see approximately a 10 nm blue shift for the solvent protected free aldehyde as evident by experimentation with several CRABPII proteins that either do not contain a Lys in the binding pocket, or were proven through other means to not form a covalent complex despite having an internal Lys. By solvent protected aldehyde, I do not mean to imply that the retinal in this case must be within the binding pocket, as even proteins with a very low affinity for retinal show a 10 nm blue shift, i.e., the wild type protein whose complete data will be presented in the next section. Perhaps simply the existence of protein in the sample mixture, even if retinal is on the outside of the binding cavity, can provide some degree of shielding.

A significant change in the retinal absorbance was not expected for the formation of a Schiff base either. There have been data published to suggest that the Schiff base will also blue shift slightly from the free aldehyde absorbance. Our experimentation, although somewhat limited in this area also seems to suggest a λ_{max} of ~365 nm for the unprotonated Schiff base. This will be discussed in more detail later. Although there is approximately a 5 nm difference between the free aldehyde and the Schiff base of retinal, we are not confident enough in being able to differentiate these two species solely by UV-vis to draw any decisive conclusions.

We can be confident however in determining if there is a protonated Schiff base present. The PSB of retinal should produce a dramatically red shifted absorbance as seen with the rhodopsin proteins, and even the formation of a PSB with n-butylamine.[34] UV-vis and the red shift of the retinal absorbance will be our primary means of deducing whether or not the protonated state of the SB exists. Although we will have MALDI-TOF analysis of the complexes, given the uncertainty in mass analysis, we cannot distinguish an unprotonated SB from a protonated one, i.e., a single mass unit.

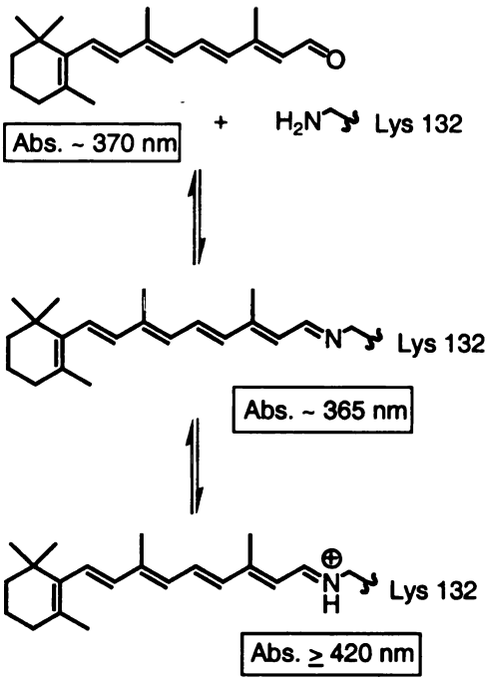

Figure II-7. Equilibrium between retinal and the protein. The free aldehyde and the Schiff base both portray similar λ_{max} values. The protonated Schiff base will show a large red shift.

In brief, we have engineered proteins that red shift to ~420 nm and some up to ~460 nm. The 460 nm absorbing species, at low equivalents (0.25 eq.) show primarily a red shift, but at a higher retinal equivalent addition, only the 380 nm peak grows while there is no change in the 460 nm peak. For proteins that absorb at ~420 nm, after more than 0.25 eq. of retinal was added, the red shifted peak began to shift back to ~380 nm (Figure II-8). This shift in absorbance does not seem to be due to a simple masking of the red shifted peak from an overbearing free aldehyde (380 nm), as second derivative analysis reveals the presence of only a single peak.[35,36] The 420 nm peak is slowly being

shifted to ~380 nm, as opposed to loss of the 420 nm peak and appearance of the 380 nm peak simultaneously, as may be expected if these are two different species.

Since there is a large amount of a non-red shifted species at higher equivalents, to better see the red shifted peak, the free retinal peak was subtracted from the spectra (see Material and Methods section for more discussion). This subtraction has no effect on the peaks already present, it solely allows the red shifted peak to be more visible, as the peaks acquired from the subtraction very closely match those seen from the second derivative of the original spectra. In doing this it can be noticed that, just as second derivative analysis revealed, the peak is red shifted at low equivalents, and gradually returns to ~375 nm, suggesting loss of the red shifted species at higher retinal concentrations (Figure II-8). The MALDI-TOF experiments (discussed in the next section) are done at retinal concentrations greater than one equivalent, and Schiff base is

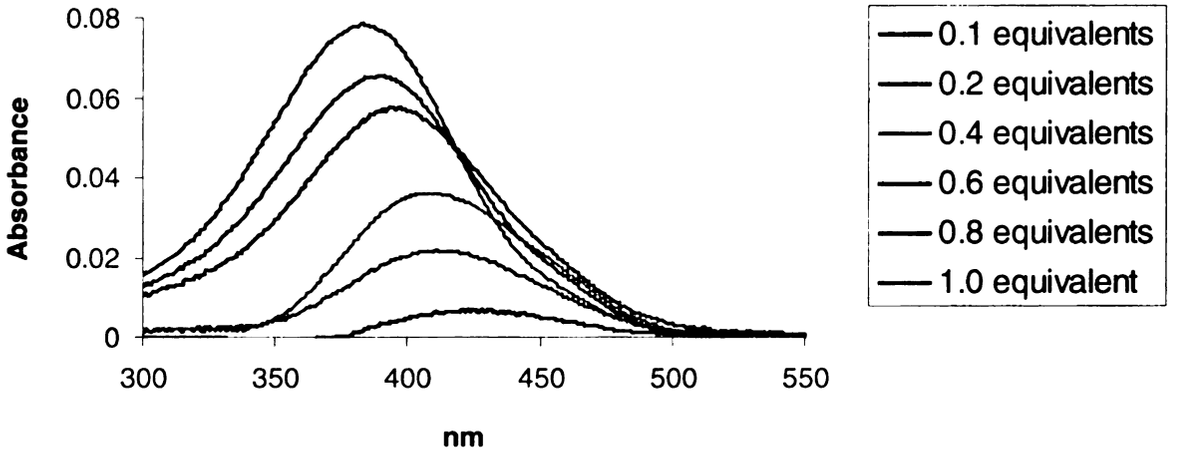

Figure II-8. Corrected UV-vis spectra of a retinal titration with R132K::Y134F::R111E::T54V. As higher retinal equivalents are added the red shift seen at low equivalents is slowly lost. The retinal peak begins at 430 nm, 0.1 equivalents, and ends at 385 nm 1.0 equivalent. The red shifted peak is not simply masked by an overwhelming free aldehyde absorbance, but is no longer present as seen from the second derivative analysis.

still visible, so loss of the red shift here may imply loss of protonation, but not loss of covalent bond formation.

At this point, for purposes of clarity, it should be pointed out that all of the spectra shown within the text are taken with approximately 0.25 equivalents of retinal present and have had an equivalent amount of 380 nm absorbing retinal subtracted from them. In the Appendix both original and subtracted spectra are given, as well as UV-vis curves with varying amounts of retinal.

MA
with
sam
con
retr
dete
TOI
of t
per
wit
be
ne
ar
p
t

B-5. MALDI-TOF

The final binding assay performed on each protein mutant involves the use of two MALDI-TOF experiments.[37] The first of these experiments is the incubation of retinal with the protein. Sufficient time is allowed for Schiff base formation to take place, the sample is then washed with ethanol and concentrated. The covalent bond between retinal and the protein, if formed, can be detected as an $[M+266]^+$ peak in the MALDI-TOF spectrum. In addition, reductive amination of this incubated sample with $NaCNBH_3$ will be performed to covalently trap the retinal molecule with the protein.[38] This covalent compound can be seen as an $[M+268]^+$ peak (Figure II-9). The necessity for both MALDI-TOF experiments arises from the fact that some Schiff bases, protonated or not, may not be stable enough to be trapped under the reductive amination reaction conditions, but will survive the work-up from the incubation long enough to be detected.

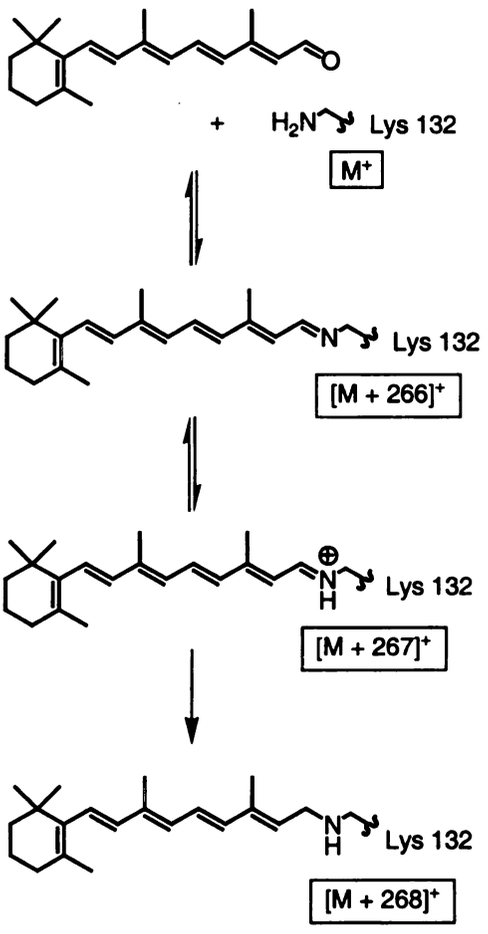

Figure II-9. Covalent bond formation between retinal and the protein can be detected by MALDI-TOF. Schiff base or PSB formation can be seen as an $[M+266]^+$ or $[M+267]^+$ peak, respectively. Both species can be reductively aminated and trapped as an $[M+268]^+$ species.

Initially, we had attempted many different procedures to separate unreacted retinal or reduced retinal from the protein before

finding a successful route. A summary of these methods is given in Table II-1. In brief, extractions, centrifugal filters, ion exchange chromatography, size exclusion chromatography, or ion affinity would not completely separate retinal and/or retinol from the protein reaction mixture. A denaturing extraction with ethyl acetate and urea did provide separation of a retinal / protein sample, however, it did not separate retinal from a protein solution (wild type) that also contained the borohydride reducing agent.

Several of these methods were also attempted with radioactive retinal, 15-^{3}H-retinal, including Sephadex and Ni^{2+}-NTA separation. Some amount of radioactivity was found in the protein (wild type and R132K::Y134F) containing fractions, but similar amounts of radioactivity were found in almost all fractions, even non-protein containing fractions. Generally, the radioactivity was spread equally in all fractions, and the majority of the radioactivity could not be accounted for, presumably stuck to the column resin which could not be solubilized well enough in the scintillation cocktail for adequate detection. While it was encouraging that most of the retinal was being separated, the fact that we could still detect retinal by UV in the protein containing fractions (wild type, no Lys in the binding cavity), meant that it may still interfere in the MALDI-TOF experiments and the determination of retinal binding to be solely within the binding cavity.

Our attempts at separating noncovalently linked chromophore from the retinal / protein incubated mixture, without disturbing the covalent bond of SB bound retinal, included concentration with Millipore centrifugal filters, washing once with EtOH and twice with water. Mass analysis will show a covalently bound retinal molecule to select proteins as a +266 adduct (retinal MW = 284 g/mole). Proteins without the engineered

Lys
sep
the
pro
de
pro
ve
no
pro
las
pe
w
d

Lys in the binding cavity will not show this adduct, proving that either all free retinal is separated from the mixture, or at least will not interfere with the results obtained as only the free protein peak is observed. Separation of retinal from a reductively aminated protein mixture was achieved through use of a Fast-Q ion exchange column. A more detailed procedural explanation can be found in the Material and Methods section.

While considering the spectra from either the incubation of retinal with the protein or the reductive amination between the two, the peak ratios between free protein versus protein revealing a covalently linked retinal molecule can only be qualitatively and not quantitatively. That is, based on peak ratios, we cannot determine how much of the protein sample is bound to a retinal molecule. Retinal absorbs near the frequency of the laser and often does not ionize as efficiently as the free protein would. Additionally, the peak ratios will vary based on how well the mixture co-crystallizes with the matrix and where the laser is actually shot. Often, one sample will produce very different peak ratios depending on where the laser is aimed.

A final note of mention in the MALDI-TOF spectra is that, as spectra are acquired as a result of co-crystallization with the matrix sinapinic acid. An adduct as a result of the matrix addition will be seen 220 mass units higher than the protein peak, and/or a dehydrated adduct 202 mass units greater than the protein mass may be seen in all MALDI-TOF spectra. This adduct does not interfere with the ability to detect the + 266-268 peak as a result of covalent bond formation with a single retinal molecule.

Table II-1. Summary of procedures attempted for retinal removal from protein solutions

Action for Removing Retinal	Result
Spin through Millipore 500 μL-centrifugal filters	1. Water wash, retinal did not wash through filter. 2. Acetonitrile wash dissolved filter
Spin through Millipore YM-3 centrifugal filters	1. EtOH wash did not pass through filter. 2. Urea wash, retinal did not pass through filter. 3. SDS wash, retinal did not pass through filter.
Extractions	1. EtOAc, retinal remained in aqueous layer. 2. EtOAc and urea: Would separate retinal from an incubated protein reaction, but would not separate retinal from a reaction where borohydride has been added. 3. Spin to dryness in speedvac, extract EtOAc, did remove some amounts of retinal, but left protein unrecoverable.
Ni^{2+}-NTA Column	1. Retinal coeluted with protein. 2. Under denaturing conditions, retinal was still visible in protein fractions by HPLC.
DEAE Column with 0 – 200 mM NaCl	Retinal coeluted with protein.
Sephadex Column	1. 6M urea buffer, retinal coeluted. 2. 50% acetonitrile in PBS, retinal containing fractions (found by UV) also contained protein (found by SDS-PAGE).
Precipitate protein with trichloroacetic acid	Retinal detected in precipitate. Protein unrecoverable.

C. Wild-Type CRABPII Binding Properties

A depiction of the wild type CRABPII protein can be seen in Figure II-10 with select amino acids in close proximity to the chromophore shown. Arg 132 and Arg 111 are 3.8 Å and 5.4 Å from the retinoic acid carbonyl carbon, respectively. The phenolic oxygen of Tyr 134 is 3.2 Å away, and the hydroxyl oxygen of Thr 54 is 3.8 Å away. Leu 121, which is the only hydrophobic residue in close proximity to the chromophore, resides 3.7 Å from the chromophore.

Previously published data shows that CRABPII has a stoichiometric binding relationship with its native substrate retinoic acid, with an approximate 2 nM dissociation constant.[6] Our experimentation has also reproduced this result (Figure II-11a). Despite retinal having a very similar structure, lack of the anionic functionality prohibits this substrate from having a tight binding to the protein. Recall that the anionic retinoic acid is held in place through hydrogen bonding with the two positively charged Arg residues. Neutral retinal however, has a very weak affinity for the wild-type protein, exhibiting a

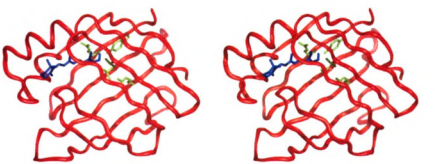

Figure II-10. Stereoview of wild-type CRABPII. Retinal is shown bound to the protein, as well as residues whose mutations will be addressed in the formation of a successful protonated Schiff base forming protein; Arg 132, Tyr 134, Leu 121, Arg 111, Thr 54.

poor dissociation constant, K_d = 6600 ± 360 nM (Figure II-11a). This low binding affinity may be due to the hydrophilic nature of the cavity, and the lack of a stabilizing feature such as the hydrogen bonding network seen in the native system.

The UV maximal absorbance of retinal when incubated with the wild-type CRABPII protein, exhibits a λ_{max} of 370 nm (Figure II-11b). The retinal absorbance value as observed in the phosphate buffered saline (PBS) blank solution is 380 nm. The 10 nm difference, as discussed before, could be due to the non-specific interaction of the protein with retinal, perhaps some amount of shielding of the hydrophobic molecule from the water environment. In addition, since there are no Lys residues within the binding site, the blue shifting cannot be due to Schiff base formation, especially since all the surface Lys residues are undoubtedly protonated at our working pH of 7.3.

MALDI-TOF analysis of the wild-type protein also produced the expected results. Neither the incubation nor the reductive amination produced a peak greater in mass than the protein peak. As a verification of our procedure, retinoic acid, which non-covalently binds the wild type protein with a 2 nM dissociation constant, was added to the protein

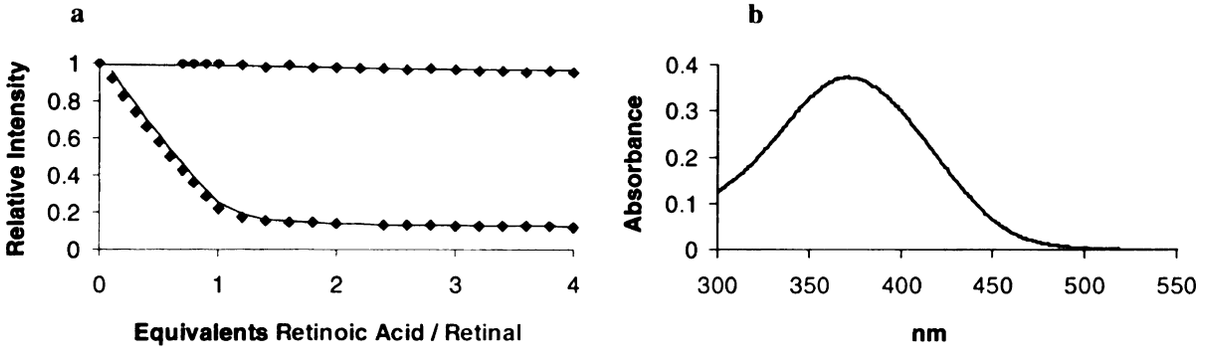

Figure II-11. **a)** Fluorescence titration curves for the retinoic acid and retinal K_d determination with wild-type CRABPII. Retinoic acid shows a stoichiometric binding relationship and K_d = 2.0 ± 1.2 nM. Retinal shows little binding affinity, K_d = 6600 ± 360 nM. **b)** UV-vis of retinal incubated with wild-type CRABPII portrays a maximal absorbance at 370 nm.

under identical reaction conditions. It also failed to produce anything other than the protein M^+ peak in the spectrum, leading us to believe that if any addition products are observed in the MALDI-TOF it must come from covalent complexes.

These results for the wild type protein validate the accuracy of our methods, as all results obtained were those expected, and we were able to reproduce the published values for the dissociation constant of retinoic acid with the wild-type CRABPII. The data gathered for this protein sets the stage for comparison of all new protein mutants made from the wild-type CRABPII.

Before proceeding with the engineering of CRABPII, we can now use the data acquired for the wild type protein and compare to the two single mutant proteins made for fluorescence enhancement, F15W and L19W. The F15W single mutant, whose crystal structure may have suggested some loss of structural integrity, actually demonstrates similar results as compared to the wild type. Fluorescence titrations produce a $K_d = 40 \pm 4$ nM for retinoic acid and $K_d = 5950 \pm 360$ nM for retinal. The retinal absorbance for the F15W protein is 375 nm. This data presents no indication of significant structural defects. Although there is a 5 nm red shift in the UV-vis, and this value is closer to the value expected for a solvent exposed retinal, given the high K_d, retinal is probably not in the binding pocket. Thus, these results offer no insight into the possible disruption of helical structure near the mouth of the cavity.

The L19W single mutant deviates a bit more from the wild-type protein, but not significantly. Retinoic acid affinity has been decreased to 170 ± 22 nM and retinal binding affinity has increased to 900 ± 38 nM. The retinal λ_{max} as bound to L19W is 378 nm, 8 nm red shifted from the wild type. While this value is closer to a solvent exposed

retinal, it cannot be ruled out that interactions with the slightly different binding pocket may force this small shift. As expected, both single mutant proteins do not deviate significantly from the wild type protein binding abilities.

D. Introduction of the Lysine Residue

To create a rhodopsin mimic, we needed to convert CRABPII from a retinoic acid binding protein to one that will bind retinal as a protonated Schiff base via a lysine residue (Figure II-12). There are 13 Lys residues present in CRABPII, however they are all on the surface of the protein. The surface Lys residues, being solvent exposed, will exist in the protonated state at physiological pH, and thus will not interfere with our attempts at engineering a specific Lys – retinal bond. Utilizing the published crystal structure and performing *in silico* mutagenesis and minimizations,[39] arginine 132 was chosen as the position for placement of the pertinent lysine residue. Insight II minimizations place the mutated lysine 2.5 Å from the carbonyl carbon of retinal, within Van der Waals distance for covalent bond formation, and should it exist, would not force the retinal far from its desired position (Figure II-13). The angle of trajectory for covalent bond formation mimics the same seen in rhodopsin as well. The Lys residue approaches the carbonyl from the side of the retinal molecule, that is the plane of the

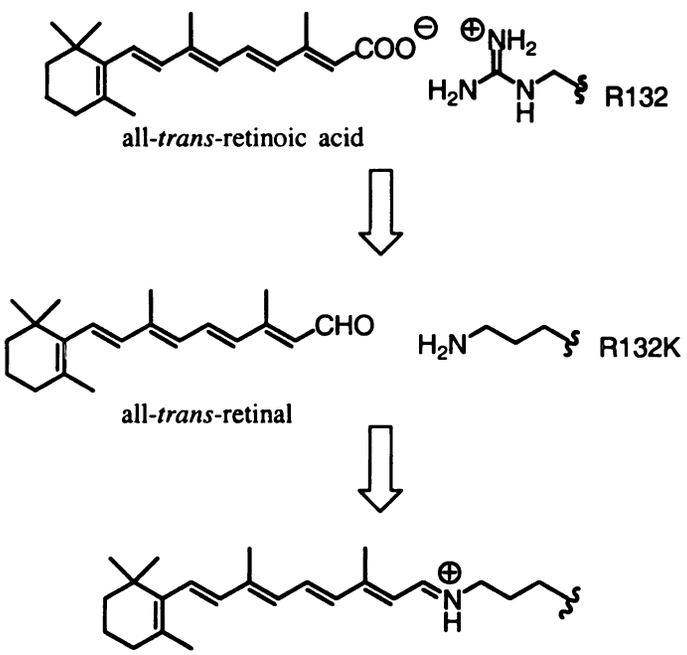

Figure II-12. To create a successful rhodopsin protein mimic, CRABPII will need to be converted from a retinoic acid binding protein to a protein that binds retinal as a protonated Schiff base.

Lys residue and that of the retinal molecule are approximately 90° to each other. Incidentally, the Lys at position 132 happens to have given us the most effective results thus far. The positive results (and covalent bond formation, which will be seen with further mutations) may be a result of the correct orientation of the engineered Lys, in which an optimal angle for attack onto the carbonyl, referred to as the Bürgi-Dünitz angle of 107° has been achieved.[40] Other positions for Lys incorporation have, and are in the process of being investigated and analyzed for effective PSB formation. Discussion of these mutants will be addressed in a later section, as I will first discuss the library of mutants containing the R132K mutation.

Mutagenesis of all CRABPII proteins, was accomplished by utilizing Stratagene's QuikChange® protocol. This method entails the use of complimentary, mutation encoding primers. Following a typical PCR process the reaction mixture will contain circular parental plasmid DNA (unmutated) and linear mutated DNA (Figure II-14). The original template DNA is unique from the mutated DNA, not only in that it is circular, but also it has methylated adenine residues. As the DNA is copied in a bacterial host,

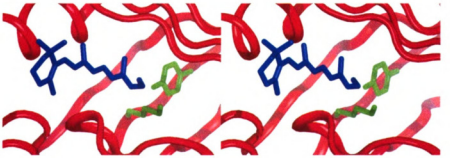

Figure II-13. Stereo view of R132K CRABPII mutant, with Tyr 134 shown. Lys 132 is 2.5 Å away from retinal. The hydroxyl group of Tyr 134 is ~2.8 Å away from the Lys amino group.

some of the adenine bases becomes methylated. The restriction enzyme DpnI recognizes the specific sequence GATC (blunt cut between A and T), but will only cut where methylated adenine residues exist. Our plasmid, pET-Blue2 contains 18 DpnI cut sites, thus incubation of the PCR product with the DpnI restriction enzyme effectively destroys the parental plasmid and leaves only the linear, mutated DNA. The desired product DNA can then be incorporated into the host strain of choice (JM109 or XL1-Blue *E. coli*).

Although Stratagene's QuikChange® method is very reliable in the production of mutations, there is one major downfall. In some instances, despite digestion with DpnI, there remains some amount of unmutated DNA, arising from an incomplete digestion reaction. Also, because we are only mutating a single amino acid at a time (three base pairs) without causing any other changes in the protein, these mutations do not typically allow for a new and unique restriction site to be engineered. The incorporation of a new restriction site would offer a quick means of deducing whether or not the desired mutation had been incorporated; a 5 mL culture could be crudely characterized by a 2 h digestion followed by a 20 min gel. Without this, the plasmid must be expressed on a

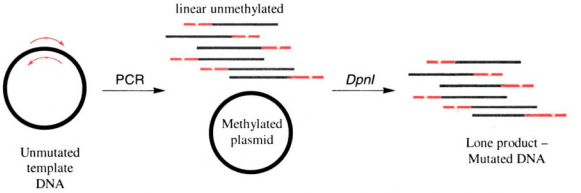

Figure II-14. Depiction of Stratagene's QuikChange® Site-Directed Mutagenesis Protocol. Through use of the restriction enzyme DpnI, the unwanted template DNA can be removed from the desired mutaed DNA product.

larger scale, purified to a high degree, and sent for sequence analysis (2 day turn around time). Once the mutation had been verified by its sequence, the protein was expressed, following IPTG induced procedures, purified by Ni-NTA column, and characterized using all the procedures mentioned previously.

By replacing the Arg residue that was responsible for the strong retinoic acid binding affinity with a Lys residue, the expected decrease in retinoic acid binding affinity (from 2 nM to 65 nM) was concomitant with an increase in retinal affinity (from 6600 nM to 280 nM) (Figure II-15a). Change of hydrophobicity within the pocket may deserve some acknowledgement for the dramatic improvement in retinal binding affinity. Arg has a hydropathic index of – 4.5 versus – 3.9 for Lys (the more positive the number, the more hydrophobic the residue).[41,42]

Fluorescence analysis is followed up by a UV-vis analysis of retinal incubated protein complex. Recall that the UV absorbance of retinal with the wild type protein had a maximal absorbance at 370 nm, and the Schiff base of retinal is expected to absorb near 365 nm. By UV-vis alone, we cannot be certain of the formation of a Schiff base because the expected difference is only 5 nm, and could potentially also be due to unique protein / substrate interactions. However, if the Schiff base is protonated the chromophore will red-shift significantly. As is the case in humans, the protonated Schiff base of 11-*cis*-retinal with rod rhodopsin red-shifts from about 380 nm to 500 nm, a 120 nm red shift.

The incorporation of a Lys residue, the single mutant R132K, did not lead to a change in the retinal absorbance as compared to the wild type, as a 370 nm peak is still observed (Figure II-15b). We expected that this single mutation would not provide PSB formation as the Lys probably still primarily exists in the protonated state due to the

continued hydrophilic nature of the binding cavity. There is however some amount of covalent species detected by both MALDI-TOF experiments. As evident from the lack of a bathochromic shift in the UV-vis, this covalent complex is SB, but not PSB. Further tuning of the pocket is necessary to promote not only substantial PSB formation, but also increased binding affinity.

The lysine responsible for Schiff base formation in rhodopsin probably exists in the unprotonated state.[43] The binding cavity of rhodopsin contains three acidic and three basic residues that exist in the middle of long stretches of hydrophobic amino acids (Figure II-16a).[44] This may allow for effective screening of the lysine residue from water molecules that could protonate it and disrupt the PSB formation.[45] Comparison to the CRABPII binding cavity shows both hydrophobic and hydrophilic amino acids (Figure II-16b). The hydrophilic residues in close proximity to the chromophore may need to be mutated to more hydrophobic residues, mimicking the hydrophobic nature of the

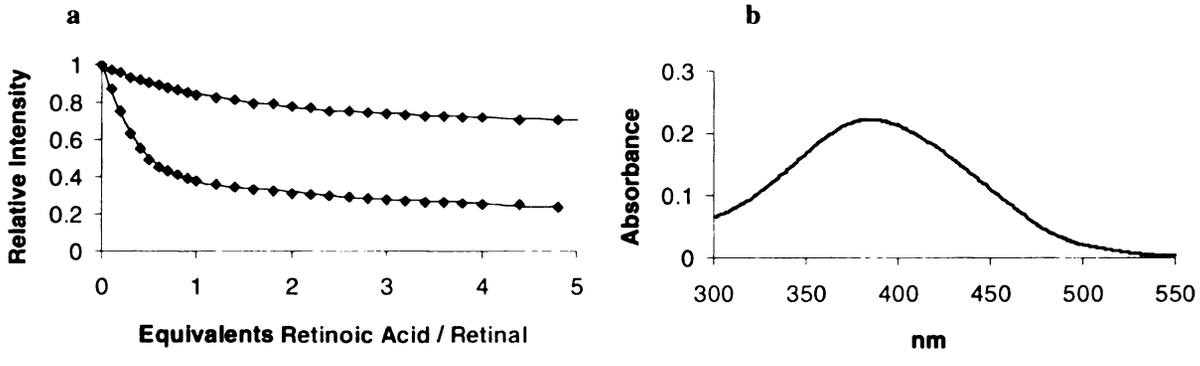

Figure II-15. **a)** Fluorescence titration curves for the retinoic acid and retinal K_d determination with the single mutant CRABPII R132K. The single amino acid mutation displays an expected drop in retinoic acid binding affinity (K_d = 65 ± 14 nM), which is concomitant with a large increase in retinal binding affinity, K_d = 280 ± 17 nM. **b)** UV-vis of retinal incubated with CRABPII R132K portrays a maximal absorbance at 370 nm, unchanged from the wild type protein and most probably due to the hydrophilic nature of the binding cavity and the Lys remaining protonated.

rhodopsin, in order to lower the pK_a of lysine and promote significant degrees of covalent bond formation.

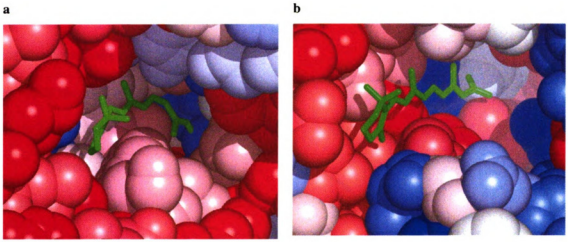

Figure II-16. **a**) View of the binding cavity of rhodopsin (hydrophobic residues are in red, hydrophilic residues are in blue). The Lys in rhodopsin is suggested to exist in the non-protonated state buried due to the extended hydrophobic nature of the binding cavity. **b**) The same view of the CRABPII cavity reveals both hydrophobic and hydrophilic amino acids. The hydrophilic residues in the cavity may need to be altered in order to reduce the pK_a of Lys so that it may exist in the non-protonated state and is available for attack and covalent bond formation with retinal.

E. Hydrophobic Tuning of the Binding Pocket

The next step in trying to achieve the ideal PSB forming mutant was to increase the hydrophobicity of the binding pocket. A more hydrophobic binding pocket will possibly increase the affinity of retinal for the cavity, and allow for the incorporated Lys residue to remain deprotonated. While we are increasing the pocket's hydrophobicity to promote the existence of a non-protonated Lys, keep in mind that we eventually want this same hydrophobic cavity to allow for a positively charged Schiff base to exist.

There were two residues that were of initial interest for possible hydrophilic to hydrophobic mutations, Tyr 134 and Arg 111. Tyr 134 is close to the carbonyl region of the retinal (3.2 Å) and may be involved in favorable hydrogen bonding with Lys 132 that prohibits the Lys from interacting with retinal. Arg 111 is further away from the chromophore (5.4 Å) than Tyr 134 but is a hydrophilic residue and its replacement could serve to make the pocket more hydrophobic.

The first of these amino acids to be mutated was Tyr 134, which was converted to a Phe. This was done for several reasons. First this is a rather conservative mutation that will increase the hydrophobicity of the binding pocket, which we believe is necessary for depressing the pK_a of Lys. Second, through structural comparison within this family of proteins, it is believed that the presence of Tyr aids in the binding of ionic substrates (retinoic acid) while the presence of a Phe group is more suitable for the binding of non-ionic substrates (retinol and retinal). And finally, this will attempt to mimic a Phe residue that exists in the rhodopsin proteins. There is a conserved Phe residue in the binding pocket of the opsin proteins. Rod rhodopsin has F91, which resides 5.9 Å from the closest point to the polyene backbone and near the carbonyl region, blue rhodopsin has

F290, which is postulated to be 5.4 Å away, and green rhodopsin has F309, which is postulated to be 5.8 Å away (in red rhodopsin, this residue is a Tyr.). This may or may not have anything to do with the stabilization of the PSB, but if we can conservatively model CRABPII with the same residues found in the rhodopsin binding cavity, we may increase either the retinal affinity for CRABPII or the possible PSB formation.

By introducing this Phe mutation and increasing the hydrophobicity within the cavity, we see dramatic differences in all of our binding assays. The fluorescence indicates that we do indeed increase the binding affinity for retinal even further (100 nM), and lose more affinity for retinoic acid (120 nM) (Figure II-17a). Most notably, the UV-vis now shows a red-shifting of the chromophore to 429 nm as can be seen in Figure II-17b. A 59 nm red-shift is a good indication that there may be PSB formation.

This 429 nm absorbing species cannot, however, be trapped with a reducing agent despite use of various reaction conditions including varying the length of incubation of retinal with the protein, increasing the reduction time with $NaCNBH_3$, and changing the pH of the reaction (Figure II-17d).

Despite being unsuccessful in trapping a covalent complex by reductive amination, we do see Schiff base formation with the incubation of the two species, before $NaCNBH_3$ addition. A $[M+266]^+$ peak can be seen in the incubation of the protein with retinal as monitored by MALDI-TOF (Figure II-17c). It is possible that the Schiff base or protonated Schiff base is too unstable in the reaction conditions for reductive amination and hydrolyzes before it can be reduced. While the MALDI-TOF results from the incubation with retinal does confirm Schiff base formation, it cannot confirm or

dismiss the existence of this species as a protonated Schiff base as the observed shift in the UV-vis may suggest.

Attempts at proving whether or not the Schiff base was protonated include addition of acid and base to the protein / substrate mixture while monitoring by UV-vis.

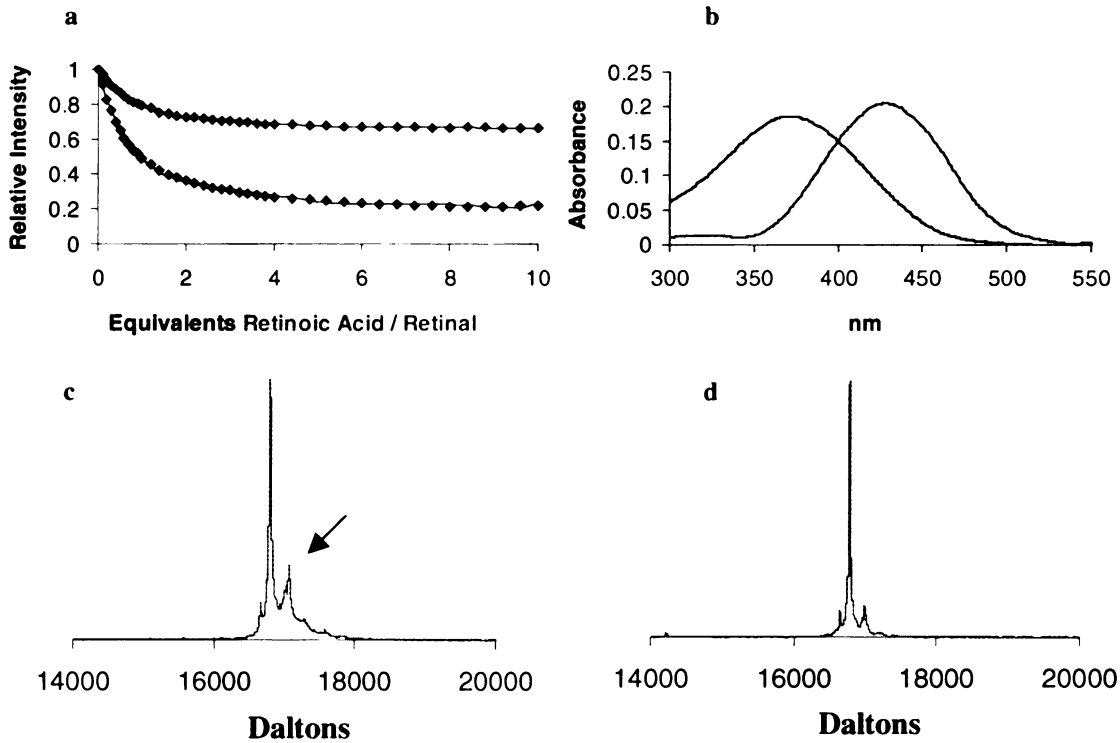

Figure II-17. **a)** Fluorescence titration curves for the retinoic acid and retinal K_d determination with the double mutant CRABPII R132K::Y134F. The additional amino acid mutation displays another expected drop in retinoic acid binding affinity (K_d = 120 ± 4.9 nM), and another expected increase in retinal binding affinity, K_d = 100 ± 7.1 nM. **b)** UV-vis of retinal incubated with CRABPII R132K::Y134F portrays a maximal absorbance at 429 nm, a 59 nm red shift as compared to the wild type CRABPII (370 nm), possibly suggesting protonated Schiff base formation. **c)** MALDI-TOF of the retinal incubated double mutant shows an M^+ = 16798.1 Da corresponding to the protein mass, calculated to be 16785.2 Da. In addition there is small amounts of a second peak (indicated by arrow), M^+ = 17067.4 Da, which is 269.3 mass units higher than the protein peak, representing a covalently linked retinal molecule (calculated mass difference 266). **d)** Reductive amination of retinal with CRABPII R132K::Y134F results in loss of the covalent complex and only the protein mass M^+ = 16788.1 Da can be detected. The small peak to the right of the major protein peak is due to matrix addition to the protein, and does not correspond to the calculated retinal addition molecular weight.

If the 429 nm absorbing species is a nonprotonated Schiff base, lowering the pH of the mixture should protonate the SB and force the retinal absorbance to red shift even more. If the 429 nm species is PSB, addition of acid should have no effect on the absorption, provided caution is taken to ensure that the protein does not denature. Upon addition of a small amount of acid to the sample, the red shift is lost, and the peak blue shifts to 384 nm (Figure II-18). This could be due to the hydrolysis of the covalent bond, whether SB or PSB, and still does not conclusively distinguish between the two. This could also mean that the red shift is not due to a PSB at all, but is observed solely because of the hydrophobic environment of the cavity. Treatment with acid changes the hydrophobicity of the retinal environment and now forces the absorption back to 384 nm.

There have been reports of a 420 nm absorbing retinal that is believed to be a non-protonated Schiff base. Initial studies by Oprian and co-workers with blue rhodopsin, which absorbs at 420 nm, suggested the nature of the bond in blue rhodopsin is a non-protonated Schiff base.[46] Mutations of the blue pigment, S289A and S87G, near the SB region failed to show significant changes in the absorbance values for retinal. If retinal was bound as a PSB, it may not be unreasonable to think that removal of two polar residues near the PSB region would affect the absorbance. The S289A mutation failed to produce any change, while the S87G mutation had a 10 nm blue shift. The protein containing the E113Q mutation failed to regenerate with retinal.

Oprian, who proposed the nonprotonated SB for the blue visual pigment, later retracted this theory.[47,48] Mutation of the human blue pigment, as well as mutation with the bovine blue pigment, to generate the E113Q mutant both failed to regenerate with retinal. Consequently, mouse UV opsin was mutated to produce two mutant clones

whose absorbance closely matched those of human (414 nm) and bovine blue (438 nm) rhodopsin. One mutation was required to mimic bovine blue and generate a 424 nm absorbing protein complex, while 7 mutations generated a 411 nm absorbing pigment. Utilizing these two new 'mouse blue' proteins, the E113Q mutation was performed. The single mutant exhibited a pH dependent equilibrium between 424 and 351 nm, while the 7 amino acid mutant displayed the expected blue shift to 369 nm. Based on these observations, Oprian concluded that the 420 nm blue pigment could in fact be a PSB.

Additionally, 11-*cis*-retinal bound to Human Cellular Retinal Binding Protein (CRALBP) also absorbs at ~420 nm.[19,49] While the exact binding nature of retinal with CRALBP has not been determined, extensive reductive amination techniques have consistently failed to produce a covalently bound retinal. Of course, this may be a result of either a solvent inaccessible cavity, or an unstable PSB that hydrolyzes before it can be trapped. However, it is believed that retinal exists in a non-covalent form, but due to the hydrophobic nature of the binding cavity, a red shift is still observed for the aldehydic substrate.[19,49]

Although we are still left without conclusive proof that retinal exists as a protonated Schiff base when bound to R132K::Y134F, crystallographic results do confirm placement of the Lys residue as being within a

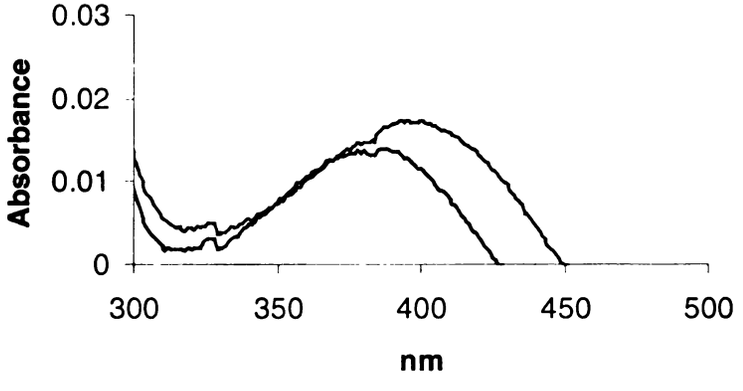

Figure II-18. Uncorrected UV-vis of the double mutant R132K::Y134F shows a retinal maximal absorbance of 400 nm. Upon lowering the pH of the sample, the red shift is lost, and the retinal maximal absorbance blue shifts to 384 nm.

suitable distance and trajectory for attack on the carbonyl. Figure II-19 shows an overlay of the retinoic acid bound wild type CRABPII and retinoic acid bound R132K::Y134F double mutant crystal structures as obtained by our collaborators. There does not seem to be any gross structural change in the overall three dimensional shape of the protein. A closer look at the binding cavity shows that the Lys residue is pointed directly at the carbonyl of retinoic acid (3.5 Å away), and should be close enough for covalent bond formation with little movement of retinal needed (provided retinal sits in the same local minima as retinoic acid).

Important to note in the crystal structure (Figure II-19b) is that the mutations within the binding cavity do not seem to perturb the desired location of the retinoic acid

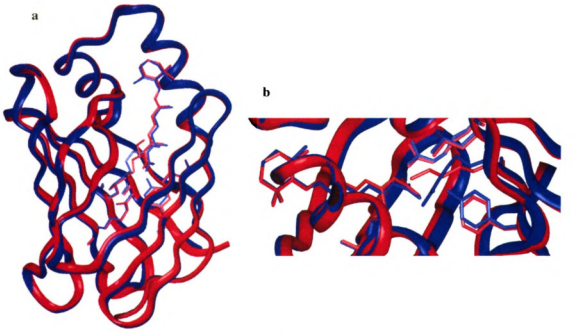

Figure II-19. **a**) Overlay of the retinoic acid bound CRABPII wild type crystal structure (1.6 Å) with the retinoic acid bound R132K::Y134F double mutant (1.8 Å). a) There is no gross structural change in the overall three dimensional shape of the protein as a result of the two amino acid mutations. **b**) A closer look in the binding pocket shows minimal movement of the chromophore, and the Lys residue pointing directly towards the carbonyl, suitably lined up for attack and covalent bond formation with retinal should it exist reside in the same position as retinoic acid.

substrate. Also, removal of the phenolic hydroxyl group and the potential hydrogen bond participant allows for the newly introduced Lys to extend directly towards the substrate, as opposed to the wild type structure where Arg 132 is pointed more towards Tyr 134. Unfortunately, due to difficulties addressed previously, a retinal bound R132K::Y134F crystal structure has yet to be obtained.

The triple mutants made for fluorescence studies, R132K::Y134F::F15W and R132K::Y134F::L19W both show diminished retinal binding abilities. Whereas the double mutant has a relatively decent binding affinity (K_d = 120 nM), both Trp triple mutants show a K_d = 680 nm. Additionally, the red shift in the UV-vis of the double mutant is now lost with the Trp triple mutants that now absorb at 374 nm (R132K::Y134F::F15W) and 367 nm (R132K::Y134F::L19W). Although the red shift is lost, just as in the double mutant, a covalent complex can be seen by MALDI-TOF by incubation of retinal with the protein, but is not trapped by the reductive amination reaction. The mutagenesis of these two residues (Phe 15 and Leu 19) does not impede SB formation, but does reduce the overall binding affinity of retinal for the proteins. The possibility of a disrupted α-helical structure near the mouth of the cavity (as was seen in the crystallographic analysis of the F15W single mutant) may be the cause of this, but again, this cannot conclusively be deduced.

In addition to Tyr 134, Arg 111 was also explored as a possible site for incorporation of a hydrophobic residue, and as we will discover, is crucial for maintaining optimal PSB formation, both in terms of the retinal maximal absorbance observed and the retinal binding affinity towards various proteins. Figure II-20 shows the

minimized structure of the binding cavity of the triple mutant R132K::Y134F::R111L, where retinal has been bound to Lys 132 as a Schiff base.

The mutant R132K::Y134F::R111L maintains a retinal binding affinity similar to the double mutant (160 nM versus 120 nM for R132K::Y134F). Also, as expected, the retinoic acid affinity was greatly reduced by removal of the final stabilizing Arg residue (1000 nM versus 100 nM for R132K::Y134F) (Figure II-21a).

Retinal absorbance still remains red shifted, similar to the double mutant, although not quite as strong (410 nm versus 429 nm for R132K::Y134F). If these species are PSB, it seems the positively charged Arg 111 (5.4 Å) allows for a larger red shift than the essentially neutral binding cavity of the triple mutant.

Despite not having as large of a red shift as the previous mutant, the Schiff base formed with this mutant seems to be more stable. The effectiveness of this amino acid mutation is highlighted in the reductive amination, whereas previously the PSB was not able to be trapped, now the covalent complex can be detected by MALDI-TOF under both the incubation only (protein plus retinal, no borohydride) and the reductive amination conditions (Figure II-21c-d).

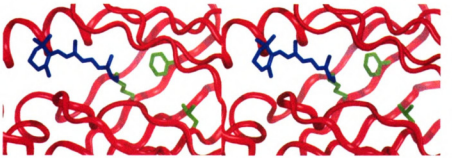

Figure II-20. Stereoview of the binding pocket of CRABPII R132K::Y134F::R111L. Retinal has been bound to Lys 132 as a Schiff base and minimized by InsightII.

We now have a CRABPII protein that we can unequivocally say is forming a Schiff base with retinal. Due to the 40 nm (R132K::Y134F::R111L) – 59 nm (R132K::Y134F) red-shift we have reason to believe that the Schiff base is protonated, although currently there is no other means by which we can prove this, even if we do obtain a crystal structure depicting the covalent Schiff base between retinal and the protein, the resolution most likely will not be high enough to detect the existence of a proton on the SB nitrogen.

All successfully red shifted retinal complexes > 440 nm produced thus far have had the R111L mutation. Experimentation has shown that neither a hydrophilic residue (Arg) or a counter anion (Glu) in this position will produce a successful PSB forming rhodopsin mimic. We have not however, probed the effect of other hydrophobic residues placed at this position, which should be done.

While the introduction of the R111L mutation has lead to the increase of stability of the SB so that it can be seen by reductive amination, it still is not as stable as we require for an ideal rhodopsin surrogate. MALDI-TOF analysis shows small amounts of the covalent complex, while the major species still remains the free protein. Recall that while retinal absorbs near the laser's frequency in the MALDI-TOF and may not always ionize very efficiently, we cannot use peak ratios for comparison of reaction or PSB formation efficiency. However, the existence of a large amount of the free protein peak does suggest a less than perfect complexation or reaction. For further PSB stabilization we began to probe the proper positioning of a suitable counter anion.

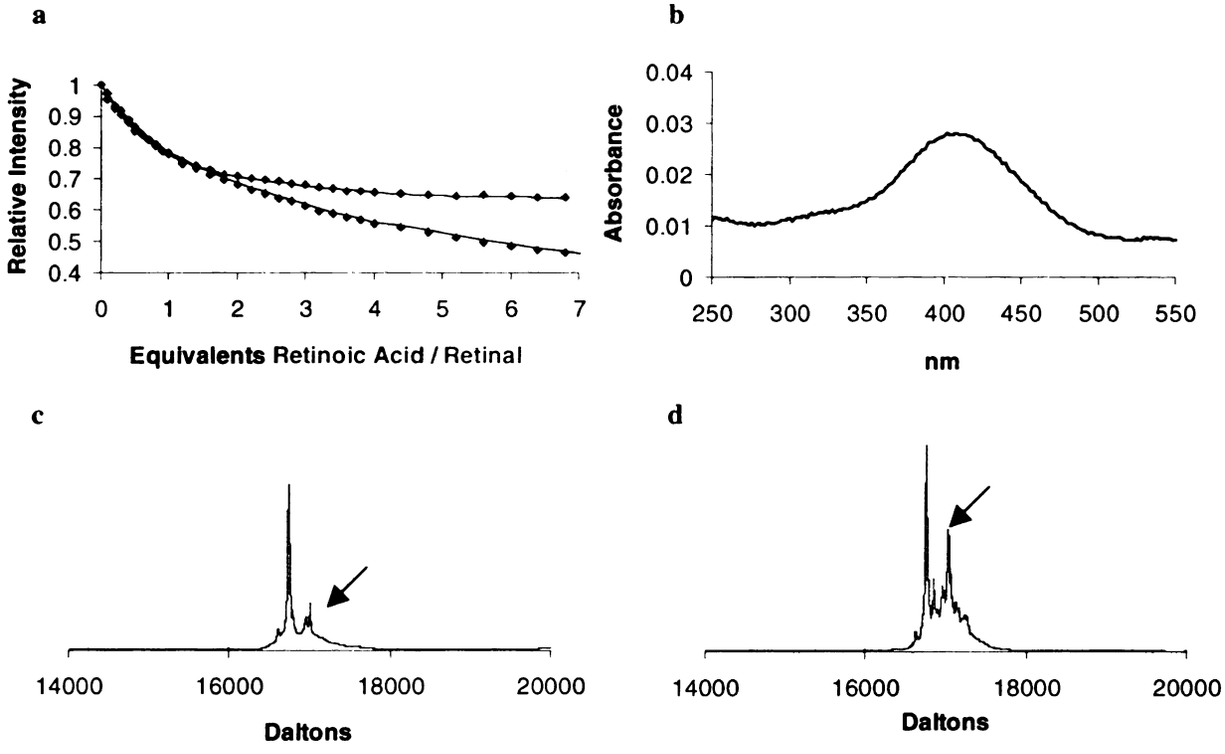

Figure II-21. **a**) Fluorescence titration curves for the retinoic acid and retinal K_d determination with the triple mutant CRABPII R132K::Y134F::R111L. Removal of the second Arg residue in the binding pocket displays an expected drop in retinoic acid binding affinity (K_d = 1000 ± 28 nM), while the hydrophobic Leu residue maintains retinal binding affinity, K_d = 160 ± 6.7 nM. **b**) UV-vis of retinal incubated with CRABPII R132K::Y134F::R111L portrays a maximal absorbance at 410 nm, a decrease from the 429 nm observed for the previous double mutant, but still a 40 nm red shift as compared to retinal incubated with the wild type CRABPII. **c**) MALDI-TOF of the retinal incubated triple mutant shows an M^+ = 16741.7 Da corresponding to the protein mass, calculated to be 16742.2 Da. In addition there is small amounts of a second peak (indicated by arrow), M^+ = 17008.4 Da, which is 266.7 mass units higher than the protein peak, representing a covalently linked retinal molecule (calculated mass difference 266). **d**) Reductive amination of retinal with CRABPII R132K::Y134F::R111L confirms Schiff base formation by trapping a single retinal molecule. Protein peak is detected at 16757.6 Da, and the enhanced covalent species is detected at 17026.8 Da, revealing a difference of 269.2 Da. Calculated addition of a single reductively aminated retinal molecule is 268 Da.

F. Positioning of the Counter anion

Incorporation of the counter anion is going to be critical in maintaining a stabilized protonated Schiff base. In bovine rhodopsin, Glu 113 serves as the counter anion to the PSB and resides 4.2 Å from the SB nitrogen.[48,50,51] It is postulated that the counter anion may reside at varying locations in other opsins which still maintain PSB formation, so although distance will be important, we may have some leniency in finding an optimum location.

Initially, we went back to the double mutant (R132K::Y134F) that had demonstrated the largest red shift thus far (429 nm), and mutated Arg 111 to a glutamic acid residue, R132K::Y134F::R111E. The counter anion in this position is 7.4 Å from the PSB (minimized structure, Figure II-22). As the data will show, this counter anion does not help to stabilize PSB formation, but actually eliminated SB formation all together. The red-shift in the UV-vis is lost (370 nm), and so has some of the binding affinity for retinal (K_d = 260 ± 12 nM) as can be seen in Entry 1 of Table II-2. Additionally, the evidence for Schiff base formation that had been seen in the MALDI-

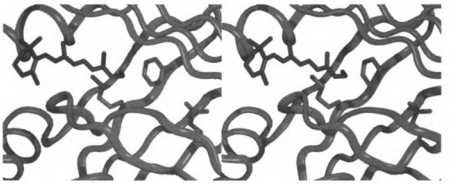

Figure II-22. Stereoview of CRABPII R132K::Y134F::R111E. Arg 111 was mutated to incorporate a counter anion for the postulated PSB, ~7.4 Å away.

Table II-2. Results of binding assays with various CRABPII mutants probing the effect of the counter anion

Entry	Protein	Rt K_d (nM)[a]	Rt λ_{max} (nm)[b]	Reductively[c] Aminates
1	R132K::Y134F::R111E	260 ± 12	370	No
2	R132K::Y134F::R111E::T54V	210 ± 8.2	414	No
3	R132K::Y134F::L121E	160 ± 9.8	370	Yes
4	R132K::Y134F::R111L::T54E	80 ± 3.4	379, 454	No
5	R132K::Y134F::R111L::L121E	200 ± 8.3	372, 464	Yes
6	R132K::Y134F::R111L::L121D	2.6 ± 7.9	365, 464	Yes
7	R132K::Y134F::R111L::L121D::T54V	30 ± 5.5	370, 466	Yes
8	R132K::Y134F::R111L::L121E::T54V	2.7 ± 7.0	378, 456	Yes

a. Dissociation constant for all-*trans*-retinal as determined by fluorescence spectroscopy.
b. Retinal maximal absorbance when incubated with protein.
c. MALDI-TOF of reductive amination.
Yes indicates the presence of a covalently bound retinal molecule.

TOF of R132K::Y134F, no longer exists for the triple mutant. The expected drop in retinoic acid binding affinity is also seen as the second stabilizing Arg residue is removed from the pocket, just as we saw with R132K::Y134F::R111L discussed in the last section. Neither the incubation or reductive amination of retinal with this new triple mutant show evidence for a covalent bond formation.

A distance of 7.4 Å might be too far to stabilize any PSB that may have formed, and perhaps the binding pocket is not yet hydrophobic enough, as we can see that retinal binding affinity has also been affected. It is interesting to note that the counter anion in this mutant will not produce a red shift and possible PSB, yet the positive charge in this position (R132K::Y134F::R111), which resides closer to the SB moiety will. This attests for the fact that there may be only a very small window of effective hydrophobicity for

existence of a deprotonated Lys residue, yet at the same time, stabilize the existence of a protonated Schiff base. By introduction of another hydrophobic residue in the cavity, perhaps we can recover the red shift and covalent complex that was observed with the R132K::Y134F double mutant. We opted to convert Thr 54 to a Val because of the conservative change as well as the large increase in hydrophobicity.

The quadruple mutant, R132K::Y134F::R111E::T54V, does indeed regain the red shift, although 15 nm blue shifted compared to the double mutant (414 nm, Entry 2, Table II-2). The increase in hydrophobicity, as we expect, does exhibit some improvement on retinal binding affinity (210 nM) as compared to the previous triple mutant (260 nM, Entry 1), although not as significant as we had imagined it would be. The retinoic acid binding affinity has been reduced even further (860 nM) as compared to the triple mutant (R132K::Y134F::R111E, 530 nM), most probably because of the removal of a hydroxyl functionality that may have helped stabilize retinoic acid binding by acting as a hydrogen bond donor.

The addition of both a counter anion and another hydrophobic residue has not had any effect on the stabilization of the PSB. The retinal is not quite as red shifted as in the R132K::Y134F double mutant case (414 nm vs. 429 nm), and the same results were seen in the MALDI-TOF experiments as was seen with the double mutant. A covalent complex, consisting of a single retinal molecule bound as a Schiff base is detected in the incubation with the quadruple mutant, but cannot be trapped and detected by reductive amination.

Since the counter anion in position 111 did not produce a protein with improved characteristics we tried to reposition it in place of Leu 121. This residue, although closer

to the SB region (5.7 Å), removes a hydrophobic residue from the binding pocket, replacing it with a hydrophilic one. The loss of hydrophobicity however does not effect the binding affinity of retinal with the triple mutant R132K::Y134F::L121E (160 nM, Entry 3, Table II-2). The addition of the negative charged Glu residue in closer proximity to the chromophore is demonstrated by the 10 fold decrease in binding affinity of retinoic acid (K_d = 1400 ± 63 nM) as compared to the double mutant without the counter anion (R132K::Y134F, 120 nM).

This triple mutant has a 370 nm λ_{max} upon incubation with retinal. Regardless of the lack of an expected blue shifting (~5 nm), this complex is still a Schiff base, just as we saw with the single mutant, R132K (370 nm). The chromophore is in a unique environment within each proteins' binding pocket, allowing for each protein to provide small variations in the wavelengths for the bound chromophore. It is for this reason UV-vis alone cannot differentiate the formation of a Schiff base, expected 5 nm blue shift, from the free aldehyde. The complex can be trapped by reductive amination and visualized in the MALDI-TOF, which does verify SB formation.

As MALDI-TOF illustrates, retinal bound to R132K::Y134F::L121E does exist as a Schiff base, however this is probably the nonprotonated Schiff base as we do not detect a red shift of retinal's maximal absorbance in the UV-vis experiment. Thus far, R132K::Y134F::R111L has been the only protein that both shows a red shift in the UV-vis and shows the covalent combination of retinal and protein in the reductive amination reaction. Given this, we chose to reintroduce the hydrophobic R111L mutation to the protein and probe for the optimum counter anion position.

Thr 54 was converted to a Glu to give the tetra mutant, R132K::Y134F::R111L::T54E. From the InsightII minimized structure (Figure II-23), the counter anion is 3.4 Å from the carbonyl carbon of retinal. As we saw in the previous case, introduction of the counter anion reduces the retinoic acid binding affinity dramatically, K_d = 2180 ± 43 nM (Entry 4, Table II-2). As the counter anion has moved closer to the carboxylate end of the substrate we expect this erosion in binding.

Having both the R111L hydrophobic mutation coupled with the counter anion in position 54 has increased the retinal binding affinity, K_d = 80 ± 3.4 nM. This protein mutant not only has increased the retinal binding affinity below 100 nM for the first time, but it also has increased the amount of red shifting seen in the UV-vis. The protein / retinal complex shows a mixture of two species, one absorbing at 379 nm, the other at 454 nm (Figure II-24). The covalent complex, presumably the 454 nm absorbing protonated Schiff base, can be detected by MALDI-TOF. However, as we have seen with R132K::Y134F and R132K::Y134F::R111E::T54V, the covalent complex can only be seen in the incubation experiment, and cannot be detected by MALDI-TOF of the reductive amination reaction.

Figure II-23. Stereoview of CRABPII R132K::Y134F::R111L::T54E. The counter anion at position 54 is 3.4 Å from the postulated PSB.

This CRABPII mutant seems to be a step in the right direction, as we now have an even more red shifted retinal peak and the retinal binding affinity has been increased significantly. This still is not an ideal rhodopsin mimic not only because the Schiff base is not stable enough to be trapped under the reductive amination reaction conditions, but also because there exists a mixture of two peaks. Some amount of what is believed to be PSB exists, but there is a significant amount of another species. The retinal binding affinity is respectable at 80 nM, but when the retinal incubated MALDI-TOF spectra was recorded, although the protein / retinal Schiff base was present, there was a significant amount of uncomplexed protein observed. The existence of free protein in the MALDI-TOF may suggest that the 379 nm peak in the UV-vis is due to the free aldehyde and not the non-protonated Schiff base. In fact, an interesting trend to note is that all of the proteins that have a ~460 nm peak in the UV-vis also have a ~375 nm peak as well. However, all of the proteins that absorb at ~420 nm have only this one peak. This could again go back to the theory of a non-covalent red shifted retinal as a result of residing in a

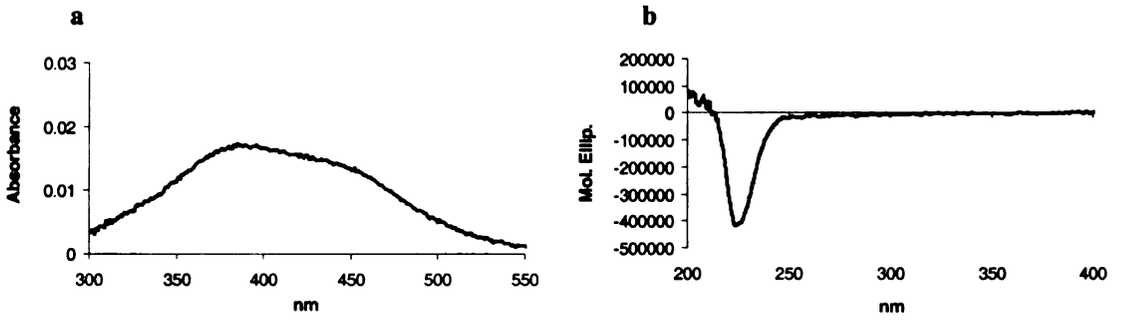

Figure II-24. **a)** UV-vis spectrum for retinal as bound to the tetra mutant R132K::Y134F::R111L::T54E. It shows the existence of two peaks, 379 nm and 454 nm. **b)** CD spectrum for the apo-R132K::Y134F::R111L::T54E shows small changes as compared to the wild type CRABPII CD spectrum. The minima is 224 nm and the distinction between the 220 nm and 230 nm peak has been lost.

hydrophobic environment, and may explain why only one species is detected in the UV-vis, and only a very little amount of SB can usually be detected by MALDI-TOF. The proteins that absorb ~460 nm generally show a stronger reductively aminated peak in the MALDI-TOF.

The question remains then, if we are constantly getting a ~375 nm / ~460 nm mixture, are there two protein isoforms that are responsible for each peak? Recall earlier evidence that seemed to suggest this possibility as well. Protein fluorescence titrations with retinal do not show as large of a drop in the overall relative intensity as compared to the native substrate retinoic acid, which may be a result of inefficient quenching with a higher absorbing retinal-PSB complex. In addition, CD analysis of the proteins reveal a change in the shape of the curve, where the characteristic 220 nm β-sheet peak is present, but the 200 nm and 230 nm region vary from protein to protein which may be a result of small structural deviations. However, these spectral deviances could be due to another protein isoform that does not bind retinal as efficiently. Either a more in depth structural analysis of the CD data or further crystallographic studies must be performed to answer this question.

Returning now to the attempts at finding the optimum counter anion position, utilizing the R111L hydrophobic mutation, the counter anion has now been repositioned to residue 121 (formerly a leucine) to generate the tetra mutant R132K::Y134F::R111L::L121E (Entry 5, Table II-2). The counter anion is 2.6 Å from the minimized Schiff base nitrogen (minimized by InsightII, Figure II-25). With the counter anion being closer to the SB nitrogen from Lys 132 than from Glu 54 (7.1 Å) from the Insight II SB minimized structure), there is evidence for an even stronger red

shift, as now there is a mixture of a 372 nm and a 464 nm absorbing species (Entry 5, Table II-2).

Removal of the hydrophobic Leu 121 residue is evident in the fluorescence titrations. The retinal binding affinity has been reduced as compared to the tetra mutant containing the Glu 54 counter anion (80 nM, Entry 4). R132K::Y134F::R111L::L121E exhibits a $K_d = 200 \pm 8.3$ nM. Although the binding affinity is not as strong as previous, MALDI-TOF reactions do provide better results. This is the first counter anion containing mutant where both the incubation and the reductive amination reactions demonstrated evidence for Schiff base formation.

In the noncovalent form, the counter anion is actually further away from the chromophore's carbonyl from position 121 (5.7 Å) as compared to the counter anion being in position 54 (3.4 Å based on InsightII minimizations). This demonstrates itself through the retinoic acid binding affinity. Recall the previous tetra mutant (R132K::Y134F::R111L::T54E, Entry 4) had a retinoic acid dissociation constant of 2180 nM whereas with the negative charge further away from the chromophore (Entry 5,

Figure II-25. Stereoview of CRABPII R132K::Y134F::R111L::L121E with Thr 54 also shown. As the covalent Schiff base complexation is formed, InsightII minimizations place the counter anion at position 121 closer to the postulated positive charge than if position 54 (Thr) was utilized for the counter anion.

Glu 121) the retinoic acid binding is not inhibited as much, $K_d = 770 \pm 61$ nM.

There is something structurally wrong with the R132K::Y134F::R111L::L121E protein however what still remains unknown to us. MALDI-TOF analysis of the protein reveals two peaks, one higher in mass (17444 Da) and one lower in mass (16660 Da) than the expected molecular weight for the protein (16758 Da). Although mass analysis shows what seems to be two protein peaks, SDS-PAGE analysis shows only one band, and it appears at a higher molecular weight than other CRABPII proteins (Figure II-26). It is not completely obvious what transformation is taking place to modify this protein from its original structure and sequence. DNA sequencing verifies the presence of the stop codon, and should this stop codon be skipped for some reason, there are several stop codons following the initial one. The mass is not large enough to be a dimer of the protein. Retransfection of the verified DNA sequence still provided the same results. Additionally, this clone was more difficult to obtain than usual, and, this protein expresses in low yields as compared to other proteins, yielding only about 10 mg of protein per liter of

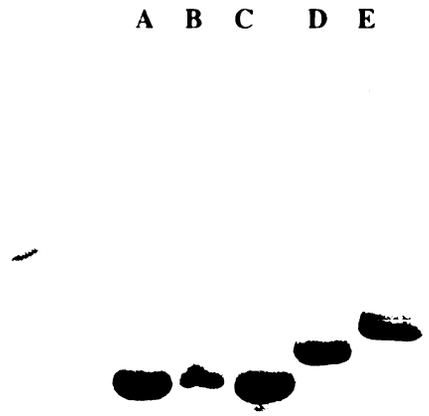

Figure II-26. Lanes A-C show SDS-PAGE analysis of WT, R132K::Y134F, and R132K::Y134F::R111L at approx. 17,000 Da, respectively. Lane D depicts R132K::Y134F:: L121E slighter higher than the others, but this protein still shows correct molecular weight by MALDI-TOF. Lane E shows the tetra mutant, R132K::Y134::R111L::L121E even higher than lane D. The tetra mutant consistently runs higher than 17,000 Da on gel. MALDI-TOF of this tetra mutant shows two peaks, one higher molecular weight and one lower molecular weight peak. The higher molecular weight peak, which is this only peak seen here, is also the only peak that demonstrates Schiff base formation with retinal.

culture.

Despite the uncertainty in protein sequence and structure, this mutant still demonstrates good retinal binding properties, in fact the best we have seen thus far. Incubation and reductive amination experiments with this protein do show Schiff base formation, however, only with the higher molecular weight protein. This agrees with the SDS-PAGE that only shows one protein peak. The second lower mass peak may be a cleavage product of the higher mass species. Also, this protein portrays almost identical retinal binding properties as compared to the pET-17b, non-His-tagged protein. The R132K::Y134F::R111L::L121E tetra mutant was prepared in the pET-17b plasmid for crystallographic studies, and interestingly does not suffer from the same structural inconsistencies as the His-tagged protein. The non-His-tagged R132K::Y134F::R111L::L121E protein has the correct molecular weight. In addition, fluorescence, UV, and MALDI-TOF data between the two proteins are in very good agreement.

There is one aspect about the pET-17b non-His-tagged protein that is different from the pET-Blue2 His-tagged protein. The codon used for the R111L amino acid is different by a single base pair (CTG used with pET-Blue2 and CTA used withpET-17b). Several attempts were made at converting the pET-Blue2 codon to match that of the pET-17b plasmid. However, the cloning attempts have yet to prove successful. Attempts at producing this clone for MALDI-TOF analysis of the molecular weight are still ongoing.

The penta mutant R132K::Y134F::R111L::L121E::F15A (Rt λ_{max} = 368 nm, Rt K_d = 110 ± 63 nM) was produced to probe the possibility of loss of structural integrity in the α-helical region as was seen in the F15W crystal structure. Comparing this protein to

the tetra mutant R132K::Y134F::R111L::L121E (Rt λ_{max} = 372, 464 nm, Rt K_d = 200 ± 8.3 nM) shows that there is not much difference in binding affinity, however, the red shift to 464 nm that was seen in the tetra mutant is lost in the penta mutant protein through the addition of the F15A mutation. Loss of structural integrity as a result of this mutation could result in a less rigid and more open binding cavity, making the PSB more solvent exposed. Only protonation, and not Schiff base formation is lost here, as both MALDI-TOF experiments still verify covalent bond formation with a single retinal molecule. Crystallographic analysis is ongoing.

The further degree of red shifting observed with the counter anion in position 121 as compared to 54, and the fact that the covalent complex, while binding affinity was not as good as previous, could be trapped in reductive amination (R132K::Y134F::R111L::T54E could not) prompted us to pursue the 121 counter anion position. We were also curious to see if this unknown protein transformation (molecular weight inconsistency observed with R132K::Y134F::R111L::L121E) will be carried through to future clones.

The Glu 121 counter anion in the tetra mutant was replaced with Asp to produce R132K::Y134F::R111L::L121D. The Asp residue (based on InsightII minimizations) minimizes to approximately the same distance from the Schiff base nitrogen (2.9 Å) as compared to Glu (3.1 Å) despite Asp having one less methylene unit in its sidechain. This small difference in distance exhibits a large effect on the retinal binding affinity, but little effect on the absorbance of retinal (Entry 6, Table II-2). While retinal bound to R132K::Y134F::R111L::L121D portrays maximal absorbance values of 365 nm and 464 nm, the dissociation constant has now dropped to achieve a stoichiometric binding

relationship with the chromophore, K_d = 2.6 ± 7.9 nM. Also, just as the corresponding protein mutant containing Glu as the counter anion, both the incubation and reductive amination experiments reveal Schiff base complexes with a single molecule of retinal (Figure II-27).

Although the 365 nm absorbing species may lead us to think that we now have a mixture of SB and PSB, the MALDI-TOF experiments still show a significant amount of free protein. Although this result may be due to unoptimized reaction conditions, the 365 nm absorbing species could not be forced to the red shifted 464 nm peak upon addition of acid. Presumably, this too is a mixture of aldehyde and PSB. We have yet to conclusively determine why, although we are getting some amount of PSB, the major species is still the free aldehyde. In a situation such as with this protein, the binding affinity is so high that we can believe that the chromophore is within the binding cavity with a stoichiometric binding relationship, yet we still cannot rule out a second isoform of the protein, that either allows for binding, but not PSB formation, or does not bind retinal.

With every hydrophobic addition to the pocket we have had increased success in at least one of the retinal binding assays. Hoping to follow this trend we decided to change Thr 54 to a Val again to produce the penta mutants R132K::Y134F::R111L::L121D::T54V and R132K::Y134F::R111L::L121E::T54V (Entries 7 and 8, respectively, Table II-2). This is one of the last residues that resides < 7 Å from the Schiff base region between retinal and Lys 132. Other residues that may be altered in future studies are further away from the chromophore, either deeper into the protein structure than the residues currently studied, or along the interior surface of the

cavity, but further along the chain of the polyene towards the ring and the opening of the cavity.

This hydrophobic addition has minimal effect on the retinal binding and PSB

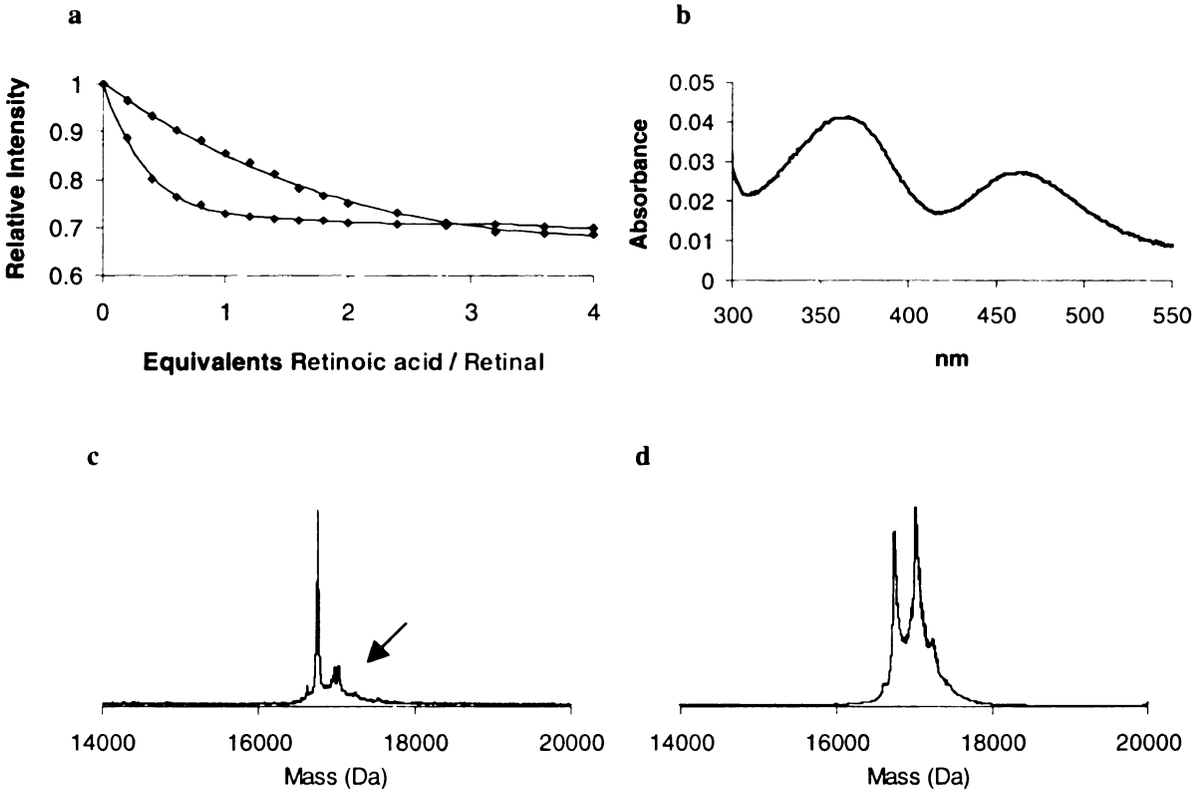

Figure II-27. **a**) Fluorescence titration curves for the retinoic acid and retinal K_d determination with the tetra mutant CRABPII R132K::Y134F::R111L::L121D. The retinoic acid dissociation constant is K_d = 200 ± 25.3 nM, and a stoichiometric retinal binding affinity, K_d = 2.6 ± 7.9 nM. **b**) UV-vis of retinal incubated with the CRABPII protein portrays maximal absorbances at 365 nm and 464 nm, a 94 nm red shift as compared to the wild type CRABPII (370 nm), possibly suggesting protonated Schiff base formation. **c**) MALDI-TOF of the retinal incubated penta mutant shows an M^+ = 16754.2 Da corresponding to the protein mass, calculated to be 16744.1 Da. In addition there is small amounts of a second peak (indicated by arrow), M^+ = 17025.1 Da, which is 270.9 mass units higher than the protein peak, representing a covalently linked retinal molecule (calculated mass difference 266). **d**) Reductive amination of retinal with CRABPII R132K::Y134F::R111L::L121E::T54V results further trapping of the covalent complex, M^+ = 16734.6 Da and 17010.6 Da (difference of 276 Da, calculated difference should be 268 Da).

formation when Asp is used as the counter anion (Entry 7, K_d = 30 nM, λ_{max} = 370 and 466 nm, positive detection of SB via MALDI-TOF). The only visible significant difference is seen in the retinoic acid binding affinity where the hydrophobic addition has hampered retinoic acid binding (760 nM) similar to trends previously reported for R132K::Y134F::R111E::T54V. The tetra mutant (R132K::Y134F::R111L::L121D), had already achieved a stoichiometric binding relationship with retinal (provided there is only one protein form), therefore we did not expect to see an increase in retinal binding affinity by this hydrophobic addition.

On the other hand, this single hydrophobic amino acid mutation has had a significant positive effect on the protein containing Glu as the counter anion. The protein retinal complex maintains a red shifted / non-red shifted mixture of two species (378 nm, 456 nm) and Schiff base is detected in both MALDI-TOF experiments. The most significant improvement is seen in the binding affinity for retinal. The tetra mutant R132K::Y134F::R111L::L121E has a K_d of 200 nM, while introduction of Val in position 54 enhanced the binding significantly with an apparent K_d of 2 nM. We have again achieved a stoichiometric binding relationship between retinal and the protein.

This protein is the best retinal PSB forming protein created thus far. It forms PSB with a single molecule of retinal as detected by MALDI-TOF and UV-vis. The tetra mutant R132K::Y134F::R111L::L121D also has a stoichiometric binding affinity with retinal and forms a red shifted PSB, but as seen in Figure II-28, the equilibrium in the penta mutant favors the PSB more so than the tetra mutant. For this reason, it is this protein that was probed further for confirmation of the PSB formation with Lys 132, and will be discussed in much more detail in the next section.

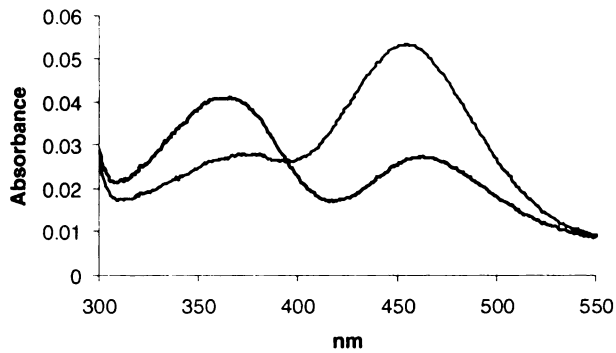

Figure II-28. Corrected UV-vis of the retinal incubated R132K::Y134F::R111L::L121E::T54V (378 nm, 456 nm) and R132K::Y134F::R111L::L121D (365nm, 464 nm) CRABPII mutants. The penta mutant has a larger amount of the red shifted peak as compared to the tetra mutant. For this reason, R132K::Y134F::R111L::L121E::T54V was probed more extensively for the existence of a protonated Schiff base with Lys 132.

G. A Successful Protonated Schiff Base Forming Protein

The penta CRABPII mutant R132K::Y134F::R111L::L121E::T54V is my most successful protonated Schiff base forming protein. It has achieved a large red shift presumably due to protonation of the Schiff base and a stoichiometric binding relationship with retinal. The success in retinal binding with R132K::Y134F::R111L::L121E::T54V is a result of both proper hydrophobic tuning and precise placement of the counter anion. Three residues had to be mutated in order to increase the hydrophobic nature of the binding pocket, Tyr 134 (3.2 Å from retinal), Arg 111 (5.5 Å from retinal), and Thr 54 (3.8 Å from retinal). As previous protein clones suggest, anything less than these three hydrophobic mutations may still achieve the same amount of red shifting as observed in this penta mutant, however, the binding affinity of retinal to the protein is dramatically reduced and unacceptable. In addition, counter anion placement only at position 121 has been fruitful in achieving both the optimal UV-vis and fluorescence results.

Figure II-29 displays the results obtained from the retinal binding assays performed with CRABPII R132K::Y134F::R111L::L121E::T54V. Fluorescence titration shows a stoichiometric binding relationship with retinal (2.7 nM), similar to that between wild type CRABPII and its native substrate retinoic acid (2.0 nM, see Figure II-11). UV-vis reveals a protein that now absorbs at 455 nm in addition to the second 378 nm peak. This is an 85 nm red shift as compared to retinal with the wild type CRABPII (370 nm). Finally, MALDI-TOF reveals very clearly a positive peak for the covalent complexation

between retinal and the protein, which can now be trapped under both incubation and reductive amination conditions.

CD spectra of the penta mutant incubated with retinal were taken in hopes of

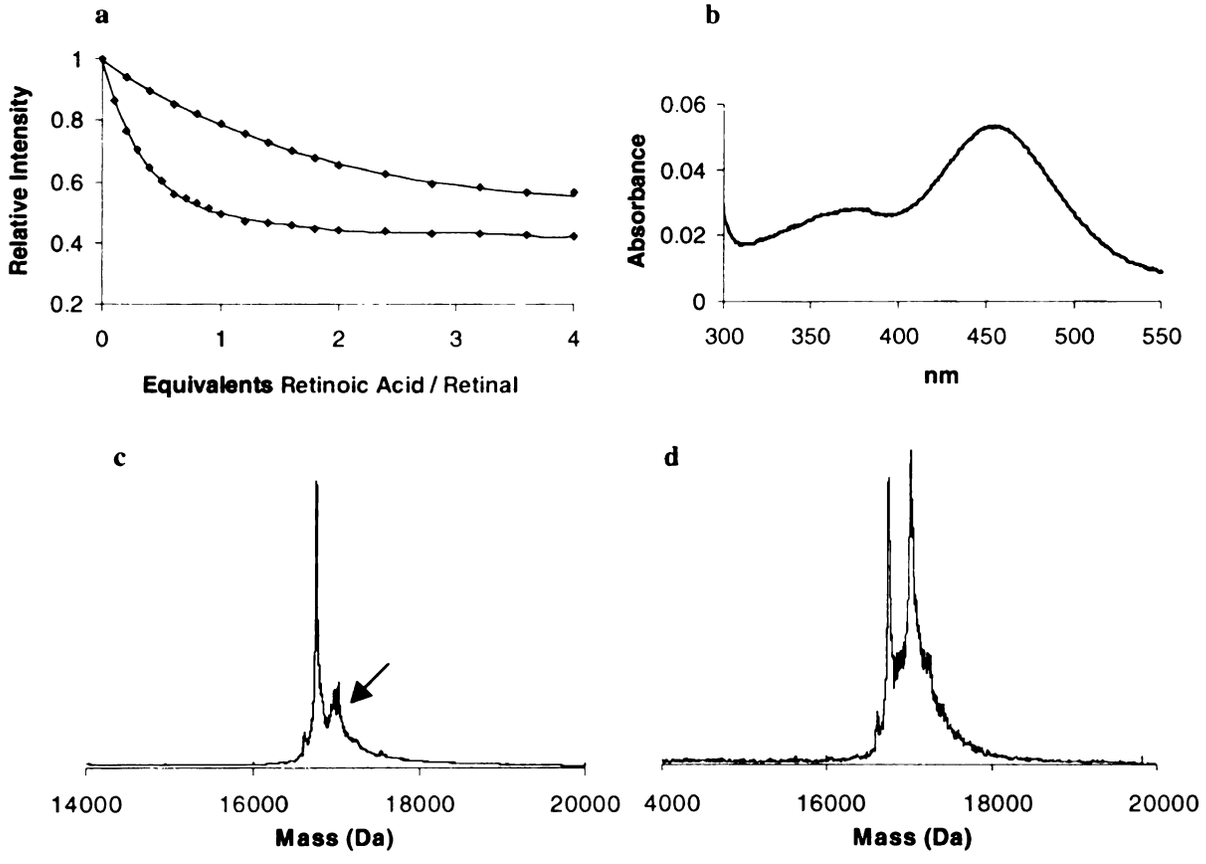

Figure II-29. **a**) Fluorescence titration curves for the retinoic acid and retinal K_d determination with the penta mutant CRABPII R132K::Y134F::R111L::L121E::T54V. The hydrophobic tuning and proper positioning of the counter anion has resulted in a retinoic acid dissociation constant of K_d = 249 ± 19.2 nM, and a stoichiometric retinal binding affinity, K_d = 2.7 ± 7.0 nM. **b**) UV-vis of retinal incubated with the CRABPII protein portrays maximal absorbances at 378 nm and 455 nm, an 86 nm red shift as compared to the wild type CRABPII (370 nm), possibly suggesting protonated Schiff base formation. **c**) MALDI-TOF of the retinal incubated penta mutant shows an M^+ = 16746.3 Da corresponding to the protein mass, calculated to be 16756.2 Da. In addition there is small amounts of a second peak (indicated by arrow), M^+ = 17018.4 Da, which is 272.1 mass units higher than the protein peak, representing a covalently linked retinal molecule (calculated mass difference 266). **d**) Reductive amination of retinal with CRABPII R132K::Y134F::R111L::L121E::T54V results further trapping of the covalent complex, M^+ = 16749.5 Da and 17016.2 Da (difference of 266.7 Da, calculated difference should be 268 Da).

obser

chrom

retinoi

When

of the

solubil

solutio

as SDS

will he

concen

II-30.

CD cu

never

condit

experi

not ha

do wi

belief

R132

:L121

best

prote

observing a bound chromophore, but has yet to be detected. Even a covalently bound chromophore may not show CD. Initially, no more than one equivalent of retinal / retinoic acid was added, as the best UV-vis results were obtained at these concentrations. When this failed to give a CD curve, presumably because of the very low concentration of the actual bound chromophore, excess chromophore was added. However, the limited solubility in water was problematic in achieving high concentrations.

A solution to the solubility problem is the addition of a detergent to the protein solution. We had experimented with CHAPSO, but additionally one may try others such as SDS or Triton-X100. An optimal detergent concentration has to be found so that it will help to solubilize the chromophore while not denature the protein. At detergent concentrations of 10 mM there was significant protein denaturation as evident in Figure II-30. Experimentation with retinal CD spectra was not pursued further than this, and a CD curve that unequivocally demonstrated the existence of a bound retinal molecule was never obtained. The conditions for the experiment may or may not have had anything to do with this, but it is our belief that although the R132K::Y134F::R111L::L121E::T54V is the best retinal binding protein we have

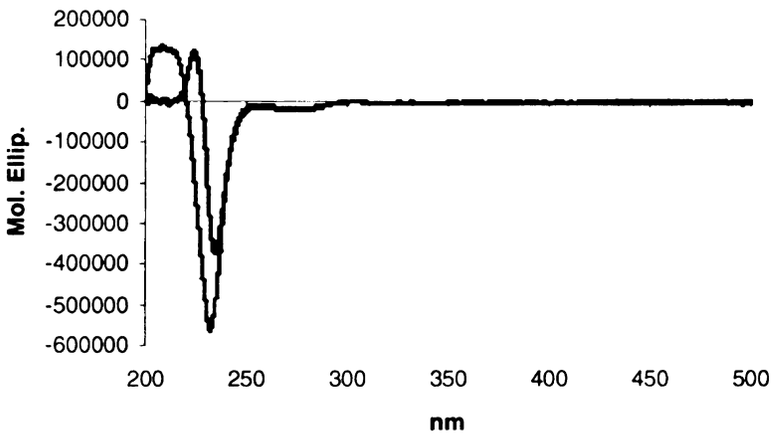

Figure II-30. The red CD spectrum is the Y134K::R132F CRABPII protein. The blue spectrum is the CD of Y134K::R132F in presence of 10 mM CHAPSO. There is not only a degradation in the 220 nm absorbing peak, but also there is perturbation in the 200 nm α-helical region.

engine

perfor

inform

set out

what th

the UV

engine

was re

with th

hydrop

the lar

second

straig

retino

± 61

affini

comp

red

R13

amir

engineered thus far, we must produce a better PSB forming protein to be able to properly perform this experiment and be able to actually detect a bound retinal molecule.

The fluorescence, UV-vis and MALDI-TOF assays have provided positive information regarding the nature of the retinal binding. Using all of this information, we set out to produce a few more CRABPII protein mutants that will help in confirming what the binding assays have already led us to believe, the red shifted peak observed in the UV-vis is a result of retinal PSB formation.

Foremost, unequivocal proof that the Lys involved in PSB formation is the engineered Lys 132 in the binding pocket comes from two protein mutants where this Lys was removed from the binding pocket. In one case the Lys was removed and replaced with the original Arg residue (Y134F::R111L::L121E), and in the other, replaced with the hydrophobic residue Leu (R132L::Y134F::R111L::L121E). Both of these proteins lose the large red shift that is visible in R132K::Y134F::R111L::T54V::L121E as well as the second peak in the MALDI-TOF representative of the covalent complex.

Analysis of the results of the binding assays for Y134F::R111L::L121E is fairly straight forward. With replacement of the Arg residue we expect to see an increase in retinoic acid binding affinity, which we do, K_d = 220 ± 28 nM, as compared to K_d = 770 ± 61 nM for R132K::Y134F::R111L::L121E. We have also lost some amount of retinal affinity due to incorporation of the more hydrophilic Arg residue, K_d = 570 ± 32 nM, as compared to K_d = 200 ± 8.3 nM for R132K::Y134F::R111L::L121E. As expected, all red shifting has been lost also, 369 nm as compared to 464 nm for R132K::Y134F::R111L::L121E (Figure II-31a). Most importantly, neither the reductive amination nor the incubation experiments show a covalently linked retinal molecule by

MALI

with t

residu

expect

either

mutan

Retina

464 n

was se

we exp

absenc

due to

shift.

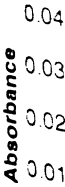

Figur

maxin

contai

Y134

Peak i

MALDI-TOF analysis (Figure II-31b), suggesting that Schiff base formation must be with the engineered Lys in the binding pocket, and not non-specifically to any other Lys residue.

The second of these mutants, R132L::Y134F::R111L::L121E, also shows the expected loss of Schiff base formation. No Schiff base is visible by MALDI-TOF from either reaction. Retinal binding affinity is slightly better than the corresponding Lys mutant protein, K_d = 180 ± 14 nM as expected due to the further hydrophobic tuning. Retinal absorbance as incubated with this protein loses the large red shift as was seen at 464 nm, but is still slightly red shifted at 402 nm. There is only this one peak present (as was seen in all the ~420 nm absorbing protein complexes), but it is more red shifted than we expected to see for a non covalent complex. From the MALDI-TOF analysis and the absence of the retinal bound protein peak, we are confident that this 30 nm red shift is not due to Schiff base formation. Discussed previously was the idea that retinal may red shift, as the aldehyde, when placed in a hydrophobic proteinacious environment.

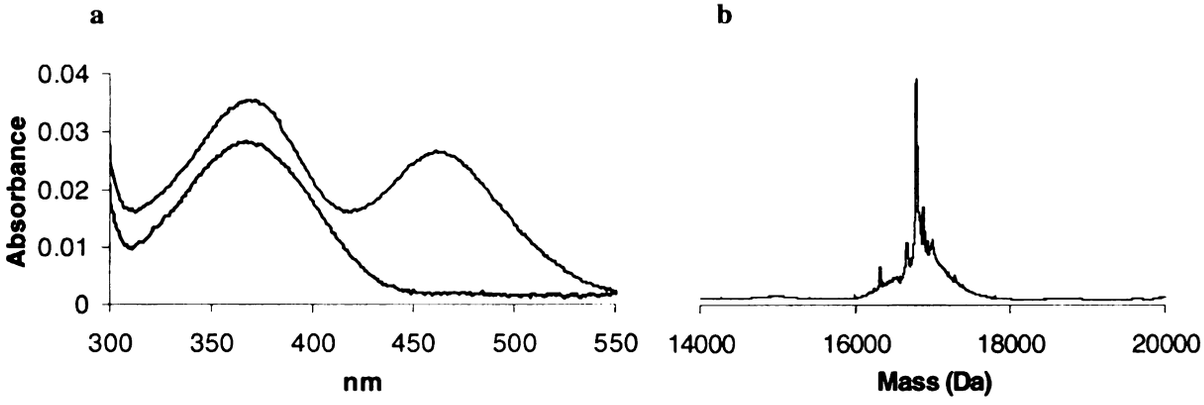

Figure II-31. **a)** UV-vis of the retinal incubated Y134F::R111L::L121E protein complex reveals a maximal absorbance of 369 nm, and loss of the red shifted peak seen in the corresponding tetra mutant containing the Lys at position 132, 372 nm and 464 nm. **b)** Reductive amination of Y134F::R111L::L121E shows the disappearance of the covalent complex here as well. The only visible peak is the protein peak, 16785.4 Da (calculated protein mass = 16786.1 Da).

Although in other mutants we have MALDI-TOF data in at least one of the two experiments to confirm SB formation, here we do not, and cannot disregard the possibility of a red shifted retinal without covalent binding.

Aside from a retinal bound crystal structure, there is one additional piece of evidence we would like to obtain for complete confirmation that retinal is bound to Lys 132. Although we are fairly confident from the previous two mutations, proteolytic cleavage of the reductively aminated species, coupled with mass analysis could further confirm the existence of a retinal molecule on the Lys 132 containing peptide fragment.

CNBr, which cleaves after Met residues, could give a maximum of five fragments, one of which would be the single Met residue at the N-terminus of the protein sequence. Trypsin , which cleaves after Arg and Lys residues, could give a maximum of 20 fragments, and chymotrypsin, which cleaves after Phe, Tyr, and Trp residues, could generate a maximum of 11 residues. All three proteolytic reactions were used in attempt to cleave reductively aminated CRABPII and isolate or detect a retinal molecule covalently attached to the Lys 132 containing fragment. Cleavage with CNBr was extensively studied based on the small number of expected fragments. Since this work was primarily the efforts of Chrysoula Vasileiou (Michigan State University), the details of the experimental optimizations will not be discussed here. However, it will be mentioned that many of the expected fragments could be found in the reaction mixture as detected by mass analysis however, the peptide fragment containing Lys 132 was not detectable in any of the cleavage reactions, probably due to its hydrophobic nature.

For complete confirmation of the retinal binding, the reaction and detection conditions of the cleavage reactions must be optimized, as this method may be the best

hope

contin

reduct

withou

being

able t

expens

sequen

than fi

14 resi

crucial

of proc

verifica

made

contain

protein

proton

PSB

R132

R132

from

hope at achieving this confirmation in a timely manner. Other means include the continuing quest for a retinal bound crystal structure, and possible sequencing of the reductively aminated complex. Sequencing will probably not be attempted, at least not without exhaustive attempts at other methods, due to the high cost and uncertainty of being able to actually detect this residue. N-terminal sequencing, while is known to be able to sequence more than 100 residues, is charged per amino acid and will very expensive. From the N-terminus of CRABPII, the Lys is 134 amino acids in. C-terminal sequencing is still quite expensive, and is not routinely performed. Acquisition of more than five amino acids cannot be guaranteed. and from the C-terminus, the desired Lys is 14 residues in.

As previous work seems to suggest, precise positioning of a counter anion is crucial for maintaining the protonated state of the Schiff base. Although the only means of proof for the PSB species is through the absorbance as seen in the UV-vis, for further verification that Glu 121 is essential for the formation of the PSB, several mutants were made that remove the counter anion and replace it with the corresponding amide containing amino acid. This was done to mimic previous work done with rhodopsin proteins, described in Chapter 1, that show this type of mutation results in loss of the protonated Schiff base, but still maintains Schiff base formation.

Four proteins were made to test the nature of the counter anion relationship to PSB maintenance, two with Gln, R132K::Y134F::R111L::L121Q and R132K::Y134F::R111L::L121Q::T54V and two with Asn, R132K::Y134F::R111L::L121N and R132K::Y134F::R111L::L121N::T54V. The results from binding assays for these four proteins are listed in Table II-3. The spatial

Tabl

Entr	
1	
2	
3	
4	

a.
b.
c.
d.

orient

remo

proto

result

maint

result

~460

count

coval

results

Table II-3. Binding Assay Results Probing the Importance of the Counter Anion

Entry	Protein	RA K_d (nM)[a]	Rt K_d (nM)[b]	Rt λ_{max} (nm)[c]	MALDI-TOF[d] Incub.	Red. Am.
1	R132K::Y134F:: R111L::L121Q	240 ± 22	530 ± 44	368	Yes	Yes
2	R132K::Y134F:: R111L::L121N	3050 ± 240	1270 ± 49	357, 467	Yes	Yes
3	R132K::Y134F:: R111L::L121Q::T54V	1720 ± 94	601 ± 66	408	Yes	Yes
4	R132K::Y134F:: R111L::L121N::T54V	420 ± 34	128 ± 15	370, 462	Yes	Yes

a. Dissociation constant for retinoic acid as determined by fluorescence spectroscopy.
b. Dissociation constant for all-*trans*-retinal as determined by fluorescence spectroscopy.
c. Retinal maximal absorbance when incubated with protein.
d. MALDI-TOF incubation and reductive amination experiments.
Yes indicates the presence of a covalently bound retinal molecule.

orientation of Glu vs. Gln and Asp vs. Asn remains the same, but in these mutants we are removing the negative charge which could be the source of stabilization for the protonated Schiff base.

The Glu to Gln mutations (Entries 1 and 3, Table II-3) show the most intriguing results. This single amino acid mutation has resulted in loss of the red shift, yet maintenance of the Schiff base as visible via both MALDI-TOF reactions, mimicking the results seen with rhodopsin E113Q mutations (Figure II-32). These results suggest the ~460 nm species is a PSB whose existence depends heavily on the presence of the counter anion, and by removing this counter anion, we lose the protonated state of the covalent complex.

The corresponding mutations with Asp to Asn mutations do not exhibit as clear results as those observed above (Entries 2 and 4, Table II-3). Both of these proteins still

maintain the existence of some amount of PSB as indicated through UV-vis. Some E113Q rhodopsin mutants also did not completely lose the protonated form of the Schiff base complex (see Chapter I for discussion).[51] One plausible reason for the continued existence of some PSB could be that not all of the protein contains the amide amino acid. The difference in mass is too small to tell the difference between the carboxylic acid moiety versus the amide functionality. Granted, we have DNA sequence verification for the amide mutation, but we cannot rule out auto hydrolysis of the amide back to the carboxylic acid.

Finally, a protein mutant was produced without the counter anion at all, R132K::Y134F::R111L::T54V. We also expected to see a loss of red shifting in this protein as well. This protein does display a relatively good binding affinity with retinal (K_d = 84 ± 12 nM) as expected with the hydrophobic nature of the binding cavity. However, as seen in the last two mutations, removal of the counter anion does not

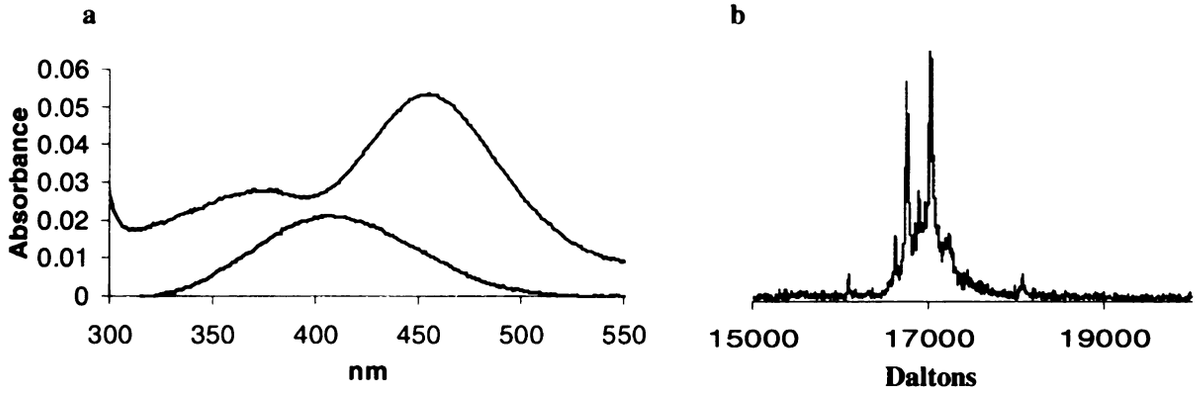

Figure II-32. a) Corrected UV-vis spectra of the penta mutant / retinal complex, R132K::Y134F::R111L::L121E::T54V, shows existence of two peaks, 378 nm and 455 nm. Replacement of the counter anion with the corresponding amide functionality, R132K::Y134F::R111L::L121Q::T54V, causes elimination of the red shifted peak , and only one peak is now present at 408 nm. b) Reductive amination of the protein still shows evidence for the Schiff base existence despite deprotonation. Protein M^+ = 16754.1 Da (calculated 16755.2 Da) and SB M^+ = 17028.1 Da (difference of 274 mass units, calculated difference is 268 Da).

compl

forma

reacti

anion

presen

counta

and e

that

hydro

probe

be a

deter

protei

absor

acid/b

nm (

base).

howe

and c

titrati

II-33)

completely eliminate the red shifted species (391 nm and 455 nm) and the covalent bond formation between the protein and chromophore is visible in both MALDI-TOF reactions. Again, the fact that the red shift is not completely lost by removing the counter anion does not discount the probability of this being a PSB. Having the counter anion present does help to increase the pK_a of the PSB. In addition, only the protein with the counter anion exhibits stoichiometric binding with retinal.

R132K::Y134F::R111L::T54V is the most hydrophobic protein we have made, and even without a counter anion it exhibits a significant amount of red shifting. Given that position 121 is presumably the best place for the counter anion, additional hydrophobic mutations should be added to R132K::Y134F::R111L::L121E::T54V to probe a possible increase in stability.

Although the above mentioned data all suggest that the red shifted complex may be a PSB with Lys 132, these next few experiments were done to help in unequivocally determining that we are indeed forming a protonated Schiff base between retinal and the protein clone at the engineered Lys position 132. First, to prove that the 455 nm absorbing species detected by UV-vis is a protonated Schiff base we performed a simple acid/base titration. At pH = 7, there exists a mixture of two species, one absorbing at 455 nm (protonated Schiff base), the other at 370 nm (free aldehyde or unprotonated Schiff base). Addition of acid to the mixture did not force the 370 nm species to red shift, however, if the mixture was treated with base first, both species shifted to 366 nm (SB) and could then all be forced to a red shifted absorbance of 450 (PSB) nm. Acid / base titrations of this sample can interconvert the 366 nm and 450 nm peaks repeatedly (Figure II-33). We know that this 450 nm peak is due to specific Schiff base formation with the

Lys in the binding pocket, as a solvent exposed PSB has been found to absorb at 445 nm by denaturation of the mixture with SDS.

From the above experiment, at pH = 7 there is approximately a 1:1 mixture of SB:PSB, thus we would expect the pK_a of the PSB to be around 7. Our attempts at measuring this pK_a produce similar results. Following similar procedures to determine the pK_a of the PSB for rhodopsin, titration of the protein solution was performed and the absorbance (A_{500}) versus the pH was plotted (Figure II-34). Fitting the data to a polynomial (3^{rd} power) yielded a $pK_a = 6.5$ for the PSB.

This is a rather low value for the pK_a in comparison with the pK_a of PSBs in various rhodopsin proteins. Most rhodopsins have a PSB pK_a estimated to be greater than 10. For bovine rhodopsin, it is suggested to be greater than 16, and is known to be at least greater than 12.[52-54] Measurement of the pK_a of bovine rhodopsin was attempted by similar experiments as just described for the CRABPII pK_a determination. The PSB was found to be unperturbed at pH ranges up to 11, but significant protein denaturation limited titration to higher pH values.[55] Alternatively, pK_a values were estimated using

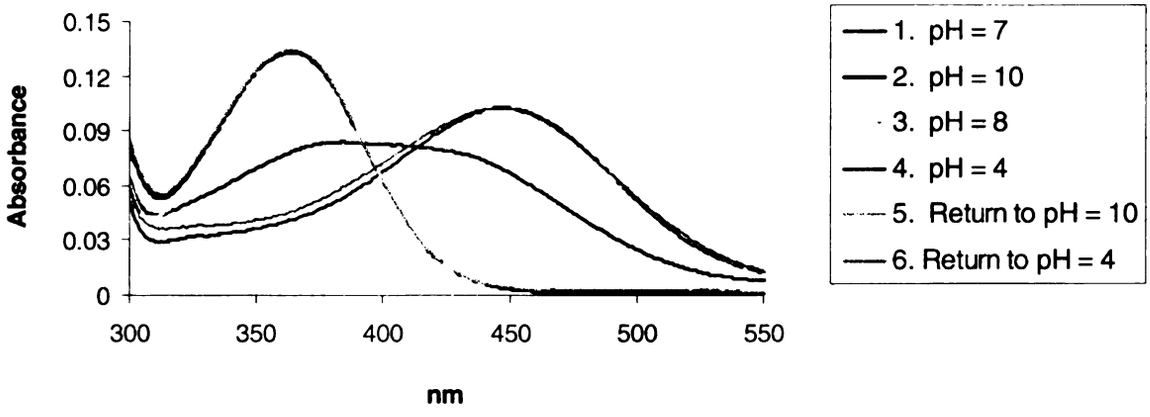

Figure II-33. Acid - base titration of the R132K::Y134F::R111L::L121E::T54V / retinal complex shows interconversion between the SB (366 nm) and the PSB (450 nm).

fluorinated retinal analogs.[56] These fluorinated derivatives typically produce pK_a values approximately 5.5 units lower than the non-fluorinated analog. Treatment of bovine rhodopsin with 11-*cis*-13-trifluoromethyl-retinal still produced a red shifted analog that was stable to pH 11. If this chromophore is 5.5 units lower than the corresponding non-fluorinated derivative (11-*cis*-retinal), the pK_a of bovine rhodopsin is again estimated to be ~16.5.[55] Interestingly however, a single amino acid mutation in bovine rhodopsin reduces the pK_a of the PSB from above 16 to approximately 6 (E113Q (pK_a = 6.0), E113N (pK_a = 6.7), and E113A (pK_a = 5.7)),[57] which attests for the fact that precise counter anion placement is critical for PSB existence.

Other opsin PSB pK_a values that have been measured include, octopus rhodopsin (10.4),[58,59] gecko cone opsin (9.9),[59] and a partially titratable bacteriorhodopsin (~13.3).[60] The relatively low value for the octopus pK_a is thought to be because of the change at position 113. In vertebrate pigments, this is the position for the counter anion, Glu, however, in invertebrate pigments this residue is replaced by the neutral Tyr.[61] Incidentally, this does not explain the low value observed for gecko opsin as it has Glu

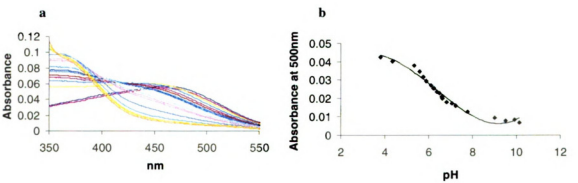

Figure II-34. **a**) The retinal incubated R132K::Y134F::R111L::L121E::T54V complex was forced completely to the 464 nm. The mixture was then titrated with base and forced completely to the 366 nm absorbing species. **b**) Plotting of the absorbance at 500 nm versus the pH of the samples revels a pKa of ~6.5 for the protonated Schiff base.

position 113. In vertebrate pigments, this is the position for the counter anion, Glu, however, in invertebrate pigments this residue is replaced by the neutral Tyr.[61] Incidentally, this does not explain the low value observed for gecko opsin as it has Glu 113.

There have been many plausible reasons suggested for the very high PSB pK_a values, most involving the possible polar nature of the PSB environment.[62,63] Stabilization could also be attributed to hydrogen bonding with nearby protein residues and the counter anion.[64] A precise arrangement of water molecules in the binding pocket that effectively directs a hydrogen bonding network can also not be ruled out.[65] Other theories include stabilization due to precise orientation of the SB with the counter anion to promote efficient proton transfer,[66,67] and differing degrees of twisting around the C14-C15 single bond that may promote stabilizing H-bond interactions.[68]

There are different possible routes to fine tune the pK_a of the PSB. First, further tuning of the amino acids in the binding pocket, including hydrophobicity changes and repositioning of the counter anion could potentially increase the stability and pK_a of the protonated Schiff base. This route to achieving the ultimate rhodopsin mimic is currently ongoing in the laboratory. Optionally, mutations on the surface of the protein may lead to an increased PSB pK_a value. Figure II-35 shows a Van der Waals structure of the surface of the CRABPII protein. There is a hole in the surface of the protein that lies above the binding cavity and directly over the top of the region where the Schiff base formation occurs. The hole is approximately 6 Å in diameter, and could potentially allow for water and/or other ions access to the cavity, reducing the isolation of the SB from the bulk solvent, and thus not effectively shielding the SB.

Attempts to close the gap seen here involved mutation at residue 61 with bulkier amino acids to produce the hexa-mutants R132K::Y134F::R111L::L121E ::T54V::T61E and R132K::Y134F::R111L::L121E ::T54V::T61F. Neither of these mutations have much effect on any of the retinal binding assays, fluorescence, UV-vis or MALDI-TOF experiments (see Appendix for data curves). All three proteins have a retinal K_d < 100 nM, exhibit 2 peaks in the UV-vis (~370 nm and ~460 nm), and display positive covalent bond formation in both MALDI-TOF experiments. Figure II-36 shows the UV-vis curves for these two mutants as well as the R132K::Y134F::R111L::L121E::T54V CRABPII mutant at pH=7. There is approximately a 1:1 mixture of two species in the penta mutant spectra, giving an approximate pK_a ~6.5 for the PSB in this protein. For an improvement and increase in the pK_a of the PSB we expect to see an increase in the amount of red shifted peak present at pH=7. As can be noticed in Figure II-36, there is no significant change in the distribution between the two species with the two new hexa mutants. Mutation at the surface residue 61 has no effect on retinal binding abilities. Further efforts are needed, either by further mutations on the surface of the protein in attempts to close the hole, or

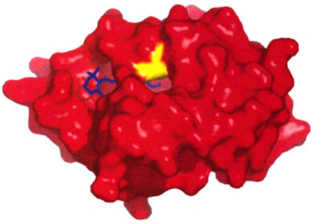

Figure II-35. A view of the Van der Waals contacts on the surface of CRABPII reveals a hole that overlooks the binding cavity and sits directly over the where Schiff base formation will occur.

further mutations in the binding cavity, to increase the PSB's pK_a value optimally to above 10 for use as a rhodopsin mimic and for probing the factors responsible for wavelength regulation.

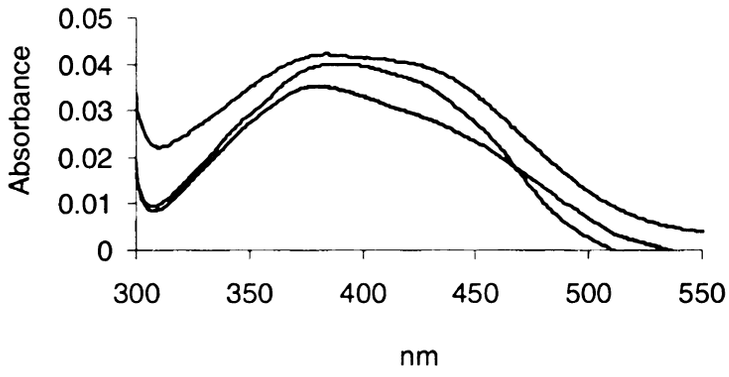

Figure II-36. UV-vis curves of the retinal incubated protein complexes R132K::Y134F::R111L::L121E::T54V, R132K::Y134F::R111L::L121E::T54V::T61E, and R132K::Y134F::R111L::L121E::T54V::T61F at pH=7. Attempts at closing the hole on the surface of the protein did not produce a stabilization of PSB and increase in the amount of the red shifted species.

H. Probing an Alternate Position for Lysine

In addition to incorporating the Lys at position 132, we also probed the possibility of having the Lys at position 134 given that this residue is the closest to the retinal carbonyl carbon. Lys at position 134 will approach the carbonyl in a different trajectory than Lys at position 132. Lys 134 approaches in a more head-on trajectory, while Lys 132 approaches from the plane perpendicular to the chromophore. Utilizing knowledge gained through previous mutagenesis and binding studies, our attempts at designing an efficient rhodopsin mimic with Lys 134 included hydrophobic tuning and probing for an effective position for the counter anion.

The single CRABPII mutant Y134K removes the hydrogen bonding phenolic amino acid and adds an additional positive charge to the binding pocket through the introduction of a Lys residue (Figure II-37). As compared to the R132K single mutant, retinoic acid binding affinity is an order of magnitude worse (630 nM versus 65 nM for R132K, Entry 1, Table II-4). This result is a little surprising given that the positively charged Arg residues, which are believed to be the reason for maintaining binding of the

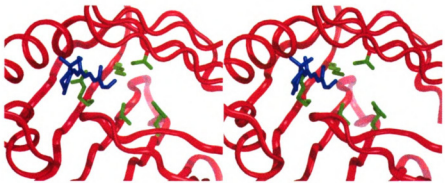

Figure II-37. Stereoview of CRABPII Y134K with Arg 132, Arg 111, Leu 121 and Thr 54 also shown. From position 134, Lys is 4.1 Å from the carbonyl of retinal.

negatively charged retinoic acid, are still intact. The charge repulsion due to incorporation of the presumably positively charged Lys, coupled with the two intact positively charged Arg residues, may force a depression of the pK_a of the less acidic amino acid. Having both an Arg and a Lys in close proximity to each other in the binding pocket may reduce the pK_a of the Lys and force it to remain non-protonated. With the single mutant Y134K however, retinal binding affinity remains unacceptably low (570 nM), and no Schiff base was detectable by MALDI-TOF.

Still utilizing the theory that two positively charged residues in close proximity to each other may force one to remain non-protonated, the double lysine mutant Y134K::R132K was prepared (Entry 2, Table II-4). This Arg to Lys mutation (Rt λ_{max} = 374 nm, Rt K_d = 270 ± 10 nM, RA K_d = 660 ± 25 nM) results in loss of retinoic acid binding affinity compared to the previous single mutant R132K (Rt λ_{max} = 370 nm, Rt K_d = 280 ± 17 nM, RA K_d = 65 ± 14 nM), however, no change in retinal binding ability was observed. Although there is still no red shift in the UV-vis of the retinal / protein complex, Schiff base formation was detected in both the incubation and reductive amination MALDI-TOF experiments. These results also mimic what was seen with R132K. The binding pocket of the Y134F::R132K CRABPII protein is very hydrophilic near the SB region, with two Lys residues and an Arg residue. It is somewhat surprising that the retinal binding affinity is down to 270 nM and that SB formation does occur. However, the lack of a red shift in the UV-vis implies further manipulation of the binding pocket is required to obtain protonation of the Schiff base. To achieve this, we began to incorporate some of the amino acids that had previously shown improvements.

Table II-4. Binding Assays Probing the Efficacy of Lysine at Position 134.

Entry	Protein	RA K_d (nM)[a]	Rt K_d (nM)[b]	Rt λ_{max} (nm)[c]	MALDI-TOF[d]	
					Incub.	Red. Am.
1	Y134K	630 ± 20	570 ± 29	370	No	No
2	Y134K::R132K	660 ± 25	270 ± 10	374	Yes	Yes
3	Y134K::R132F	180 ± 7.3	78 ± 11	415	No	No
4	Y134K::R132L	800 ± 19	340 ± 16	432	Yes	No
5	Y134K::R132F::R111L	570 ± 26	7.9 ± 7.2	415	Yes	No
6	Y134K::R132F::R111L::L121E	1000 ± 51	220 ± 16	364	Yes	Yes
7	Y134K::R132F::R111L::T54E	120 ± 10	41 ± 6.6	434	Yes	Yes
8	Y134K::R132L::R111L	3300 ± 264	210 ± 7.8	423	Yes	Yes
9	Y134K::R132L::L121E	450 ± 19	110 ± 6.7	423	No	No
10	Y134K::R132L::R111L::L121E	1069 ± 38	570 ± 30	367	Yes	Yes

a. Dissociation constant for retinoic acid as determined by fluorescence spectroscopy.
b. Dissociation constant for all-*trans*-retinal as determined by fluorescence spectroscopy.
c. Retinal maximal absorbance when incubated with protein.
d. MALDI-TOF incubation and reductive amination experiments.
Yes indicates the presence of a covalently bound retinal molecule.

Given the initial success of the R132K::Y134F double mutant, we opted to add the hydrophobic Phe residue at position 132 to produce the double mutant, Y134K::R132F. As an alternative, Arg 132 was also mutated to Leu. This mutation also increases the hydrophobicity of the binding pocket, yet is a more spatially conservative mutation than Arg to Phe. Both of these protein mutants exhibit similar results compared to the previous R132K::Y134F double mutant (429 nm), producing a retinal λ_{max} of 415

nm (Y134K::R132F, Entry 3, Table II-4) and 432 nm (Y134K::R132L, Entry 4, Table II-4). The dissociation constant of Y134K::R132F (78 nM) is comparable to the double mutant R132K::Y134F (100 nM) where both proteins have identical hydrophobic environments. CRABPII Y134K::R132L has a slightly higher K_d (340 nM), but still fits well with the previously seen results. Also mimicking the results seen with R132K::Y134, neither of these double mutants could trap a covalently bound retinal by reductive amination. Y134K::R132L does demonstrate Schiff base formation through the incubation with retinal but Y134K::R132F does not.

As we cannot say with any degree of certainty whether or not this ~420 nm species is a PSB, further tuning of the pocket is still necessary. The binding affinity of retinal for the protein needs to be increased, as well as the stability of the Schiff base.

In keeping with the same strategy as the previous series of CRABPII mutants, an additional hydrophobic mutation was incorporated at the Arg 111 site (changed to Leu) to generate the triple mutants Y134K::R132F::R111L (Entry 5, Table II-4) and Y134K::R132L::R111L (Entry 8, Table II-4). Incorporation of the additional hydrophobic residue in R132K::Y134F::R111L did not have much effect on either the binding affinity of retinal (160 nM) with the protein, or retinal's λ_{max} (410 nm) when incubated with the protein, but it did allow for trapping of the covalent complex by reductive amination, as R132K::Y134F did not. That trend is again repeated in the Y134K series of mutants as well. The R111L mutation in Y134K::R132L::R111L does not generate much change in retinal binding affinity (210 nM) or UV-vis absorbance (423 nm). MALDI-TOF analysis of the retinal incubated complex and the reductively aminated complex both demonstrate SB formation. Similarly, the triple mutant

Y134K::R132F::R111L has an absorbance of 415 nm, and although the SB in observed with the incubation of retinal, it cannot be trapped by reductive amination. Interestingly, this triple mutant, whose hydrophobicity closely matches Y134K::R132L::R111L, has a dramatically lower dissociation constant (8 nM). Despite this very good binding affinity, this protein still needs further tuning to stabilize SB formation.

We next began to probe optimal placement of the counter anion. Initially, the counter anion was placed at position 121, as this had been the best in previous studies with the Lys 132 series of mutants. In the two tetra mutants Y134K::R132F::R111L::L121E (Entry 6, Table II-4) and Y134K::R132L::R111L::L121E (Entry 10, Table II-4) the red shift that was visible in each of their respective previous triple mutants has now been lost, 415 nm (Y134K::R132F::R111L) shifted to 364 nm, and 423 nm (Y134K::R132L::R111L) to 367 nm upon addition of Glu 121. Although these absorbance values do not indicate PSB formation from the lack of red shift in the UV-vis, reductive amination and MALDI-TOF reveal the formation of Schiff base. Also in both the tetra mutant proteins, addition of Glu 121 results in some loss of retinal binding affinity. Y134K::R132L::R111L::L121E has dropped to a K_d of 570 nm and Y134K::R132F::R111L::L121E has dropped significantly to 220 nM. A 220 nM K_d for this protein, although dramatically worse than the 8 nM observed for the triple mutant Y134K::R132F::R111L, is the expected K_d when compared to the analogous protein in the Lys 132 series, R132K::Y134F::R111L::L121E (200 nM).

Two additional mutants were made in this series in efforts towards establishing the proper counter anion placement and environment. Y134K::R132L::L121E (Entry 9,

Table II-4), which still has the hydrophilic, positively charged Arg 111 residue, did manage to maintain a red shift (423 nm) and lower the binding affinity for retinal (110 nM), however not low enough to be of significant use as the optimal rhodopsin protein mimic. This protein serves as another piece of evidence for the theory that the ~420 nm absorbing species may not be PSB. All of the other ~420 nm absorbing complexes demonstrate SB formation in one of the two experiments, however this protein shows no indication of SB formation with either MALDI-TOF experiment.

Besides position 121 for the putative counter anion, position 54 (originally a Thr) was also probed. Y134K::R132F::R111L::T54E (Entry 7, Table II-3), was effective in that it had a relatively low dissociation constant (K_d = 41 nM, best in the Lys 134 series), and exhibited a 64 nm red shift (λ_{max} = 434 nm, the best in this series of proteins). Additionally, the retinal complex was stable enough to be trapped under the reductive amination reaction conditions and detected by MALDI-TOF. Although Glu at position 121 may have served Lys 132 the best, Glu at position 54 may be best suited for Lys 134. Unlike the previous series of proteins though, the Lys 134 series was never able to demonstrate a red shift up ~460 nm. The largest red shift seen was only up to 434 nm. The Lys 134 position has yet to produce adequate PSB forming protein that would be suitable to serve as a rhodopsin mimic, and further tuning of the Y134K::R132F::R111L::T54E protein is necessary.

I. Investigating 11-*cis*-Retinal as the Substrate

In humans, the native substrate of rhodopsin is 11-*cis*-retinal, although other isomeric forms (9-*cis*- and all-*trans*-retinal) are also known to both efficiently bind some opsins as a PSB, and efficiently promote activation of the G-protein, transducin, *in vitro*. Additionally, tadpoles have an extra conjugated double bond in the β-ionone ring which allows them to see into the IR wavelengths.[69] Some insects have lost the double bond in the β-ionone ring of retinal, and can see into the UV wavelengths.[70] These various retinal analogs seem to suggest that we do have some flexibility in the structure of the retinylidene chromophore while still maintaining the same PSB forming, red-shifted properties. Additionally, even if our protein would not bind the 11-*cis* isomer, it should not hinder our studies to utilize the all-*trans* isomer.

Initially, all of the binding assays performed on the CRABPPII mutants were performed with all-*trans*-retinal. This was done in part because of the very sensitive nature of 11-*cis*-retinal (even small amounts of natural light will isomerize the 11-*cis* bond to *trans*) and the lengthy means of obtaining pure samples (either via isomerization of all-*trans*-retinal and HPLC purification,[71,72] or synthesis and purification of the compound in the absence of natural light). Attempts were made at separation of an isomerized retinal mixture, however, this did not lead to isolation of pure compounds in acceptable yields. Instead, the molecule was synthesized following a published procedure.[73]

Several of the CRABPII mutants capable of binding all-*trans*-retinal were chosen for binding analysis with the 11-*cis*-retinal isomer. Results of the fluorescence titrations,

Table II-5. Results of binding assays with 11-*cis*-Retinal

Entry	Protein	Rt K_d (nM)[a]	Rt λ_{max} (nm)[b]	Reductively[c] Aminates
1	Wild-Type	>1000	373	No
2	R132K	50 ± 16	356	Yes
3	R132K::Y134F	630 ± 53	373	No
4	R132L::Y134F::R111L::L121E	-	385	-[d]
5	R132K::Y134F::R111L::L121E::T54V	210 ± 18	360	Yes
6	R132K::Y134F::R111L::L121D	320 ± 19	360	-
7	Y134K	1680 ± 140	384	No
8	Y134K::R132F	-	394	-
9	Y134K::R132F::R111L::L121E	-	371	-
10	Y134K::R132F::R111L::T54E	1000 ± 100	381, 418	-
11	L19W	2120 ± 300	380	-

a. Fluorescence titration with 11-*cis*-retinal to determine K_d values.
b. 11-*cis*-retinal UV-vis absorbance when incubated with protein.
c. Reductive amination measured by MALDI-TOF.
Yes indicates the covalent complex between 11-*cis*-retinal and protein was detected.
d. Results indicated with a – were not completed.

UV-vis incubation and MALDI-TOF reductive aminations are summarized in Table II-5 (graphs are presented in the Appendix). There was no single protein that exhibited positive results in all three experiments, i.e., binding efficiency, red shifted λ_{max}, and positive reductive amination. The wild type protein (Entry 1), L19W (Entry 11), and the tetra mutant R132L::Y134F::R111L::L121E (Entry 4) were all analyzed as controls, as they all lack the active site lysine. None of these three proteins showed a red shift in the UV-vis, and reductive amination with the wild type protein confirms the absence of the SB.

The single mutant R132K (Entry 2, Table II-5) was the only protein among those tested that had a binding affinity less than 100 nM (K_d = 50 nM). It was also one of only two proteins that displayed a positive covalent complexation as detected by MALDI-TOF. R132K incubated with 11-*cis*-retinal does not however generate a red shifted absorbance (365 nm).

The penta mutant R132K::Y134F::R111L::L121E::T54V (Entry 5) and the tetra mutant R132K::Y134F::R111L::L121D (Entry 6), which were the best all-*trans*-retinal binding proteins (2 nM K_ds), were the next best 11-*cis*-retinal binding proteins with 200 nM and 320 nM dissociation constants, respectively. Only R132K::Y134F::R111L::L121E::T54V was tested for reductive amination (due to insufficient supply of the chromophore), and does indeed show SB formation. Both of these mutants absorb at 360 nm, which may only suggest SB formation as opposed to PSB formation. The double mutant R132K::Y134F (Entry 3, Table II-5) has also lost the red shift (373 nm) that was seen as a result of complexation of the all-*trans*-retinal (429 nm). Binding affinity is also worse with 11-*cis*-retinal (630 nM) as compared to all-*trans*-retinal (100 nM). SB formation is not detected in the reductive amination either.

UV-vis analysis of 11-*cis*-retinal with these CRABPII mutant proteins did not produce many red shifted species. In fact, none of the proteins with the Lys in position 132 red shifted at all. The two proteins that revealed Schiff base formation via MALDI-TOF (R132K and R132K::Y134F::R111L::L121E::T54V), as well as R132K::Y134F::R111L::L121D whose reductive amination was not attempted, exhibit retinal λ_{max} values that are actually blue shifted as compared to the noncovalent wild type

/ retinal mixture. Again, this blue shifted absorbance may be indicative of Schiff base formation, however in the unprotonated state.

Most of the Lys 134 proteins tested do red shift from the wild type absorbance, unfortunately, a current lack of ample quantities of the 11-*cis*-retinal substrate has not allowed for a complete analysis of this series of proteins as is necessary. There were two proteins with the Lys in position 134 that exhibited a small degree of red shifting. The double mutant Y134K::R132F (Entry 8) showed a retinal peak at 394 nm, a red shift of 21 nm as compared to the wild type. This is a 10 nm improvement over the Y134K single mutant which absorbs at 384 nm (Entry 7). Hydrophobic tuning and placement of the counter anion at position 121 (Entry 9) also did not red shift, but the tetra mutant Y134K::R132F::R111L::T54E (Entry 10) does show a 45 nm red shift, with peaks at 381 nm and 418 nm.

This is a particularly interesting result, since as opposed to the previous ~420 nm absorbing all-*trans* complexes that only showed the one peak, this protein does show two peaks as was seen with the ~460 nm absorbing species (Figure II-38). This red shifted peak could be due to a small amount of PSB, or alternatively, it could be bound aldehyde, which absorbs at a different wavelength than retinal in solution, as the K_d is fairly high, equilibrium may not favor substrate binding.

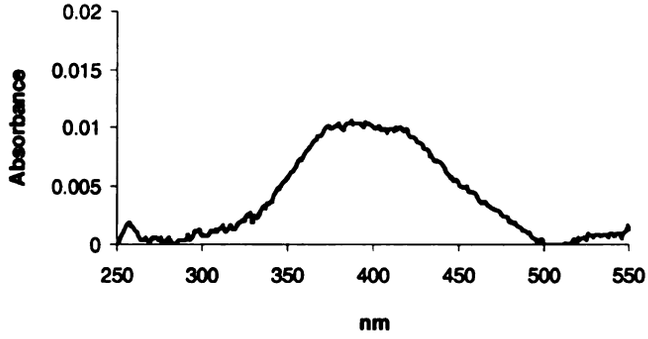

Figure II-38. UV-vis of 11-*cis*-retinal as bound to Y134K::R132F::R111L::T54E. This is the largest bathochromic shift observed thus far for the11-*cis* isomer, 381 nm and 418 nm.

Figure II-39 shows 11-*cis*-

retinal in the binding cavity of Y134K::R132F::R111L::T54E. Lys 134 is positioned 6.6 Å from the carbonyl of the chromophore and Glu 54 is 2.7 Å. The hydrophobic Leu residues 121 and 111 are 3.5 Å and 7.2 Å from retinal, respectively. Compared to the all-*trans*-retinal binding position, the ionone ring has not moved, but as a result of the double bond isomerization, the carbonyl region has shifted ~3 Å.

The binding affinity for this protein, as well as all Lys 134 proteins analyzed, is very poor (K_d > 1000 nM). This series has yet to be tested for SB formation with 11-*cis*-retinal by reductive amination and MALDI-TOF.

Preliminary binding analyses with 11-*cis*-retinal indicate that Lys in position 134 coupled with Glu in position 54 may be the most beneficial for PSB formation. However, sterics may prohibit 11-*cis*-retinal from achieving a suitable binding affinity with Lys 134. The Lys 132 series may be more suited for binding, and with proper counter anion placement may promote PSB formation.

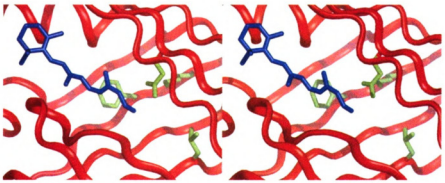

Figure II-39. Stereoview of Y134K::R132F::R111L::T54E with 11-*cis*-retinal bound. Lys 134 is 6.6 Å from the substrate, and the counter anion Glu 54 is 2.7 Å from the substrate (InsightII minimizations).

J. Monitoring the Schiff Base via ^{13}C-^{15}N NMR

Another means by which we hope to monitor Schiff base formation is via NMR, more specifically, ^{15}N and ^{13}C NMR. The carbonyl carbon of retinal should exhibit different chemical shifts for free aldehyde, SB, and PSB. We hope to be able to couple the results already uncovered through fluorescence, UV-vis and MALDI-TOF with NMR experiments to further probe the nature and extent of retinal binding.

Although one may conceivably be able to follow the ^{13}C peak of retinal's aldehydic carbon in the NMR, relating the chemical shifts seen to different species, i.e., unbound, Schiff base, and protonated Schiff base, we will also couple this with a ^{15}N-Lys132 protein for more conclusive results. Following the ^{13}C signal only may not be conclusive due to the existence of multiple species present. By coupling the ^{13}C labeled retinal with the ^{15}N labeled protein, we will attempt to acquire ^{13}C-^{15}N HMQC data to demonstrate with more certainty if indeed the retinal is covalently attached, and specifically to the Lys we desire. If retinal is covalently attached, the ^{13}C peak should show correlation to the ^{15}N peak.

Additionally, determination of the pK_a of the active site PSB will be attempted through use of both the labeled retinal and labeled protein. Retinal will be incubated with protein samples at different pH values and probed for SB formation. Following similar procedures used in the UV-vis determination of the PSB pK_a, chemical shifts of either the carbon or nitrogen will be plotted against pH and the pK_a can be deduced. We already have a fully ε-^{15}N-Lys labeled R132K::Y134F protein, and are working on acquiring a 132-ε-^{15}N-Lys only.

The synthesis of 15-[^{13}C]-retinal (**II-a**) to be used in these experiments has been completed and is outlined in Scheme II-1. Ethyl diphenylphosphinite (**II-b**) was heated with chloroacetonitrile, neat, to produce ylide **II-c** which was deprotonated with *t*-BuOK and reacted with β-ionone to give primarily the *E* isomer of **II-d**. Dibal reduction of the cyano derivative gave aldehyde **II-e** in 70% yield.[74] This aldehyde was used in another Horner-Wadsworth-Emmons (HWE) reaction with ylide **II-f** to produce the ester **II-g**. Treatment of ester **II-g** with TMSCl and MeLi yielded methyl ketone **II-h** in 46% yield.[75,76] Although the low yielding step from **II-g** to **II-h** only results in a 46% yield of the product, 29% of the starting material is recovered and can be recycled. Pushing the reaction with longer times only resulted in degradation of the olefin and lower yields in the range of 20%.

The final two reactions incorporate the labeled carbon via another HWE reaction. 1-^{13}C-Acetonitrile is treated with two equivalents of *n*-BuLi and stirred for 10 min at –60 °C. Chlorodiethylphosphite was added into the reaction and stirred for an additional 30 min at low temperatures, first generating the ylide, then deprotonating it. Ketone **II-h** was added, and the reaction mixture was stirred for 1 h at –60 °C and then allowed to slowly warm to room temperature. Intermediate **II-i** was quenched and extracted, but not purified. It was taken directly into Et_2O for Dibal reduction, and after column chromatography yielded 30% of 15-^{13}C-retinal, **II-a**.[77] The recovery is a bit low, but it is over two steps. The reaction seems fairly clean by TLC and there is no recovery of other materials. The low yielding step is the recovery of **II-a** from the silica gel work-up. Even after several extractions the silica gel still maintains a yellow / orange color presumably from the retinal.

Attempts are currently ongoing to acquire suitable NMR spectra with the ^{13}C labeled retinal and fully ε-^{15}N-Lys labeled protein to detect different retinal / protein complexes.

Scheme II-1

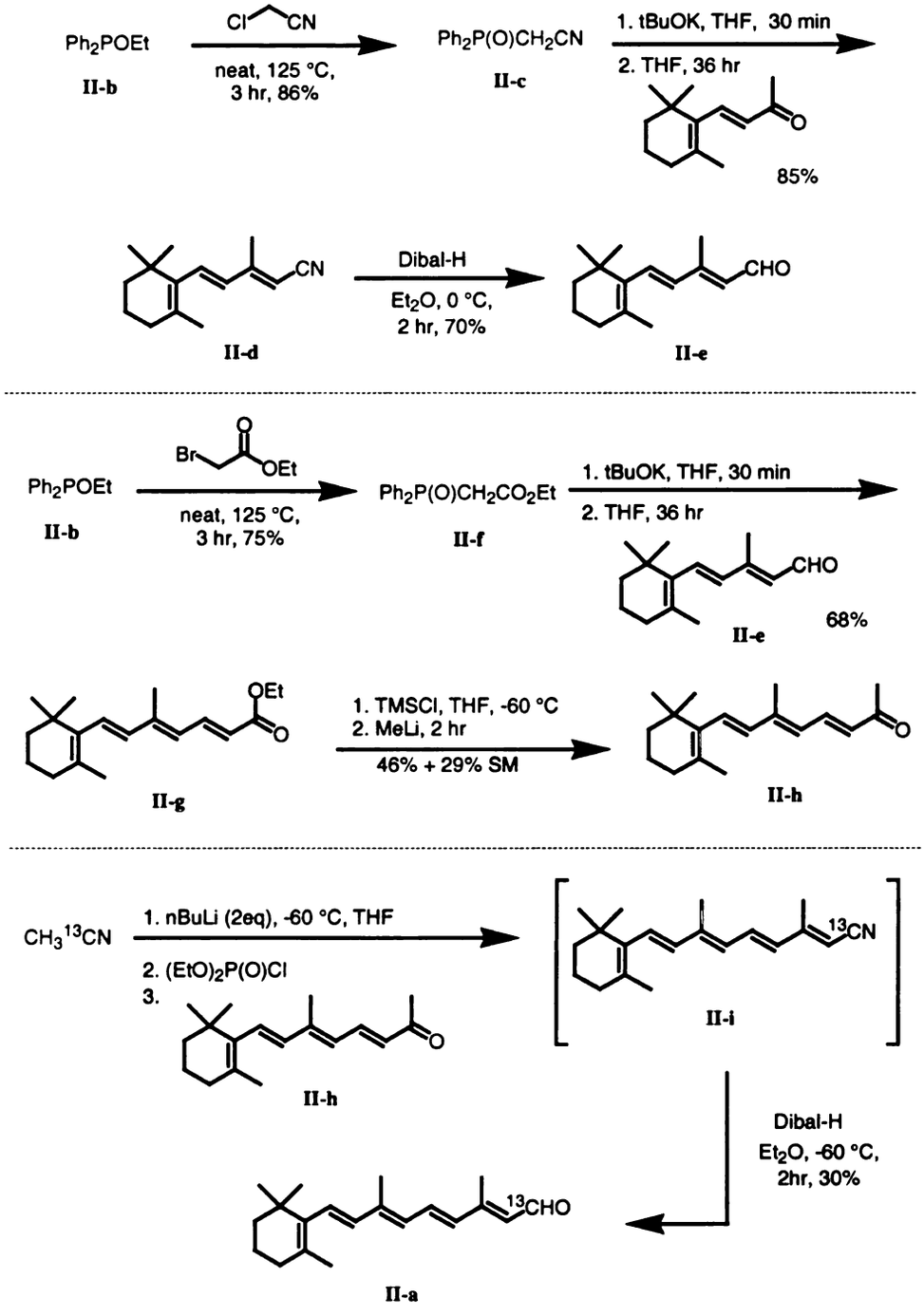
Ph2POEt
II-b
Cl CN
neat, 125 °C,
3 hr, 86%
Ph2P(O)CH2CN
II-c
1. tBuOK, THF, 30 min
2. THF, 36 hr
O
85%
CN
Dibal-H
Et2O, 0 °C,
2 hr, 70%
CHO
II-d
II-e
Ph2POEt
II-b
Br OEt
O
neat, 125 °C,
3 hr, 75%
Ph2P(O)CH2CO2Et
II-f
1. tBuOK, THF, 30 min
2. THF, 36 hr
CHO
II-e
68%
OEt
O
II-g
1. TMSCl, THF, -60 °C
2. MeLi, 2 hr
46% + 29% SM
O
II-h
CH3 13CN
1. nBuLi (2eq), -60 °C, THF
2. (EtO)2P(O)Cl
3.
O
II-h
13CN
II-i
Dibal-H
Et2O, -60 °C,
2hr, 30%
13CHO
II-a

K. Summary

Mutagenesis of Human Cellular Retinoic Acid Binding Protein II has afforded a protein that will now bind retinal with binding affinity comparable to that of the native protein with its native substrate (K_d = 2 nM). Additionally, retinal will bind as a protonated Schiff base with an engineered Lys in an appropriately tuned binding cavity. The best PSB forming protein is the penta mutant R132K::Y134F::R111L::L121E::T54V, that includes mutations to not only introduce the pertinent Lys residue, but also to increase the hydrophobicity of the binding cavity and correctly position a counter anion for the positively charged iminium ion.

Through our mutagenesis studies, we have found that position 132 seems to be best suited for the Lys location, coupled with a counter anion at position 121, for binding with all-*trans*-retinal. Preliminary binding studies with 11-*cis*-retinal indicate that perhaps position 134, coupled with a counter anion at position 54, would be best suited. The optimal all-*trans*-retinal PSB forming protein and 11-*cis*-retinal PSB forming protein do not necessarily have to be the same protein, and indeed they probably will not be. Efforts at probing the mechanisms responsible for wavelength regulation can, and will, be applied to both chromophores and their respective proteins.

Hydrophobic tuning is essential, not necessarily to form PSB, but to increase the binding affinity to acceptable levels (K_d < 100 nM). Particularly, the Arg residue at position 111 seems to be critical for hydrophobic incorporation. No red-shifted retinal species > 440 nm was ever obtained in a protein that did not have the R111L mutation. Studies are currently ongoing to probe the effect of other hydrophobic amino acids at this position. Precise positioning of the counter anion is also critical in forcing the PSB

species to become favored at equilibrium, as shortening the distance of the counter anion (Glu mutated to Asp) in our best PSB forming protein shows not only a slight decrease in the binding affinity, but also that the equilibrium has shifted to favor the 380 nm species more than the 460 nm PSB.

The pK_a of R132K::Y134F::R111L::L121E::T54V has been measured to be 6.5, which is considerably lower than pK_a values measured for various rhodopsin proteins (generally > 10). Our efforts at increasing this value have just begun, and is still being heavily pursued. Once complete however, the ultimate task at hand will begin, probing the underlying principles of wavelength regulation. Site-directed mutagenesis on the protein will include adding varying charges, dipoles, and sterics at positions all along the polyene backbone and measuring the effect on retinal's maximal absorbance.

L. Materials and Methods

Typical PCR Conditions for Stratagene's QuikChange Site-Directed Mutagenesis Protocol: For the PCR reaction, the following materials are mixed together in a 500 mL eppendorf tube: 50 – 100 μg template plasmid DNA; 15 pmol each of complimentary, mutation containing primers; 1 μL of 10 mM pre-mixed dNTP; 5 μL of a 10x reaction buffer; sterile water, diluted up to a reaction volume of 49 μL; 1 μL of pfu turbo polymerase (This should be added last.).

Temperature cycles for the PCR:

~95 °C (0.5 min), one time

~95 °C (0.5 min), ~55 °C (1 min), 70 °C (8 min), repeat 16-20 times depending on the number of base pairs being mutated

~70 °C (10 min), one time

Following the PCR reaction and agarose gel verification, 1 μL of DpnI is added to the reaction tube and allowed to incubate at 37 °C for 1 h, after which time 1 – 5 μL of reaction is transformed into 100 μL of either JM109 or XL1-Blue competent cells.

A typical transformation procedure:

A 100 μL aliquot of competent cells was allowed to thaw on ice about five min. One microliter (usually 1 and never more than 10 μL) was added to the cells, gently mixed, and allowed to incubate on ice 30 min. The cells were then heat shocked in a 42 °C water bath for 2 min and incubated on ice 2 min. A 500 μL aliquot of LB was added, mixed gently, and incubated at 37 °C for 1 h. After which time the cells were spun down,

500 μL of supernatant removed, resuspended in remaining liquid, and plated on appropriate antibiotic containing plates.

Plasmid Purification:

Following successful transformation into either JM109 or XL1-Blue competent cells (Tet resistant), a colony was grown up in 500 mL LB (containing appropriate antibiotics) and purified with via Qiagen® column purification. Upon completion of the Qiagen® purification, the recovered DNA was resuspended in approximately 400 μL sterile water, and analyzed by UV-vis for concentration determination and purity.

Concentration of DNA sample (μg / μL) =

Abs_{260} x (50 μg / 1000 μL) x (volume of DNA used / total volume UV sample)

Purity of DNA sample = Abs_{260} / Abs_{280}

= 1.8, pure

>1.8, RNA contamination

< 1.8, protein contamination

Sample preparation for sequencing DNA:

In a sterilized 0.5 mL eppendorf tube, combine 1 μg DNA and 30 pmol primer (5' CGTTGTAAAACGACGGCCAGCG, for pET-Blue2 plasmid, approximately 75 base pairs upstream from the desired sequence starting position) in a combined total volume of 12 μL with sterile water. The DNA should have been purified by a Qiagen column and

resuspended in sterile water. Failure to do this will result in poor sequence data. In addition, the sequence sample should be diluted with sterile water, not buffer.

Protein Expression of a Clone with a Histidine Purification Tag:

A 100 mL LB culture was inoculated with the appropriate plasmid (pET-Blue2 + CRABPII, Amp resistant) containing cell (Tuner(DE3)pLacI, Clm resistant), antibiotics were added (ampicillin, 100 mg/mL and chloramphenicol, 25 mg/mL) and grown overnight at 37 °C with shaking. This culture was then used to inoculate one liter of LB (containing appropriate antibiotics) and grown at 37 °C with shaking until the absorbance at 600 nm reached 0.6 - 0.8. At this time, iso-propylthiogalactoside (IPTG) was added to a final concentration of 1.0 mM and allowed to grow at 32 °C with shaking for an additional 5 h. The cells were harvested (6,000 rpm, 20 min, 4 °C), resuspended in minimal (20 - 50 mL) binding buffer (50 mM NaH_2PO_4, 300 mM NaCl, 10 mM imidazole, pH = 8), and frozen overnight at –20 °C.

Expression temperatures may need to be optimized to find the highest level of protein production. For this clone, 32 °C was found to be the best from 28 °C – 37 °C expressions.

Lysis of a Cell Pellet:

The following morning the frozen cell pellet was allowed to thaw on ice, after which time lysozyme (0.5-1.0 mg/mL) was added and allowed to incubate on ice for 30 min. Optionally, the lysate was either subjected to 2-3 more cycles of freezing and thawing, or was sonicated for three one minute cycles. Finally, benzonase (25 U/mL,

Novagen) and magnesium (1 mM) were added and allotted 30 min on ice. Following this, the cell mixture was spun down (6,000 rpm, 30 min, 4 °C) and the lysate containing soluble protein separated from the cell pellet.

Purification of a Clone with a Histidine Purification Tag:

The lysate, containing the His tag encoded protein, is applied to a nickel resin for purification (Novagen). The lysate was allowed to flow through the column, after which time it was washed (2 x 10 mL) with the wash buffer (50 mM NaH_2PO_4, 300 mM NaCl, 20 mM imidazole, pH = 8). The protein was eluted with the elution buffer (50 mM NaH_2PO_4, 300 mM NaCl, 250 mM imidazole, pH = 8), and the fractions were then analyzed by SDS-PAGE. The fractions containing protein were then concentrated with Amicon Centriplus YM-10 filters, and buffer exchanged to 4 mM NaH_2PO_4, 16 mM Na_2HPO_4, and 150 mM NaCl at pH = 7.3. Protein concentration can be resolved via experimentally determined extinction coefficient or BioRad standard protocol.

Imidazole from the elution buffer may be removed by a variety of methods, but care must be taken to ensure that it is indeed all removed from the protein sample. Imidazole absorbs at 280 nm, the same wavelength as the protein signature peak occurs. Any imidazole left in the sample will interfere in protein concentration determination, which may cause incorrect interpretations of spectroscopic data.

Purification of 6x-His Protein Under Denaturing Conditions:

After the cell culture has been spun down, it is resuspended in one of two binding buffers (Buffer 1: 6 M GndHCl, 0.1 M NaH_2PO_4, 0.01 M Tris HCl, pH = 8, lysozyme = 1 mg/mL or Buffer 2: 8 M Urea, 0.1 M NaH_2PO_4, 0.01 M Tris HCl, pH = 8, lysozyme = 1 mg/mL. Following a 30 minute incubation time on ice to allow for complete cell lysis, it is applied to the column and washed out with the wash buffer (8 M Urea, 0.1 M NaH_2PO_4, 0.01 M Tris HCl, pH = 6.3), then eluted with the first elution buffer (8 M Urea, 0.1 M NaH_2PO_4, 0.01 M Tris HCl, pH=5.9), followed by complete elution with 8 M Urea, 0.1 M NaH_2PO_4, 0.01 M Tris HCl, pH = 4.5. The fractions collected are then analyzed by SDS-PAGE.

Ni^{2+} Resin Regeneration:

Resin is regenerated and recycled after each use by first stripping the column of all Ni^{2+} ions and anything bound to them. The column is washed with three column lengths of the strip buffer (100 mM EDTA, 0.5 M NaCl, 20 mM TrisHCl, pH = 7.9), followed by three column lengths of sterile distilled water. The column is then recharged with five column lengths of a fresh, clean Ni^{2+} source utilizing the charge buffer (50 mM $NiSO_4$). Finally, the column is equilibrated with three column lengths of binding buffer (50 mM NaH_2PO_4, 300 mM NaCl, 10 mM imidazole, pH = 8) to wash away any unbound Ni^{2+} ions. The column can be recycled as long as it retains a blue / green color after the cleaning.

Extended Ni^{2+} Resin Regeneration:

When the flow rate of the column slows dramatically, or does not turn a strong blue/green after being washed with charge buffer, the following wash should be done (for a 2.5 mL column bed):

1. 5 mL of 6 M guanidine HCl, 0.2 M Acetic Acid
2. 5 mL sterile distilled water
3. 2.5 mL 2% SDS
4. 2.5 mL 25% EtOH
5. 2.5 mL 50% EtOH
6. 2.5 mL 75% EtOH
7. 12.5 mL 100% EtOH
8. 2.5 mL 75% EtOH
9. 2.5 mL 50% EtOH
10. 2.5 mL 25% EtOH
11. 2.5 mL sterile distilled water
12. 12.5 100 mM EDTA, pH = 8.0
13. 7.5 mL sterile distilled water
14. 7.5 20% EtOH (for prolonged storage)

Note that the SDS solutions and the SDS wash steps cannot be done in the cold room as the detergent precipitates out of solution. Also, the column should be stored in 20% EtOH when not in use for long periods of time because bacteria can grow in the agarose resin.

Extinction coefficient determination:

Using the method of Gill and von Hippel,[13] first the number of tryptophan, tyrosine, and cysteine residues in the protein must be determined, and used to calculate the extinction coefficient of the denatured protein (ε_{den}) by:

$$\varepsilon_{den} = a\varepsilon_{tyr} + b\varepsilon_{trp} + c\varepsilon_{cys}$$

where a, b, and c represent the number of respective amino acids per molecule of protein, and their ε values have been determined experimentally (ε_{tyr} = 5690 M^{-1} cm^{-1}, ε_{trp} = 1280 M^{-1} cm^{-1}, ε_{cys} = 120 M^{-1} cm^{-1}, wild type CRABPII protein contains 3 Trp, 2 Tyr, and 3 Cys residues).

Two protein solutions are made, at identical concentrations, one in the native buffer (4 mM NaH_2PO_4, 16 mM Na_2HPO_4, 150 mM NaCl, pH = 7.3) and the other in a denaturing buffer (6 M guanidine•HCl, 4 mM NaH_2PO_4, 16 mM Na_2HPO_4, 150 mM NaCl), and the Abs_{280} for each sample is measured.

To determine the extinction coefficient for the natured protein (ε_{nat}), we utilize Beer's Law:

$$Abs_{den} \div \varepsilon_{den} = c_{den}$$

$$Abs_{nat} \div \varepsilon_{nat} = c_{nat}$$

Since the concentration of both samples is the same, we can equate the two equations and solve for the extinction coefficient by:

$$\varepsilon_{nat} = (Abs_{nat})(\varepsilon_{den}) \div (Abs_{den})$$

UV-Vis titrations of CRABPII with retinal:

A stock solution of retinal (Toronto Research Company, ε = 48,000 M^{-1}, cm^{-1}, λ_{max} = 380 nm) is made in 95% spectroscopy grade EtOH, keeping in mind that we want to keep < 2% volume of EtOH after adding two equivalents of chromophore to our 1 mL protein sample. For a $5x10^{-6}$ M protein solution in PBS (4 mM NaH_2PO_4, 16 mM Na_2HPO_4, 150 mM NaCl, pH = 7.3), the retinal stock solution is made at 2.5 mM. In this case, 2 μL of the retinal solution will be 0.1 equivalents.

Additions from 0.1 – 2.0 equivalents at 0.1 equivalent increments were added and spectra recorded at room temperature from 200 - 600 nm (Lambda 40, Perkin Elmer). This retinal titration was done for both the protein samples, and PBS only to serve as our blank. Due to the low binding affinity of retinal with most protein mutants, and the overwhelming presence of the 380 nm free aldehyde peak, the retinal titration performed in buffer only was subtracted from the retinal protein titration curve, i.e., 0.2 equivalents of retinal measured in buffer only was subtracted from the 0.2 retinal equivalent protein spectrum. This was done for every point taken solely to help deconvolute the red shifted peak from the rest of the spectra. Spectra were considered in both the uncorrected form (raw data), and this corrected form. The peaks appearing in the corrected UV-vis spectra very closely correlate to peaks present in the uncorrected spectra, as deconvoluted by taking the second derivative.

Fluorescence Titrations

The cuvette is allowed to sit with 3 mL of a 0.01% gelatin containing PBS (4 mM NaH_2PO_4, 16 mM Na_2HPO_4, 150 mM NaCl, pH=7.3) for 30-60 min. This buffer is dumped and the cell rinsed once with distilled water. The cuvettes are all handled while wearing gloves so as to avoid both fingerprints and lint. Then 3 mL of a room temperature $5e^{-7}$ M protein is added to the cell. The sample is excited at 283 nm with a slit width about 1.5 nm; this varies a little to ensure the intensity of each sample remains below one million counts. The fluorescence is measured at the peak maximum, about 345 nm, but again varies somewhat for each protein. The chromophore is added in at varying equivalents from a $1.5e^{-3}$ M stock (in 95% spectroscopy grade EtOH) sample maintained in the dark. A measurement is taken for each chromophore addition at the same wavelength. This is plotted as concentration of chromophore versus relative fluorescence intensity. When the curve levels off, the titration is complete.

If the chromophore is retinoic acid (Sigma, ε = 45,000 M^{-1}, cm^{-1}, λ_{max} = 350 nm), the data can be plotted as is. There is minimal effect of RA on Trp emission as seen in a blank titration run with N-acetyltryptophanamide.

If the chromophore is retinal (Toronto Research Company, ε = 48,000 M^{-1}, cm^{-1}, λ_{max} = 380 nm), a blank titration must be run with 3 mL of $1.5e^{-6}$ M N-acetyltryptophanamide. The peak maximum for the blank is at 365 nm. This curve is plotted as concentration of retinal versus change in intensity. The retinal seems to absorb some of the emission observed through the Trp residues. This will be added back into each of the protein / chromophore titrations.

The correction for the retinal titrations involves a four step calculation after the completion of both the protein titration and the blank titration.[33]

1. Determine a value of α for every point on the curve.

$$\alpha = \frac{F_{max} - F}{F_{max} - F_o}$$

F_{max} = Fluorescence upon saturation

F_o = initial fluorescence

F = observed fluorescence

α = fraction of free binding sites

2. Determine the free ligand concentration, R.

$R = R_o - nP_o(1-\alpha)$

R_o = ligand concentration

n = # binding sites / protein, assume n=1

P_o = protein concentration

3. Find fluorescence contribution of free ligand, F_R, to be deduced from blank.

4. Subtract fluorescence contribution of free ligand from actual readings, plot vs. ligand concentration.

$(F-F_R)$ vs. R_o

5. Using the values in 4, the correction can be repeated a second time, calculating new α values. I have found this to mostly be unnecessary.

An example of the correction procedure is given below. First, a titration is performed with retinal into a 3 mL solution of $1.5e^{-6}$ M N-acetyltryptophanamide in PBS. Results of this experiment are shown below (not all data points are shown). The Trp fluorescence intensity is recorded at 365 nm for each addition of retinal, which is then converted to a relative intensity by dividing all intensity values by the initial intensity reading, 964,278. Relative values are used so that all titration curves will be plotted on the same scale. This is then converted to a relative drop in intensity by subtracting 1 from all relative intensity values. This is the amount of Trp fluorescence that is quenched by addition of retinal through nonspecific interactions. This is the amount that will have to be added back into the protein titrations.

These data points are then plotted as relative loss in intensity versus retinal concentration, and fitted to a curve to generate the equation:

$$y = 5E\text{-}05x^2 - 0.012x - 0.0257$$

Blank Titration:

[Rt]	Int.@ 365	Rel. Int.	Rel.Int. Drops
0	964278	1	0
5E-08	959078	0.994607364	-0.005392636
1E-07	955294	0.990683185	-0.009316815
1.5E-07	953848	0.989183617	-0.010816383
2E-07	949388	0.984558395	-0.015441605
2.5E-07	945508	0.980534659	-0.019465341
3E-07	940945	0.975802621	-0.024197379
3.5E-07	937699	0.972436372	-0.027563628
4E-07	934734	0.969361533	-0.030638467
4.5E-07	933820	0.968413673	-0.031586327
5E-07	931027	0.965517206	-0.034482794
6E-07	925228	0.95950338	-0.04049662
7E-07	920940	0.955056529	-0.044943471
8E-07	920313	0.954406302	-0.045593698
9E-07	913937	0.947794101	-0.052205899
0.000001	912989	0.946810982	-0.053189018
1.1E-06	909661	0.943359695	-0.056640305
1.2E-06	906673	0.940261004	-0.059738996
1.3E-06	902660	0.936099341	-0.063900659
1.4E-06	898651	0.931941826	-0.068058174
1.5E-06	898440	0.931723009	-0.068276991
1.6E-06	894297	0.927426531	-0.072573469
1.7E-06	893585	0.926688154	-0.073311846
1.8E-06	891899	0.924939696	-0.075060304
1.9E-06	889804	0.922767086	-0.077232914
0.000002	887847	0.920737588	-0.079262412
2.2E-06	884439	0.917203338	-0.082796662
2.4E-06	875525	0.907959116	-0.092040884
2.6E-06	870287	0.902527072	-0.097472928
2.8E-06	864625	0.896655321	-0.103344679
0.000003	863185	0.895161976	-0.104838024
3.2E-06	858753	0.890565791	-0.109434209
3.4E-06	855040	0.886715242	-0.113284758
3.6E-06	856515	0.888244884	-0.111755116
3.8E-06	849367	0.880832084	-0.119167916
0.000004	846137	0.877482427	-0.122517573
4.2E-06	841318	0.872484906	-0.127515094
4.4E-06	840170	0.871294378	-0.128705622
4.6E-06	837721	0.868754654	-0.131245346
4.8E-06	832851	0.863704243	-0.136295757
0.000005	830434	0.861197704	-0.138802296
0.000006	809284	0.839264196	-0.160735804
0.000007	788857	0.818080471	-0.181919529
0.000008	763795	0.79209004	-0.20790996
0.000009	747983	0.77569228	-0.22430772
0.00001	732321	0.759450076	-0.240549924
0.000012	701834	0.727833675	-0.272166325

The same retinal solution is used to titrate the desired CRABPII protein. Fluorescence intensity is measured at approximately 347 nm (protein dependent), the buffer fluorescence intensity (20,000) is subtracted from each reading, and these values are again converted to relative intensity readings as each value is divided by the initial fluorescence value, 700,961.

Protein Titration:

[Rt]	Eq. Rt	Int.@ 347	Int.-Buffer	Rel. Int.
0	0	720961	700961	1
5E-08	0.1	681694	661694	0.944
1E-07	0.2	658226	638226	0.9105
1.5E-07	0.3	637356	617356	0.8807
2E-07	0.4	620959	600959	0.8573
2.5E-07	0.5	604324	584324	0.8336
3E-07	0.6	593778	573778	0.8186
3.5E-07	0.7	579156	559156	0.7977
4E-07	0.8	568257	548257	0.7822
4.5E-07	0.9	562746	542746	0.7743
5E-07	1	551233	531233	0.7579
6E-07	1.2	539687	519687	0.7414
7E-07	1.4	520801	500801	0.7144
8E-07	1.6	516569	496569	0.7084
9E-07	1.8	505580	485580	0.6927
1E-06	2	499195	479195	0.6836
1.1E-06	2.2	494367	474367	0.6767
1.2E-06	2.4	489180	469180	0.6693
1.3E-06	2.6	484524	464524	0.6627
1.4E-06	2.8	478871	458871	0.6546
1.5E-06	3	475910	455910	0.6504
1.6E-06	3.2	470680	450680	0.6429
1.7E-06	3.4	465571	445571	0.6357
1.8E-06	3.6	460387	440387	0.6283
1.9E-06	3.8	456924	436924	0.6233
2E-06	4	454661	434661	0.6201
2.2E-06	4.4	448260	428260	0.611
2.4E-06	4.8	441761	421761	0.6017
2.6E-06	5.2	438803	418803	0.5975
2.8E-06	5.6	433270	413270	0.5896
3E-06	6	428892	408892	0.5833
3.2E-06	6.4	424475	404475	0.577
3.4E-06	6.8	421554	401554	0.5729
3.6E-06	7.2	418126	398126	0.568
3.8E-06	7.6	412626	392626	0.5601
4E-06	8	409594	389594	0.5558
4.2E-06	8.4	408353	388353	0.554
4.4E-06	8.8	403923	383923	0.5477
4.6E-06	9.2	398838	378838	0.5405
4.8E-06	9.6	396139	376139	0.5366
5E-06	10	392218	372218	0.531

As plotted, without the correction, there is no leveling off or saturation point in the curve.

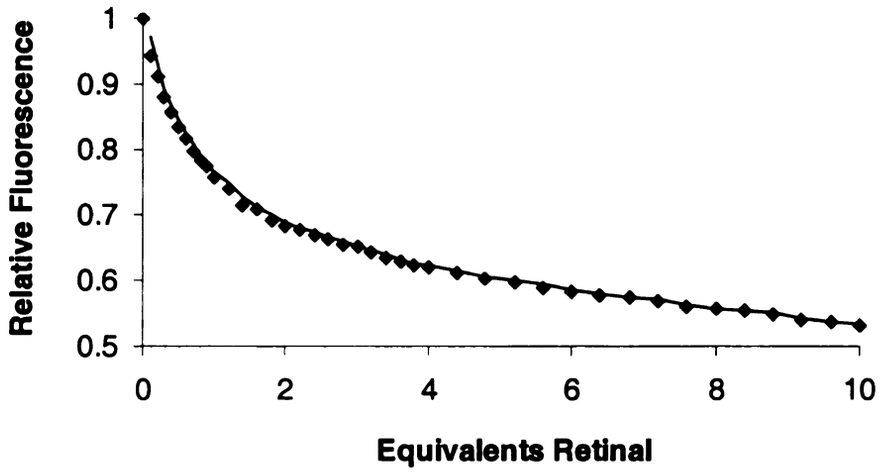

Correction procedures begin with calculation of the fraction of free binding sites, α, using the equation:

$$\alpha = \frac{F_{max} - F}{F_{max} - F_o}$$

F_{max} = Fluorescence upon saturation = 0.53

F_o = initial fluorescence = 1

F = observed fluorescence

This value is used to determine the free ligand concentration, R, for each measurement.

$$R = R_o - nP_o(1-\alpha)$$

R_o = ligand concentration at that fluorescent measurement

n = # binding sites / protein, assume n=1

P_o = protein concentration = $5e^{-7}$ M

Next, the fluorescence contribution of free ligand, F_R, is to be deduced from the equation acquired during the blank titration and the free ligand concentration, R, as just determined.

$$F_R = 5E\text{-}05R^2 - 0.012R - 0.0257$$

Finally, the fluorescence contribution of free ligand is subtracted from the actual intensity readings and plotted versus retinal concentration or equivalents.

$(F\text{-}F_R)$ vs. R_o

Corrected Protein Titration:

α	R	F_R	F-F_R
1	0	0	1
0.921561	1.08E-08	-0.0259583	0.96994
0.874682	3.73E-08	-0.0265946	0.937096
0.832993	6.65E-08	-0.0272927	0.908021
0.800239	1E-07	-0.0280974	0.885433
0.767009	1.34E-07	-0.0288959	0.8625
0.745943	1.73E-07	-0.0298393	0.848398
0.716734	2.08E-07	-0.0306848	0.828384
0.694963	2.47E-07	-0.0316186	0.813769
0.683954	2.92E-07	-0.0326802	0.806969
0.660956	3.3E-07	-0.0335981	0.791462
0.637892	4.19E-07	-0.0357049	0.777097
0.600166	5E-07	-0.0376345	0.752084
0.591712	5.96E-07	-0.0399087	0.74832
0.569761	6.85E-07	-0.0420194	0.734754
0.557007	7.79E-07	-0.0442356	0.727861
0.547362	8.74E-07	-0.0464851	0.723223
0.537001	9.69E-07	-0.0487225	0.718061
0.5277	1.06E-06	-0.0509688	0.713665
0.516408	1.16E-06	-0.0531881	0.707819
0.510493	1.26E-06	-0.0554669	0.705874
0.500046	1.35E-06	-0.0576888	0.700635
0.48984	1.44E-06	-0.05991	0.695567
0.479485	1.54E-06	-0.0621258	0.690388
0.472567	1.64E-06	-0.0643781	0.687699
0.468047	1.73E-06	-0.0666545	0.686747
0.45526	1.93E-06	-0.0711525	0.682114
0.442278	2.12E-06	-0.0756333	0.677323
0.436369	2.32E-06	-0.0801805	0.67765
0.425317	2.51E-06	-0.0846532	0.674229
0.416571	2.71E-06	-0.0891371	0.672468
0.407748	2.9E-06	-0.0936048	0.670634
0.401913	3.1E-06	-0.0980912	0.670953
0.395066	3.3E-06	-0.1025506	0.670522
0.384079	3.49E-06	-0.1069479	0.667073
0.378022	3.69E-06	-0.1113854	0.667185
0.375543	3.89E-06	-0.1158475	0.669877
0.366694	4.08E-06	-0.1202227	0.667932
0.356536	4.28E-06	-0.124568	0.665023
0.351145	4.48E-06	-0.1289509	0.665556
0.343313	4.67E-06	-0.1332914	0.664302

Plotting the corrected relative fluorescence values ($F - F_R$) versus retinal concentration (or equivalents) shows how the curve now levels off to clearly indicate the saturation point.

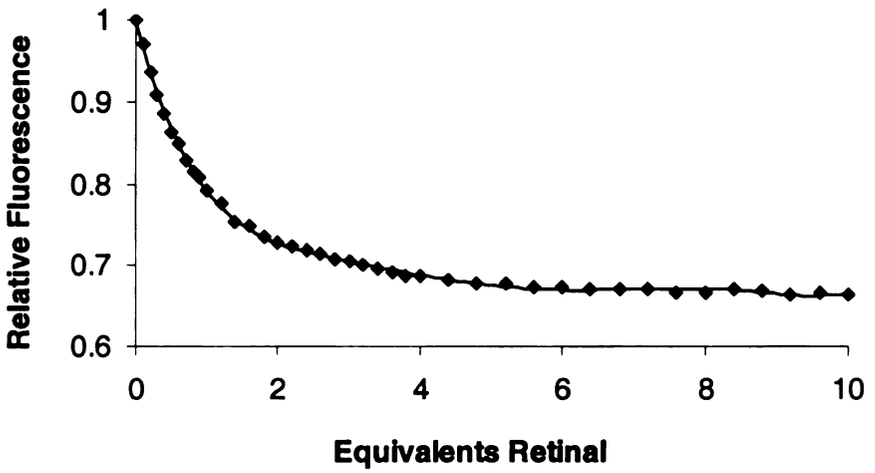

The dissociation constant is calculated with the program SigmaPlot through non-linear least square regression analysis.[6.22] Within SigmaPlot, the corrected relative fluorescence intensities are plotted against the concentration of retinal. The protein concentration and the final fluorescence intensity upon saturation are the other two values needed for solving the equation for the dissociation constant:

$$\frac{F}{F_f} = 1 + \left(\frac{F_b}{F_f} - 1\right) \times \left(\frac{P_t + R_t + K_d - \sqrt{(P_t + R_t + K_d)^2 - 4P_tR_t}}{2P_t}\right)$$

F = observed fluorescence

F_f = fluorescence of free protein

F_b = fluorescence of bound protein

P_t = total protein concentration

R_t = total chromophore concentration

As input into SigmaPlot:

$$y = p1+p1*((p2/p1-1)*(p3+x+k-((p3+x+K_d)^2-4*p3*x)^0.5))/(2*p3)$$

y = fluorescence value

x = chromophore concentration

p1 = initial fluorescence intensity = 1

p2 =fluorescence intensity upon saturation = 0.53

p3 = protein concentration = 5*10^(-7)

Cleaning of Fluorescence Cuvettes:

As both fingerprints and protein residue on the surface of the fluorescence cells may cause interference in the measurements, they should be thoroughly cleaned regularly, depending on volume of use. A proper cleaning procedure entails:

1. Soak 24 h in chromic acid, then rinse with water.
2. Soak 8 h in a KOH / MeOH solution (20 pellets / 100 mL), then rinse with water.
3. Soak 4 h in HNO_3, then rinse with water.

CD Measurements:

A 5 μM solution of protein in PBS (4 mM NaH_2PO_4, 16 mM Na_2HPO_4, 150 mM NaCl, pH=7.3) was used for CD measurement (JASCO). CD was scanned from 500 nm to 200 nm at 100 nm / min with a bandwidth of 1 nm. Extended degassing of the sample chamber with nitrogen must be done to ensure quality spectra near the 200 nm region.

MALDI-TOF Experimental Parameters:

System: Applied Biosystems Voyager STR MALDI-TOF mass spectrometer

Mode of operation: Linear

Acquisition mass range: 5000 – 20000 Da

Number of laser shots: 250/spectrum

Nitrogen Laser: 337 nm

Laser intensity: 3013-3024*

Laser Rep Rate: 5.2 Hz

Calibration type: External (apomyoglobin, MW = 16952.6 Da)

Calibration matrix: Sinapic acid (Fluka)

MALDI-TOF Measurement of Retinal incubated Protein Samples:

Approximately 0.5 mg of CRABPII protein in 1 mL PBS was mixed with 1.0 eq retinal from an ethanol stock (final ethanol volume less than 30 μL). The mixture was incubated at 25 °C, dark for 1 h. The reactions were exposed to light, transferred into micro-centrifuge filters (Millipore Ultrafree® 0.5 Centrifugal Filters, NMWL: 5000) and concentrated. The yellow samples were washed once with 95% EtOH, to wash off excess

free retinal and then twice with ddH_2O (2 x 500 μL), to desalt. From a final volume of 20 μL, 0.5 μL of each reaction was mixed with 0.5 μL of matrix solution in the MALDI plate, and upon co-crystallization, the MALDI-TOF spectrum was obtained.

MALDI-TOF Reductive Amination Procedure:

Approximately 0.5 mg of CRABPII protein in 1 mL PBS was mixed with 1.0 eq retinal from an ethanol stock (final ethanol volume less than 30 μL). The mixture was incubated at 25 °C, dark for 1 h after which 10 μL of 5M $NaCNBH_3$ in 1N NaOH were added. The reaction was left for an additional hour before being exposed to light. The light yellow crude reaction mixture was then run through a Q Sepharose™ Fast Flow column (quaternary ammonium resin, strong anion exchanger, Column: 3 x 1.5 cm) leaving a yellow residue on the top layer of the resin (PBS contains 150 mM NaCl, hence the crude reaction had to be diluted to a final volume of ~8 mL to reduce salt concentration and enhance FQ binding before loading onto the column). The column was washed with 10 mM Tris HCl, pH = 8 and the protein was eluted using 10 mM Tris HCl, 100 mM NaCl, pH = 8 buffer. The protein containing fractions were identified using UV-vis (A_{280}) and concentrated to a 50 μL final volume using micro-centrifuge filters (Millipore Ultrafree® 0.5 Centrifugal Filters, NMWL: 5000). 0.5 μL of each reaction were mixed with 0.5 μL of matrix solution in the MALDI plate, and upon co-crystallization, the MALDI-TOF spectrum was obtained.

GeneClean® Protocol for purifying DNA fragments:

Digested DNA should be run on a 0.5% agarose gel, and the desired band cut out. Chop up this fragment, place in a 1.5 mL eppendorf tube, and add GeneClean Turbo Salt Solution (100 μL /0.1 g agarose). Heat this at 55 °C for 5 min and mix well. Transfer 500 μL of this solution at a time to a Turbo Column, spin for 5 seconds, empty catch tube, and repeat until all solution has been washed through the column. Next, add 500 μL of Turbo Wash Solution, spin 5 seconds, empty catch tube, and repeat. The column should then be spun for 4 min to dry. Finally, place column in a fresh catch tube, add 30 μL Turbo Elution Solution, allow to sit for 5 min at room temperature, spin 1 minute, and quantify eluted DNA by agarose gel.

Melting temperature calculation for primers:

Primers should ideally have melting points ≥ 78 °C, and end in at least one, if not more, GC base pair

$$T_m = 81.5\ °C + (0.41)(\%\ GC) - 675 / N - \%\ Mismatch$$

where N = primer length

Molecular Modeling:

Computational results were obtained using software programs from Accelrys. Dynamics and minimizations were done using the Discover 3® program, using the CVFF forcefield from within the InsightII 2000 molecular modeling system.

Protein figures were generated using PyMol Molecular Graphics System, version 0.93, copyright by DeLano Scientific LLC.

PCR conditions for introducing BamHI cut sites on both CRABPII termini from pET-17b:

REACTANT		AMOUNT (μL)	PCR Cycles	
Template DNA (147 ng/μL)		1	1x	94°C for 5 min
bbb0013	(9.9 μM)	5	30x	94°C for 2 min
bbb0014	(10.8 μM)	4.6		55°C for 2 min
Thermopol rxn buffer (10x)		10		72°C for 2 min
dNTP	(10mM)	2	1x	72°C for 10 min
$MgSO_4$	(100 mM)	0.6	1x	23°C for 10 min
Water		76		
Deep Vent polymerase		1		

bbb0013 5' CGCGGATCCTCACTCTCGGACGTA

bbb0014 5' CGCGGATCCCATATGCCAAACTTC

CRABPII and pET-30a ligation:

REACTANT	AMOUNT (μL)
pET-30a ÷ BamHI (200 ng/μL)	1
CRABPII PCR ÷ BamHI (100 ng/μL)	1.6
Ligase Buffer (10x)	1
T4 DNA ligase	2
TE	4.4

The above reaction was allowed to sit at room temperature overnight (~12 h) and transformed into both JM109 and BL21(DE3)pLysS.

To trouble shoot a ligation reaction, several different conditions can be varied. Plasmid vector to gene insert ratios should be varied from 1:3 to 1:10, always using excess of the smaller gene insert. Total DNA concentrations between 10 ng – 500 ng can be tried. Also, vary cleavage times from 2-24 h, ligation times from 2-24 h, ligation temperatures at 16 °C and 23 °C, reaction volumes at 10 μL and 20 μL, and T4 DNA ligase volume from 1-2 μL.

PCR conditions for incorporating NcoI and XhoI cut sites on CRABPII for pET-Blue2 ligation:

REACTANT	AMOUNT (μL)	PCR Cycles	
Template DNA (10 ng/μL)	5	1x	95 °C for 0.5 min
bbb0024 (12.5 pmol/μL)	4	16x	95 °C for 0.5 min
bbb0026 (12.2 pmol/μL)	4		55 °C for 1 min
Thermopol buffer (10x)	10		70 °C for 8 min
dNTP (10mM)	2	1x	70 °C for 10 min
Water	73.5	1x	23 °C for 10 min
Deep Vent polymerase	1		

bbb0024 5' GGGCCATGGCGCCAAACTTCTCTGGCAAC

bbb0026 5' GGGCTCGAGCTCTCGGACGTAGAC

CRABPII and pET-Blue2 ligation:

REACTANT	AMOUNT (μL)
PET-30a ÷ NcoI, XhoI (200 ng/ μL)	1
CRABPII PCR ÷ NcoI, XhoI (175 ng/μL)	1.6
Ligase Buffer (10x)	1
T4 DNA ligase	2
TE	4.4

The above reaction was allowed to sit at room temperature overnight (~12 h) and transformed into JM109. Once the plasmid was verified, it was then transformed into BL21(DE3)pLysS.

PCR conditions for R132K Mutation of CRABPII in pET-Blue2:

REACTANT	AMOUNT (μL)	PCR Cycles	
Template DNA (10 ng/μL)	5	1x	95 °C for 0.5 min
bbb0027 (4.3 pmol/μL)	2.6	16x	95 °C for 0.5 min
bbb0028 (9.5 pmol/μL)	1.2		55 °C for 1 min
pfu turbo rxn buffer (10x)	5		70 °C for 8 min
dNTP (10mM)	1	1x	70 °C for 10 min
Water	34.2	1x	23 °C for 10 min
Pfu turbo polymerase	1		

bbb0027 5' CTCTCGGACGTAGACCTTGGTGCACACAACGTC

bbb0028 5' GACGTTGTGTGCACCAAGGTCTACGTCCGAGAG

After the PCR was complete, 10 μL was taken out for gel analysis, and 1 μL DpnI was added to the remaining solution. The reaction was incubated for 1 h at 37 °C, then transformed into either JM109 or XL1-Blue *E. coli* competent cells. For best results, super competent cells were used (Stratagene, 10^6 – 10^8 cfu / μg) as self prepared competent cells were usually not efficient enough (10^3 cfu / μg). These steps are standard practice, and were performed after every mutagenesis PCR.

PCR conditions for Y134F Mutation of CRABPII R132K in pET-Blue2:

REACTANT	AMOUNT (μL)	PCR Cycles	
Template DNA (10 ng/μL)	5	1x	95 °C for 0.5 min
bbb0030 (8.7 pmol/μL)	1.2	16x	95 °C for 0.5 min
bbb0031 (7.2 pmol/μL)	1.5		55 °C for 1 min
pfu turbo rxn buffer (10x)	5		70 °C for 8 min
dNTP (10mM)	1	1x	70 °C for 10 min
Water	35.3	1x	23 °C for 10 min
Pfu turbo polymerase	1		

bbb0030 5' GTTGTGTGCACCAAGGTCTTCGTCCGAGAGCTCGAG

bbb0031 5' CTCGAGCTCTCGGACGAAGACCTTGGTGCACACAAC

PCR conditions for R111E Mutation of CRABPII R132K::Y134F in pET-Blue2:

REACTANT	AMOUNT (μL)	PCR Cycles	
Template DNA (10 ng/μL)	5	1x	95 °C for 0.5 min
bbb0033 (10.9 pmol/μL)	1.4	16x	95 °C for 0.5 min
bbb0034 (13.7 pmol/μL)	1.1		55 °C for 1 min
pfu turbo rxn buffer (10x)	5		70 °C for 8 min
dNTP (10mM)	1	1x	70 °C for 10 min
Water	35.5	1x	23 °C for 10 min
Pfu turbo polymerase	1		

bbb0033 5' TCGTGGACCGAGGAACTGACC

bbb0034 5' GGTGACTTCCTCGGTCCACGA

PCR conditions for T54V Mutation of CRABPII R132K::Y134F::R111E in pET-Blue2:

REACTANT	AMOUNT (μL)	PCR Cycles	
Template DNA (10 ng/μL)	5	1x	95 °C for 3.5 min
bbb0067 (7.5 pmol/ μL)	2	20x	95 °C for 0.5 min
bbb0068 (6.7 pmol/ μL)	2.24		55 °C for 1 min
pfu turbo rxn buffer (10x)	5		70 °C for 8 min
dNTP (10 mM)	2	1x	70 °C for 10 min
Water	31.76	1x	23 °C for 10 min
Pfu turbo polymerase	2		

bbb0067 5' CTACATCAAAGTCTCCACCACCGTGCG

bbb0068 5' CGCACGGTGGTGGAGACTTTGATGTAG

PCR conditions for L121E Mutation of CRABPII R132K::Y134F in pET-Blue2:

REACTANT		AMOUNT (uL)	PCR Cycles	
Template DNA (10 ng/uL)		5	1x	95 °C for 0.5 min
bbb0037	(6.1 pmol/uL)	1.4	16x	95 °C for 0.5 min
bbb0038	(8.3 pmol/uL)	1.2		55 °C for 1 min
pfu turbo rxn buffer (10x)		5		70 °C for 8 min
dNTP	(10 mM)	1	1x	70 °C for 10 min
Water		35.4	1x	23 °C for 10 min
Pfu turbo polymerase		1		

bbb0037 5' GATGGGGAACTGATCGAGACCATGACGGCGGATGAC

bbb0038 5' GTCATCCGCCGTCATGGTCTCGATCAGTTCCCCATC

PCR conditions for R111L Mutation of CRABPII R132K::Y134F in pET-Blue2:

REACTANT		AMOUNT (uL)	PCR Cycles	
Template DNA (10 ng/uL)		5	1x	95 °C for 0.5 min
bbb0039	(7.7 pmol/uL)	1.6	16x	95 °C for 0.5 min
bbb0040	(8.8 pmol/uL)	1.2		55 °C for 1 min
pfu turbo rxn buffer (10x)		5		70 °C for 8 min
dNTP	(10 mM)	1	1x	70 °C for 10 min
Water		35.2	1x	23 °C for 10 min
Pfu turbo polymerase		1		

bbb0039 5' CCCAAGACCTCGTGGACCCTGGAACTGACCAACGATGGG

bbb0040 5' CCCATCGTTGGTCAGTTCCAGGGTCCACGAGGTCTTGGG

PCR conditions for T54E Mutation of CRABPII R132K::Y134F::R111L in pET-Blue2:

REACTANT	AMOUNT (μL)	PCR Cycles	
Template DNA (10 ng/μL)	5	1x	95 °C for 3.5 min
bbb0065 (11 pmol/ μL)	1.36	20x	95 °C for 0.5 min
bbb0066 (8.7 pmol/ μL)	1.72		55 °C for 1 min
pfu turbo rxn buffer (10x)	5		70 °C for 8 min
dNTP (10 mM)	2	1x	70 °C for 10 min
Water	32.92	1x	23 °C for 10 min
Pfu turbo polymerase	2		

bbb0065 5' CTACATCAAAGAGTCCACCACCGTGCG

bbb0066 5' CGCACGGTGGTGGACTCTTTGATGTAG

PCR conditions for L121E Mutation of CRABPII R132K::Y134F::R111L in pET-Blue2:

REACTANT	AMOUNT (uL)	PCR Cycles	
Template DNA (10 ng/uL)	5	1x	95 °C for 0.5 min
bbb0037 (6.1 pmol/uL)	1.4	16x	95 °C for 0.5 min
bbb0038 (8.3 pmol/uL)	1.2		55 °C for 1 min
pfu turbo rxn buffer (10x)	5		70 °C for 8 min
dNTP (10 mM)	1	1x	70 °C for 10 min
Water	35.4	1x	23 °C for 10 min
Pfu turbo polymerase	1		

bbb0037 5' GATGGGGAACTGATCGAGACCATGACGGCGGATGAC

bbb0038 5' GTCATCCGCCGTCATGGTCTCGATCAGTTCCCCATC

PCR conditions for R111L Mutation of CRABPII R132K::Y134F::L121E in pET-Blue2:

REACTANT		AMOUNT (μL)	PCR Cycles	
Template DNA (10 ng/μL)		5	1x	95 °C for 0.5 min
bbb0082	(4.4 pmol/μL)	3.41	16x	95 °C for 0.5 min
bbb0083	(7.2 pmol/μL)	2.08		55 °C for 1 min
pfu turbo rxn buffer (10x)		5		70 °C for 8 min
dNTP	(10 mM)	1	1x	70 °C for 10 min
Water		32.51	1x	23 °C for 10 min
Pfu turbo polymerase		1		

bbb0082 5' CCCAAGACCTCGTGGACCCTAGAACTGACCAACGATGGG

bbb0083 5' CCCATCGTTGGTCAGTTCTAGGGTCCACGAGGTCTTGGG

PCR conditions for L121Q Mutation of CRABPII R132K::Y134F::R111L::L121E in pET-Blue2:

REACTANT		AMOUNT (μL)	PCR Cycles	
Template DNA (10 ng/μL)		7	1x	95 °C for 1 min
bbb0096	(7.20 pmol/ μL)	2.10	20x	95 °C for 1 min
bbb0097	(11.0 pmol/ μL)	1.40		55 °C for 1 min
pfu turbo rxn buffer (10x)		5		72 °C for 8 min
dNTP (10 mM)		1	1x	72 °C for 10 min
Water		32.50	1x	23 °C for 10 min
Pfu turbo polymerase		1		

bbb0096 5' GGGGAACTGATCCAGACCATGACGGCG

bbb0097 5' CGCCGTCATGGTCTGGATCAGTTCCCC

PCR conditions for R132R Mutation of CRABPII R132K::Y134F::R111L::L121E in pET-Blue2:

REACTANT	AMOUNT (μL)	PCR Cycles	
Template DNA (10 ng/μL)	7	1x	95 °C for 1 min
bbb0088 (13.5 pmol/ μL)	1.11	20x	95 °C for 1 min
bbb0089 (9.6 pmol/ μL)	1.56		55 °C for 1 min
pfu turbo rxn buffer (10x)	5		72 °C for 8 min
dNTP (10 mM)	1	1x	72 °C for 10 min
Water	33.33	1x	23 °C for 10 min
Pfu turbo polymerase	1		

bbb0088 5' CGTTGTGTGCACCAGGGTCTTCGTCCG

bbb0089 5' CGGACGAAGACCCTGGTGCACACAACG

PCR conditions for R132L Mutation of CRABPII R132K::Y134F::R111L::L121E in pET-Blue2:

REACTANT	AMOUNT (μL)	PCR Cycles	
Template DNA (10 ng/μL)	7	1x	95 °C for 1 min
bbb0086 (16.1 pmol/ μL)	0.93	20x	95 °C for 1 min
bbb0087 (4.8 pmol/ μL)	3.12		55 °C for 1 min
pfu turbo rxn buffer (10x)	5		72 °C for 8 min
dNTP (10 mM)	1	1x	72 °C for 10 min
Water	31.95	1x	23 °C for 10 min
Pfu turbo polymerase	1		

bbb0086 5' CGTTGTGTGCACCCTGGTCTTCGTCCG

bbb0087 5'CGGACGAAGACCAGGGTGCACACAACG

PCR conditions for F15A Mutation of CRABPII R132K::Y134F::R111L::L121E in pET-Blue2:

REACTANT	AMOUNT (μL)	PCR Cycles	
Template DNA (10 ng/μL)	7	1x	95 °C for 1 min
bbb0092 (9.2 pmol/ μL)	1.60	20x	95 °C for 1 min
bbb0093 (5.8 pmol/ μL)	2.60		55 °C for 1 min
pfu turbo rxn buffer (10x)	5		72 °C for 8 min
dNTP (10 mM)	1	1x	72 °C for 10 min
Water	31.80	1x	23 °C for 10 min
Pfu turbo polymerase	1		

bbb0092 5' CGATCGGAAAACGCCGAGGAATTGCTC

bbb0093 5' GAGCAATTCCTCGGCGTTTTCCGATCG

PCR conditions for T54V Mutation of CRABPII R132K::Y134F::R111L::L121E in pET-Blue2:

REACTANT	AMOUNT (μL)	PCR Cycles	
Template DNA (10 ng/μL)	5	1x	95 °C for 1 min
bbb0067 (7.5 pmol/ μL)	2.00	20x	95 °C for 1 min
bbb0068 (6.7 pmol/ μL)	2.24		55 °C for 1 min
pfu turbo rxn buffer (10x)	5		72 °C for 8 min
dNTP (10 mM)	1	1x	72 °C for 10 min
Water	29.76	1x	23 °C for 10 min
Pfu turbo polymerase	1		

bbb0067 5' CTACATCAAAGTCTCCACCACCGTGCG

bbb0068 5' CGCACGGTGGTGGAGACTTTGATGTAG

PCR conditions for L121Q Mutation of CRABPII R132K::Y134F::R111L::L121E::T54V in pET-Blue2:

REACTANT	AMOUNT (μL)	PCR Cycles	
Template DNA (10 ng/μL)	5	1x	95 °C for 1 min
bbb0096 (7.20 pmol/ μL)	2.10	20x	95 °C for 1 min
bbb0097 (11.0 pmol/ μL)	1.40		55 °C for 1 min
pfu turbo rxn buffer (10x)	5		72 °C for 8 min
dNTP (10 mM)	1	1x	72 °C for 10 min
Water	32.50	1x	23 °C for 10 min
Pfu turbo polymerase	1		

bbb0096 5' GGGGAACTGATCCAGACCATGACGGCG

bbb0097 5' CGCCGTCATGGTCTGGATCAGTTCCCC

PCR conditions for T54V Mutation of CRABPII R132K::Y134F::R111L in pET-Blue2:

REACTANT	AMOUNT (μL)	PCR Cycles	
Template DNA (10 ng/μL)	5	1x	95 °C for 1 min
bbb0067 (7.5 pmol/ μL)	2.00	20x	95 °C for 1 min
bbb0068 (6.7 pmol/ μL)	2.24		55 °C for 1 min
pfu turbo rxn buffer (10x)	5		72 °C for 8 min
dNTP (10 mM)	1	1x	72 °C for 10 min
Water	29.76	1x	23 °C for 10 min
Pfu turbo polymerase	1		

bbb0067 5' CTACATCAAAGTCTCCACCACCGTGCG

bbb0068 5' CGCACGGTGGTGGAGACTTTGATGTAG

PCR conditions for L121D Mutation of CRABPII R132K::Y134F::R111L::L121E in pET-Blue2:

REACTANT	AMOUNT (μL)	PCR Cycles	
Template DNA (10 ng/μL)	7	1x	95°C for 1 min
bbb0090 (7.6 pmol/ μL)	2.00	20x	95°C for 1 min
bbb0091 (11.4 pmol/ μL)	1.30		55°C for 1 min
pfu turbo rxn buffer (10x)	5		72°C for 8 min
dNTP (10 mM)	1	1x	72°C for 10 min
Water	32.70	1x	23°C for 10 min
Pfu turbo polymerase	1		

bbb0090 5' GGGGAACTGATCGACACCATGACGGCG

bbb0091 5' CGCCGTCATGGTGTCGATCAGTTCCCC

PCR conditions for L121N Mutation of CRABPII R132K::Y134F::R111L::L121E in pET-Blue2:

REACTANT	AMOUNT (μL)	PCR Cycles	
Template DNA (10 ng/μL)	5	1x	95 °C for 1 min
bbb0102 (10.4 pmol/ μL)	1.45	20x	95 °C for 1 min
bbb0103 (12.1 pmol/ μL)	1.24		55 °C for 1 min
pfu turbo rxn buffer (10x)	5		72 °C for 8 min
dNTP (10 mM)	1	1x	72 °C for 10 min
Water	35.31	1x	23 °C for 10 min
Pfu turbo polymerase	1		

bbb0102 5' GGGGAACTGATCAACACCATGACGGCG

bbb0103 5' CGCCGTCATGGTGTTGATCAGTTCCCC

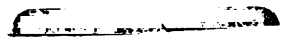

PCR conditions for T54V Mutation of CRABPII R132K::Y134F::R111L::L121D in pET-Blue2:

REACTANT	AMOUNT (μL)	PCR Cycles	
Template DNA (10 ng/μL)	5	1x	95 °C for 1 min
bbb0096 (7.20 pmol/ μL)	2.10	20x	95 °C for 1 min
bbb0097 (11.0 pmol/ μL)	1.40		55 °C for 1 min
pfu turbo rxn buffer (10x)	5		72 °C for 8 min
dNTP (10 mM)	1	1x	72 °C for 10 min
Water	32.50	1x	23 °C for 10 min
Pfu turbo polymerase	1		

bbb0096 5' GGGGAACTGATCCAGACCATGACGGCG

bbb0087 5' CGCCGTCATGGTCTGGATCAGTTCCCC

PCR conditions for T54V Mutation of CRABPII R132K::Y134F::R111L::L121N in pET-Blue2:

REACTANT	AMOUNT (μL)	PCR Cycles	
Template DNA (10 ng/μL)	5	1x	95 °C for 1 min
bbb0067 (7.5 pmol/ μL)	2.00	20x	95 °C for 1 min
bbb0068 (6.7 pmol/ μL)	2.24		55 °C for 1 min
pfu turbo rxn buffer (10x)	5		72 °C for 8 min
dNTP (10 mM)	1	1x	72 °C for 10 min
Water	29.76	1x	23 °C for 10 min
Pfu turbo polymerase	1		

bbb0067 5' CTACATCAAAGTCTCCACCACCGTGCG

bbb0068 5' CGCACGGTGGTGGAGACTTTGATGTAG

PCR conditions for T61E Mutation of CRABPII R132K::Y134F::R111L::L121E::T54V in pET-Blue2:

REACTANT	AMOUNT (µL)	PCR Cycles	
Template DNA (10 ng/µL)	5	1x	95 °C for 1 min
bbb0107 (9.0 pmol/ µL)	1.67	20x	95 °C for 1 min
bbb0108 (5.8 pmol/ µL)	2.59		55 °C for 1 min
pfu turbo rxn buffer (10x)	5		72 °C for 8 min
dNTP (10 mM)	1	1x	72 °C for 10 min
Water	33.74	1x	23 °C for 10 min
Pfu turbo polymerase	1		

bbb0107 5' CCGTGCGCACCGAGGAGATTAACTTC

bbb0108 5' GAAGTTAATCTCCTCGGTGCGCACGG

PCR conditions for T61F Mutation of CRABPII R132K::Y134F::R111L::L121E::T54V in pET-Blue2:

REACTANT	AMOUNT (µL)	PCR Cycles	
Template DNA (10 ng/µL)	5	1x	95 °C for 1 min
bbb0105 (8.7 pmol/ µL)	1.72	20x	95 °C for 1 min
bbb0106 (6.4 pmol/ µL)	2.34		55 °C for 1 min
pfu turbo rxn buffer (10x)	5		72 °C for 8 min
dNTP (10 mM)	1	1x	72 °C for 10 min
Water	33.94	1x	23 °C for 10 min
Pfu turbo polymerase	1		

bbb0105 5' CCGTGCGCACCTTCGAGATTAACTTC

bbb0106 5' GAAGTTAATCTCGAAGGTGCGCACGG

PCR conditions for Y134K Mutation of CRABPII Wild-Type in pET-Blue2:

REACTANT	AMOUNT (μL)	PCR Cycles	
Template DNA (10 ng/μL)	5	1x	95 °C for 3.5 min
bbb0061 (9 pmol/ μL)	1.67	20x	95 °C for 0.5 min
bbb0062 (13.4 pmol/ μL)	1.12		55 °C for 1 min
pfu turbo rxn buffer (10x)	5		70 °C for 8 min
dNTP (10 mM)	2	1x	70 °C for 10 min
Water	33.21	1x	23 °C for 10 min
Pfu turbo polymerase	2		

bbb0061 5' GCACCAGGGTCAAGGTCCGAGAGC

bbb0062 5' GCTCTCGGACCTTGACCCTGGTGC

PCR conditions for Y134K Mutation of CRABPII R132K in pET-Blue2:

REACTANT	AMOUNT (μL)	PCR Cycles	
Template DNA (10 ng/μL)	5	1x	95 °C for 3.5 min
bbb0063 (7.4 pmol/ μL)	2.03	20x	95 °C for 0.5 min
bbb0064 (14.1 pmol/ μL)	1.06		55 °C for 1 min
pfu turbo rxn buffer (10x)	5		70 °C for 8 min
dNTP (10 mM)	2	1x	70 °C for 10 min
Water	32.91	1x	23 °C for 10 min
Pfu turbo polymerase	2		

bbb0063 5' GCACCAAGGTCAAGGTCCGAGAGC

bbb0064 5' GCTCTCGGACCTTGACCTTGGTGC

PCR conditions for R132F Mutation of CRABPII Y134K in pET-Blue2:

REACTANT	AMOUNT (μL)	PCR Cycles	
Template DNA (10 ng/μL)	10	1x	95 °C for 3.5 min
bbb0071 (13.4 pmol/ μL)	1.12	20x	95 °C for 0.5 min
bbb0075 (11.2 pmol/ μL)	1.34		55 °C for 1 min
pfu turbo rxn buffer (10x)	5		70 °C for 8 min
dNTP (10 mM)	2	1x	70 °C for 10 min
Water	28.5	1x	23 °C for 10 min
Pfu turbo polymerase	1		

bbb0071 5' CGTTGTGTGCACCTTCGTCAAGGTCCG

bbb0075 5' CGGACCTTGACGAAGGTGCACACAACG

PCR conditions for R132L Mutation of CRABPII Y134K in pET-Blue2:

REACTANT	AMOUNT (μL)	PCR Cycles	
Template DNA (10 ng/μL)	10	1x	95 °C for 3.5 min
bbb0069 (12.1 pmol/ μL)	1.65	20x	95 °C for 0.5 min
bbb0070 (8.5 pmol/ μL)	2.35		55 °C for 1 min
pfu turbo rxn buffer (10x)	5		70 °C for 8 min
dNTP (10 mM)	2	1x	70 °C for 10 min
Water	28	1x	23 °C for 10 min
Pfu turbo polymerase	1		

bbb0069 5' CGTTGTGTGCACCCTGGTCAAGGTCCG

bbb0070 5' CGGACCTTGACCAGGGTGCACACAACG

PCR conditions for R111L Mutation of CRABPII Y134K::R132F in pET-Blue2:

REACTANT	AMOUNT (μL)	PCR Cycles	
Template DNA (10 ng/μL)	5	1x	95 °C for 3.5 min
bbb0082 (4.4 pmol/ μL)	3.41	20x	95 °C for 0.5 min
bbb0083 (7.2 pmol/ μL)	2.08		55 °C for 1 min
pfu turbo rxn buffer (10x)	5		70 °C for 8 min
dNTP (10 mM)	1	1x	70 °C for 10 min
Water	32.51	1x	23 °C for 10 min
Pfu turbo polymerase	1		

bbb0082 5' CCCAAGACCTCGTGGACCCTAGAACTGACCAACGATGGG

bbb0083 5' CCCATCGTTGGTCAGTTCTAGGGTCCACGAGGTCTTGGG

PCR conditions for L121E Mutation of CRABPII Y134K::R132F::R111L in pET-Blue2:

REACTANT	AMOUNT (μL)	PCR Cycles	
Template DNA (10 ng/μL)	5	1x	95 °C for 3.5 min
bbb0037 (6.1 pmol/ μL)	2.50	20x	95 °C for 0.5 min
bbb0038 (8.3 pmol/ μL)	1.80		55 °C for 1 min
pfu turbo rxn buffer (10x)	5		70 °C for 8 min
dNTP (10 mM)	1	1x	70 °C for 10 min
Water	33.70	1x	23 °C for 10 min
Pfu turbo polymerase	1		

bbb0037 5' GATGGGGAACTGATCGAGACCATGACGGCGGATGAC

bbb0038 5' GTCATCCGCCGTCATGGTCTCGATCAGTTCCCCATC

PCR conditions for T54E Mutation of CRABPII Y134K::R132F::R111L in pET-Blue2:

REACTANT	AMOUNT (μL)	PCR Cycles	
Template DNA (10 ng/μL)	7	1x	95 °C for 1 min
bbb0065 (11.0 pmol/ μL)	1.40	20x	95 °C for 1 min
bbb0066 (8.7 pmol/ μL)	1.70		55 °C for 1 min
pfu turbo rxn buffer (10x)	5		72 °C for 8 min
dNTP (10 mM)	1	1x	72 °C for 10 min
Water	32.90	1x	23 °C for 10 min
Pfu turbo polymerase	1		

bbb0065 5' CTACATCAAAGAGTCCACCACCGTGCG

bbb0066 5' CGCACGGTGGTGGACTCTTTGATGTAG

PCR conditions for R111L Mutation of CRABPII Y134K::R132L in pET-Blue2:

REACTANT	AMOUNT (μL)	PCR Cycles	
Template DNA (10 ng/μL)	5	1x	95 °C for 3.5 min
bbb0082 (4.4 pmol/ μL)	3.41	20x	95 °C for 0.5 min
bbb0083 (7.2 pmol/ μL)	2.08		55 °C for 1 min
pfu turbo rxn buffer (10x)	5		70 °C for 8 min
dNTP (10 mM)	1	1x	70 °C for 10 min
Water	32.51	1x	23 °C for 10 min
Pfu turbo polymerase	1		

bbb0082 5' CCCAAGACCTCGTGGACCCTAGAACTGACCAACGATGGG

bbb0083 5' CCCATCGTTGGTCAGTTCTAGGGTCCACGAGGTCTTGGG

PCR conditions for L121E Mutation of CRABPII Y134K::R132L in pET-Blue2:

REACTANT	AMOUNT (μL)	PCR Cycles	
Template DNA (10 ng/μL)	5	1x	95 °C for 1 min
bbb0067 (6.1 pmol/ μL)	1.4	20x	95 °C for 1 min
bbb0068 (8.3 pmol/ μL)	1.2		55 °C for 1 min
pfu turbo rxn buffer (10x)	5		72 °C for 8 min
dNTP (10 mM)	1	1x	72 °C for 10 min
Water	35.4	1x	23 °C for 10 min
Pfu turbo polymerase	1		

bbb0037 5' GATGGGGAACTGATCGAGACCATGACGGCGGATGAC

bbb0038 5' GTCATCCGCCGTCATGGTCTCGATCAGTTCCCCATC

PCR conditions for L121E Mutation of CRABPII Y134K::R132L::R111L in pET-Blue2:

REACTANT	AMOUNT (μL)	PCR Cycles	
Template DNA (10 ng/μL)	5	1x	95 °C for 3.5 min
bbb0037 (6.1 pmol/ μL)	2.50	20x	95 °C for 0.5 min
bbb0038 (8.3 pmol/ μL)	1.80		55 °C for 1 min
pfu turbo rxn buffer (10x)	5		70 °C for 8 min
dNTP (10 mM)	1	1x	70 °C for 10 min
Water	33.70	1x	23 °C for 10 min
Pfu turbo polymerase	1		

bbb0037 5' GATGGGGAACTGATCGAGACCATGACGGCGGATGAC

bbb0038 5' GTCATCCGCCGTCATGGTCTCGATCAGTTCCCCATC

PCR conditions for F15W Mutation of Wild Type CRABPII in pET-Blue2:

REACTANT	AMOUNT (μL)	PCR Cycles	
Template DNA (10 ng/μL)	5	1x	95 °C for 0.5 min
bbb0049 (6.1 pmol/μL)	1.4	16x	95 °C for 0.5 min
bbb0050 (8.3 pmol/μL)	1.2		55 °C for 1 min
pfu turbo rxn buffer (10x)	5		70 °C for 8 min
dNTP (10 mM)	1	1x	70 °C for 10 min
Water	35.4	1x	23 °C for 10 min
Pfu turbo polymerase	1		

bbb0049 5' CGATCGGAAAACTGGGAGGAATTGCTC

bbb0051 5' GAGCAATTCCTCCCAGTTTTCCGATCG

PCR conditions for F15W Mutation of CRABPII R132K::Y134F in pET-Blue2:

REACTANT	AMOUNT (μL)	PCR Cycles	
Template DNA (10 ng/μL)	5	1x	95 °C for 0.5 min
bbb0049 (6.1 pmol/μL)	1.4	16x	95 °C for 0.5 min
bbb0050 (8.3 pmol/μL)	1.2		55 °C for 1 min
pfu turbo rxn buffer (10x)	5		70 °C for 8 min
dNTP (10 mM)	1	1x	70 °C for 10 min
Water	35.4	1x	23 °C for 10 min
Pfu turbo polymerase	1		

bbb0049 5' CGATCGGAAAACTGGGAGGAATTGCTC

bbb0051 5' GAGCAATTCCTCCCAGTTTTCCGATCG

PCR conditions for L19W Mutation of Wild Type CRABPII in pET-Blue2:

REACTANT		AMOUNT (μL)	PCR Cycles	
Template DNA	(10 ng/μL)	5	1x	95 °C for 0.5 min
bbb0047	(6.1 pmol/μL)	1.4	16x	95 °C for 0.5 min
bbb0048	(8.3 pmol/μL)	1.2		55 °C for 1 min
pfu turbo rxn buffer (10x)		5		70 °C for 8 min
dNTP	(10 mM)	1	1x	70 °C for 10 min
Water		35.4	1x	23 °C for 10 min
Pfu turbo polymerase		1		

bbb0047 5' CGAGGAATTGTGGAAAGTGCTGGGG

bbb0048 5' CCCCAGCACTTTCCACAATTCCTCG

PCR conditions for L19W Mutation of CRABPII R132K::Y134F in pET-Blue2:

REACTANT		AMOUNT (μL)	PCR Cycles	
Template DNA	(10 ng/μL)	5	1x	95 °C for 0.5 min
bbb0047	(6.1 pmol/μL)	1.4	16x	95 °C for 0.5 min
bbb0048	(8.3 pmol/μL)	1.2		55 °C for 1 min
pfu turbo rxn buffer (10x)		5		70 °C for 8 min
dNTP	(10 mM)	1	1x	70 °C for 10 min
Water		35.4	1x	23 °C for 10 min
Pfu turbo polymerase		1		

bbb0047 5' CGAGGAATTGTGGAAAGTGCTGGGG

bbb0048 5' CCCCAGCACTTTCCACAATTCCTCG

$Ph_2P(O)CH_2CN$

Synthesis of (Diphenyl-phosphinoyl)-acetonitrile (II-c):

Ethyl diphenylphosphinite (21.71 mmol) was placed into a sealed tube. To the sealed tube was added chloroacetonitrile (23.9 mmol). The mixture was heated at 125 °C for 3 h. After allowing the reaction to cool, the mixture solidified and was taken up in $CHCl_3$. This was then transferred to an RB and solvent was removed under reduced pressure. Dichloromethane (15 mL) was added to the solid and, under gentle heating, the compound dissolved. The product was precipitated by addition of Et_2O, filtered and placed under high vacuum to yield 86% of a fine white powder. ^1H NMR (300 MHz, $CDCl_3$): δ 3.32 (2H, d, J = 15.1 Hz); 7.51-7.67 (5H, m); 7.78-7.88 (5H, m). Matches previously published spectral data.[77]

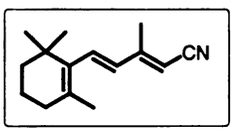

Synthesis of 3-Methyl-5-(2,6,6-trimethyl-cyclohex-1-enyl)-penta-2,4-dienenitrile (II-d): Ylide **II-c** (18.7 mmol) was dissolved in 75 mL of dry THF. Potassium *t*-butoxide (18.7 mmol) was added and allowed to stir at room temperature for 30 min After this time, β-ionone (9.35 mmol) was added, and allowed to stir at room temperature for 36 h. Et_2O was added to precipitate the phosphate, which was then celite filtered. The filtrate was concentrated under reduced pressure and applied directly to a silica column. The compound was eluted with 10% EtOAc/Hex to yield 85% of a yellow oil. ^1H NMR (300 MHz, $CDCl_3$): δ 1.00 (6H, s); 1.46 (2H, m); 1.58 (2H, m); 1.68 (3H, s);

2.02 (2H, m); 2.18 (3H, s); 5.13 (1H, s); 6.11 (1H, d, J = 15.9 Hz); 6.53 (1H, d, J = 15.9 Hz). Matches previously published spectral data.[77]

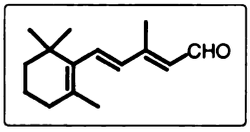

Synthesis of 3-Methyl-5-(2,6,6-trimethyl-cyclohex-1-enyl)-penta-2,4-dienal (II-e):

Compound **II-d** (9.35 mmol) was dissolved in 85 mL of dry Et_2O and cooled to 0 °C. Four equivalents of Dibal-H were added and allowed to stir at 0 °C for 2 h. The reaction was quenched by adding wet silica and NH_4Cl, and stirred vigorously for 1 h. The mixture was celite filtered, and the organic phase washed with brine, dried over Na_2SO_4, and concentrated under reduced pressure. The crude reaction mixture was applied directly to a silica column and eluted with 10% EtOAc/Hex to yield 70% of a yellow oil. ^1H NMR (300 MHz, $CDCl_3$): δ 1.02 (6H, s); 1.47 (2H, m); 1.60 (2H, m); 1.70 (3H, s); 2.01 (2H, m); 2.29 (3H, s); 5.91 (1H, d, J = 8.5 Hz); 6.19 (1H, d, J = 16.2 Hz); 6.72 (1H, d, J = 15.7 Hz); 10.10 (1H, d, J = 8.0 Hz). ^{13}C NMR (75 MHz, $CDCl_3$): δ 191.37, 155.05, 137.01, 135.66, 135.55, 132.73, 128.74, 39.45, 34.23, 33.18, 28.89, 21.72, 18.99, 12.91. Matches previously published spectral data.[77]

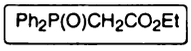

Synthesis of (Diphenyl-phosphinoyl)-acetic acid ethyl ester (II-f):

Ethyl diphenylphosphinite (21.71 mmol) was placed into a sealed tube. To the reaction vessel was added bromoethylacetate (23.9 mmol). The mixture was heated at 125 °C for 3 h. After allowing the reaction to cool, the mixture solidified and was taken

up in $CHCl_3$. This was then transferred to an RB and solvent removed under reduced pressure. Dichloromethane (15 mL) was added to the solid and under gentle heating, the compound was dissolved. The product was precipitated by addition of Et_2O, filtered and placed under high vacuum to yield 75% of a fine white powder. ^1H NMR (300 MHz, $CDCl_3$): δ 1.01 (3H, t, J = 7.14 Hz); 3.47 (2H, d, J = 15.11 Hz); 3.98 (2H, q, J = 7.14 Hz); 7.56-7.43 (6H, m); 7.82-7.45 (4H, m). Matches previously published spectral data.[77]

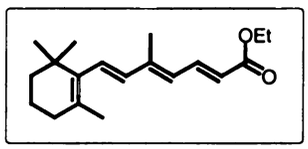

Synthesis of 5-Methyl-7-(2,6,6-trimethyl-cyclohex-1-enyl)-hepta-2,4,6-trienoic acid ethyl ester (II-g): Ylide **II-f** (18.7 mmol) was taken up in 100 mL THF. KOtBu (18.7 mmol) was added and allowed to stir for 30 min at room temperature. Aldehyde **II-e** (9.35 mmol) was added and allowed to stir for 24 h at room temperature. After the reaction was complete Et_2O was added to precipitate the phosphate, which was celite filtered and concentrated under reduced pressure. Flash chromatography (10% EtOAc/Hex) yielded 68% of a yellow oil. ^1H NMR (300 MHz, $CDCl_3$): δ 1.00 (6H, s); 1.28 (3H, t, J = 7.14 Hz); 1.46-1.42 (3H, m); 1.61-1.55 (3H, m); 1.69 (3H, s); 2.02 (3H, s); 4.19 (2H, q, J = 7.14 Hz); 5.84 (1H, d, J = 15.11 Hz); 6.12 (2H, d, J = 15.66 Hz); 6.36 (1H, d, J = 15.93 Hz); 7.66 (1H, dd, J = 15.11 Hz, 3.30 Hz). ^{13}C NMR (75 MHz, $CDCl_3$): δ 197.29, 167.56, 144.35, 140.65, 136.72, 130.82, 130.68, 127.25, 120.01, 60.18, 39.54, 34.23, 33.09, 28.92, 21.74, 19.14, 14.33, 13.00. Matches previously published spectral data.[77]

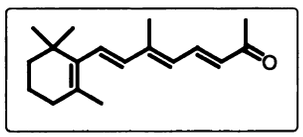

Synthesis of 6-Methyl-8-(2,6,6-trimethyl-cyclohex-1-enyl)-octa-3,5,7-trien-2-one (II-h): Ester **II-g** (5.90 mmol) was suspended in 30 mL THF, cooled to –100 °C, and an excess of freshly distilled TMSCl (29.5 mmol) was added. This mixture was stirred for 30 min to allow for formation of the silyl enol ether. MeLi (1 eq.) was added dropwise in 0.25 eq. aliquots over 30 min and allowed to stir for an additional 2 h. After this time, the mixture was warmed to room temperature, quenched with sat. NH_4Cl, and extracted. The aqueous layer was washed with Et_2O three times. The combined organic layers were washed with brine, dried over Na_2SO_4, and concentrated under reduced pressure. The reaction was purified via flash chromatography (10% EtOAc/Hex) to recover 46% of the desired compound (yellow oil) plus 29% unreacted starting material. ^1H NMR (300 MHz, $CDCl_3$): δ 1.00(6H, s); 1.46-1.42 (3H, m); 1.63-1.55 (3H, m); 1.69 (3H, s); 2.02 (3H, s); 2.73 (3H, s); 6.17-6.12 (3H, m); 6.39 (1H, d, J = 15.93 Hz); 7.55 (1H, dd, J=15.11 Hz, 3.57 Hz). ^{13}C NMR (75 MHz, $CDCl_3$): δ 198.52, 139.30, 137.44, 136.67, 131.26, 131.01, 129.25, 127.67, 100.30, 39.53, 34.22, 33.12, 28.92, 27.66, 21.74, 19.11, 13.09. Matches previously published spectral data.[77]

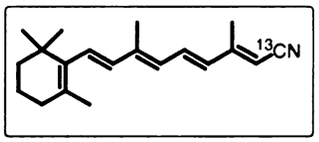

Synthesis of 3,7-Dimethyl-9-(2,6,6-trimethyl-cyclohex-1-enyl)-nona-2,4,6,8-tetraene-^{13}C-nitrile (II-i): THF (5 mL) was cooled to –60 °C. 1-^{13}C-acetonitrile (0.581 mmol) was added, followed by *n*-BuLi (1.16 mmol), and was stirred for 10 min at –60 °C. Chlorodiethylphosphite (0.581 mmol) was added to the now brown reaction mixture and allowed to stir for 30 min at –60 °C, generating and deprotonating the ylide. Methyl ketone **II-h** (0.232 mmol) taken up in 2 mL THF was added to the reaction. It was stirred for 1 h at –60 °C after which time the cryo-cooler was turned off and the reaction allowed to warm to room temperature very slowly (4 h). The reaction was quenched with sat. NH_4Cl and extracted with Et_2O three times. The combined organic layers were washed with brine, dried over Na_2SO_4, and concentrated under reduced pressure. The crude reaction mixture was used in the synthesis of **II-a**. ^{1}H NMR (300 MHz, $CDCl_3$): δ 1.00 (6H, s); 1.46-1.42 (3H, m); 1.63-1.55 (3H, m); 1.68 (3H, s); 2.18 (3H, s); 5.13 (1H, s); 6.11 (1H, d, J = 16.21 Hz); 6.54 (1H, d, J = 15.66 Hz). Matches previously published spectral data.[76]

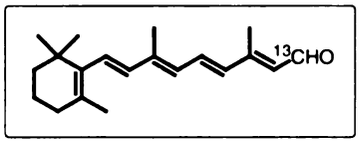

Synthesis of 15-[^{13}C]-retinal (II-a):

The crude mixture of **II-i** (0.232 mmol) was taken up in 5 mL Et_2O and cooled to –60 °C. Dibal (0.928 mmol) was added and stirred for 2 h at –60 °C. The reaction mixture was stirred for an additional 2 h over a NH_4Cl / silica gel slurry after which time the mixture filtered over celite, and the silica gel washed three times with Et_2O. The combined organic layers were dried over Na_2SO_4 and concentrated under reduced pressure. The mixture was purified by flash chromatography (10% EtOAc/Hex) to yield 30% of the desired compound (yellow oil). ^{1}H NMR (300 MHz, $CDCl_3$): δ 1.01 (6H, s); 1.47-1.43 (3H, m); 1.62-1.57 (3H, m); 1.70 (3H, s); 2.01 (3H, s); 2.31 (3H, s); 5.95 (1H, d, J = 8.24 Hz); 6.18-6.11 (2H, m); 6.37-6.29 (2H, m); 7.12 (1H, dd, JHH = 15.11 Hz, 3.57 Hz); 10.08 (1H, dd, J_{HH} = 8.24 Hz, J_{HC} = 161.52 Hz). ^{13}C NMR (75 MHz, $CDCl_3$): δ 191.14, 155.63, 141.29, 137.60, 137.05, 134.43, 132.53, 130.53, 129.73, 129.36, 128.61, 39.57, 34.24, 33.14, 28.95, 23.71, 19.16, 13.00. Matches previously published spectral data.[76,77]

M. References

1. Flower, D. R. "Experimentally determined lipocalin structures." *Biochim. Biophys. Acta-Protein Struct. Molec. Enzym.* **2000**, *1482*, 46-56.
2. Flower, D. R.; North, A. C. T.; Sansom, C. E. "The lipocalin protein family: structural and sequence overview." *Biochim. Biophys. Acta-Protein Struct. Molec. Enzym.* **2000**, *1482*, 9-24.
3. Skerra, A. "Lipocalins as a scaffold." *Biochim. Biophys. Acta-Protein Struct. Molec. Enzym.* **2000**, *1482*, 337-350.
4. Akerstrom, B.; Flower, D. R.; Salier, J. P. "Lipocalins: unity in diversity." *Biochim. Biophys. Acta-Protein Struct. Molec. Enzym.* **2000**, *1482*, 1-8.
5. Kleywegt, G. J.; Bergfors, T.; Senn, H.; Le Motte, P.; Gsell, B.; Shudo, K.; Jones, T. A. "Crystal structures of cellular retinoic acid binding proteins I and II in complex with all-*trans* retinoic acid and a synthetic retinoid." *Structure* **1994**, *2*, 1241-1258.
6. Wang, L.; Li, Y.; Yan, H. "Structure-function relationships of Cellular Retinoic Acid-binding proteins." *J. Biol. Chem.* **1997**, *272*, 1541-1547.
7. Stoeckenius, W.; Lozier, R. H.; Bogomolni, R. A. *Biochim. Biophys. Acta* **1979**, *505*, 215-278.
8. Bornhorst, J. A.; Falke, J. J., Purification of proteins using polyhistidine affinity tags. In *Methods in Enzymology*, ed.; Thorner, J.; Emr, S. D.; Abelson, J. N., Academic Press: London, 2000; Vol. 326, pp 245-254.

9. Sambrook, J.; Russell, D. W., Expression of cloned genes in *Escherichia coli*. In *Molecular cloning. A laboratory manual*, ed.; Sambrook, J.; Russell, D. W., Cold Spring Harbor Laboratory Press: Cold Spring Harbor, NY, 2001; Vol. 3, pp 15.1-15.65.

10. Sambrook, J.; Russell, D. W., Plasmids and their usefulness in molecular cloning. In *Molecular cloning. A laboratory manual*, ed.; Sambrook, J.; Russell, D. W., Cold Spring Harbor Laboratory Press: Cold Spring Harbor, NY, 2001; Vol. 1, pp 1.1-1.70.

11. Mueller, U.; Buessow, K.; Diehl, A.; Bartl, F. J.; Niesen, F. H.; Nyarsik, L.; Heinemann, U. "Rapid purification and crystal structure analysis of a small protein carrying two terminal affinity tags." *J. Struct. Funct. Genomics* **2003**, *4*, 217-225.

12. Kim, K. M.; Yi, E. C.; Baker, D.; Zhang, K. Y. J. "Post-translational modification of the N-terminal His tag interferes with the crystallization of the wild-type and mutant SH3 domains form chicken src tyrosine kinase." *Acta Crystallogr. D* **2001**, *D57*, 759-762.

13. Gill, S. C.; von Hippel, P. H. "Calculation of protein extinction coefficients from amino acid sequence data." *Anal. Biochem.* **1989**, *182*, 319-326.

14. Edelhoch, H. "Spectroscopic determination of tryptophan and tryosine in proteins." *Biochemistry* **1967**, 1948-1954.

15. Walker, J. M., *Protein Protocols Handbook*. 2nd ed.; Humana Press, Inc.: Totowa, NJ, 2002; p 11-14.

16. Venyaminov, S. Y.; Yang, J. T., Determination of protein secondary structure. In *Circular dichroism and the conformational analysis of biomolecules.*, ed.; Fasman, G. D., Plenum Press: New York, NY, 1996; pp 69-107.

17. Woody, R. W.; Dunker, A. K., Aromatic and cystine side-chain circular dichroism in proteins. In *Circular dichroism and the conformational analysis of biomolecules.*, ed.; Fasman, G. D., Plenum Press: New York, NY, 1996; pp 109-157.

18. Zhang, J.; Liu, Z. P.; Jones, T. A.; Gierasch, L.; Sambrook, J. F. "Mutating the charged residues in the binding posket of Cellular Retinoic Acid Binding Protein simultaneously reduces its binding affinity to retinoic acid and increases its thermostability." *Proteins: Struc. Func. Gen.* **1992**, *13*, 87-99.

19. Crabb, J. W.; Carlson, A.; Chen, Y.; Goldflam, S.; Intres, R.; West, K. A.; Hulmes, J. D.; Kapron, J. T.; Luck, L. A.; Horwitz, J.; Bok, D. "Structural and functional characterization of recombinant cellular retinaldehyde-binding protein." *Protein Science* **1998**, *7*, 746-757.

20. Tan, Q.; Lou, J.; Borhan, B.; Karnaukhova, E.; Berova, N.; Nakanishi, K. "Absolute sense of twist of the C12-C13 bond of the retinal chromophore in bovine rhodopsin based on exciton-coupled CD spectra of 11,12-dihydroretinal analogues." *Angew. Chemie Intl. Ed.* **1997**, *36*, 2089-2093.

21. Chen, X.; Tordova, M.; Gilliland, G. L.; Wang, L.; Li, Y.; Yan, H.; Ji, X. "Crystal structure of apo cellular retinoic acid bind protein type II (R111M) suggests a mechanism of ligand entry." *J. Mol. Biol.* **1998**, *278*, 641-653.

22. Norris, A. W.; Cheng, L.; Giguere, V.; Rosenberger, M.; Li, E. "Measurement of Subnanomolar Retinoic Acid-Binding Affinities for Cellular Retinoic Acid-Binding Proteins by Fluorometric Titration." *Biochim. Biophys. Acta-Protein Struct. Molec. Enzym.* **1994**, *1209*, 10-18.

23. Rost, B. "Protein structures sustain evolutionary drift." *Fold. Des.* **1997**, *2*, S19-S24.

24. Gally, J. A.; Edelman, G. M. "The effect of temperature of the fluorescence of some aromatic amino acids and proteins." *Biochim. Biophys. Acta* **1962**, *60*, 499-509.

25. Miller, J. N., Standards in fluorescence spectrometry. In *Techniques in visible and ultra-violet spectroscopy.*, ed.; Miller, J. N., Chapman and Hall: New York, 1981; Vol. 2, pp 1-7.

26. Kronman, M. J. "Fluorescence studies of teh molecular conformation of α-lactalbumin." *Biochim. Biophys. Acta* **1967**, *133*, 19-32.

27. Steiner, R. F.; Edelhoch, H. "Effect of thermally induced structural transitions on the ultra-violet fluorescence of proteins." *Nature* **1962**, *193*, 375-376.

28. Valeur, B., Characteristics of fluorescence emission. In *Molecular Fluorescence*, ed.; Wiley-VCH: Weinham, Germany, 2002; pp 34-71.

29. White, A. "Effect of pH on fluorescence of tyrosine, tryptophan and related compounds." *Biochem. J.* **1959**, *71*, 217-220.

30. Chen, R. F., Extrinsic and intrinsic fluorescence in the study of protein structure. In *Fluorescence: Theory, Instrumentation, and Practice*, ed.; Guilbault, G. G., Marcel Dekker, Inc.: New York, 1967; pp 443-509.

31. Eftink, M. R., Intrinsic fluorescence of proteins. In *Topics in Fluorescence Spectroscopy*, ed.; Lakowicz, J. R., Kulwer Academic / Plenum Publishers: New York, 2000; Vol. 6, pp 1-15.

32. Konev, S. V., *Fluorescence and phosphorescence of proteins and nucleic acids.* ed.; Plenum Press: New York, 1967; p 69-79.

33. Cogan, U.; Kopelman, M.; Mokady, S.; Shinitzky, M. "Binding affinities of retinol and related compounds to retinal binding proteins." *Eur. J. Biochem.* **1976**, *65*, 71-78.

34. Blatz, P. E.; Baumgartner, N.; Balasubramaniyan, B.; Balasubramaniyan, P.; Stedman, F. "Wavelength regulation in visual pigment chromophore. Large induced bathochromic shifts in retinol and related polyenes." *Photochem. Photobiol.* **1971**, *14*, 531-549.

35. Abasolo, M. I.; Bekerman, D. G.; Rodrigo, G. A.; Fernandez, B. M. "Second derivative UV-VIS absorption spectroscopy: A successful method to follow kinetics of organic reactions, when two bands are strongly overlapped in the fundamental spectra." *An. Asoc. Quim. Argent.* **1997**, *85*, 9-15.

36. Kus, S.; Marczenko, Z.; Obarski, N. "Derivative UV-VIS spectrophotometry in analytical chemistry." *Chem. Anal.* **1996**, *41*, 899-929.

37. All MALDI-TOF measurements were performed by Chrysoula Vasileiou, and a more detailed discussion of these can be found in her thesis.

38. Hermanson, G. T., Zero-Length Cross-linkers. In *Bioconjugate Techniques*, ed.; Academic Press: San Diego, CA, 1996; pp 169-186.

39. Computational results obtained using software programs from Accelrys, Inc. Minimization calculations performed with the Discover program using CVFF force field. Graphical displays were generated with the Insight II molecular modeling system.

40. Midland, M. M.; Kwon, Y. C. "Stereochemistry of hydroboration of α-chiral olefins and reduction of a-chiral ketones. An unusual anti-Cram selectivity with dialkylboranes." *J. Am. Chem. Soc.* **1983**, *105*, 3725-3727.

41. Kyte, J.; Doolittle, R. F. "A simple method for displaying the hydropathic character of a protein." *J. Mol. Biol.* **1982**, *157*, 105-132.

42. Hoop, T. P.; Woods, K. R. "Prediction of protein antigenic determinants from amino acid sequences." *Proc. Natl. Acad. Sci. U. S. A.* **1981**, *78*, 3824-3828.

43. Pajares, M. A.; Rando, R. R. "The active-site environment of rhodopsin." *J. Biol. Chem.* **1989**, *264*, 6804-6809.

44. Hargrave, P. A.; McDowell, J. H.; Curtis, D. R.; Wang, J. K.; Juszczak, E.; Fong, S. L.; Mohanna Rao, J. K.; Argos, P. "The structure of bovine rhodopsin." *Biophys. Struct. Mech.* **1983**, *9*, 235-244.

45. Honig, B.; Hubbell "Stablility of "salt bridges" in membrane proteins." *Proc. Natl. Acad. Sci. U. S. A.* **1984**, *81*, 5412-5416.

46. Jager, S.; Palczewski, K.; Hoffmann, K. P. "Opsin / all-*trans*-retinal complex activates transducin by different mechanism than photolyzed rhodopsin." *Biochemistry* **1996**, *35*, 2901-2908.

47. Fasick, J. I.; Applebury, M. L.; Oprian, D. D. "Spectral tuning in the mammalian short-wavelength sensitive cone pigments." *Biochemistry* **2002**, *41*, 6860-6865.

48. Zhukovsky, E. A.; Oprian, D. D. "Effect of carboxylic side chains on the absorption maximum of visual pigments." *Science* **1989**, *246*, 928-930.

49. Crabb, J. W.; Nie, Z.; Chen, Y.; Hulmes, J. D.; West, K. A.; Kapron, J. T.; Ruuska, S. E.; Noy, N.; Saari, J. C. "Cellular retinaldehyde-binding protein ligand interactions." *J. Biol. Chem.* **1998**, *273*, 20712-20720.

50. Nathans, J. "Determinants of visual pigment absorbance: Role of charged amino acids in the putative transmembrane segments." *Biochemistry* **1990**, *29*, 937-942.

51. Sakmar, T. P.; Franke, R. R.; Khorana, H. G. "Glutamic acid-113 serves as the retinylidene Schiff base counterion in bovine rhodopsin." *Proc. Natl. Acad. Sci., USA* **1989**, *86*, 8309-8313.

52. Lythgoe, R. J. "The absorption spectra of visual purple and of indicator yellow." *J. Physiol.* **1937**, *89*, 331-358.

53. Wald, G. "On rhodopsin in solution." *J. Gen. Physiol.* **1938**, *21*, 795-832.

54. Koutalos, Y. "High pH form of bovine rhodopsin." *Biophys. J.* **1992**, *61*, 272-275.

55. Steinberg, G.; Ottolenghi, M.; Sheves, M. "pK_a of the protonated Schiff base of bovine rhodopsin." *Biophys. J.* **1993**, *64*, 1499-1502.

56. Sheves, M.; Albeck, A.; Friedman, N.; Ottolenghi, M. "Controlling the pK_a of the bacteriorhodopsin Schiff base by use of artificial retinal analogues." *Proc. Natl. Acad. Sci. U. S. A.* **1986**, *83*, 3262-3266.

57. Sakmar, T. P.; Franke, R. R.; Khorana, G. "The role of retinylidene Schiff base counterion in rhodopsin in determining wavelength absorbance and Schiff base pK_a." *Proc. Natl. Acad. Sci., USA* **1991**, *88*, 3079-3083.

58. Koutalos, Y.; Ebrey, T. G.; Gilson, H. R.; Honig, B. "Octopus photoreceptor membranes. Surface charge density and pK of the Schiff base of the pigments." *Biophys. J.* **1990**, *58*, 493-501.

59. Liang, J.; Steinberg, G.; Livnah, N.; Sheves, M.; Ebrey, T. G.; Tsuda, M. "The pK_a of the protonated Schiff bases of gecko cone and octopus visual pigments." *Biophys. J.* **1994**, *67*, 848-854.

60. Drukman, S.; Ottolenghi, M.; Pande, A.; Callender, R. "Acid-base equilibrium of the Schiff base in bacteriorhodopsin." *Biochemistry* **1982**, *21*, 4953-4959.

61. Nakagawa, M.; Iwasa, T.; Kikkawa, M.; Tsuda, M.; Ebrey, T. G. "How vertebrate and invertebrate visual pigments differ in their mechanism of photoactivation." *Proc. Natl. Acad. Sci. U. S. A.* **1999**, *96*, 6189-6192.

62. Gat, Y.; Sheves, M. "A mechanism for controlling the pK_a of the retinal protonated Schiff base in retinal proteins. A study with model compounds." *J. Am. Chem. Soc.* **1993**, *115*, 3772-3773.

63. Warshel, A.; Russel, S.; Churg, A. "Macroscopic models for studies of electrostatic interactions in proteins: Limitations and applicability." *Proc. Natl. Acad. Sci. U. S. A.* **1984**, *81*, 4785-.

64. Honig, B.; Ebrey, T. G.; Callender, R.; Dinur, U.; Ottolenghi, M. "Photoisomerization, energy storage, and charge separation: A model for light energy transduction in visual pigments and bacteriorhodopsin." *Proc. Natl. Acad. Sci. U. S. A.* **1979**, *76*, 2503-2507.

65. DuPuis, P.; Harosi, I.; Sandorfy, C.; Leclerq, J.; Vocelle, D. "First step in vision: proton transfer or isomerization?" *Rev. Can. Biol.* **1980**, *39*, 247-258.

66. Scheiner, S.; Duan, X. "Effect of intermolecular orientation upon proton transfer within a polarization medium." *Biophys. J.* **1991**, *60*, 874-883.

67. Scheiner, S.; Hillenbrand, E. "Modification of p*K* values caused by change in H-bond geometry." *Proc. Natl. Acad. Sci. U. S. A.* **1985**, *82*, 2741-2745.

68. Schulten, K.; Tavan, P. *Nature* **1979**, *272*, 85.

69. Bridges, C. D. B. "Rversible visual pigment changes in tadpoles exposed to light and darkness." *Nature* **1970**, *227*, 956-957.

70. Pande, C.; Deng, H.; Rath, P.; Callender, R. H.; Schwemer, J. "Resonance Raman spectroscopy of an ultraviolet sensitive insect rhodopsin." *Biochemistry* **1987**, *26*, 7426-7430.

71. Tsukida, K.; Kodama, A.; Ito, M. "A rapid and convenient acquisition of the pure 11-*cis*-retinal specimen by preparative high performance liquid chromatography." *J. Nutr. Sci. Vitaminol.* **1978**, *24*, 593-596.

72. Liu, R. S. H.; Asato, A. E. "Synthesis and photochemistry of stereoisomers of retinal." *Methods in Enzymology* **1982**, *88*, 506-516.

73. Borhan, B.; Souto, M. L.; Um, J. M.; Zhou, B.; Nakanishi, K. "Efficient synthesis of 11-*cis*-retinoids." *Chem. Eur. J.* **1999**, *5*, 1172-1175.

74. Dugger, R. W.; Heathcock, C. H. "An efficient preparation of *trans*, *trans*-β-ionylideneacetaldehyde." *Syn. Comm.* **1980**, *10*, 509-515.

75. Cooke, M. P. J. "Acylation of organolithium reagents by esters in the presence of chlorotrimethylsilane." *J. Org. Chem.* **1986**, *51*, 951-953.

76. Verdegem, P. J. E.; Monnee, M. C. F.; Lugtenburg, J. "Simple and efficient preparation of [10,20-$^{13}C_2$]-and [10-CH_3, 13-$^{13}C_2$]-10-methylretinal: Introduction

of substituents at the position of 2,3-unsaturated nitriles." *J. Org. Chem.* **2001**, *66*, 1269-1282.

77. Groesbeek, M.; Lugtenburg, J. "Synthesis of doubly and multiply isotopically labeled retinals." *Photochem. Photobiol.* **1992**, *56*, 903-908.

Chapter 3

Probing a Possible Mode of Wavelength Regulation: Twisting of the Chromophore's Single Bonds

A. Synthesis of Model Derivatives for Solid State NMR Optimization

Recall one of the possible modes of wavelength regulation entails the degree of twisting about the single bonds within retinal (Figure III-1). It is proposed that different steric constraints in the various rhodopsin proteins may force different degrees of twisting, resulting in different amounts of orbital overlap or conjugation, and ultimately, different retinal maximal absorbances. We propose to investigate this theory through the use of an isotopically labeled retinal coupled with solid state NMR experiments that may probe the degree of single bond twisting. Use of 11,14-[^{13}C]$_2$-11-*cis*-retinal (Figure III-2) will provide the means to measure the dihedral angle between the two isotopic labels, and thus give us the degree of twisting about the C12/C13 single bond. The labeled retinal will be bound to each of the four rhodopsin proteins (rod, red, green, and blue) and the dihedral angle will be measured as a function of the coupling of the ^{13}C tensors by solid state NMR (collaboration with Professor David Weliky, Department of

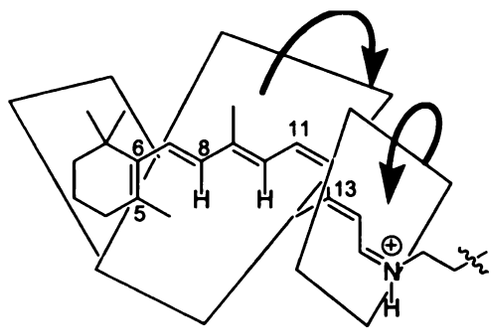

Figure III-1. Twisting of the single bonds will reduce the degree of π orbital overlap, and thus will lead to different maximal wavelengths. Individual rhodopsin proteins may modulate this by altering the steric restrictions placed on the chromophore, resulting in different degrees of conjugation and ultimately different maximal wavelengths.

Chemistry, Michigan State University).[1-3] We would expect the amount of twisting to be minimal when bound to red rhodopsin, as this has the largest maximal wavelength (570 nm) and would require the largest degree of orbital overlap. By the same arguments, we would then expect the blue rhodopsin to display the largest degree of twisting resulting in the largest disruption in conjugation and smallest λ_{max} (420 nm).

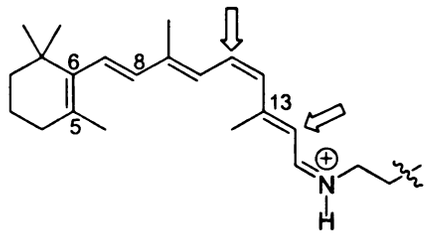

Figure III-2. ^{13}C labels will be incorporated at positions 11 and 14 as indicated by the arrows. This compound will be bound to each of the four opsin proteins and the dihedral angle, i.e., the twist of the C12/C13 single bond, will be measured.

The technique involved in this study will measure the relative orientation of chemical shift anisotropy (CSA) tensors of labeled olefinic carbons. The CSA depends on how the functional groups from the nuclei are positioned relative to the external magnetic field. Solid state NMR, rather than solution NMR is the most viable approach for this experiment not only because of the size of the protein, but also because it is a membrane bound protein which will be in a more structurally robust environment under solid state NMR conditions.

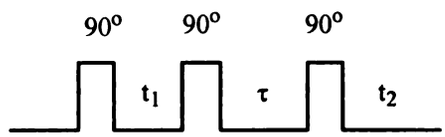

Figure III-3. Simplified pulse sequence of Magic Angle Spinning spectroscopy. t_1 and t_2 represent where NMR spectrum is recorded. τ represents the exchange time where magnetization transfer takes place.

Two-dimensional spectra in the solid state are acquired through rotor-synchronized Magic Angle Spinning spectroscopy, whose simplified pulse sequence is shown in Figure III-3. Magnetization transfer between the ^{13}C during τ (exchange time) gives rise to crosspeaks in the two-dimensional spectra. The intensities of these

crosspeaks can then be compared to simulated data and constraints placed on the dihedral angles between the labeled carbons.

The two isomers of 1,4-diphenyl-2-ethoxycarbonylbutadiene (*Z,E* isomer **III-a**, and *E,E* isomer **III-b**, Figure III-6) are meant to serve as model compounds to mimic the diene nature of the final desired bis-labeled 11-*cis*-retinal compound (Figure III-2).[4] Similar compounds have been synthesized before,[5] but we required a route to acquire 1,4-bis-labeled butadienes from readily available and inexpensive ^{13}C labeled precursors. These two molecules contain the same olefinic labeling pattern as the proposed 11-*cis*-retinal, i.e.; 1,4-[^{13}C]$_2$-labels. The isomeric phenyl group at C1 of **III-a** and **III-b** leads to different torsional twists within the C2/C3 single bond. We have performed conformational analyses of these molecules (Monte Carlo) and have determined the theoretical dihedral angles between the olefinic planes (dihedral angles between C1-C2-C3-C4) for each compound. As illustrated in Figure III-4, the planes defined by the two olefins in the *Z,E* isomer **III-a** are twisted by about 20°. However, the same two planes in the *E,E* isomer **III-b** are twisted by 41°. For both compounds **III-a** and **III-b**, the *s-cis* conformations were more stable as compared to their corresponding *s-trans* conformations by 1.2 and 1.4 Kcal/mol, respectively (PM3, Spartan V.5.1.3). The *s-cis* conformation for both compounds was obtained by starting the minimization from various starting geometries including *s-trans*.

The synthetic route for synthesis of (*Z*, *E*)-2-ethoxycarbonyl-1,4-[^{13}C]$_2$-diphenylbutadiene (**III-a**) is outlined in Scheme III-1. The *Z,E* isomer **III-a** was synthesized by employing a double Horner-Wadsworth-Emmons (HWE) strategy in a similar fashion which was reported by Minami et al.[6] Selenation of triethyl-2-

phosphonopropionate (**III-b**) proceeded smoothly to furnish **III-c**, which was oxidized promptly with *m*CPBA to yield the *syn*-eliminated product **III-d** in high yield.

Due to the lower cost and toxicity of sulfur as compared to selenium compounds, we initially tried several aromatic sulfur compounds in progression towards **III-d**. Phenyl disulfide, 4-nitrobenzenesulfenyl chloride, and 1,4-dinitrobenzenesulfenyl chloride all provided > 90% yields of the sulfur analog of **III-c**. Oxidation of these compounds with either *m*CPBA or $NaIO_4$ provided the sulfoxide intermediates again in > 90% yields. The *syn*-eliminated product (**III-d**) was only obtained upon high temperature Kugelrohr distillation and in yields < 50%. Use of phenylselenyl chloride provided the eliminated product in 95% yield directly from **III-c** upon treatment with *m*CPBA. No further reaction or heating was required to afford **III-d** in high yield and purity.

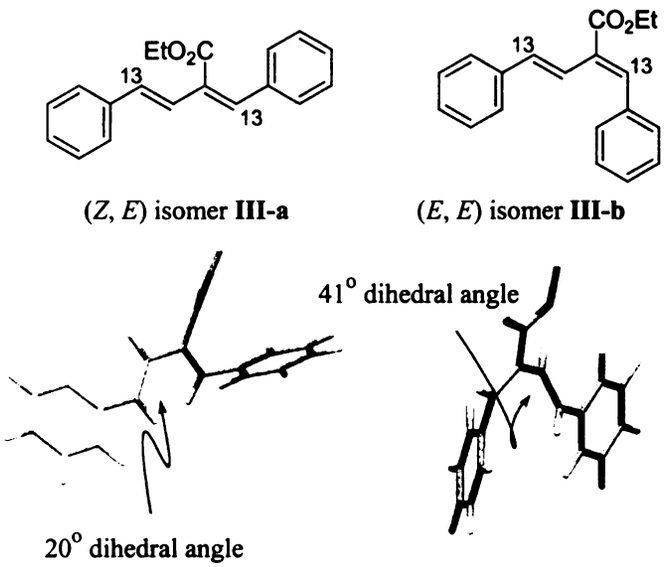

Figure III-4. Conformational analysis and minimizations (MacroModel, version 7.0) reveal a 20° dihedral twist of the single bond between the two isotopic labels for the *Z*, *E* isomer (III-a). The *E*, *E* isomer (III-b) exhibits a 41° dihedral twist of the same bond.

The olefinic carbons in **III-d** are the unlabeled carbons C2 and C3 in the final product. The double HWE reaction at these two carbon centers with ^{13}C-carbonyl labeled benzaldehyde would deliver the 1,4-bis-^{13}C-labeled compounds. The double HWE was

initiated by the 1,4-addition of diethylphosphite to obtain the bis-phosphate **III-e**. Deprotonation of **III-e** with *s*-BuLi and addition of labeled benzaldehyde delivered intermediate **III-f**, which was treated with another equivalent of *s*-BuLi and labeled benzaldehyde to deliver a 6:1 isomeric mixture of **III-a**:**III-b** in 39% yield over the latter steps. The *Z,E* isomer **III-a** was purified by HPLC.

Our attempts at a one pot synthesis from **III-d** → **III-a,** by utilizing the enolate generated after the Michael addition of diethylphosphite to **III-d** for the subsequent HWE reactions produced low yields of the desired final compound and was not reproducible. It was therefore necessary to isolate **III-e** and proceed forward. The bis-olefination of **III-e** allows for the introduction of commercially available ^{13}C-labeled carbonyl compounds such as benzaldehyde or other ketones or aldehydes as the last step of the synthesis. In

Scheme III-1

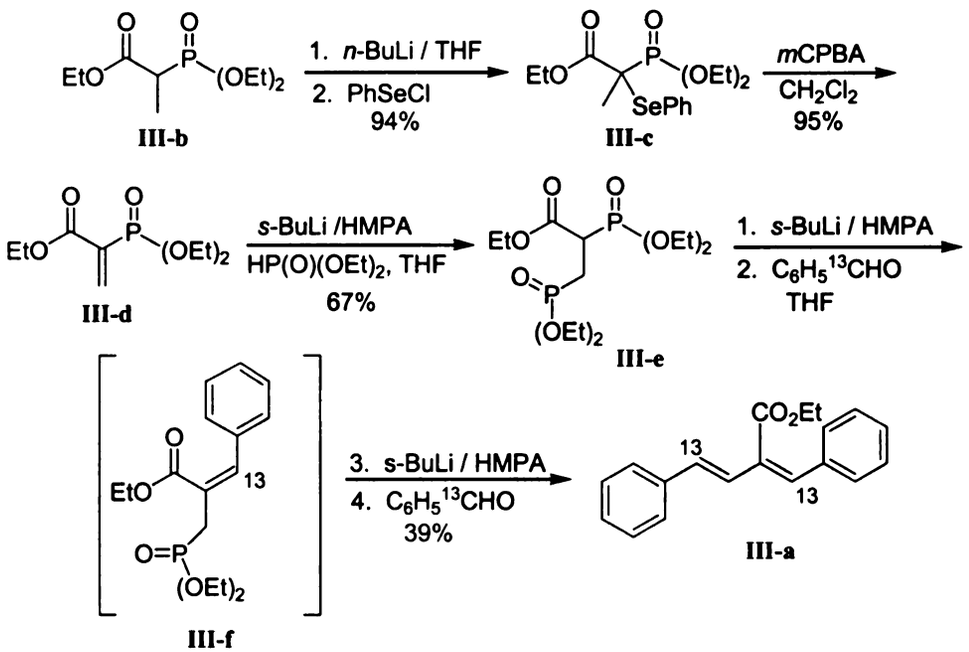

this manner, we can introduce both labels at once at the end of the scheme. This could enable us to quickly create a small library of 1,4-[$^{13}C]_2$-butadine compounds if needed.

Synthesis of the *E,E* isomer **III-b** is illustrated in Scheme III-2.[7] The Baylis-Hillman reaction between labeled benzaldehyde and ethyl acrylate proceeded smoothly to furnish the allyl alcohol **III-h**,[8] which upon treatment with HBr in concentrated sulfuric acid rearranged to yield the allyl bromide **III-i** in excellent yield.[9] As reported by Aggarwal and coworkers, we also noticed a substantial decrease in reaction time required for the Baylis-Hillman reaction catalyzed by 1,8-diazabicyclo[5.4.0]undec-7-ene (DBU) (1 day) as compared to DABCO (7 days).[10] Ylide **III-j** was obtained in quantitative yield from the reaction of **III-i** with triphenylphosphine, which was subsequently deprotonated and reacted with labeled benzaldehyde to afford the desired *E,E* diene **III-b** in good yield and high isomeric purity (20:1 ratio of **III-b**:**III-a**). Although we had to use the labeled benzaldehyde in the first step of the synthesis, because the yields of the subsequent reactions were high, we did not deem this as a major problem.

Scheme III-2

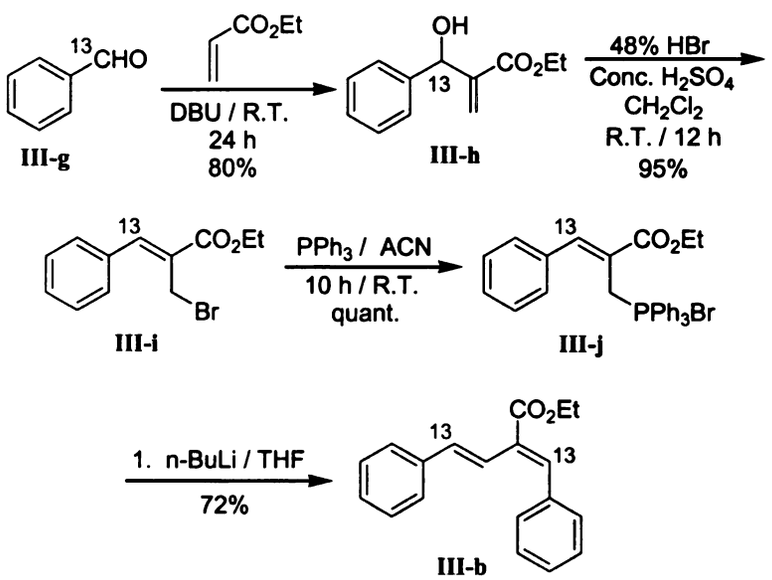

The stereoisomers **III-a** and **III-b** were characterized by one and two-dimensional NMR spectroscopy. The stereochemistry of the olefinic bonds were confirmed by NOESY. In particular, strong coupling of H1 and H3 protons was observed in **III-a**, which was absent in **III-b**. ^{13}C NMR analysis of the resulting **III-a** revealed doubly enhanced signals at 132.5 and 131 ppm, while **III-b** displayed enhanced signals at 139 and 135 ppm, corresponding to enriched C_1 and C_4 of the 1,4-bis-^{13}C-butadiene system.

These compounds are ready for analysis by solid state NMR experiments. If successful measurements are made, and it is found that the difference in dihedral angle of the two isomers can be distinguished through these means, synthesis of 11,14-[^{13}C]$_2$-11-*cis*-retinal and isolation of the rhodopsin pigments will commence.

B. Proposed Synthesis of 11,14-[$^{13}C]_2$-11-*cis*-retinal

The proposed route to synthesize the bis-labeled retinal analog is depicted in Scheme III-3. The sources of ^{13}C will be incorporated through ethyl bromoacetate (**III-k**) and carbon tetrabromide. Deprotection and oxidation of the allylic alcohol will provide compound **IIII-n**, which is set up for a Corey-Fuchs type reaction and incorporation of the second isotopic label. The synthesis of vinyl iodide **III-q** will follow published procedures,[11, 12] and will undergo a Sonogashira coupling with the bis-^{13}C-labeled fragment **III-o** to produce the 11-yne retinal precursor (**III-r**).[13] For final conversion to the desired compound, DIBAL reduction of the ester will afford the alcohol, the triple bond will be selectively reduced to furnish 11-*cis*-retinol as previously reported, and oxidation with activated MnO_2 should afford the desired adduct, 11,14-[$^{13}C]_2$-11-*cis*-retinal (**III-s**).[14] Although the isotopic labels appear early in the synthetic plan, we do not deem this a major problem given that many of the further steps are well established.

The efforts on this portion of the wavelength regulation project have stopped here, with the synthesis of the labeled adipic and succinic model derivatives **III-a** and **III-b**, and preliminary investigations into the synthesis of the bis-labeled retinal, **III-s**. Provided successful solid state NMR measurements and conditions are obtained from the model butadienes, this project will be continued with the completion of the synthesis of **III-s** as described above, and isolation of the rhodopsin pigments. Regeneration of rod rhodopsin and the cone rhodopsins from their opsins will be performed following previously published protocols.[15-17] Since neither the protein nor the chromophore is

altered structurally or chemically, the result of the regeneration will be the wild type pigments with ^{13}C-labels incorporated within the polyene.

Solid state NMR experiments should reveal the degree of twist within the C12 / C13 single bond of retinal as bound to different rhodopsins. If this proves to be a successful method for analysis of dihedral angles of bound chromophores, one could employ this same procedure to investigate the twist of other single bonds in 11-*cis*-retinal as it is bound to different rhodopsins, using alternative bis-^{13}C-labeled 11-*cis*-retinals with placement of the labels before and after the single bond to be analyzed.

Scheme III-3

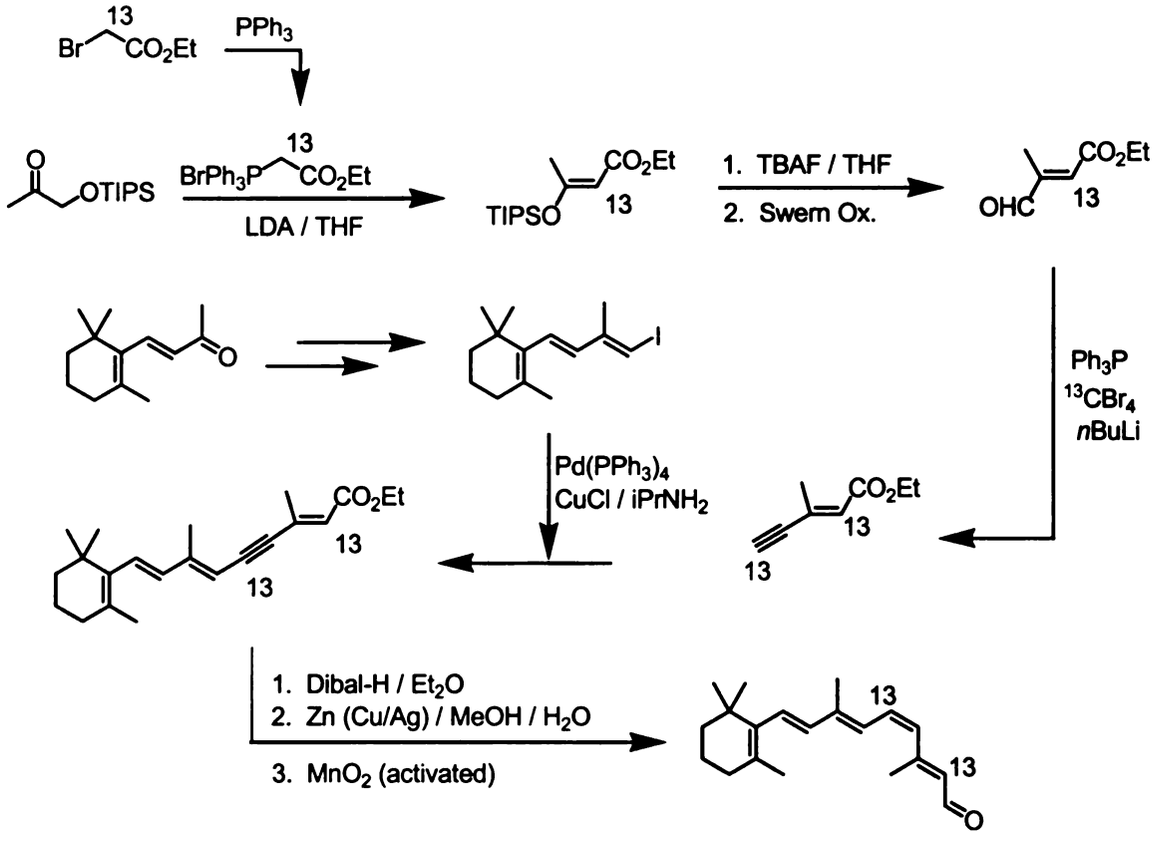

C. Materials and Methods

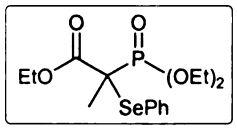

Preparation of 2-(Diethoxyphosphoryl)-2-phenylselanyl-propionic acid ethyl ester (III–c) : A 0.75 M solution of triethyl-2-phosphonopropionate in THF was cooled to –78 °C. One equivalent (2.1 mmol) of *n*-BuLi (1.2 M in hexane) was added to the mixture and allowed to warm to room temperature. Upon reaching room temperature a 0.85 M (2.1 mmol / 2.5 mL THF) solution of phenylselenyl chloride was added and stirred for 4 hours. The reaction was quenched with 10% HCl, extracted with Et_2O, dried over anhydrous Na_2SO_4, and concentrated under reduced pressure. The product was isolated in 94% yield, and used without further purification. ^1H NMR (300 MHz, $CDCl_3$): δ 1.22 (3H, t, J = 8.1 Hz); 1.34 (6H, m); 1.55 (3H, d, J = 15.8 Hz); 4.0-4.2 (4H, m); 4.25 (2H, q, J = 8.1 Hz); 7.26-7.43 (4H, m); 7.68 (1H, dd, J = 1.4, 7.5 Hz). Matches previously published spectral data.[18]

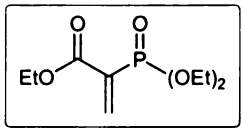

Preparation of 2-(Diethoxyphosphoryl)-acrylic acid ethyl ester (III–d) :

A 0.17 M (2.1 mmol / 12.4 mL) solution of mCPBA in CH_2Cl_2 was added dropwise to a 0.1 M solution (2.1 mmol / 21 mL) of **III-c** in CH_2Cl_2 at –78 °C. After complete addition, the reaction was allowed to warm to room temperature and stir for 20 hours. The mixture was washed with saturated $NaHCO_3$, brine, dried over anhydrous

Na_2SO_4 and concentrated under reduced pressure. The product was purified by Kugelrohr distillation to yield 95% of a colorless oil. ^1H NMR (300 MHz, $CDCl_3$): δ 1.33 (3H, t); 1.35 (3H, t); 4.18 (2H, m); 4.28 (2H, q, J = 7.14 Hz); 6.74 (1H, dd, J_{HH} = 1.9 Hz, J_{HP} = 20.3 Hz); 6.98 (1H, dd, J_{HH} = 1.9, J_{HP} = 42.0 Hz). Matches previously published spectral data.[18]

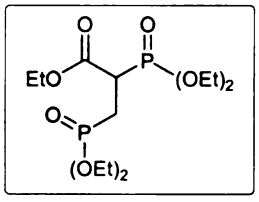

Preparation of 2,3-Bis-(diethoxyphosphoryl)-propionic acid ethyl ester (III–e) :

A 0.15 M (59.1 mmol) solution of diethylphosphite in THF was cooled to –78 °C, NaHMDS (69 mmol) was added and stirred for one hour. Then 19.7 mmol of **III-d**, diluted in THF (5 mL), was added via canula and allowed to stir overnight. The reaction was quenched with 2% HCl, extracted with Et_2O, dried over Na_2SO_4 and concentrated under reduced pressure. The crude reaction mixture was purified with flash chromatography, washed with 70% EtOAc / hexane, then eluted with 10% MeOH / $CHCl_3$ to yield 67% product. ^1H NMR (300 MHz, $CDCl_3$): δ 1.3 (15H, m); 2.2 (1H, dd, J = 16.4, 19 Hz); 2.5 (1H, dq, J = 2.1, 16.4 Hz); 3.23 (1H, dt, J = 13.6, 24.5 Hz); 4.15 (8H, m); 4.3 (2H, m). Matches previously published spectral data.[5]

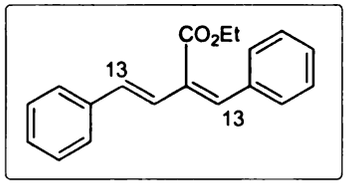

Preparation of (*Z*, *E*)-2-ethoxycarbonyl-1,4-[$^{13}C]_2$-diphenylbutadiene (III–a) :

A 0.1 M (0.24 mmol / 2.4 mL) solution of **III-e** in THF was cooled to 0 °C, 0.24 mmol of *s*-BuLi (1.2 M in hexane) was added, 0.24 mmol of HMPA was added, and stirred for 10 minutes. The reaction was then cooled to –78 °C and 0.24 mmol of Ph^{13}CHO, diluted in THF was added. The reaction was allowed to stir for 3-4 hours, until complete by TLC. The mixture was then cooled to 0 °C again, 0.24 mmol sBuLi added, 0.24 mmol HMPA added, and allowed to stir for 20 minutes. It was then cooled to –78 °C and another 0.24 mmol of Ph^{13}CHO, diluted in THF was added and monitored by TLC. Upon completion, the crude reaction mixture was purified by flash chromatography using 1% EtOAc / hexane to yield a 6:1 isomeric mixture of **III-a**:**III-b** in 39% yield. The isomers were then separated by HPLC (Perkin Elmer LC-75 system, normal phase column Altex Ultra Shere-Si, under isocratic conditions, 3% EtOAc/Hex, 5 mL/min, detection at 325 nm) to recover 30% of the desired isomer **III-a**. ^{1}H NMR (300 MHz, $CDCl_3$): δ 1.2 (3H, t, J = 7.14 Hz) ; 4.34 (2H, q, J = 7.14 Hz); 6.65 (1H, dd, J_{HH} = 16.5 Hz, $^1J_{HC}$ = 156 Hz); 6.75 (1H, d, $^1J_{HC}$ = 155.2 Hz); 6.89 (1H, m); 7.2 – 7.5 (10H, m). ^{13}C NMR (75 MHz, $CDCl_3$): δ 13.9; 61.4; 126.6 (d, $^3J_{CC}$ = 2.3 Hz); 127.4 (d, $^1J_{CC}$ = 43.8 Hz); 128.0; 128.2; 128.3; 128.5 (d, $^2J_{CC}$ = 4.6 Hz); 128.7 (d, $^2J_{CC}$ = 4.6 Hz); 131.0 (d, $^3J_{CC}$ = 8.0 Hz); 132.7 (d, $^3J_{CC}$ = 9.2 Hz); 134.2 (d, $^1J_{CC}$ = 58.5 Hz); δ 135.4 (d, $^1J_{CC}$ = 55.5 Hz); 136.7 (d, $^1J_{CC}$ = 55.5 Hz); 168.9. Matches previously published spectral data.[5]

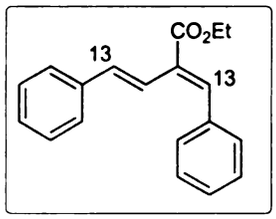

NMR data of (*E*, *E*)-2-ethoxycarbonyl-1,4-[$^{13}C]_2$-diphenylbutadiene (III–b) :

^{1}H NMR: (500 MHz, $CDCl_3$): δ 1.38 (3H, t, J = 7 Hz); 4.35 (2H, q, J = 7 Hz); 7.03 (1H, dd, J = 3.3 Hz, 17 Hz); 7.20 – 7.48 (11H, m); 7.57 (1H, d, $^1J_{HC}$ = 134 Hz). ^{13}C NMR (75 MHz, $CDCl_3$): δ 14.5; 61.0; 121.6 (d, $^1J_{CC}$ = 73.3 Hz); 126.7; 127.8; 128.4 (d, $^2J_{CC}$ = 4.6 Hz); 128.6; 128.7; 130.0 (d, $^1J_{CC}$ = 70.9 Hz); 130.1; 134.7 (d, $^3J_{CC}$ = 5.7 Hz); 135.5 (d, $^1J_{CC}$ = 55.5 Hz); 138.8 (d, $^3J_{CC}$ = 5.7 Hz); 167.5. Matches previously published spectral data.[5]

D. References

1. Weliky, D. P.; Tycko, R. "Determination of peptide conformations by two-dimensional magic angle spinning NMR exchange spectroscopy with rotor synchronization." *J. Am. Chem. Soc.* **1996**, *118*, 8487-8488.
2. Tycko, R.; Weliky, D. P.; Berger, A. E. "Investigation of molecular structure in solids by two-dimensional exchange spectroscopy with magic angle spinning." *J. Chem. Phys.* **1996**, *105*, 7915-7926.
3. Weliky, D. P.; Bennett, A. E.; Zvi, A.; Anglister, J.; Steinbach, P. J.; Tycko, R. "Solid state NMR evidence for an antibody-dependent conformation of V3 loop of HIV gp120." *Nature Struc. Biol.* **1999**, *6*, 141-145.
4. Crist, R. M.; Reddy, P. V.; Borhan, B. "Synthesis of isomeric 1,4-[$^{13}C]_2$-labeled 2-ethoxycarbonyl-1,4-diphenylbutadienes." *Tetrahedron Lett.* **2001**, *42*, 619-621.
5. Janecki, T.; Bodalski, R. "A convenient Horner-Emmons approach to the synthesis of substituted ethyl 1,3-butadiene-2-carboxylates and related compounds." *Synthesis* **1989**, *7*, 506-510.
6. Minami, T.; Tokumasu, S.; Hirao, I. "Reactions of vinylphosphonates. 3. One-pot synthesis of dienes and their analogs from vinylphosphonates, aldehydes and diethyl phosphonate." *Bull. Chem. Soc. Jpn.* **1985**, *58*, 2139-2140.
7. This work was performed in collaboration with post-doctoral fellow, Dr. Pulgam Veera Reddy.
8. Fort, Y.; Berthe, M. C.; Caubere, P. "The 'Baylis-Hillman Reaction' mechanism and applications revisited." *Tetrahedron* **1992**, *48*, 6371-6384.

9. Buchholz, R.; Hoffmann, H. M. R. "α-Methylidene- and α-alkylidene-β-lactams from nonproteinogenic amino acids." *Helv. Chim. Acta* **1991**, *74*, 1213-1220.

10. Aggarwal, V. K.; Mereu, A. "Superior amine catalysts for the Baylis-Hillman reaction: the use of DBU and its implications." *Chem. Commun.* **1999**, *22*, 2311-2312.

11. Negishi, E.; Valente, L. F.; Kobayashi, M. "Palladium-catalyzed cross-coupling reaction of homoallylic or homopropargylic organozincs with alkenyl halides as a new selective route to 1,5-dienes and 1,5-enynes." *J. Am. Chem. Soc.* **1980**, *102*, 3298-3299.

12. Negishi, E.; King, A. O.; Tour, J. M., Conversion of methyl ketones into terminal alkynes. In *Organic Syntheses*, ed.; Kende, A. S., American Chemical Society: Bloomington, 1985; Vol. 64, pp 44-49.

13. Sonogashira, K.; Tohda, Y.; Hagihara, N. "A convenient synthesis of acetylenes: Catalytic substitutions of acetylenic hydrogen with bromoalkenes, iodoarenes, and bromopyridines." *Tetrahedron Lett.* **1975**, *16*, 4467-4470.

14. Borhan, B.; Souto, M. L.; Um, J. M.; Zhou, B.; Nakanishi, K. "Efficient synthesis of 11-*cis*-retinoids." *Chem. Eur. J.* **1999**, *5*, 1172-1175.

15. Oprian, D. D.; Asenjo, A. B.; Lee, N.; Pelletier, S. L. "Design, chemical synthesis, and expression of genes for the 3 human color vision pigments." *Biochemistry* **1991**, *30*, 11367-11372.

16. Papermaster, D. S. "Preparation of retinal rod outer segments." *Methods in Enzymology; Academic Press: New York* **1982**, *81*, 48-52.

17. Kochendoerfer, G. G.; Wang, Z.; Oprian, D. D.; Mathies, R. A. "Resonance Raman examination of the wavelength regulation mechanism in human visual pigments." *Biochemistry* **1997**, *36*, 6577-6587.

18. Kleschick, W. A.; Heathcock, C. H. "Synthesis and chemistry of ethyl 2-diethylphosphonoacrylate." *J. Org. Chem.* **1978**, *43*, 1256-1259.

EXPLORING THE UNDERLYING CHEMICAL BASIS FOR COLOR VISION: DESIGNING A PROTEIN MIMIC OF RHODOPSIN

Volume II

By

Rachael M. Crist

A DISSERTATION

Submitted to
Michigan State University
in partial fulfillment of the requirements
for the degree of

DOCTOR OF PHILOSOPHY

Department of Chemistry

2004

APPENDIX

APPENDIX

Data Collect

WILD TYPE
R132K....
R132K...Y
R132K...Y
R132K...Y
R132K...Y
R132K...Y
R132K...Y
R132K...Y
R132K...Y
Y134F...R
R132L...Y
R132K...Y
R132K...Y
R132K...Y
R132K...Y
R132K...Y
R132K...Y
R132K...Y
R132K...Y
R132K...Y
R132K...Y
R132K...Y
Y134K...
Y134K...
Y134K...
Y134K...
Y134K...
Y134K...
Y134K...
Y134K...
Y134K...
Y134K...
Y134K...
F15W...
R132K...
L19W...
R132K...

Data Collected for:

Summary of Protein Properties for all His-tagged CRABPII Mutants

Entry	Protein	Molecular Weight (Da) Calculated	Molecular Weight (Da) Experimental	Extinction Coefficient ($M^{-1}cm^{-1}$)	CD (nm)

Summary of Protein Properties for all His-tagged CRABPII Mutants

Entry	Protein	Molecular Weight (Da) Calculated	Molecular Weight (Da) Experimental	Extinction Coefficient ($M^{-1}cm^{-1}$)	CD (nm)
1	Wild-Type	16829.21	16821.88	20215	221
2	R132K	16801.20	16803.61	19202	225
3	R132K::Y134F	16785.20	16788.17	18317	221
4	R132K::Y134F::R111E	16758.13	16759.39	16698	266
5	R132K::Y134F::R111E::T54V	16756.16	16759.61	17214	220
6	R132K::Y134F::L121E	16801.16	16794.78	18422	224
7	R132K::Y134F::R111L	16742.17	16740.58	16654	220
8	R132K::Y134F::R111L::T54E	16770.18	16770.79	18430	224
9	R132K::Y134F::R111L::L121E	16758.13	16660.13, 17444.16	21625	218
10	R132K::Y134F::R111L::L121Q	16757.14	16752.33	17397	229
11	Y134F::R111L::L121E	16786.14	16781.69	19432	218
12	R132L::Y134F::R111L::L121E	16743.11	16747.01	19415	220
13	R132K::Y134F::R111L::L121E::F15A	16682.03	16679.48	19450	223
14	R132K::Y134F::R111L::L121E::T54V	16756.16	16765.81	19362	222
15	R132K::Y134F::R111L::L121Q::T54V	16755.17	16754.61	22821	224
16	R132K::Y134F::R111L::T54V	16740.10	16740.26	17798	218
17	R132K::Y134F::R111L::L121D	16744.10	16753.46	19138	218
18	R132K::Y134F::R111L::L121N	16743.12	16742.27	20266	222
19	R132K::Y134F::R111L::L121D::T54V	16742.13	16739.97	22056	226
20	R132K::Y134F::R111L::L121N::T54V	16741.14	16740.55	21766	225
21	R132K::Y134F::R111L::L121E::T54V::T61E	16784.17	16781.07	17283	218
22	R132K::Y134F::R111L::L121E::T54V::T61F	16802.23	16799.90	18847	218

Summary of Protein Properties for all His-tagged CRABPII Mutants

Entry	Protein	Molecular Weight (Da)		Extinction Coefficient (M⁻¹cm⁻¹)	CD (nm)
		Calculated	Experimental		

Summary of Protein Properties for all His-tagged CRABPII Mutants

Entry	Protein	Molecular Weight (Da) Calculated	Molecular Weight (Da) Experimental	Extinction Coefficient ($M^{-1}cm^{-1}$)	CD (nm)
23	Y134K	16794.21	16796.09	20990	219
24	Y134K::R132K	16766.20	16769.94	19332	226
25	Y134K::R132F	16785.20	16792.29	19393	225
26	Y134K::R132L	16751.18	16763.65	18697	228
27	Y134K::R132F::R111L	16742.17	16737.13	18056	225
28	Y134K::R132F::R111L::L121E	16758.13	16757.11	20200	225
29	Y134K::R132F::R111L::T54E	16770.18		21110	228
30	Y134K::R132F::R111L	16708.15	16745.94	19931	219
31	Y134K::R132L::L121E	16767.14	16764.97	19315	224
32	Y134K::R132L::R111L::L121E	16724.11	16723.00	19152	218
33	F15W	16868.25	16873.72	28022	217
34	R132K::Y134F::F15W	16824.24	16823.60	37716	222
35	L19W	16902.27	16901.30	26639	219
36	R132K::Y134F::L19W	16858.25	16858.97	25582	217

Summary of Binding Assay Results for all His-tagged CRABPII Mutants

Entry	Protein	RA K_d (nM)	Rt K_d (nM)	Rt λ_{max} (nm) 2nd Deriv.	Corr.	MALDI-TOF Incubation

Summary of Binding Assay Results for all His-tagged CRABPII Mutants

Entry	Protein	RA K_d (nM)	Rt K_d (nM)	Rt λ_{max} (nm) 2nd Deriv.	Corr.	MALDI-TOF Incubation	Red. Am.
1	Wild-Type	2.0 ± 1.2	6600 ± 360	375	378	No	No
2	R132K	65 ± 14	280 ± 17	375	378	Yes	Yes
3	R132K::Y134F	100 ± 7.1	120 ± 4.9	400	420	Yes	No
4	R132K::Y134F::R111E	530 ± 31	260 ± 12	376	370	No	No
5	R132K::Y134F::R111E::T54V	860 ± 36	210 ± 8.2	398	414	Yes	No
6	R132K::Y134F::L121E	1400 ± 63	160 ± 9.8	373	370	No	Yes
7	R132K::Y134F::R111L	1000 ± 28	160 ± 6.7	391	410	Yes	Yes
8	R132K::Y134F::R111L::T54E	2180 ± 43	80 ± 3.4	379, 410	379, 454	Yes	No
9	R132K::Y134F::R111L::L121E	770 ± 61	200 ± 8.3	377, 430	372, 464	Yes	Yes
10	R132K::Y134F::R111L::L121Q	240 ± 22	530 ± 44	379	363	Yes	Yes
11	Y134F::R111L::L121E	220 ± 28	570 ± 32	378	369	No	No
12	R132L::Y134F::R111L::L121E	160 ± 21	180 ± 14	393	402	No	No
13	R132K::Y134F::R111L::L121E::F15A	370 ± 35	110 ± 63	373	368	Yes	Yes
14	R132K::Y134F::R111L::L121E::T54V	250 ± 19	2.7 ± 7.0	385, 437	378, 456	Yes	Yes
15	R132K::Y134F::R111L::L121Q::T54V	1730 ± 94	600 ± 66	377	408	Yes	Yes
16	R132K::Y134F::R111L::T54V	900 ± 64	84 ± 12	412	391, 456	Yes	Yes
17	R132K::Y134F::R111L::L121D	200 ± 25	2.6 ± 7.9	377, 445	365, 464	Yes	Yes
18	R132K::Y134F::R111L::L121N	3050 ± 240	1270 ± 49	375	357, 467	Yes	Yes
19	R132K::Y134F::R111L::L121D::T54V	760 ± 43	30 ± 5.5	378	370, 466	Yes	Yes
20	R132K::Y134F::R111L::L121N::T54V	420 ± 34	180 ± 15	402	370, 462	Yes	Yes
21	R132K::Y134F::R111L::L121E::T54V::T61E	3380 ± 230	9.2 ± 28	373, 442	458	Yes	Yes
22	R132K::Y134F::R111L::L121E::T54V::T61F	1020 ± 24	96 ± 44	376, 428	452	Yes	Yes

Summary of Binding Assay Results for all His-tagged CRABPII Mutants

Entry	Protein	RA K_d (nM)	Rt K_d (nM)	Rt λ_{max} (nm) 2nd Deriv.	Corr.	MALDI-TOF Incubation	Red. Am.
23	Y134K	630 ± 20	570 ± 29	376	370	No	No
					374	Yes	Yes

Summary of Binding Assay Results for all His-tagged CRABPII Mutants

Entry	Protein	RA K_d (nM)	Rt K_d (nM)	Rt λ_{max} (nm) 2nd Deriv.	Corr.	MALDI-TOF Incubation	Red. Am.
23	Y134K	630 ± 20	570 ± 29	376	370	No	No
24	Y134K::R132K	660 ± 25	270 ± 10	377	374	Yes	Yes
25	Y134K::R132F	180 ± 7.3	78 ± 11	403	415	No	No
26	Y134K::R132L	800 ± 19	340 ± 16	402	432	Yes	No
27	Y134K::R132F::R111L	570 ± 26	7.9 ± 7.2	401	415	Yes	No
28	Y134K::R132F::R111L::L121E	1000 ± 51	220 ± 16	366	364	Yes	Yes
29	Y134K::R132F::R111L::T54E	120 ± 10	41 ± 6.6	396	434		Yes
30	Y134K::R132F::R111L	3300 ± 260	210 ± 7.8	402	423	Yes	Yes
31	Y134K::R132L::L121E	450 ± 19	110 ± 6.7	395	423	No	No
32	Y134K::R132L::R111L::L121E	1070 ± 38	570 ± 30	375	367	Yes	Yes
33	F15W	40 ± 4.3	5960 ± 350	375	372	No	No
34	R132K::Y134F::F15W	340 ± 14	680 ± 30	376	374	Yes	No
35	L19W	170 ± 22	900 ± 38	378	378	No	No
36	R132K::Y134F::L19W	1000 ± 38	680 ± 20	377	367	Yes	No

Summary of 11-*cis*-Retinal Assays for His-tagged CRABPII Mutants

Entry	Protein	Rt K_d (nM)	Rt λ_{max} (nm) 2nd Deriv.	Corr.	Reductively Aminates

Summary of 11-*cis*-Retinal Assays for His-tagged CRABPII Mutants

Entry	Protein	Rt K_d (nM)	Rt λ_{max} (nm)		Reductively Aminates
			2nd Deriv.	Corr.	
1	Wild-Type	> 1000	383	373	No
2	R132K	50 ± 16	370	356	Yes
3	R132K::Y134F	630 ± 53	380	373	No
12	R132L::Y134F::R111L::L121E	-	386	385	-
14	R132K::Y134F::R111L::L121E::T54V	210 ± 18	368	360	Yes
17	R132K::Y134F::R111L::L121D	320 ± 19	371	360	-
23	Y134K	1680 ± 140	386	384	No
25	Y134K::R132F	-	397	394	-
28	Y134K::R132F::R111L::L121E	-	373	371	-
29	Y134K::R132F::R111L::T54E	1000 ± 100	379, 421	381, 418	-
35	L19W	2120 ± 300	381	380	-

CRABPII Wild-Type

Cloning Information:

Cloned into pl·T Blue2 vector (~3.6 Kb) from a pl·T 17b CRABPII containing plasmid.
Cloned between the restriction sites NcoI (5') and XhoI (3').
Construct size ~ 4.1 Kb Gene size ~ 0.5 Kb

CRABPII Wild-Type

Cloning Information:

Cloned into pET-Blue2 vector (~3.6 Kb) from a pET-17b CRABPII containing plasmid.
Cloned between the restriction sites NcoI (5') and XhoI (3').
Construct size : ~4.1 Kb Gene size : ~0.5 Kb

Primers Used:

bbb24 5' GGG CCA TGG CGC CAA ACT TCT CTG GCA AC
bbb26 5' GGG CTC GAG CTC TCG GAC GTA GAC

DNA Sequence of CRABPII WT as cloned into pET-Blue2

atggcgccaaacttctctggcaactggaaaatcatccgatcggaaaacttcgaggaattgctcaaa
gtgctgggggtgaatgtgatgctgaggaagattgctgtggctgcagcgtccaagccagcagtgga
gatcaaacaggagggagacactttctacatcaaaacctccaccaccgtgcgcaccacagagatta
acttcaaggttggggaggagtttgaggagcagactgtggatgggaggccctgtaagagcctggtg
aaatgggagagtgagaataaaatggtctgtgagcagaagctcctgaagggagagggccccaaga
cctcgtggaccagagaactgaccaacgatggggaactgatcctgaccatgacggcggatgacgtt
gtgtgcaccagggtctacgtccgagagctcgagcaccaccaccaccaccac

Protein Sequence of CRABPII WT as cloned into pET-Blue2

MAPNFSGNWKIIRSENFEELLKVLGVNVMLRKIAVA
AASKPAVEIKQEGDTFYIKTSTTVRTTEINFKVGEEF
EEQTVDGRPCKSLVKWESENKMVCEQKLLKGEGPK
TSWTRELTNDGELILTMTADDVVCTRVYVRELEHH
HHHH

** The third residue, Pro, is referenced as residue number one to maintain the same amino acid numbering as the original, non 6x-His-tag wild-type protein. The Met residue does not express in that system, and the Ala had to be added during the cloning into pET-Blue2.

CRABPII Wild-Type

Molecular Weight :

16829.21 Da

Calculated from http://us.expasy.org/tools/pi_tool.html

CRABPII Wild-Type

Molecular Weight :

16829.21 Da

Calculated from http://us.expasy.org/tools/pi_tool.html

Extinction Coefficient :

20,215 $M^{-1}cm^{-1}$

CD

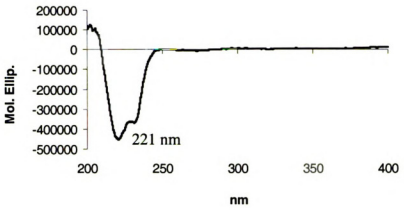

CRABPII Wild-Type
CD, Retinoic Acid

CRABPII Wild-Type

CD, Retinoic Acid

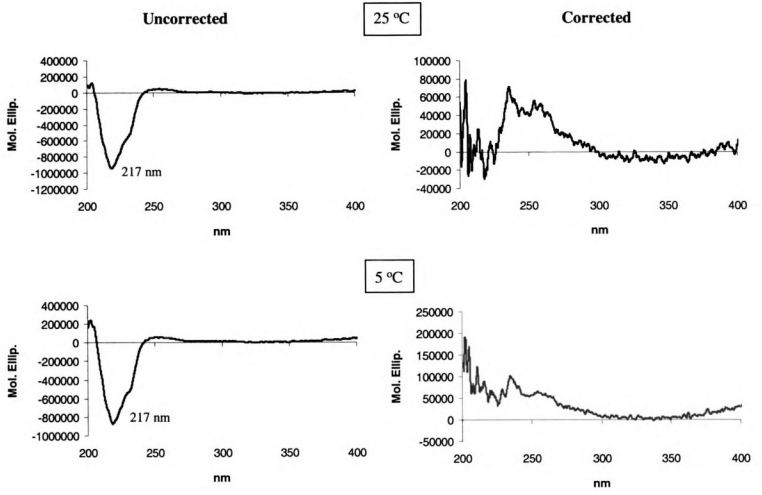

CRABPII Wild-Type
Fluorescence Titrations

CRABPII Wild-Type
Fluorescence Titrations

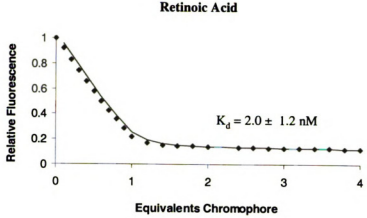

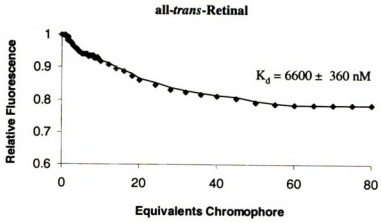

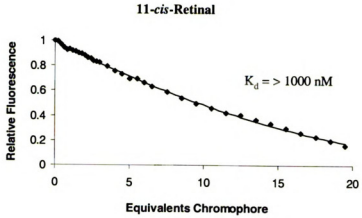

cRABPII Wild-Type

UV-vis Titrations, all-trans-Retinal

0.2 equivalents
0.4 equivalents
0.6 equivalents

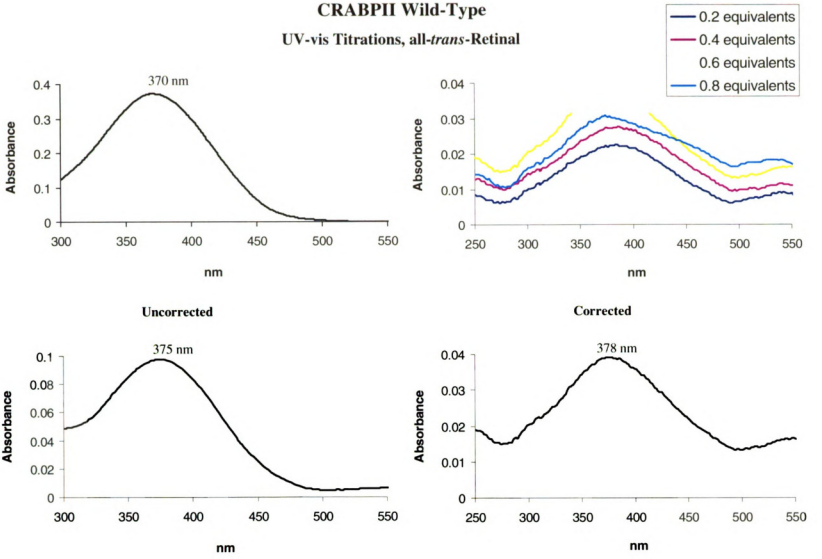
CRABPII Wild-Type
UV-vis Titrations, all-trans-Retinal
0.2 equivalents
0.4 equivalents
0.6 equivalents
0.8 equivalents
370 nm
Absorbance
nm
Uncorrected
375 nm
Corrected
378 nm

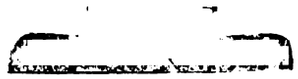

CRABPII Wild-Type
UV-vis Titrations, 11-cis-Retinal
Uncorrected

0.12 equivalents
0.24 equivalents

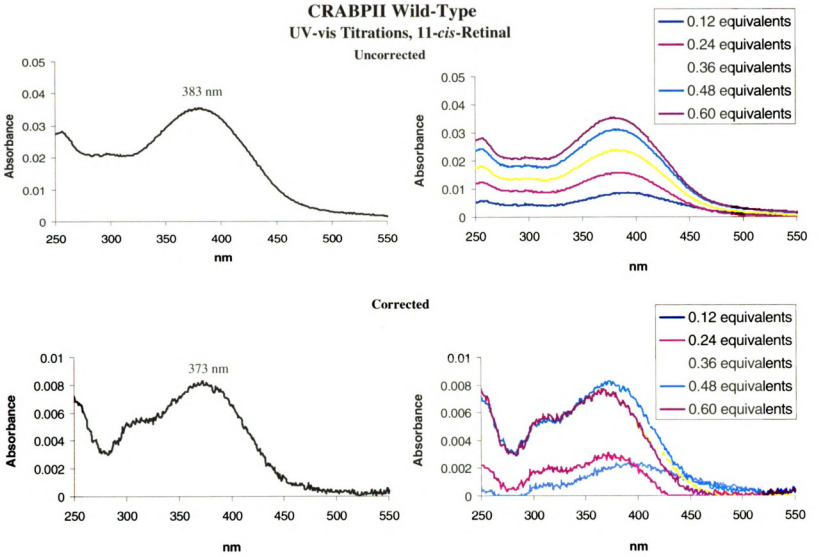
CRABPII Wild-Type
UV-vis Titrations, 11-cis-Retinal
Uncorrected
383 nm
Absorbance
nm
0.12 equivalents
0.24 equivalents
0.36 equivalents
0.48 equivalents
0.60 equivalents
Corrected
373 nm

CRABPII Wild-Type
MALDI-TOF, Protein

Calculated Mass = 16829.21 Da

CRABPII Wild-Type

MALDI-TOF, Protein

Calculated Mass = 16829.21 Da

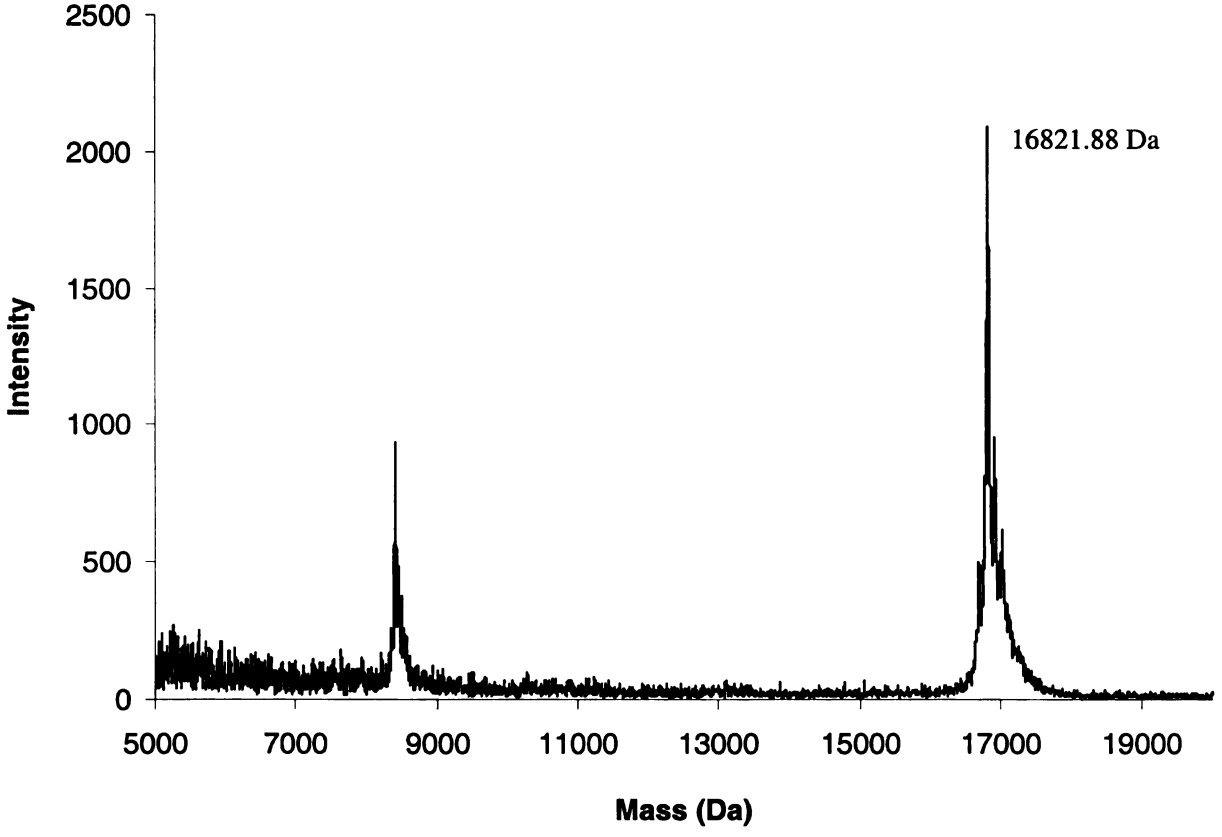

CRABPII Wild-Type
MALDI-TOF, Incubation with all-*trans*-Retinal
Protein Mass = 16829.21 Da
Positive Covalent Bond Formation = Protein Mass + 266

1000

CRABPII Wild-Type

MALDI-TOF, Incubation with all-*trans*-Retinal

Protein Mass = 16829.21 Da

Positive Covalent Bond Formation = Protein Mass + 266

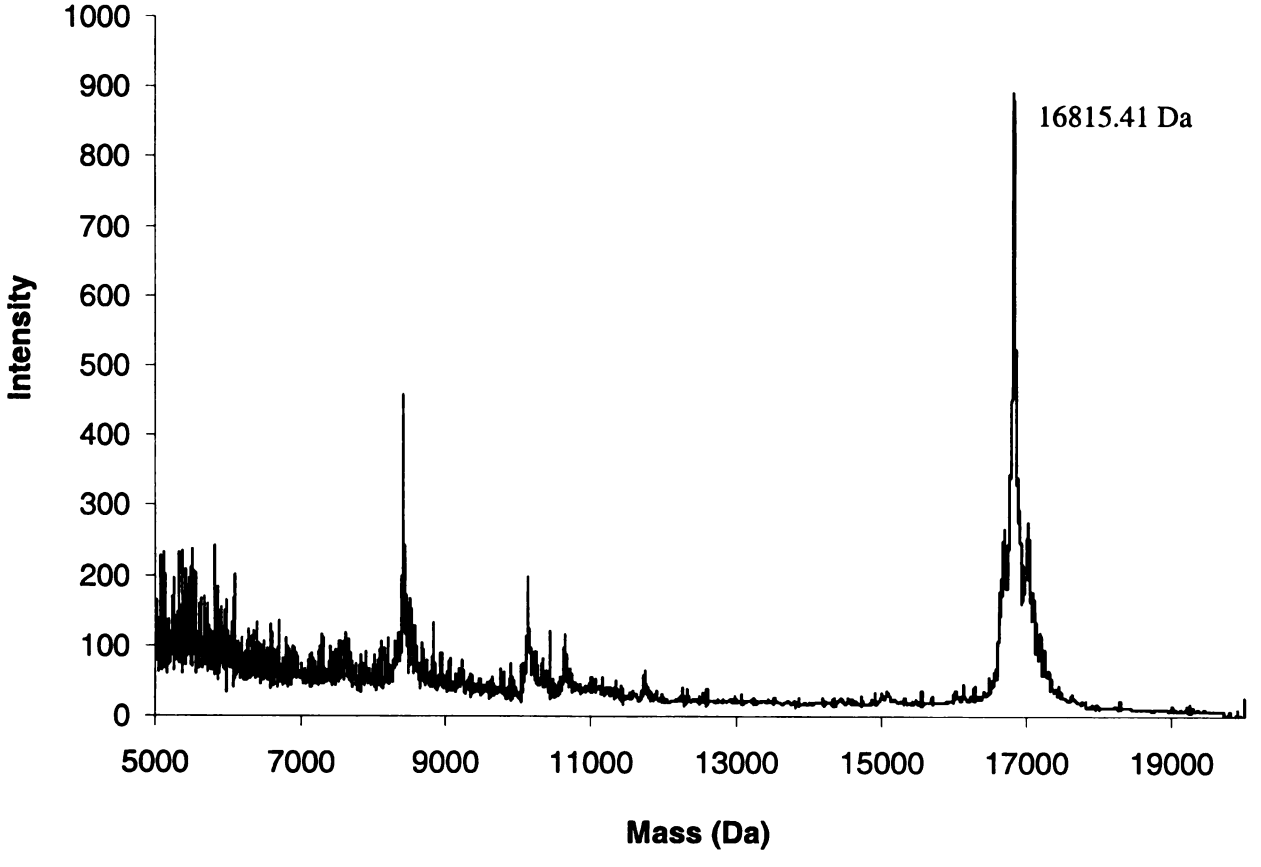

CRABPII Wild-Type

***MALDI-TOF*, Reductive Amination with all-*trans*-Retinal**

Protein Mass = 16829.21 Da

CRABPII Wild-Type

MALDI-TOF, Reductive Amination with all-*trans*-Retinal

Protein Mass = 16829.21 Da

Positive Reductive Amination = Protein Mass + 268

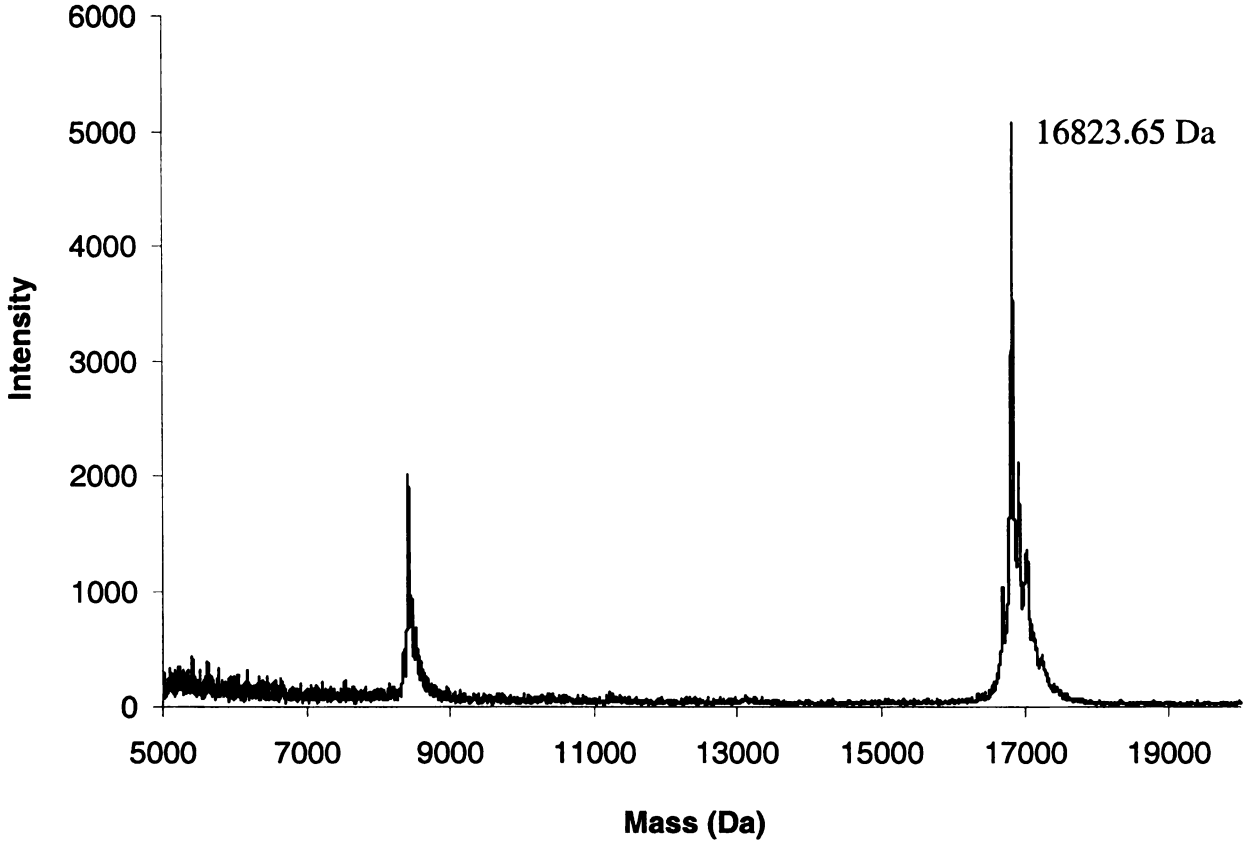

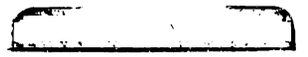

CRABPII Wild-Type
***MALDI-TOF*, Reductive Amination with 11-*cis*-Retinal**
Protein Mass = 16829.21 Da

CRABPII Wild-Type

MALDI-TOF, Reductive Amination with 11-*cis*-Retinal

Protein Mass = 16829.21 Da

Positive Reductive Amination = Protein Mass + 268

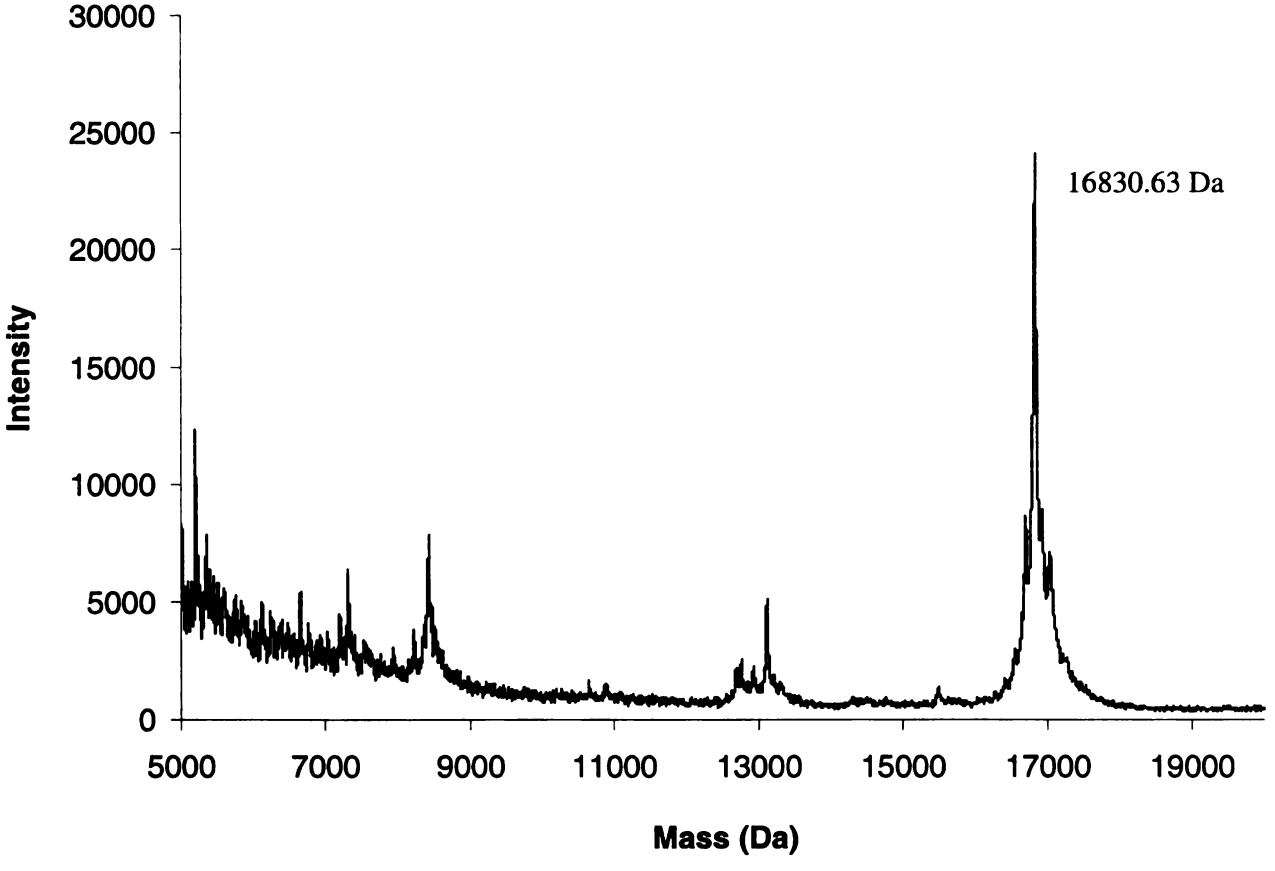

CRABPII Wild-Type
MALDI-TOF, Incubation with Retinoic Acid
Protein Mass = 16829.21 Da

CRABPII Wild-Type

MALDI-TOF, Incubation with Retinoic Acid

Protein Mass = 16829.21 Da

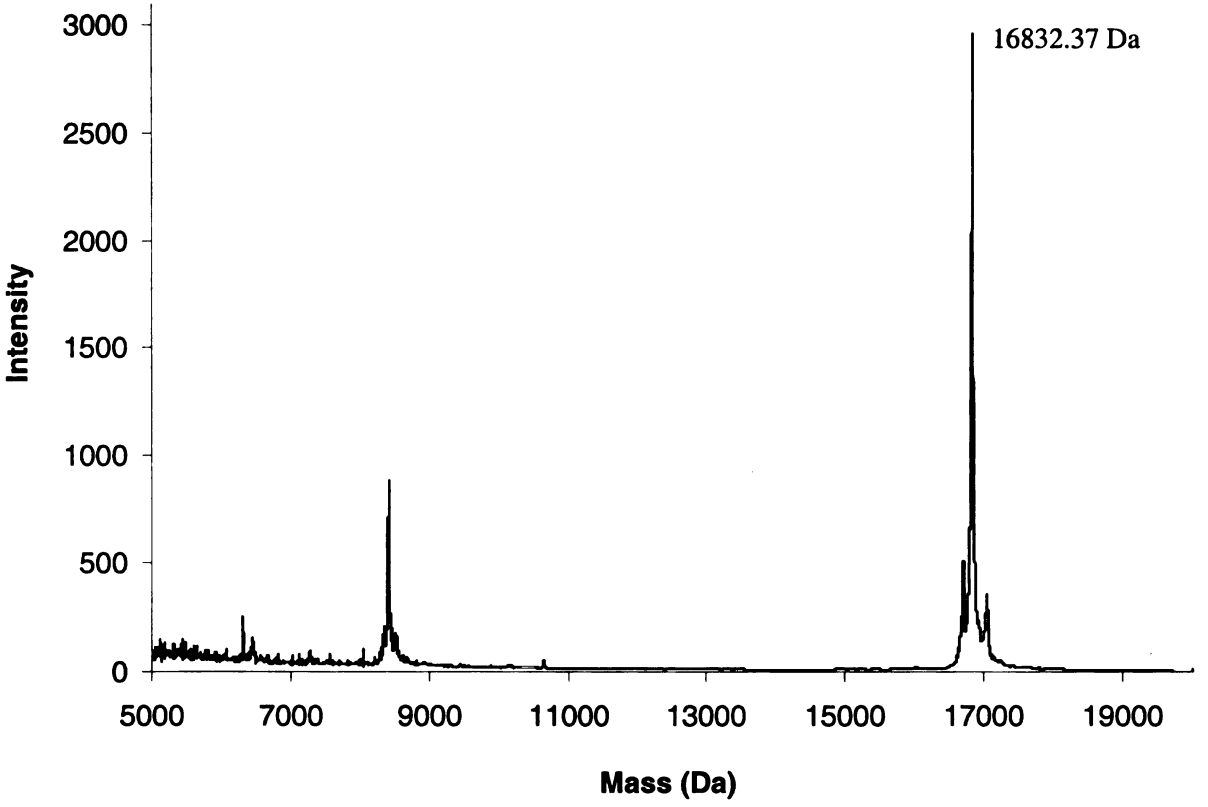

CRABPII R132K

Molecular Weight :
16801.20 Da

Extinction Coefficient :

CRABPII R132K

Molecular Weight :

16801.20 Da

Extinction Coefficient :

19,202 M^{-1} cm^{-1}

Primers :

bbb 27 5' CTC TCG GAC GTA GAC CTT GGT GCA CAC AAC GTC

bbb 28 5' GAC GTT GTG TGC ACC AAG GTC TAC GTC CGA GAG

(Primers given are to introduce the last mutation listed in the name.)

CD

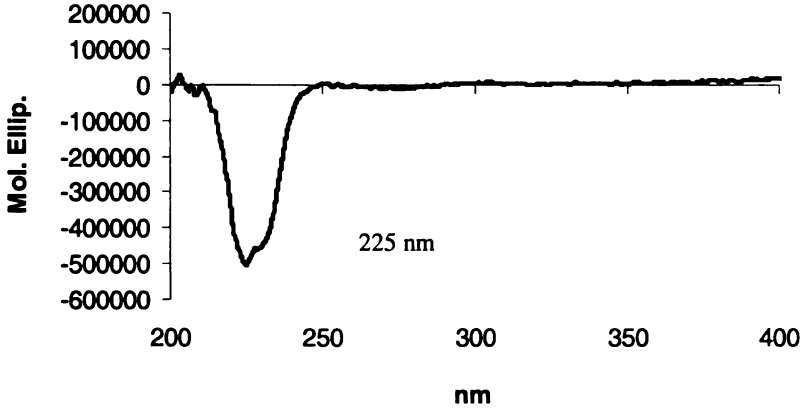

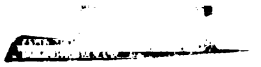

CRABPII R132K
Sequence BB 48

CRABPII R132K

Sequence BB 48

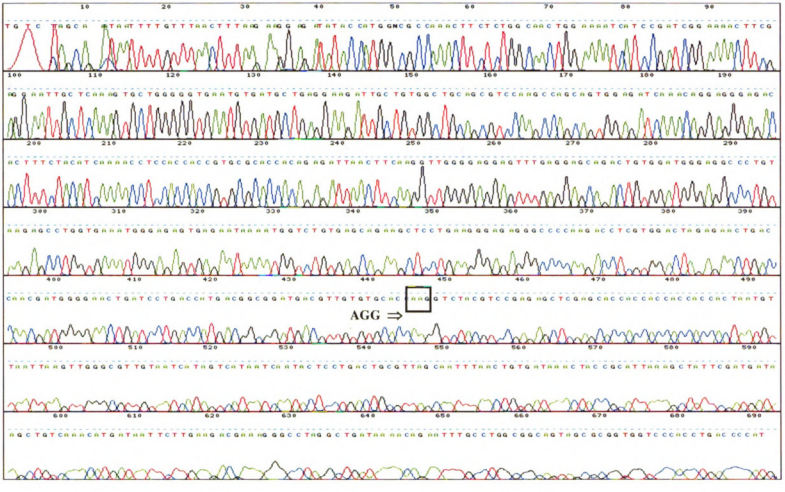

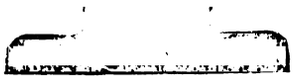

CRABPII R132K
Fluorescence Titrations

CRABPII R132K
Fluorescence Titrations

Retinoic Acid

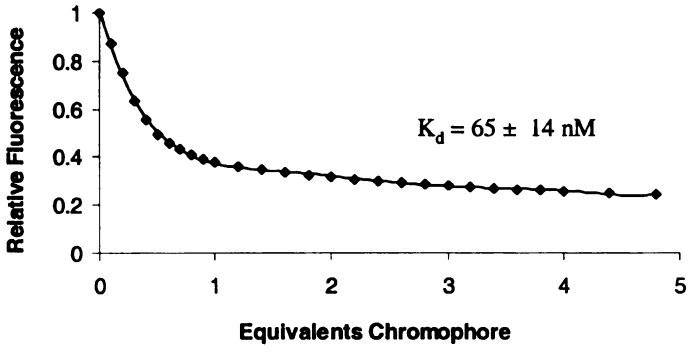

all-*trans*-Retinal

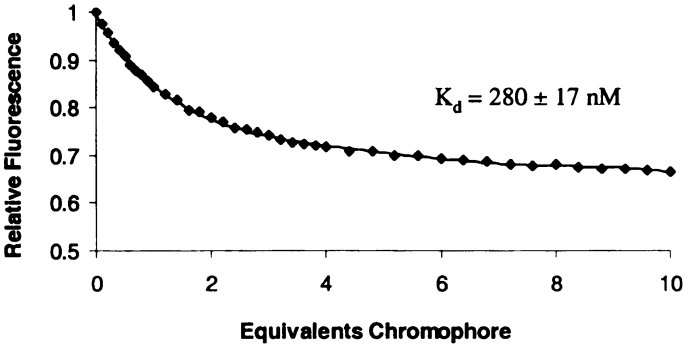

11-*cis*-Retinal

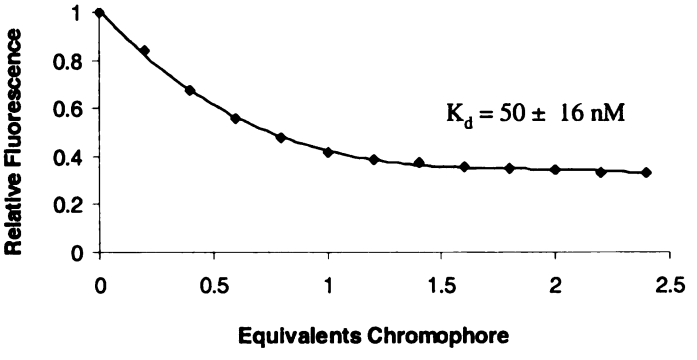

CRABPII R132K
***UV-vis* Titrations, all-*trans*-Retinal**

CRABPII R132K

UV-vis Titrations, all-*trans*-Retinal

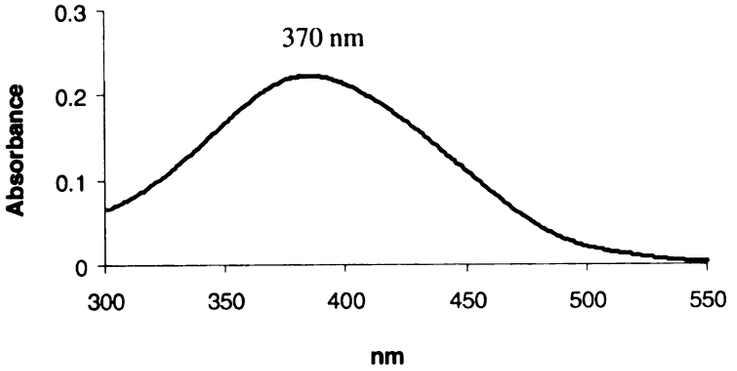

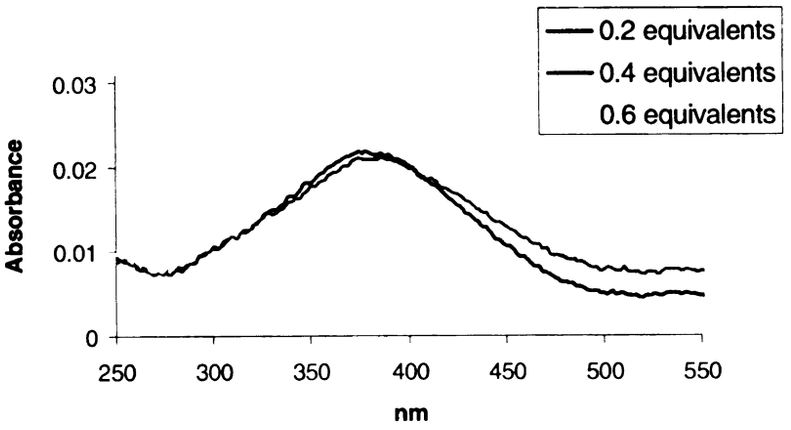

Uncorrected

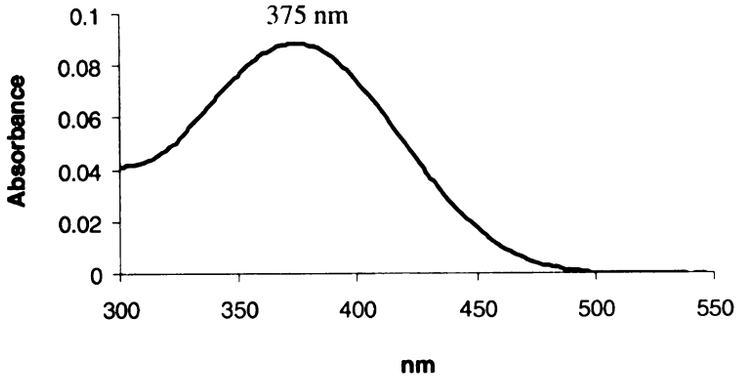

Corrected

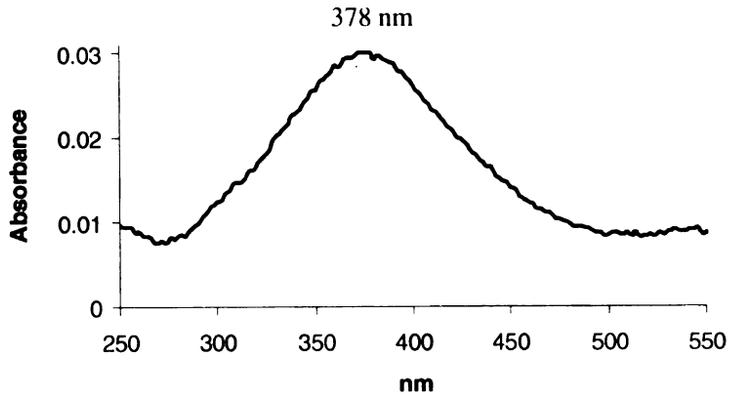

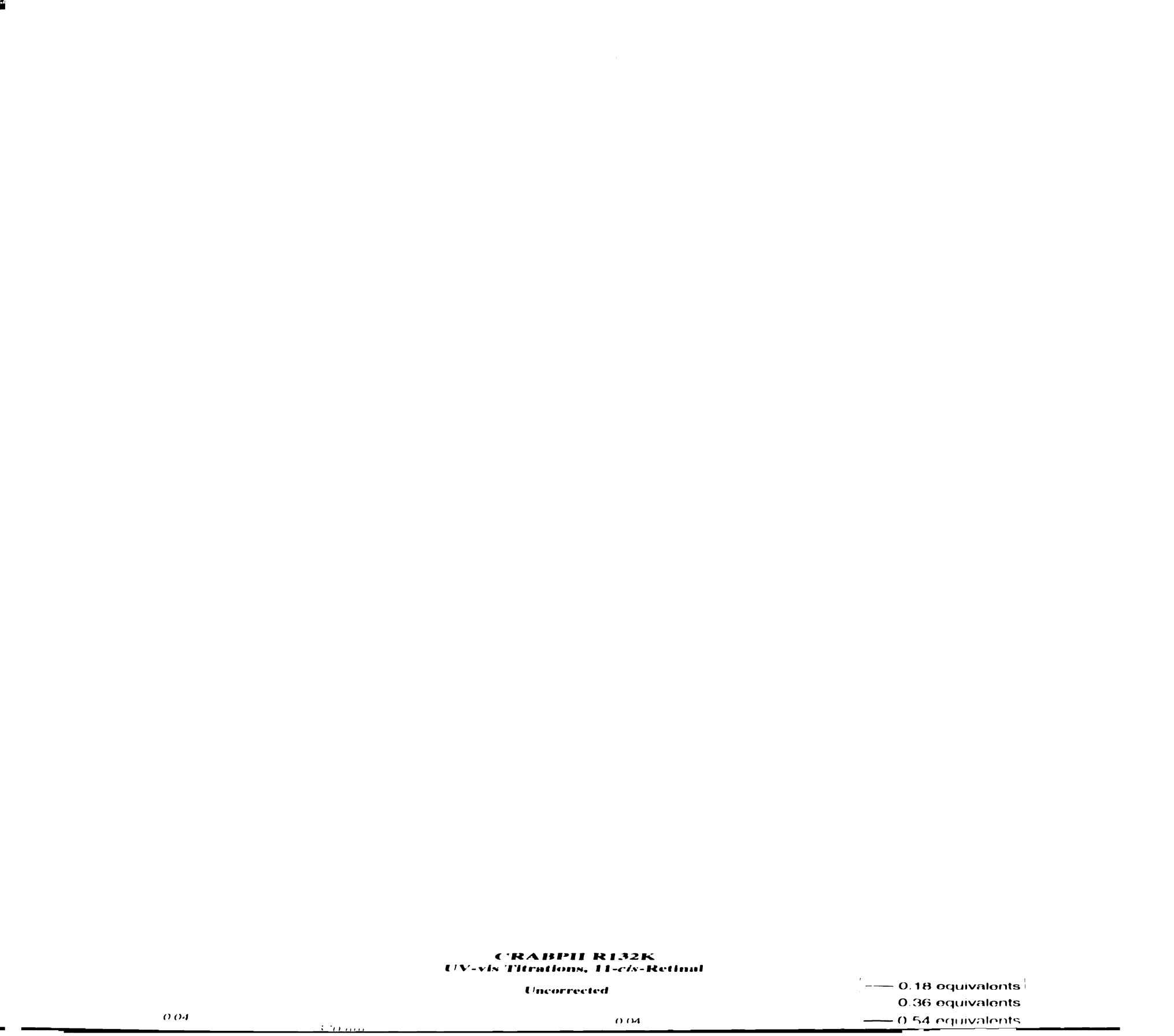
CRABPII R132K
UV-vis Titrations, 11-cis-Retinal
Uncorrected
0.18 equivalents
0.36 equivalents
0.54 equivalents
0.04
0.04

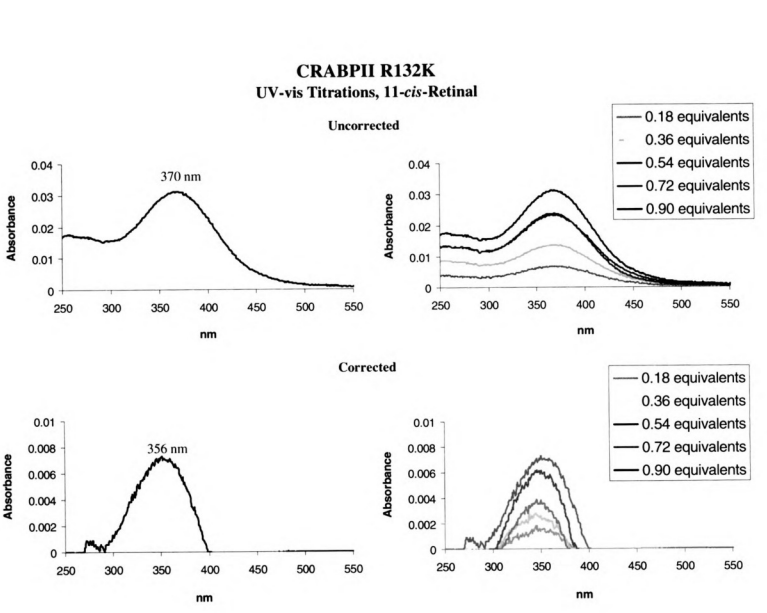
CRABPII R132K
UV-vis Titrations, 11-cis-Retinal
Uncorrected
370 nm
Absorbance
nm
0.18 equivalents
0.36 equivalents
0.54 equivalents
0.72 equivalents
0.90 equivalents
Corrected
356 nm
Absorbance
nm
0.18 equivalents
0.36 equivalents
0.54 equivalents
0.72 equivalents
0.90 equivalents

CRABPII R132K

MALDI-TOF, Protein

Calculated Mass = 16801.20 Da

CRABPII R132K

MALDI-TOF, Protein

Calculated Mass = 16801.20 Da

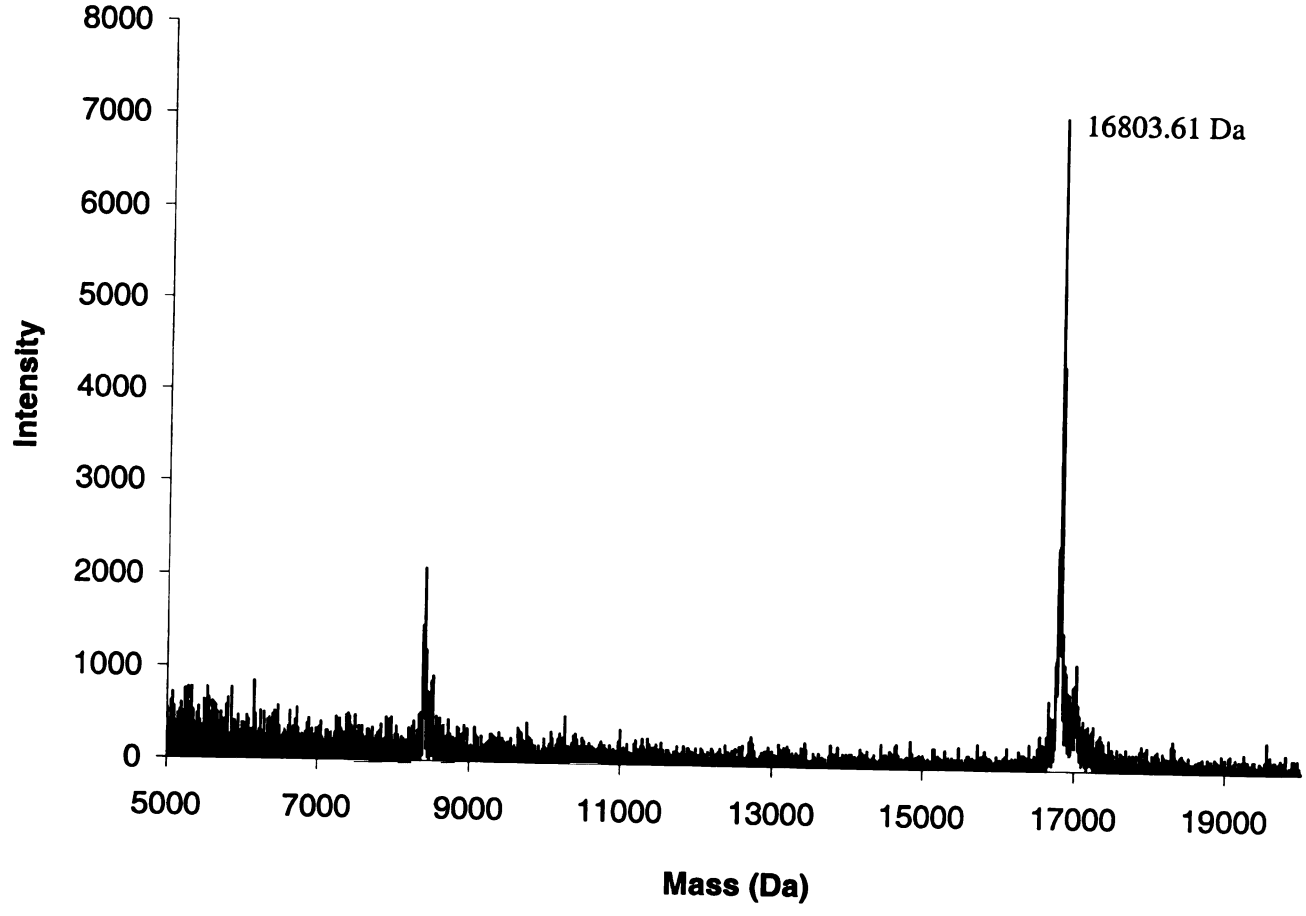

CRABPII R132K
MALDI-TOF, Incubation with all-*trans*-Retinal
Protein Mass = 16801.20 Da

CRABPII R132K

MALDI-TOF, Incubation with all-*trans*-Retinal

Protein Mass = 16801.20 Da

Positive Covalent Bond Formation = Protein Mass + 266

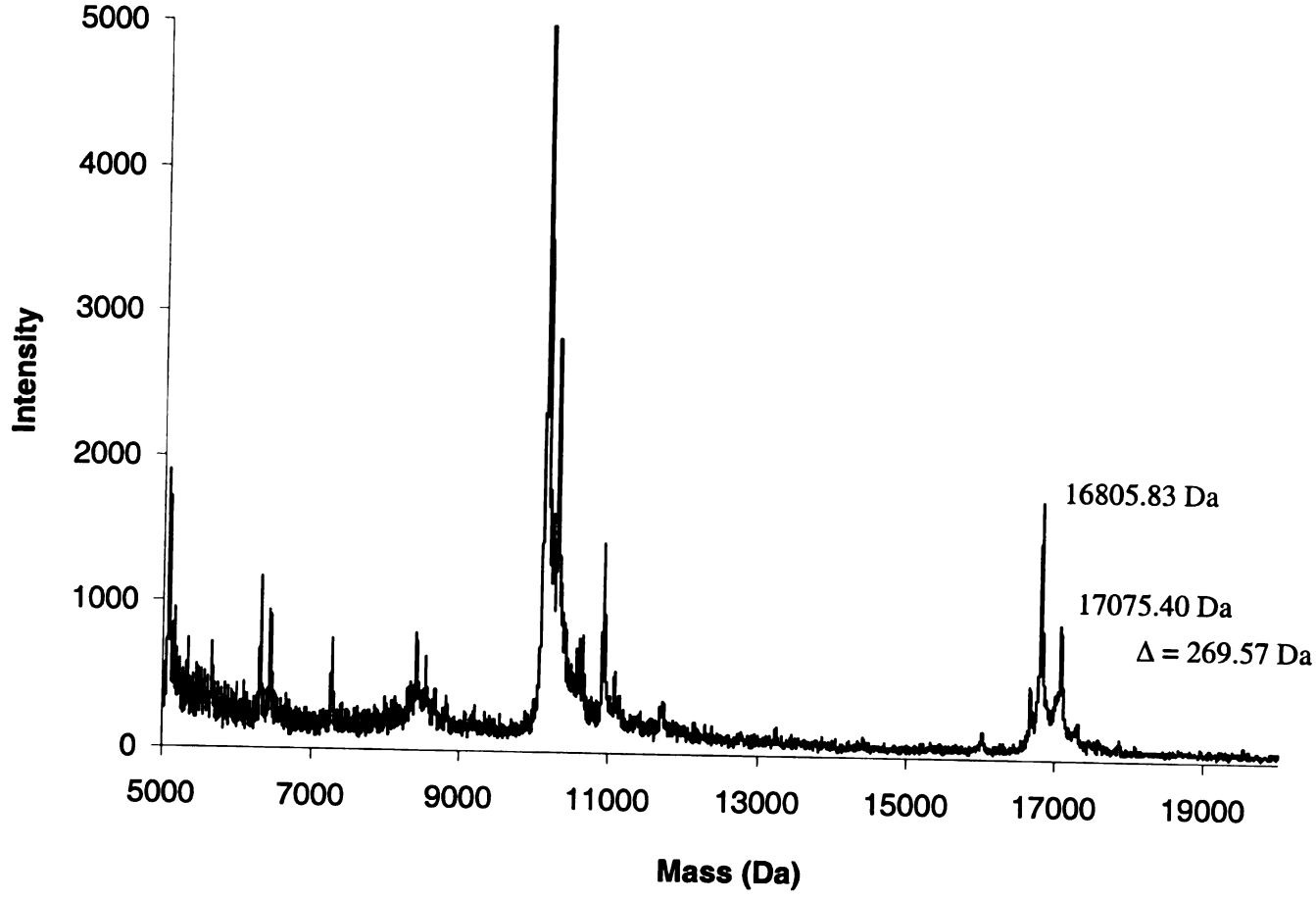

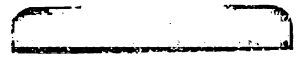

CRABPII R132K
***MALDI-TOF*, Reductive Amination with all-*trans*-Retinal**
Protein Mass = 16801.20 Da

CRABPII R132K

MALDI-TOF, Reductive Amination with all-*trans*-Retinal

Protein Mass = 16801.20 Da

Positive Reductive Amination = Protein Mass + 268

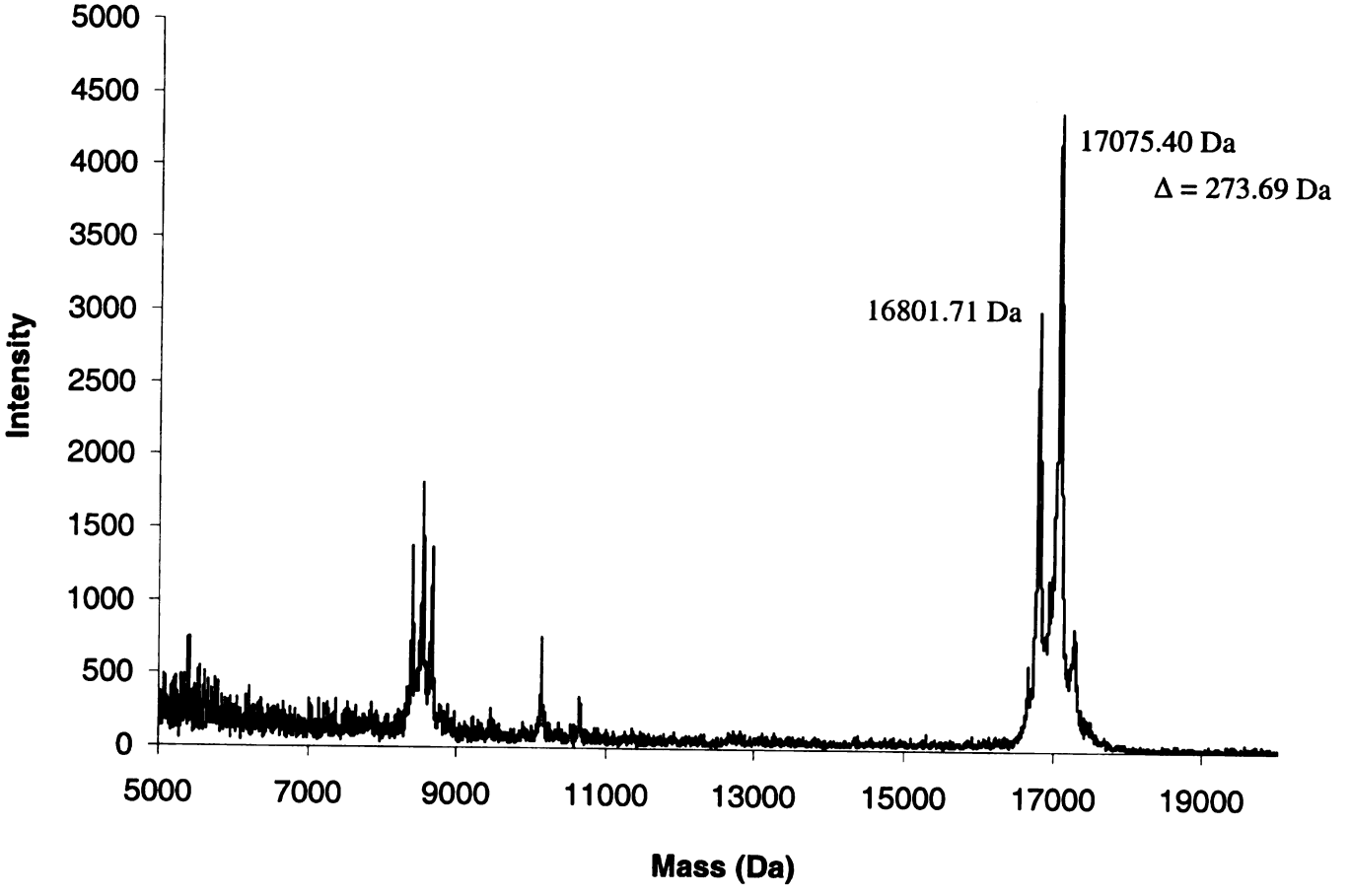

CRABPII R132K
MALDI-TOF, Reductive Amination with 11-*cis*-Retinal
Protein Mass = 16801.20 Da
Positive Reductive Amination = Protein Mass + 268

12000

CRABPII R132K

MALDI-TOF, Reductive Amination with 11-*cis*-Retinal

Protein Mass = 16801.20 Da

Positive Reductive Amination = Protein Mass + 268

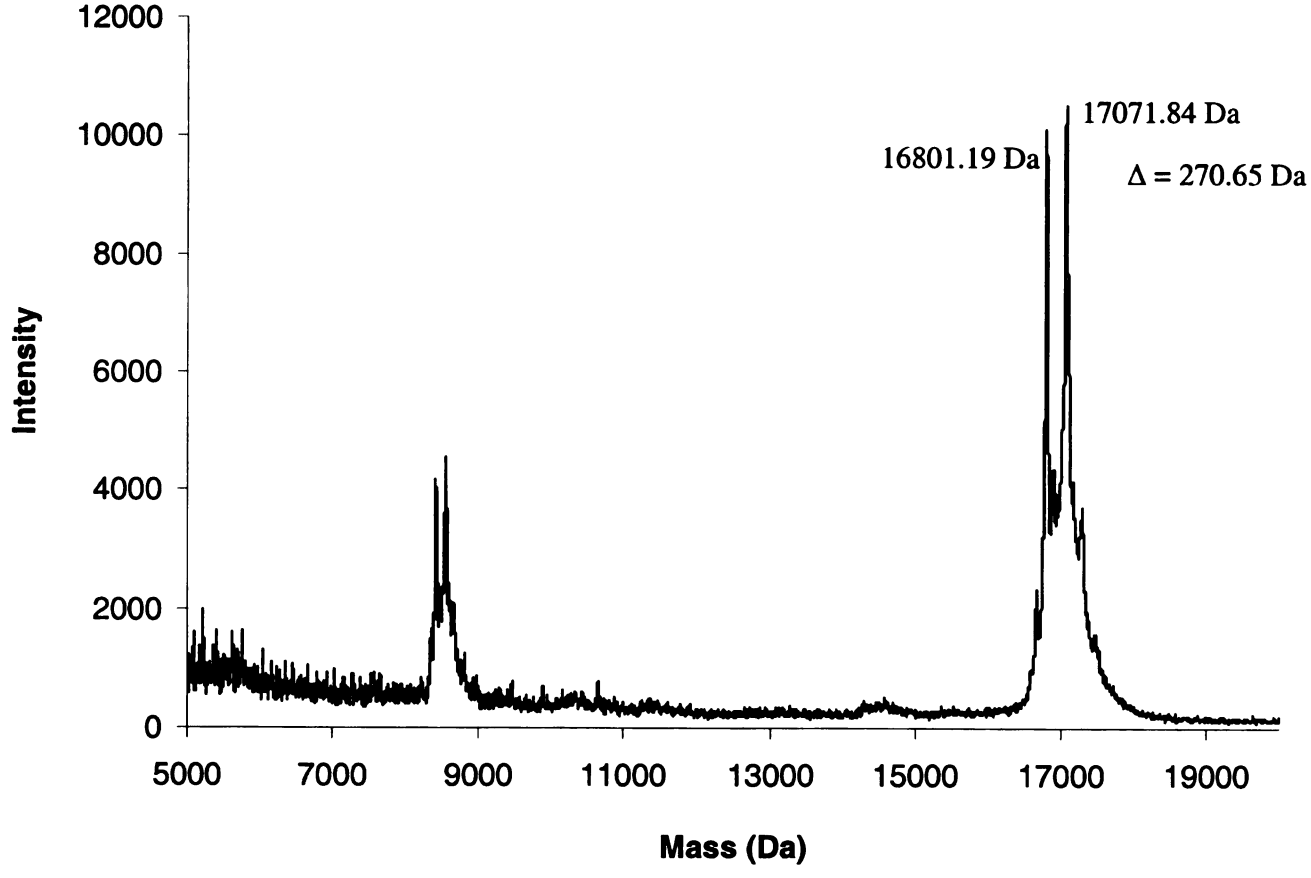

CRABPII R132K::Y134F

Molecular Weight :

16785.20 Da

CRABPII R132K::Y134F

Molecular Weight :
16785.20 Da

Extinction Coefficient :
18,317 M^{-1} cm^{-1}

Primers :
bbb30 5' GTT GTG TGC ACC AAG GTC TTC GTC CGA GAG CTC GAG
bbb31 5' CTC GAG CTC TCG GAC GAA GAC CTT GGT GCA CAC AAC

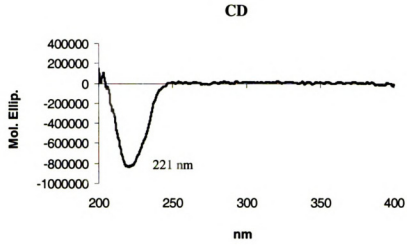

CRABPII R132K::Y134F
Sequence BB 171

CRABPII R132K::Y134F
Sequence BB 171

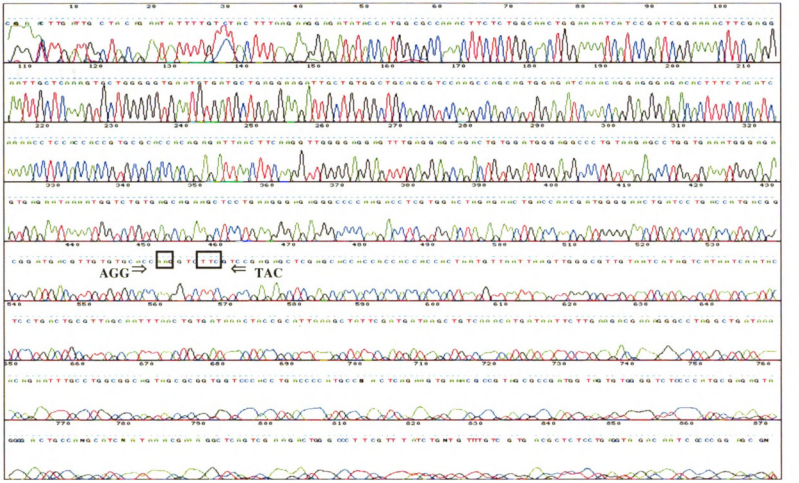

CRABPII R132K::Y134F
Fluorescence Titrations

Retinoic Acid

CRABPII R132K::Y134F
Fluorescence Titrations

Retinoic Acid

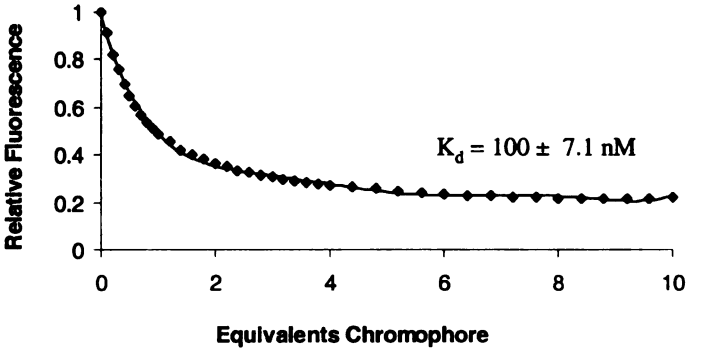

all-*trans*-Retinal

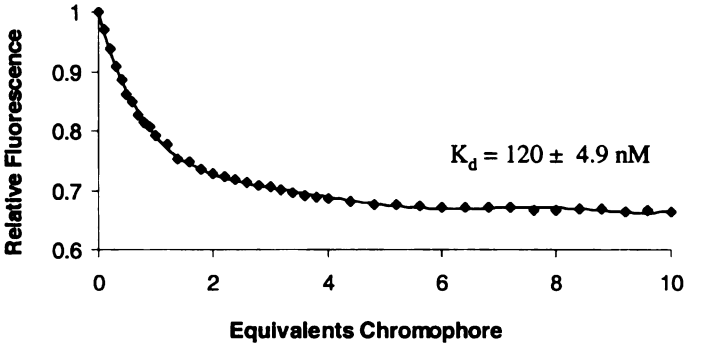

11-*cis*-Retinal

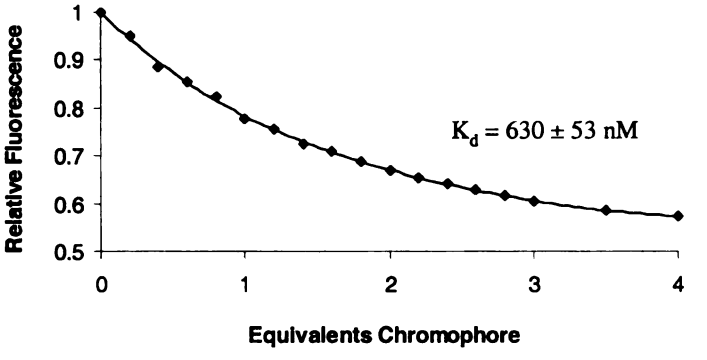

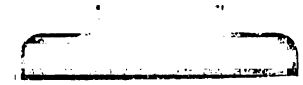

CRABPII R132K::Y134F
***UV-vis* Titrations, all-*trans*-Retinal**

0.2 equivalents
0.4 equivalents

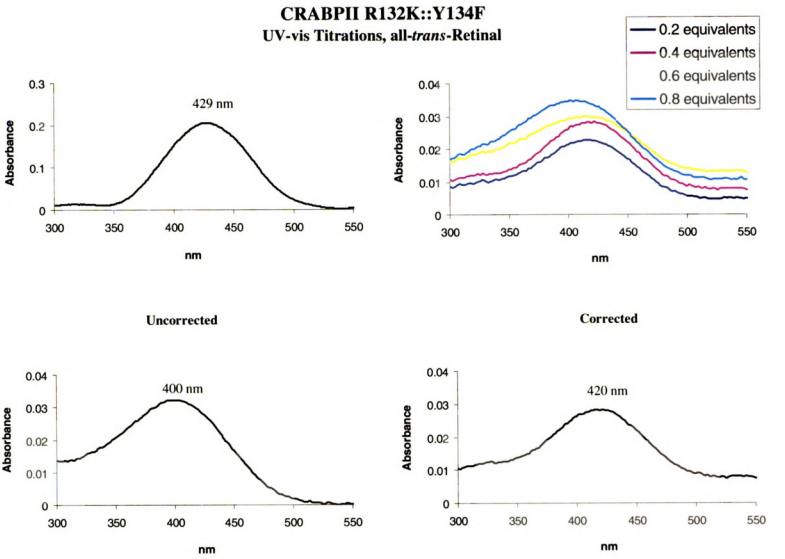
CRABPII R132K::Y134F
UV-vis Titrations, all-trans-Retinal
0.2 equivalents
0.4 equivalents
0.6 equivalents
0.8 equivalents
429 nm
Absorbance
nm
Uncorrected
Corrected
400 nm
420 nm

CRABPII R132K::Y134F
***UV-vis* Titrations, 11-*cis*-Retinal**

Uncorrected

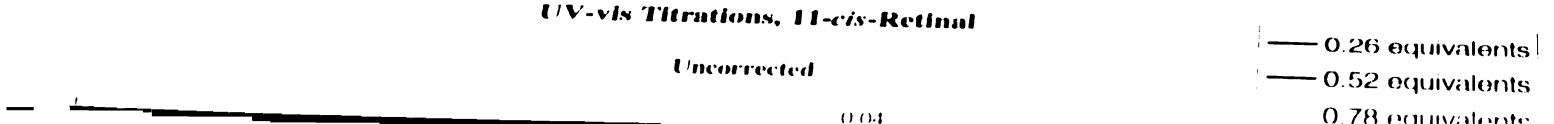

CRABPII R132K::Y134F

UV-vis Titrations, 11-*cis*-Retinal

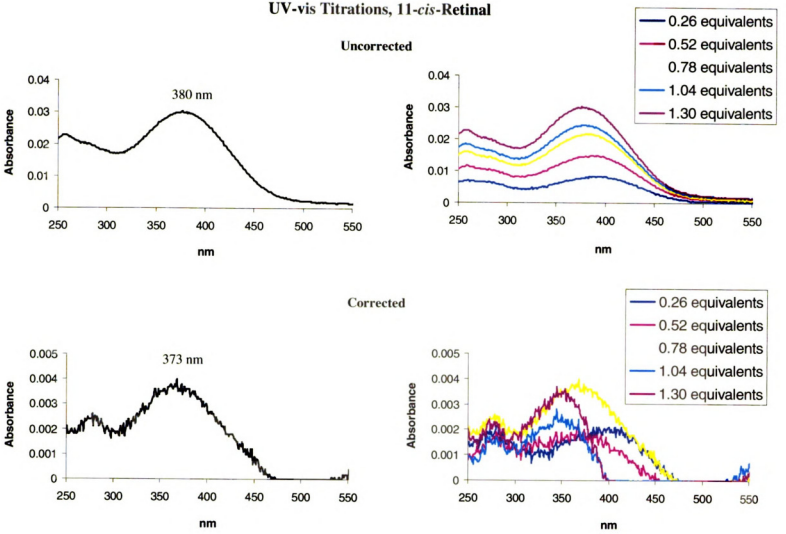

CRABPII R132K::Y134F
MALDI-TOF, Protein
Calculated Mass = 16785.20 Da

7000

CRABPII R132K::Y134F

MALDI-TOF, Protein

Calculated Mass = 16785.20 Da

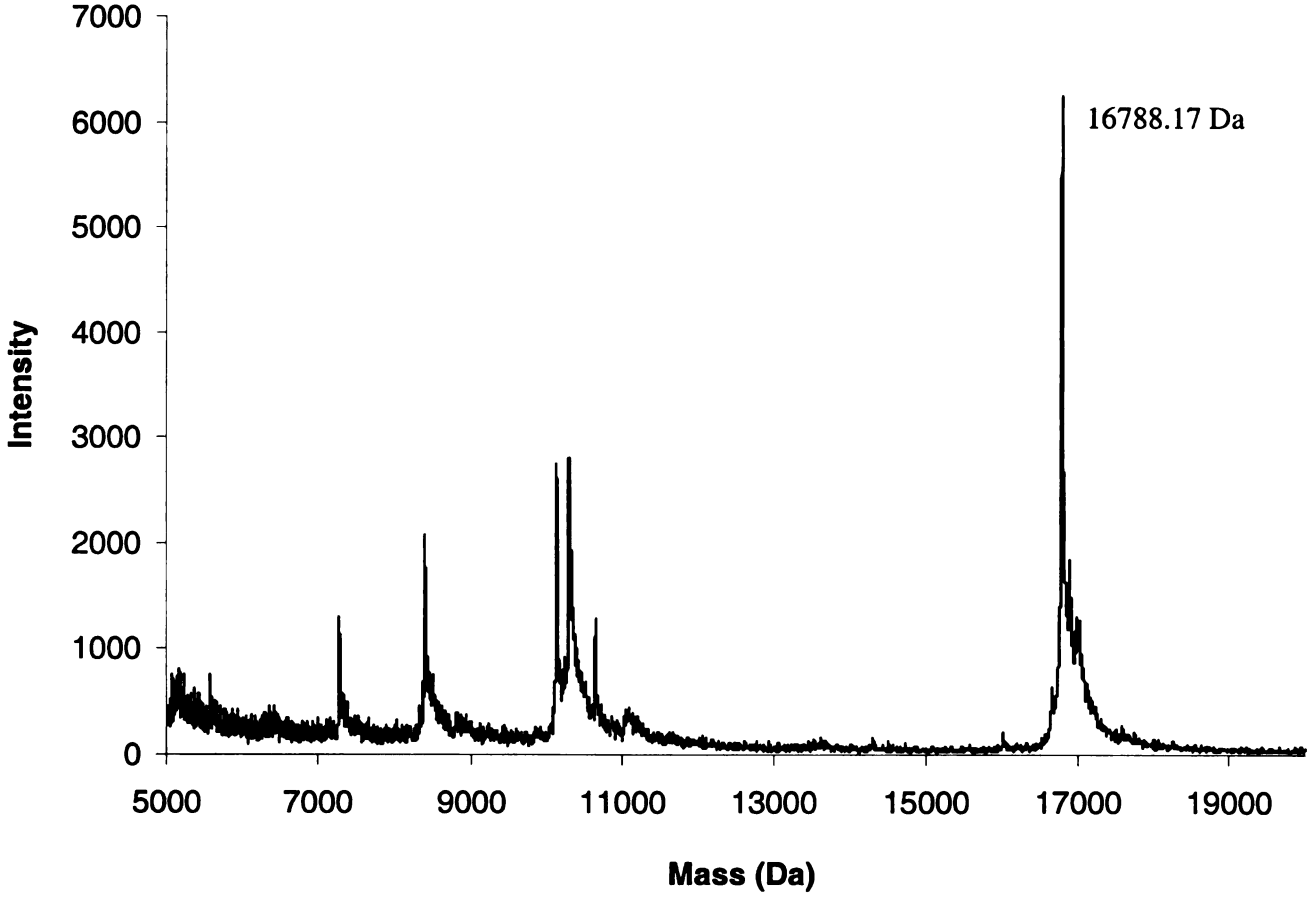

CRABPII R132K::Y134F

***MALDI-TOF*, Incubation with all-*trans*-Retinal**

CRABPII R132K::Y134F

MALDI-TOF, Incubation with all-*trans*-Retinal

Protein Mass = 16785.20 Da

Positive Covalent Bond Formation = Protein Mass + 266

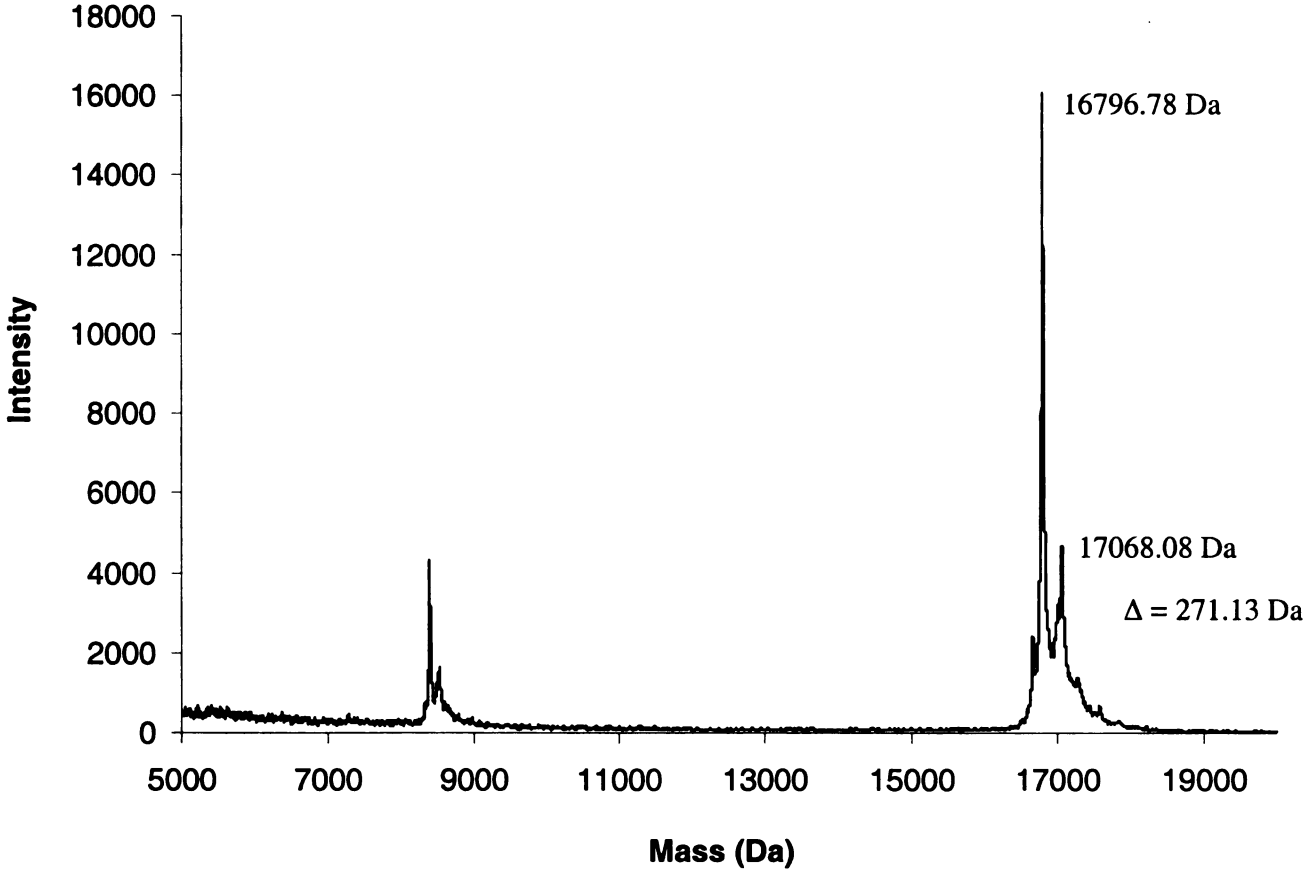

CRABPII R132K::Y134F

MALDI-TOF, Reductive Amination with all-*trans*-Retinal

Protein Mass = 16785.20 Da

Positive Reductive Amination = Protein Mass + 268

8000

CRABPII R132K::Y134F

MALDI-TOF, Reductive Amination with all-*trans*-Retinal

Protein Mass = 16785.20 Da

Positive Reductive Amination = Protein Mass + 268

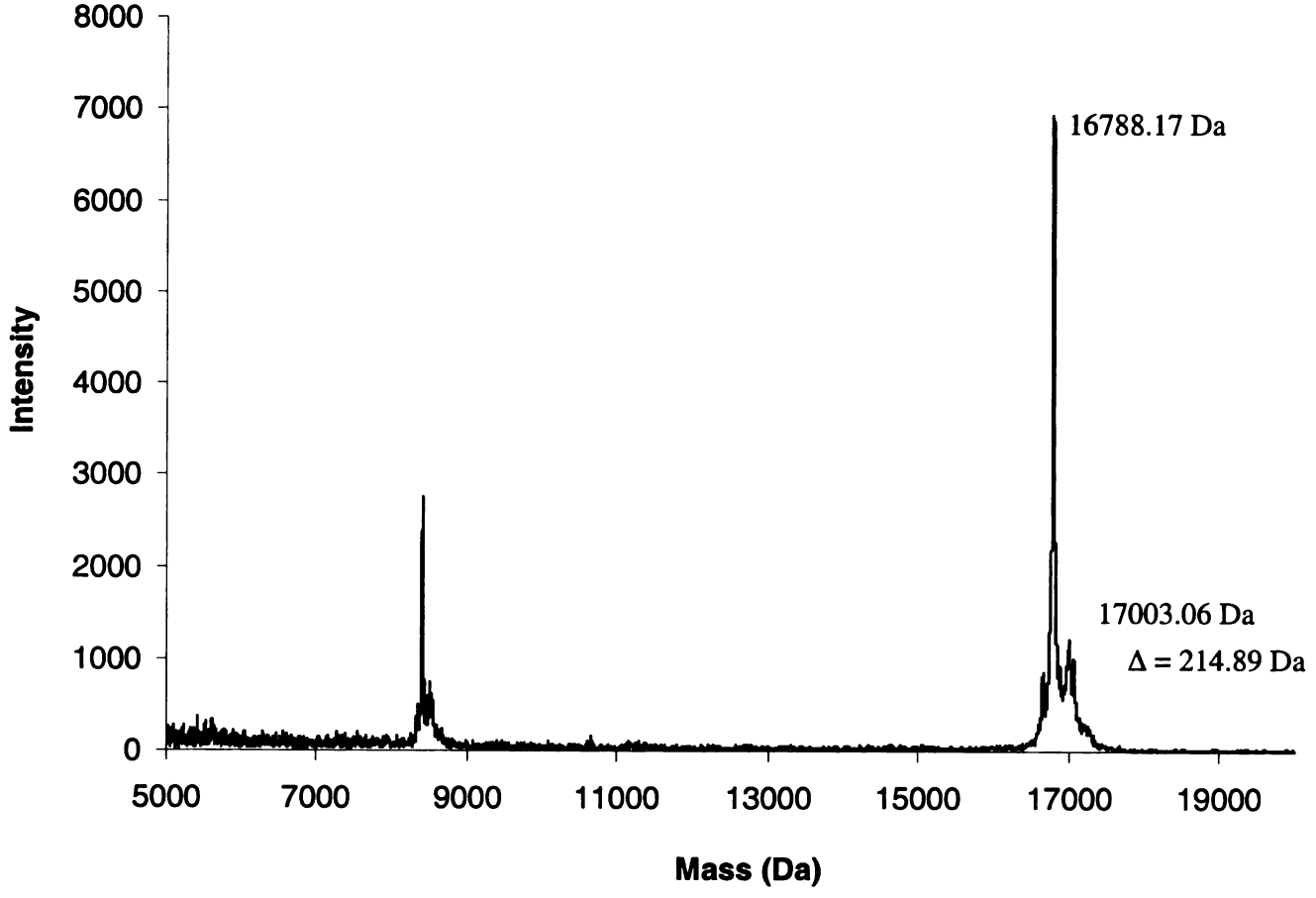

CRABPII R132K::Y134F

MALDI-TOF, Reductive Amination with 11-*cis*-Retinal

Protein Mass = 16785.20 Da

Positive Reductive A

5000

CRABPII R132K::Y134F

MALDI-TOF, Reductive Amination with 11-*cis*-Retinal

Protein Mass = 16785.20 Da

Positive Reductive Amination = Protein Mass + 268

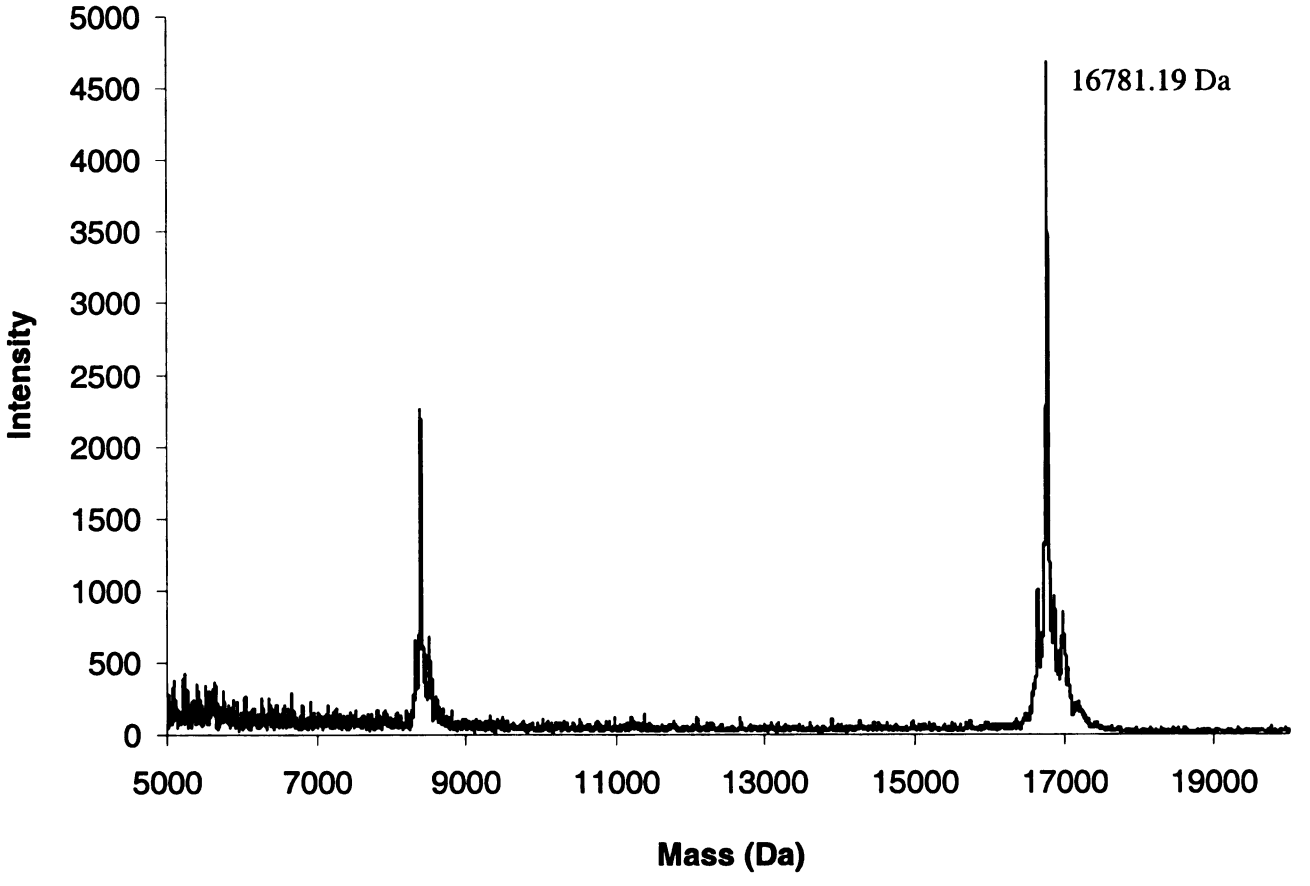

CRABPII R132K::Y134F::R111E

Molecular Weight :

16758.13 Da

Extinction Coefficient :

CRABPII R132K::Y134F::R111E

Molecular Weight :

16758.13 Da

Extinction Coefficient :

16,698 M^{-1} cm^{-1}

Primers :

bbb33 5' TCG TGG ACC GAG GAA CTG ACC
bbb34 5' GGT CAG TTC CTC GGT CCA CGA

CD

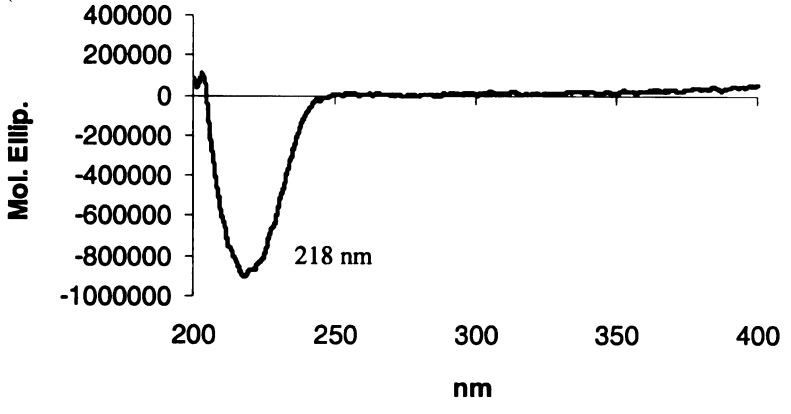

CRABPII R132K::Y134F::R111E
Sequence BB 172

CRABPII R132K::Y134F::R111E

Sequence BB 172

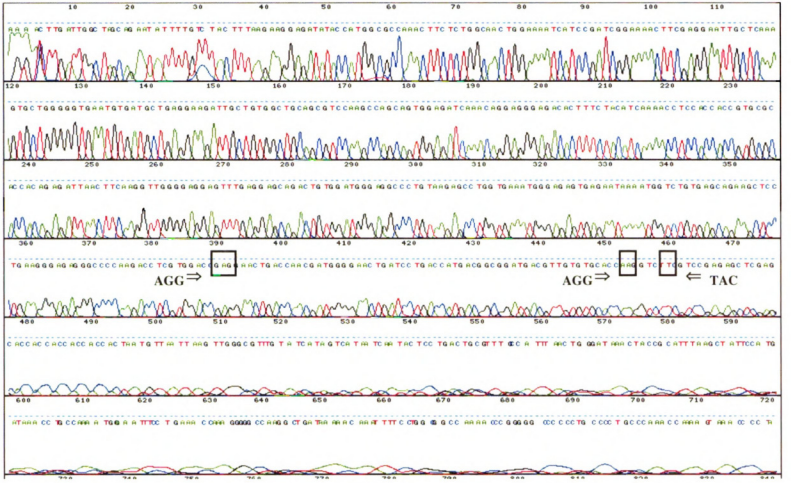

CRABPII R132K::Y134F::R111E
Fluorescence Titrations

Retinoic Acid

all-*trans*-Retinal

CRABPII R132K::Y134F::R111E

Fluorescence Titrations

Retinoic Acid

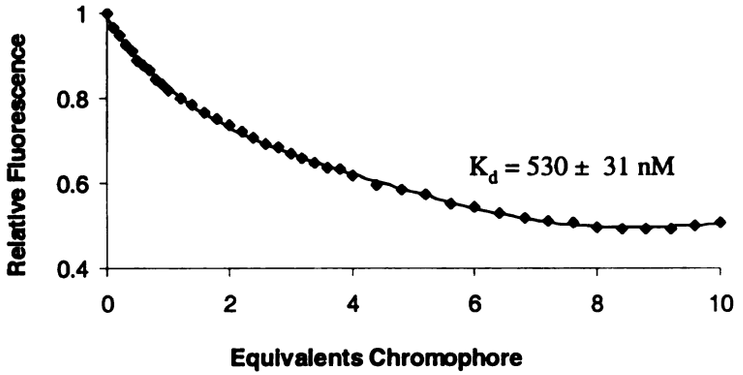

all-*trans*-Retinal

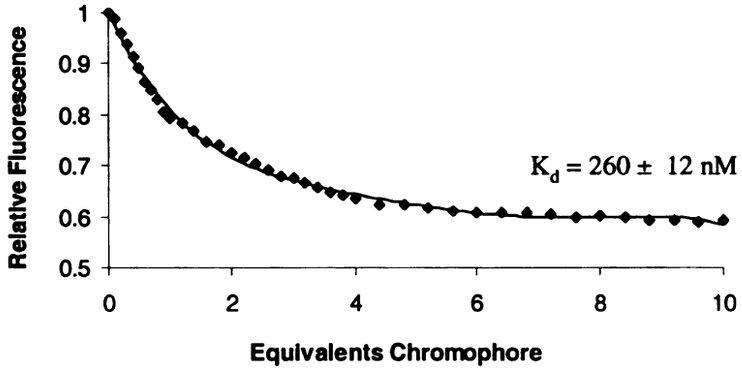

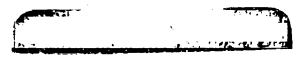

CRABPII R132K::Y134F::R111E

All-trans-Retinal

CRABPII R132K::Y134F::R111E

UV-vis Titrations, all-*trans*-Retinal

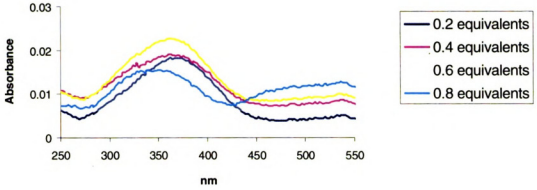

Uncorrected

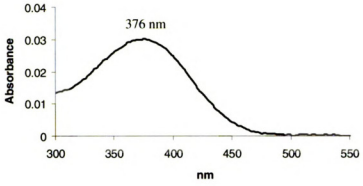

Corrected

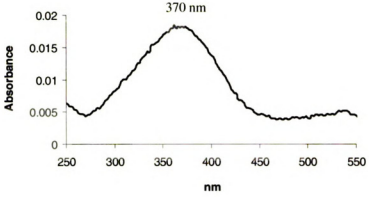

CRABPII R132K::Y134F::R111E
MALDI-TOF, Protein
Calculated Mass = 16758.13 Da

CRABPII R132K::Y134F::R111E

MALDI-TOF, Protein

Calculated Mass = 16758.13 Da

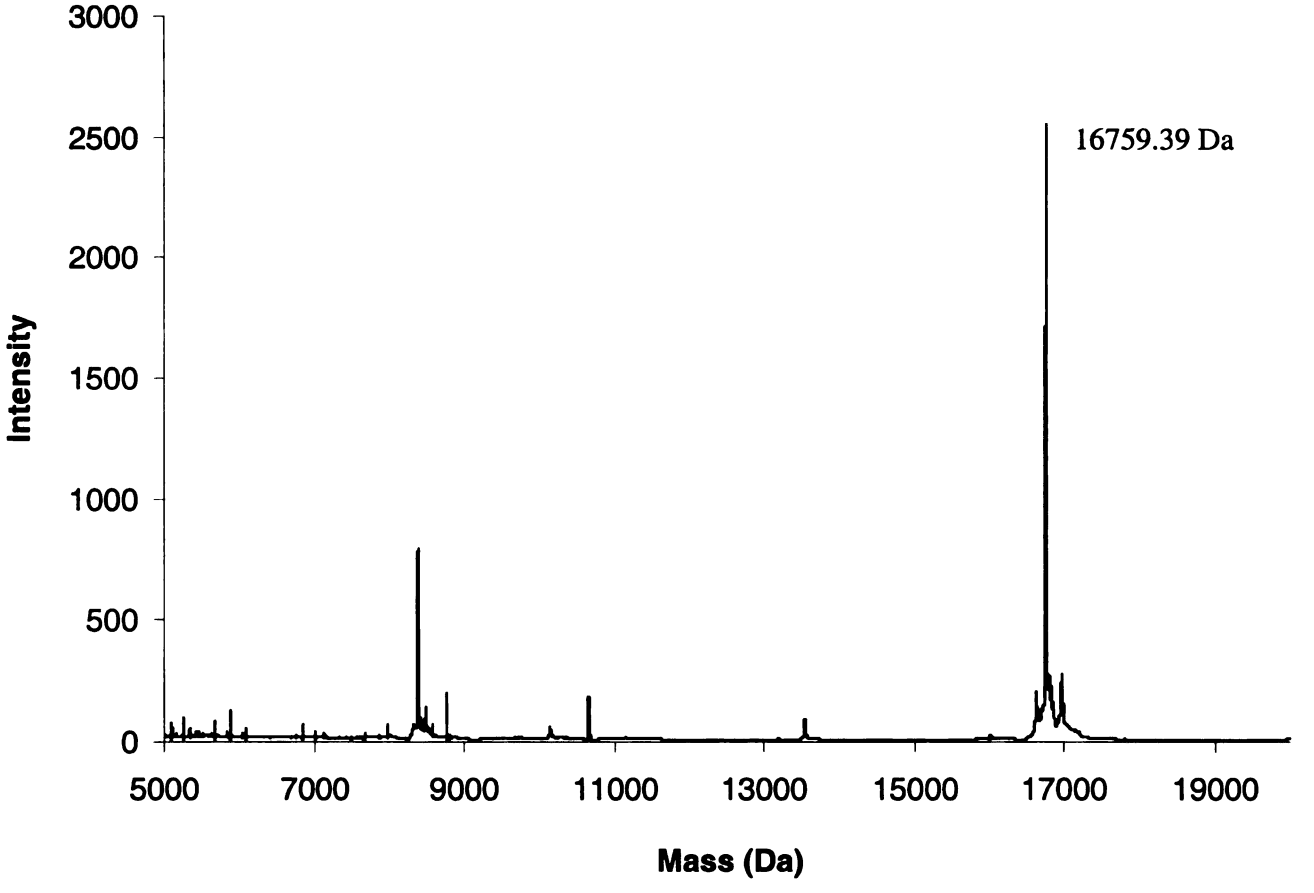

CRABPII R132K::Y134F::R111E

MALDI-TOF, Incubation with all-*trans*-Retinal

Protein Mass = 16758.13 Da

Schiff Base Formation = Protein Mass + 266

20000

CRABPII R132K::Y134F::R111E

MALDI-TOF, Incubation with all-*trans*-Retinal

Protein Mass = 16758.13 Da

Positive Covalent Bond Formation = Protein Mass + 266

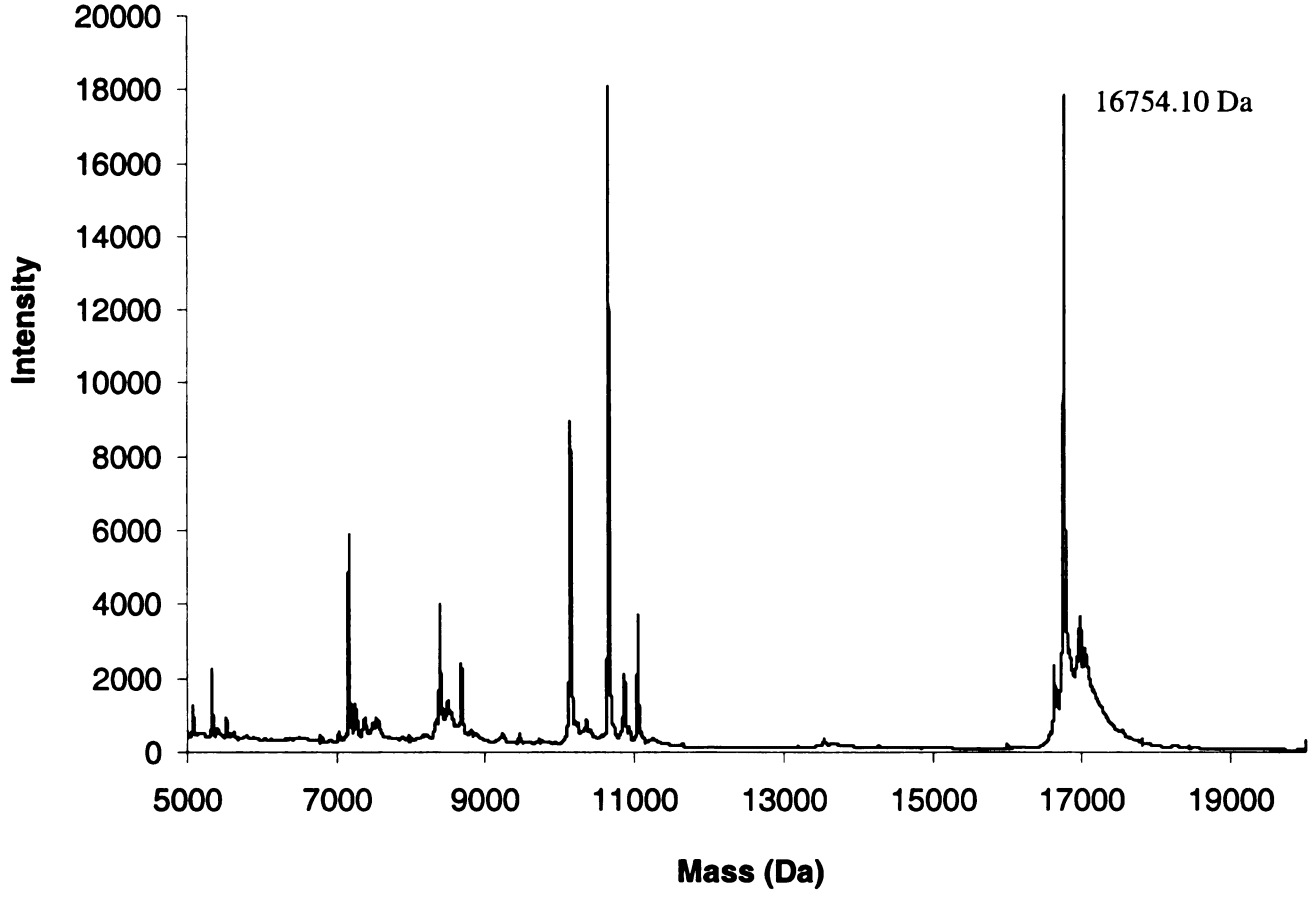

CRABPII R132K::Y134F::R111E
MALDI-TOF, Reductive Amination with all-*trans*-Retinal
Protein Mass = 16758.13 Da
Positive Reductive Amination = Protein Mass + 268

CRABPII R132K::Y134F::R111E

MALDI-TOF, Reductive Amination with all-*trans*-Retinal

Protein Mass = 16758.13 Da

Positive Reductive Amination = Protein Mass + 268

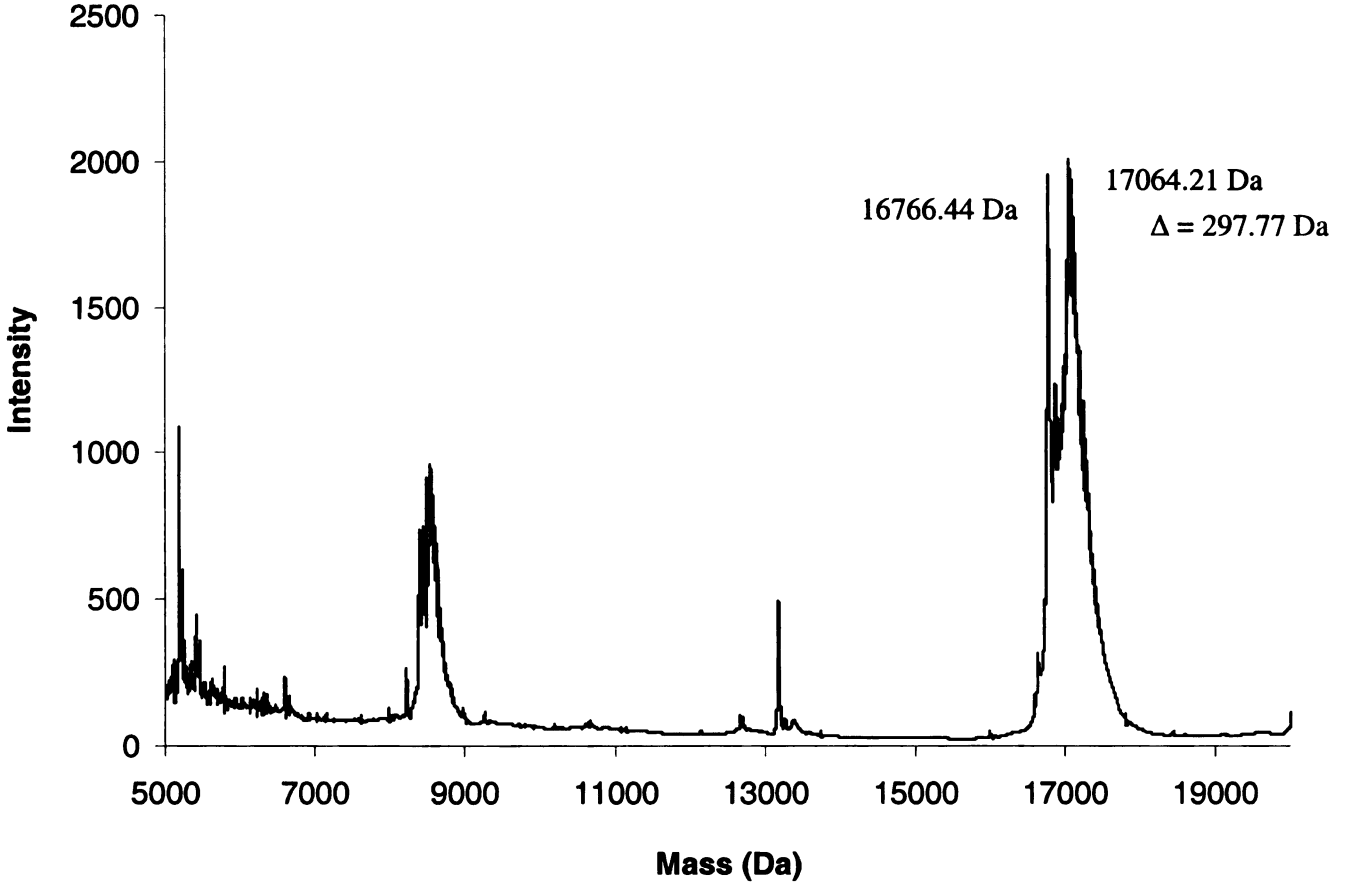

CRABPII R132K::Y134F::R111E::T54V

Molecular Weight :

16756.16 Da

CRABPII R132K::Y134F::R111E::T54V

Molecular Weight :

16756.16 Da

Extinction Coefficient :

17,214 M^{-1} cm^{-1}

Primers :

bbb67 5' CTA CAT CAA AGT CTC CAC CAC CGT GCG
bbb68 5' CGC ACG GTG GTG GAG ACT TTG ATG TAG

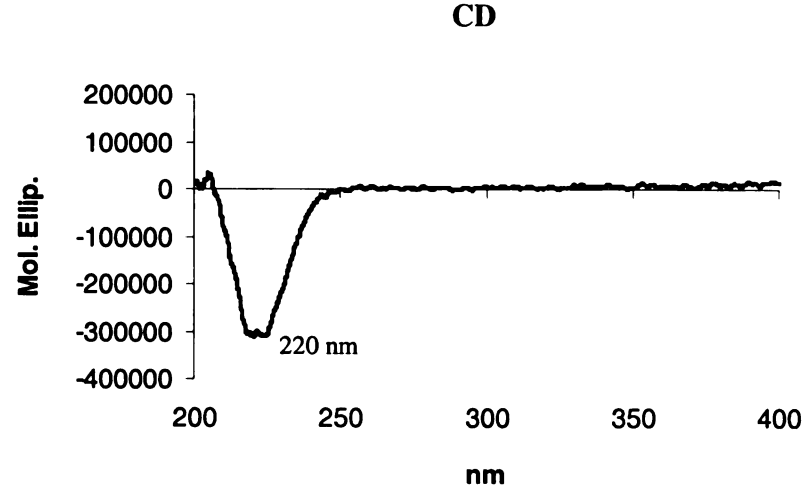

CRABPII R132K::Y134F::R111E::T54V
Sequence BB 174

CRABPII R132K::Y134F::R111E::T54V

Sequence BB 174

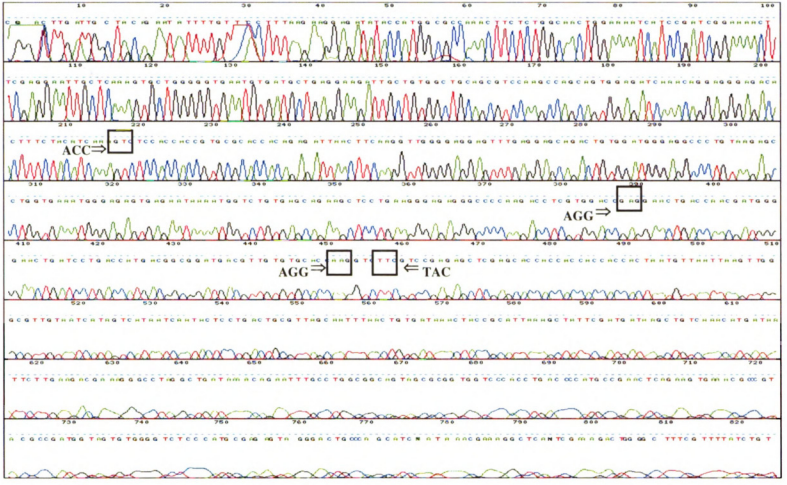

CRABPII R132K::Y134F::R111E::T54V
Fluorescence Titrations

Retinoic Acid **all-*trans*-Retinal**

CRABPII R132K::Y134F::R111E::T54V

Fluorescence Titrations

Retinoic Acid

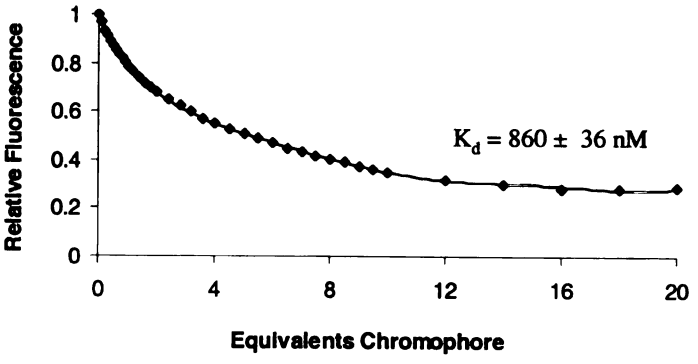

all-*trans*-Retinal

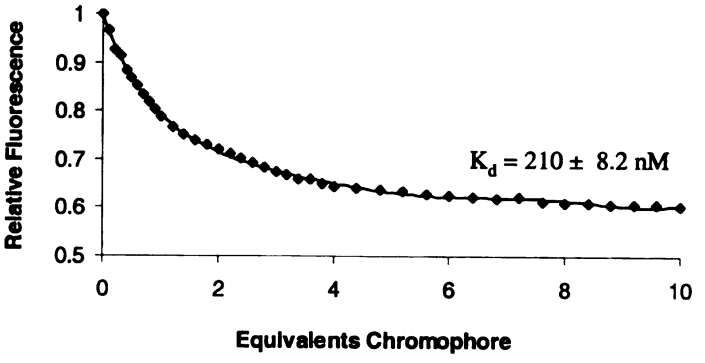

UV-vis Titrations, all-trans-Retinal

CRABPII R132K::Y134F::R111E::T54V

UV-vis Titrations, all-*trans*-Retinal

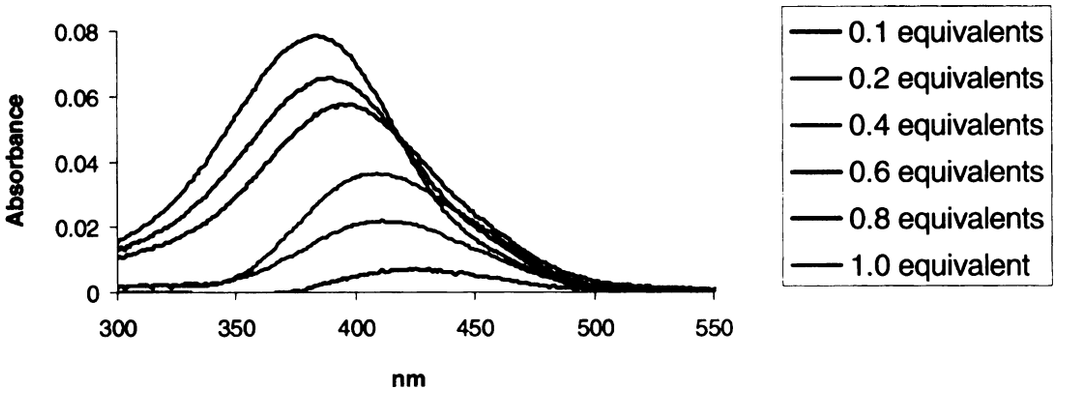

Uncorrected

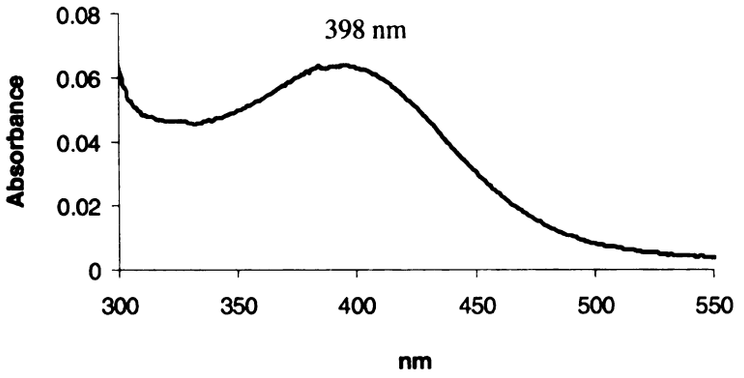

Corrected

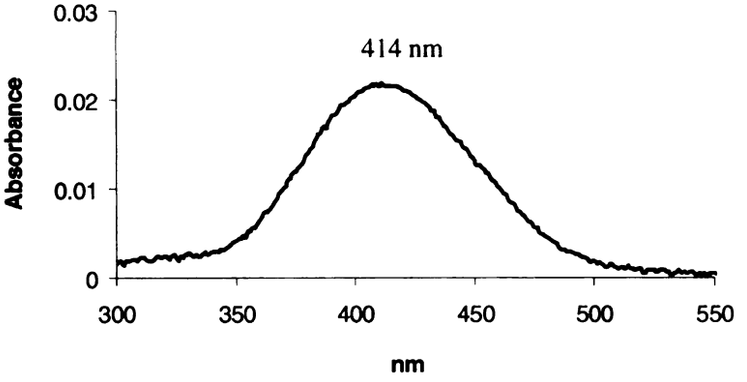

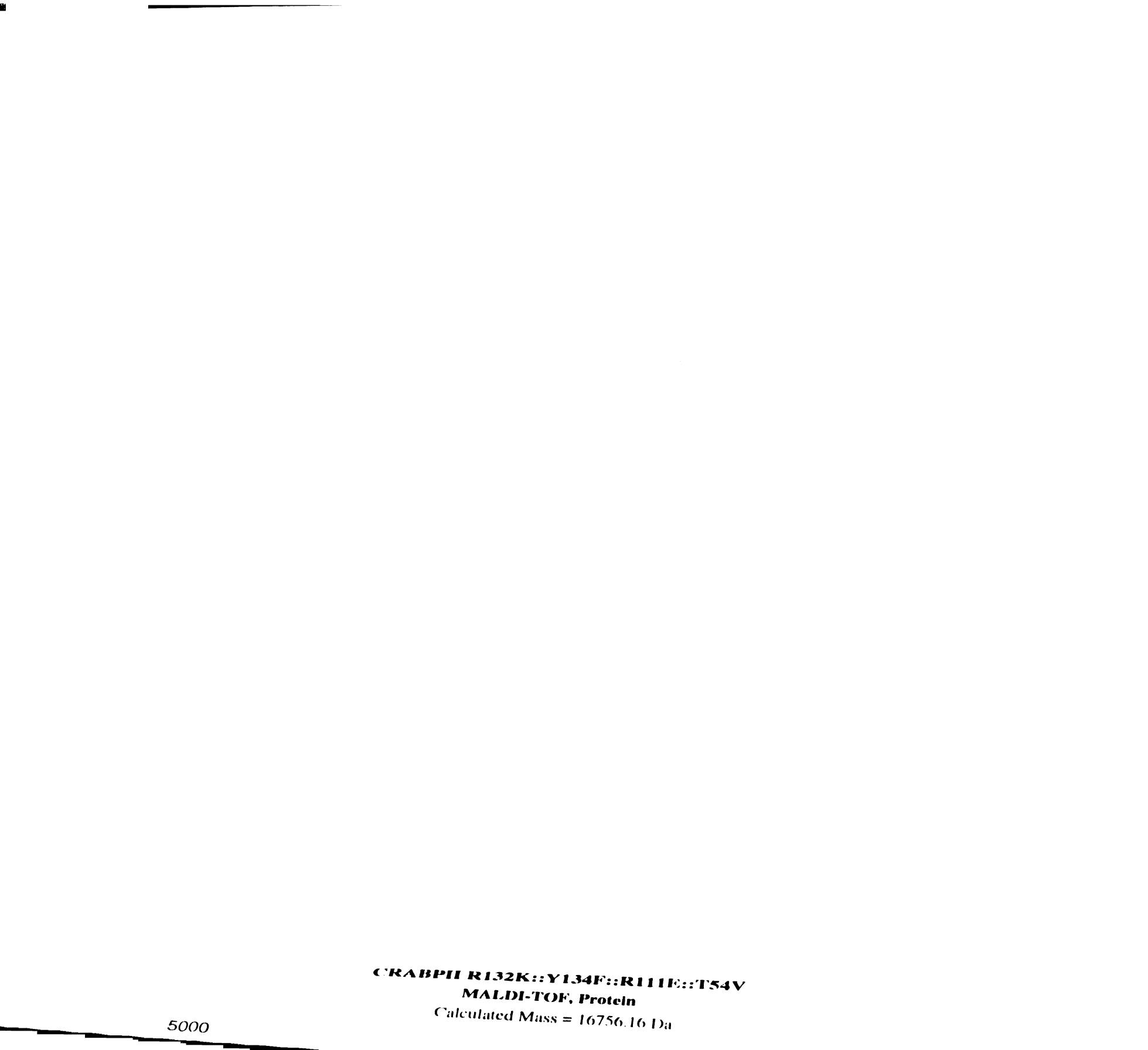
CRABPII R132K::Y134F::R111E::T54V
MALDI-TOF, Protein
Calculated Mass = 16756.16 Da
5000

CRABPII R132K::Y134F::R111E::T54V

MALDI-TOF, Protein

Calculated Mass = 16756.16 Da

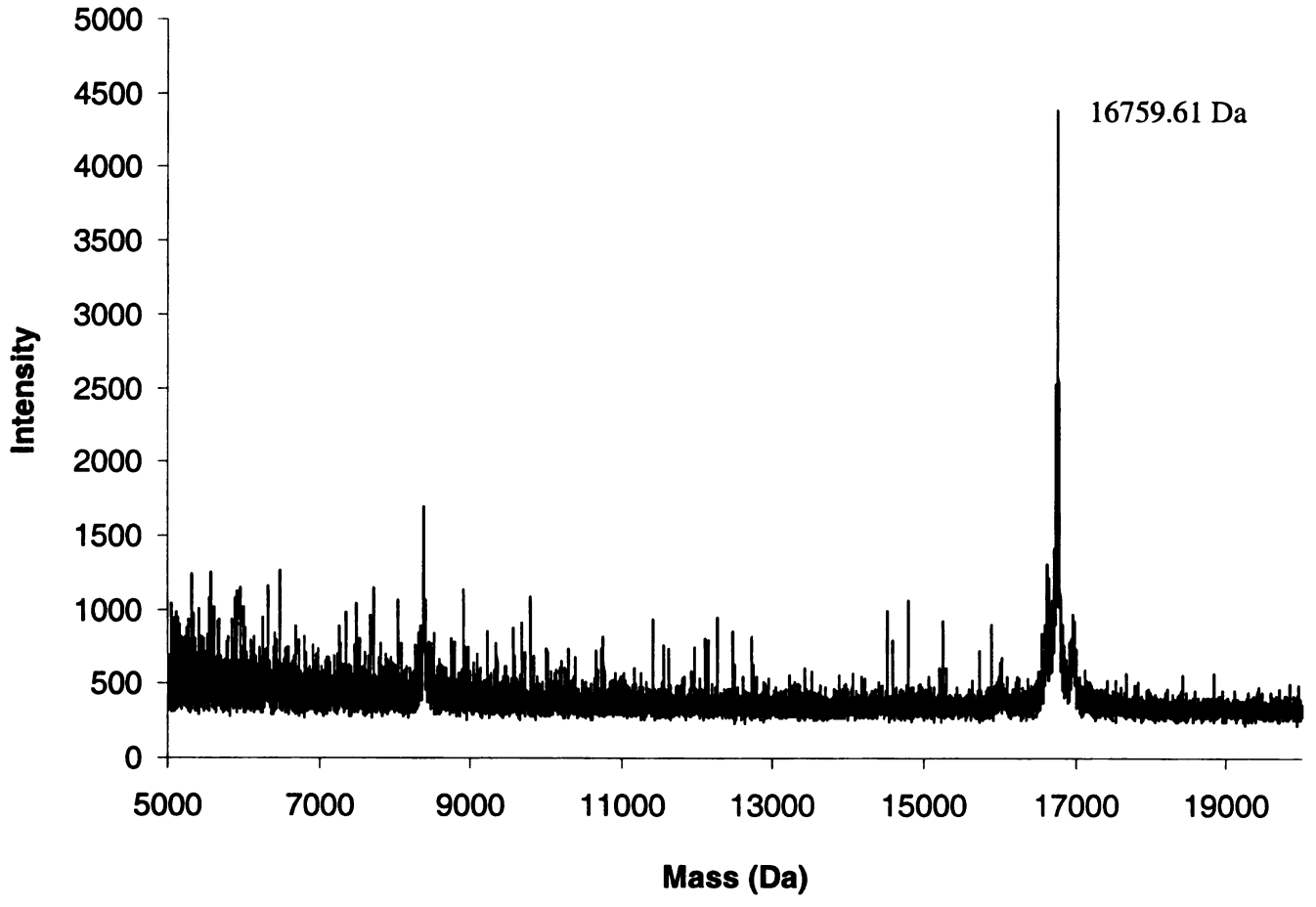

CRABPII R132K::Y134F::R111E::T54V

MALDI-TOF, Incubation with all-*trans*-Retinal

Protein Mass = 16756.16 Da

Positive Covalent Bond Formation = Protein Mass + 266

CRABPII R132K::Y134F::R111E::T54V

MALDI-TOF, Incubation with all-*trans*-Retinal

Protein Mass = 16756.16 Da

Positive Covalent Bond Formation = Protein Mass + 266

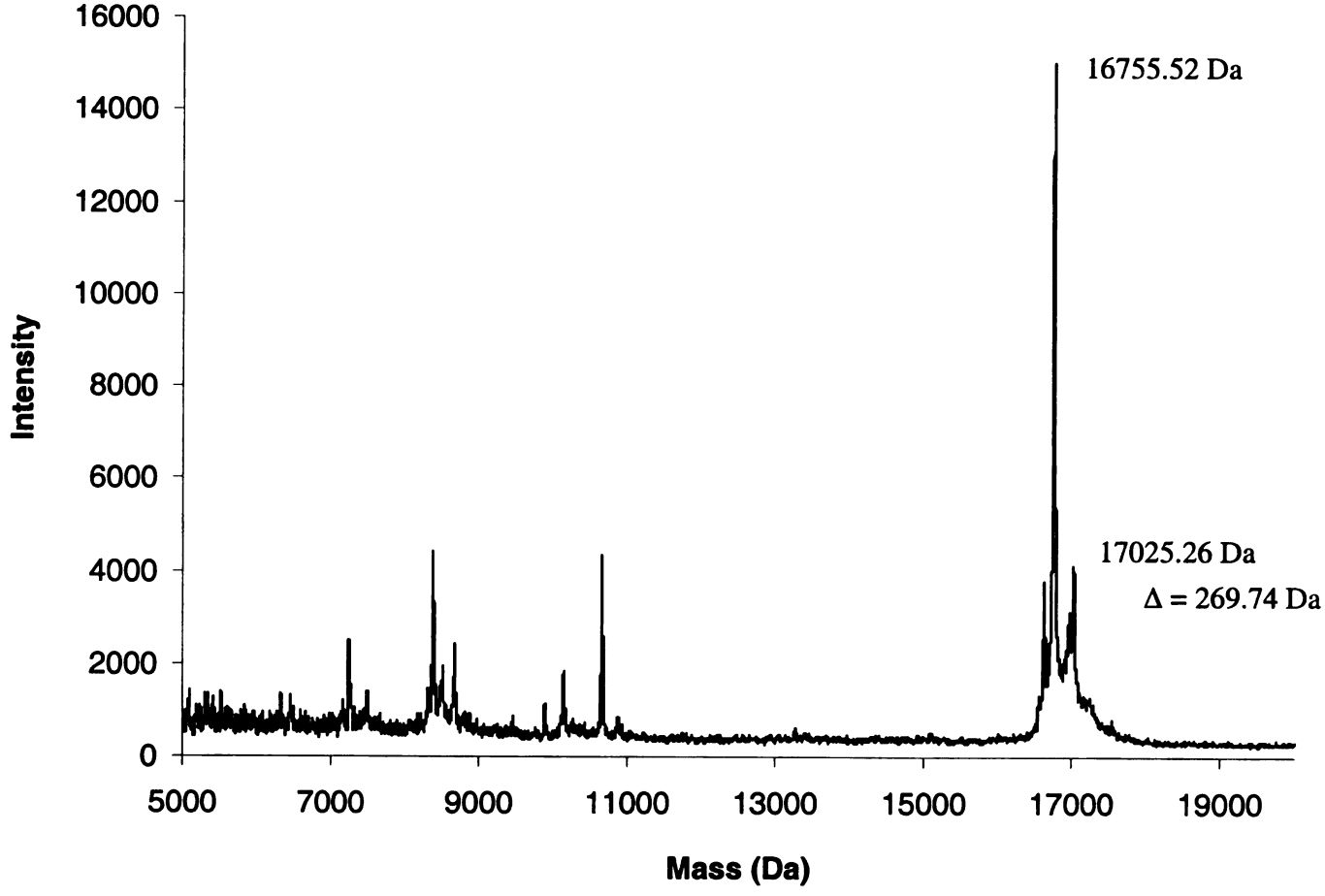

CRABPII R132K::Y134F::R111E::T54V

***MALDI-TOF*, Reductive Amination with all-*trans*-Retinal**

Protein Mass = 16756.16 Da

Positive Reductive Amination = Protein Mass + 268

CRABPII R132K::Y134F::R111E::T54V

MALDI-TOF, Reductive Amination with all-*trans*-Retinal

Protein Mass = 16756.16 Da

Positive Reductive Amination = Protein Mass + 268

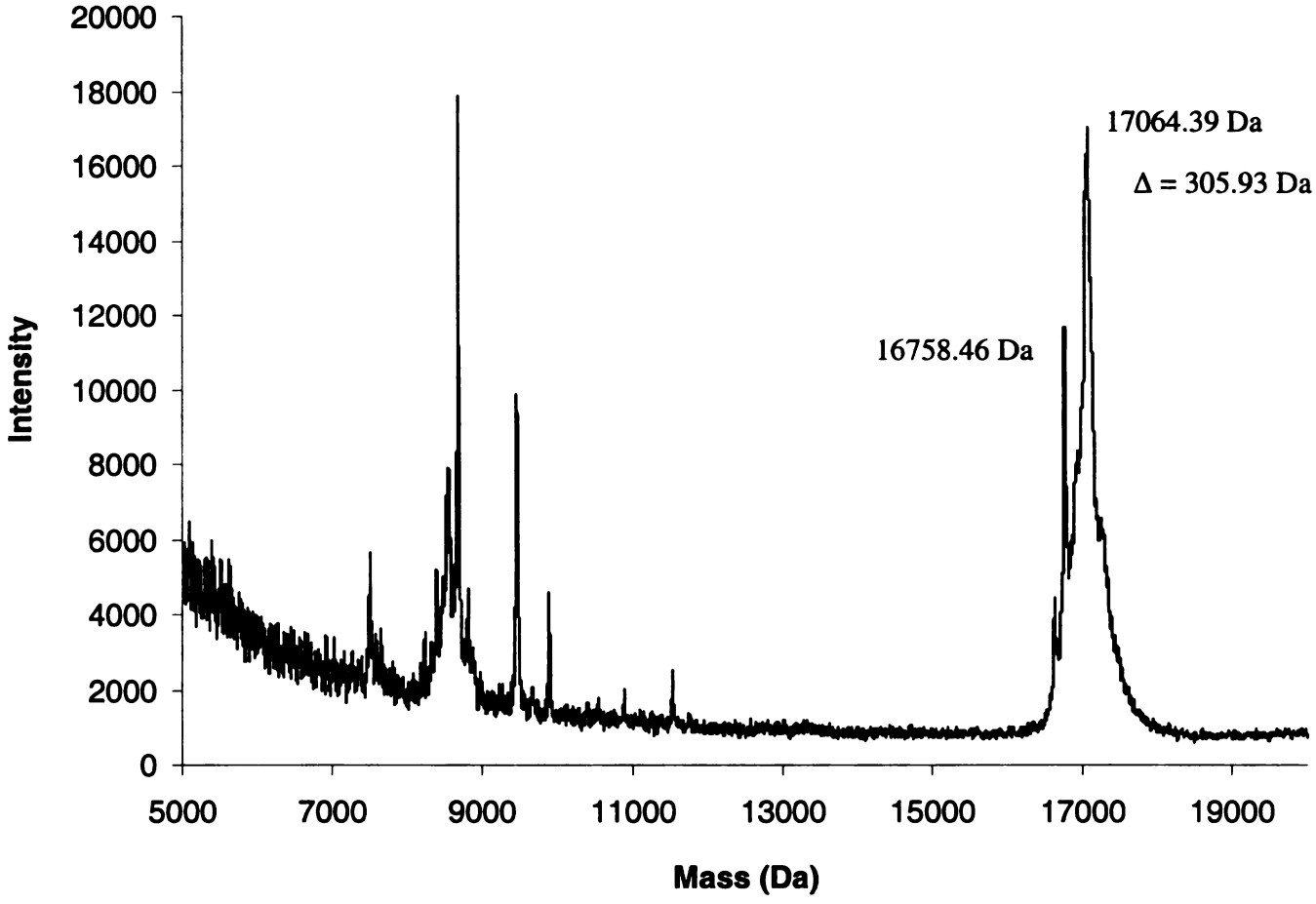

CRABPII R132K::Y134F::L121E

Molecular Weight :

CRABPII R132K::Y134F::L121E

Molecular Weight :

16801.16 Da

Extinction Coefficient :

18,422 M^{-1} cm^{-1}

Primers :

bbb37 5' GAT GGG GAA CTG ATC GAG ACC ATG ACG GCG GAT GAC
bbb38 5' GTC ATC CGC CGT CAT GGT CTC GAT CAG TTC CCC ATC

CD

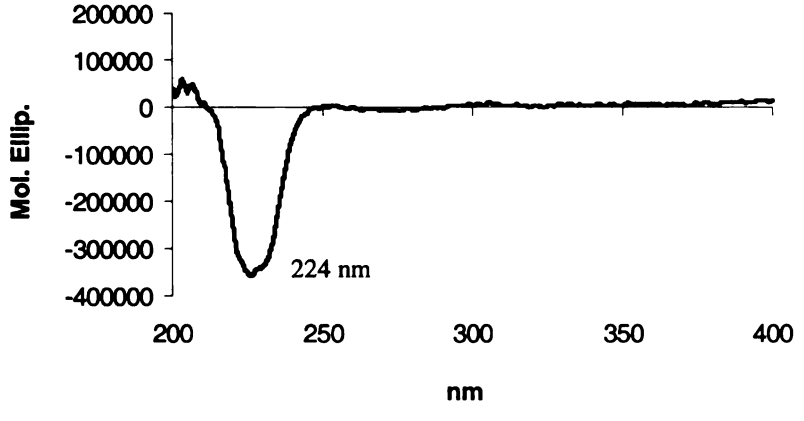

CRABPII R132K::Y134F::L121E
Sequence BB 173

CRABPII R132K::Y134F::L121E

Sequence BB 173

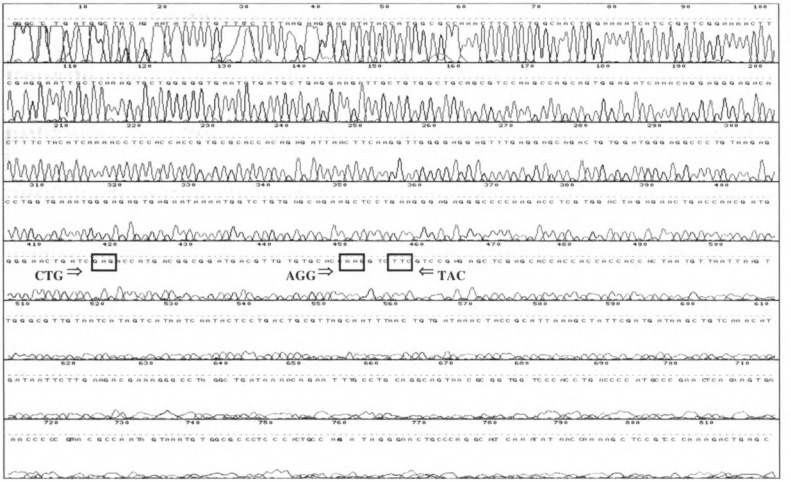

CRABPII R132K::Y134F::L121E
Fluorescence Titrations

CRABPII R132K::Y134F::L121E
Fluorescence Titrations

Retinoic Acid

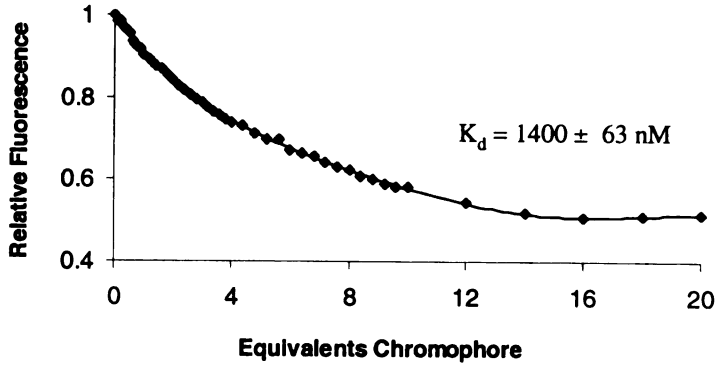

all-*trans*-Retinal

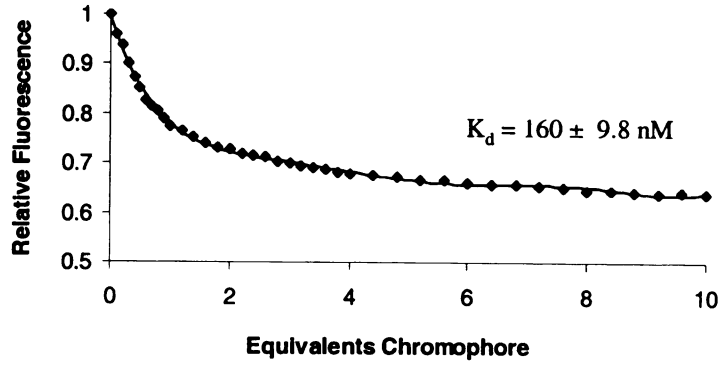

CRABPII R132K::Y134F::L121E
UV-vis Titrations, all-*trans*-Retinal

CRABPII R132K::Y134F::L121E

UV-vis Titrations, all-*trans*-Retinal

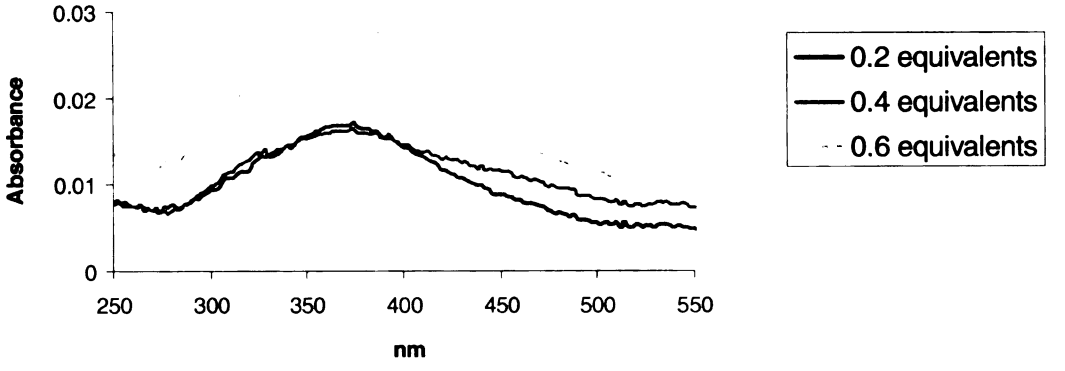

Uncorrected

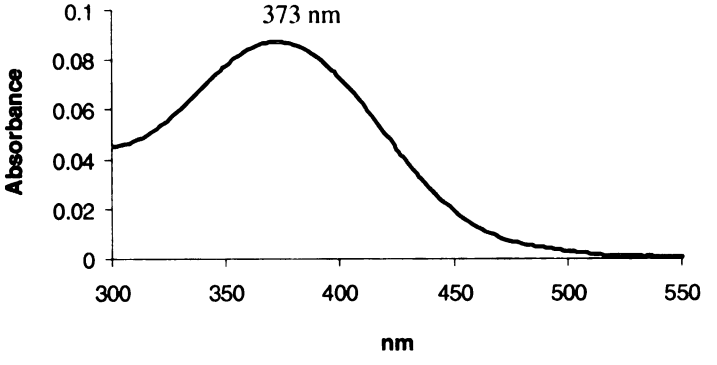

Corrected

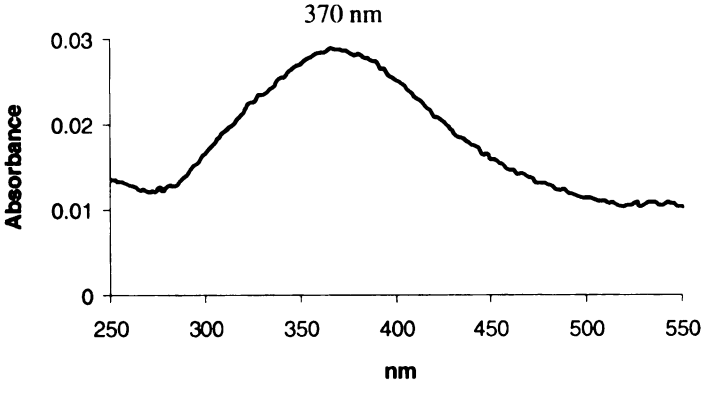

CRABPII R132K::Y134F::L121E
MALDI-TOF, Protein
Calculated Mass = 16801.16 Da

2500

CRABPII R132K::Y134F::L121E

MALDI-TOF, Protein

Calculated Mass = 16801.16 Da

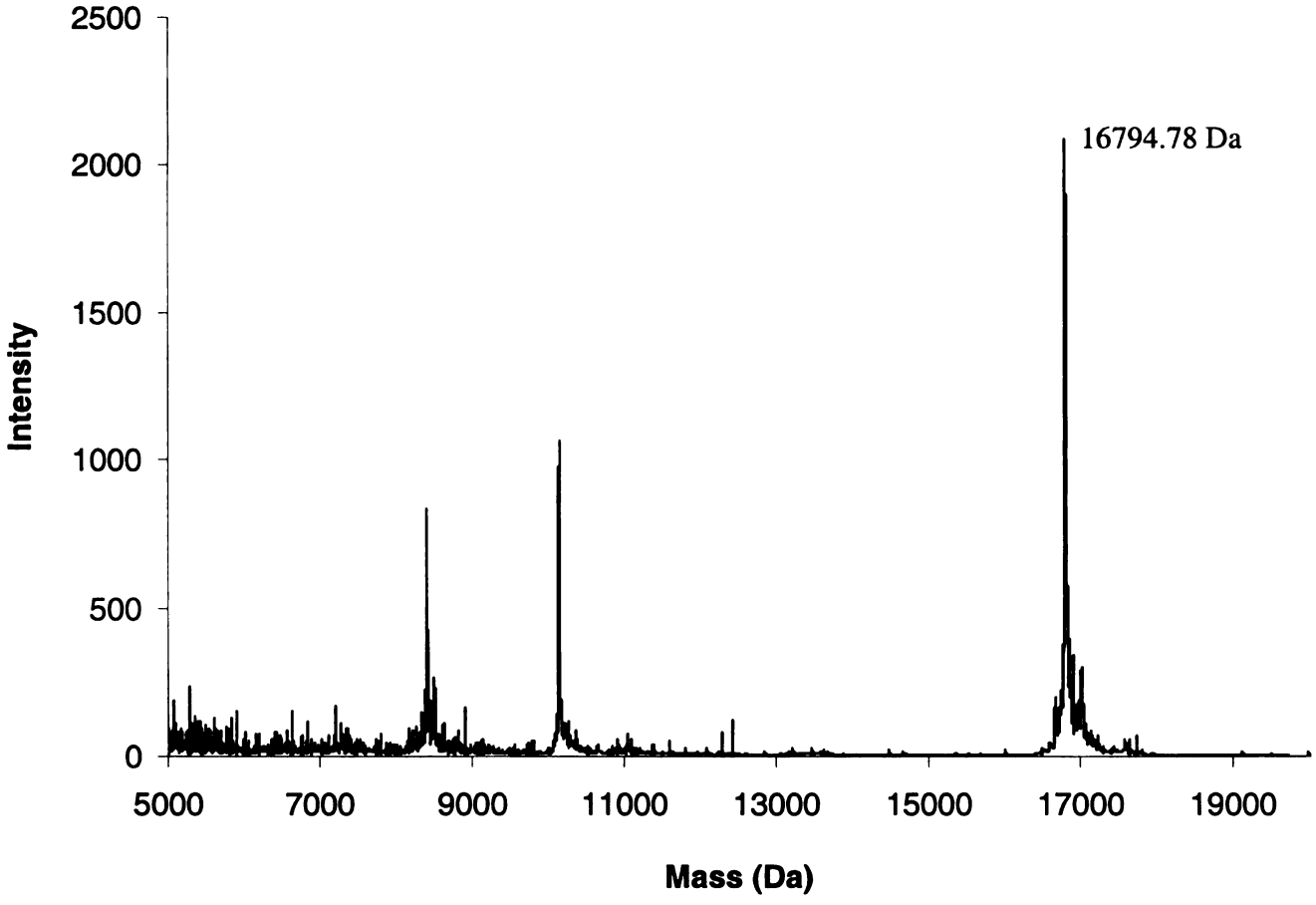

CRABPII R132K::Y134F::L121E

MALDI-TOF, Incubation with all-trans-Retinal

Protein Mass = 16801.16 Da

Positive Covalent Bond Formation = Protein Mass + 266

CRABPII R132K::Y134F::L121E

MALDI-TOF, Incubation with all-*trans*-Retinal

Protein Mass = 16801.16 Da

Positive Covalent Bond Formation = Protein Mass + 266

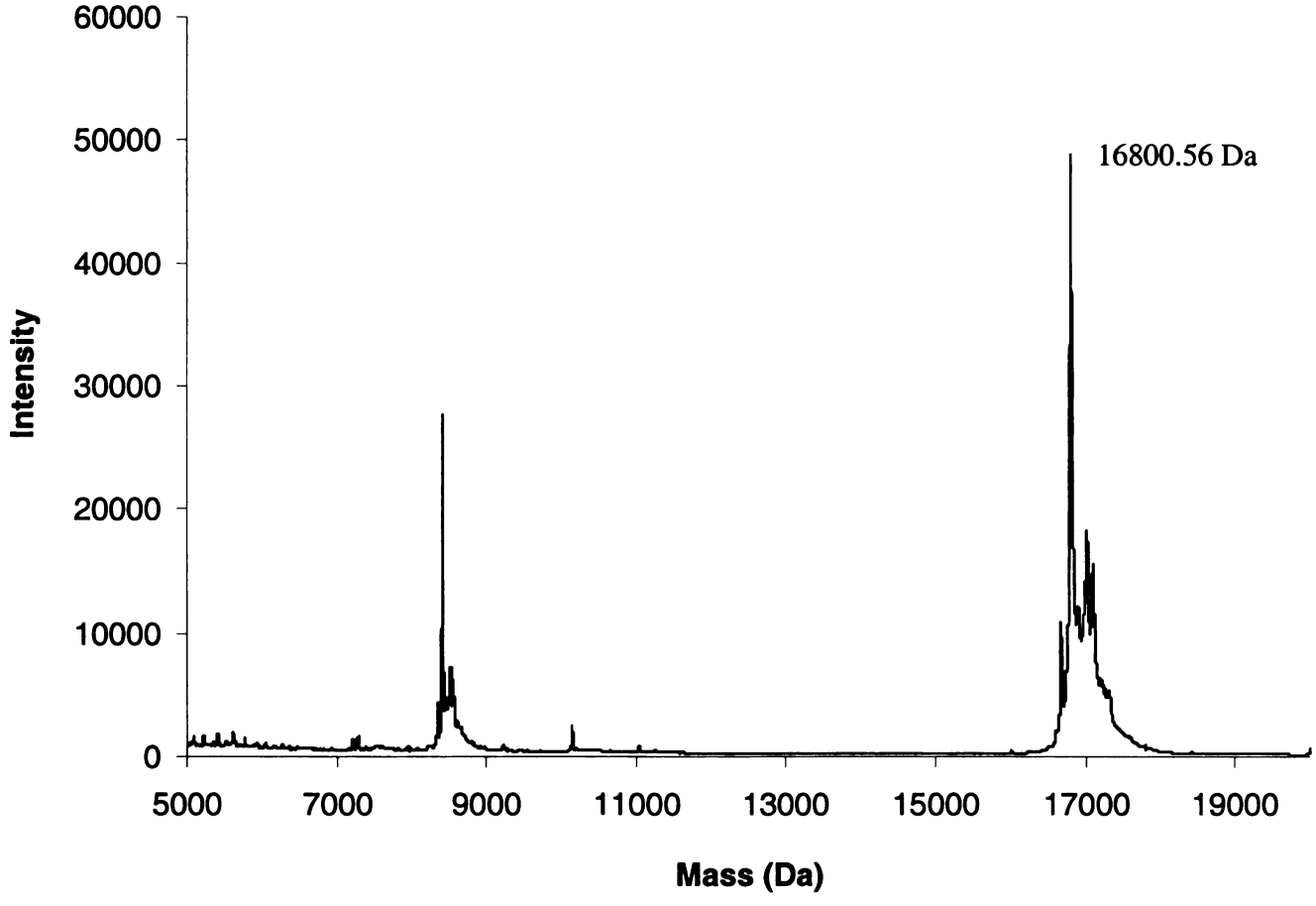

CRABPII R132K::Y134F::L121E
MALDI-TOF, Reductive Amination with all-*trans*-Retinal
Protein Mass = 16801.16 Da
Positive Reductive Amination = Protein Mass + 268

CRABPII R132K::Y134F::L121E

MALDI-TOF, Reductive Amination with all-*trans*-Retinal

Protein Mass = 16801.16 Da

Positive Reductive Amination = Protein Mass + 268

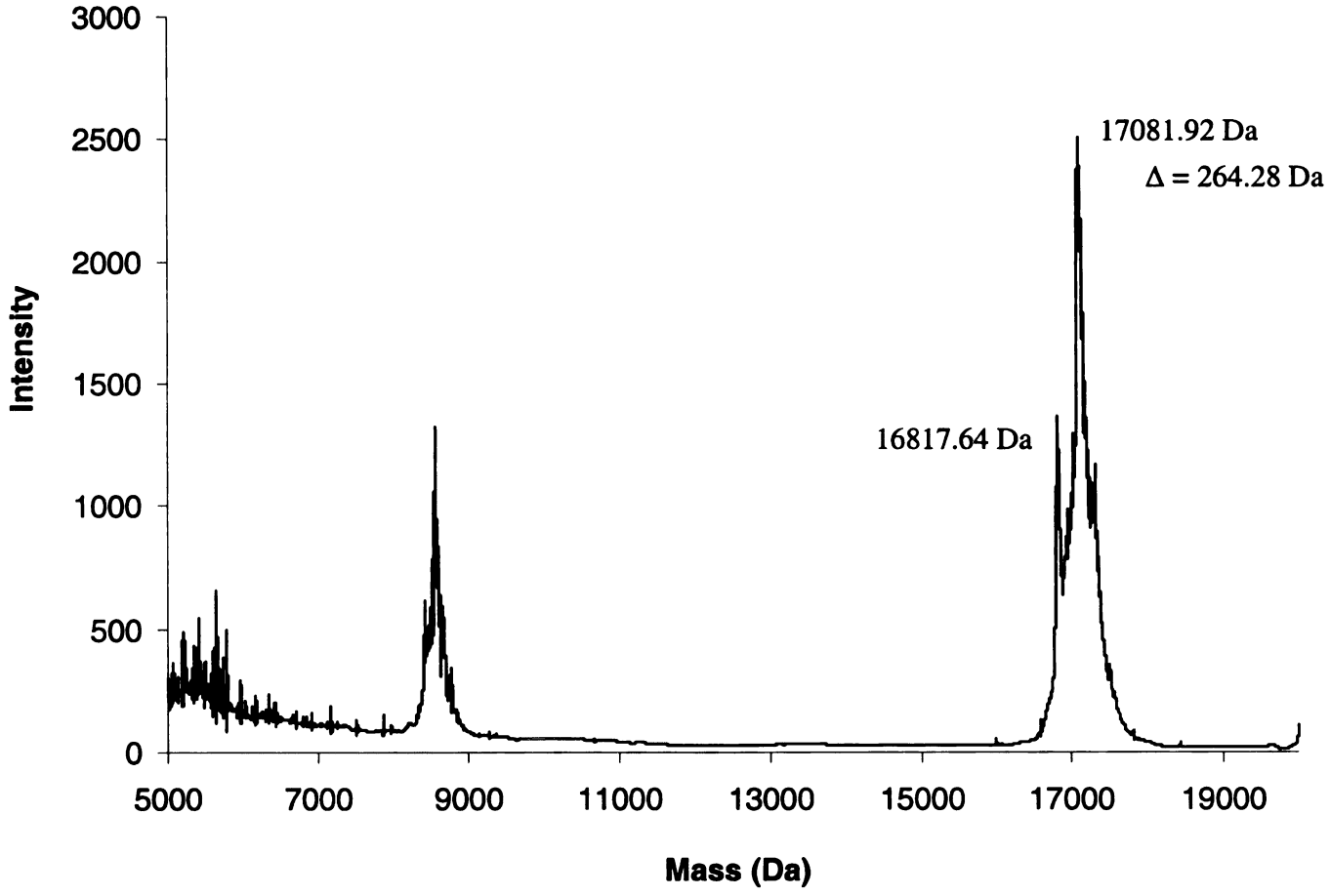

CRABPII R132K::Y134F::R111L

Molecular Weight :

16742.17 Da

Extinction Coefficient :

16,654 M^{-1} cm^{-1}

Primers :

bbb39 5' CCC AAG ACC TCG TGG ACC CTG GAA CTG ACC AAC GAT GGG

bbb40 5' CCC ATC GTT GGT CAG TTG CAG GGT CCA CGA GGT CTT GGG

CD

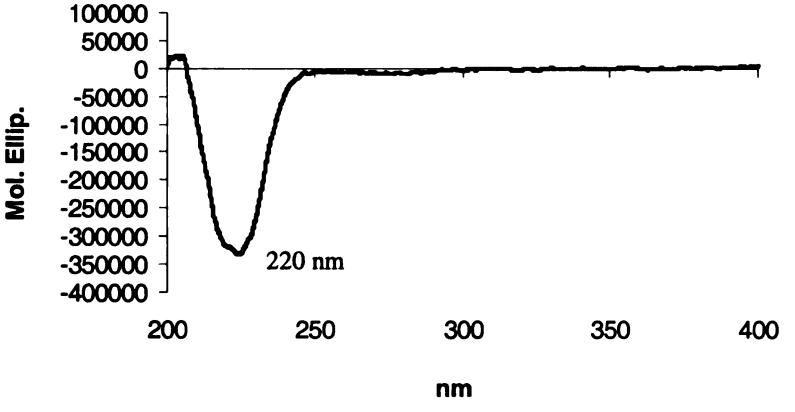

CRABPII R132K::Y134F::R111L
Sequence BB 19

CRABPII R132K::Y134F::R111L

Sequence BB 19

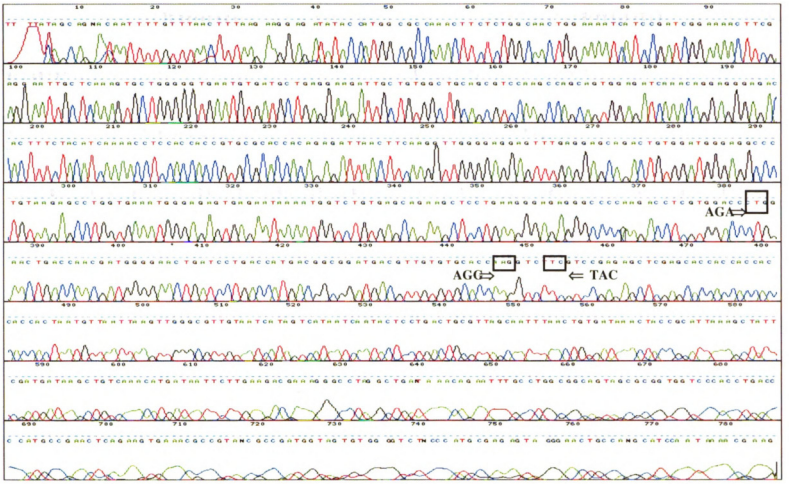

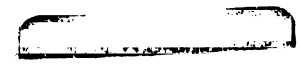

CRABPII R132K::Y134F::R111L
Fluorescence Titrations

CRABPII R132K::Y134F::R111L
Fluorescence Titrations

Retinoic Acid

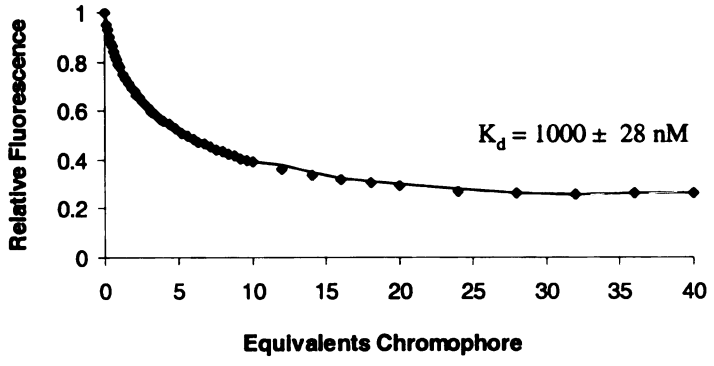

all-*trans*-Retinal

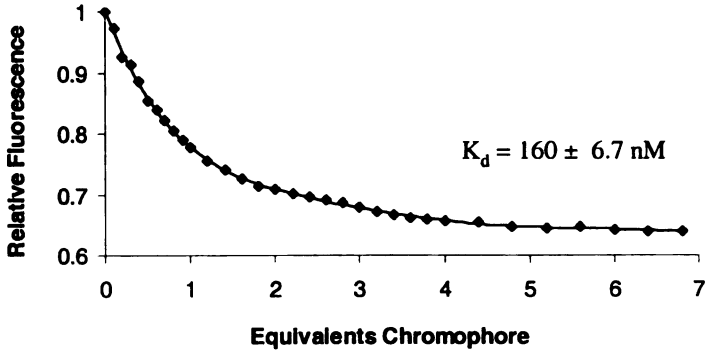

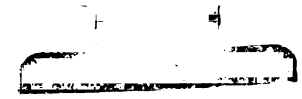

CRABPII R132K::Y134F::R111L

CRABPII R132K::Y134F::R111L

UV-vis Titrations, all-*trans*-Retinal

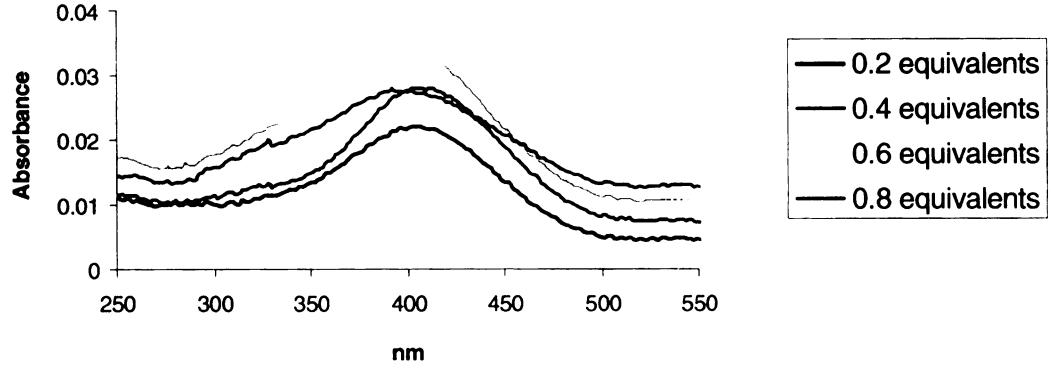

Uncorrected

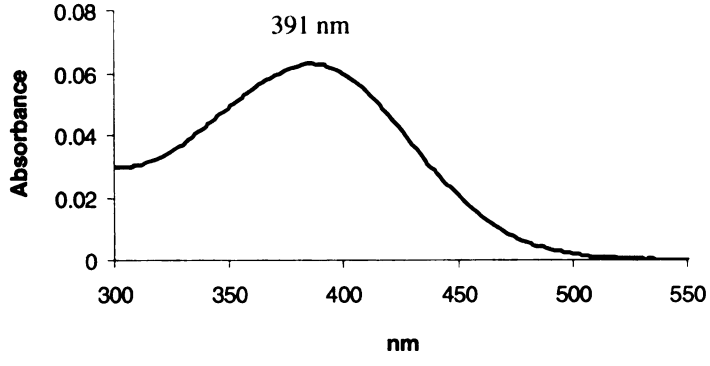

Corrected

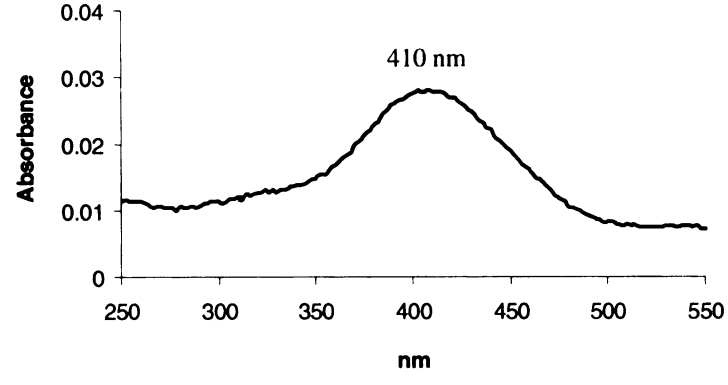

CRABPII R132K::Y134F::R111L
MALDI-TOF, Protein
Calculated Mass = 16742.17 Da

CRABPII R132K::Y134F::R111L

MALDI-TOF, Protein

Calculated Mass = 16742.17 Da

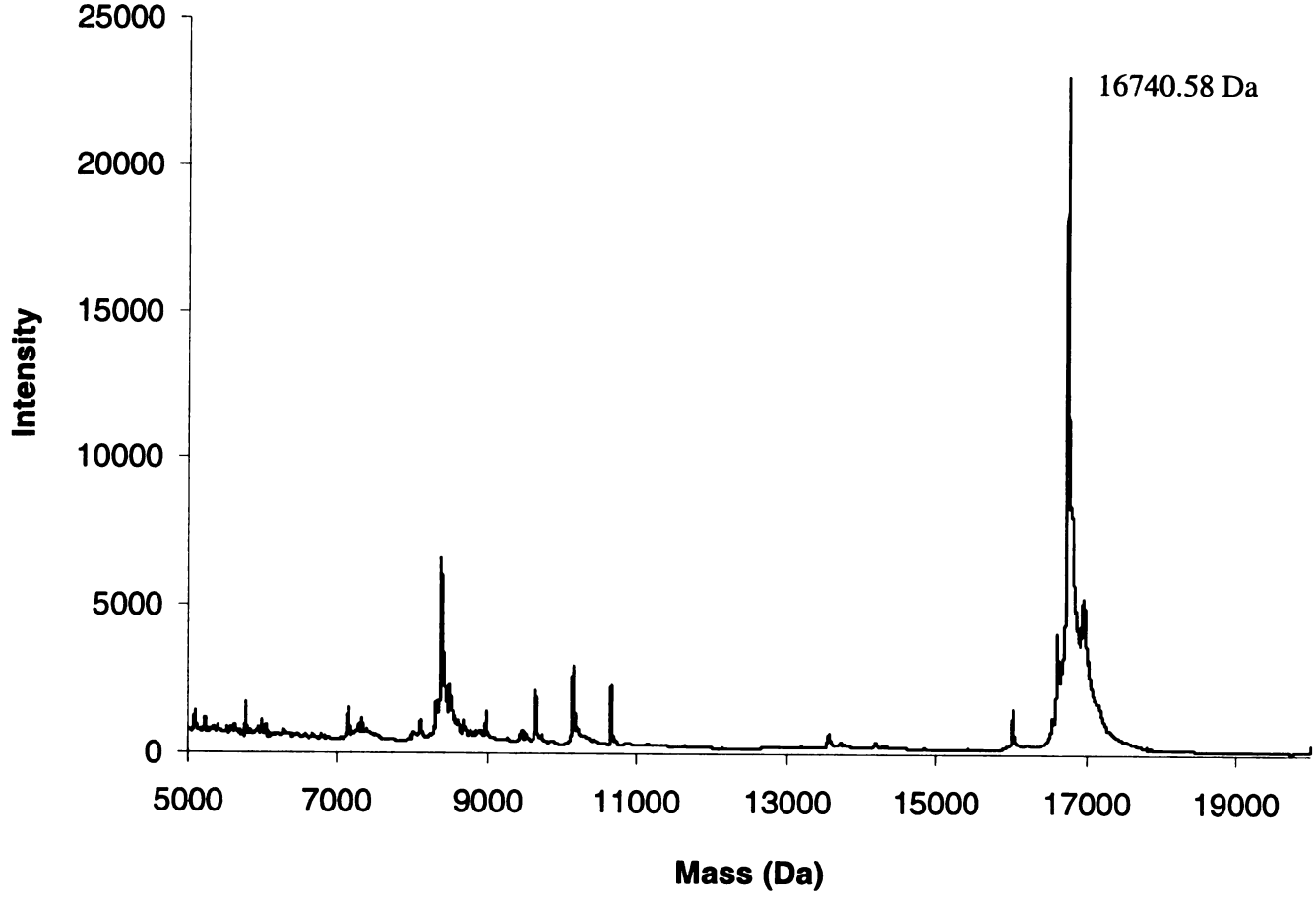

CRABPII R132K::Y134F::R111L
MALDI-TOF, Incubation with all-*trans*-Retinal

CRABPII R132K::Y134F::R111L

MALDI-TOF, Incubation with all-*trans*-Retinal

Protein Mass = 16742.17 Da

Positive Covalent Bond Formation = Protein Mass + 266

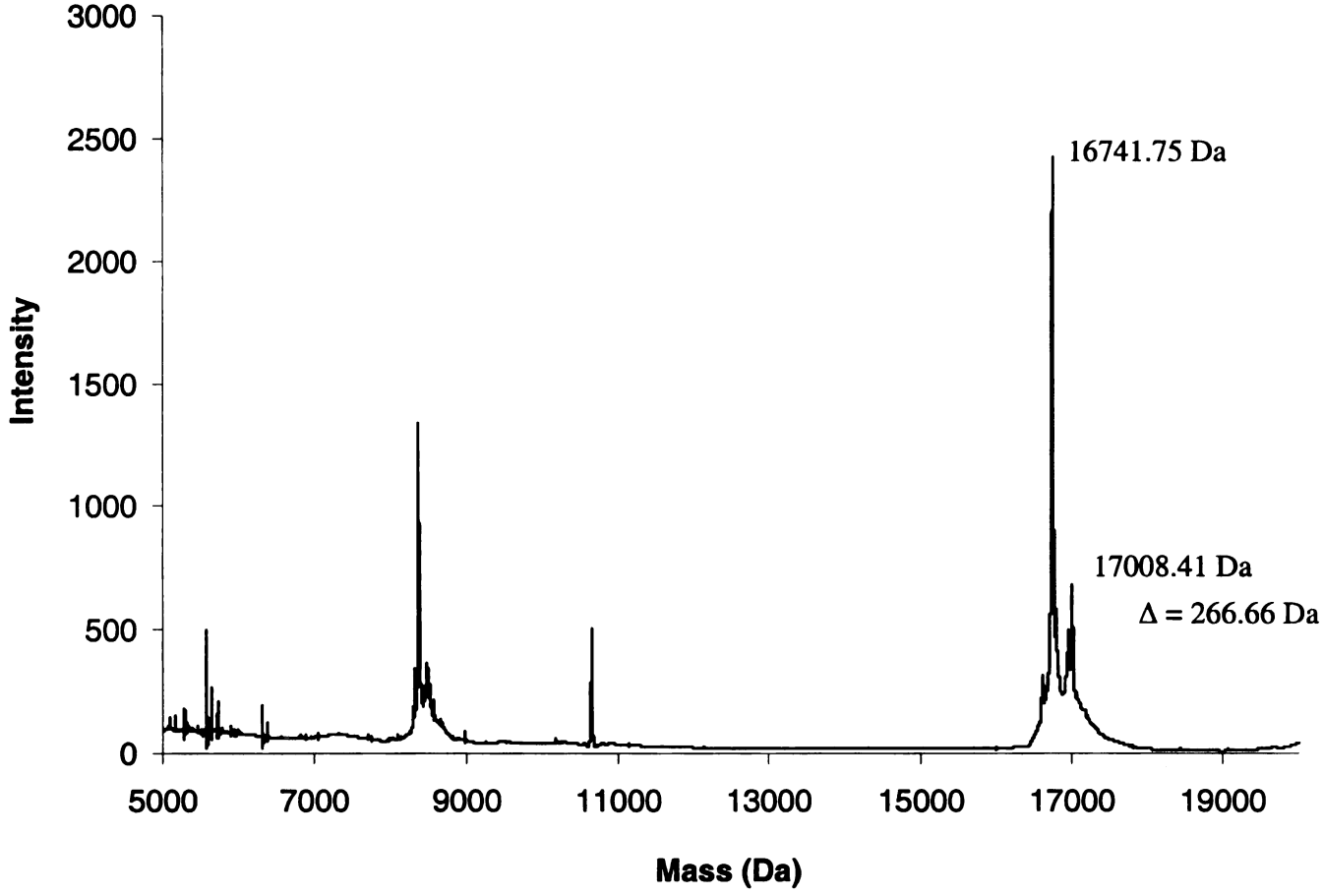

CRABPII R132K::Y134F::R111L
MALDI-TOF, Reductive Amination with all-*trans*-Retinal

CRABPII R132K::Y134F::R111L

MALDI-TOF, Reductive Amination with all-*trans*-Retinal

Protein Mass = 16742.17 Da

Positive Reductive Amination = Protein Mass + 268

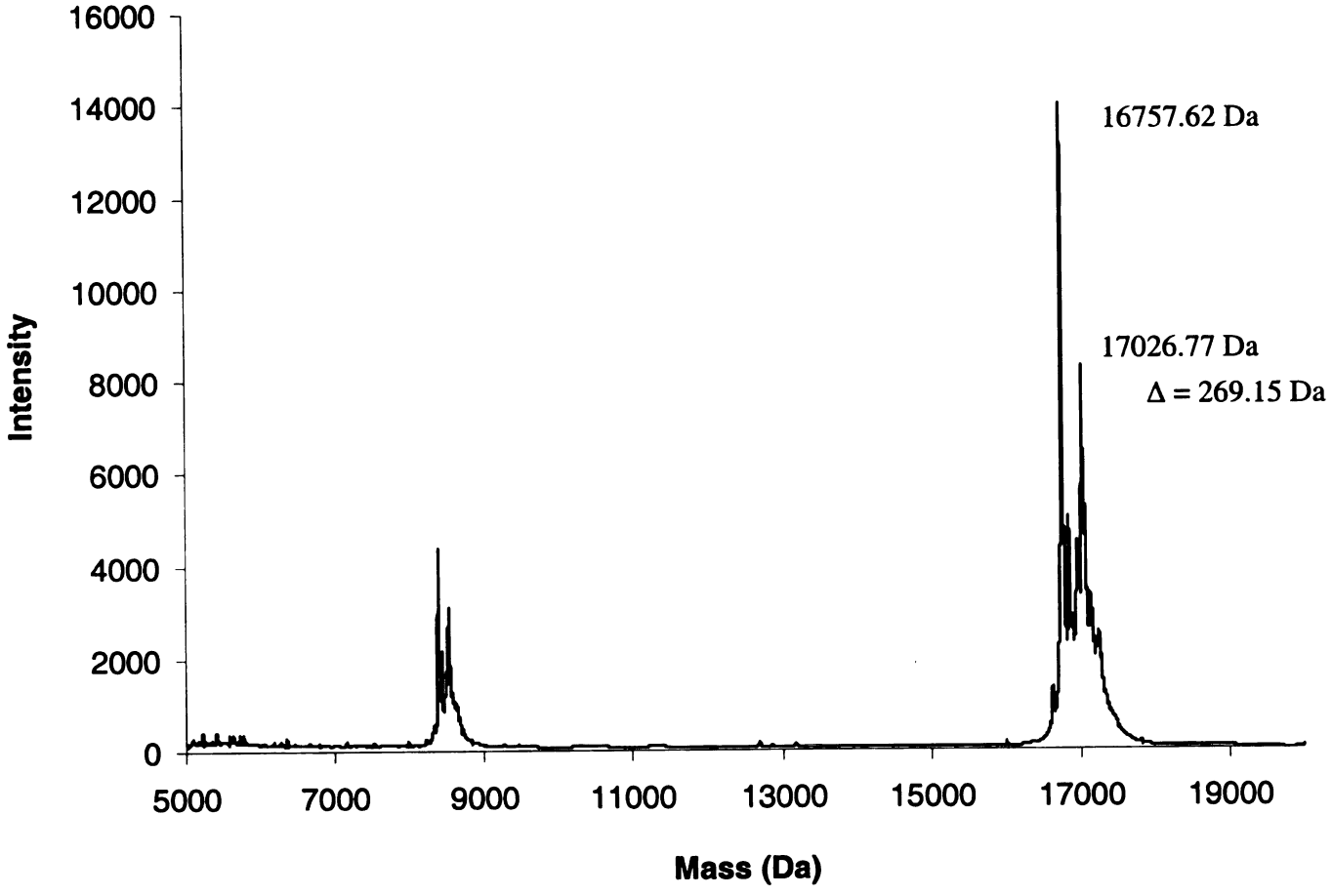

CRABPII R132K::Y134F::R111L::T54E

Molecular Weight :

16770.18 Da

Extinction Coefficient :

18,430 M^{-1} cm^{-1}

Primers :

bbb65 5' CTA CAT CAA AGA GTC CAC CAC CGT GCG

bbb66 5' CGC ACG GTG GTG GAC TCT TTG ATG TAG

CD

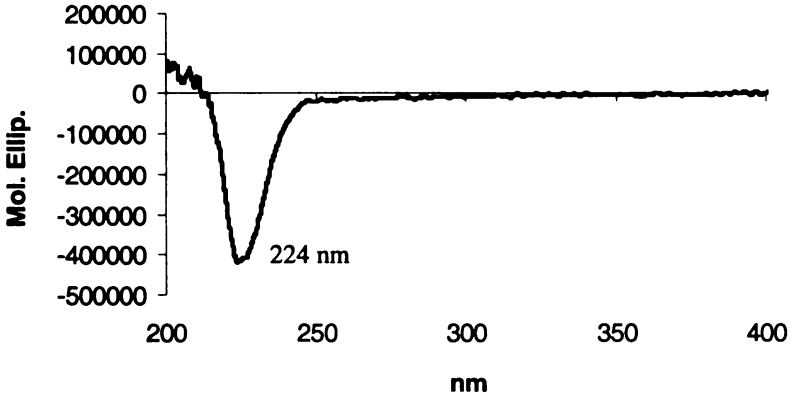

CRABPII R132K::Y134F::R111L::T54E
Sequence BB 47

CRABPII R132K::Y134F::R111L::T54E

Sequence BB 47

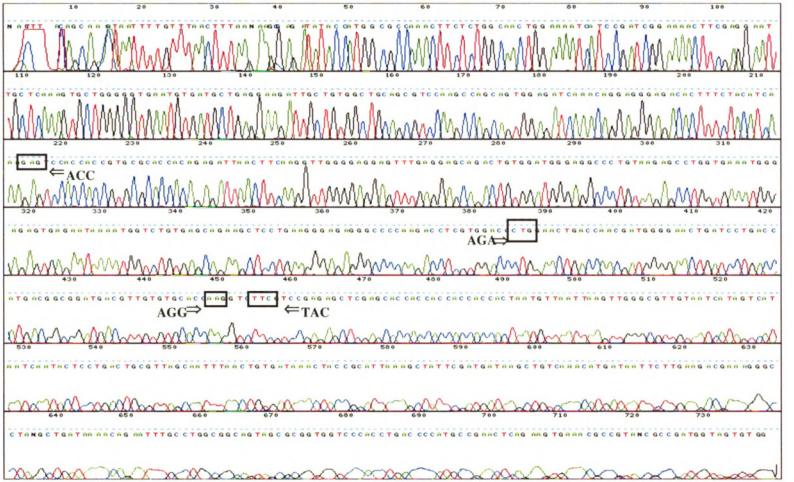

CRABPII R132K::Y134F::R111L::T54E

Fluorescence Titrations

CRABPII R132K::Y134F::R111L::T54E

Fluorescence Titrations

Retinoic Acid

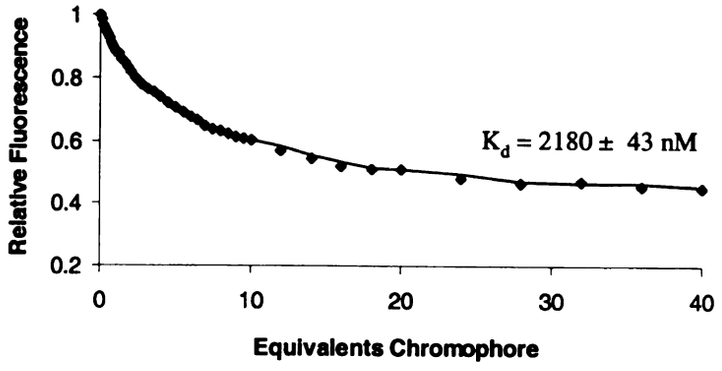

all-*trans*-Retinal

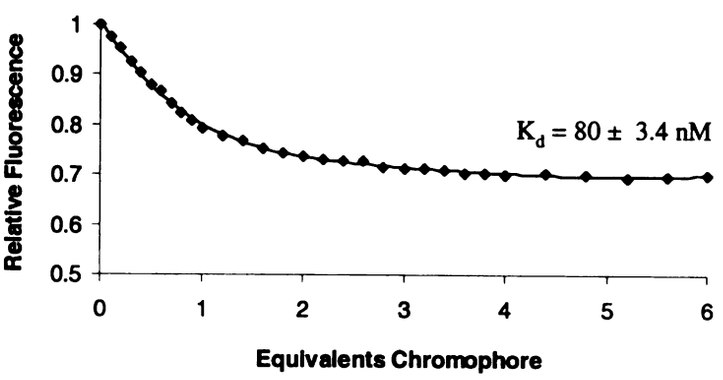

CRABPII R132K::Y134F::R111L::T54E
UV-vis Titrations, all-trans-Retinal

CRABPII R132K::Y134F::R111L::T54E

UV-vis Titrations, all-*trans*-Retinal

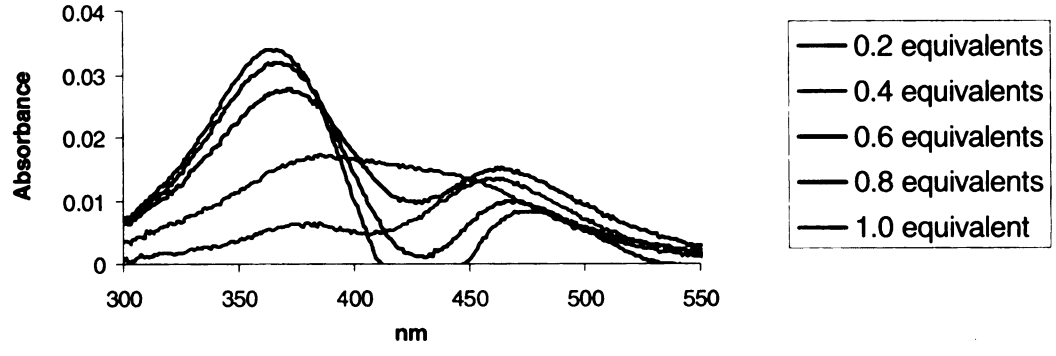

Uncorrected

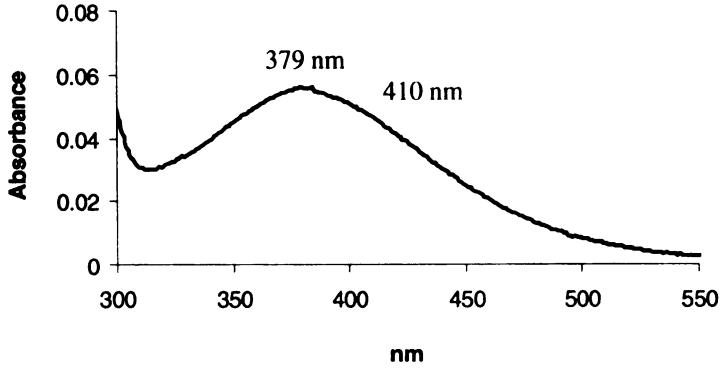

Corrected

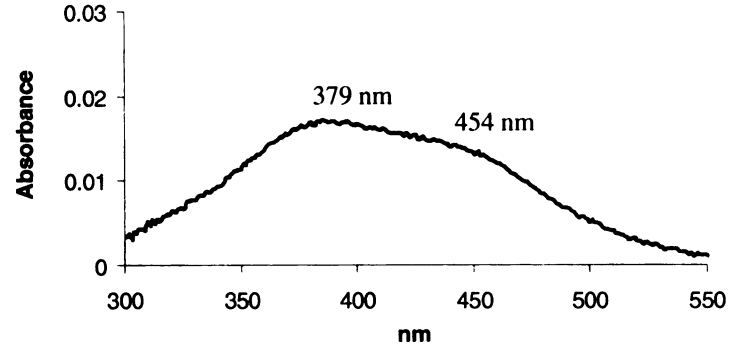

CRABPII R132K::Y134F::R111L::T54E
MALDI-TOF, Protein
Calculated Mass = 16770.18 Da

CRABPII R132K::Y134F::R111L::T54E

MALDI-TOF, Protein

Calculated Mass = 16770.18 Da

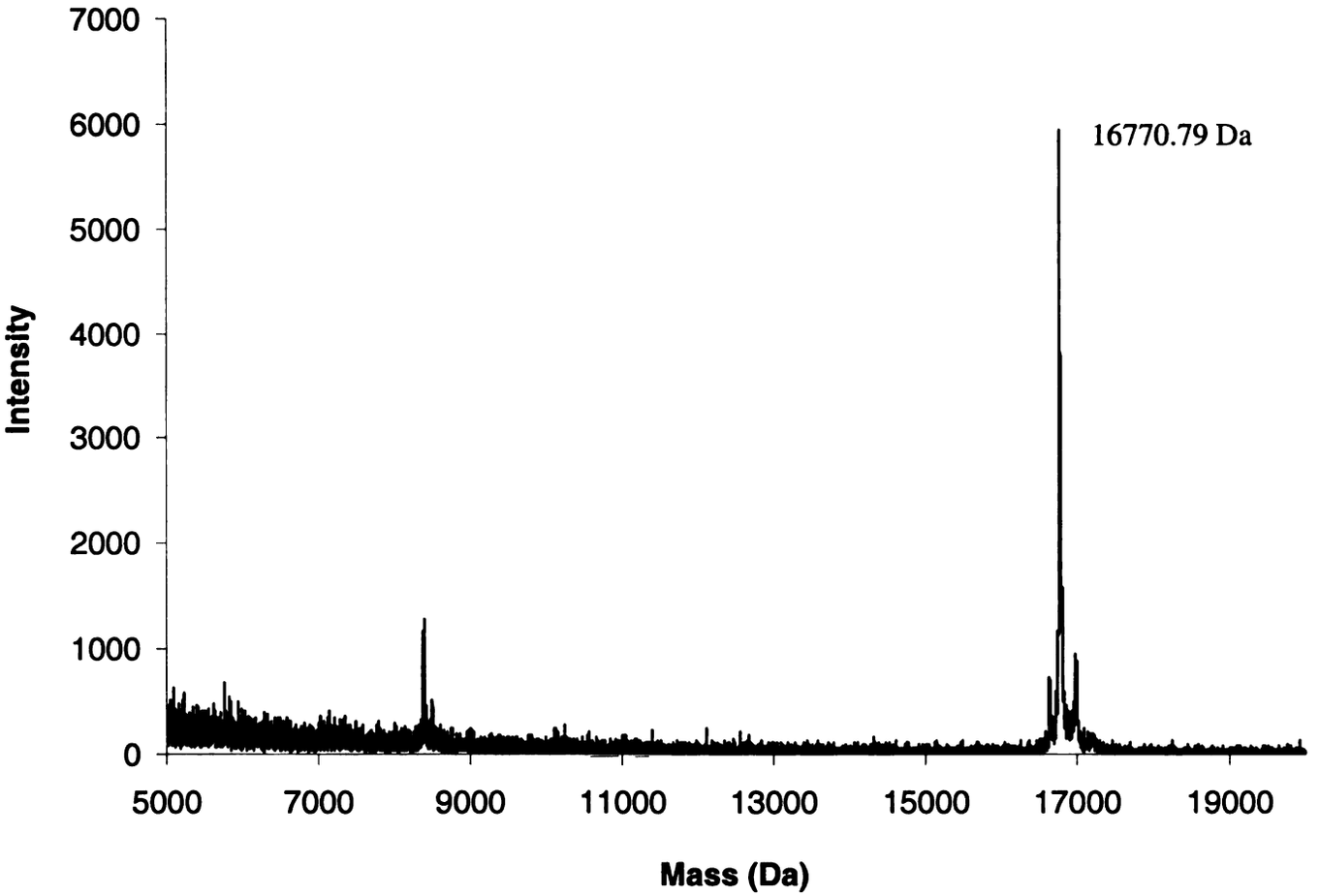

CRABPII R132K::Y134F::R111L::T54E
MALDI-TOF, Incubation with all-trans-Retinal
Protein Mass = 16770.18 Da
Positive Covalent Bond Formation = Protein Mass + 266

CRABPII R132K::Y134F::R111L::T54E

MALDI-TOF, Incubation with all-*trans*-Retinal

Protein Mass = 16770.18 Da

Positive Covalent Bond Formation = Protein Mass + 266

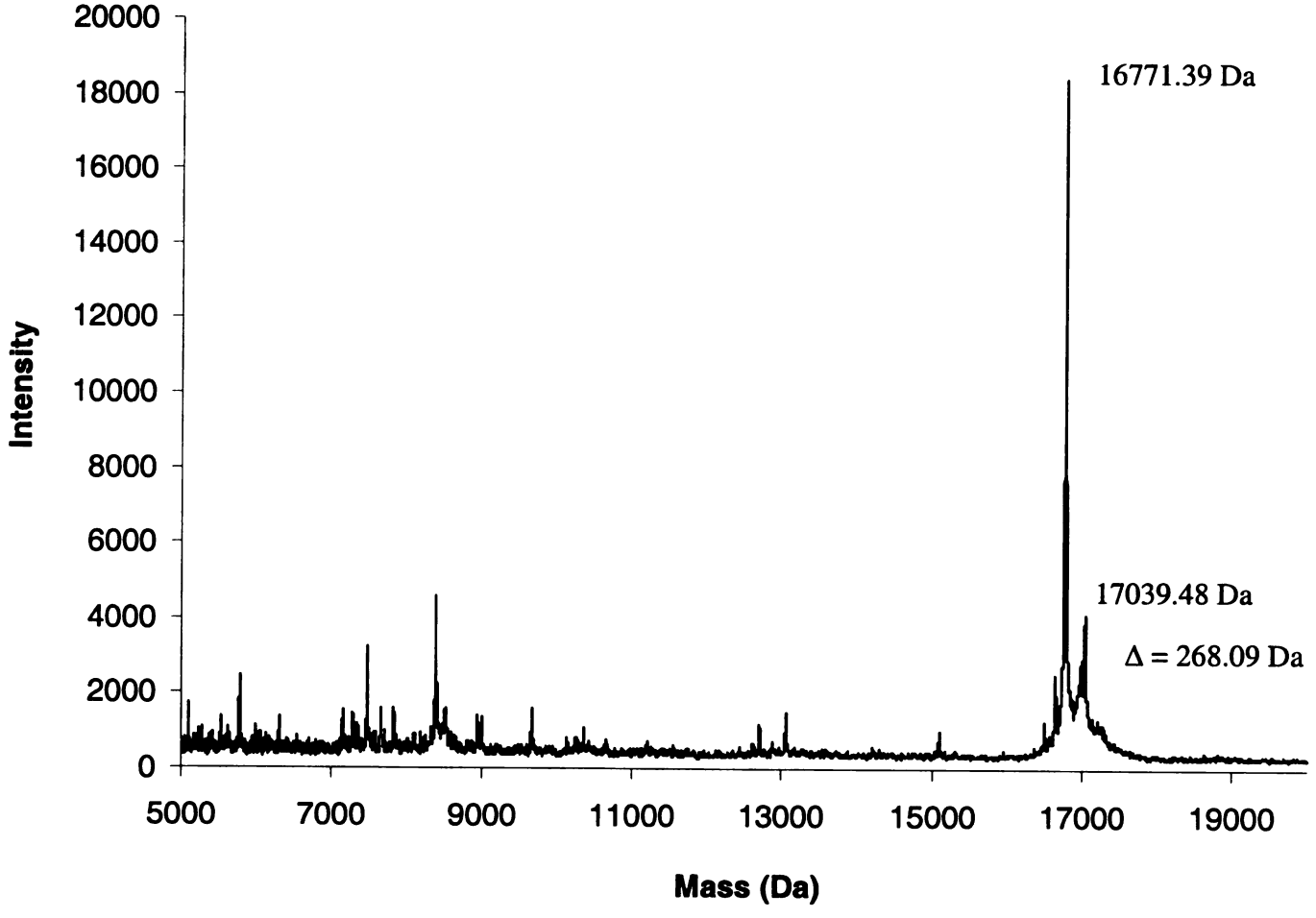

CRABPII R132K::Y134F::R111L::T54E
MALDI-TOF, Reductive Amination with all-*trans*-Retinal
Protein Mass = 16770.18 Da
Positive Reductive Amination = Protein Mass + 268

CRABPII R132K::Y134F::R111L::T54E

MALDI-TOF, Reductive Amination with all-*trans*-Retinal

Protein Mass = 16770.18 Da

Positive Reductive Amination = Protein Mass + 268

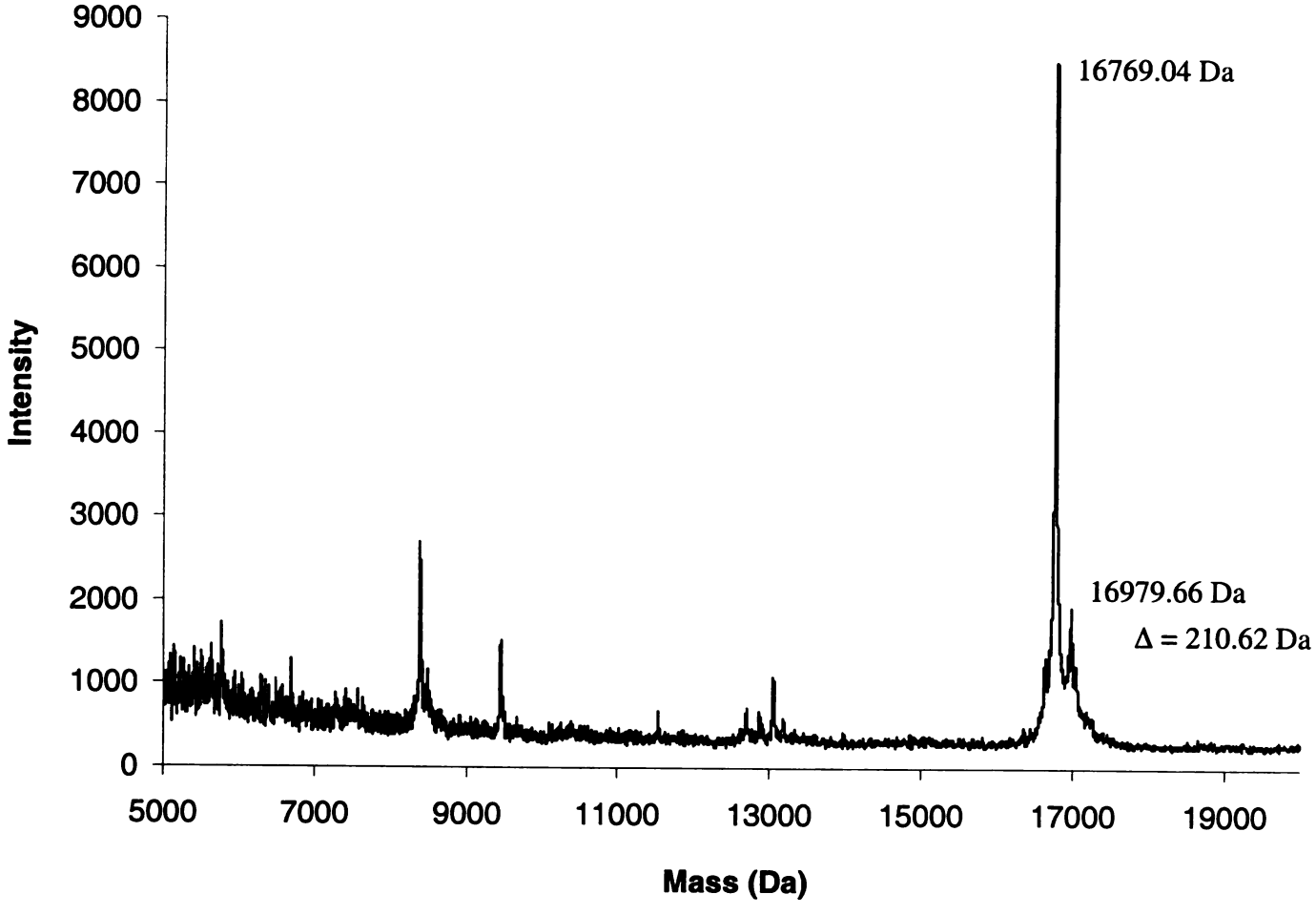

CRABPII R132K::Y134F::R111L::L121E

Molecular Weight :
16758.13 Da

Extinction Coefficient :
21,625 M^{-1} cm^{-1}

Primers :
bbb37 5' GAT GGG GAA CTG ATC GAG ACC ATG ACG GCG GAT GAC
bbb38 5' GTC ATC CGC CGT CAT GGT CTC GAT CAG TTC CCC ATC

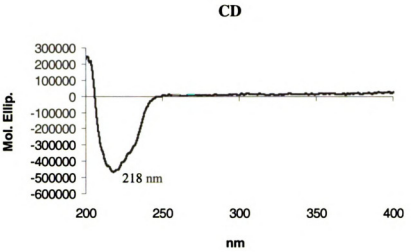

CRABPII R132K::Y134F::R111L::L121E

Sequence BB 27

CRABPII R132K::Y134F::R111L::L121E

Sequence BB 27

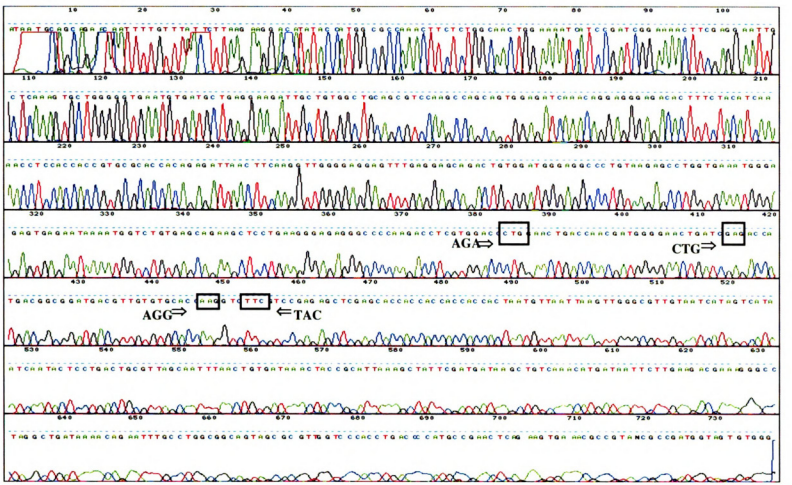

CRABPII R132K::Y134F::R111L::L121E

Fluorescence Titrations

CRABPII R132K::Y134F::R111L::L121E

Fluorescence Titrations

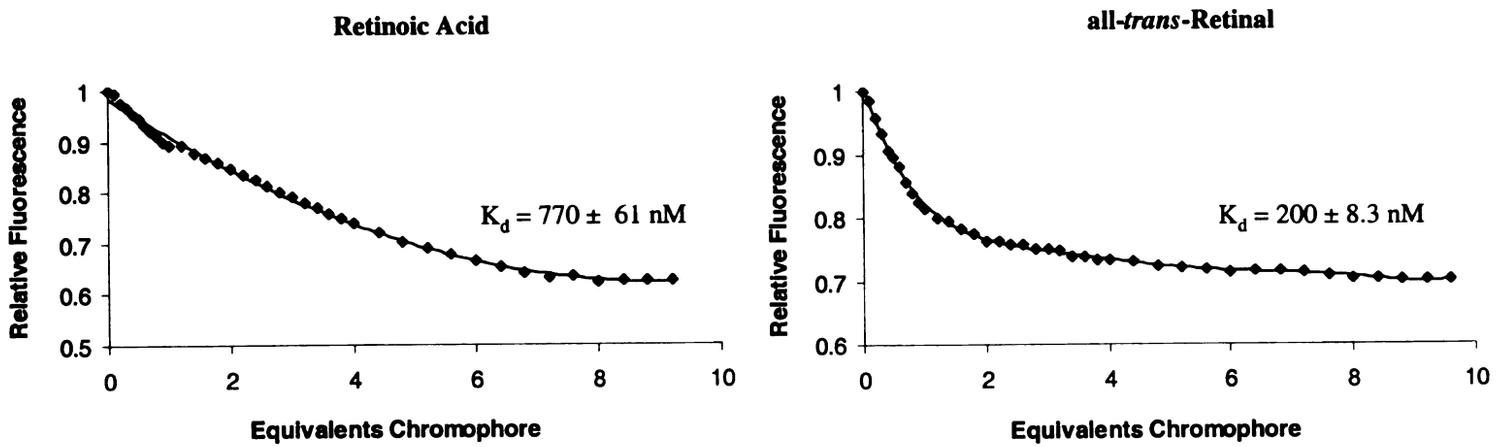


CRABPII R132K::Y134F::R111L::L121E
UV-vis Titrations, all-trans-Retinal
0.2 equivalents

CRABPII R132K::Y134F::R111L::L121E

UV-vis Titrations, all-*trans*-Retinal

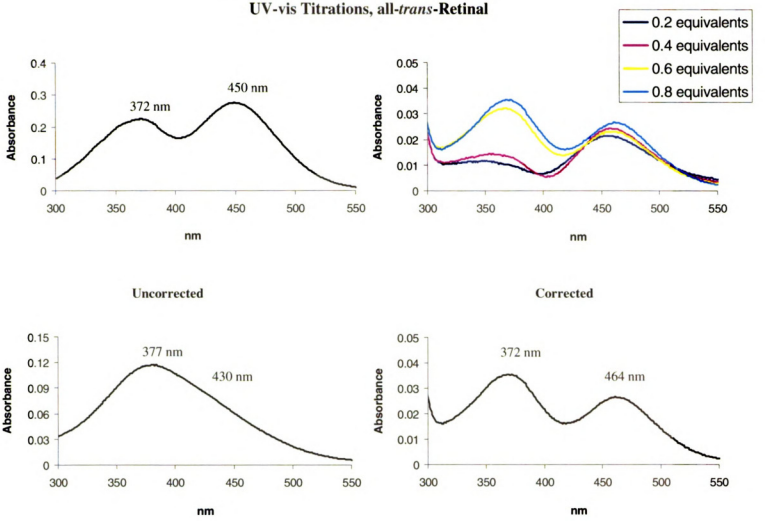

CRABPII R132K::Y134F::R111L::L121E
MALDI-TOF, Protein

CRABPII R132K::Y134F::R111L::L121E

MALDI-TOF, Protein

Calculated Mass = 16758.13 Da

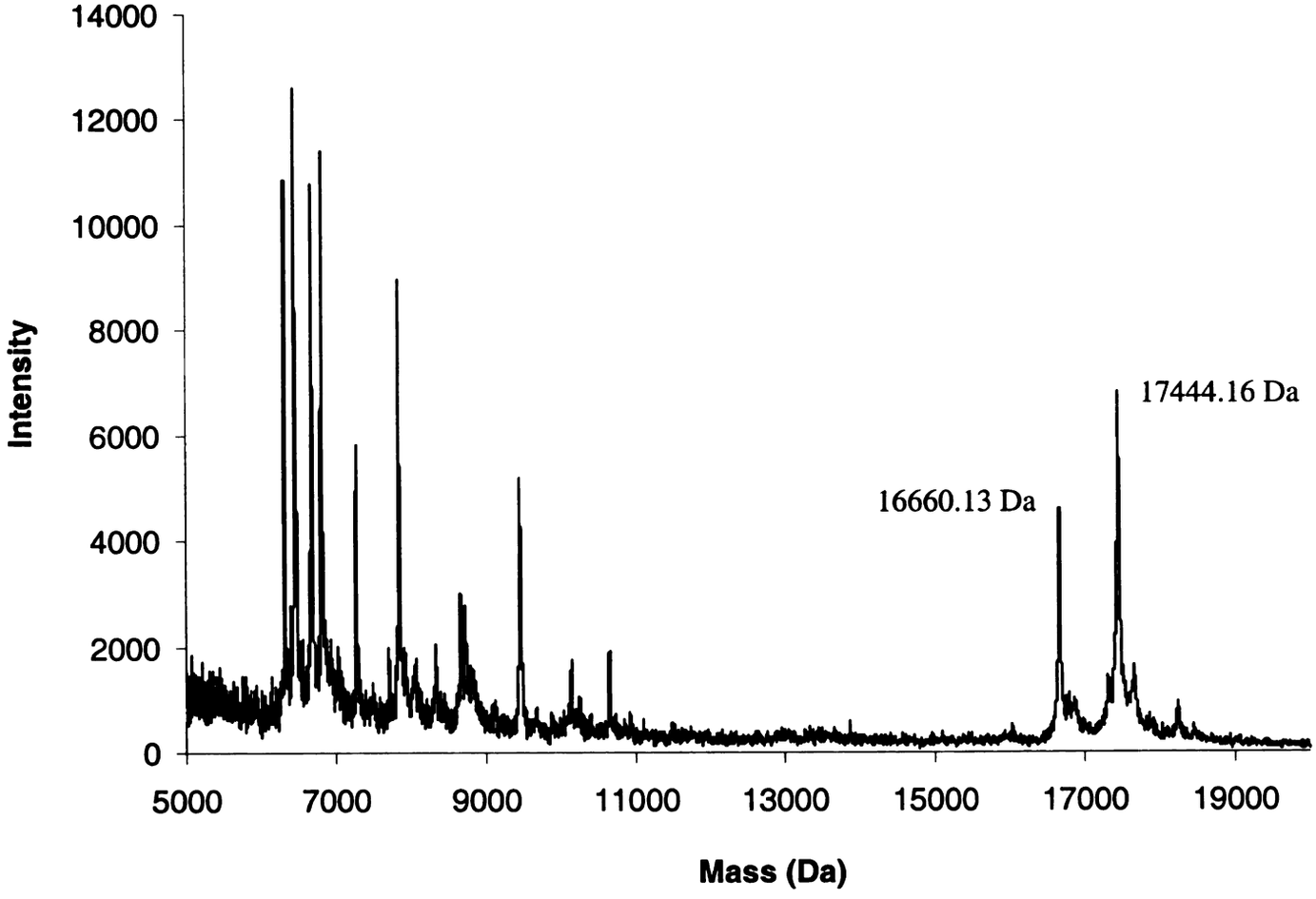

CRABPII R132K::Y134F::R111L::L121E
MALDI-TOF, Incubation with all-trans-Retinal
Protein Mass = 16758.13 Da

CRABPII R132K::Y134F::R111L::L121E

MALDI-TOF, Incubation with all-*trans*-Retinal

Protein Mass = 16758.13 Da

Positive Covalent Bond Formation = Protein Mass + 266

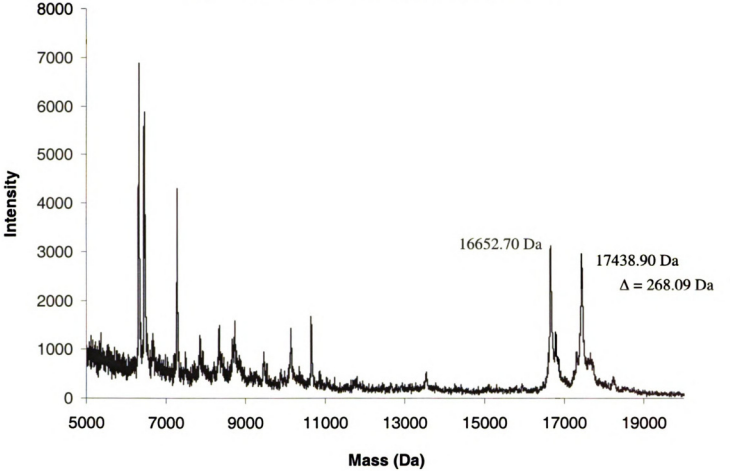

CRABPII R132K::Y134F::R111L::L121E
***MALDI-TOF*, Reductive Amination with all-*trans*-Retinal**
Protein Mass = 16758.13 Da
Positive Reductive Amination = Protein Mass + 268

CRABPII R132K::Y134F::R111L::L121E

MALDI-TOF, Reductive Amination with all-*trans*-Retinal

Protein Mass = 16758.13 Da

Positive Reductive Amination = Protein Mass + 268

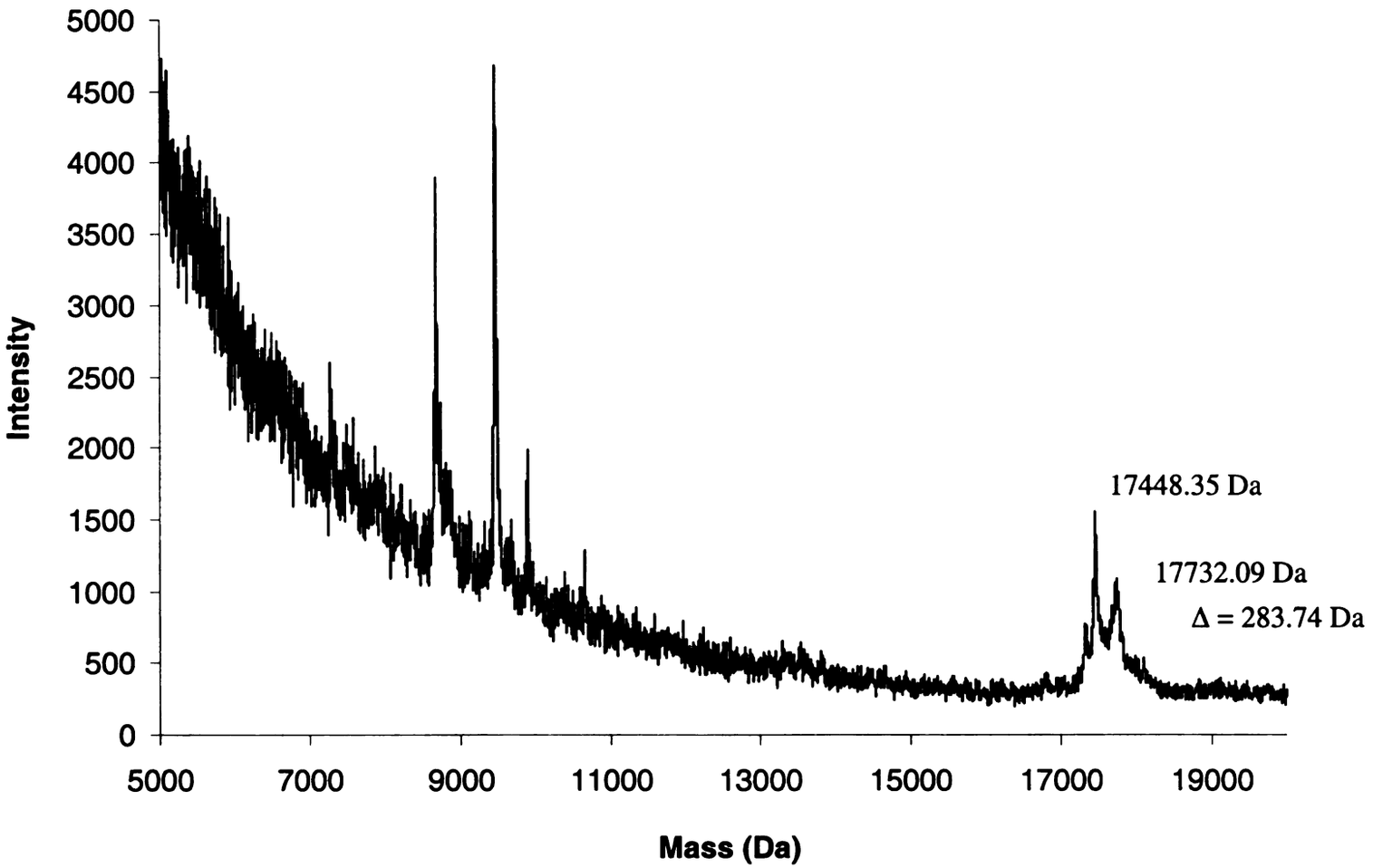

CRABPII R132K::Y134F::R111L::L121Q

Molecular Weight :

16757.14 Da

Extinction Coefficient :

17,397 M^{-1} cm^{-1}

Primers :

bbb96 5' GGG GAA CTG ATC CAG ACC ATG ACG GCG
bbb97 5' CGC CGT CAT GGT CTG GAT CAG TTC CCC

CD

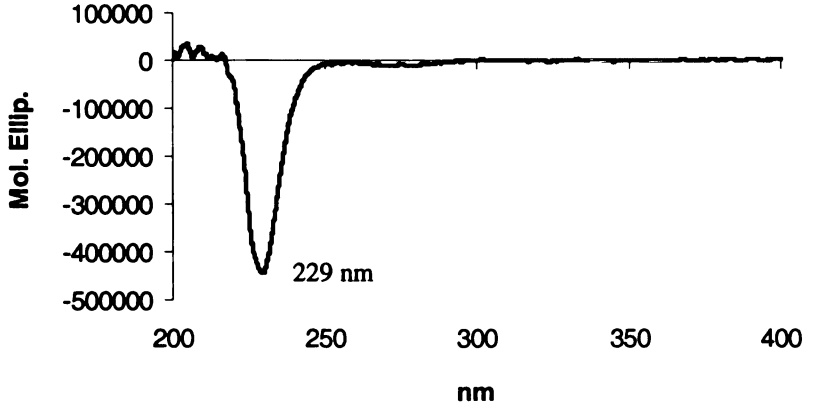

CRABPII R132K::Y134F::R111L::L121Q

Sequence BB 152

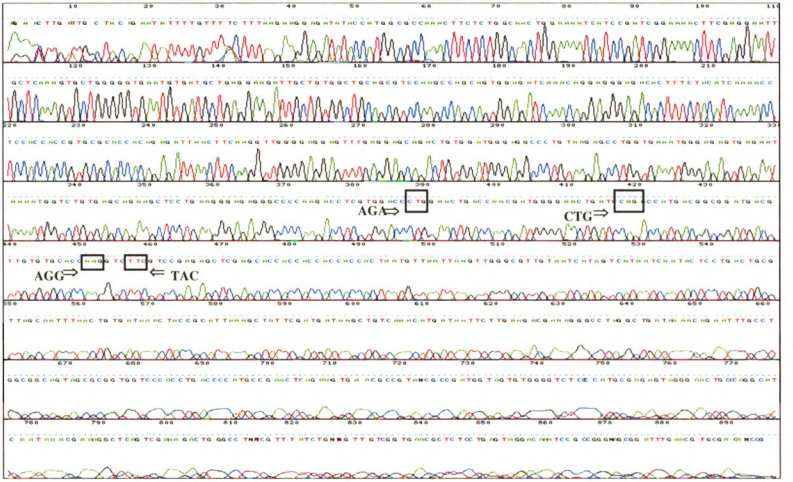

CRABPII R132K::Y134F::R111L::L121Q
Fluorescence Titrations

CRABPII R132K::Y134F::R111L::L121Q

Fluorescence Titrations

Retinoic Acid

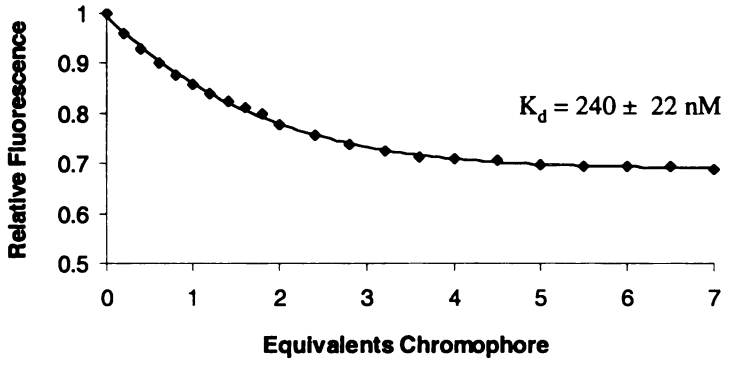

all-*trans*-Retinal

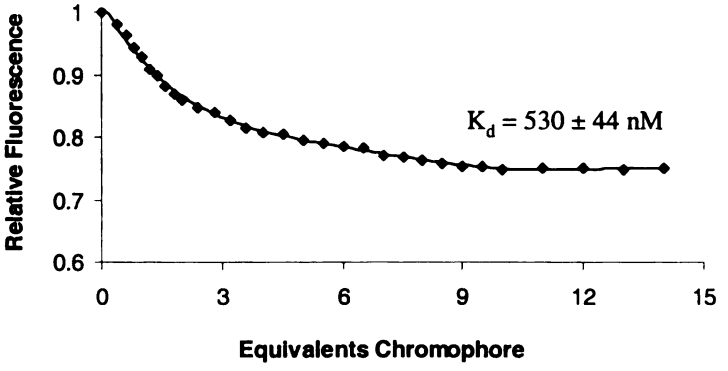

CRABPII R132K::Y134F::R111L::L121Q
UV-vis Titrations, all-*trans*-Retinal

0.3 equivalents

CRABPII R132K::Y134F::R111L::L121Q

UV-vis Titrations, all-*trans*-Retinal

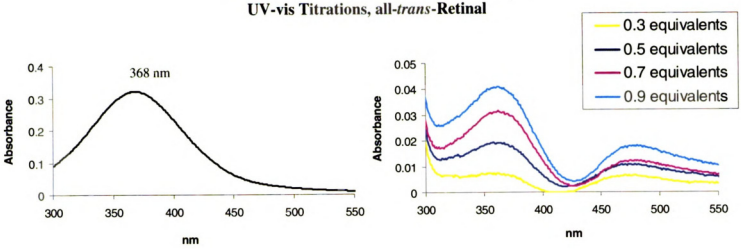

Uncorrected

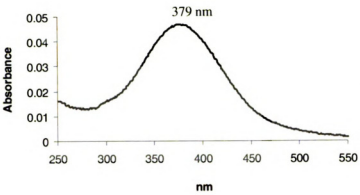

Corrected

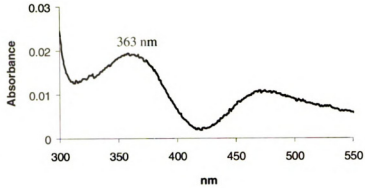

CRABPII R132K::Y134F::R111L::L121Q
MALDI-TOF, Protein
Calculated Mass = 16757.14 Da

CRABPII R132K::Y134F::R111L::L121Q

MALDI-TOF, Protein

Calculated Mass = 16757.14 Da

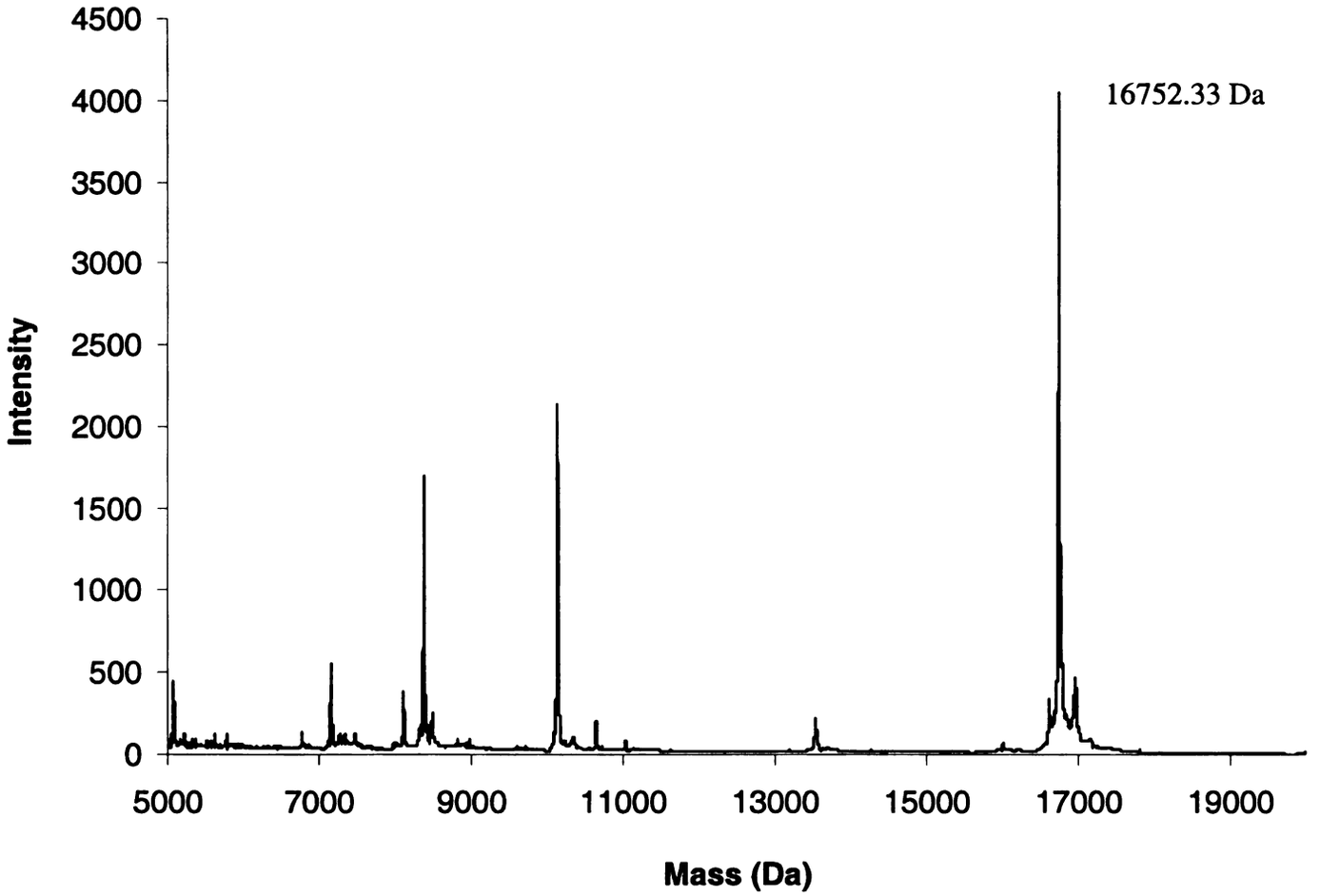

CRABPII R132K::Y134F::R111L::L121Q
MALDI-TOF, Incubation with all-*trans*-Retinal
Protein Mass = 16767.14 Da

CRABPII R132K::Y134F::R111L::L121Q

MALDI-TOF, Incubation with all-*trans*-Retinal

Protein Mass = 16757.14 Da

Positive Covalent Bond Formation = Protein Mass + 266

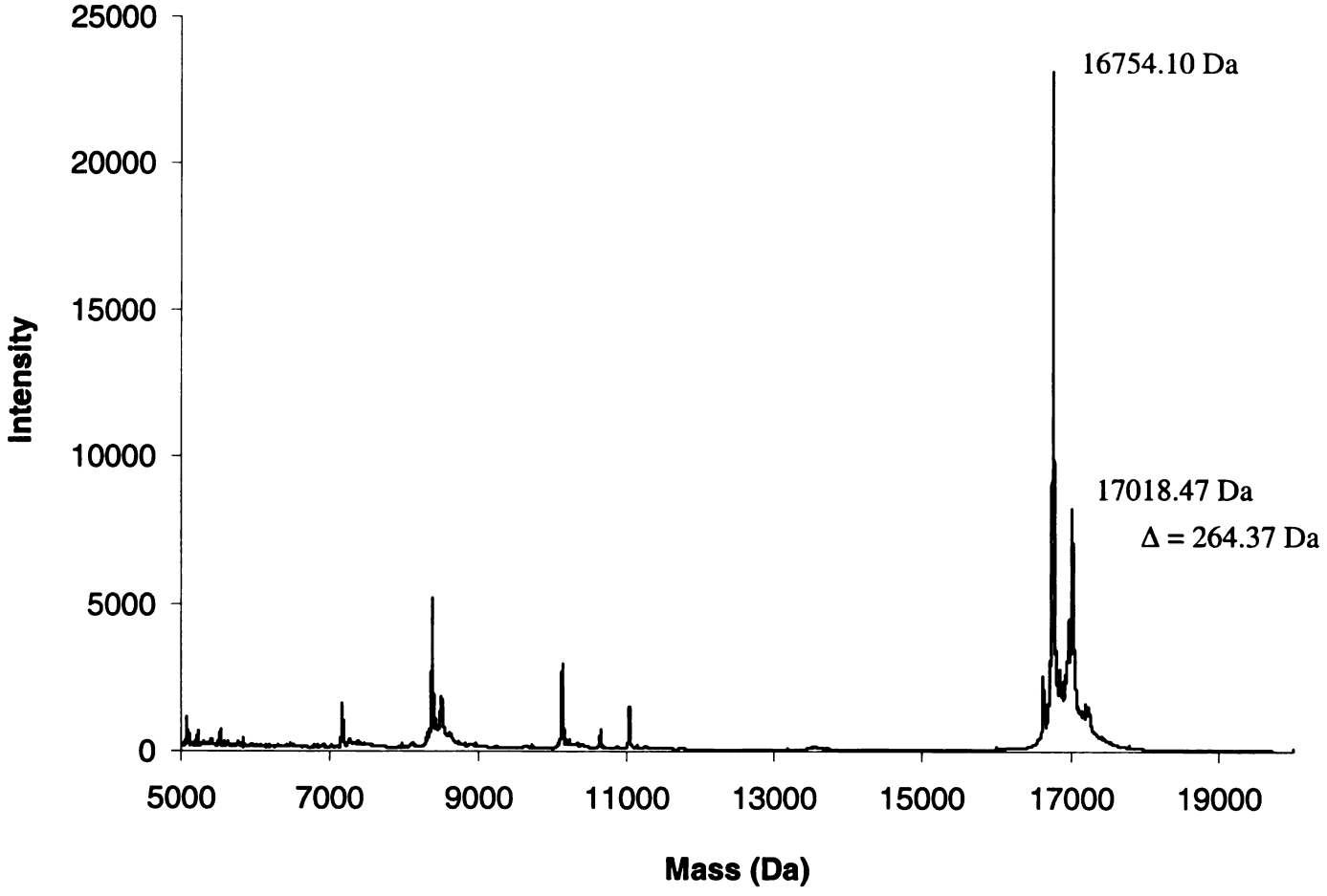

CRABPII R132K::Y134F::R111L::L121Q
MALDI-TOF, Reductive Amination with all-*trans*-Retinal
Protein Mass = 16757.14 D

CRABPII R132K::Y134F::R111L::L121Q

MALDI-TOF, Reductive Amination with all-*trans*-Retinal

Protein Mass = 16757.14 Da

Positive Reductive Amination = Protein Mass + 268

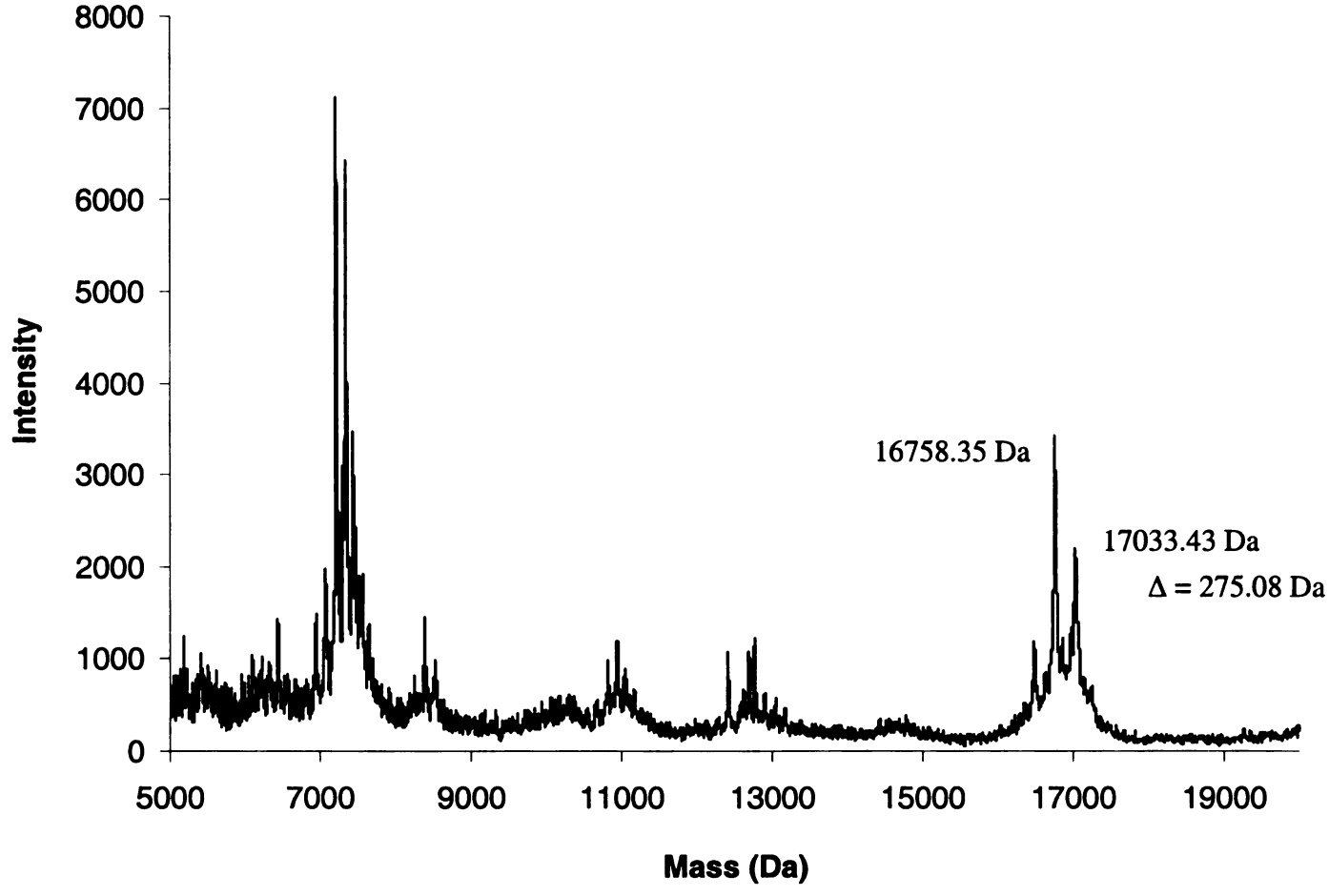

Molecular Weight :

CRABPII Y134F::R111L::L121E

Molecular Weight :

16786.14 Da

Extinction Coefficient :

19,432 M^{-1} cm^{-1}

Primers :

bbb88 5' CGT TGT GTG CAC CAG GGT CTT CGT CCG

bbb89 5' CGG ACG AAG ACC CTG GTG CAC ACA ACG

(Primers given for K132R.)

CD

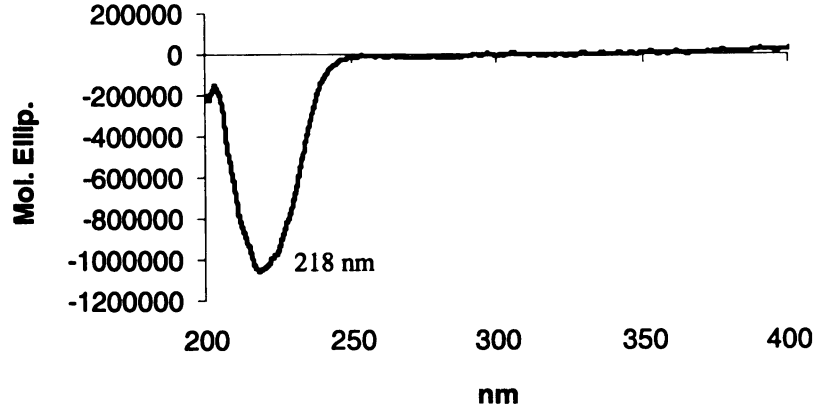

CRABPII Y134F::R111L::L121E

Sequence BB 141

CRABPII Y134F::R111L::L121E

Sequence BB 141

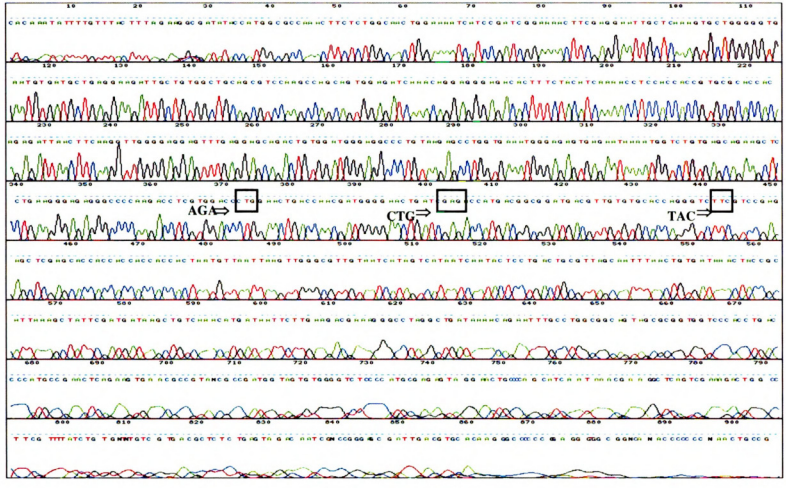

CRABPII Y134F::R111L::L121E

Fluorescence Titrations

Retinoic Acid

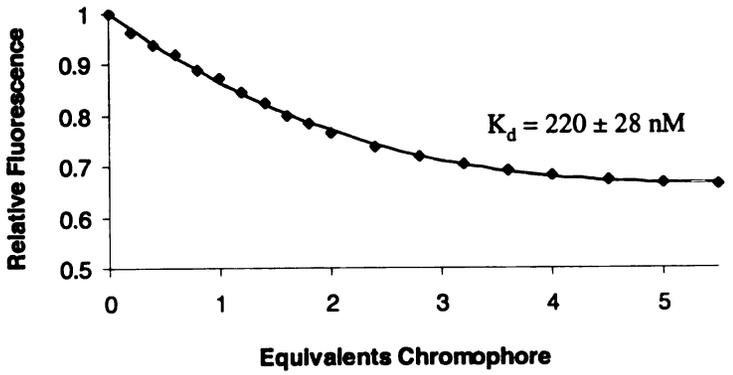

all-*trans*-Retinal

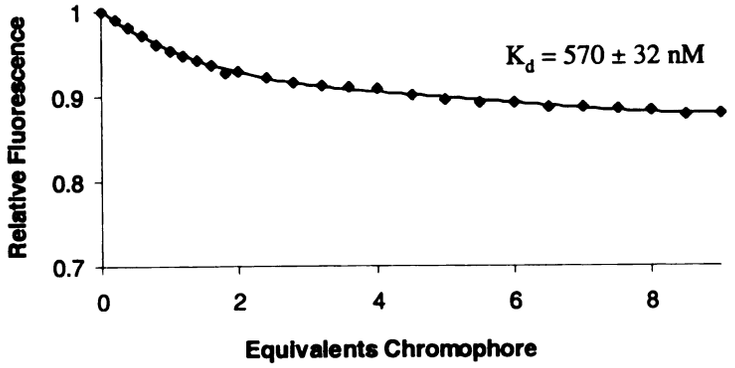

CRABPII Y134F::R111L::L121E
UV-vis Titrations, all-*trans*-Retinal

CRABPII Y134F::R111L::L121E

UV-vis Titrations, all-*trans*-Retinal

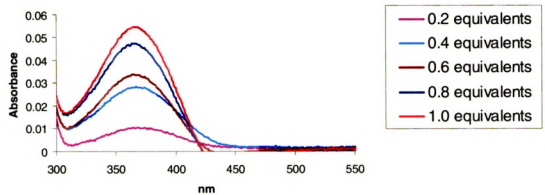

Uncorrected

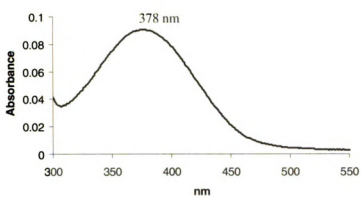

Corrected

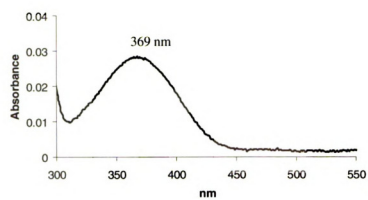

CRABPII Y134F::R111L::L121E
MALDI-TOF, Protein

CRABPII Y134F::R111L::L121E

MALDI-TOF, Protein

Calculated Mass = 16786.14 Da

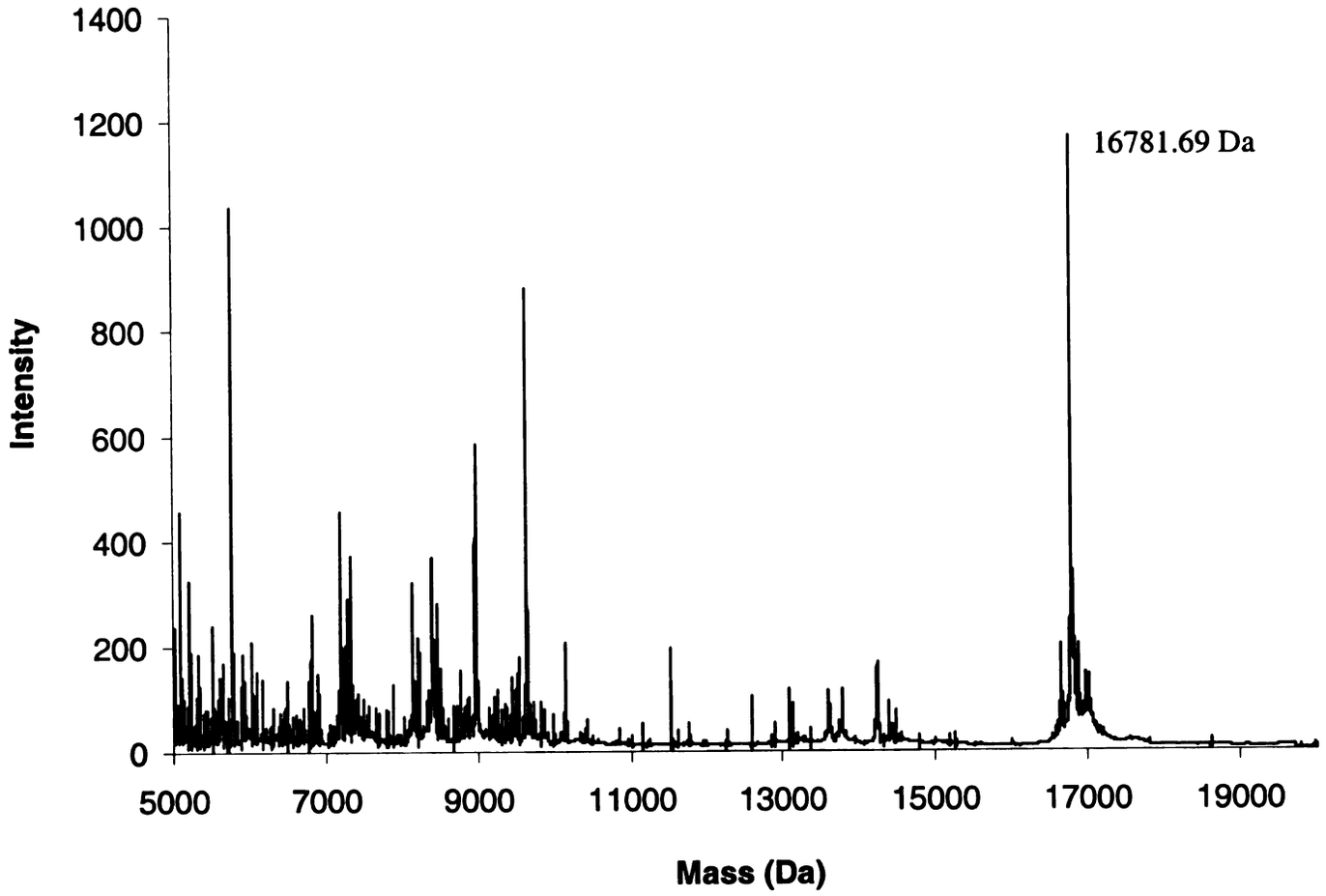

CRABPII Y134F::R111L::L121E
MALDI-TOF, Incubation with all-*trans*-Retinal

CRABPII Y134F::R111L::L121E

MALDI-TOF, Incubation with all-*trans*-Retinal

Protein Mass = 16786.14 Da

Positive Covalent Bond Formation = Protein Mass + 266

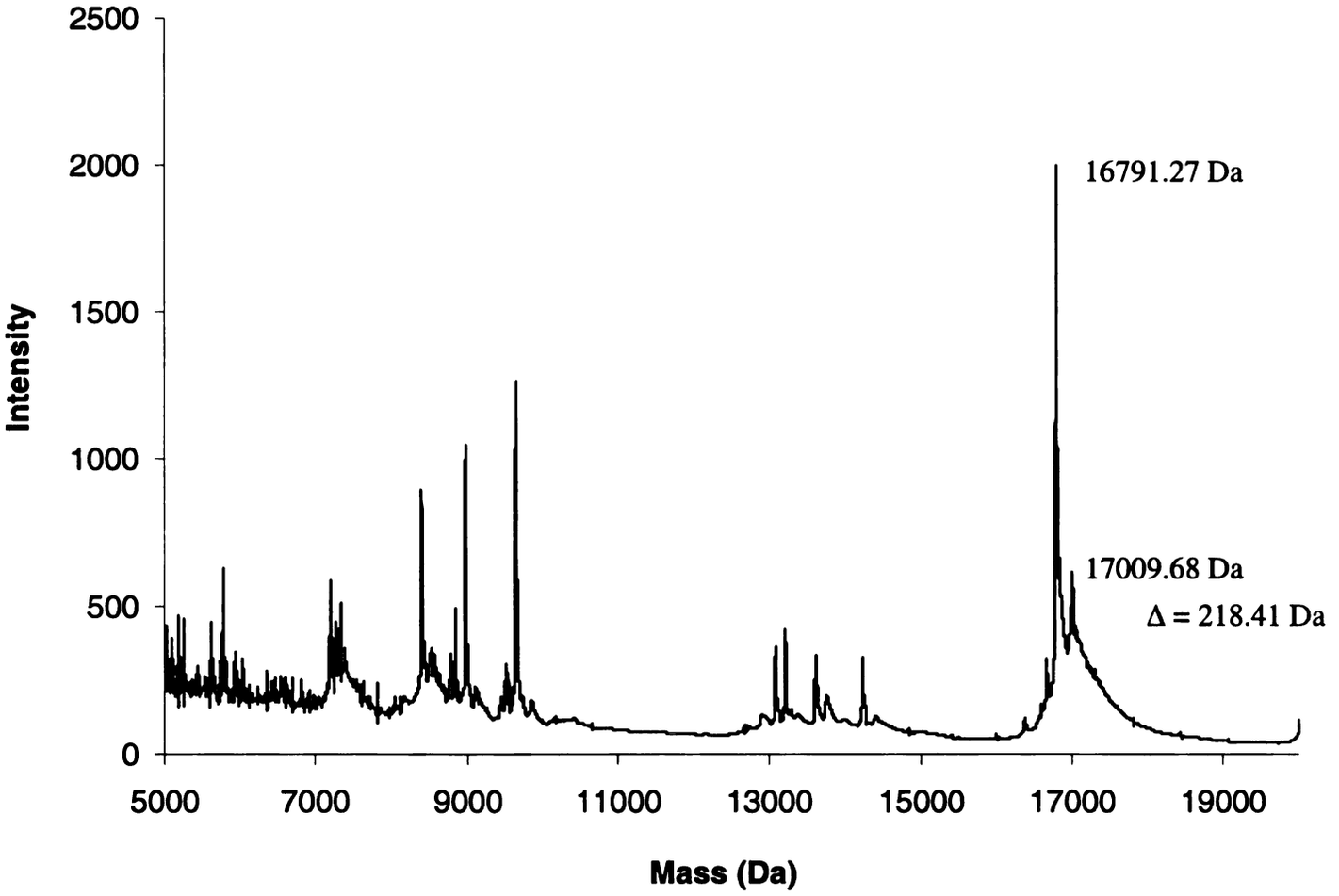

CRABPII Y134F::R111L::L121E

MALDI-TOF, Reductive Amination with all-*trans*-Retinal

CRABPII Y134F::R111L::L121E

MALDI-TOF, Reductive Amination with all-*trans*-Retinal

Protein Mass = 16786.14 Da

Positive Reductive Amination = Protein Mass + 268

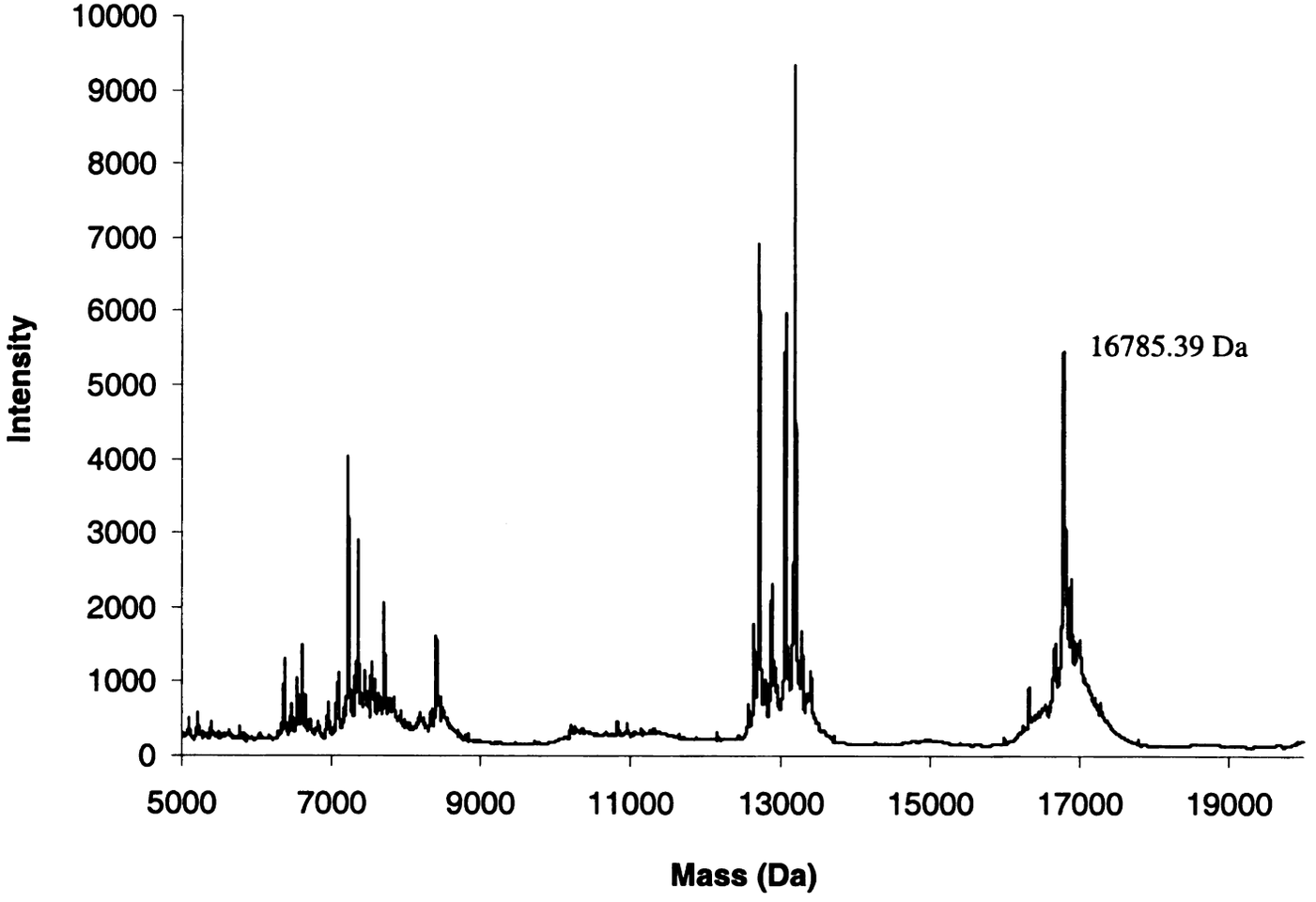

CRABPII R132L::Y134F::R111L::L121E

Molecular Weight :

16743.11 Da

Extinction Coefficient :

19,415 M^{-1} cm^{-1}

Primers :

bbb86 5' CGT TGT GTG CAC CCT GGT CTT CGT CCG

bbb87 5' CGG ACG AAG ACC AGG GTG CAC ACA ACG

(Primers given for R132L.)

CD

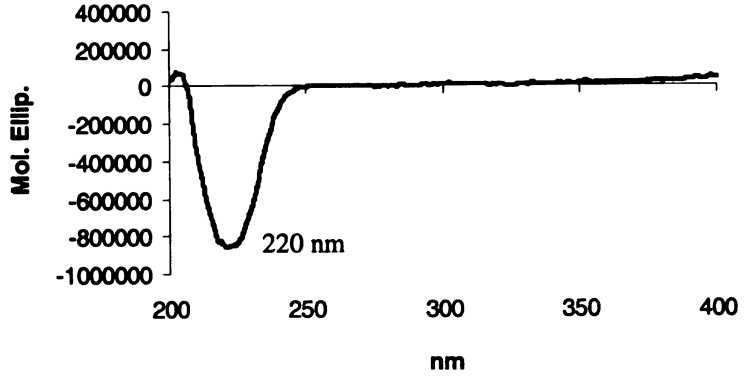

CRABPII R132L::Y134F::R111L::L121E

Sequence BB 142

CRABPII R132L::Y134F::R111L::L121E

Sequence BB 142

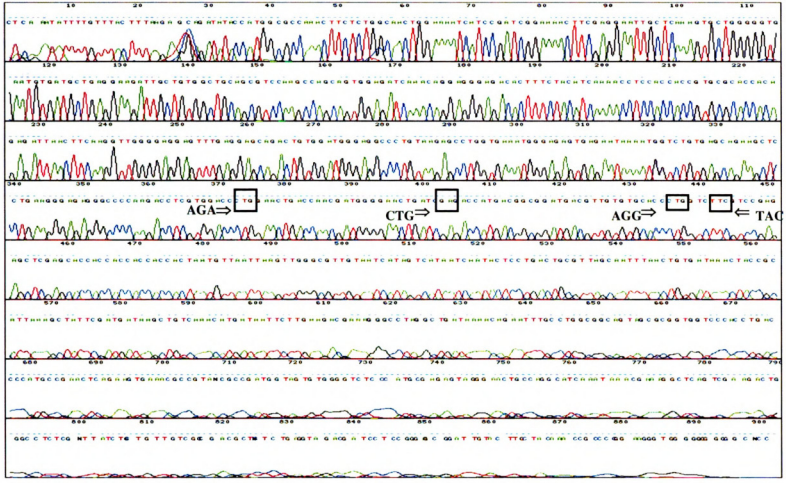

CRABPII R132L::Y134F::R111L::L121E

Fluorescence Titrations

CRABPII R132L::Y134F::R111L::L121E

Fluorescence Titrations

Retinoic Acid

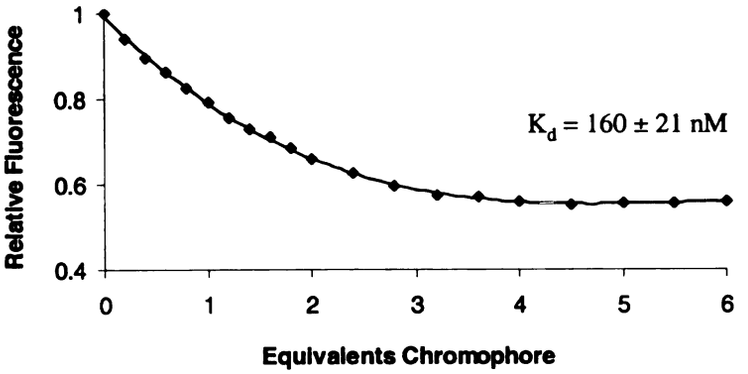

all-*trans*-Retinal

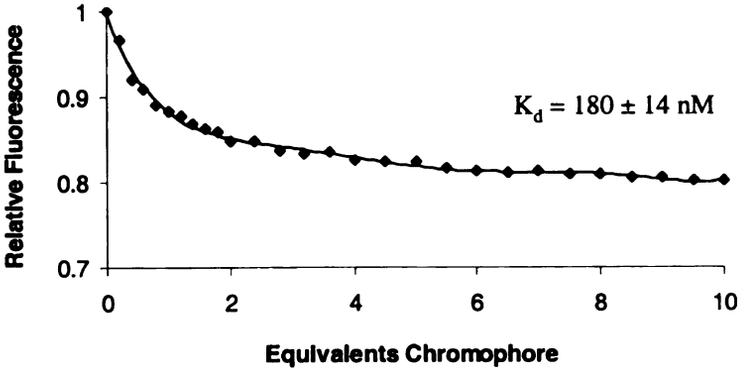

CRABPII R132L::Y134F::R111L::L121E
UV-vis Titrations, all-*trans*-Retinal

CRABPII R132L::Y134F::R111L::L121E

UV-vis Titrations, all-*trans*-Retinal

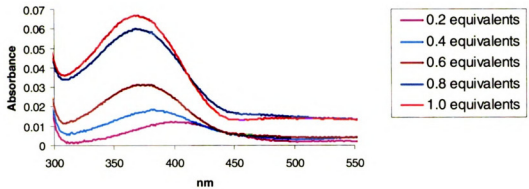

Uncorrected

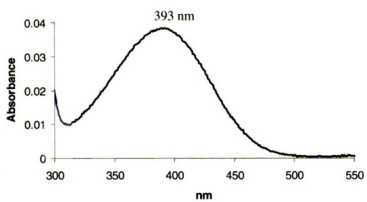

Corrected

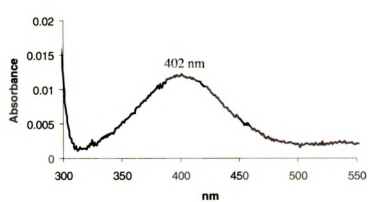

CRABPII R132L::Y134F::R111L::L121E
UV-vis Titrations, 11-cis-Retinal

CRABPII R132L::Y134F::R111L::L121E

UV-vis Titrations, 11-*cis*-Retinal

Uncorrected

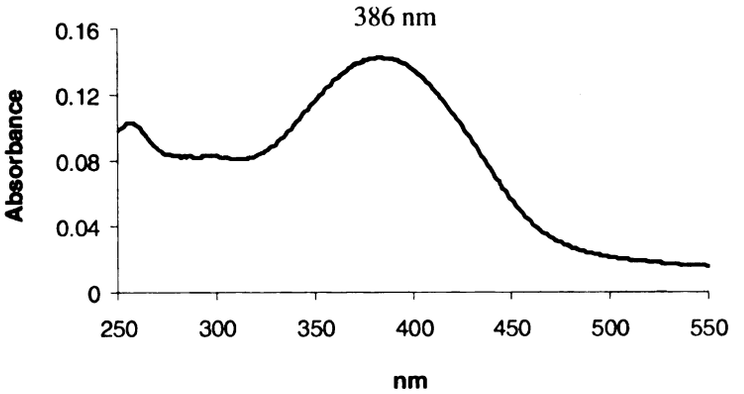

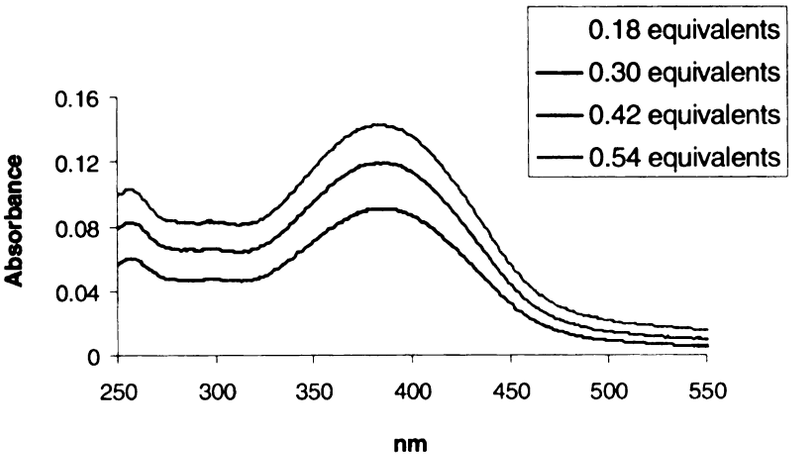

Corrected

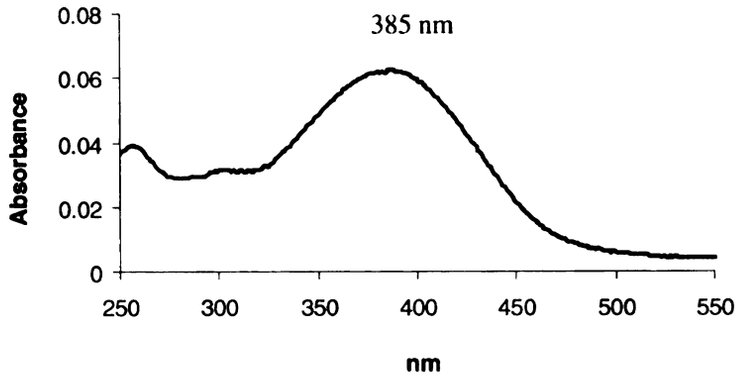

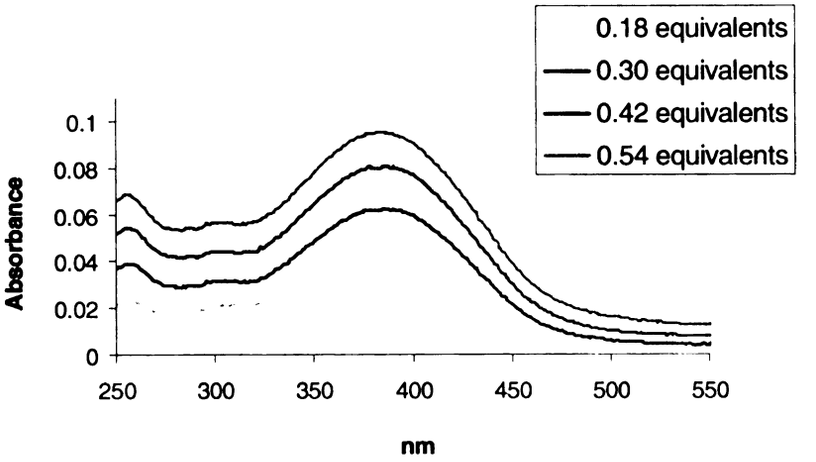

CRABPII R132L::Y134F::R111L::L121E
MALDI-TOF, Protein

CRABPII R132L::Y134F::R111L::L121E

MALDI-TOF, Protein

Calculated Mass = 16743.11 Da

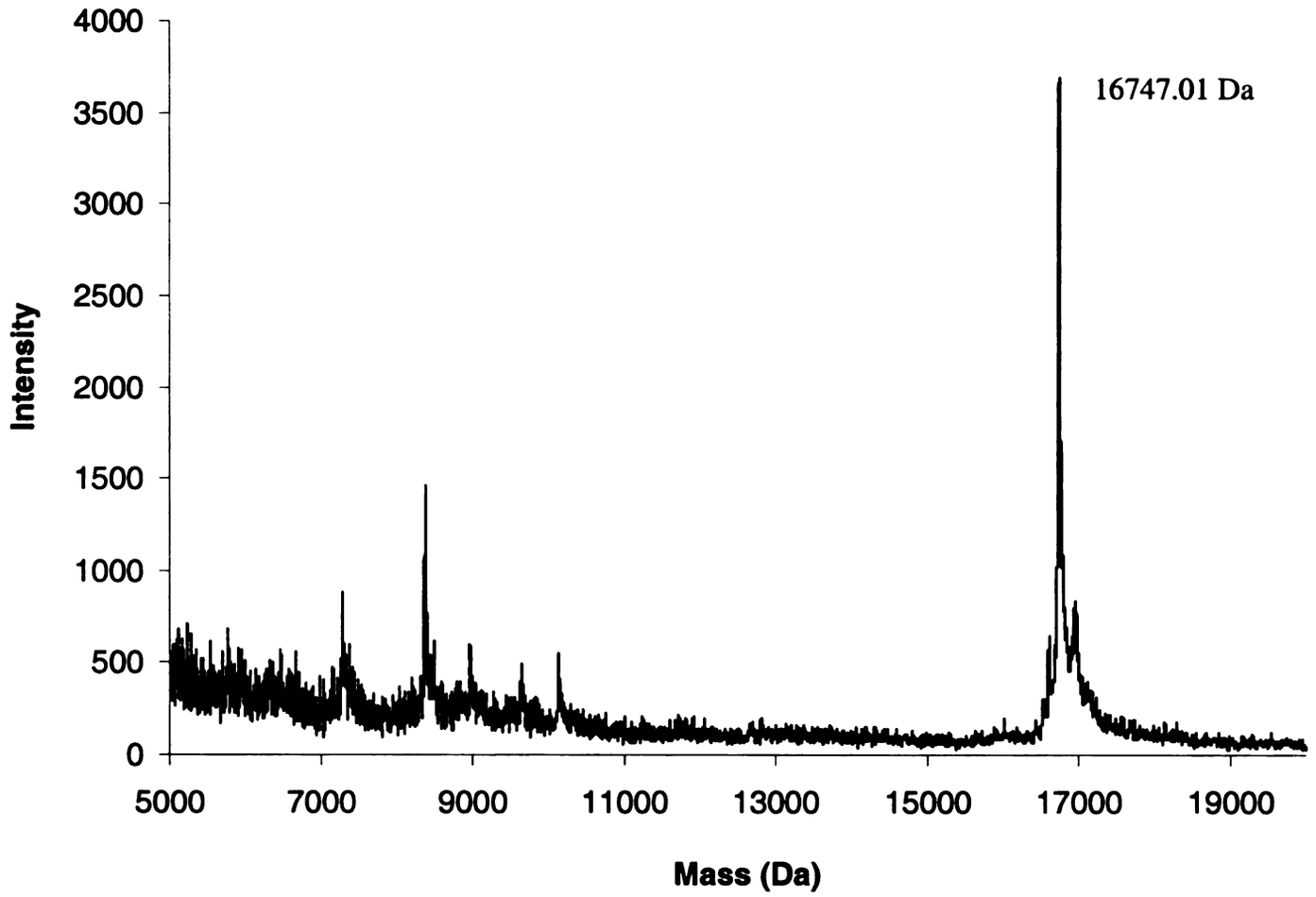

CRABPII R132L::Y134F::R111L::L121E
***MALDI-TOF*, Incubation with all-*trans*-Retinal**

CRABPII R132L::Y134F::R111L::L121E

MALDI-TOF, Incubation with all-*trans*-Retinal

Protein Mass = 16743.11 Da

Positive Covalent Bond Formation = Protein Mass + 266

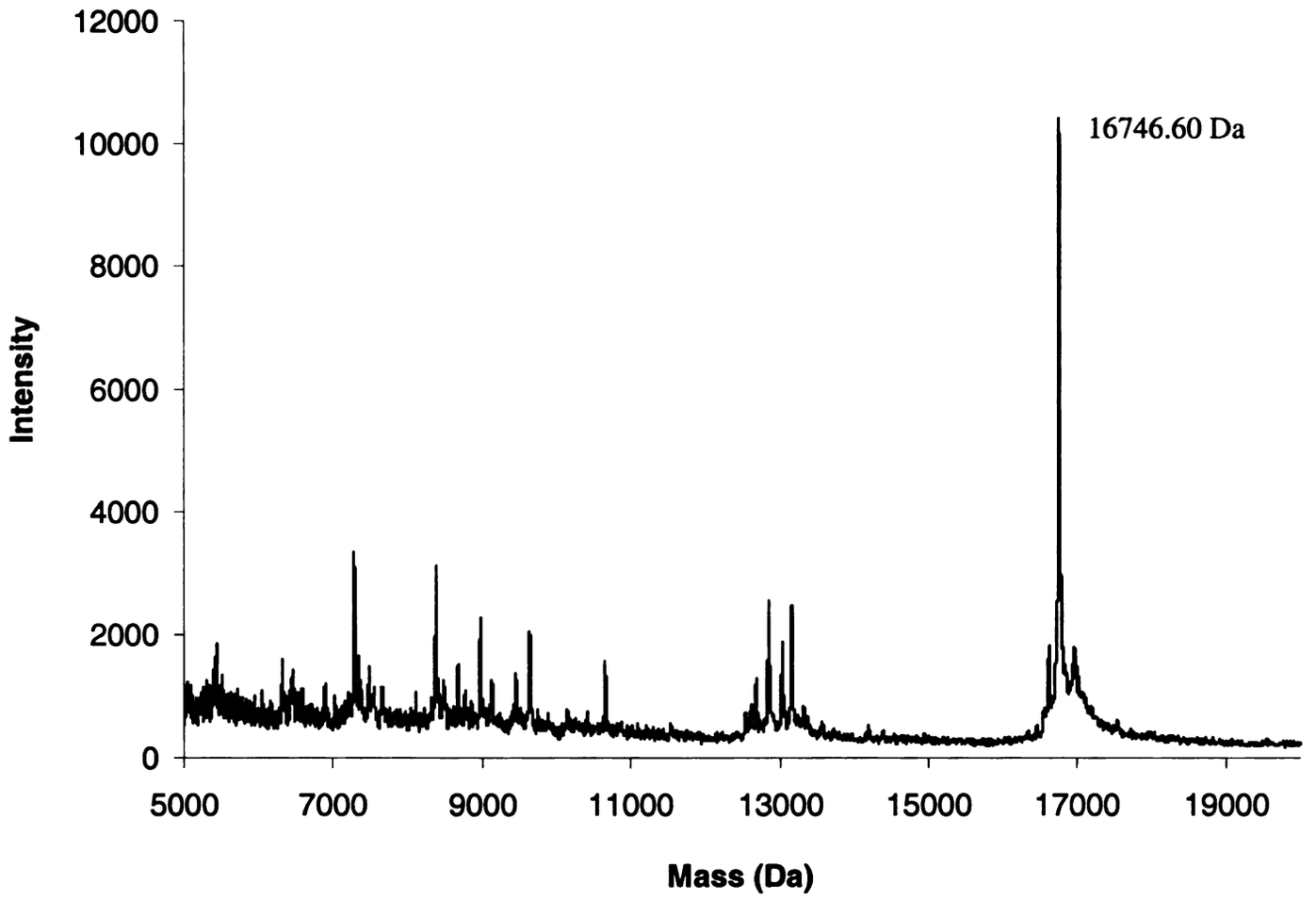

CRABPII R132L::Y134F::R111L::L121E
MALDI-TOF, Reductive Amination with all-trans-Retinal

CRABPII R132L::Y134F::R111L::L121E

MALDI-TOF, Reductive Amination with all-*trans*-Retinal

Protein Mass = 16743.11 Da

Positive Reductive Amination = Protein Mass + 268

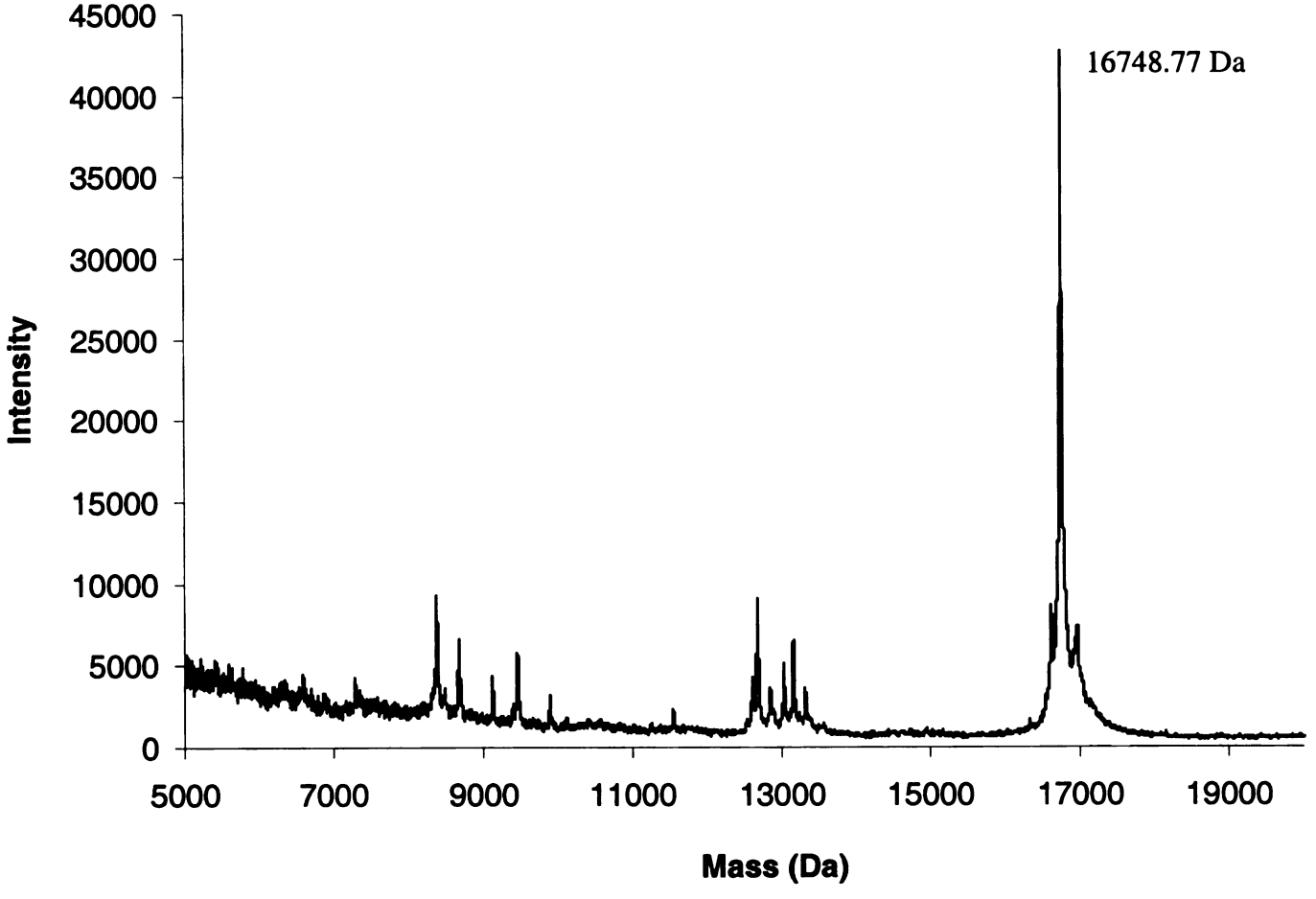

CRABPII R132K::Y134F::R111L::L121E::F15A

Molecular Weight :

16682.03 Da

Extinction Coefficient :

19,450 M^{-1} cm^{-1}

Primers :

bbb92 5' CGA TCG GAA AAC GCC GAG GAA TTG CTC

bbb93 5' GAG CAA TTC CTC GGC GTT TTC CGA TCG

CD

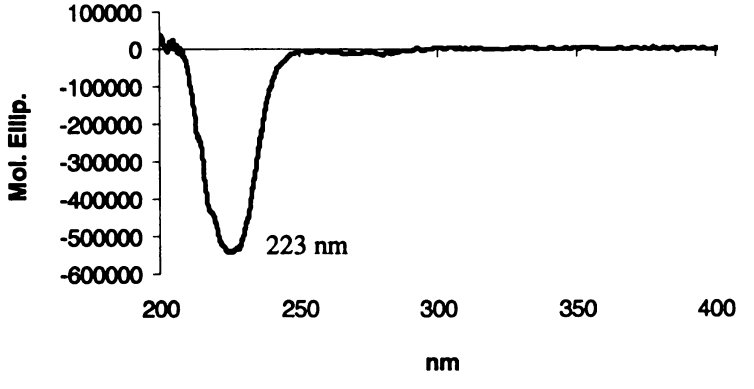

CRAIBPII R132K::Y134F::R111L::L121E::F15A
Sequence BB 180

CRABPII R132K::Y134F::R111L::L121E::F15A

Sequence BB 180

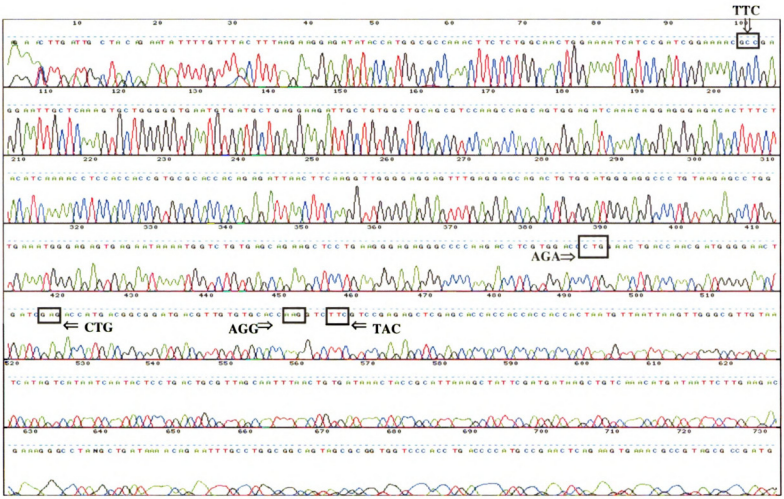

CRABPII R132K::Y134F::R111L::L121E::F15A

Fluorescence Titrations

CRABPII R132K::Y134F::R111L::L121E::F15A

Fluorescence Titrations

Retinoic Acid

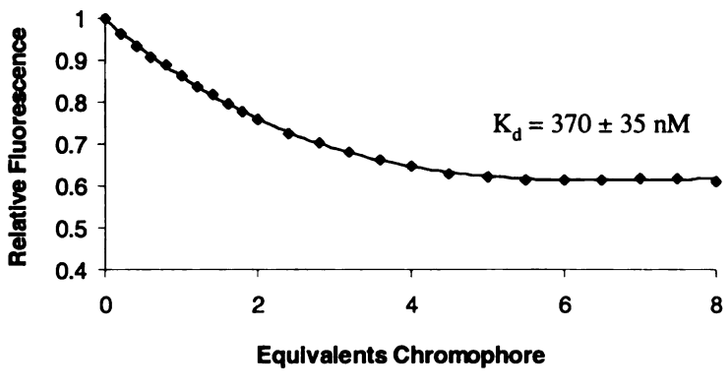

all-*trans*-Retinal

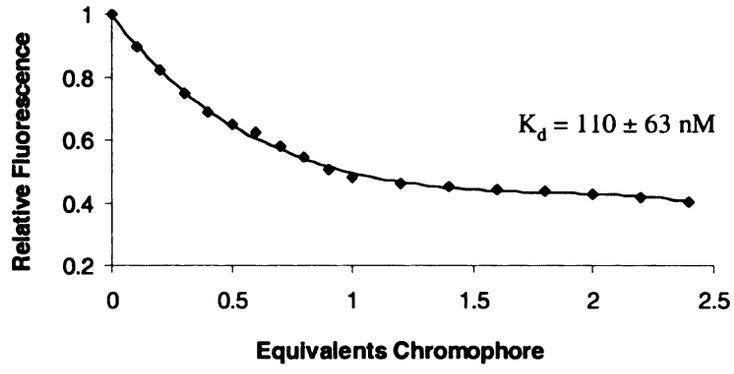

CRABPII R132K::Y134F::R111L::L121E::F15A

UV-vis Titrations, all-*trans*-Retinal

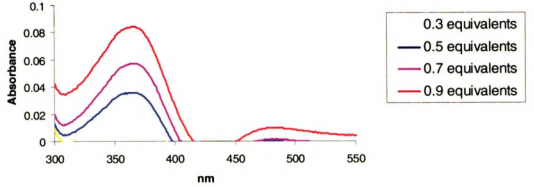

Uncorrected

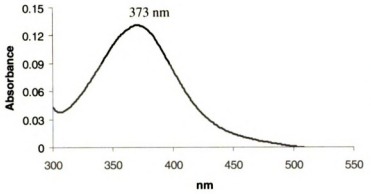

Corrected

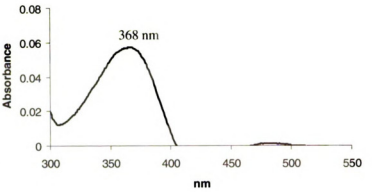

CRABPII R132K::Y134F::R111L::L121E::F15A

MALDI-TOF, Protein

CRABPII R132K::Y134F::R111L::L121E::F15A

MALDI-TOF, Protein

Calculated Mass = 16682.03 Da

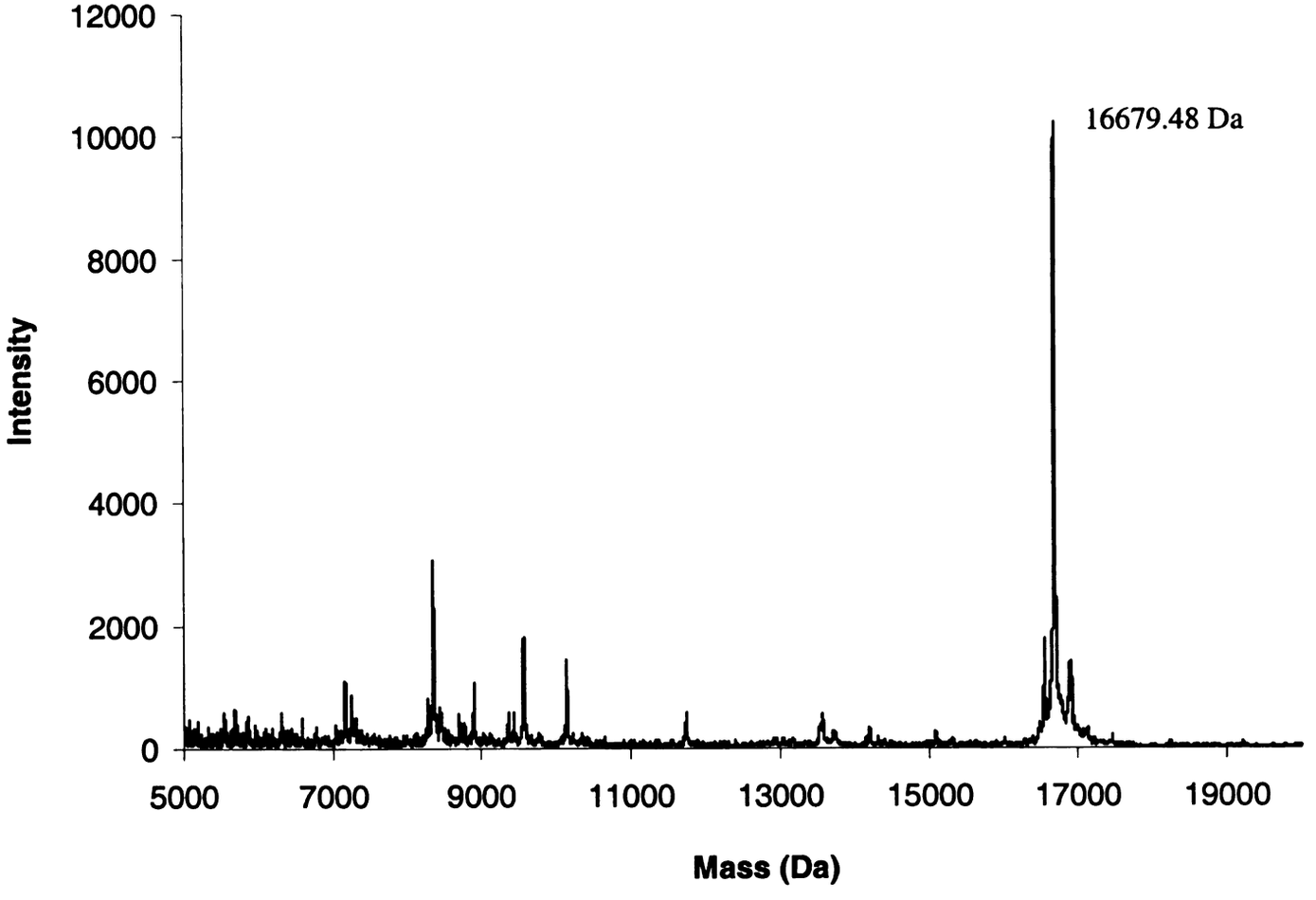

CRABPII R132K::Y134F::R111L::L121E::F15A
MALDI-TOF, Incubation with all-*trans*-Retinal

CRABPII R132K::Y134F::R111L::L121E::F15A

MALDI-TOF, Incubation with all-*trans*-Retinal

Protein Mass = 16682.03 Da

Positive Covalent Bond Formation = Protein Mass + 266

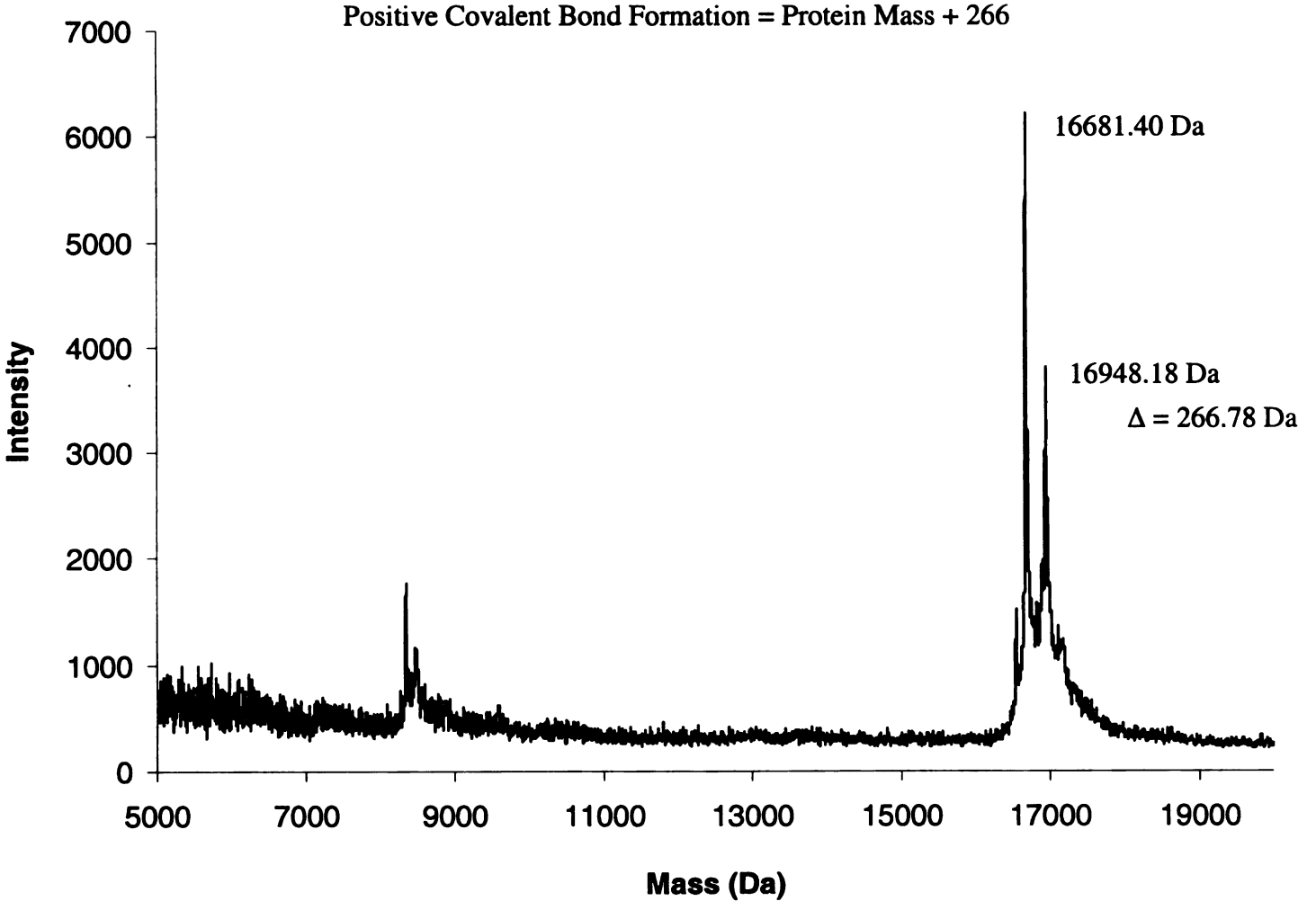

CRABPII R132K::Y134F::R111L::L121E::F15A

***MALDI-TOF*, Reductive Amination with all-*trans*-Retinal**

CRABPII R132K::Y134F::R111L::L121E::F15A

MALDI-TOF, Reductive Amination with all-*trans*-Retinal

Protein Mass = 16682.03 Da

Positive Reductive Amination = Protein Mass + 268

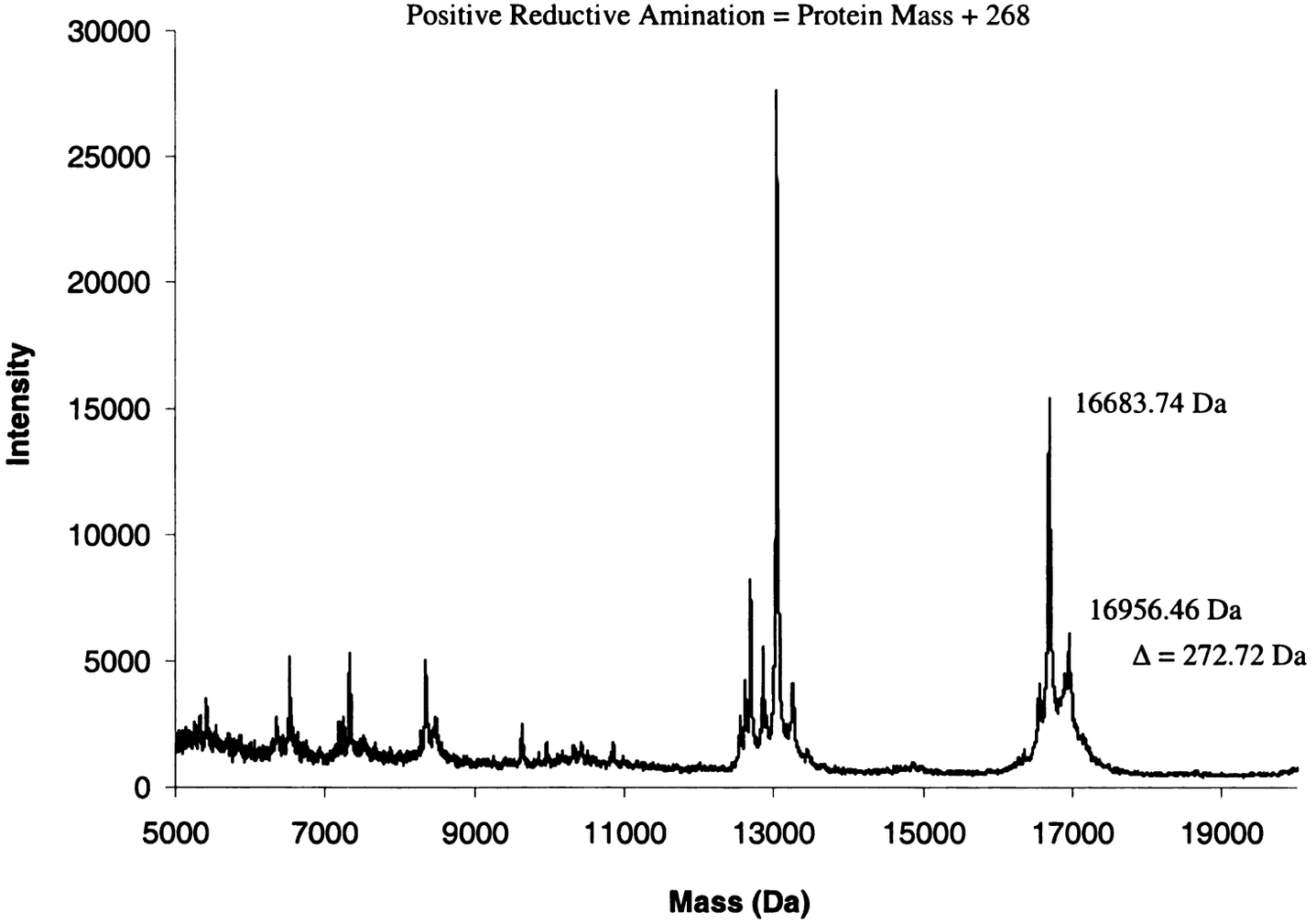

CRABPII R132K::Y134F::R111L::L121E::T54V

Molecular Weight :
16756.16 Da

Extinction Coefficient :
19,362 M^{-1} cm^{-1}

Primers :
bbb67 5' CTA CAT CAA AGT CTC CAC CAC CGT GCG
bbb68 5' CGC ACG GTG GTG GAG ACT TTG ATG TAG

CD

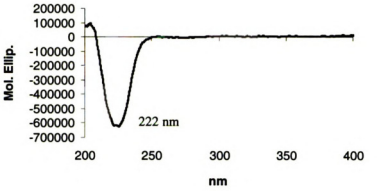

CRABPII R132K::Y134F::R111L::L121E::T54V
CD, Retinal

CRABPII R132K::Y134F::R111L::L121E::T54V

CD, Retinal

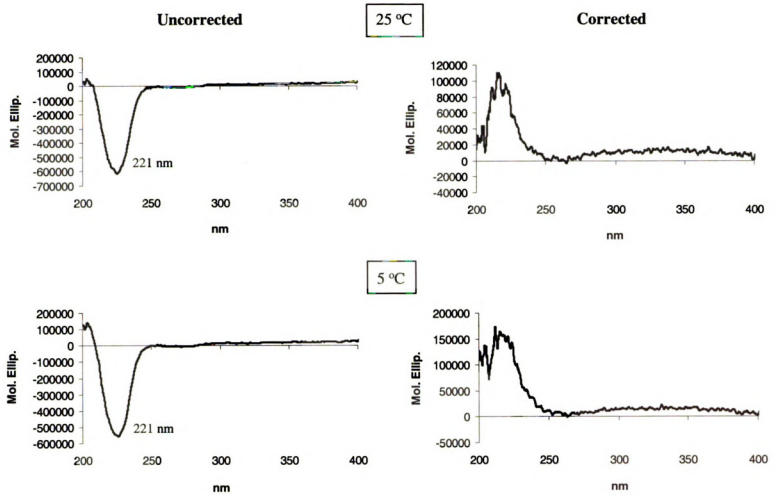

CRABPII R132K::Y134F::R111L::L121E::T54V

Sequence BB 184

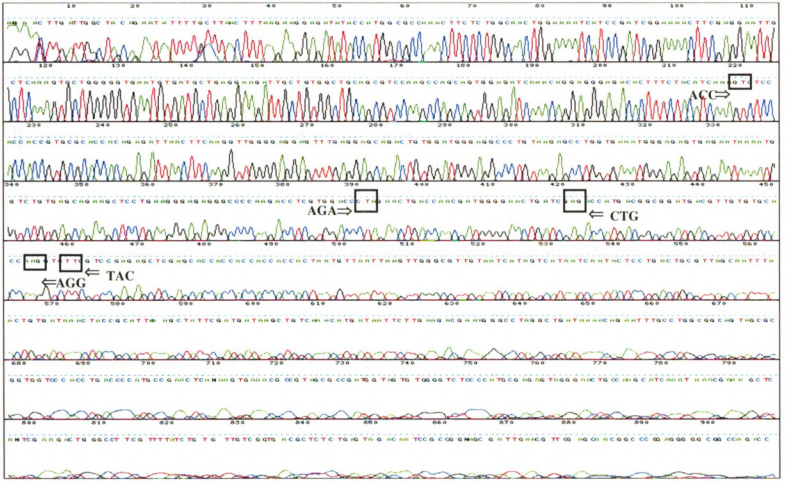

CRABPII R132K::Y134F::R111L::L121E::T54V

Fluorescence Titrations

Retinoic Acid

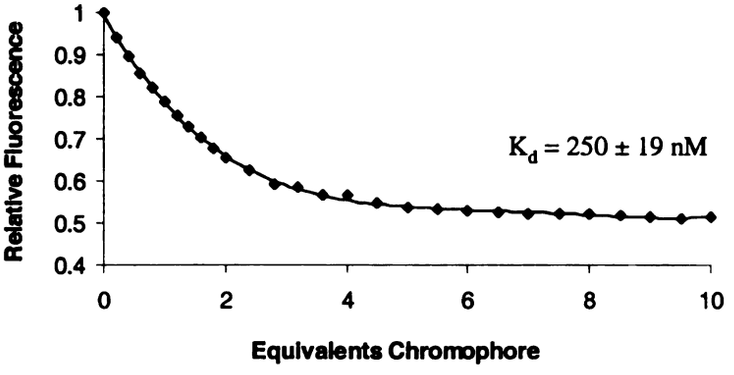

all-*trans*-Retinal

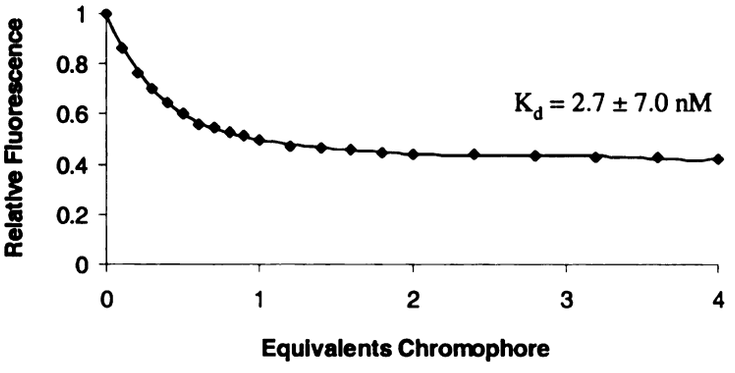

11-*cis*-Retinal

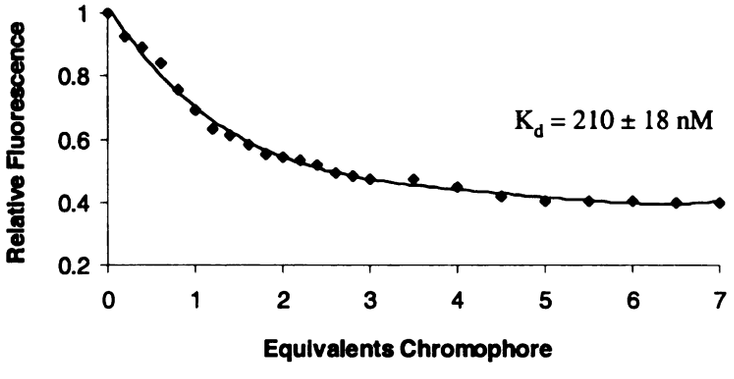

CRABPII R132K::Y134F::R111L::L121E::T54V

UV-vis Titrations, all-*trans*-Retinal

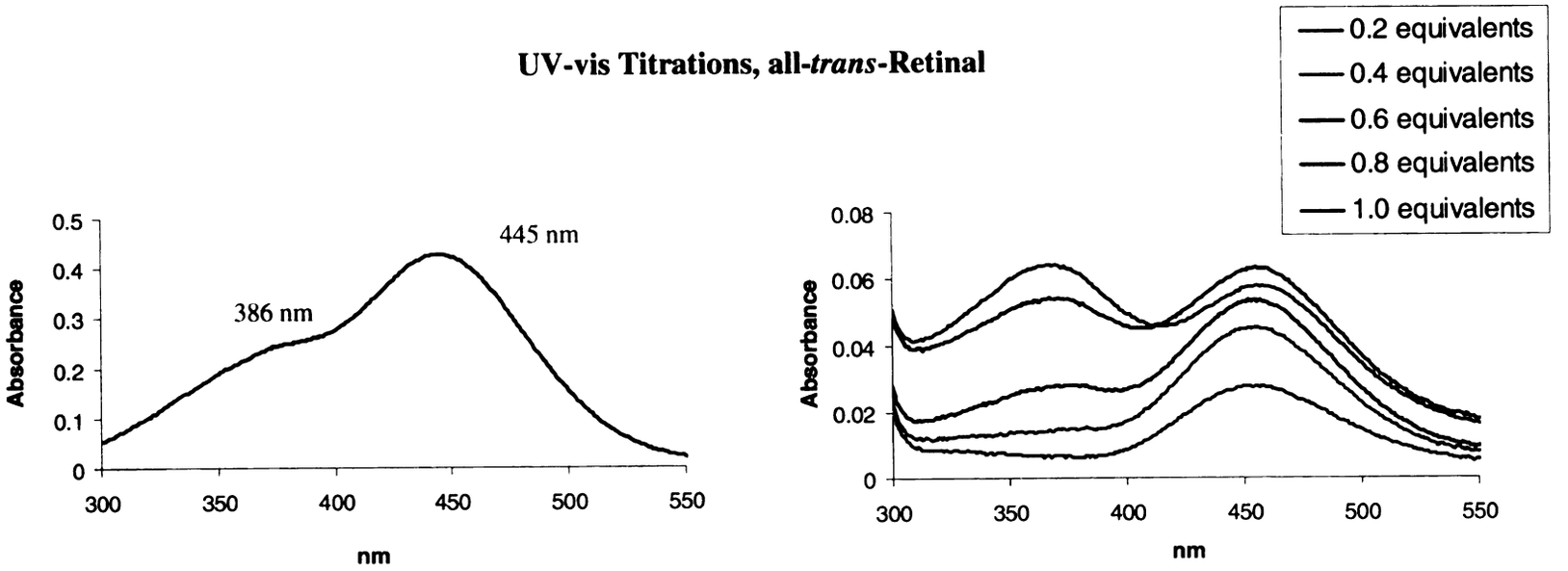

Uncorrected

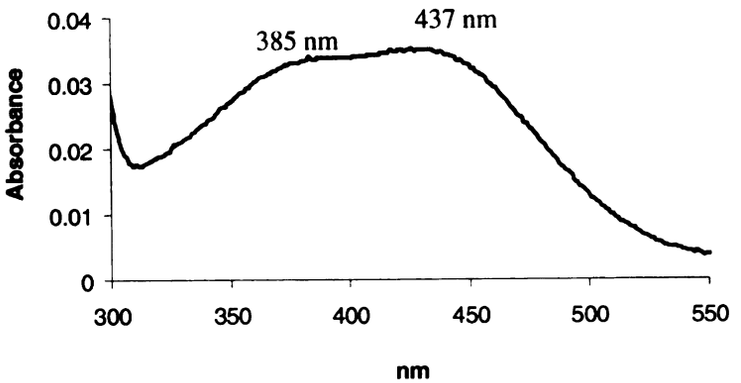

Corrected

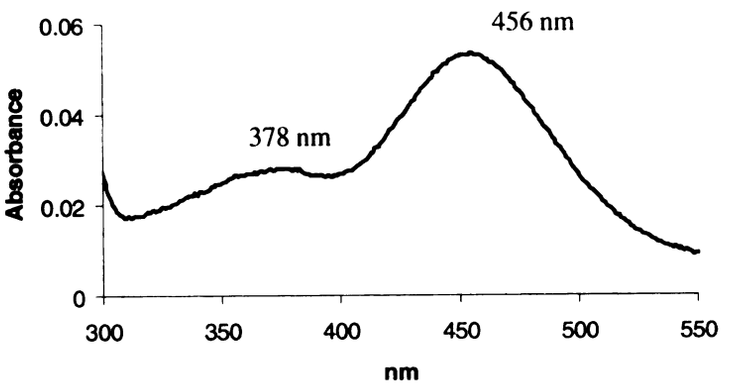

CRABPII R132K::Y134F::R111L::L121E::T54V

UV-vis Titrations, 11-*cis*-Retinal

Uncorrected

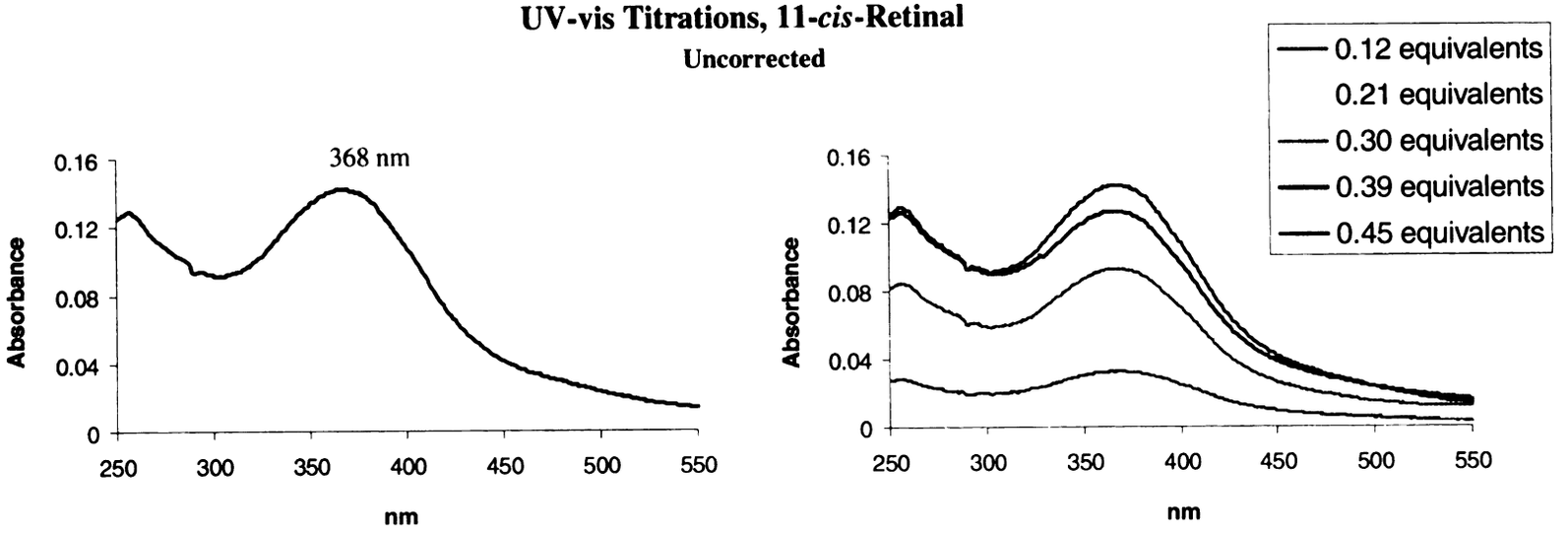

Corrected

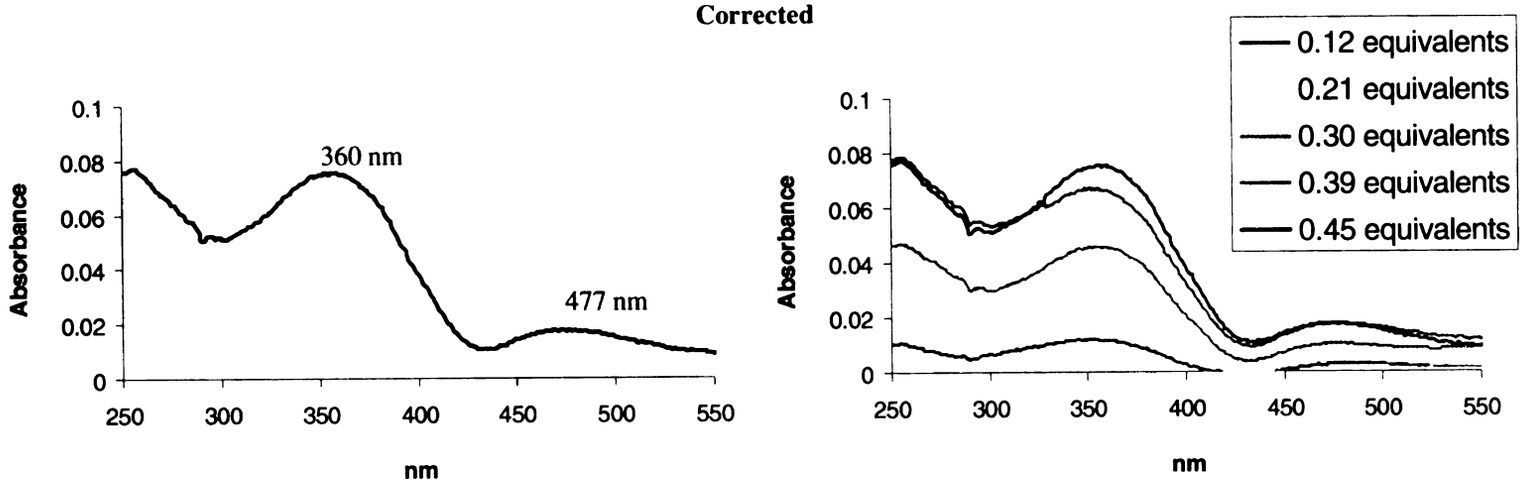

CRABPII R132K::Y134F::R111L::L121E::T54V

UV-vis Acid/Base Titrations, all-*trans*-Retinal

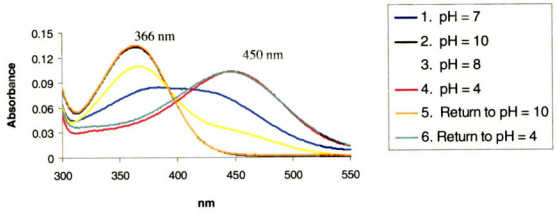

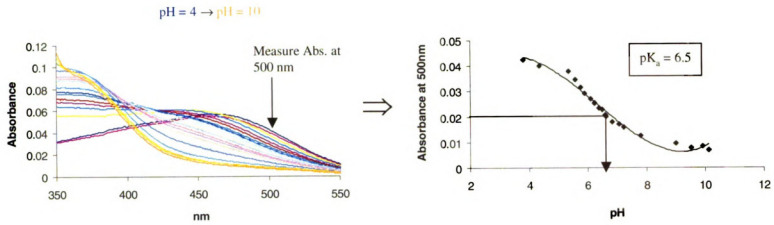

CRABPII R132K::Y134F::R111L::L121E::T54V

MALDI-TOF, Protein

Calculated Mass = 16756.16 Da

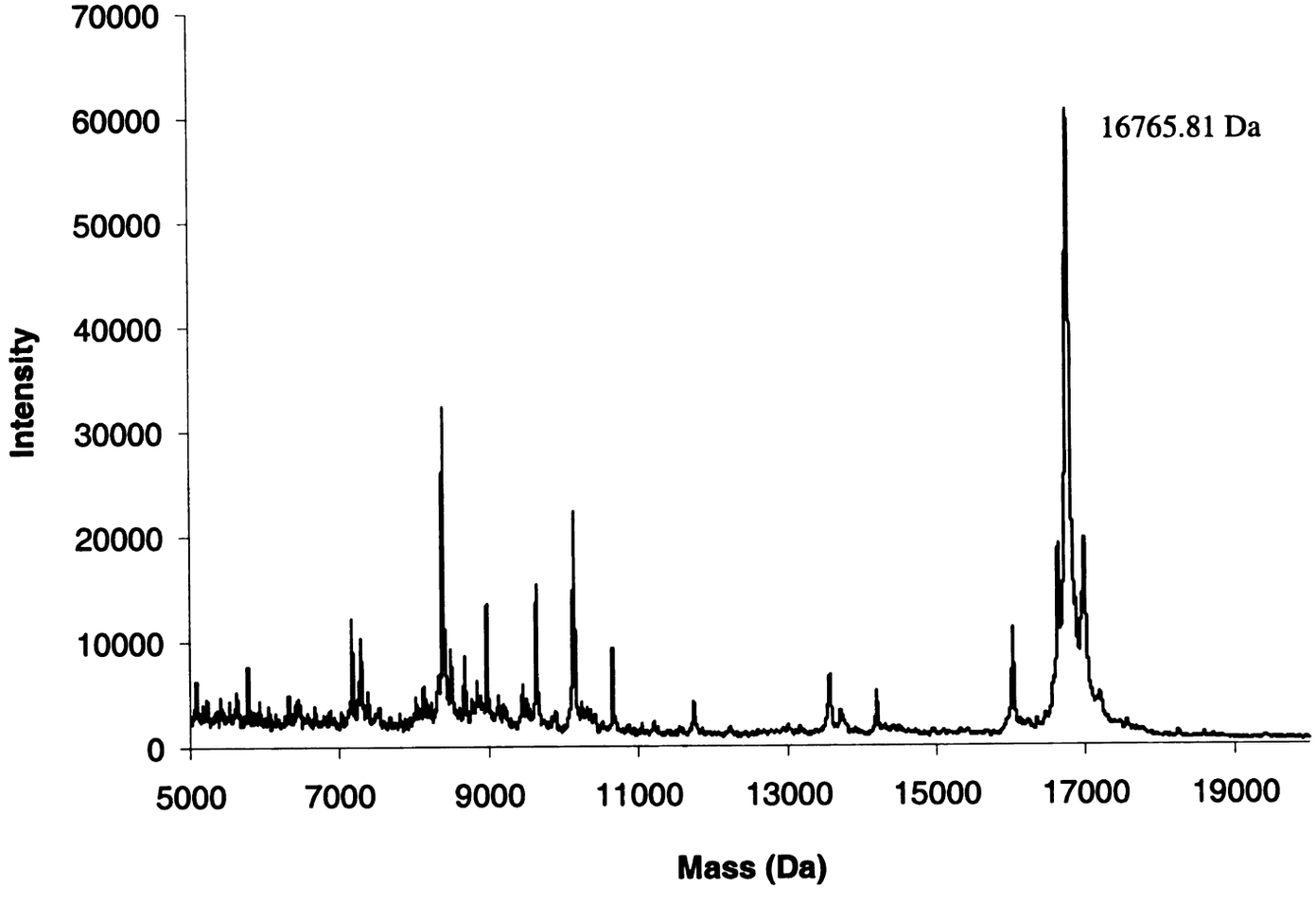

CRABPII R132K::Y134F::R111L::L121E::T54V

MALDI-TOF, Incubation with all-*trans*-Retinal

Protein Mass = 16756.16 Da

Positive Covalent Bond Formation = Protein Mass + 266

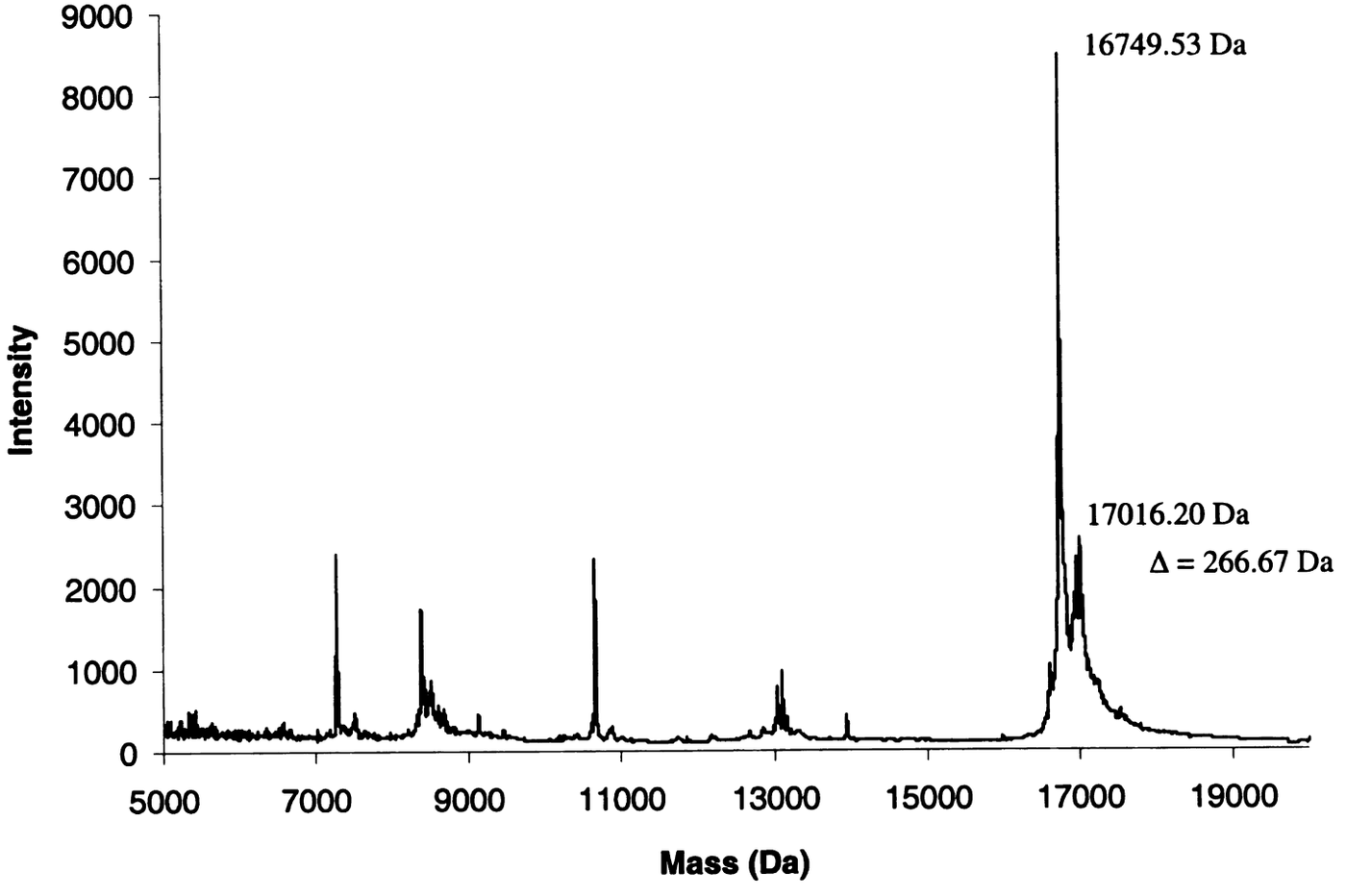

CRABPII R132K::Y134F::R111L::L121E::T54V

MALDI-TOF, Reductive Amination with all-*trans*-Retinal

Protein Mass = 16756.16 Da

Positive Reductive Amination = Protein Mass + 268

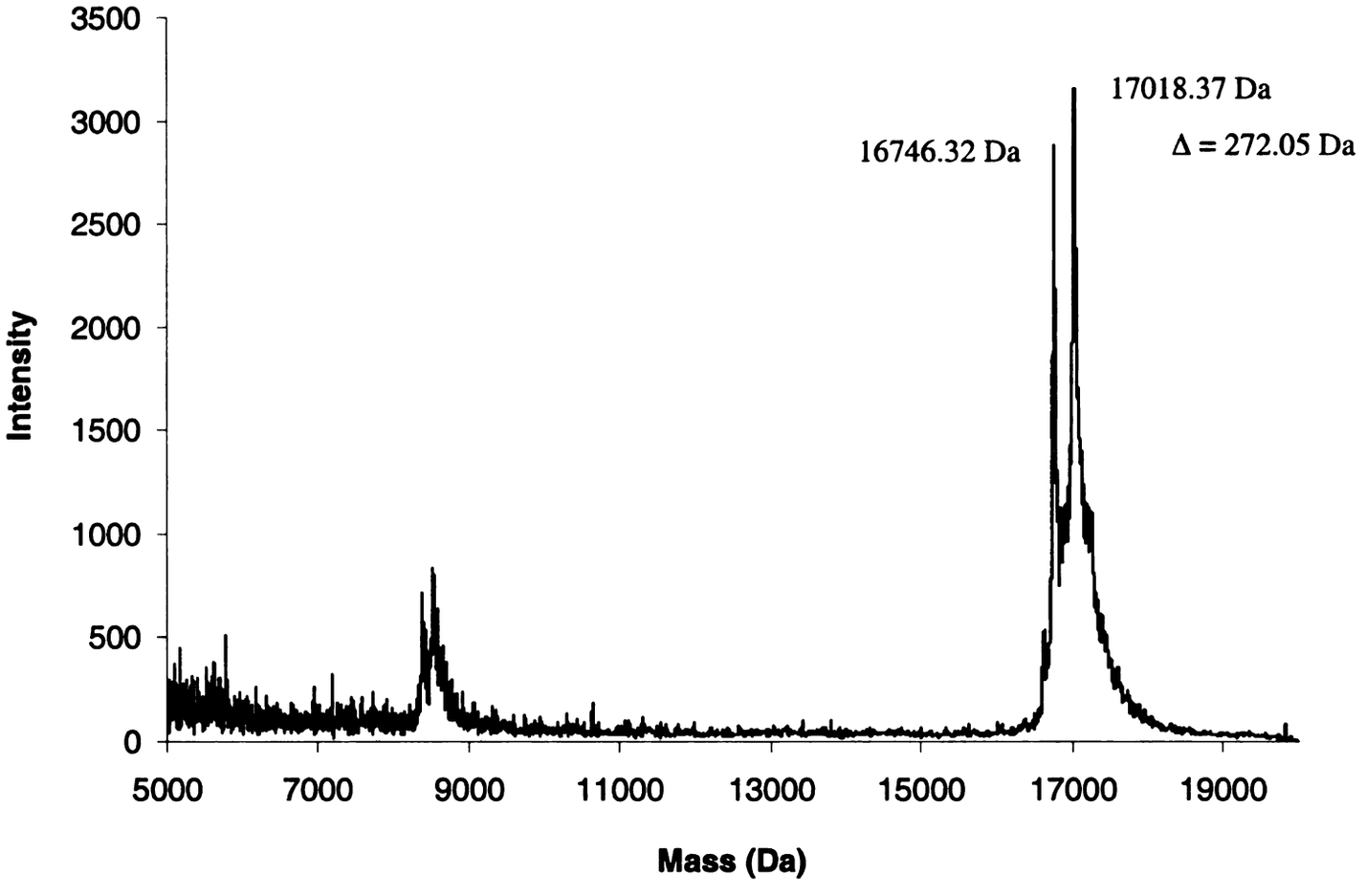

CRABPII R132K::Y134F::R111L::L121E::T54V

MALDI-TOF, Reductive Amination with 11-*cis*-Retinal

Protein Mass = 16756.16 Da

Positive Reductive Amination = Protein Mass + 268

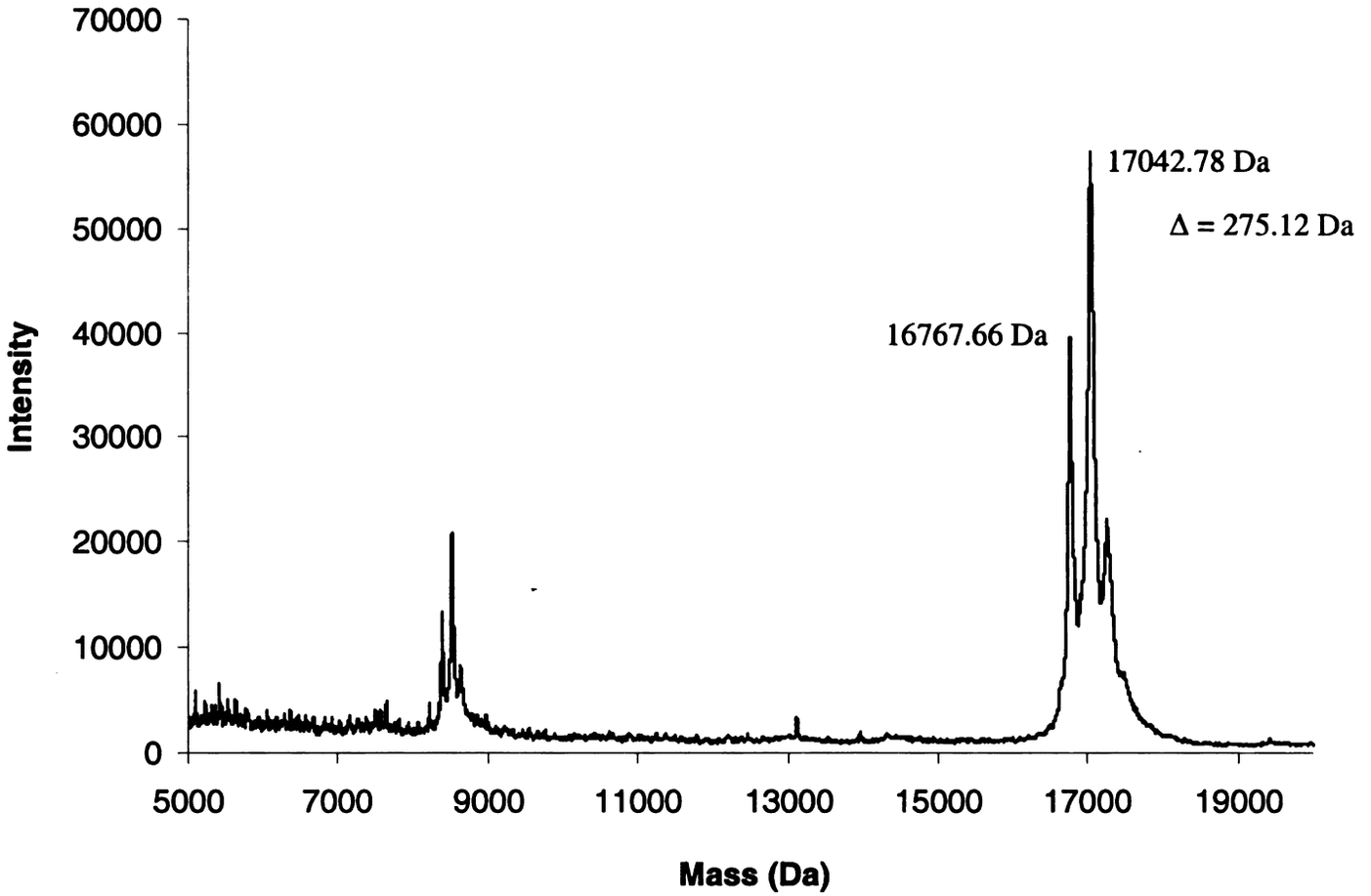

CRABPII R132K::Y134F::R111L::L121Q::T54V

Molecular Weight :

16755.16 Da

Extinction Coefficient :

22,821 M^{-1} cm^{-1}

Primers :

bbb67 5' CTA CAT CAA AGT CTC CAC CAC CGT GCG
bbb68 5' CGC ACG GTG GTG GAG ACT TTG ATG TAG

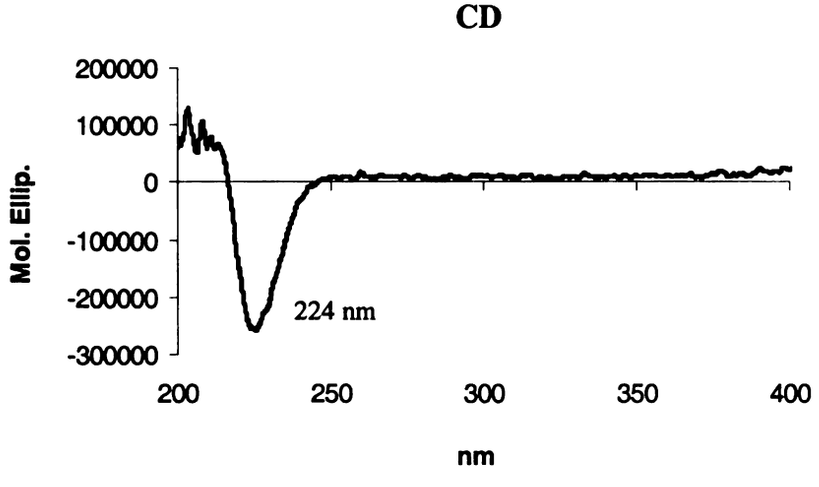

CRABPII R132K::Y134F::R111L::L121Q::T54V

Sequence BB 186

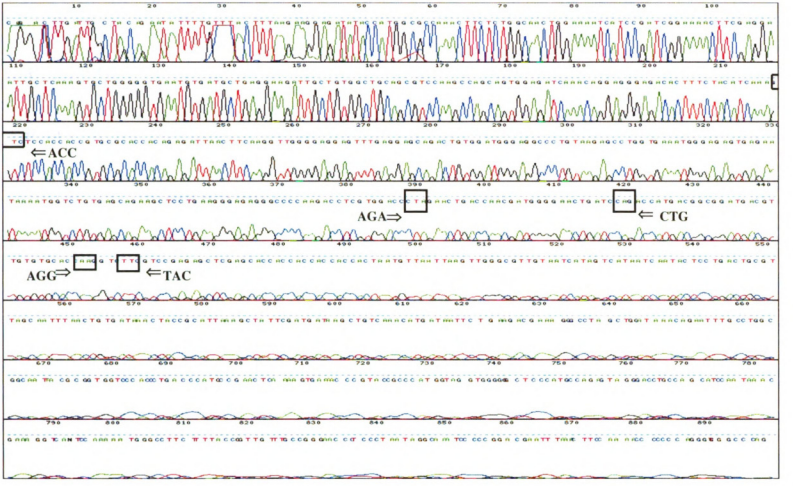

CRABPII R132K::Y134F::R111L::L121Q::T54V

Fluorescence Titrations

Retinoic Acid

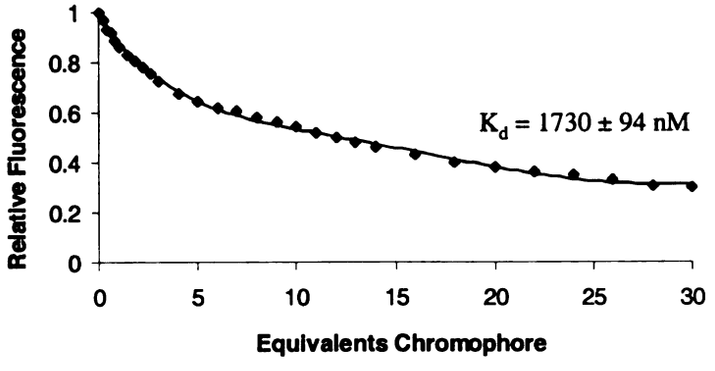

all-*trans*-Retinal

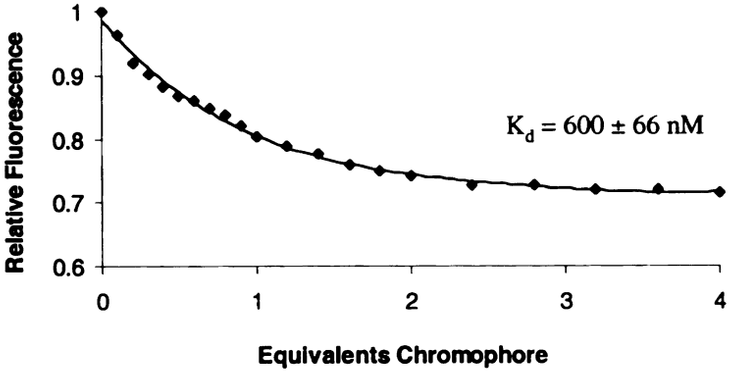

CRABPII R132K::Y134F::R111L::L121Q::T54V

UV-vis Titrations, all-*trans*-Retinal

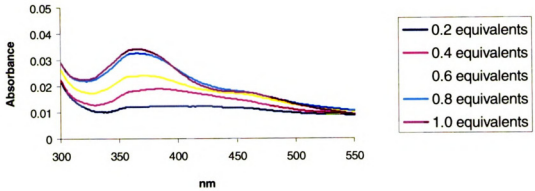

Uncorrected

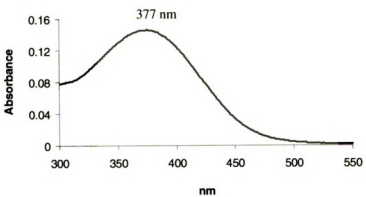

Corrected

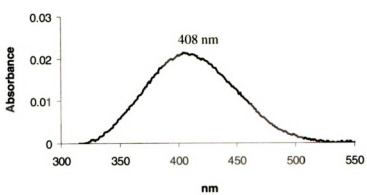

CRABPII R132K::Y134F::R111L::L121Q::T54V

MALDI-TOF, Protein

Calculated Mass = 16755.16 Da

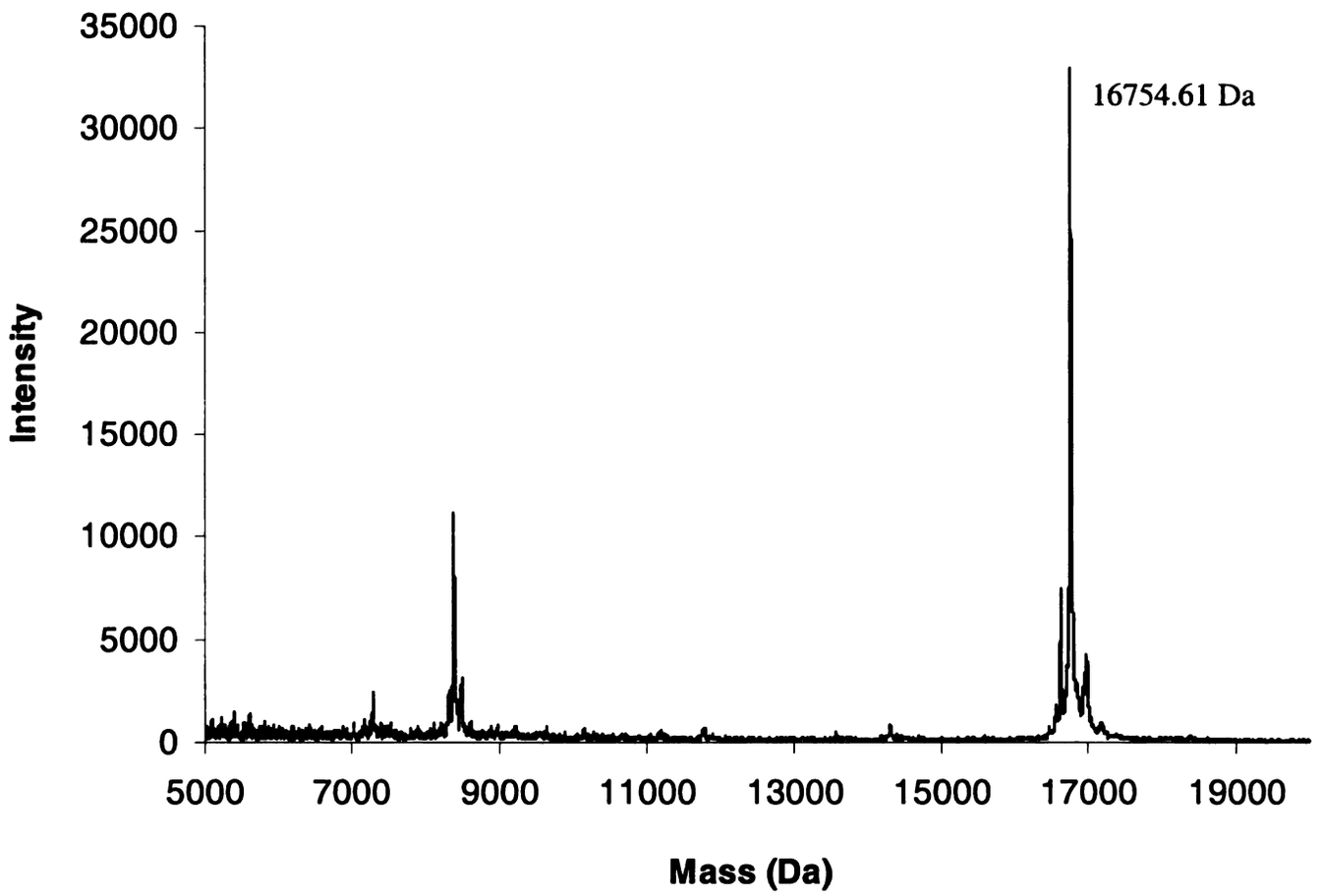

CRABPII R132K::Y134F::R111L::L121Q::T54V

MALDI-TOF, Incubation with all-*trans*-Retinal

Protein Mass = 16755.16 Da

Positive Covalent Bond Formation = Protein Mass + 266

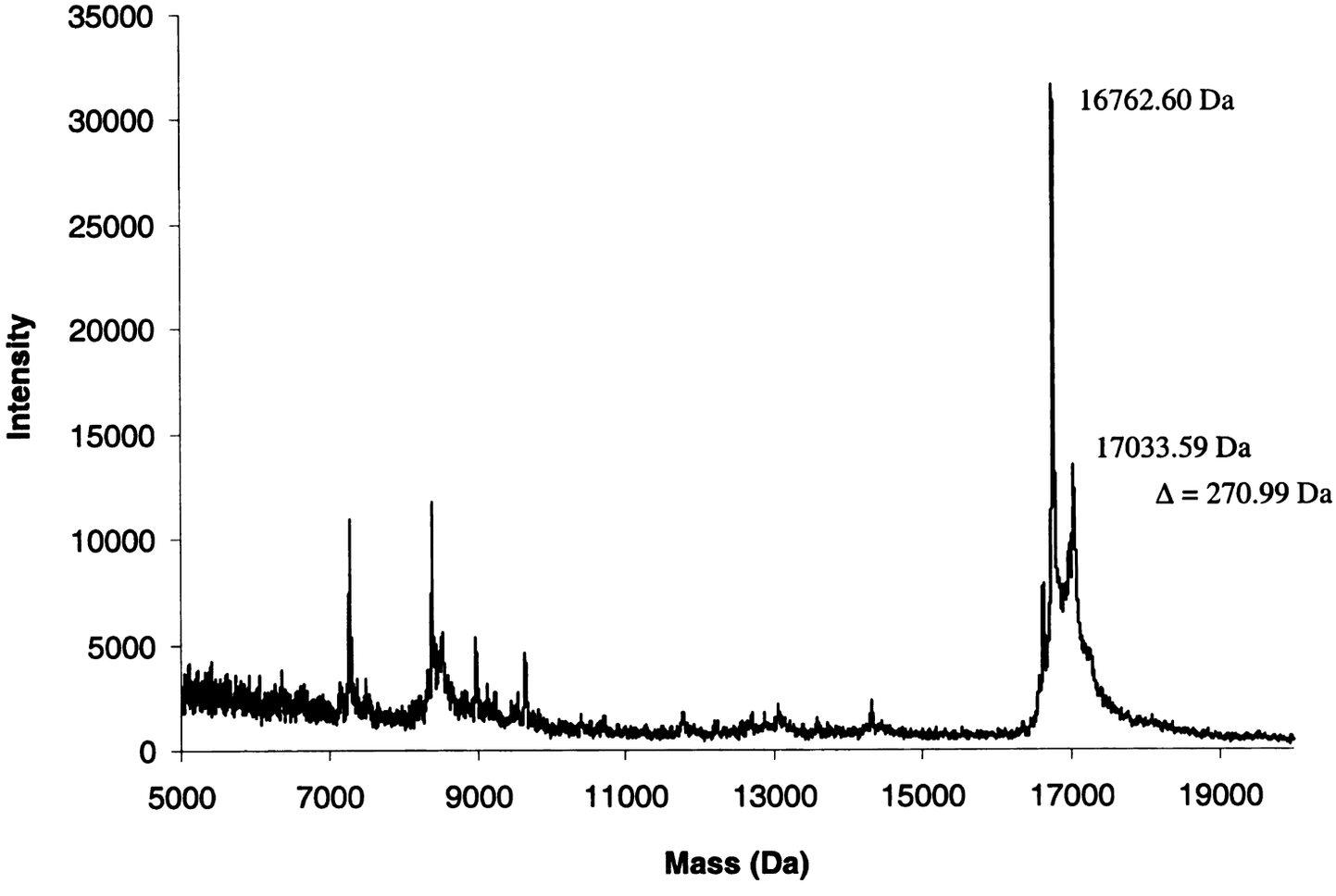

CRABPII R132K::Y134F::R111L::L121Q::T54V

MALDI-TOF, Reductive Amination with all-*trans*-Retinal

Protein Mass = 16755.16 Da

Positive Reductive Amination = Protein Mass + 268

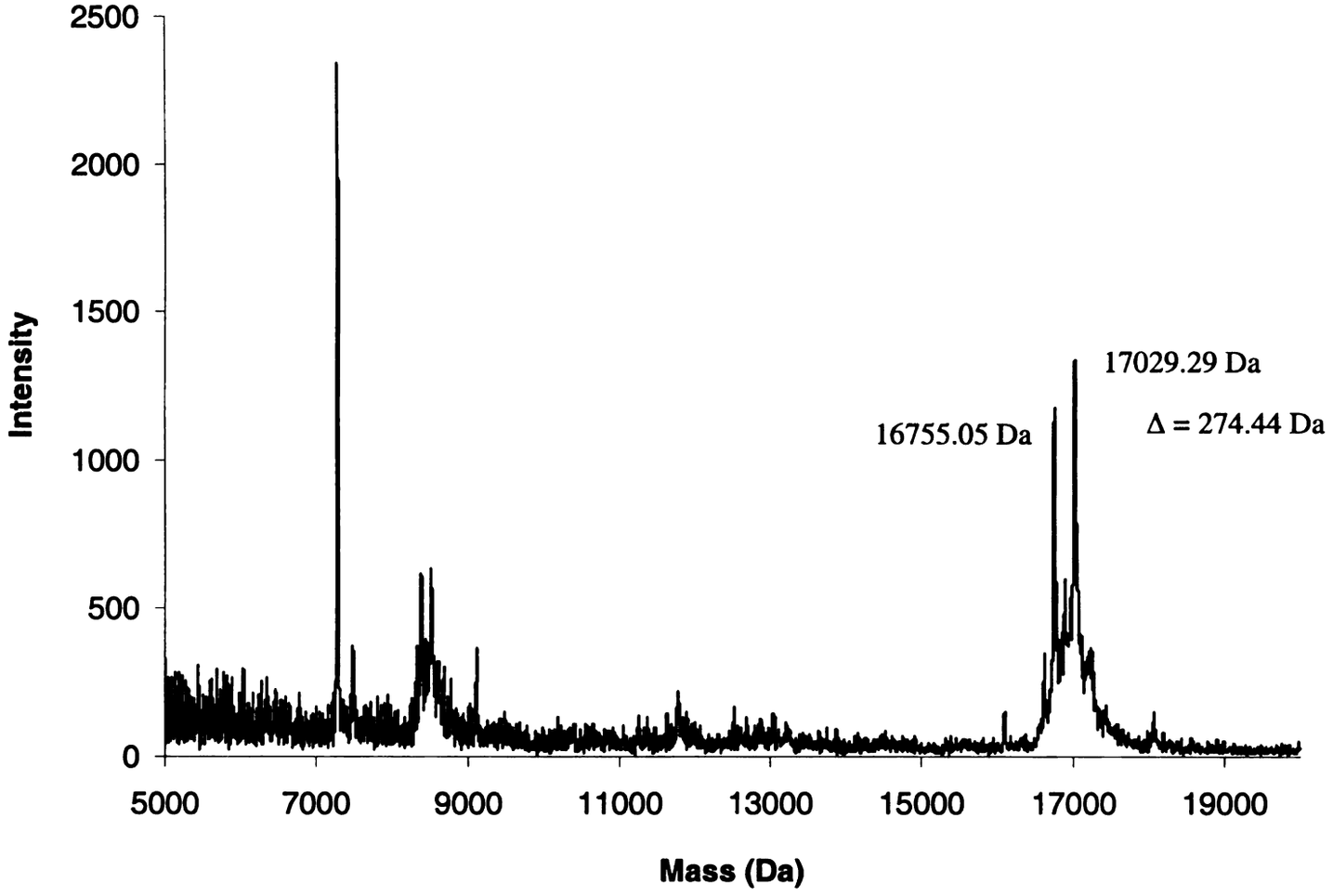

CRABPII R132K::Y134F::R111L::T54V

Molecular Weight :

16740.20 Da

Extinction Coefficient :

17,798 M^{-1} cm^{-1}

Primers :

bbb67 5' CTA CAT CAA AGT CTC CAC CAC CGT GCG
bbb68 5' CGC ACG GTG GTG GAG ACT TTG ATG TAG

CD

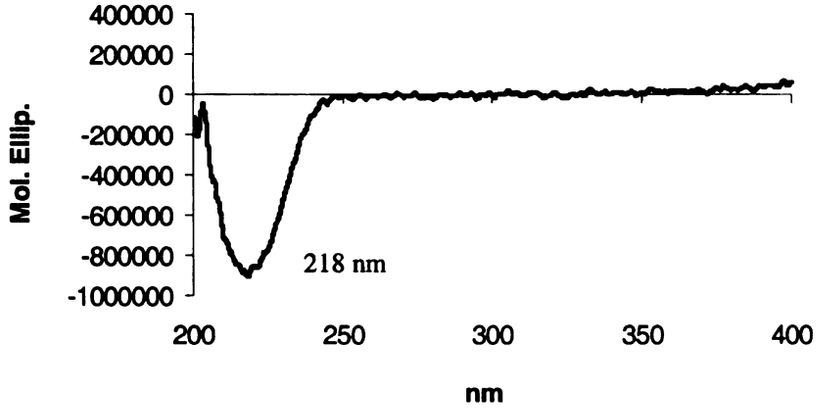

CRABPII R132K::Y134F::R111L::T54V

Sequence BB 196

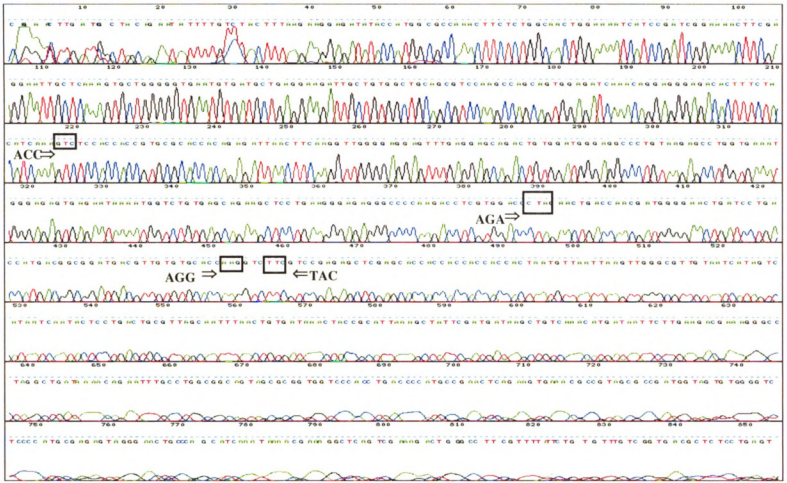

CRABPII R132K::Y134F::R111L::T54V

Fluorescence Titrations

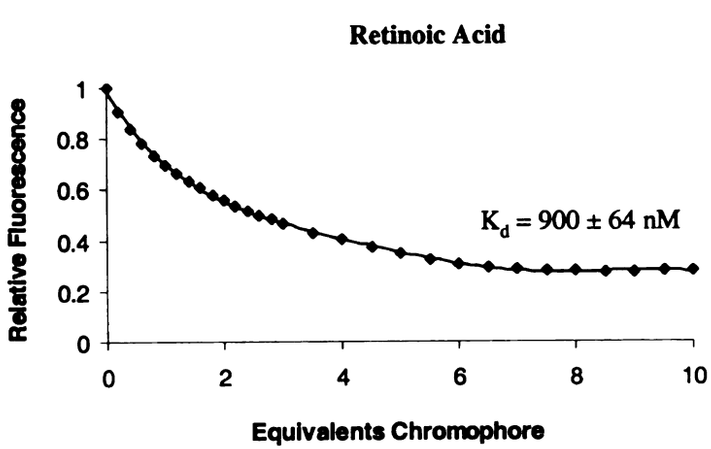

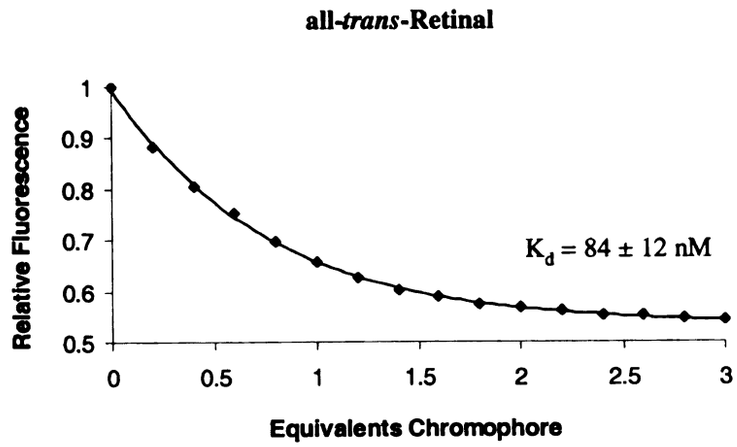

CRABPII R132K::Y134F::R111L::T54V

UV-vis Titrations, all-*trans*-Retinal

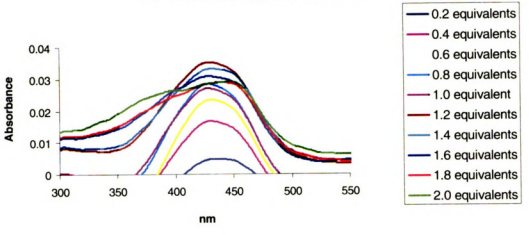

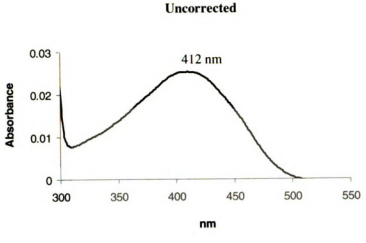

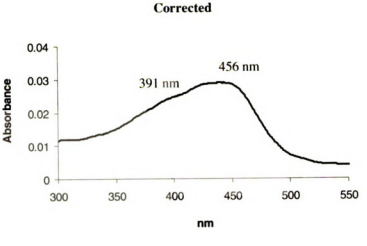

CRABPII R132K::Y134F::R111L::T54V

MALDI-TOF, Protein

Calculated Mass = 16740.20 Da

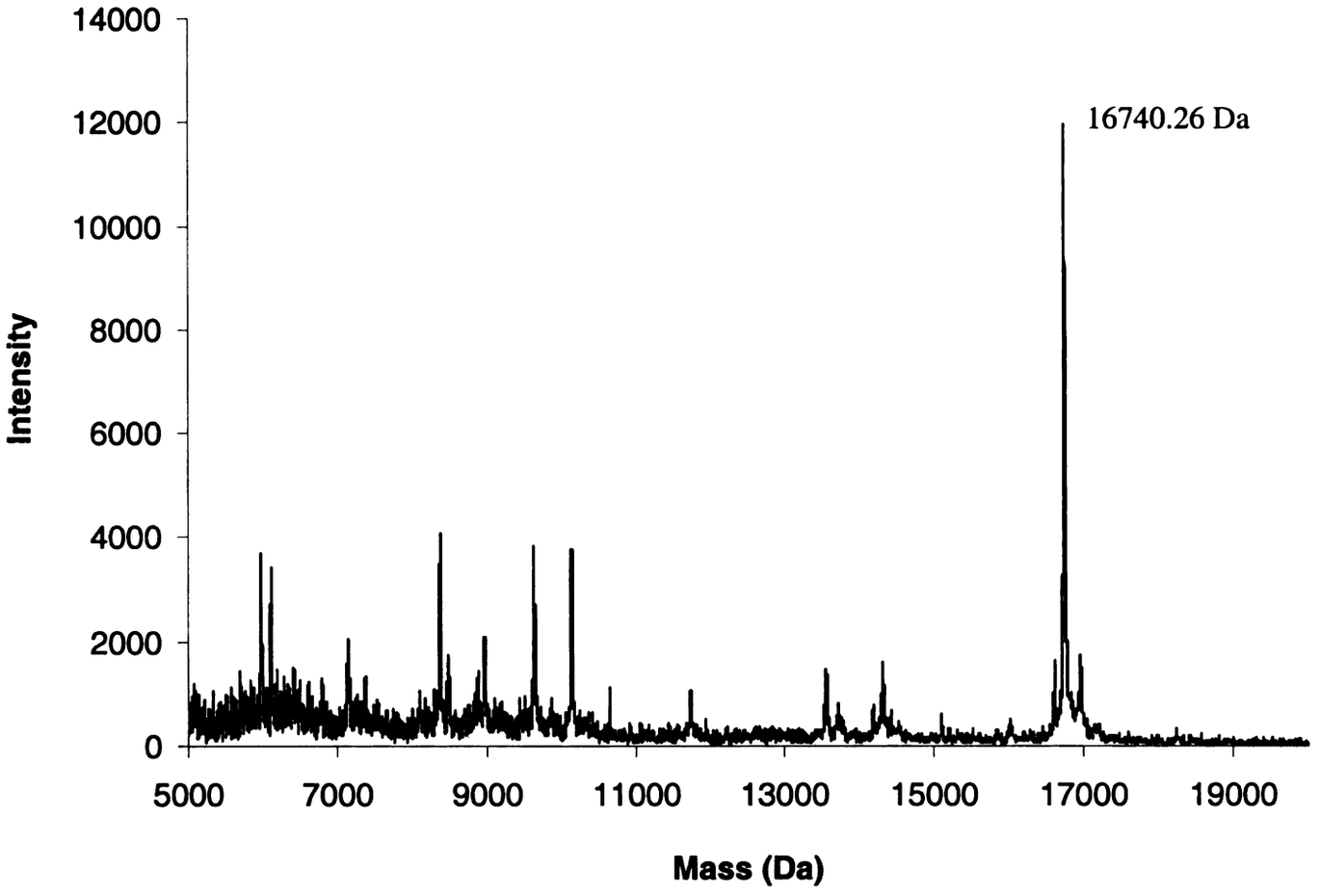

CRABPII R132K::Y134F::R111L::T54V

MALDI-TOF, Incubation with all-*trans*-Retinal

Protein Mass = 16740.20 Da

Positive Covalent Bond Formation = Protein Mass + 266

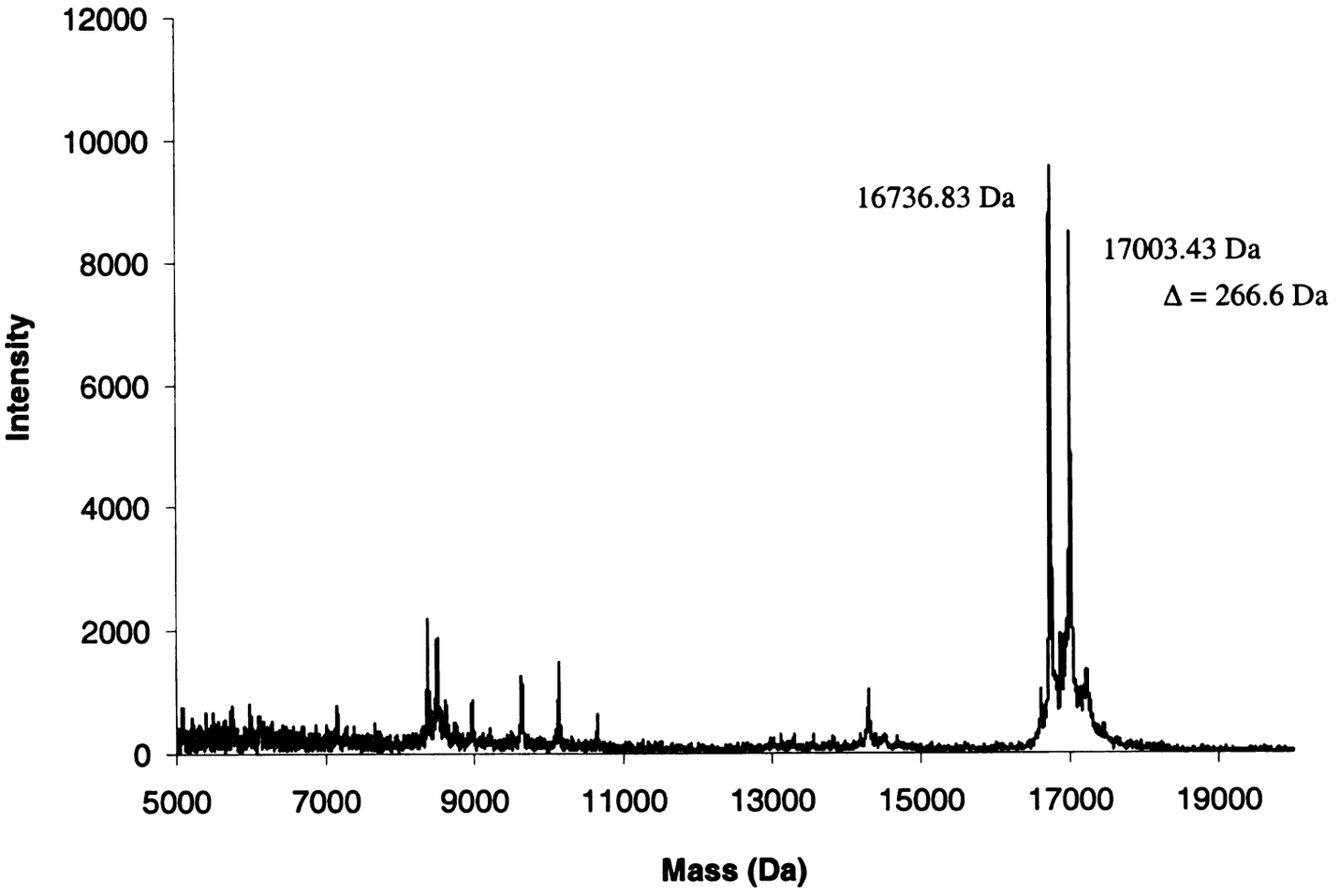

CRABPII R132K::Y134F::R111L::T54V

MALDI-TOF, Reductive Amination with all-*trans*-Retinal

Protein Mass = 16740.20 Da

Positive Reductive Amination = Protein Mass + 268

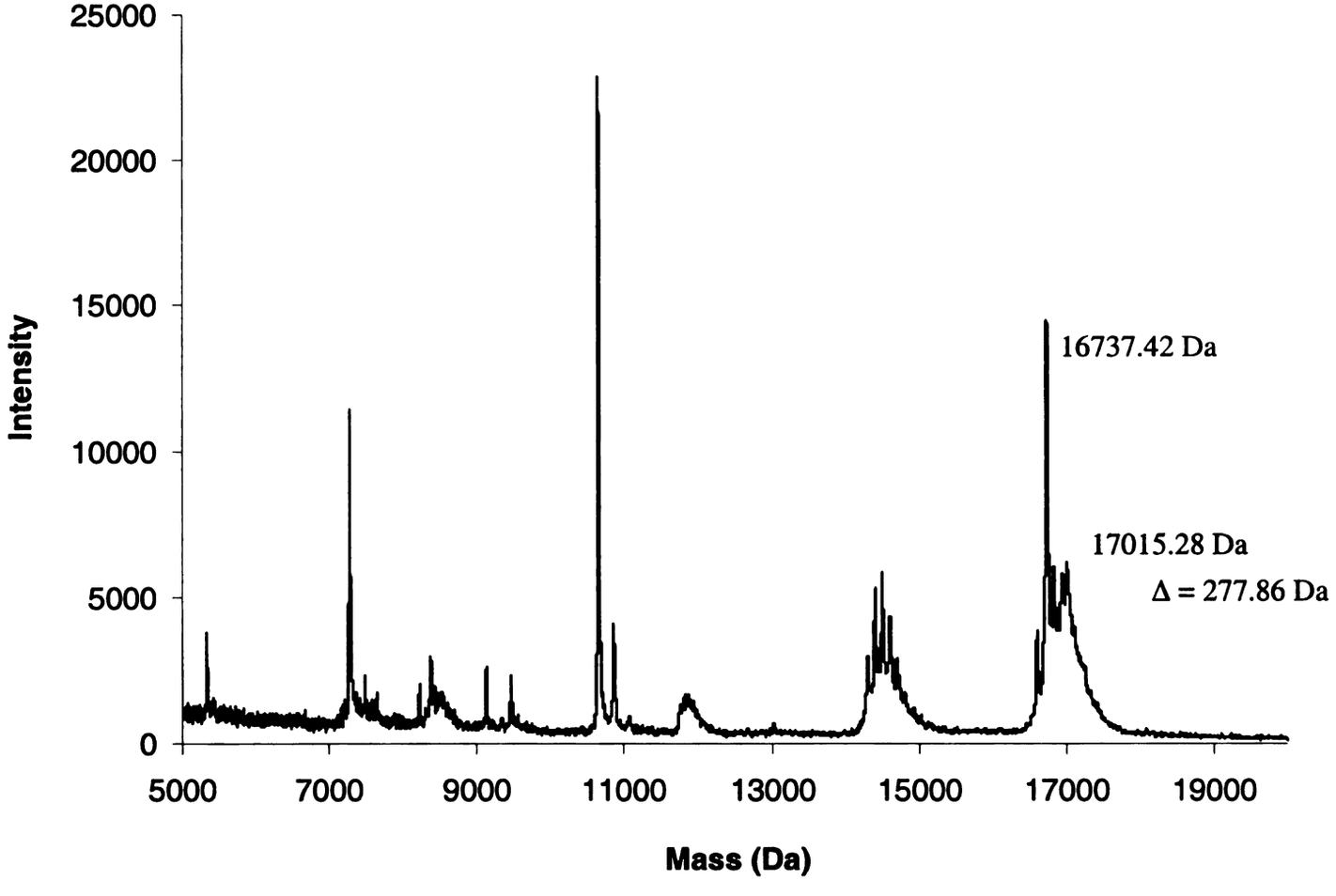

CRABPII R132K::Y134F::R111L::L121D

Molecular Weight :

16744.10 Da

Extinction Coefficient :

19,138 M^{-1} cm^{-1}

Primers :

bbb90 5' GGG GAA CTG ATC GAC ACC ATG ACG GCG

bbb91 5' CGC CGT CAT GGT GTC GAT CAG TTC CCC

CD

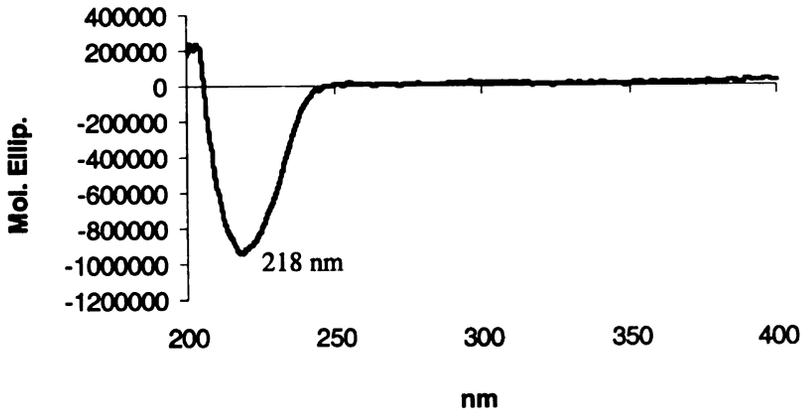

CRABPII R132K::Y134F::R111L::L121D

Sequence BB 148

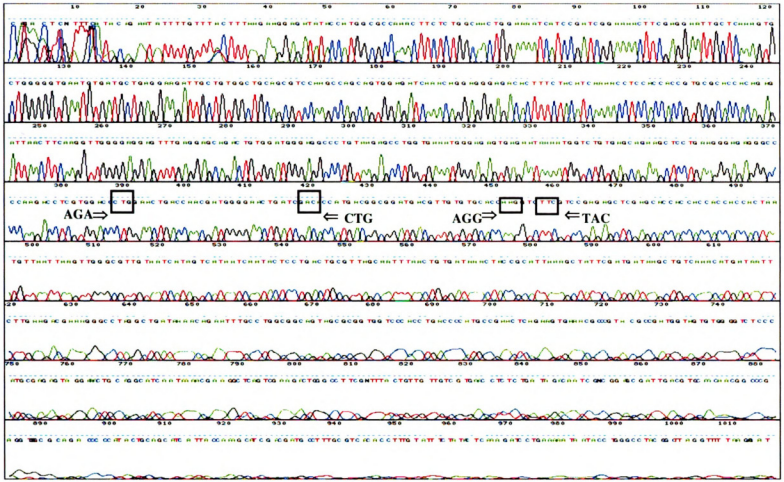

CRABPII R132K::Y134F::R111L::L121D

Fluorescence Titrations

Retinoic Acid

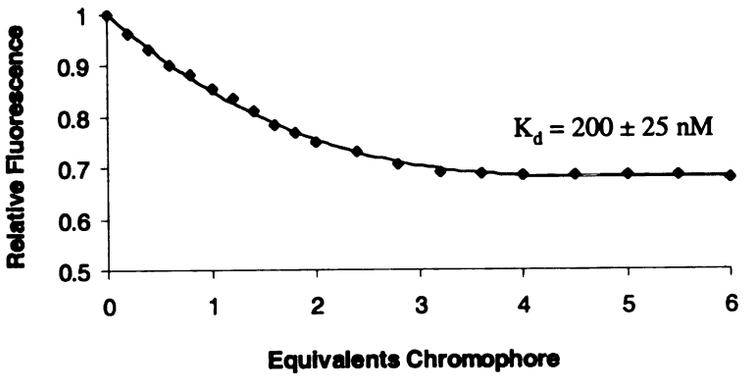

all-*trans*-Retinal

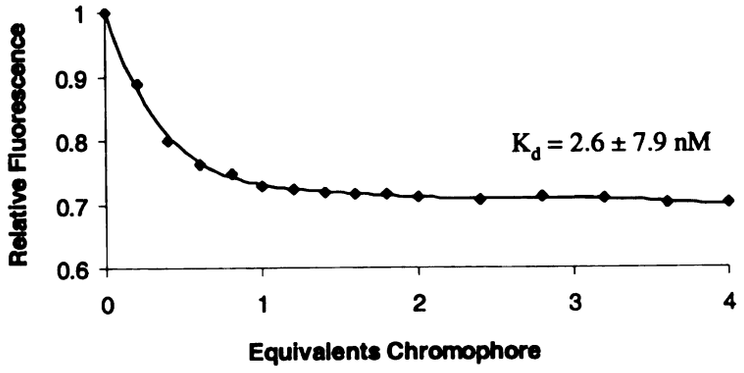

11-*cis*-Retinal

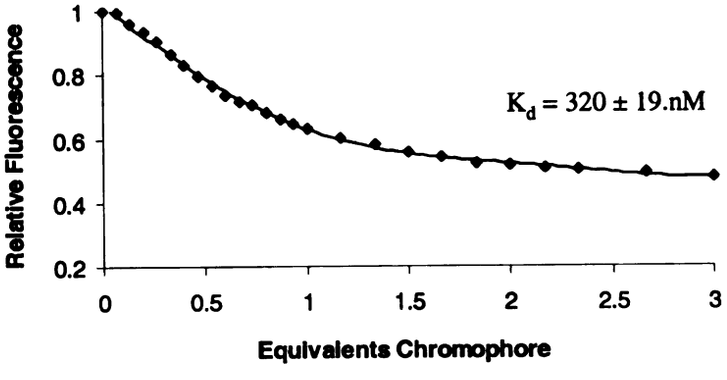

CRABPII R132K::Y134F::R111L::L121D

UV-vis Titrations, all-*trans*-Retinal

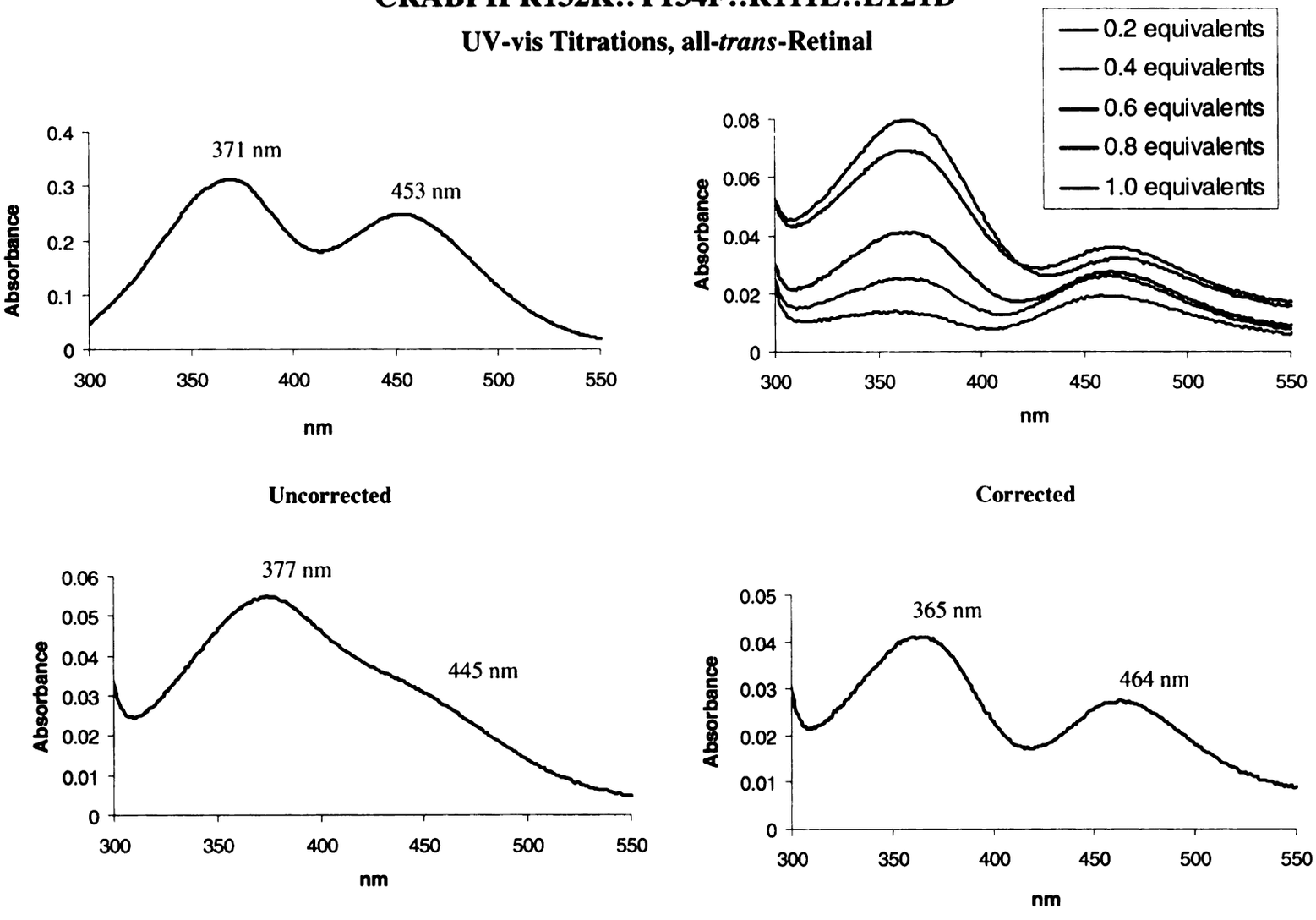

CRABPII R132K::Y134F::R111L::L121D

UV-vis Titrations, 11-*cis*-Retinal

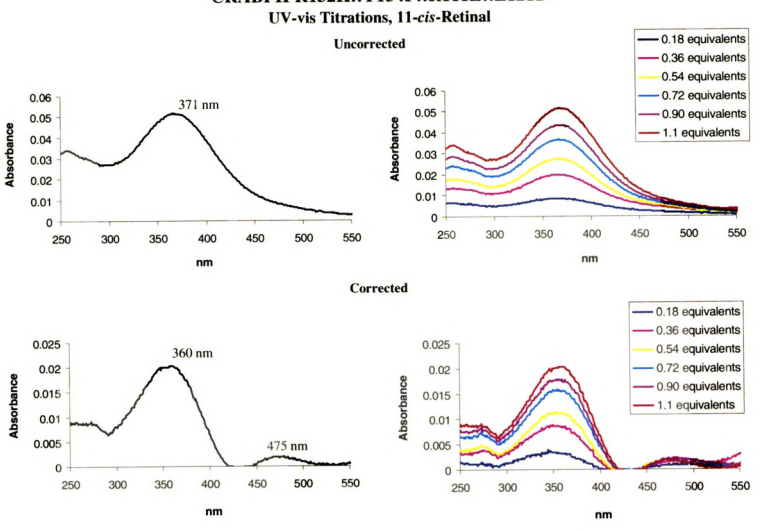

CRABPII R132K::Y134F::R111L::L121D

MALDI-TOF, Protein

Calculated Mass = 16744.10 Da

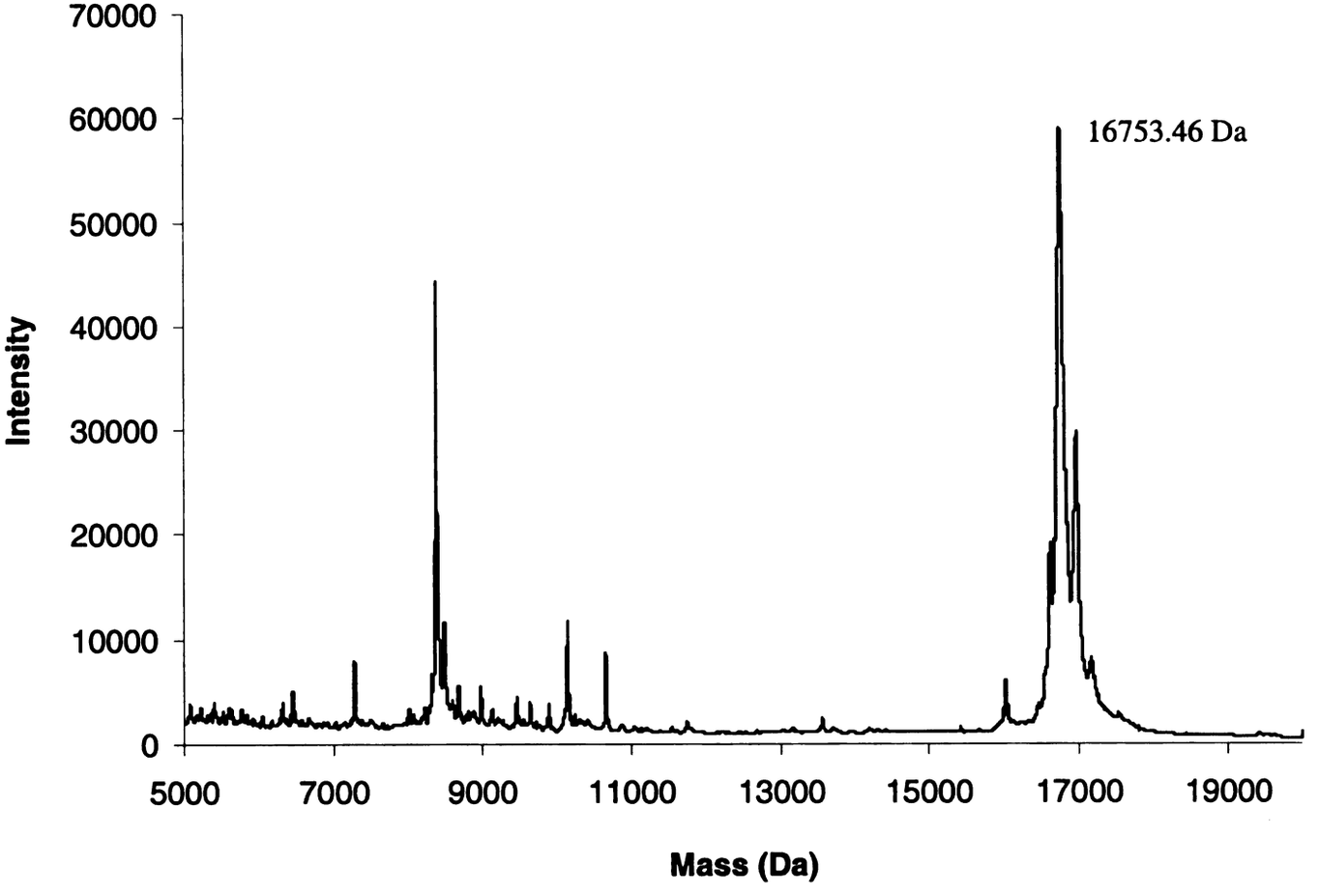

CRABPII R132K::Y134F::R111L::L121D

MALDI-TOF, Incubation with all-*trans*-Retinal

Protein Mass = 16744.10 Da

Positive Covalent Bond Formation = Protein Mass + 266

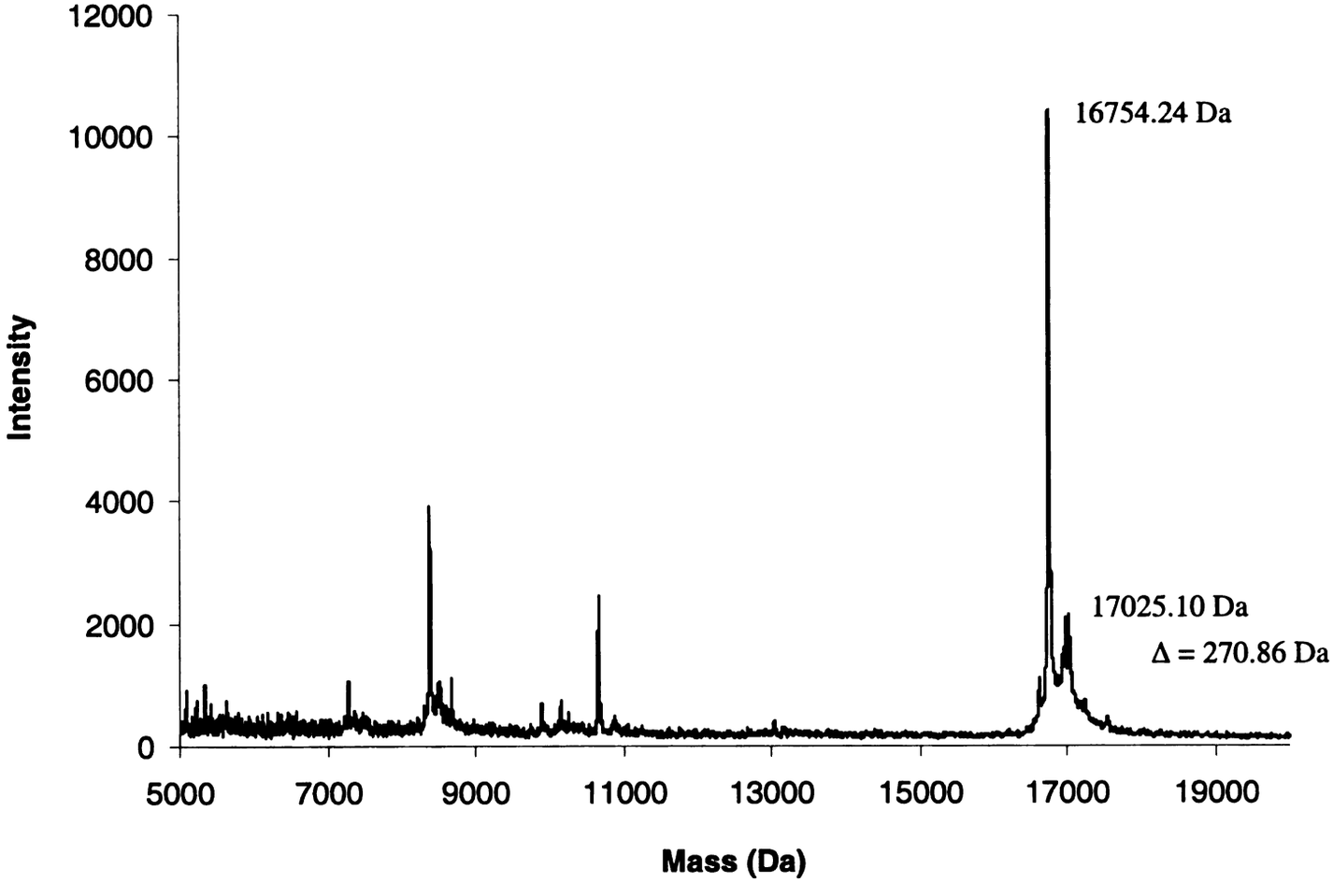

CRABPII R132K::Y134F::R111L::L121D

MALDI-TOF, Reductive Amination with all-*trans*-Retinal

Protein Mass = 16744.10 Da

Positive Reductive Amination = Protein Mass + 268

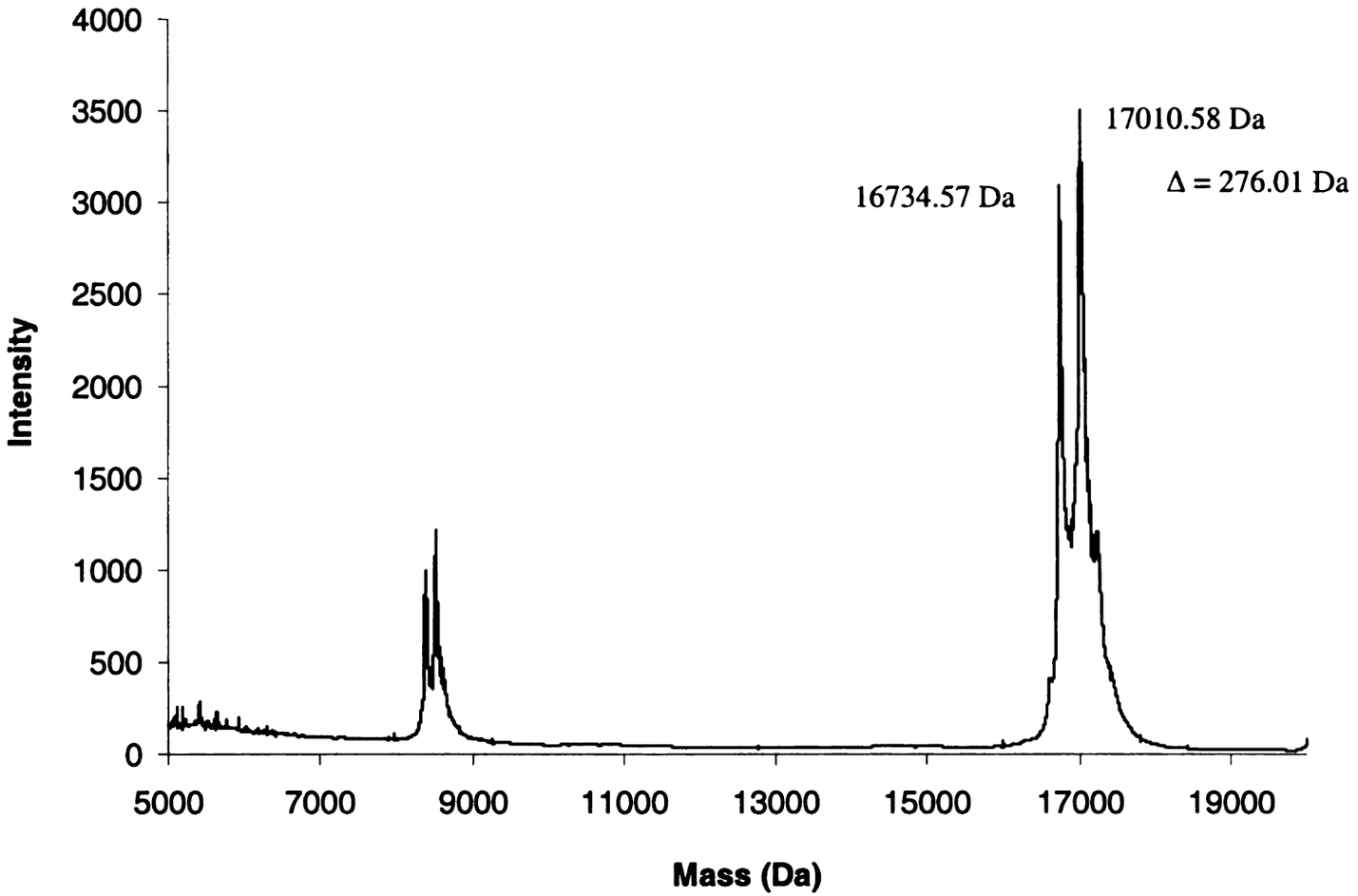

CRABPII R132K::Y134F::R111L::L121N

Molecular Weight :

16743.12 Da

Extinction Coefficient :

20,266 M^{-1} cm^{-1}

Primers :

bbb102 5' GGG GAA CTG ATC AAC ACC ATG ACG GCG

bbb103 5' CGC CGT CAT GGT GTT GAT CAG TTC CCC

CD

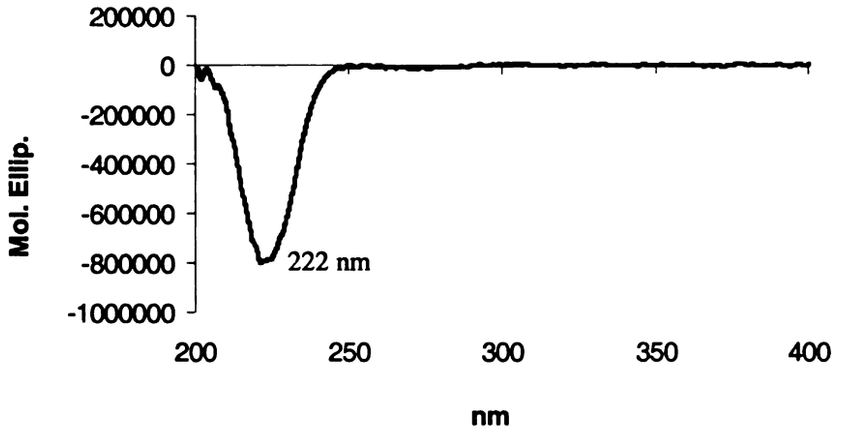

CRABPII R132K::Y134F::R111L::L121N

Sequence BB 166

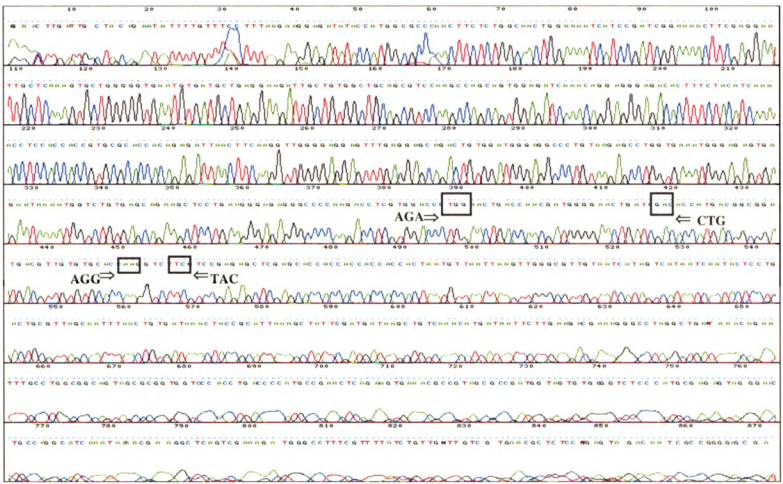

CRABPII R132K::Y134F::R111L::L121N

Fluorescence Titrations

Retinoic Acid

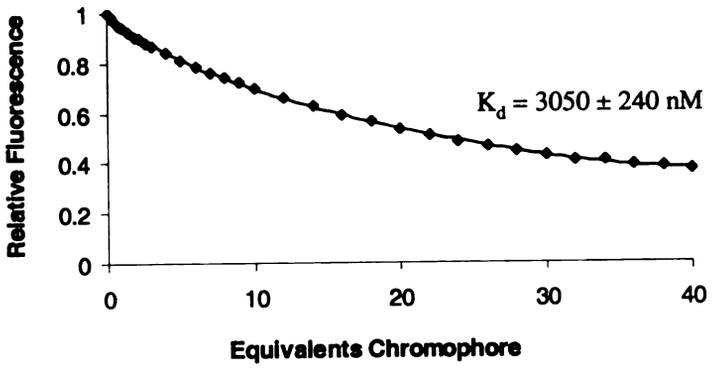

all-*trans*-Retinal

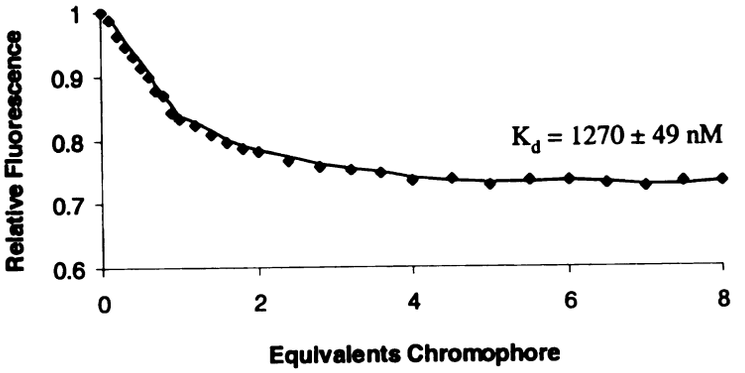

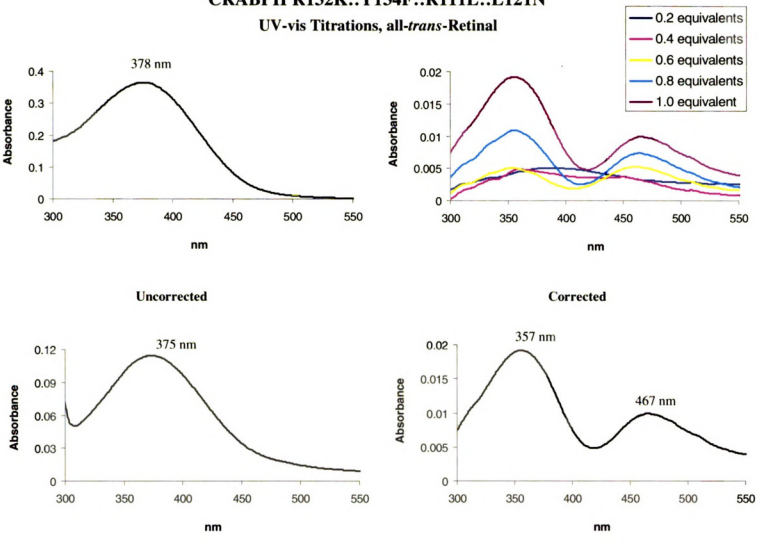
CRABPII R132K::Y134F::R111L::L121N
UV-vis Titrations, all-trans-Retinal
0.2 equivalents
0.4 equivalents
0.6 equivalents
0.8 equivalents
1.0 equivalent
378 nm
Absorbance
nm
Uncorrected
375 nm
Corrected
357 nm
467 nm

CRABPII R132K::Y134F::R111L::L121N

MALDI-TOF, Protein

Calculated Mass = 16743.12 Da

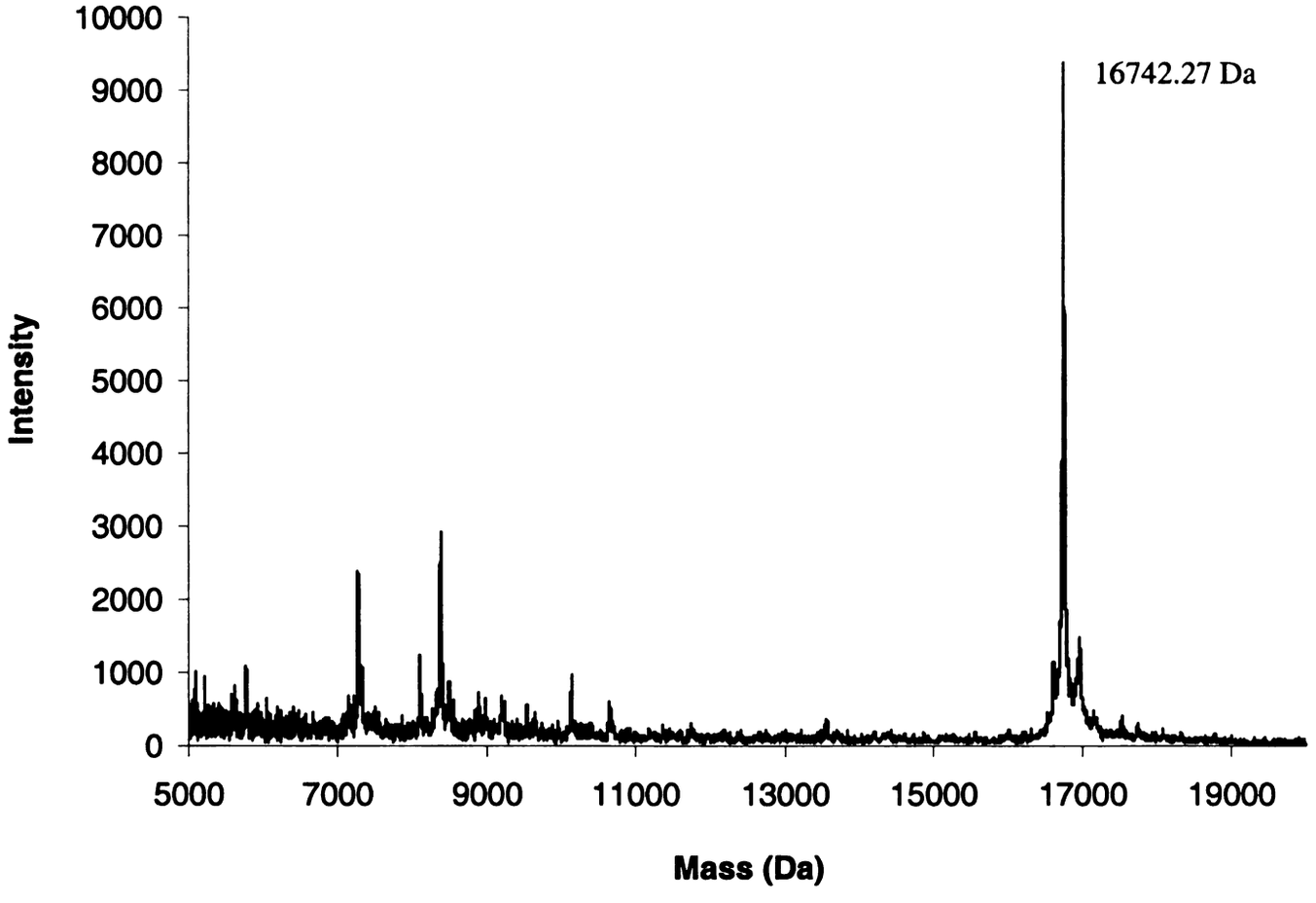

CRABPII R132K::Y134F::R111L::L121N

MALDI-TOF, Incubation with all-*trans*-Retinal

Protein Mass = 16743.12 Da

Positive Covalent Bond Formation = Protein Mass + 268

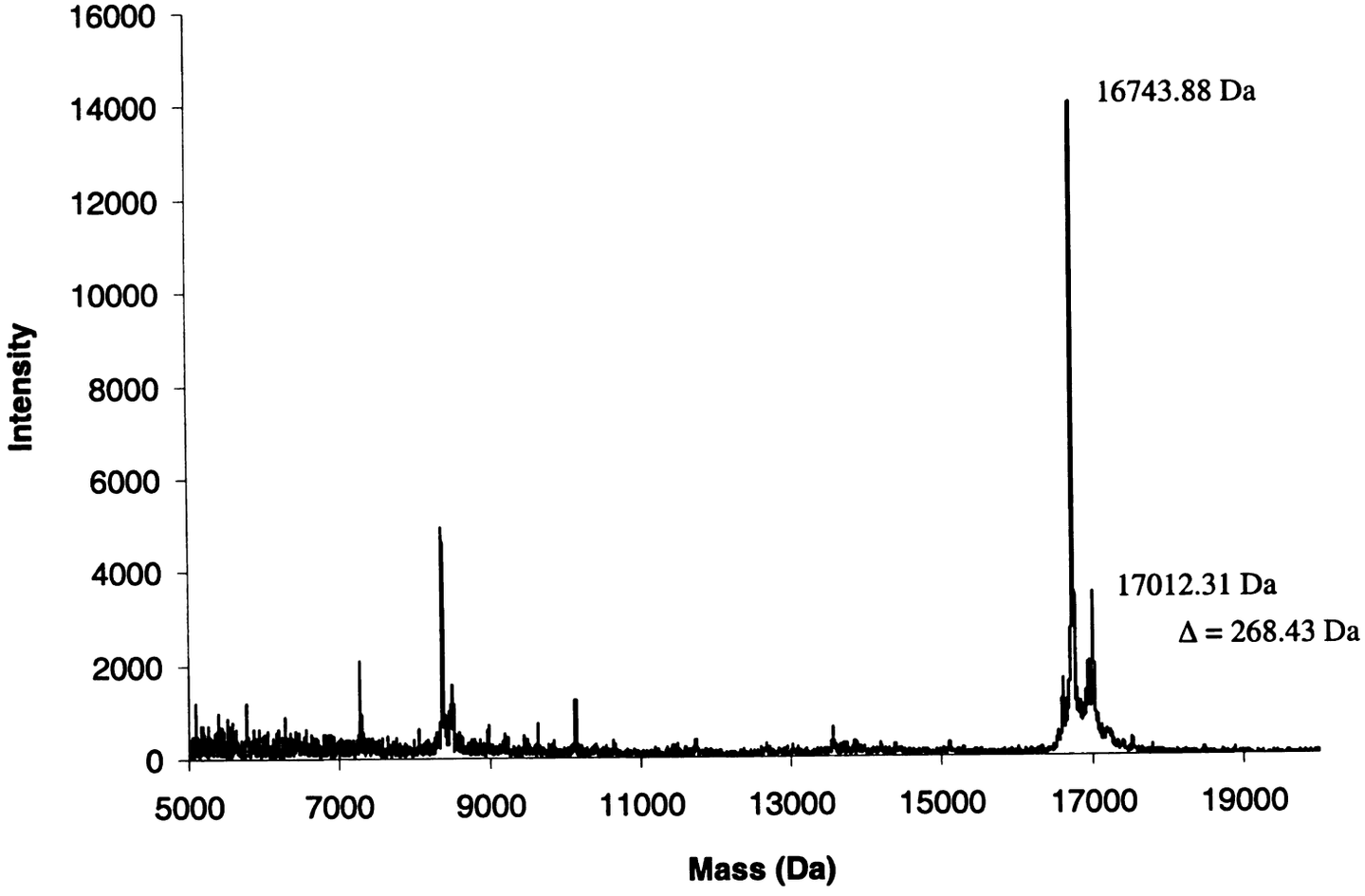

CRABPII R132K::Y134F::R111L::L121N

MALDI-TOF, Reductive Amination with all-*trans*-Retinal

Protein Mass = 16743.12 Da

Positive Reductive Amination = Protein Mass + 268

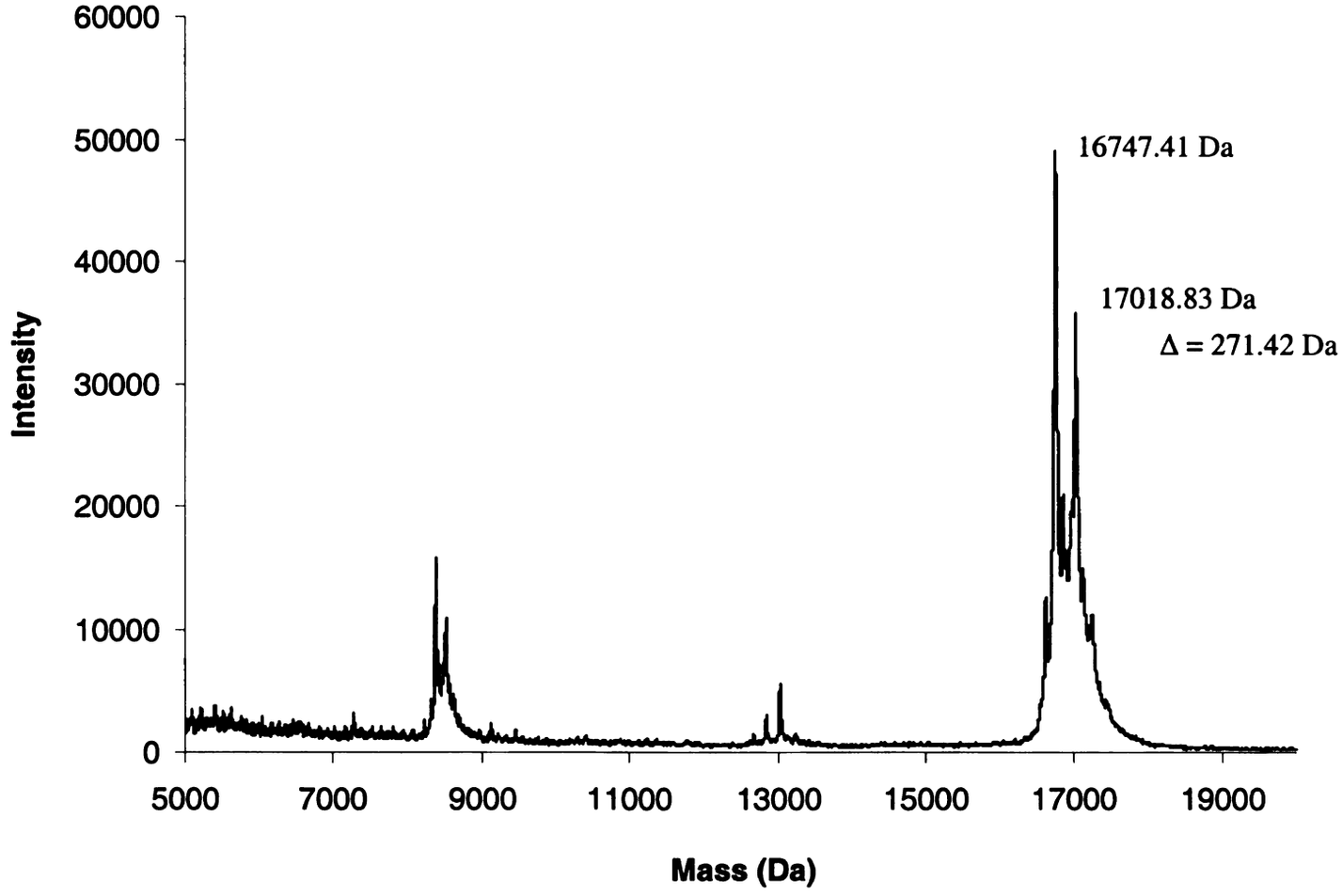

CRABPII R132K::Y134F::R111L::L121D::T54V

Molecular Weight :

16742.13 Da

Extinction Coefficient :

22,056 M^{-1} cm^{-1}

Primers :

bbb67 5' CTA CAT CAA AGT CTC CAC CAC CGT GCG

bbb68 5' CGC ACG GTG GTG GAG ACT TTG ATG TAG

CD

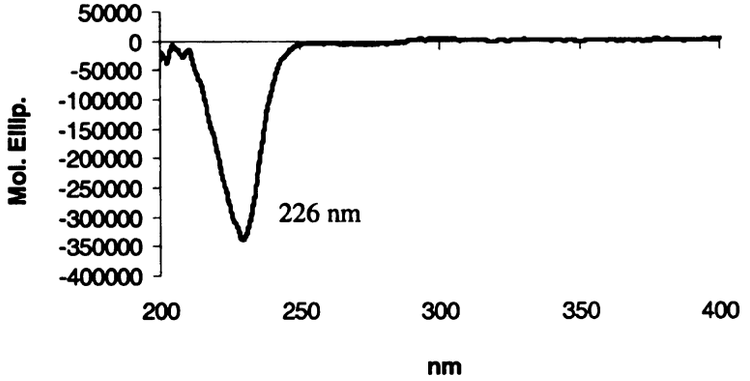

CRABPII R132K::Y134F::R111L::L121D::T54V

Sequence BB 168

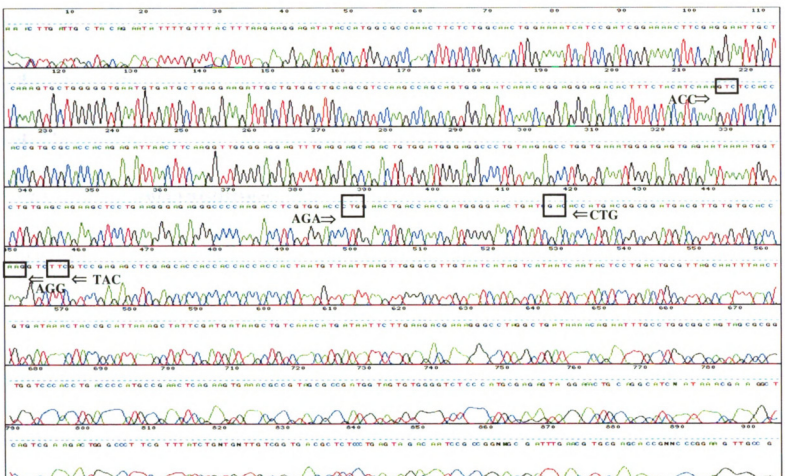

CRABPII R132K::Y134F::R111L::L121D::T54V

Fluorescence Titrations

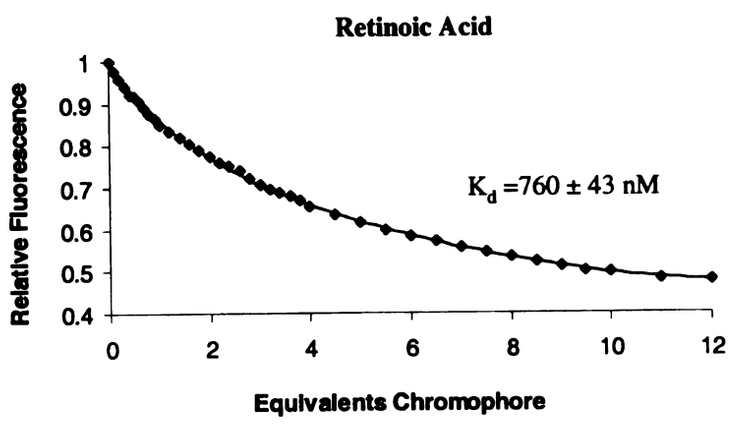

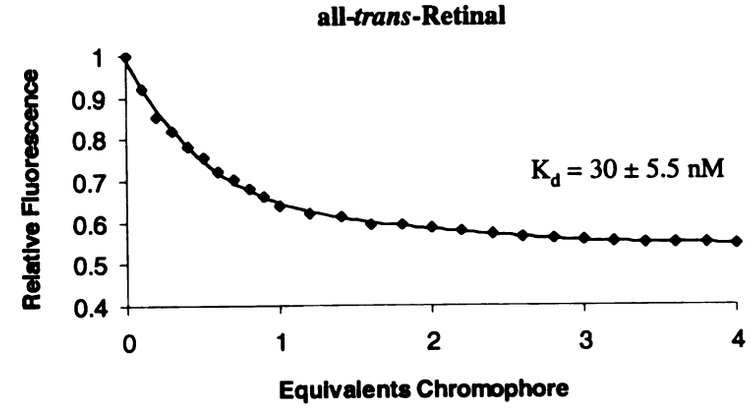

CRABPII R132K::Y134F::R111L::L121D::T54V

UV-vis Titrations, all-*trans*-Retinal

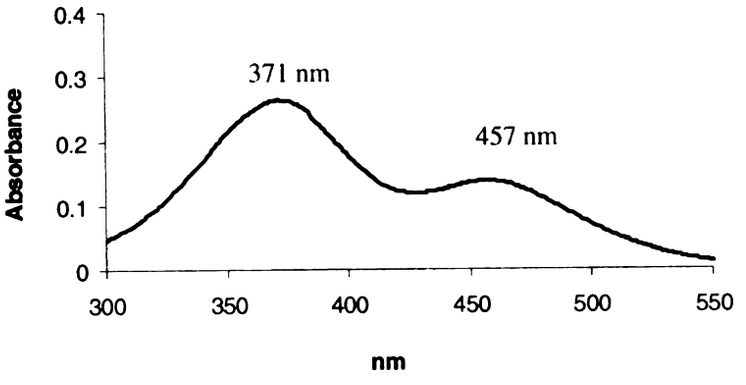

Uncorrected

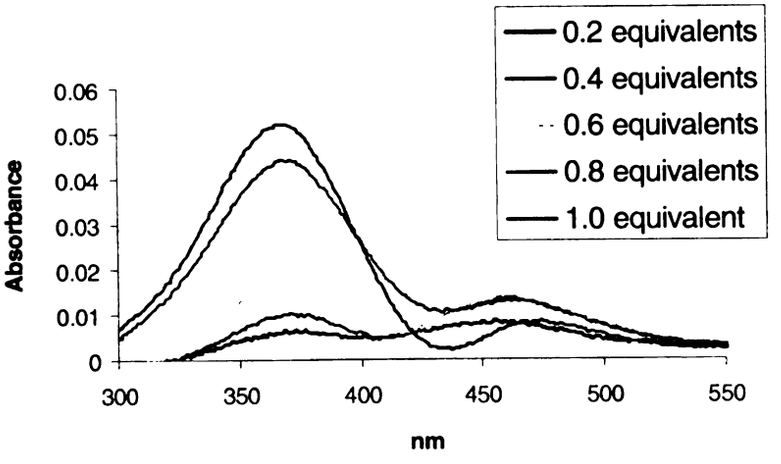

Corrected

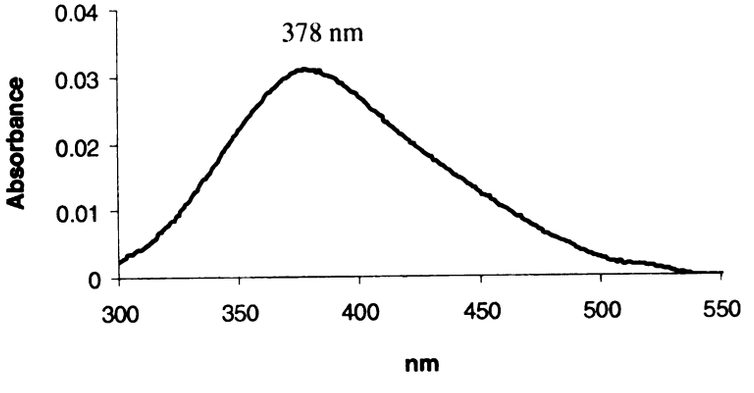

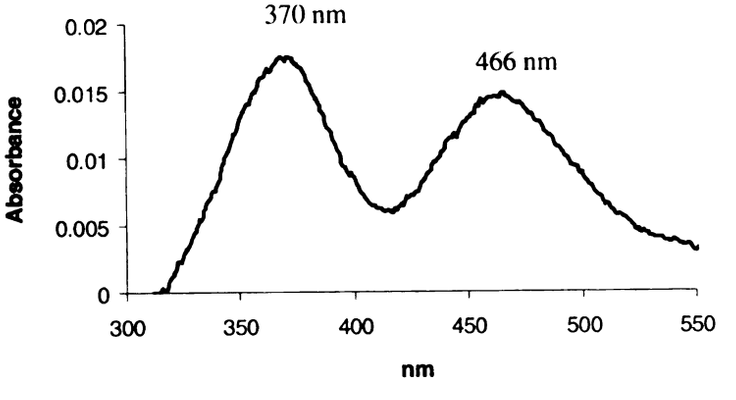

CRABPII R132K::Y134F::R111L::L121D::T54V

MALDI-TOF, Protein

Calculated Mass = 16742.13 Da

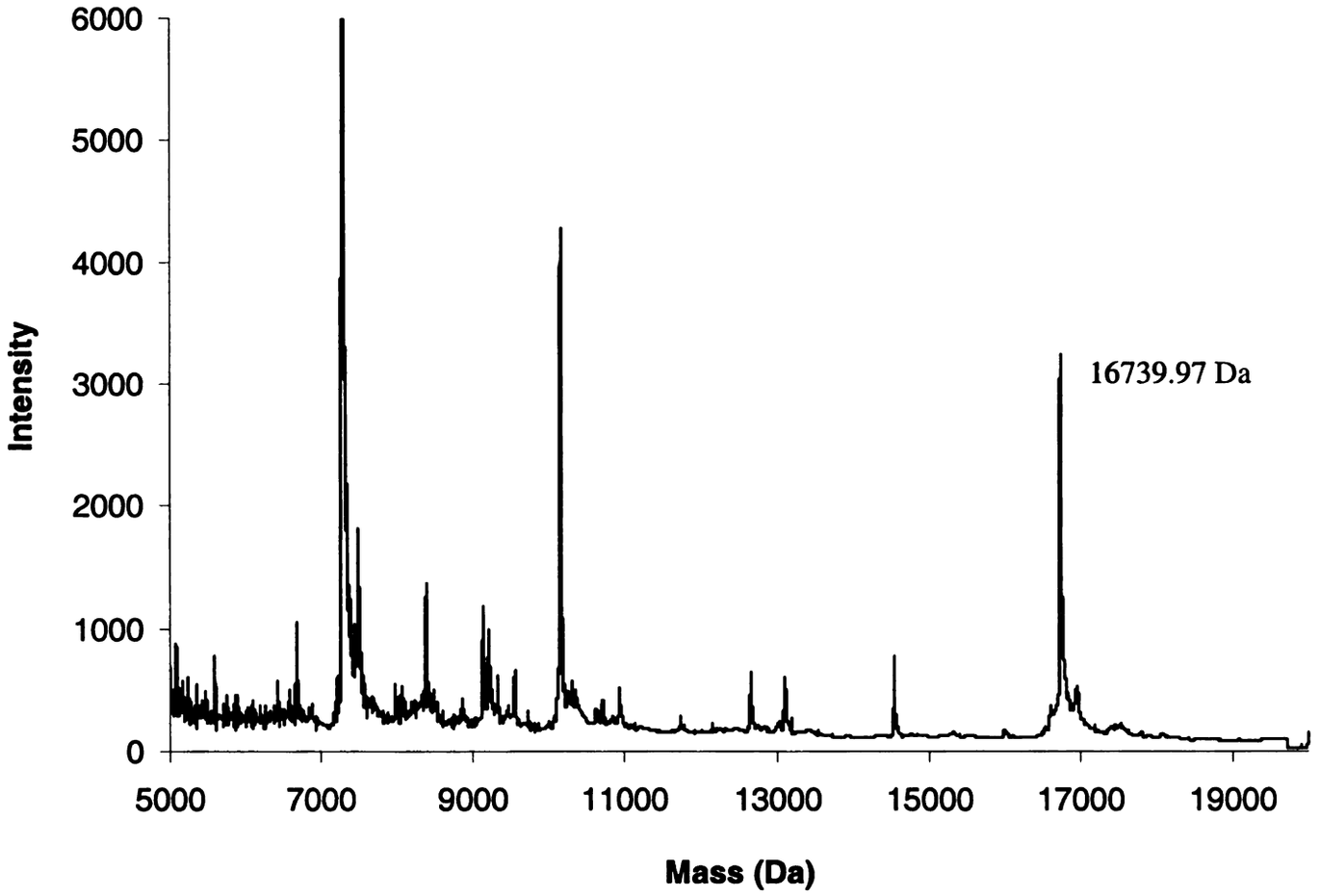

CRABPII R132K::Y134F::R111L::L121D::T54V

MALDI-TOF, Incubation with all-*trans*-Retinal

Protein Mass = 16742.13 Da

Positive Covalent Bond Formation = Protein Mass + 266

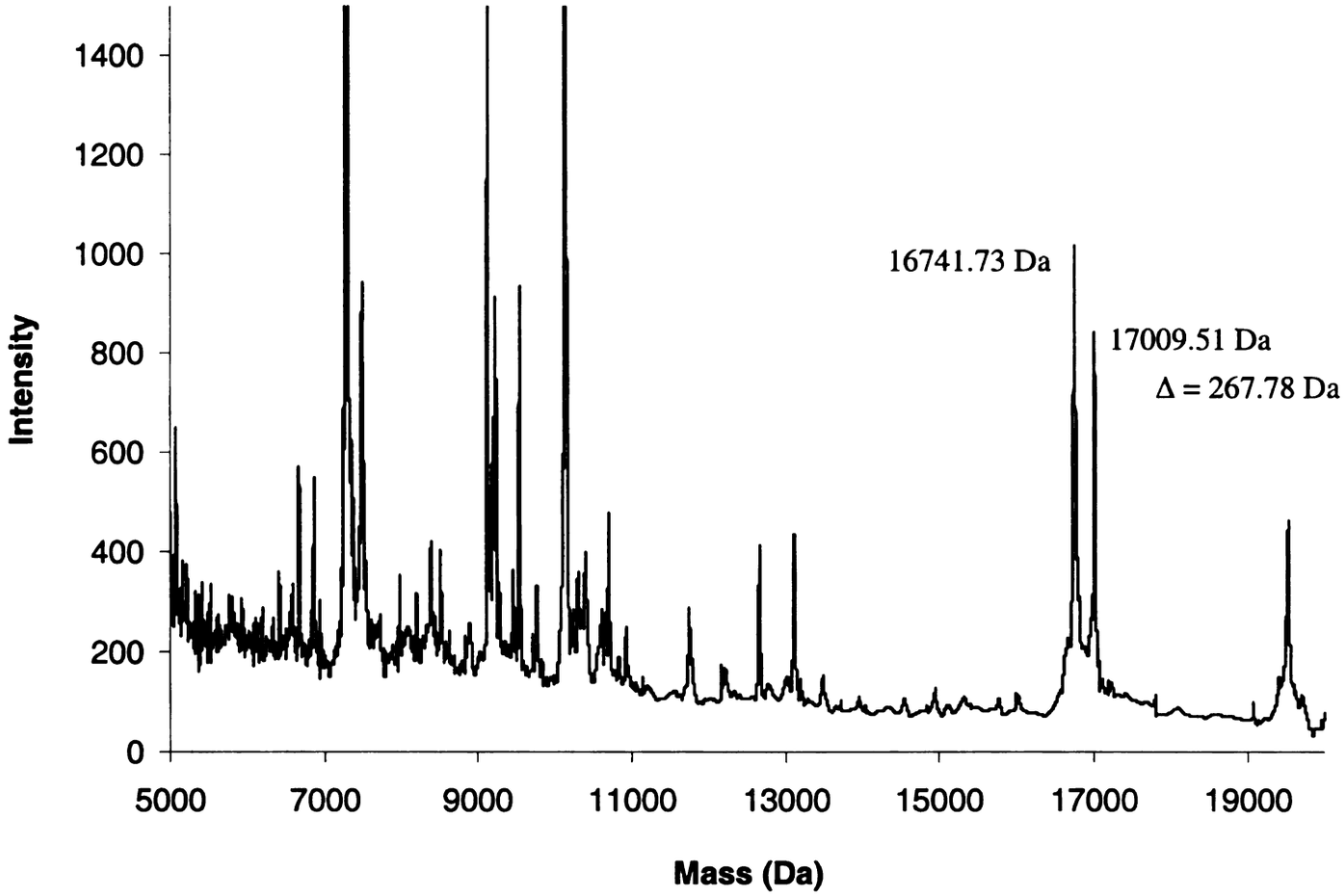

CRABPII R132K::Y134F::R111L::L121D::T54V

MALDI-TOF, Reductive Amination with all-*trans*-Retinal

Protein Mass = 16742.13 Da

Positive Reductive Amination = Protein Mass + 268

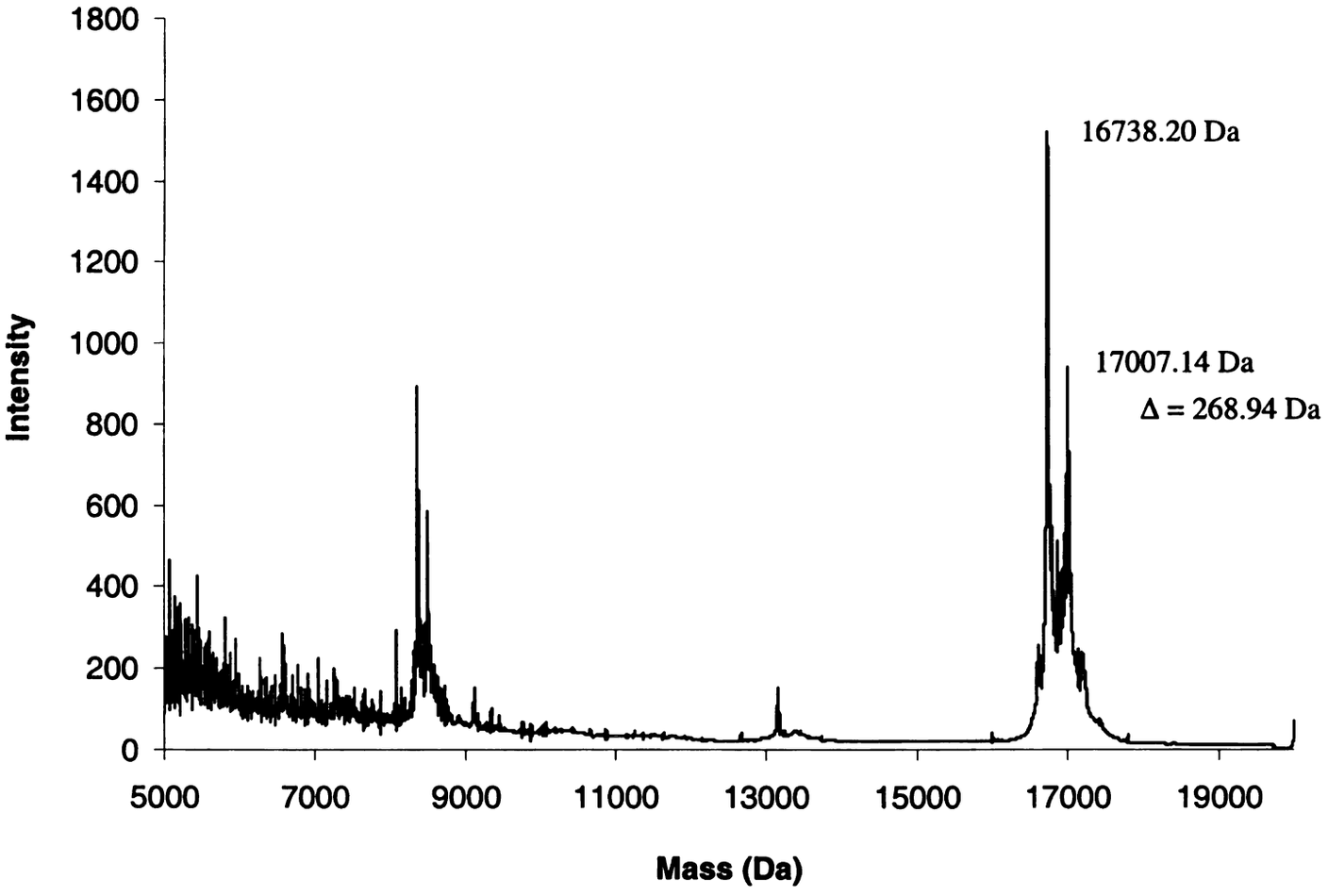

CRABPII R132K::Y134F::R111L::L121N::T54V

Molecular Weight :

16741.14 Da

Extinction Coefficient :

21,766 M^{-1} cm^{-1}

Primers :

bbb67 5' CTA CAT CAA AGT CTC CAC CAC CGT GCG

bbb68 5' CGC ACG GTG GTG GAG ACT TTG ATG TAG

CD

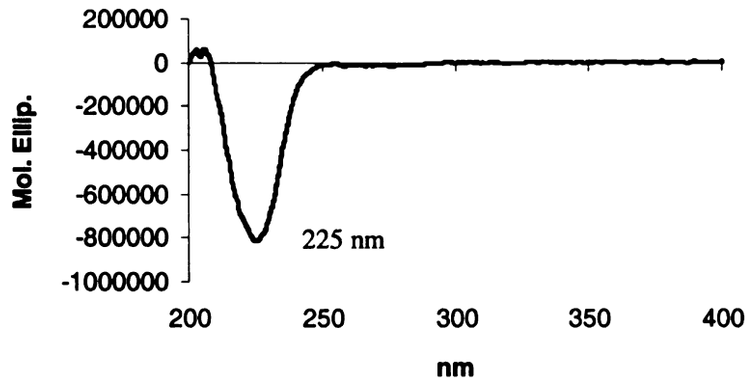

CRABPII R132K::Y134F::R111L::L121N::T54V

Sequence BB 167

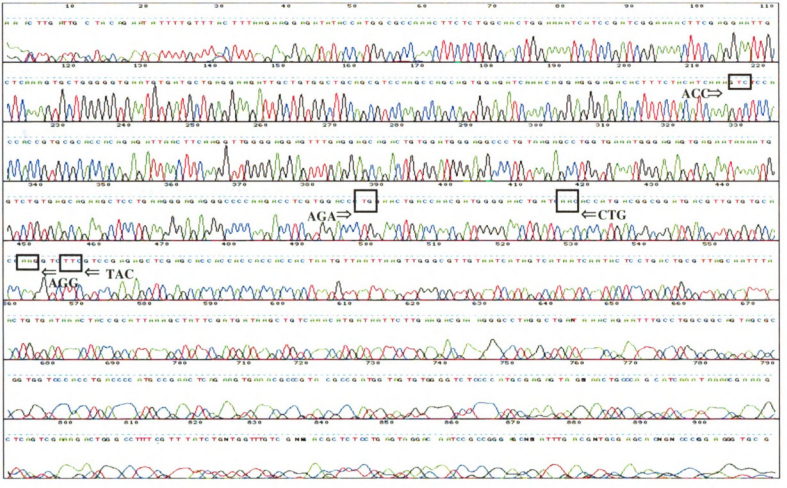

CRABPII R132K::Y134F::R111L::L121N::T54V

Fluorescence Titrations

Retinoic Acid

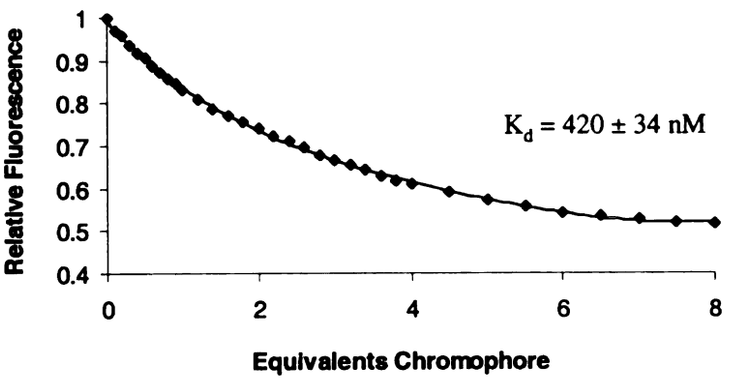

all-*trans*-Retinal

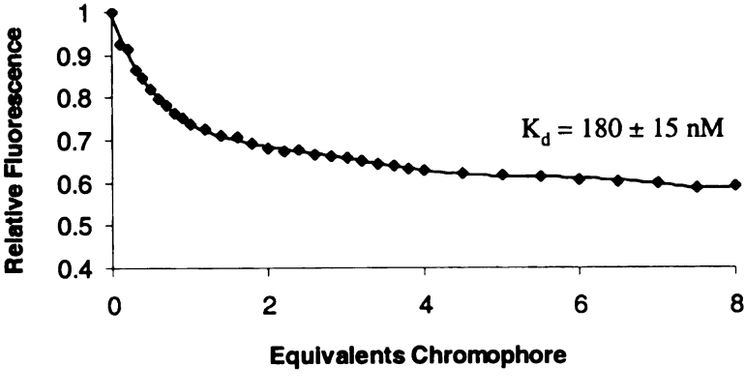

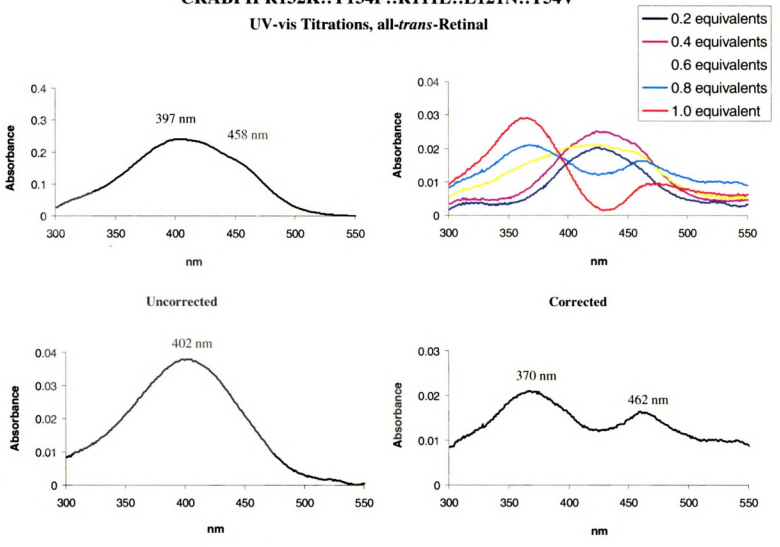
CRABPII R132K::Y134F::R111L::L121N::T54V
UV-vis Titrations, all-trans-Retinal
0.2 equivalents
0.4 equivalents
0.6 equivalents
0.8 equivalents
1.0 equivalent
Absorbance
nm
397 nm
458 nm
Uncorrected
Corrected
402 nm
370 nm
462 nm

CRABPII R132K::Y134F::R111L::L121N::T54V

MALDI-TOF, Protein

Calculated Mass = 16741.14 Da

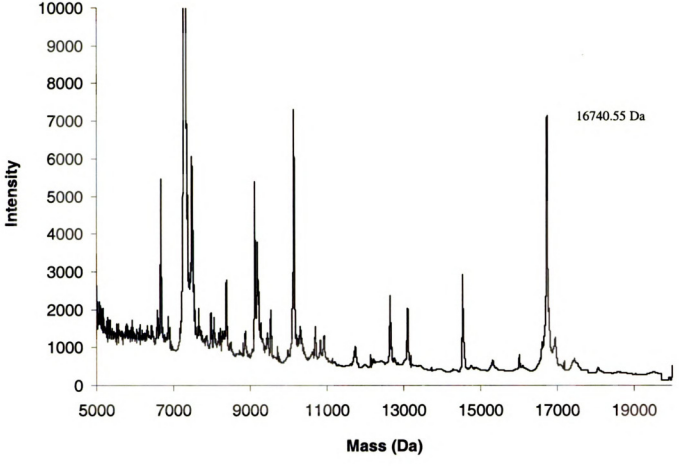

CRABPII R132K::Y134F::R111L::L121N::T54V

MALDI-TOF, Incubation with all-*trans*-Retinal

Protein Mass = 16741.14 Da

Positive Covalent Bond Formation = Protein Mass + 266

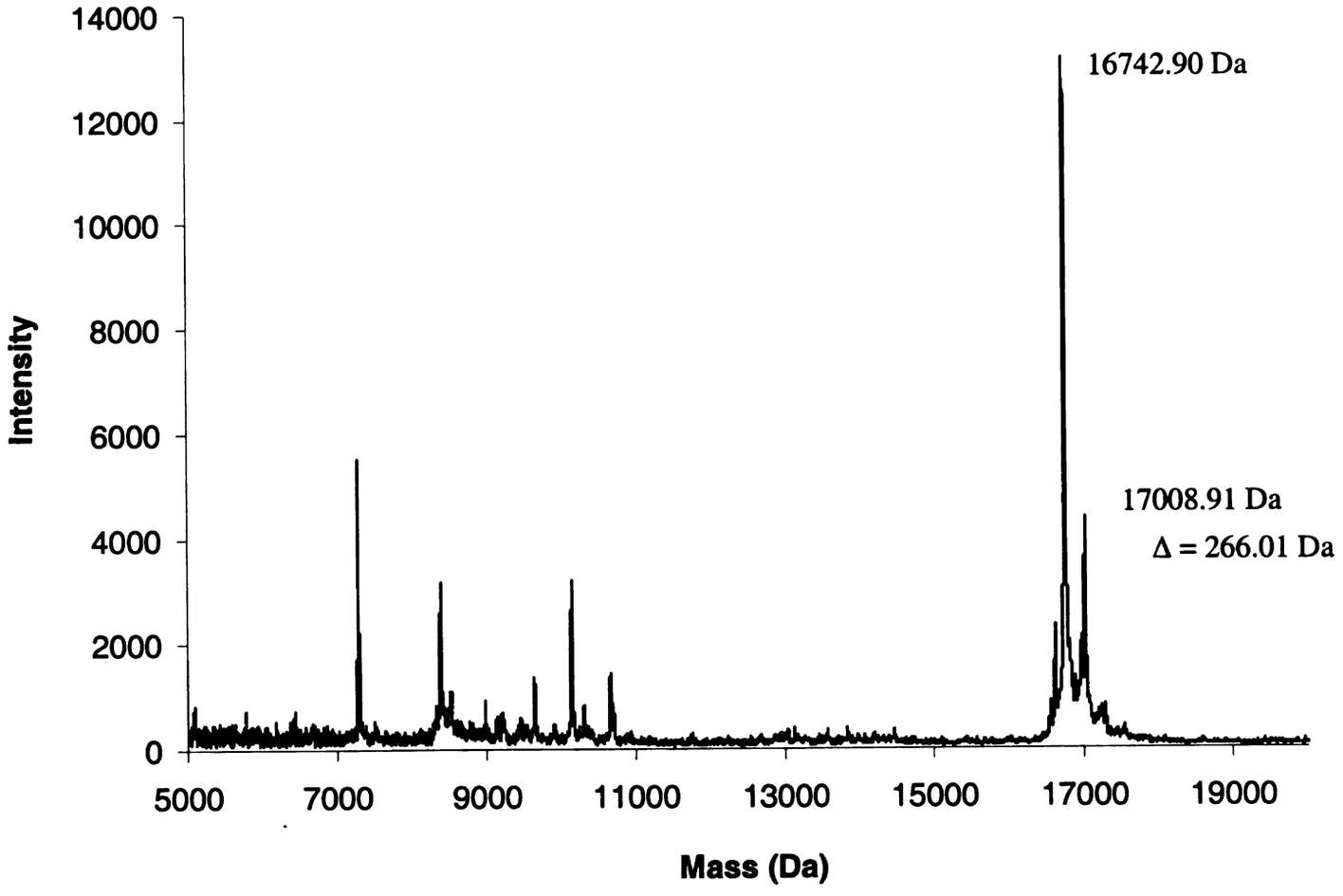

CRABPII R132K::Y134F::R111L::L121N::T54V

MALDI-TOF, Reductive Amination with all-*trans*-Retinal

Protein Mass = 16741.14 Da

Positive Reductive Amination = Protein Mass + 268

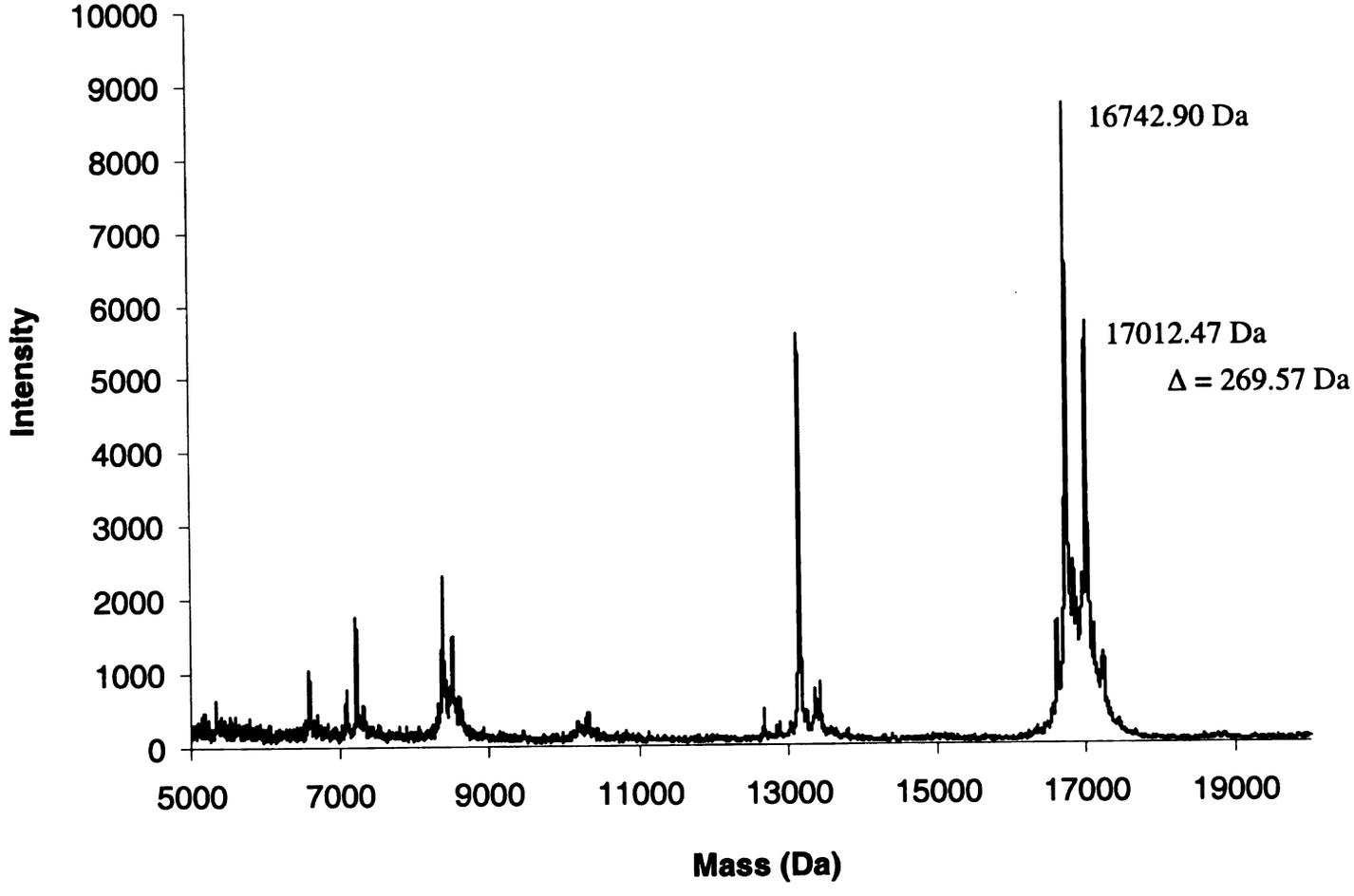

CRABPII R132K::Y134F::R111L::L121E::T54V::T61E

Molecular Weight :
16784.17 Da

Extinction Coefficient :
17,283 M^{-1} cm^{-1}

Primers :
bbb107 5' CCG TGC GCA CCG AGG AGA TTA ACT TC
bbb108 5' GAA GTT AAT CTC CTC GGT GCG CAC GG

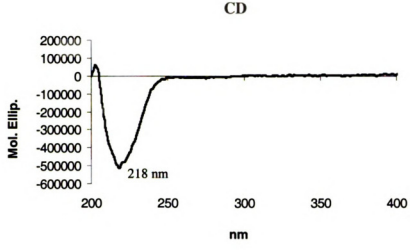

CRABPII R132K::Y134F::R111L::L121E::T54V::T61E

Sequence BB 189

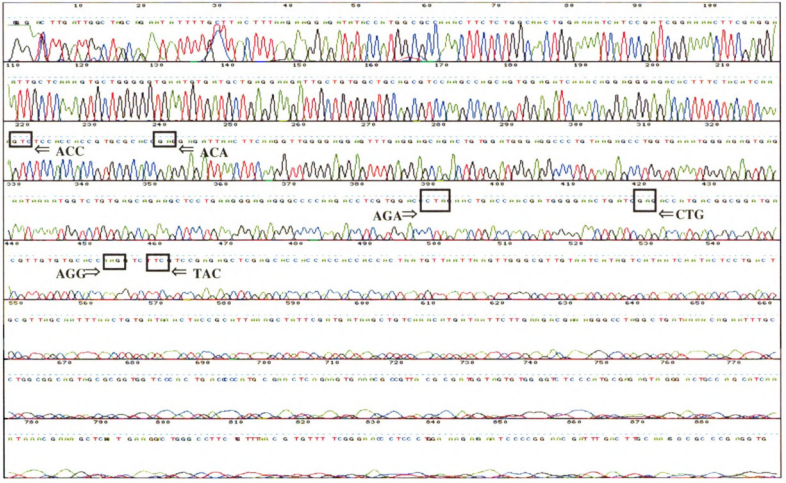

CRABPII R132K::Y134F::R111L::L121E::T54V::T61E

Fluorescence Titrations

Retinoic Acid

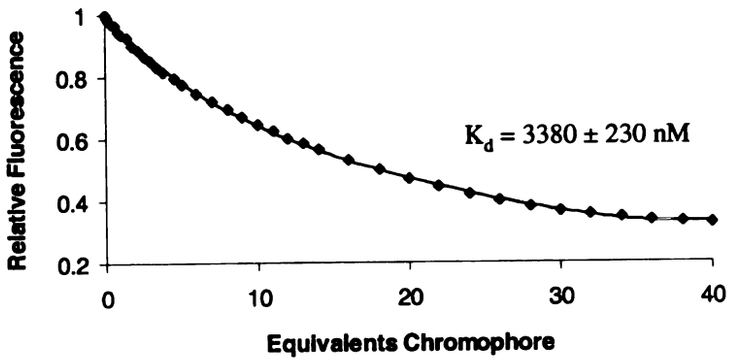

all-*trans*-Retinal

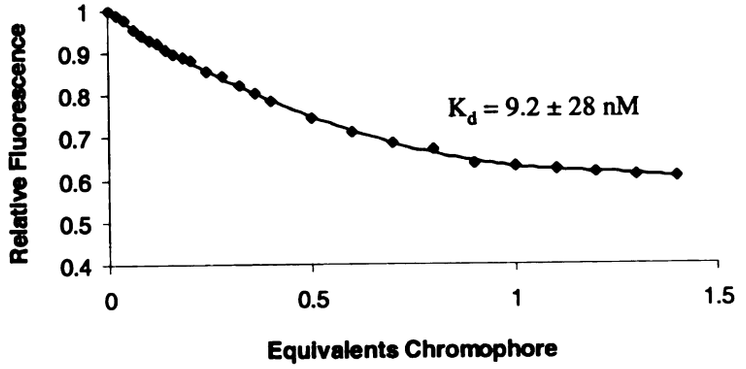

CRABPII R132K::Y134F::R111L::L121E::T54V::T61E

UV-vis Titrations, all-*trans*-Retinal

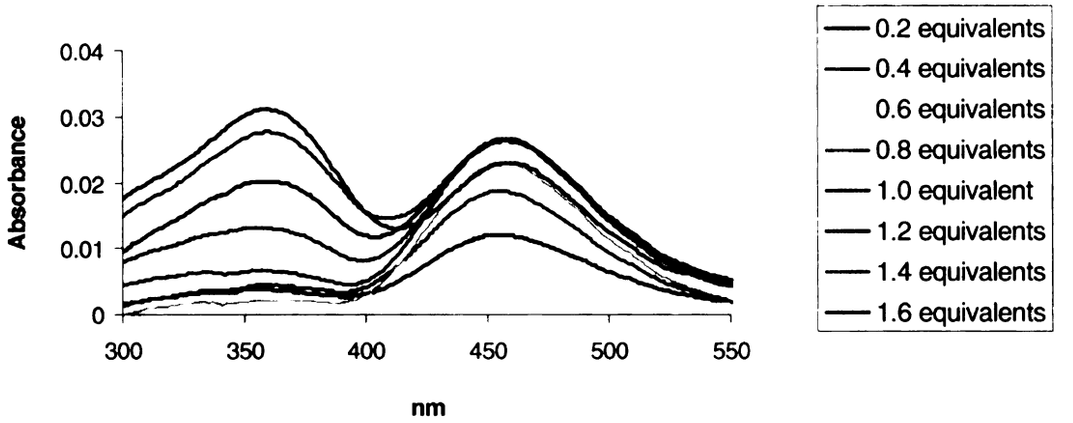

Uncorrected

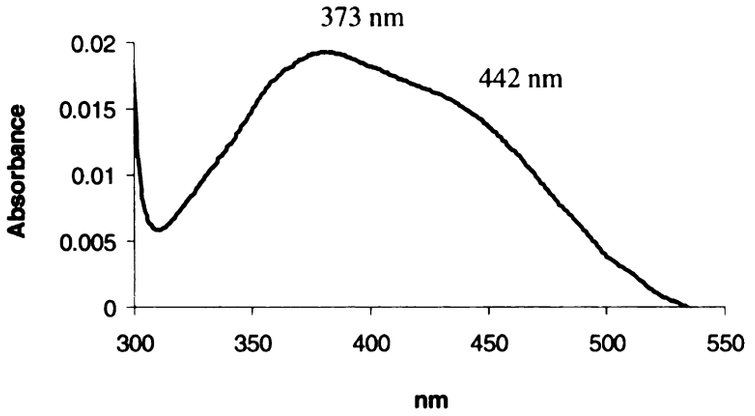

Corrected

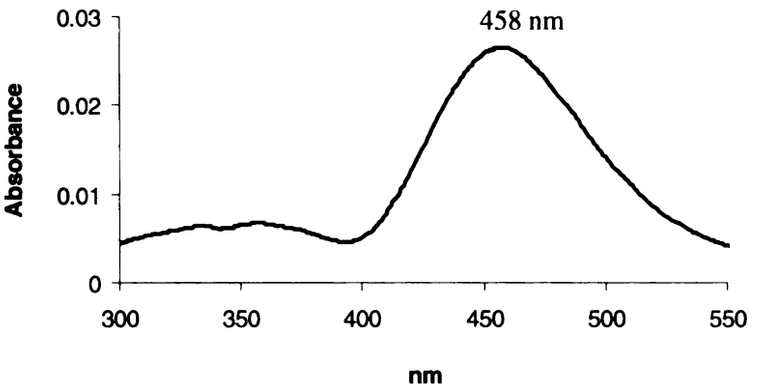

CRABPII R132K::Y134F::R111L::L121E::T54V::T61E

UV-vis Acid/Base Titrations, all-*trans*-Retinal

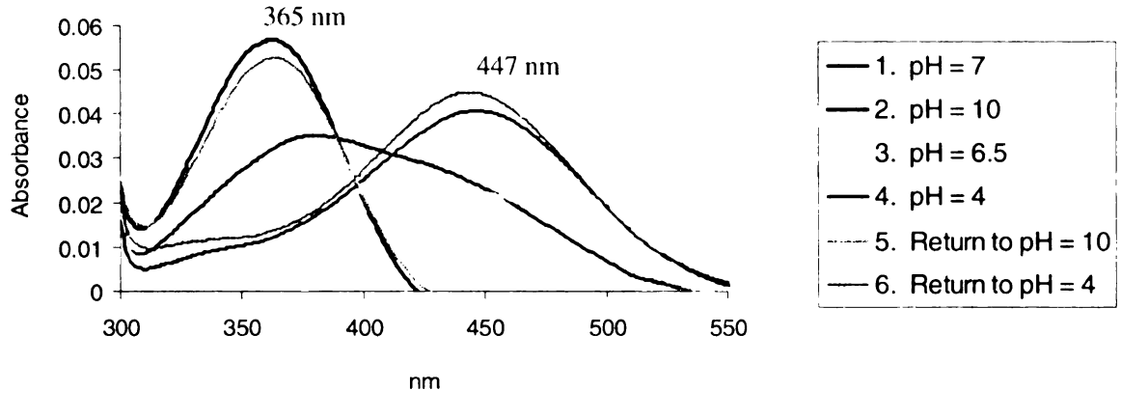

CRABPII R132K::Y134F::R111L::L121E::T54V::T61E

MALDI-TOF, Protein

Calculated Mass = 16784.17 Da

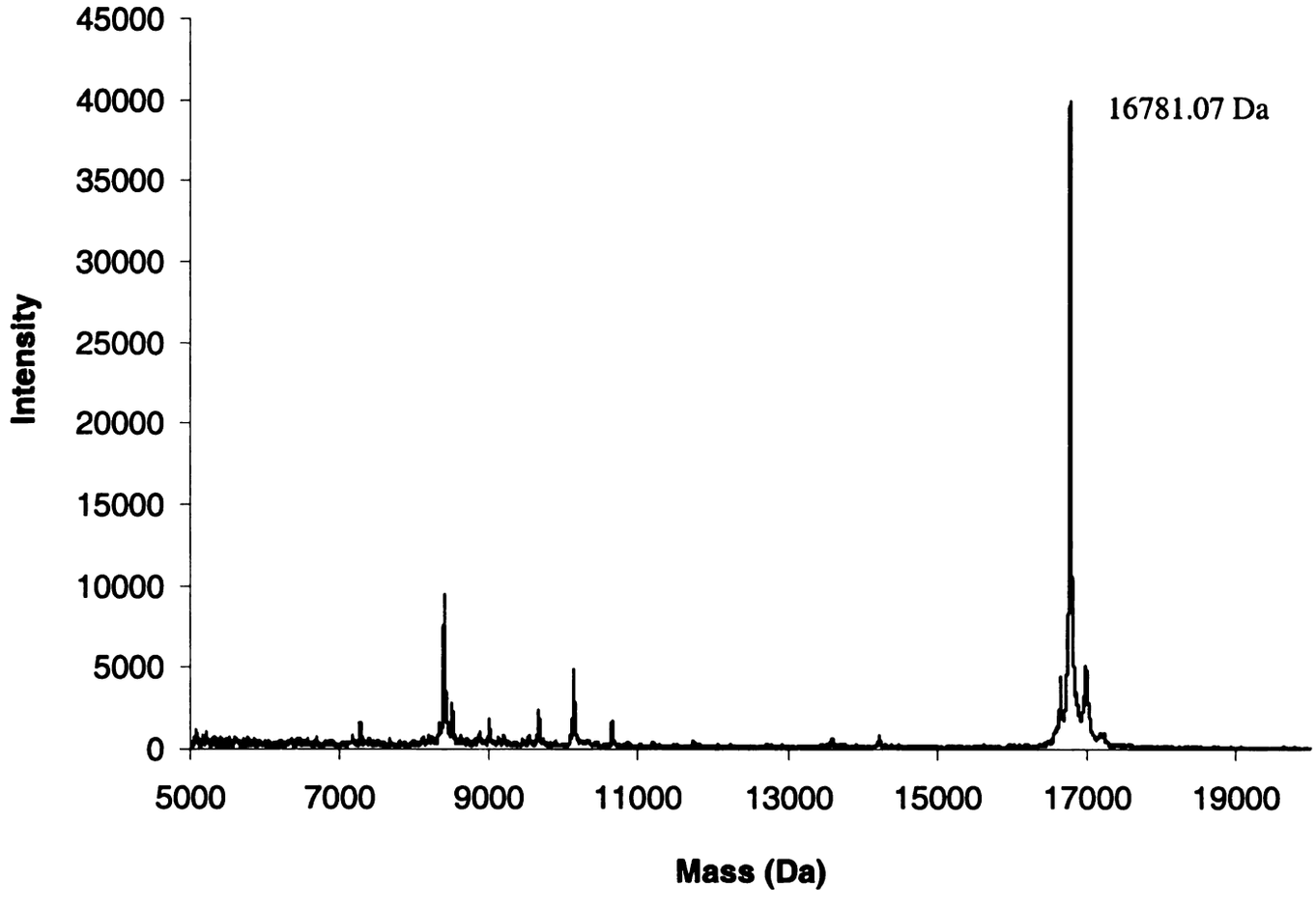

CRABPII R132K::Y134F::R111L::L121E::T54V::T61E

MALDI-TOF, Incubation with all-*trans*-Retinal

Protein Mass = 16784.17 Da

Positive Covalent Bond Formation = Protein Mass + 268

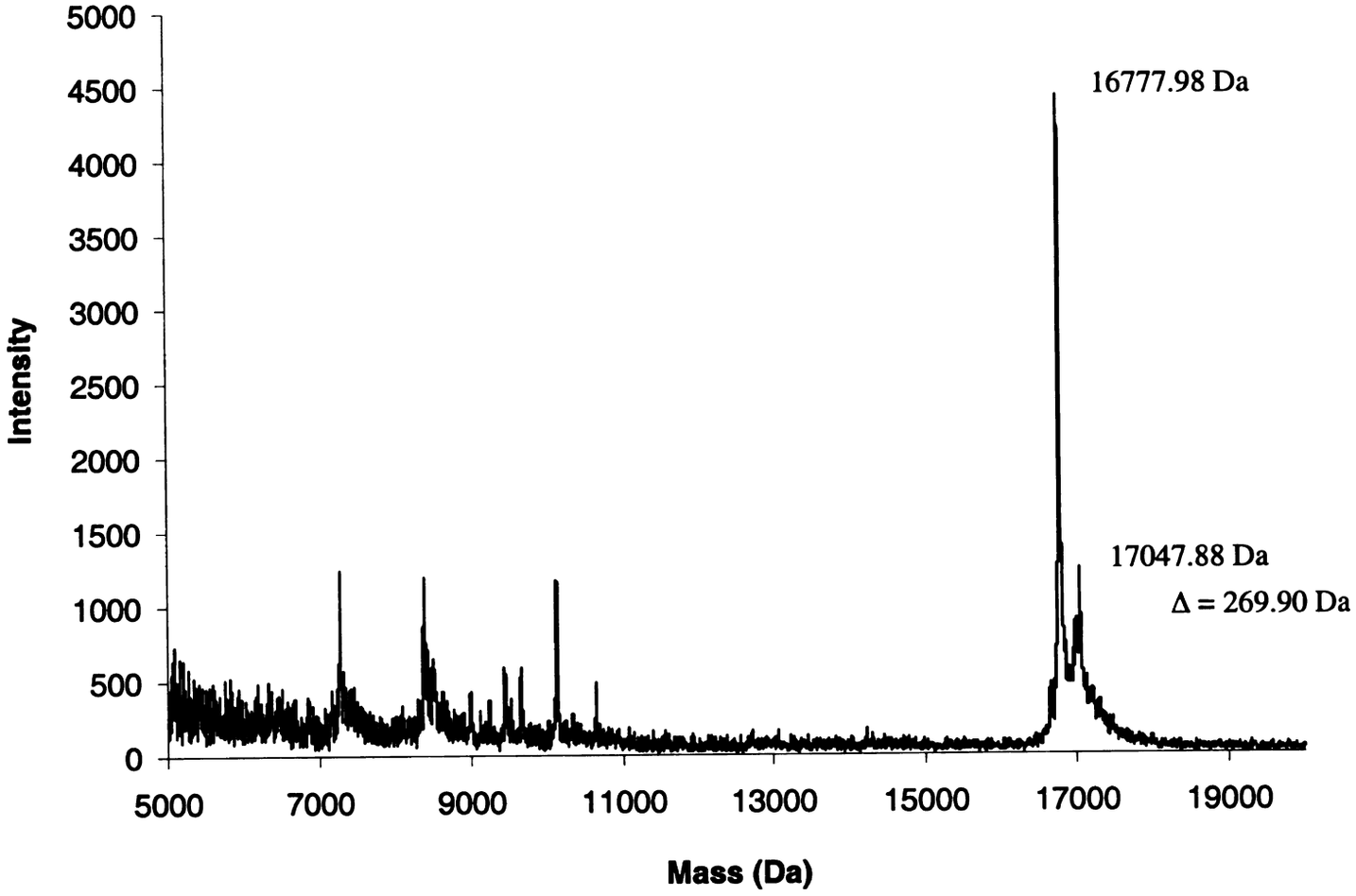

CRABPII R132K::Y134F::R111L::L121E::T54V::T61E

MALDI-TOF, Reductive Amination with all-*trans*-Retinal

Protein Mass = 16784.17 Da

Positive Reductive Amination = Protein Mass + 268

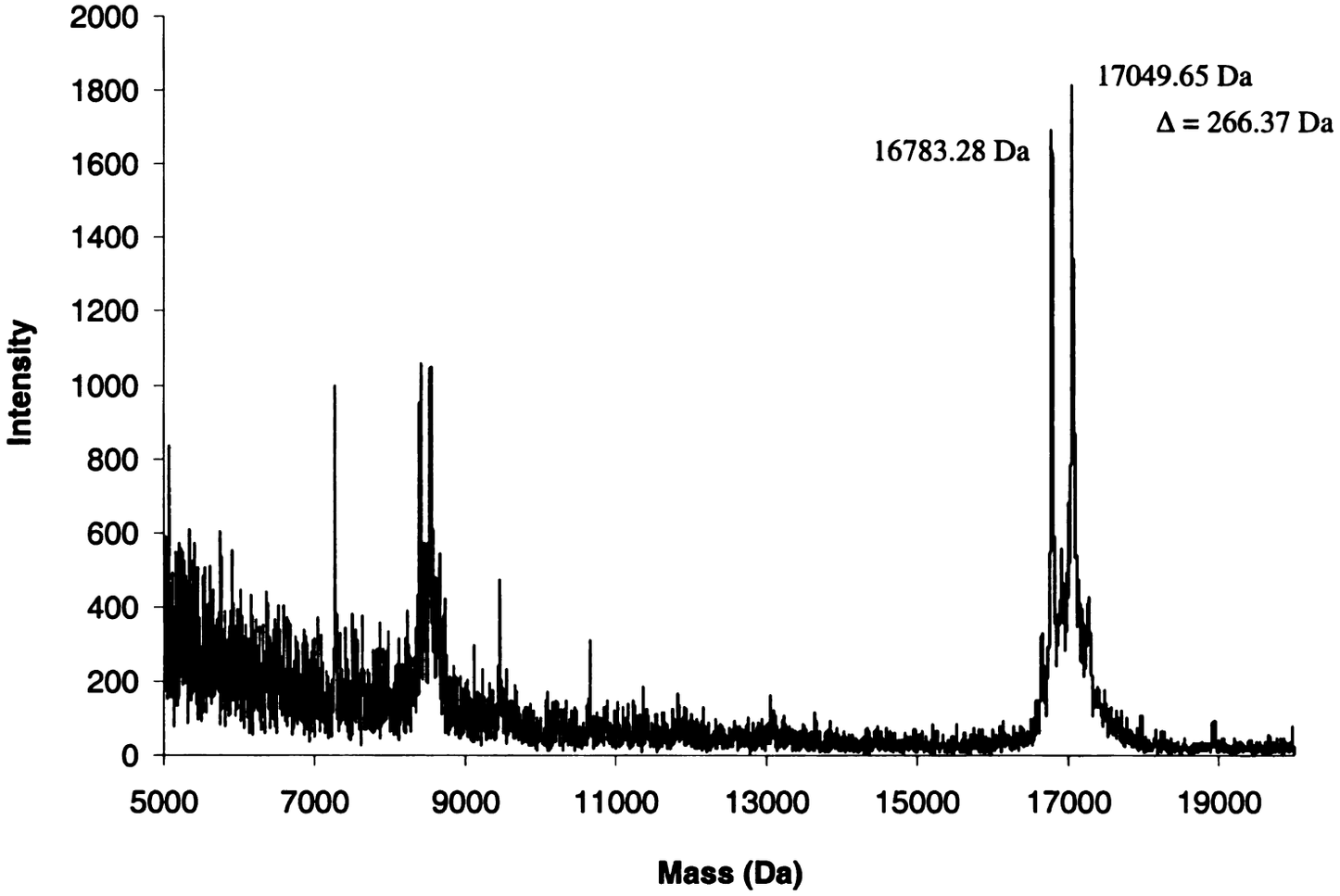

CRABPII R132K::Y134F::R111L::L121E::T54V::T61F

Molecular Weight :

16802.23 Da

Extinction Coefficient :

18,847 M^{-1} cm^{-1}

Primers :

bbb105 5' CCG TGC GCA CCT TCG AGA TTA ACT TC
bbb106 5' GAA GTT AAT CTC GAA GGT GCG CAC GG

CD

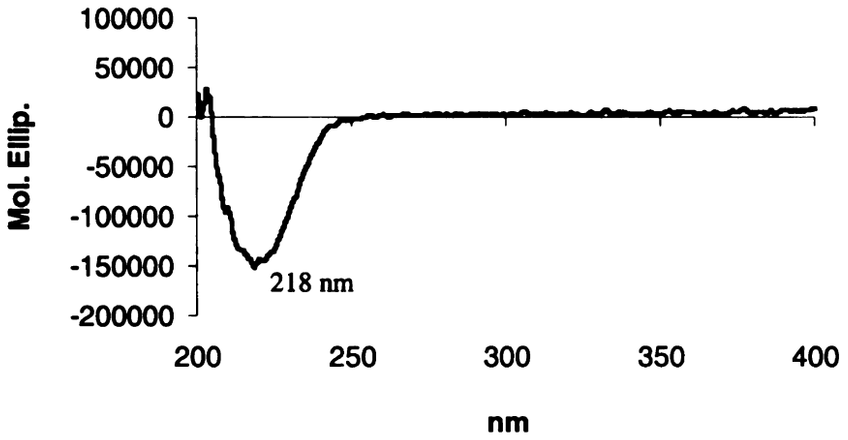

CRABPII R132K::Y134F::R111L::L121E::T54V::T61F

Sequence BB 185

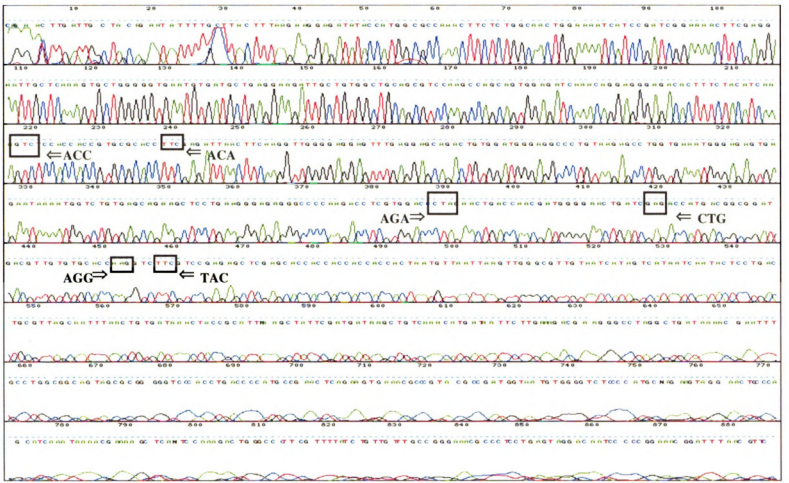

CRABPII R132K::Y134F::R111L::L121E::T54V::T61F

Fluorescence Titrations

Retinoic Acid

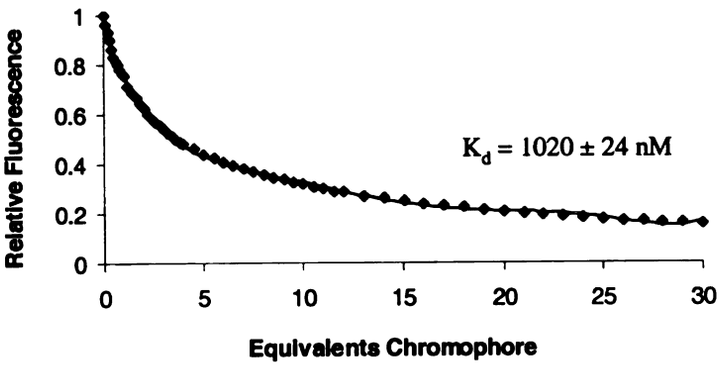

all-*trans*-Retinal

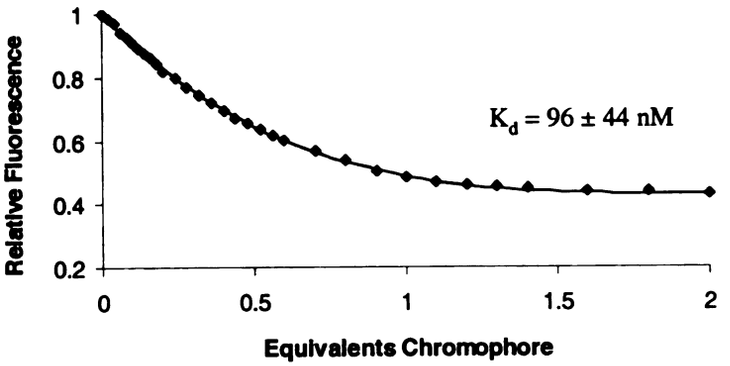

CRABPII R132K::Y134F::R111L::L121E::T54V::T61F

UV-vis Titrations, all-*trans*-Retinal

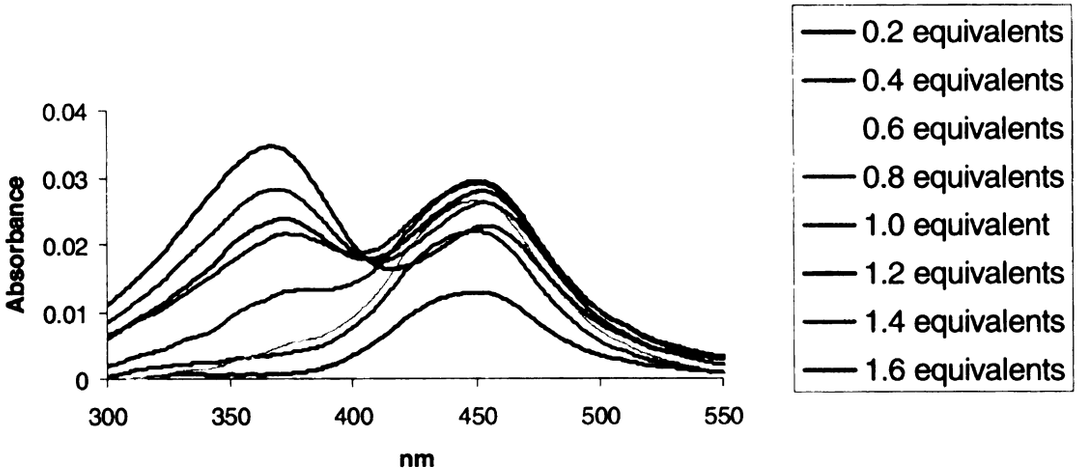

Uncorrected

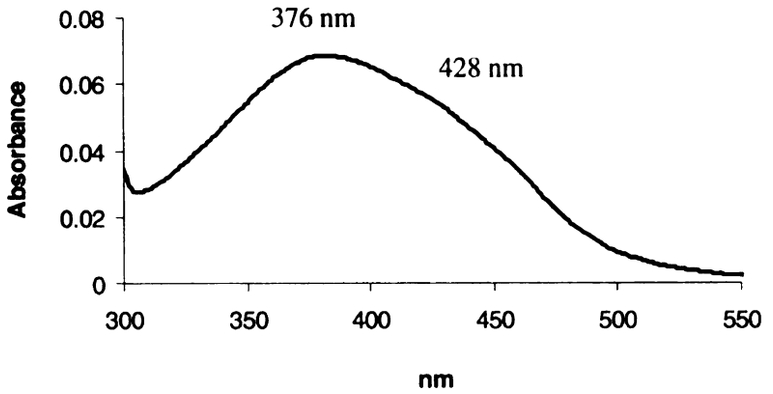

Corrected

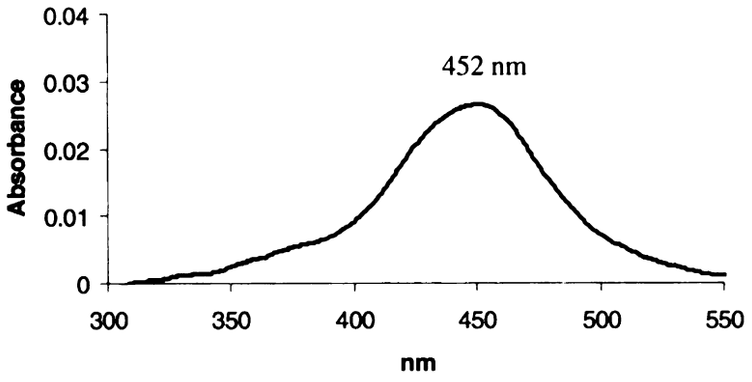

CRABPII R132K::Y134F::R111L::L121E::T54V::T61F

UV-vis Acid/Base Titrations, all-*trans*-Retinal

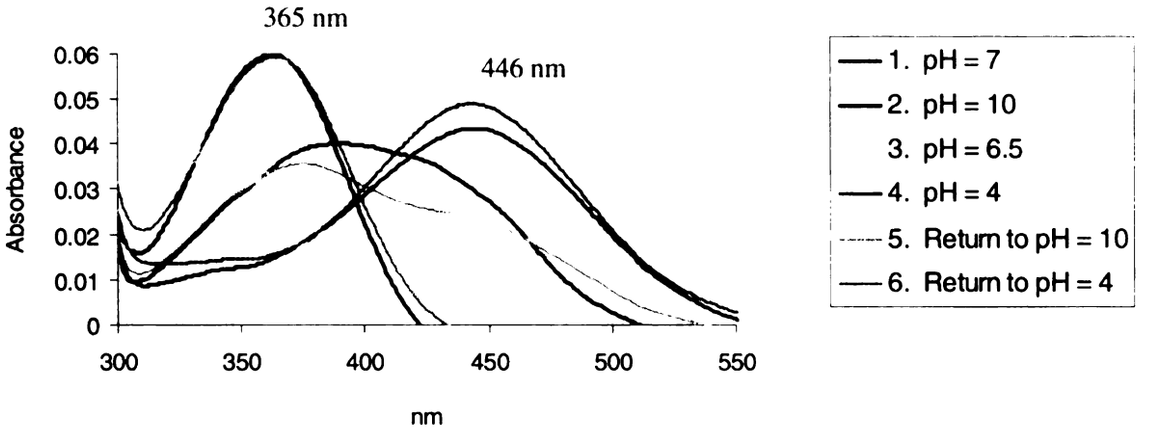

CRABPII R132K::Y134F::R111L::L121E::T54V::T61F

MALDI-TOF, Protein

Calculated Mass = 16802.23 Da

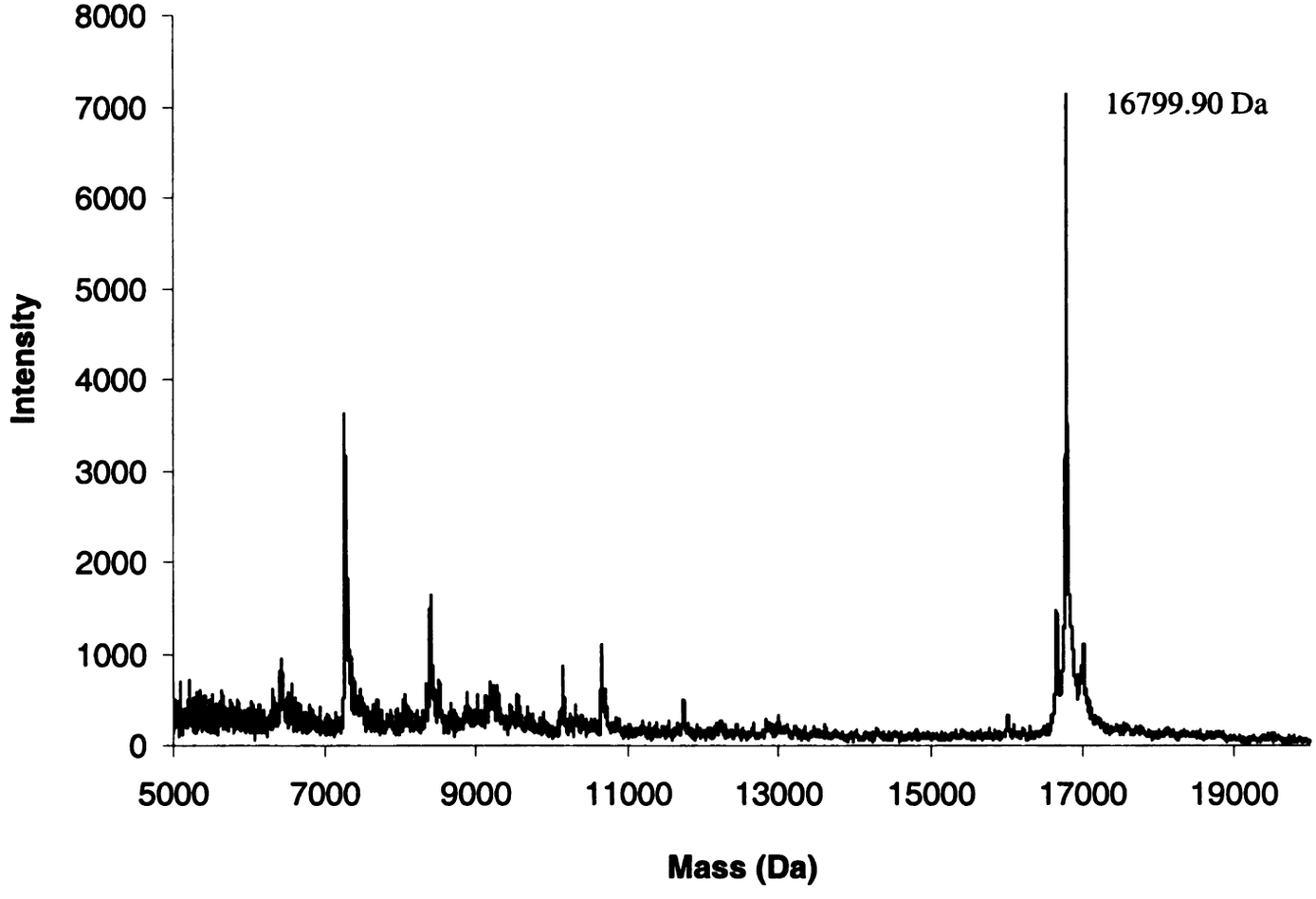

CRABPII R132K::Y134F::R111L::L121E::T54V::T61F

MALDI-TOF, Incubation with all-*trans*-Retinal

Protein Mass = 16802.23 Da

Positive Covalent Bond Formation = Protein Mass + 268

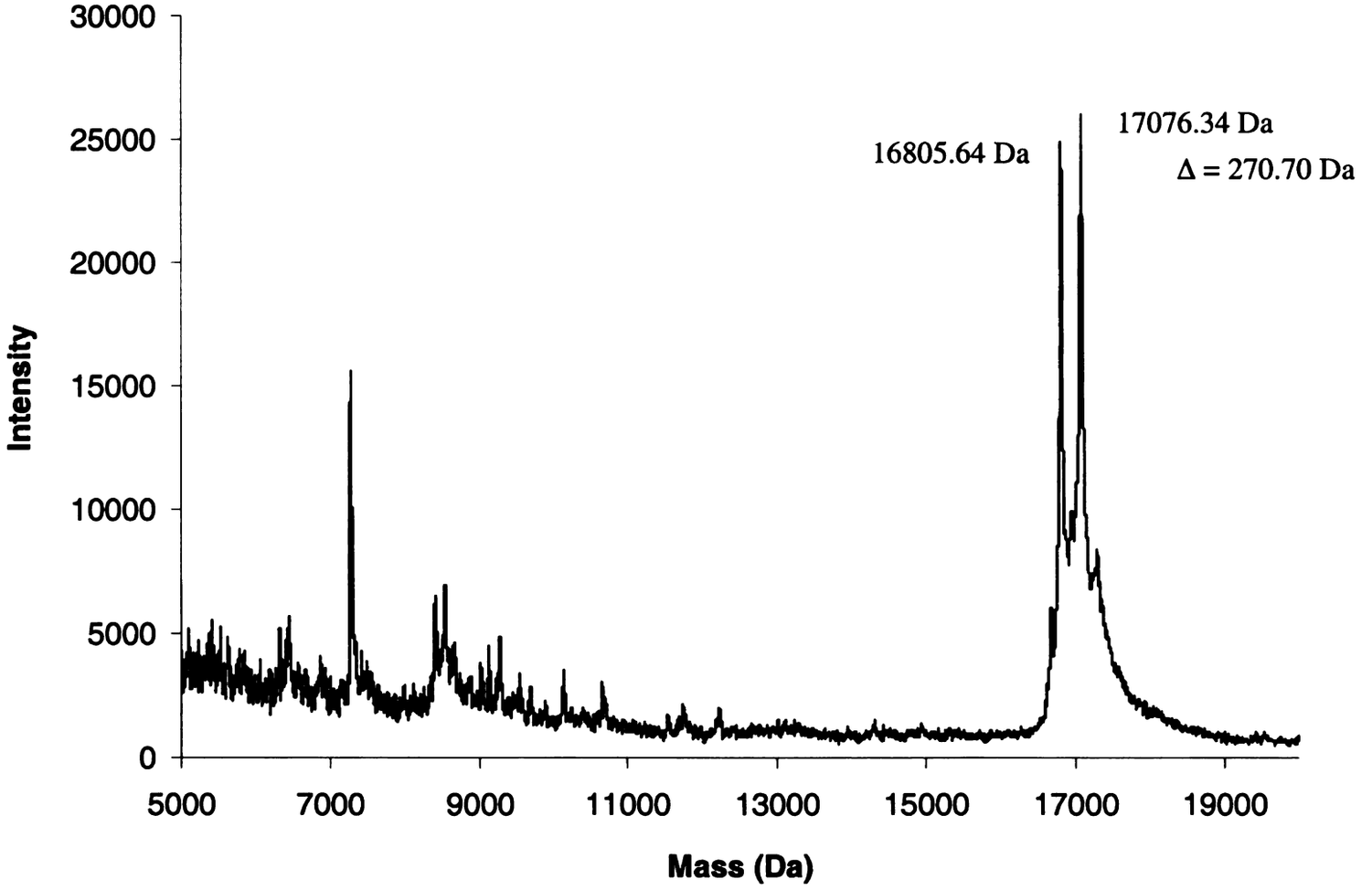

CRABPII R132K::Y134F::R111L::L121E::T54V::T61F

MALDI-TOF, Reductive Amination with all-*trans*-Retinal

Protein Mass = 16802.23 Da

Positive Reductive Amination = Protein Mass + 268

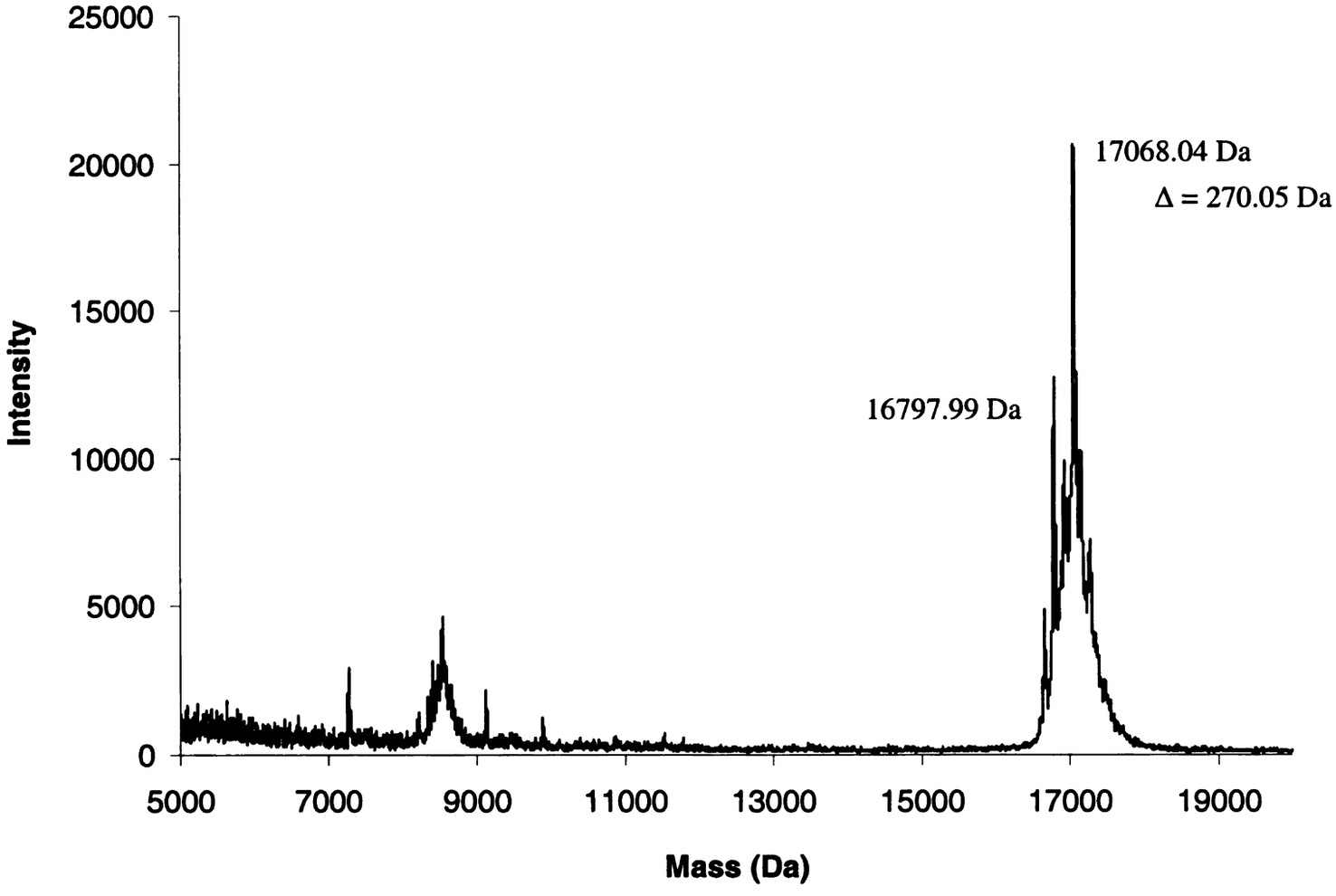

CRABPII Y134K

Molecular Weight :
16794.21 Da

Extinction Coefficient :
20,990 M^{-1} cm^{-1}

Primers :

bbb61 5' GCA CCA GGG TCA AGG TCC GAG AGC
bbb62 5' GCT CTC GGA CCT TGA CCC TGG TGC

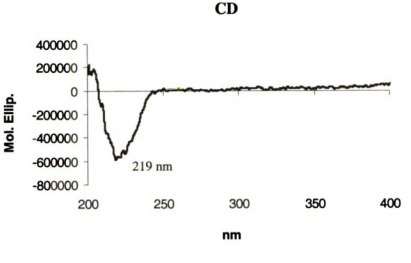

CRABPII Y134K

Sequence BB 42

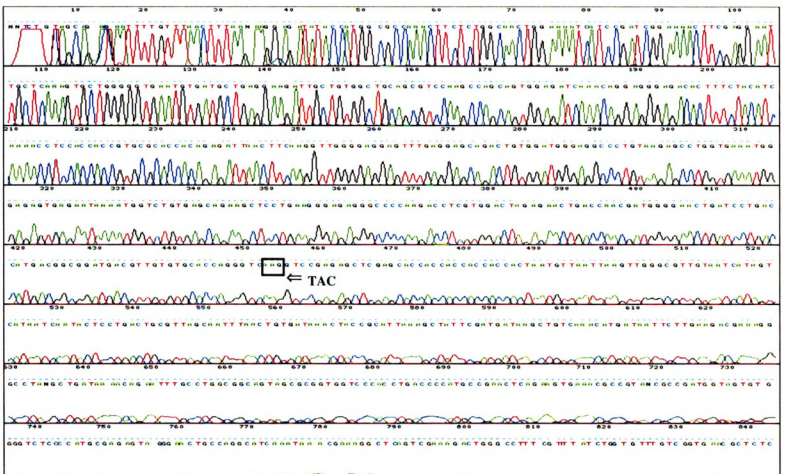

CRABPII Y134K

Fluorescence Titrations

Retinoic Acid

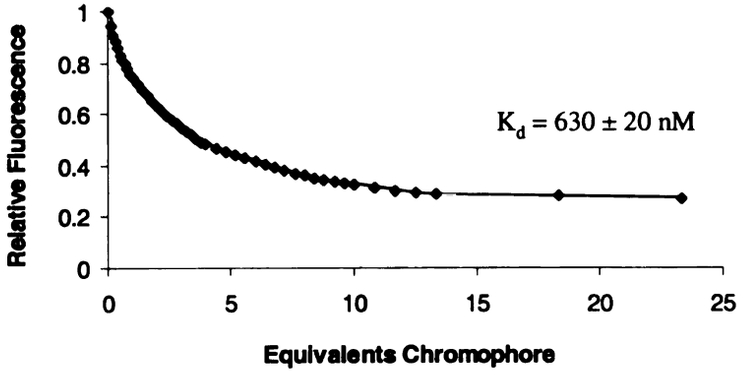

all-*trans*-Retinal

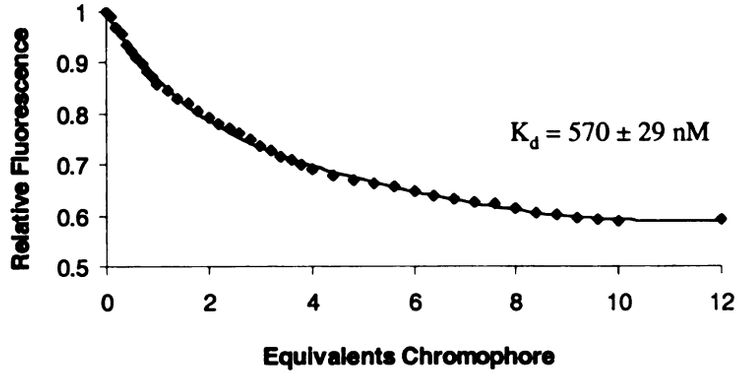

11-*cis*-Retinal

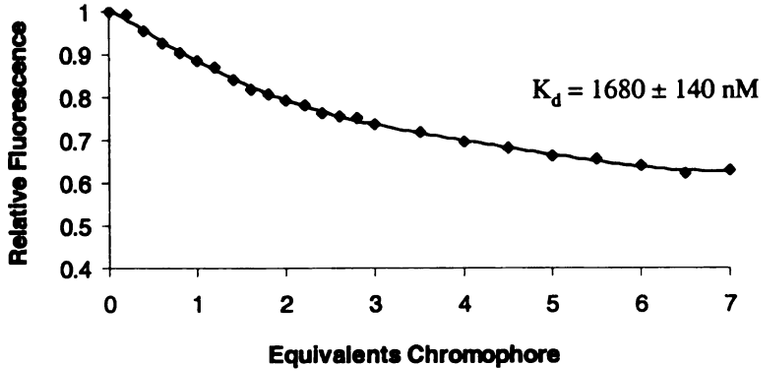

CRABPII Y134K

UV-vis Titrations, all-*trans*-Retinal

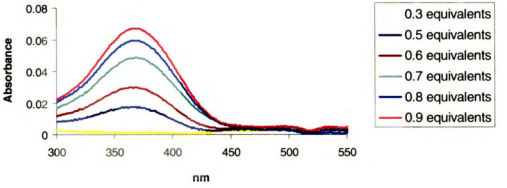

Uncorrected

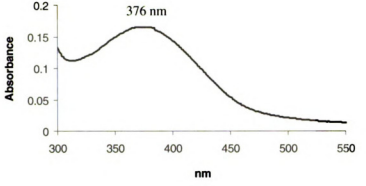

Corrected

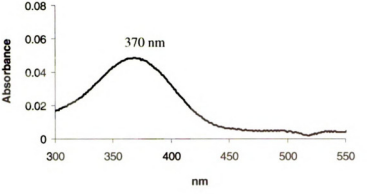

CRABPII Y134K

UV-vis Titrations, 11-*cis*-Retinal

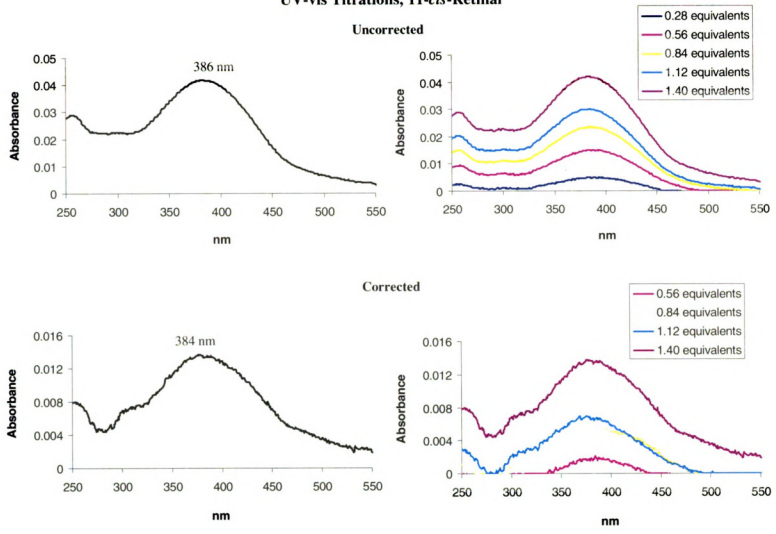

CRABPII Y134K

MALDI-TOF, Protein

Calculated Mass = 16794.21 Da

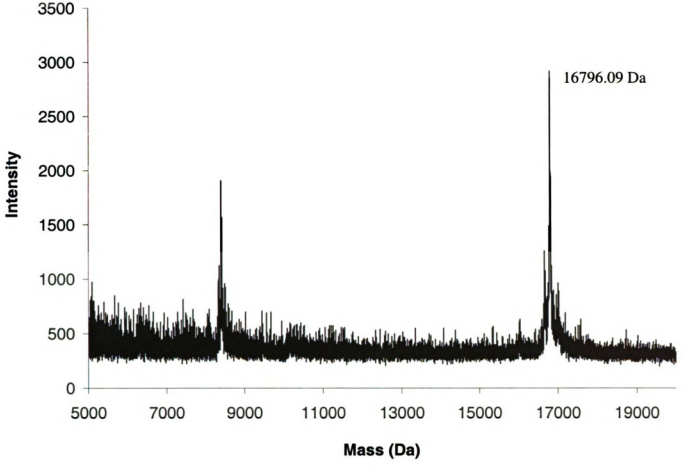

CRABPII Y134K

MALDI-TOF, Incubation with all-*trans*-Retinal

Protein Mass = 16794.21 Da

Positive Covalent Bond Formation = Protein Mass + 268

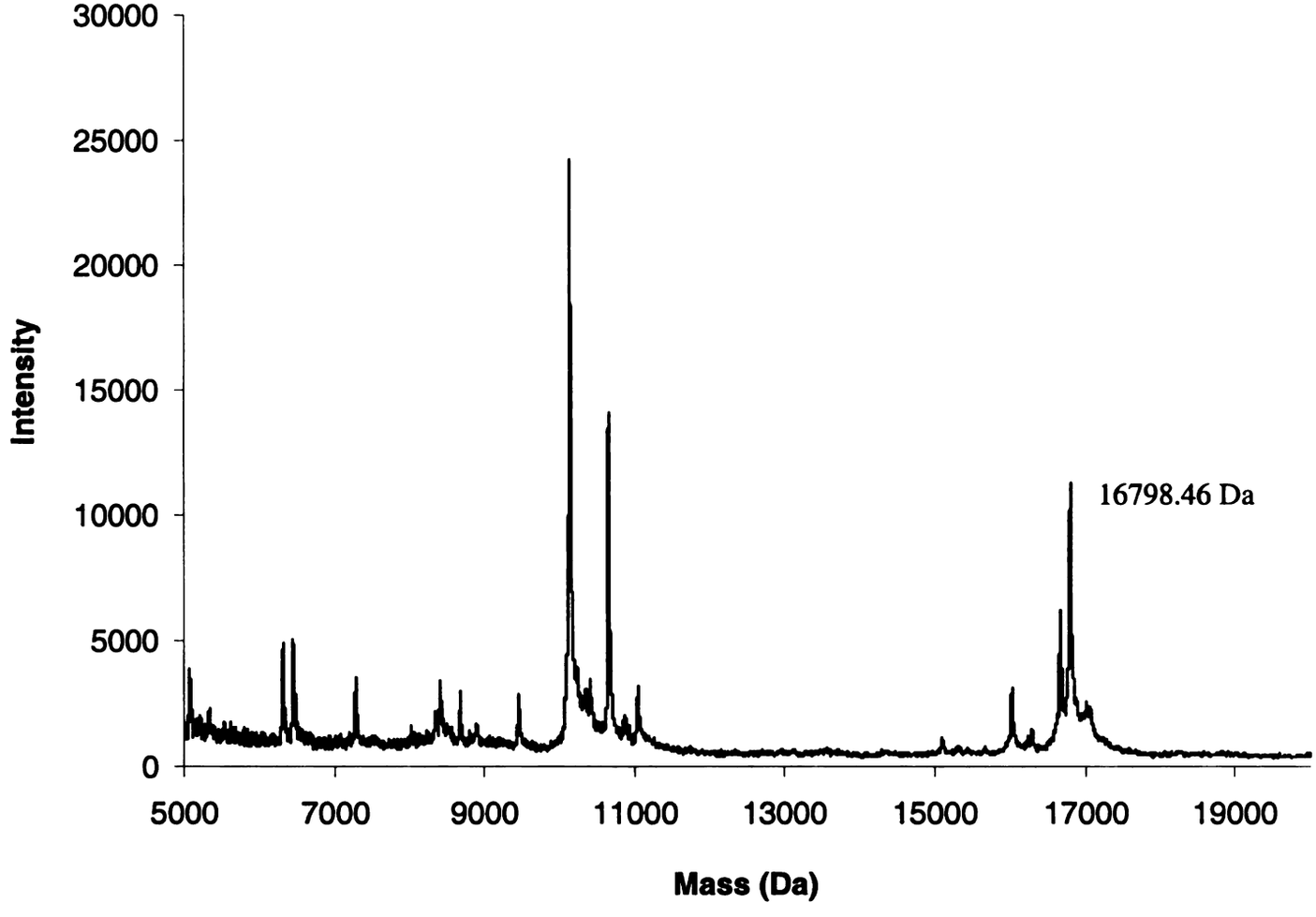

CRABPII Y134K

MALDI-TOF, Reductive Amination with all-*trans*-Retinal

Protein Mass = 16794.21 Da

Positive Reductive Amination = Protein Mass + 268

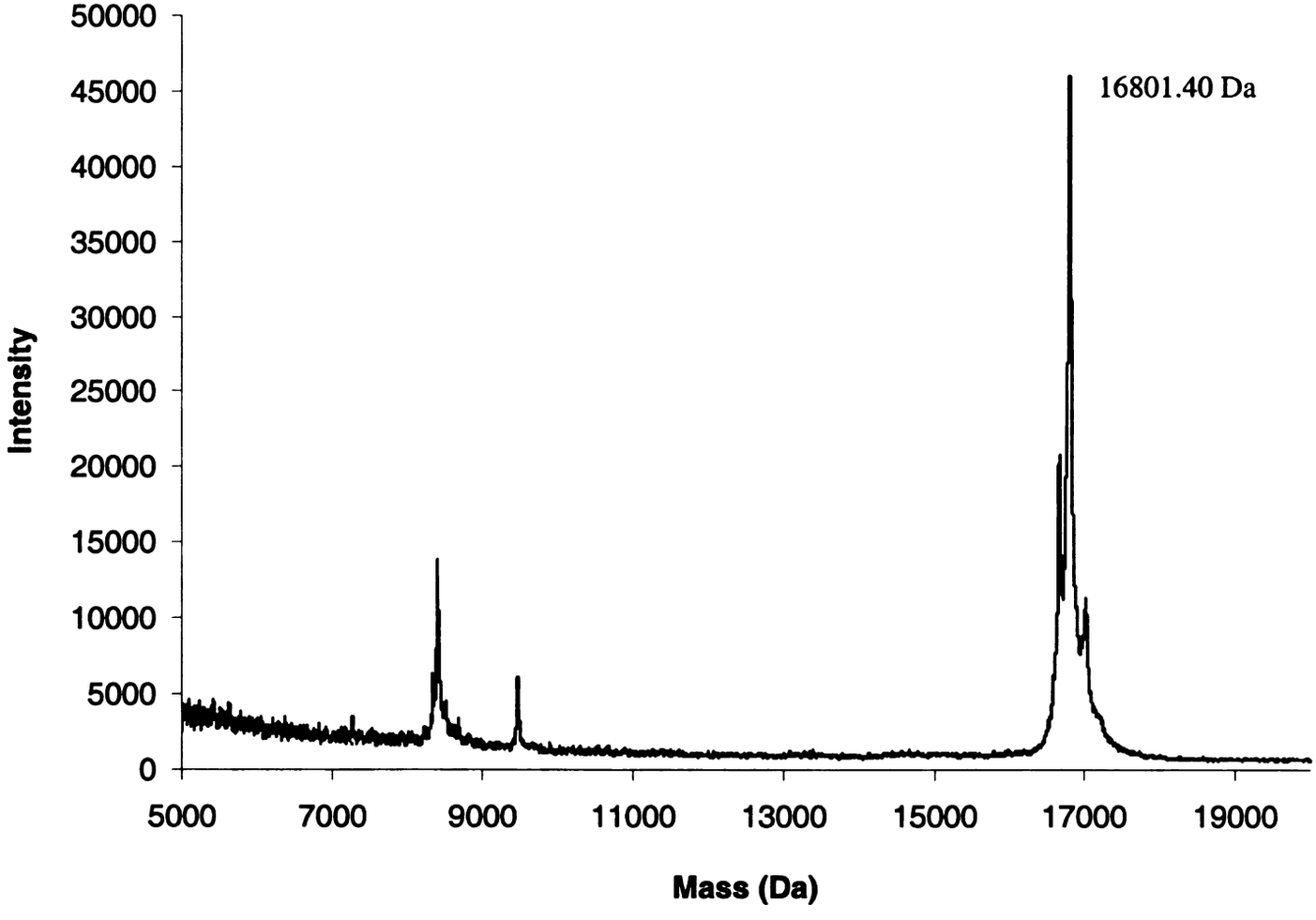

CRABPII Y134K

MALDI-TOF, Reductive Amination with 11-*cis*-Retinal

Protein Mass = 16794.21 Da

Positive Reductive Amination = Protein Mass + 268

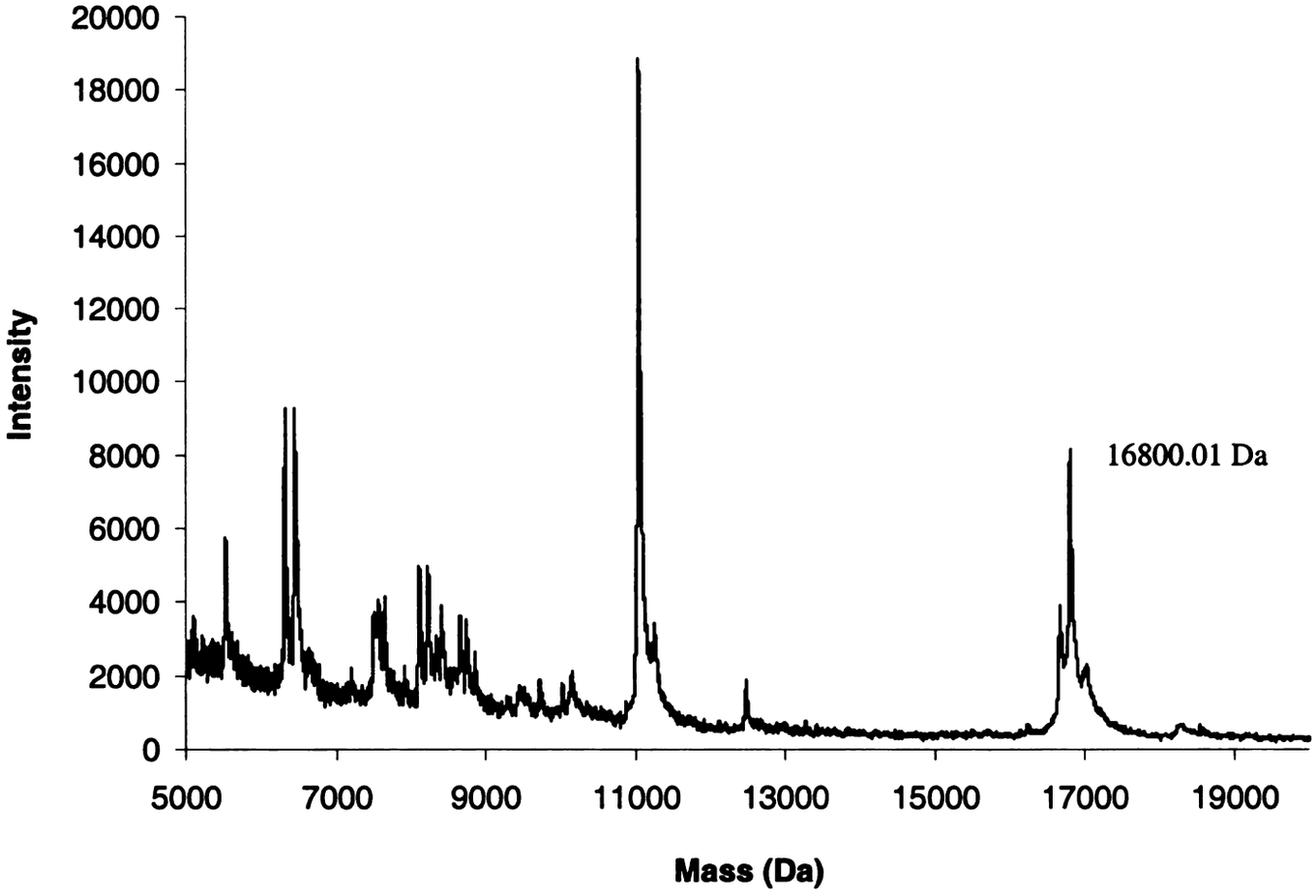

CRABPII Y134K::R132K

Molecular Weight :

16766.20 Da

Extinction Coefficient :

19,332 M^{-1} cm^{-1}

Primers :

bbb63 5' GCA CCA AGG TCA AGG TCC GAG AGC
bbb64 5' GCT CTC GGA CCT TGA CCT TGG TGC

CD

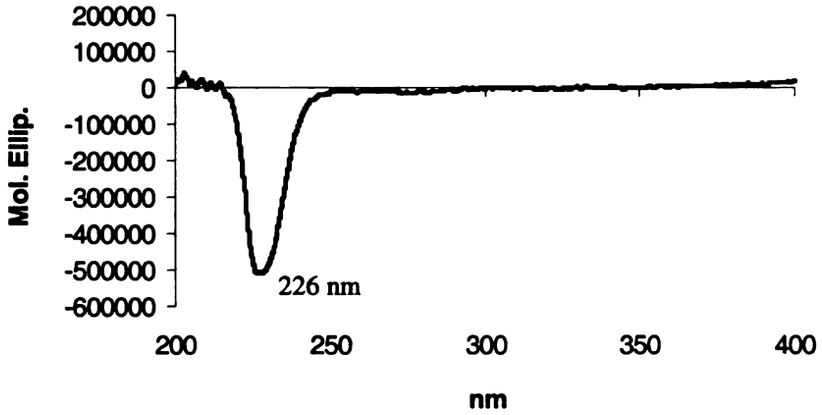

CRABPII Y134K::R132K

Sequence BB 83

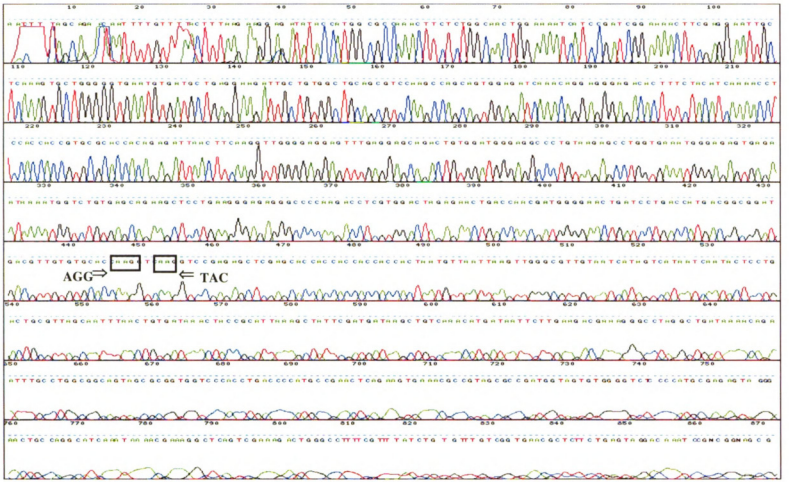

CRABPII Y134K::R132K

Fluorescence Titrations

Retinoic Acid

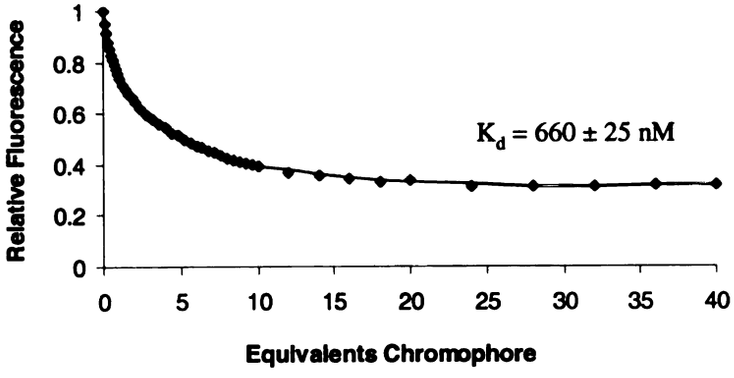

all-*trans*-Retinal

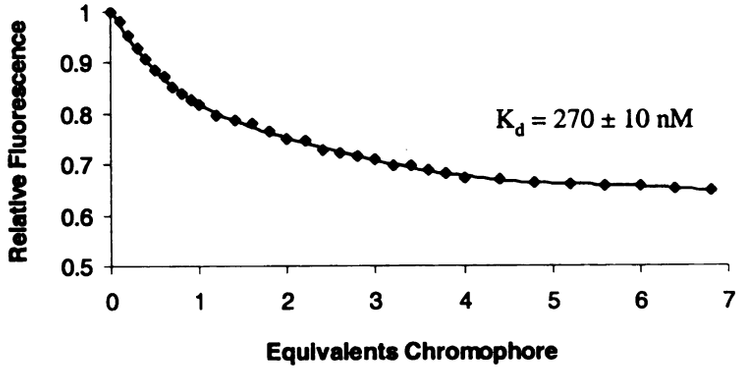

CRABPII Y134K::R132K

UV-vis Titrations, all-*trans*-Retinal

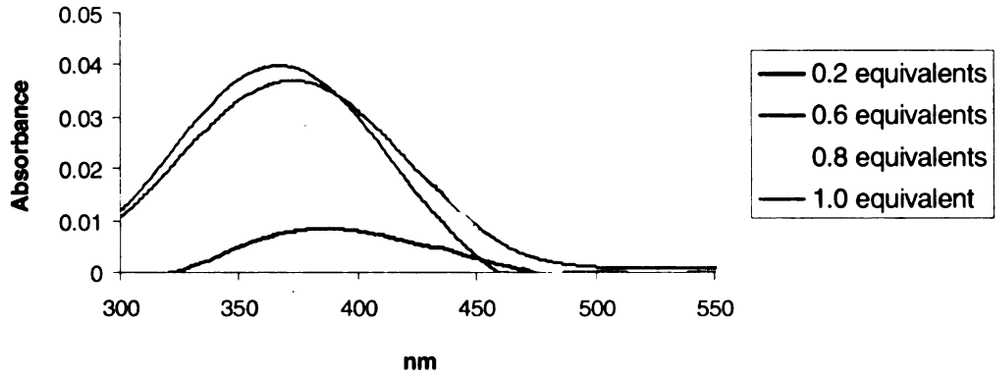

Uncorrected

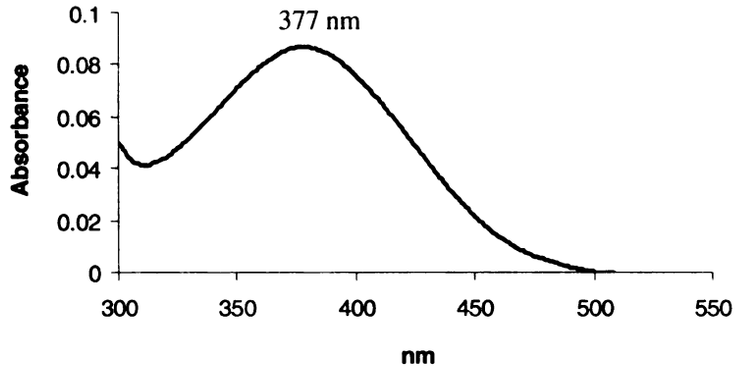

Corrected

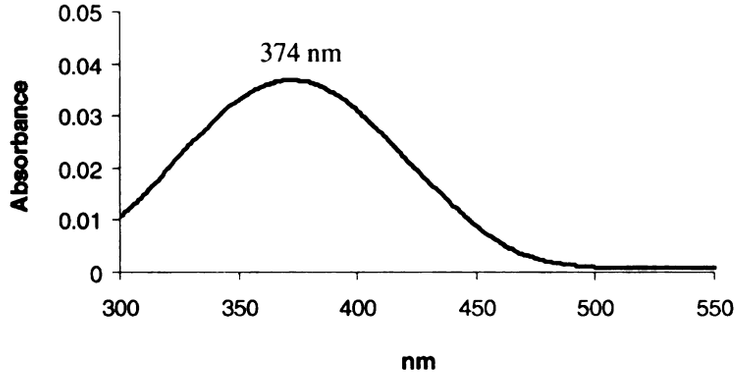

CRABPII Y134K::R132K

MALDI-TOF, Protein

Calculated Mass = 16766.20 Da

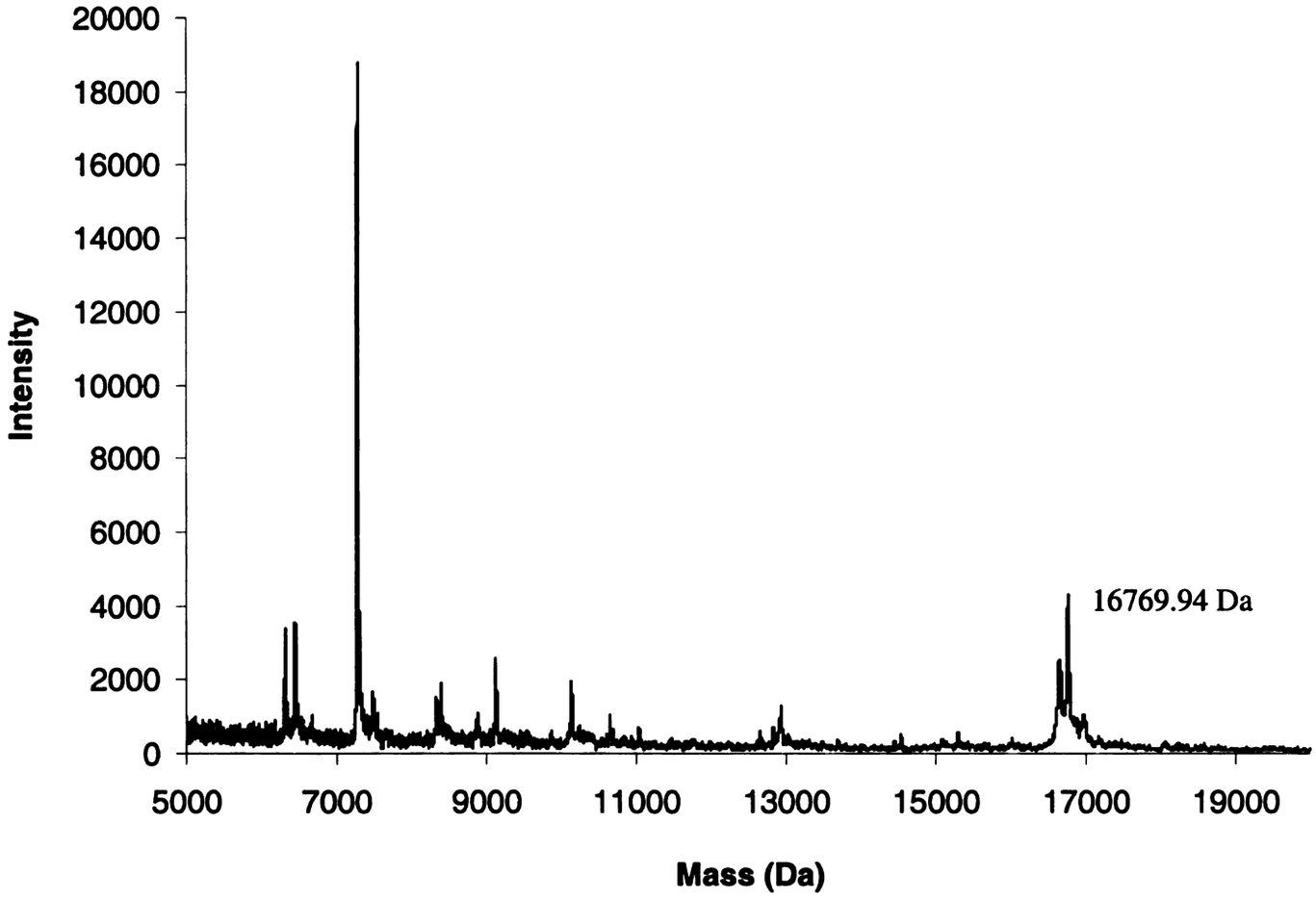

CRABPII Y134K::R132K

MALDI-TOF, Incubation with all-*trans*-Retinal

Protein Mass = 16766.20 Da

Positive Covalent Bond Formation = Protein Mass + 268

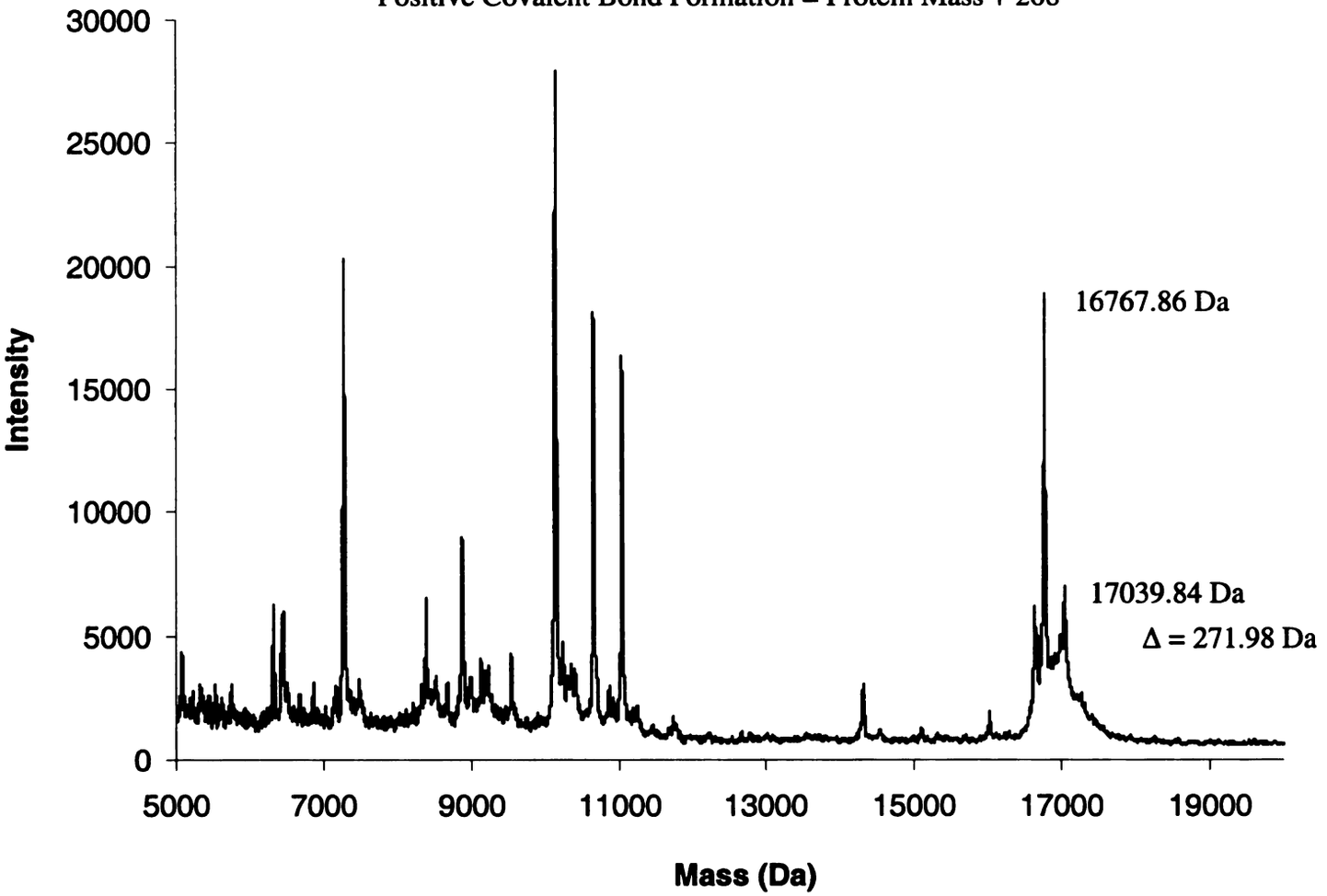

CRABPII Y134K::R132K

MALDI-TOF, Reductive Amination with all-*trans*-Retinal

Protein Mass = 16766.20 Da

Positive Reductive Amination = Protein Mass + 268

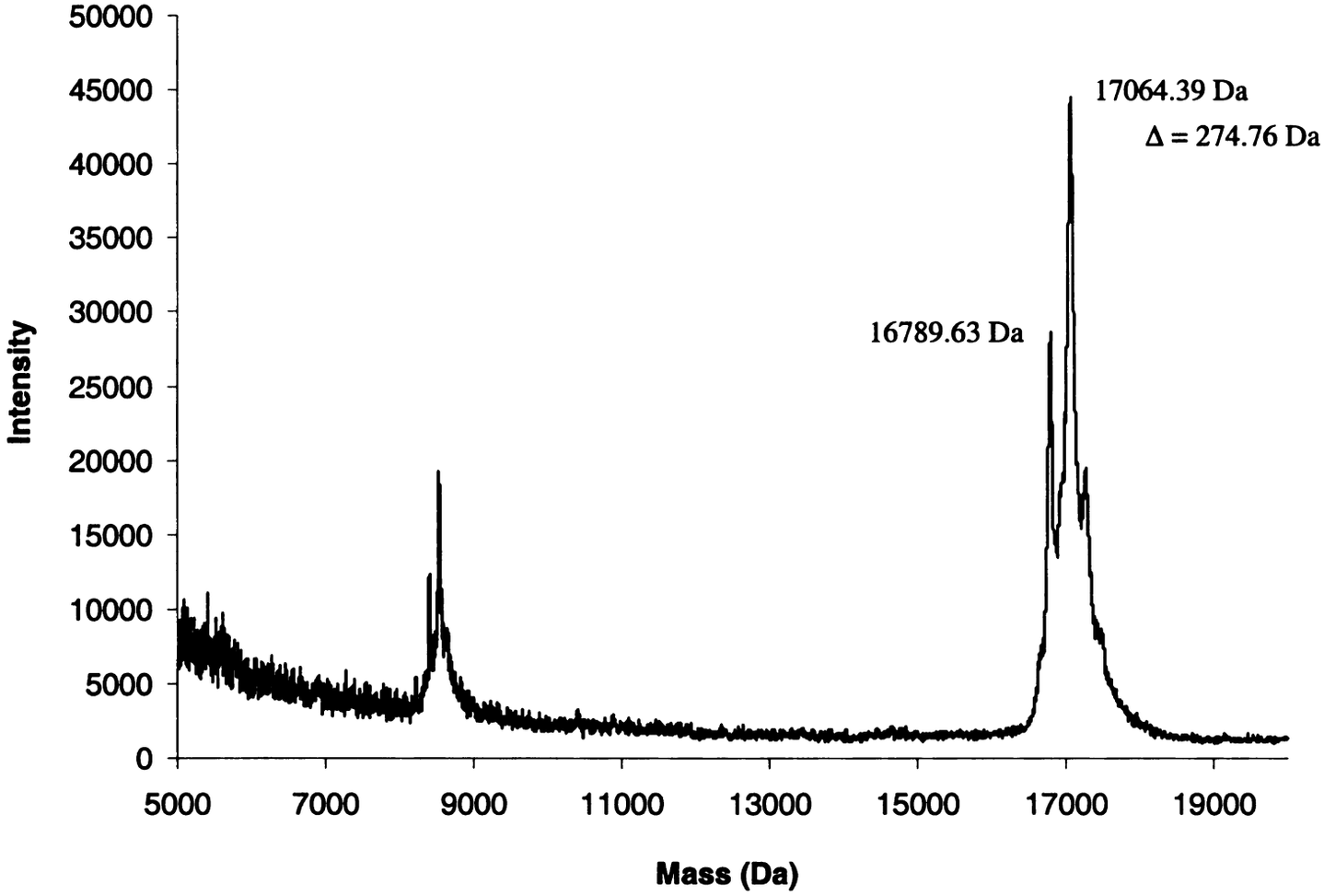

CRABPII Y134K::R132F

Molecular Weight :

16785.20 Da

Extinction Coefficient :

19,393 M^{-1} cm^{-1}

Primers :

bbb71 5' CGT TGT GTG CAC CTT CGT CAA GGT CCG

bbb75 5' CGG ACC TTG ACG AAG GTG CAC ACA ACG

CD

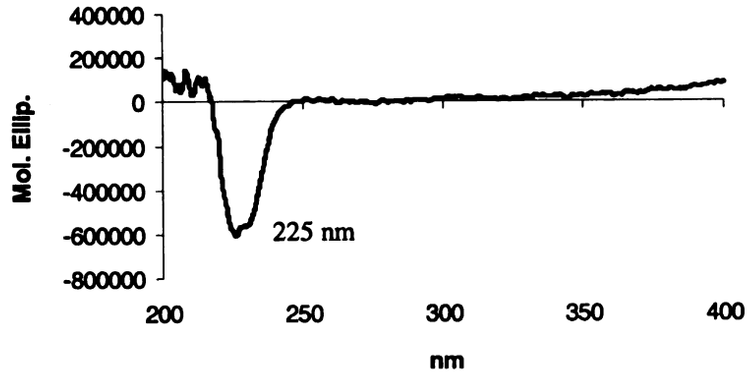

CRABPII Y134K::R132F

Sequence BB 60

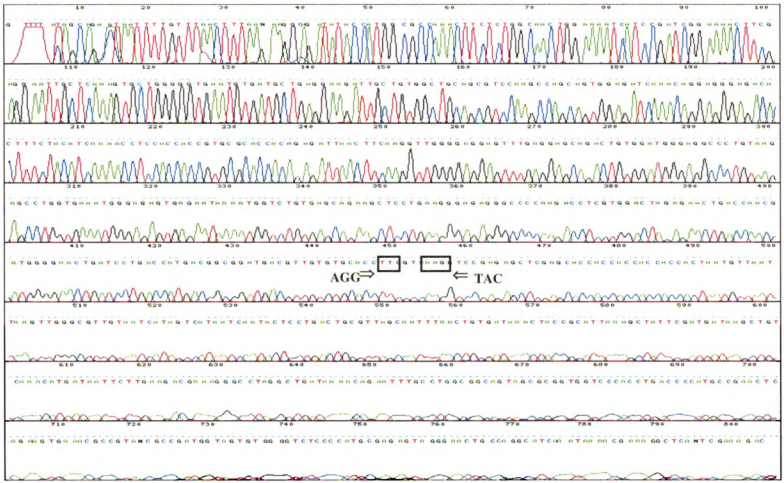

CRABPII Y134K::R132F

Fluorescence Titrations

Retinoic Acid

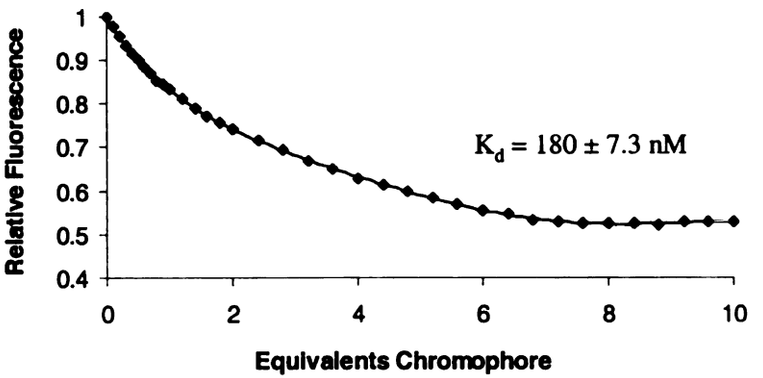

all-*trans*-Retinal

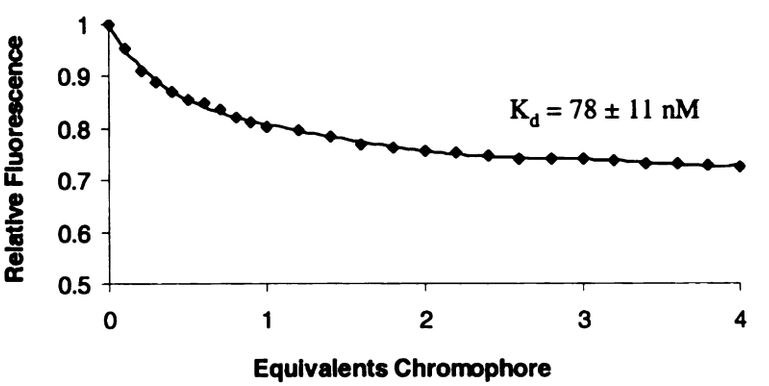

CRABPII Y134K::R132F

UV-vis Titrations, all-*trans*-Retinal

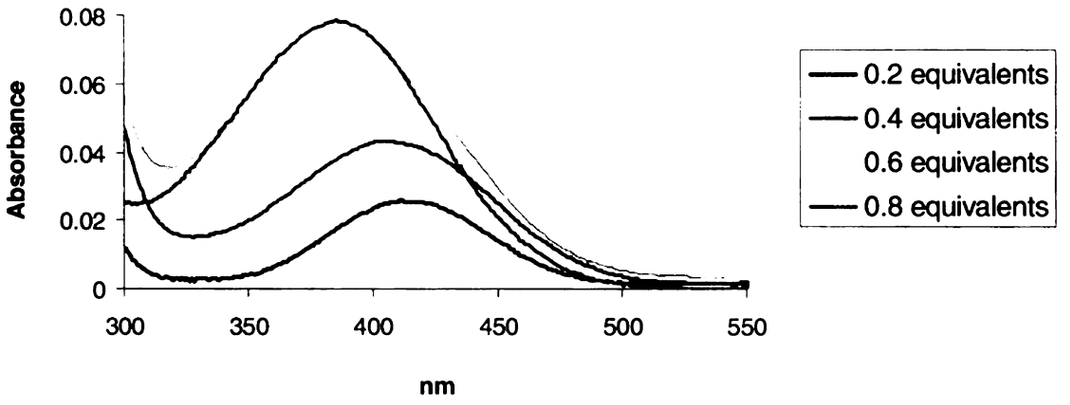

Uncorrected

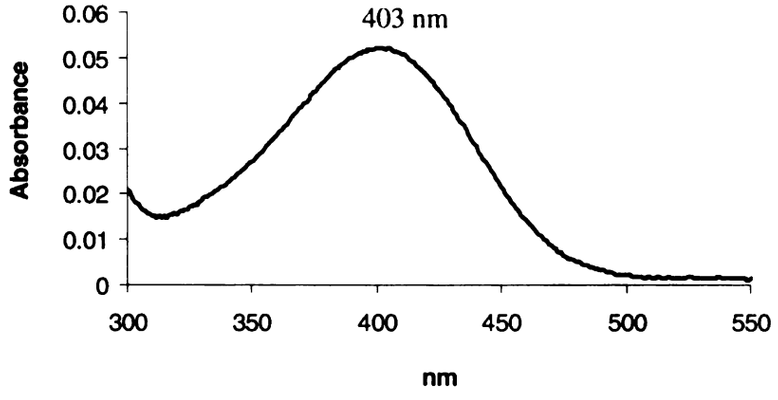

Corrected

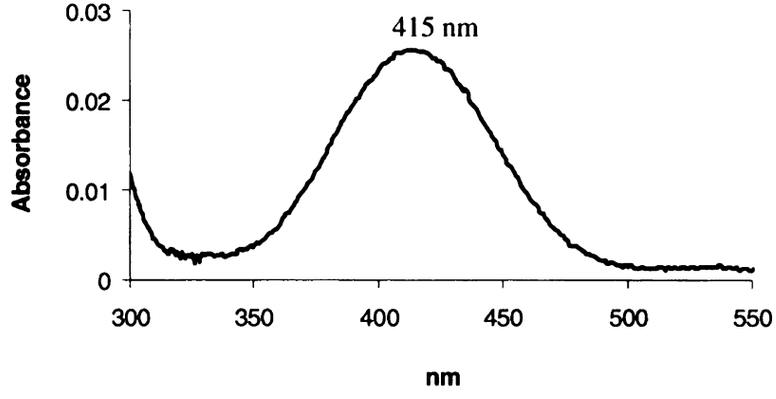

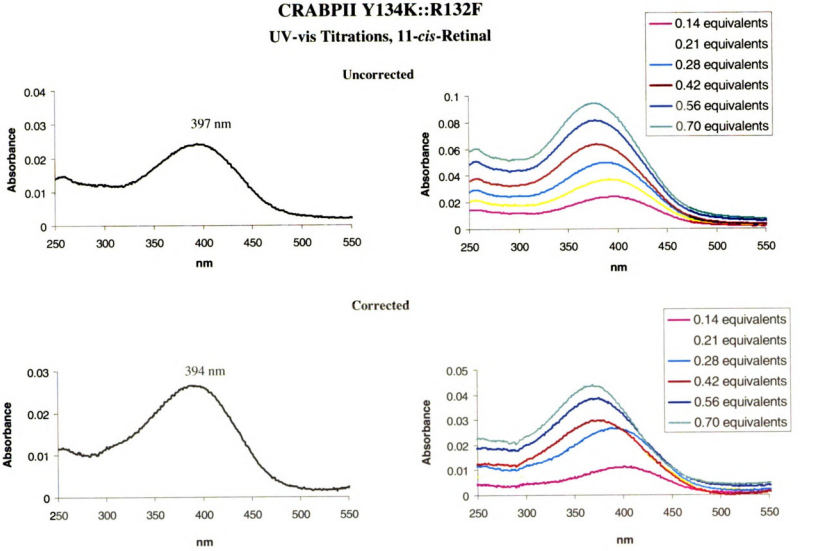
CRABPII Y134K::R132F
UV-vis Titrations, 11-cis-Retinal
Uncorrected
397 nm
Absorbance
nm
0.14 equivalents
0.21 equivalents
0.28 equivalents
0.42 equivalents
0.56 equivalents
0.70 equivalents
Corrected
394 nm
Absorbance
nm
0.14 equivalents
0.21 equivalents
0.28 equivalents
0.42 equivalents
0.56 equivalents
0.70 equivalents

CRABPII Y134K::R132F

MALDI-TOF, Protein

Calculated Mass = 16785.20 Da

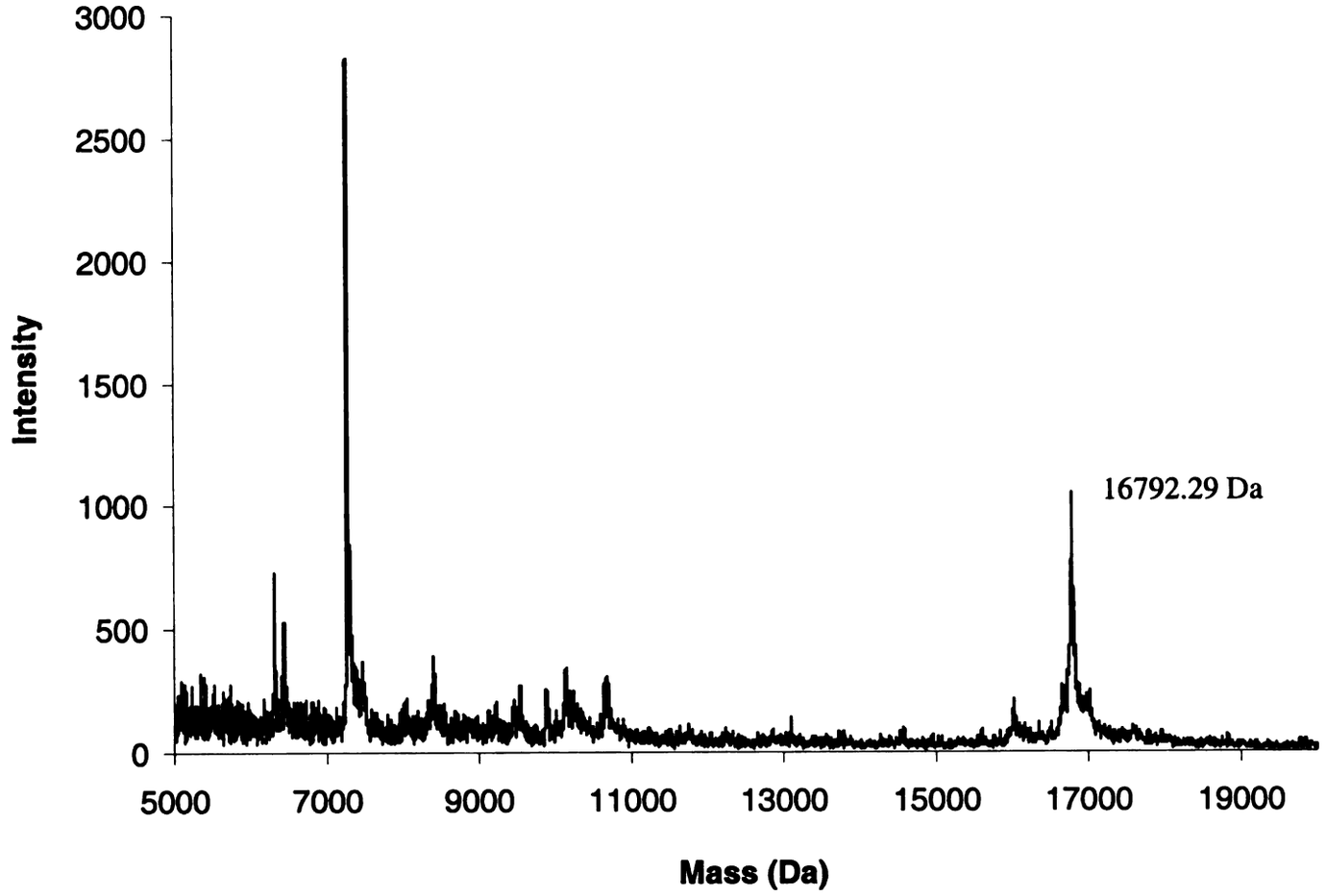

CRABPII Y134K::R132F

MALDI-TOF, Incubation with all-*trans*-Retinal

Protein Mass = 16785.20 Da

Positive Covalent Bond Formation = Protein Mass + 268

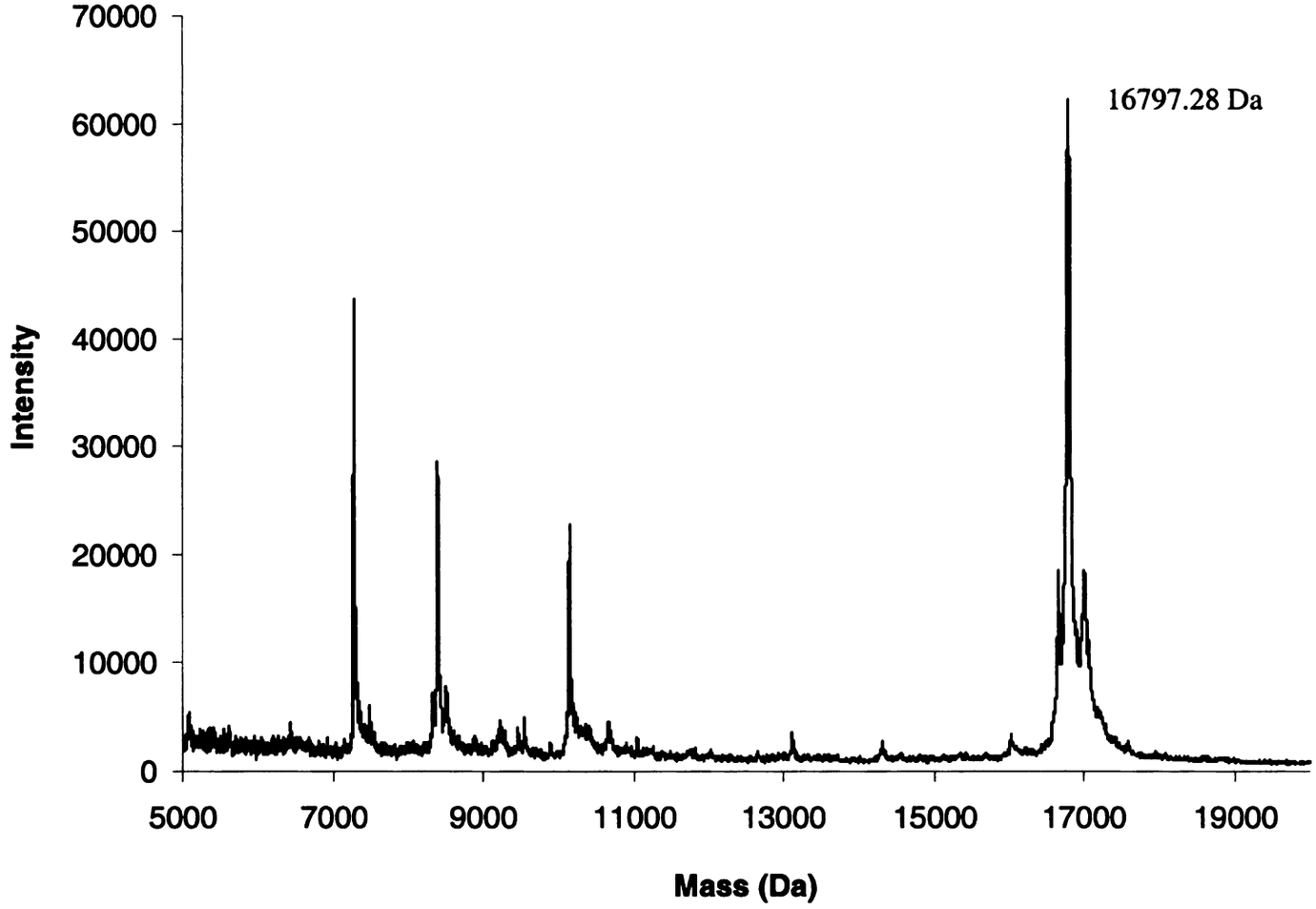

CRABPII Y134K::R132F

MALDI-TOF, Reductive Amination with all-*trans*-Retinal

Protein Mass = 16785.20 Da

Positive Reductive Amination = Protein Mass + 268

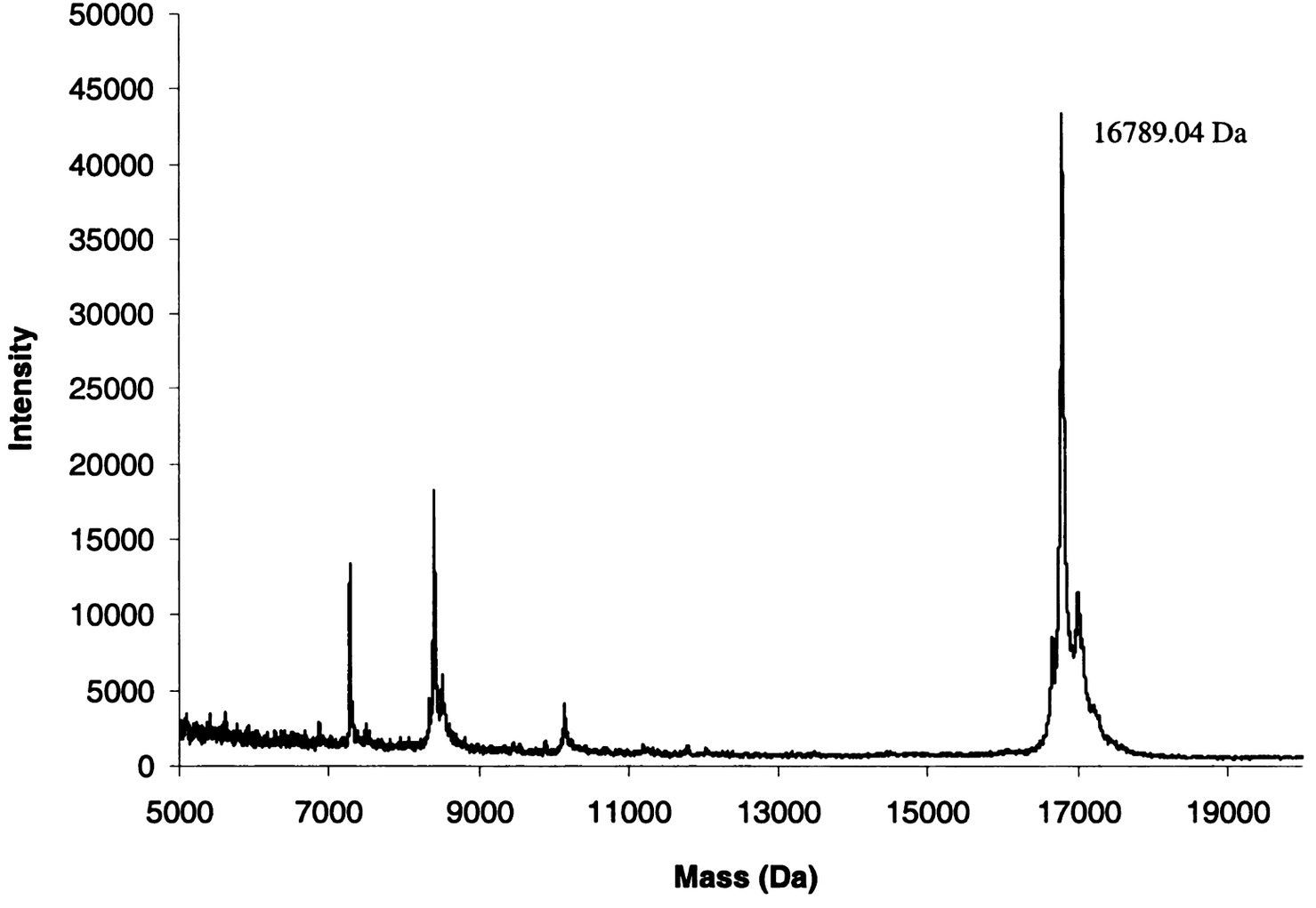

CRABPII Y134K::R132L

Molecular Weight :
16751.18 Da

Extinction Coefficient :
18,697 M^{-1} cm^{-1}

Primers :
bbb69 5' CGT TGT GTG CAC CCT GGT CAA GGT CCG
bbb70 5' CGG ACC TTC ACC AGG GTG CAC ACA ACG

CD

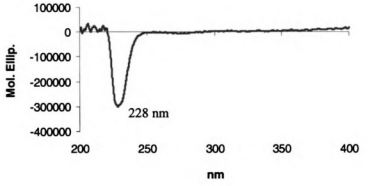

CRABPII Y134K::R132L

Sequence BB 176

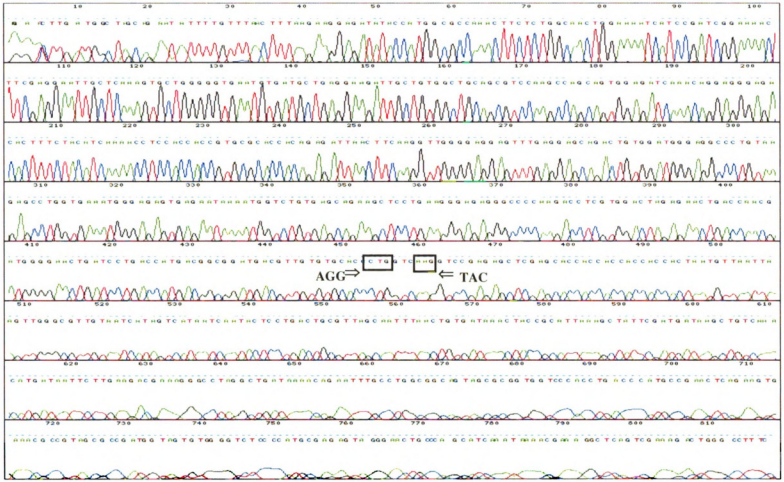

CRABPII Y134K::R132L

Fluorescence Titrations

Retinoic Acid

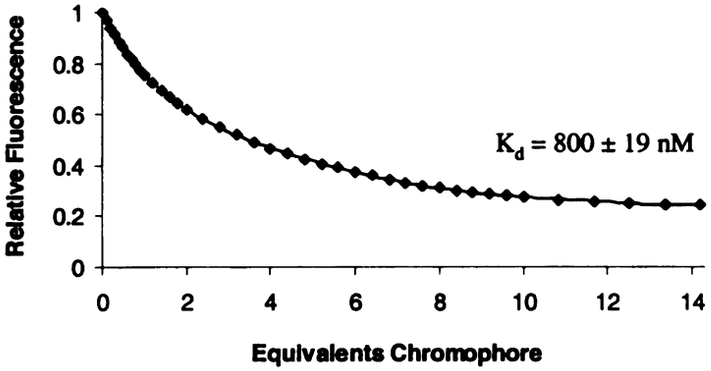

all-*trans*-Retinal

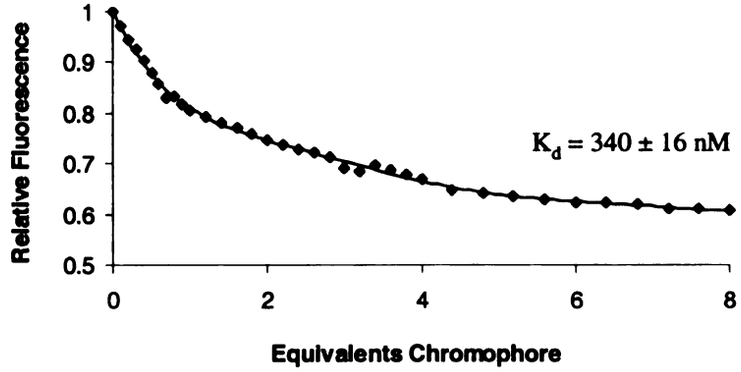

CRABPII Y134K::R132L

UV-vis Titrations, all-*trans*-Retinal

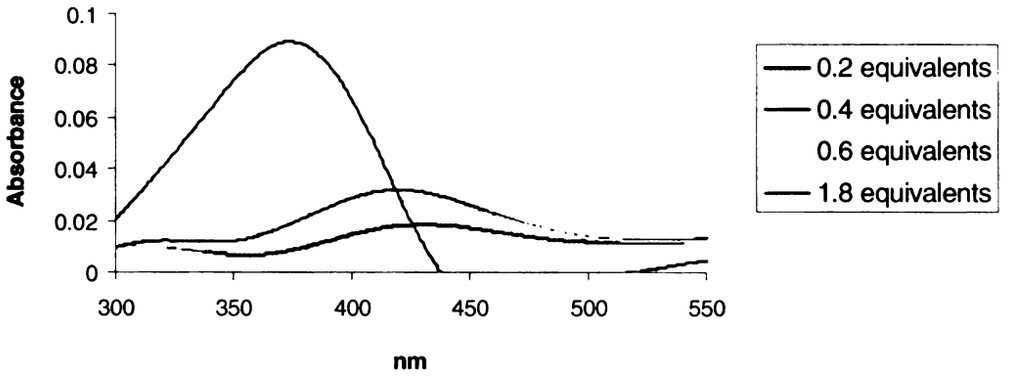

Uncorrected

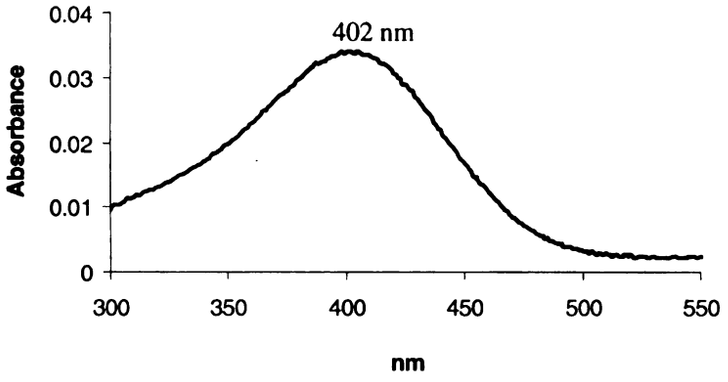

Corrected

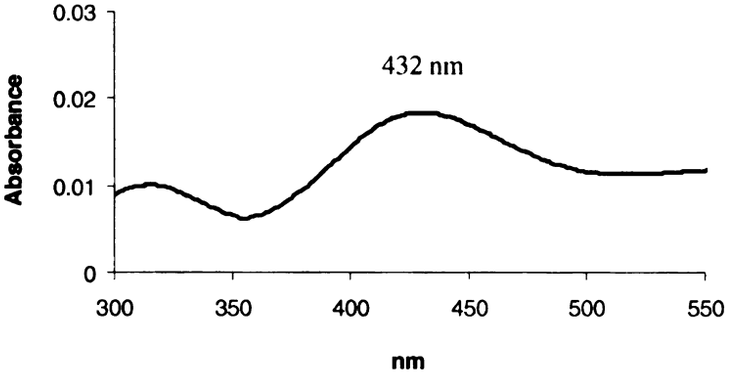

CRABPII Y134K::R132L
MALDI-TOF, Protein
Calculated Mass = 16751.18 Da

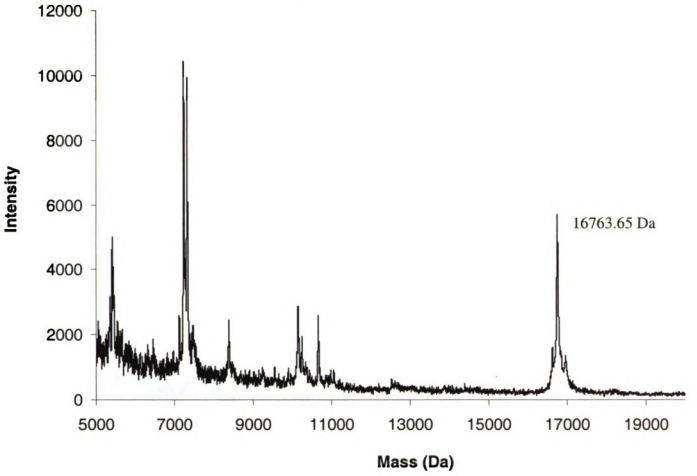

CRABPII Y134K::R132L

MALDI-TOF, Incubation with all-*trans*-Retinal

Protein Mass = 16751.18 Da

Positive Covalent Bond Formation = Protein Mass + 268

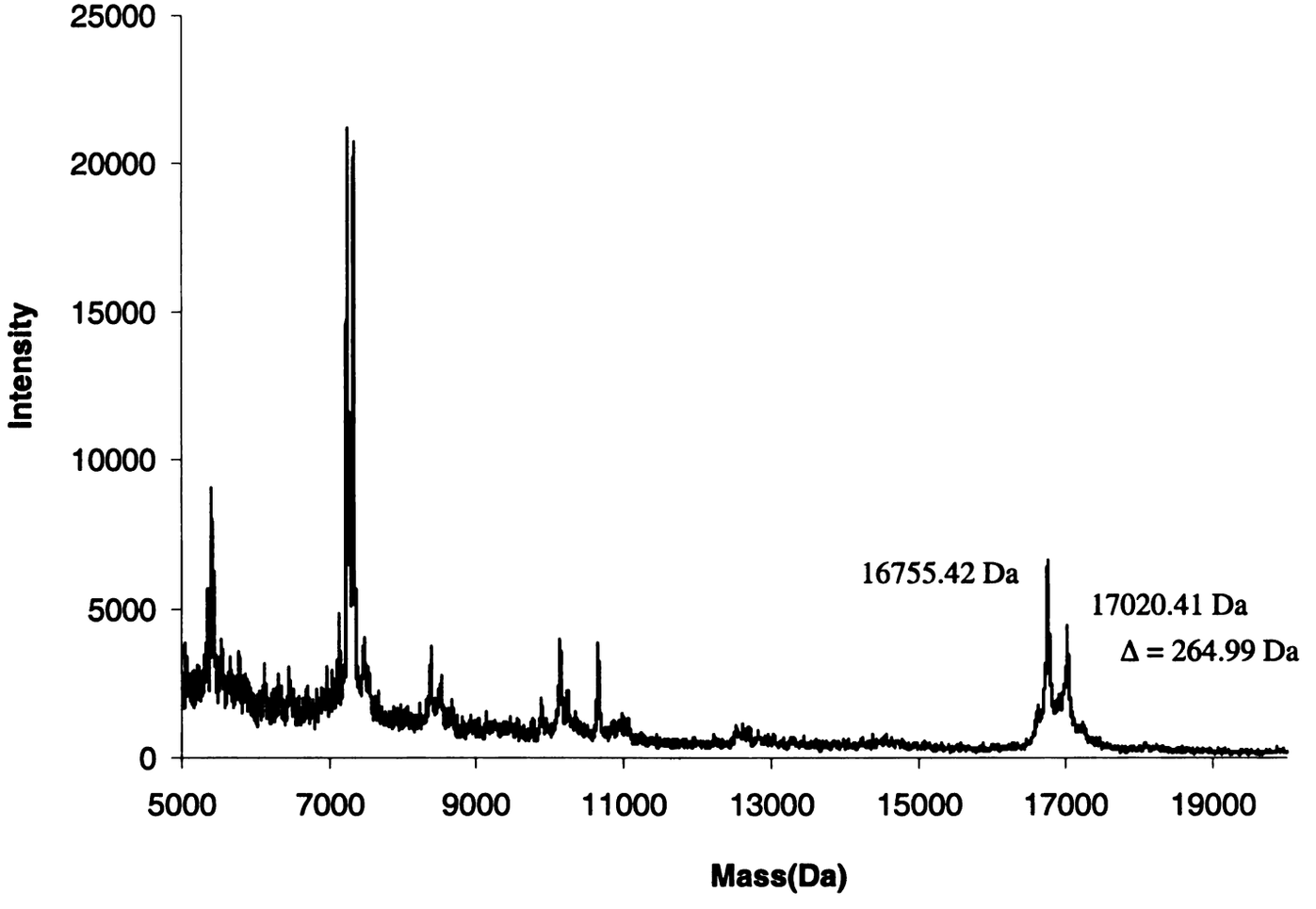

CRABPII Y134K::R132L

MALDI-TOF, Reductive Amination with all-*trans*-Retinal

Protein Mass = 16751.18 Da

Positive Reductive Amination = Protein Mass + 268

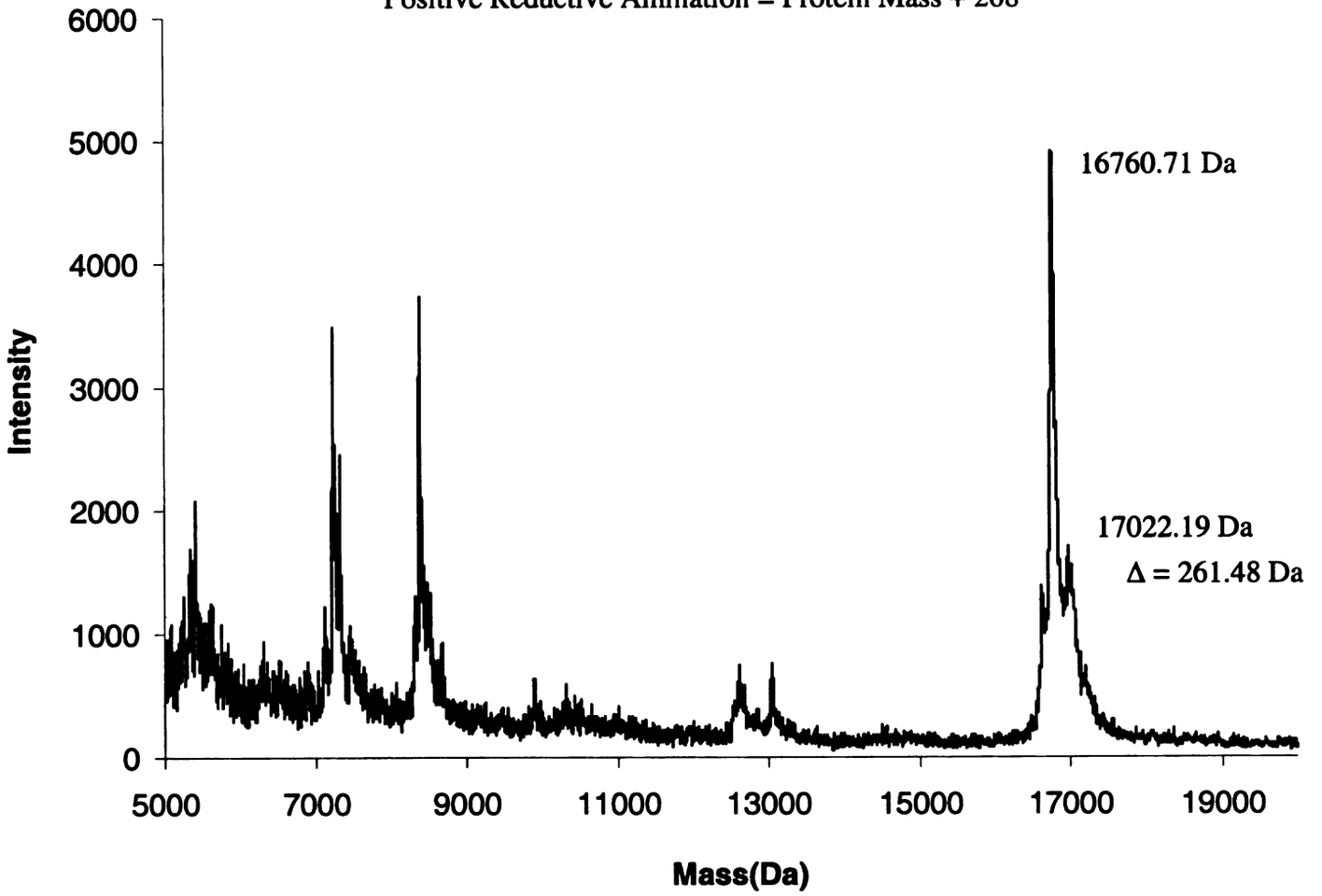

CRABPII Y134K::R132F::R111L

Molecular Weight :

16742.17 Da

Extinction Coefficient :

18,056 M^{-1} cm^{-1}

Primers :

bbb39 5' CCC AAG ACC TCG TGG ACC CTG GAA CTG ACC AAC GAT GGG

bbb40 5' CCC ATC GTT GGT CAG TTG CAG GGT CCA CGA GGT CTT GGG

CD

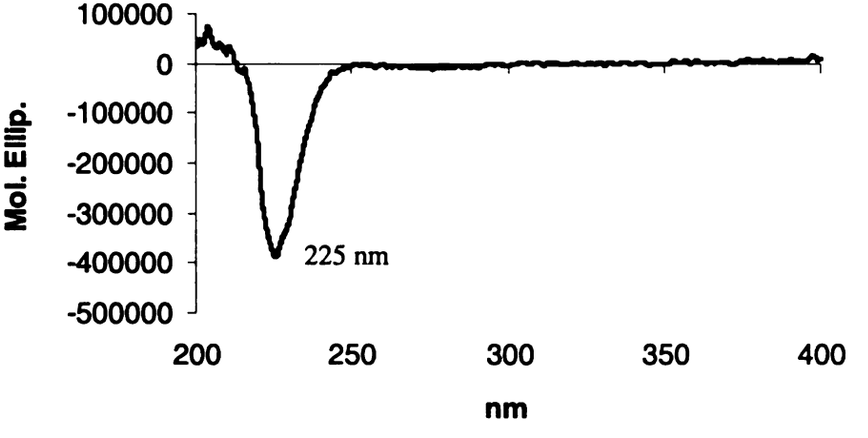

CRABPII Y134K::R132F::R111L

Sequence BB 109

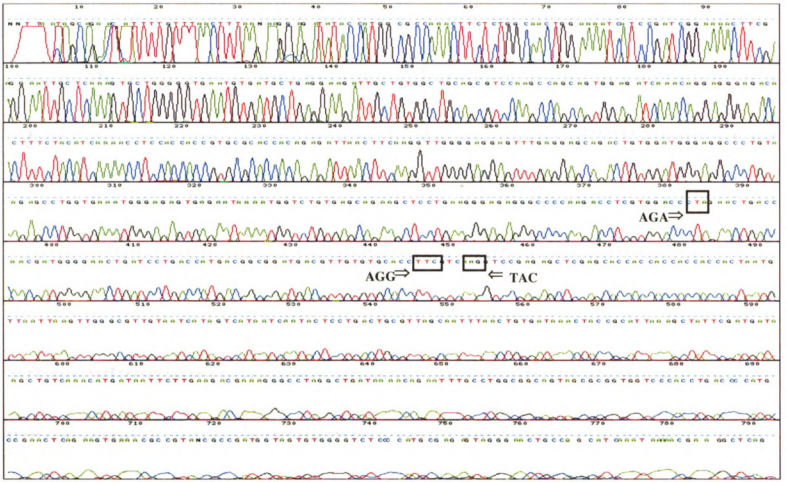

CRABPII Y134K::R132F::R111L

Fluorescence Titrations

Retinoic Acid

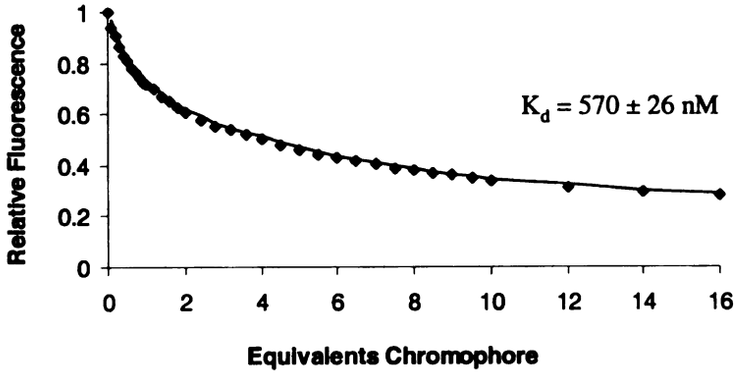

all-*trans*-Retinal

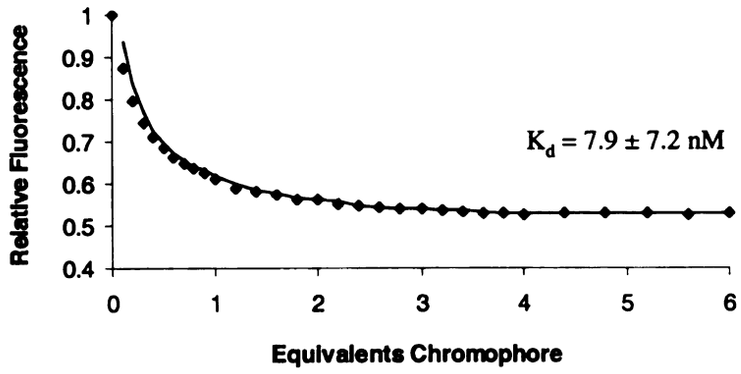

CRABPII Y134K::R132F::R111L

UV-vis Titrations, all-*trans*-Retinal

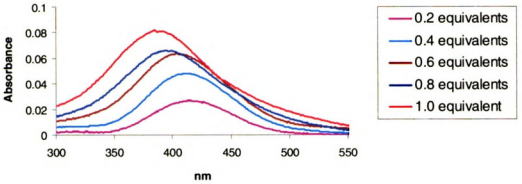

Uncorrected

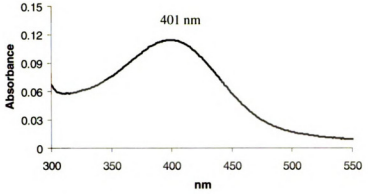

Corrected

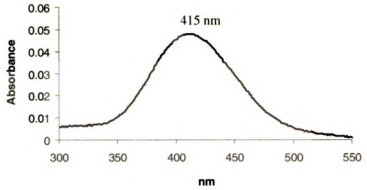

CRABPII Y134K::R132F::R111L

MALDI-TOF, Protein

Calculated Mass = 16742.17 Da

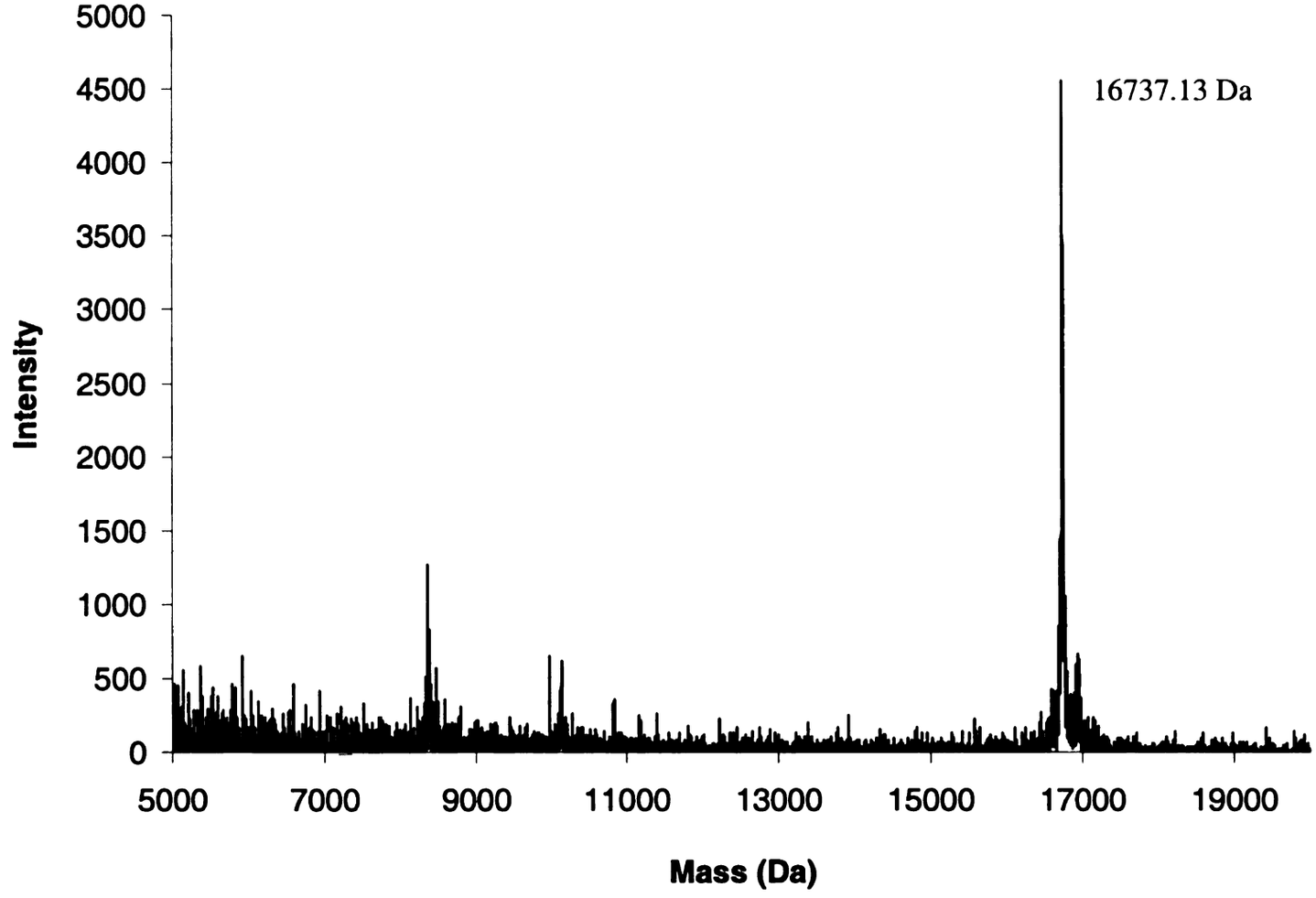

CRABPII Y134K::R132F::R111L

MALDI-TOF, Incubation with all-*trans*-Retinal

Protein Mass = 16742.17 Da

Positive Covalent Bond Formation = Protein Mass + 268

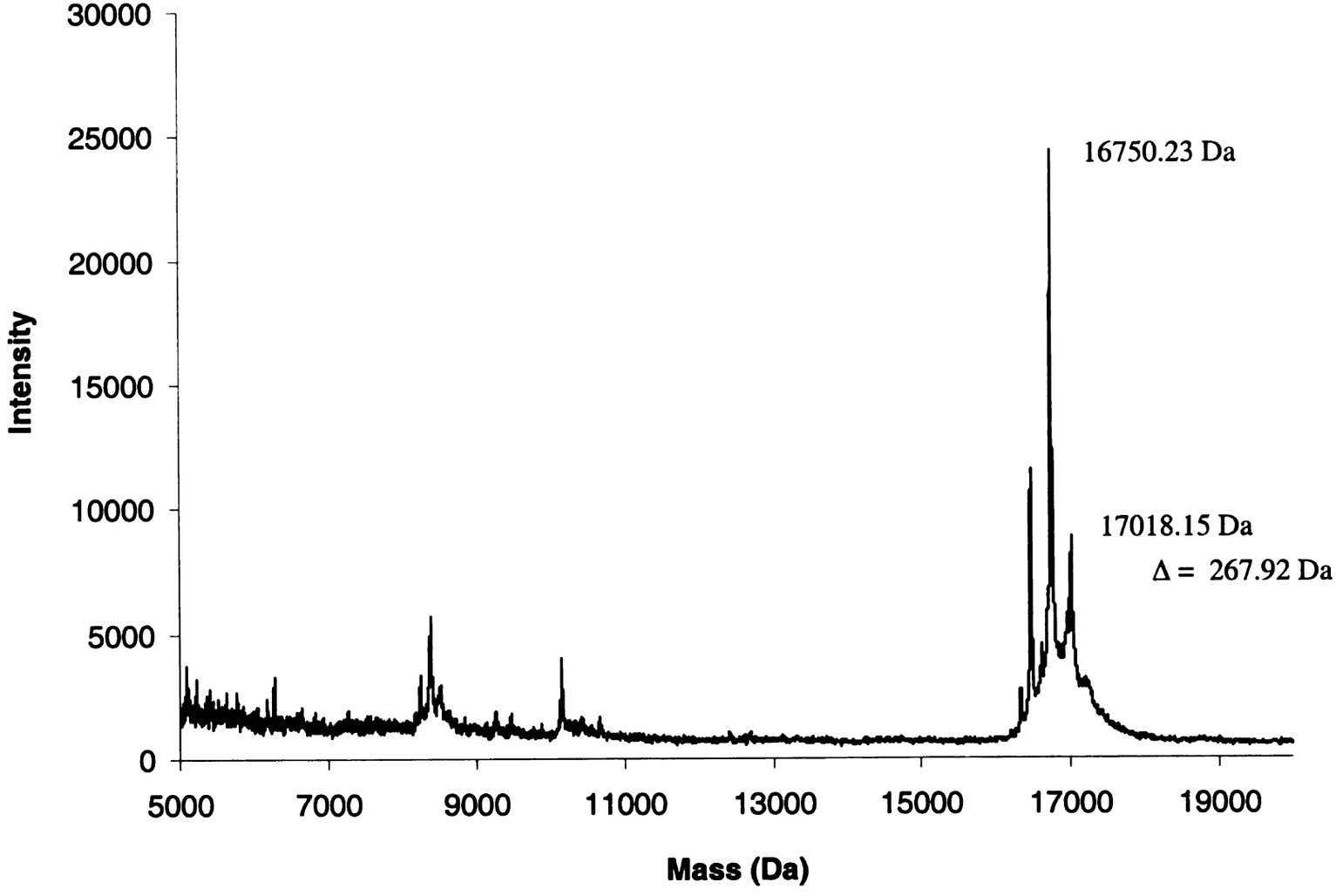

CRABPII Y134K::R132F::R111L

MALDI-TOF, Reductive Amination with all-*trans*-Retinal

Protein Mass = 16742.17 Da

Positive Reductive Amination = Protein Mass + 268

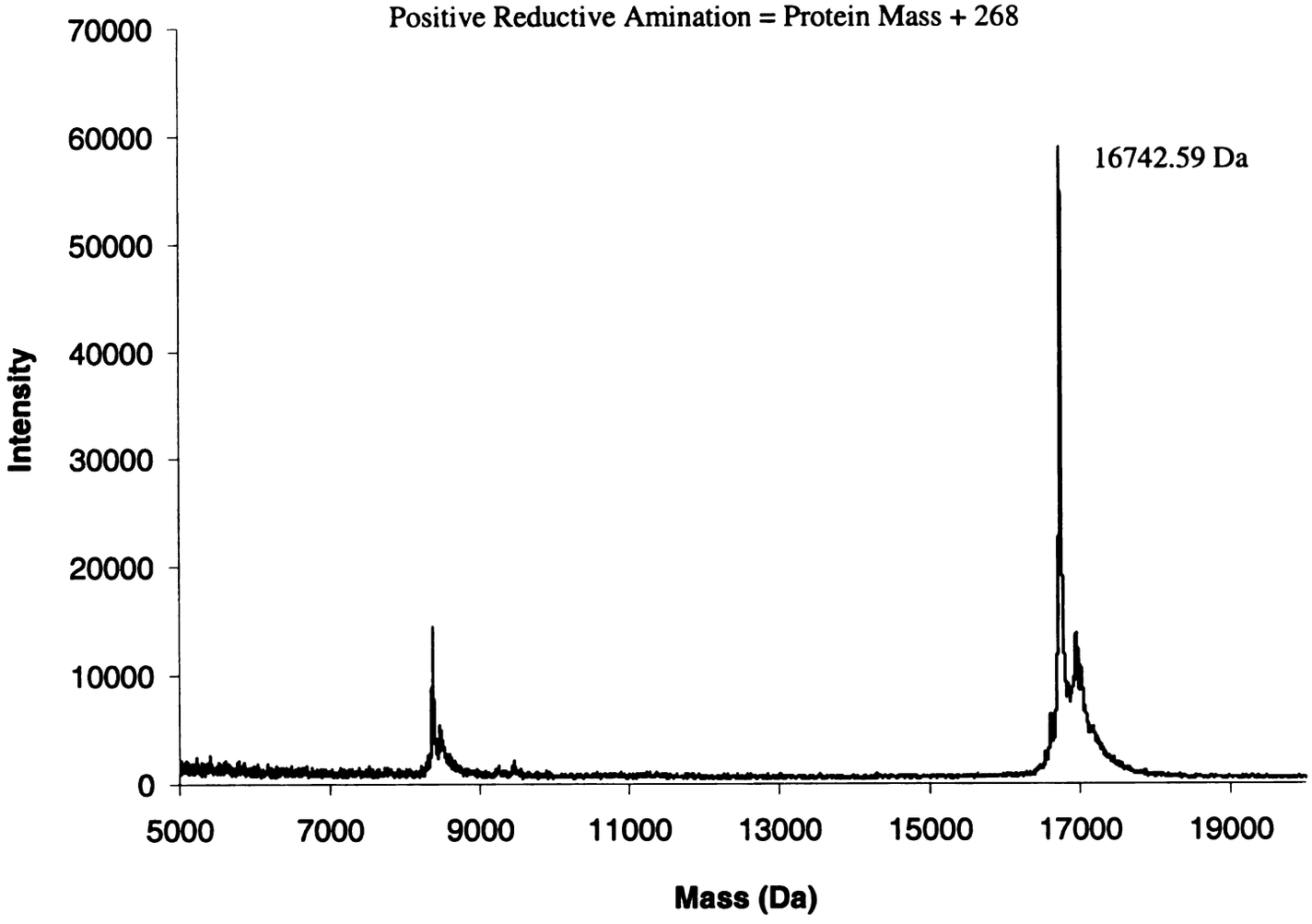

CRABPII Y134K::R132F::R111L::L121E

Molecular Weight :

16758.13 Da

Extinction Coefficient :

20,200 M^{-1} cm^{-1}

Primers :

bbb37 5' CGT TGT GTG CAC CCT GGT CTT CGT CCG
bbb38 5' CGG ACG AAG ACC AGG GTG CAC ACA ACG

CD

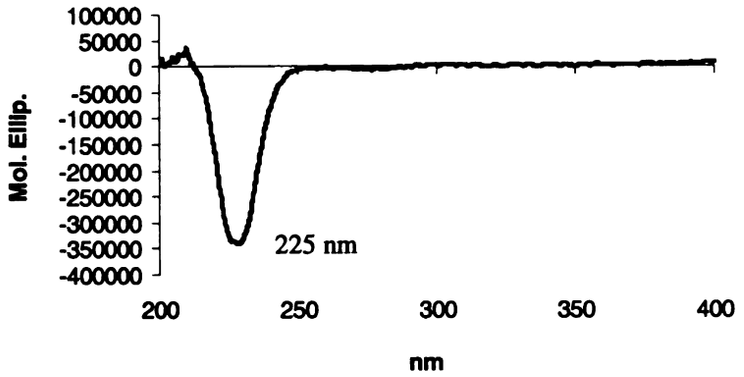

CRABPII Y134K::R132F::R111L::L121E

Sequence BB 177

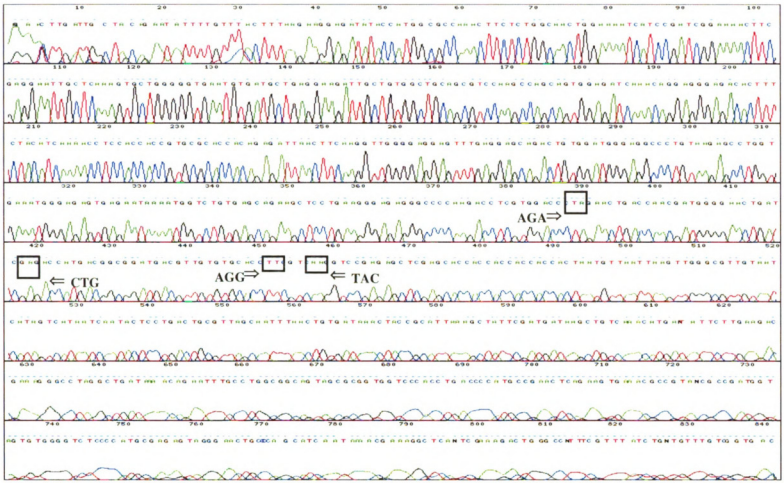

CRABPII Y134K::R132F::R111L::L121E

Fluorescence Titrations

Retinoic Acid

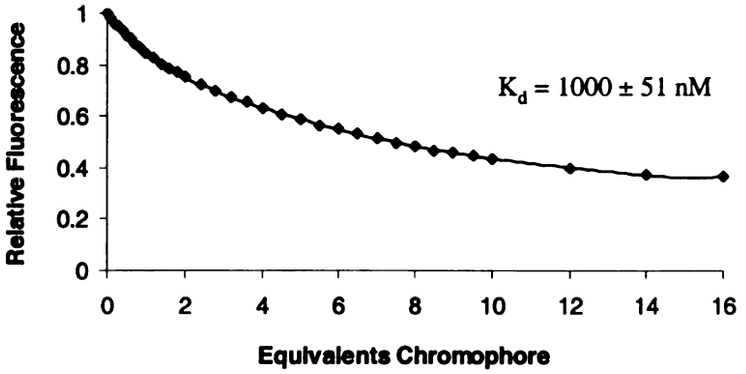

all-*trans*-Retinal

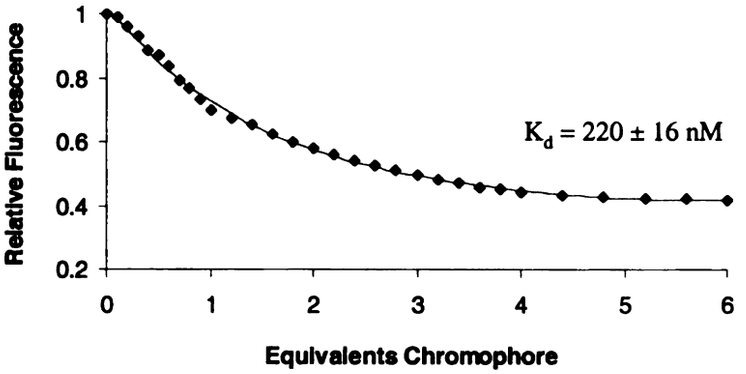

CRABPII Y134K::R132F::R111L::L121E

UV-vis Titrations, all-*trans*-Retinal

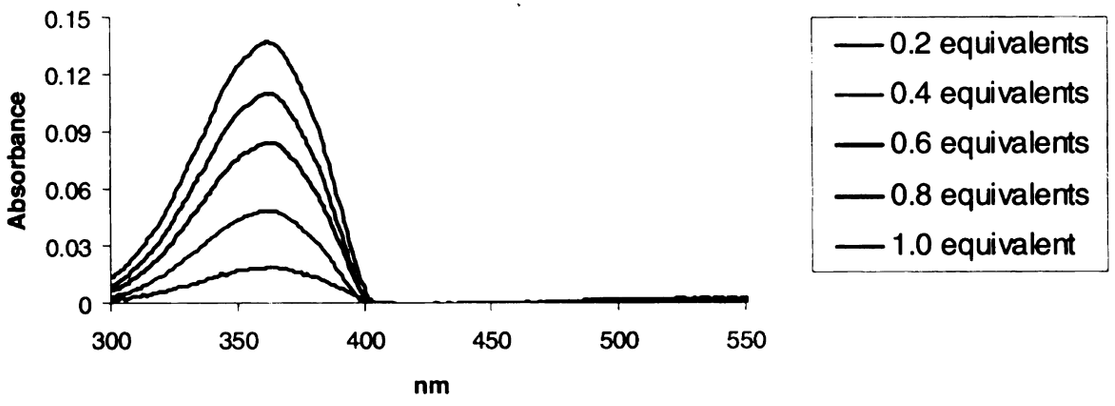

Uncorrected

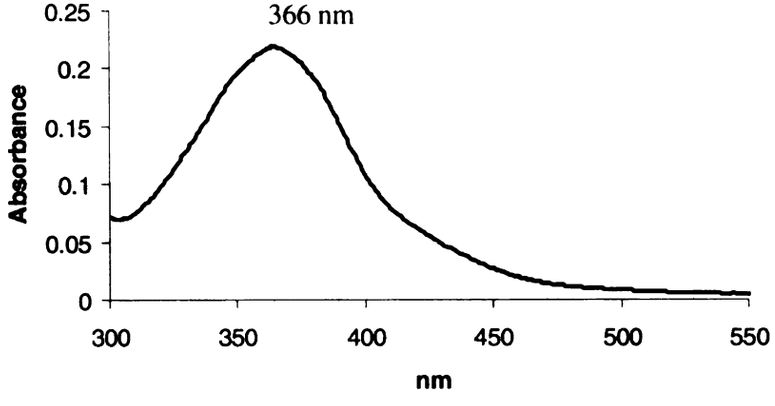

Corrected

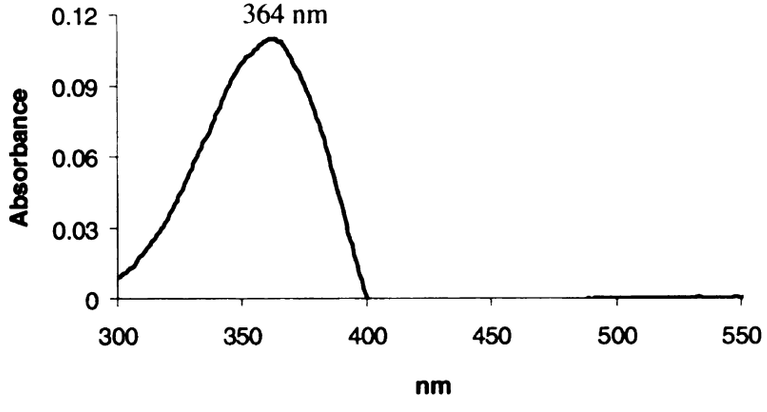

CRABPII Y134K::R132F::R111L::L121E

UV-vis Titrations, 11-*cis*-Retinal

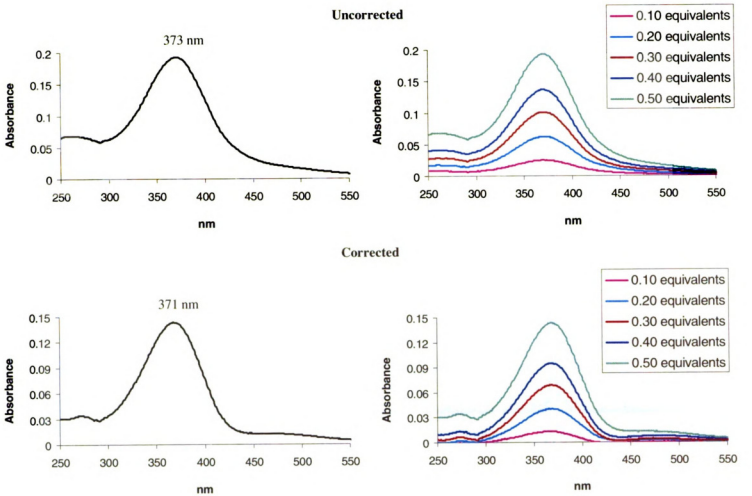

CRABPII Y134K::R132F::R111L::L121E

MALDI-TOF, Protein

Calculated Mass = 16758.13 Da

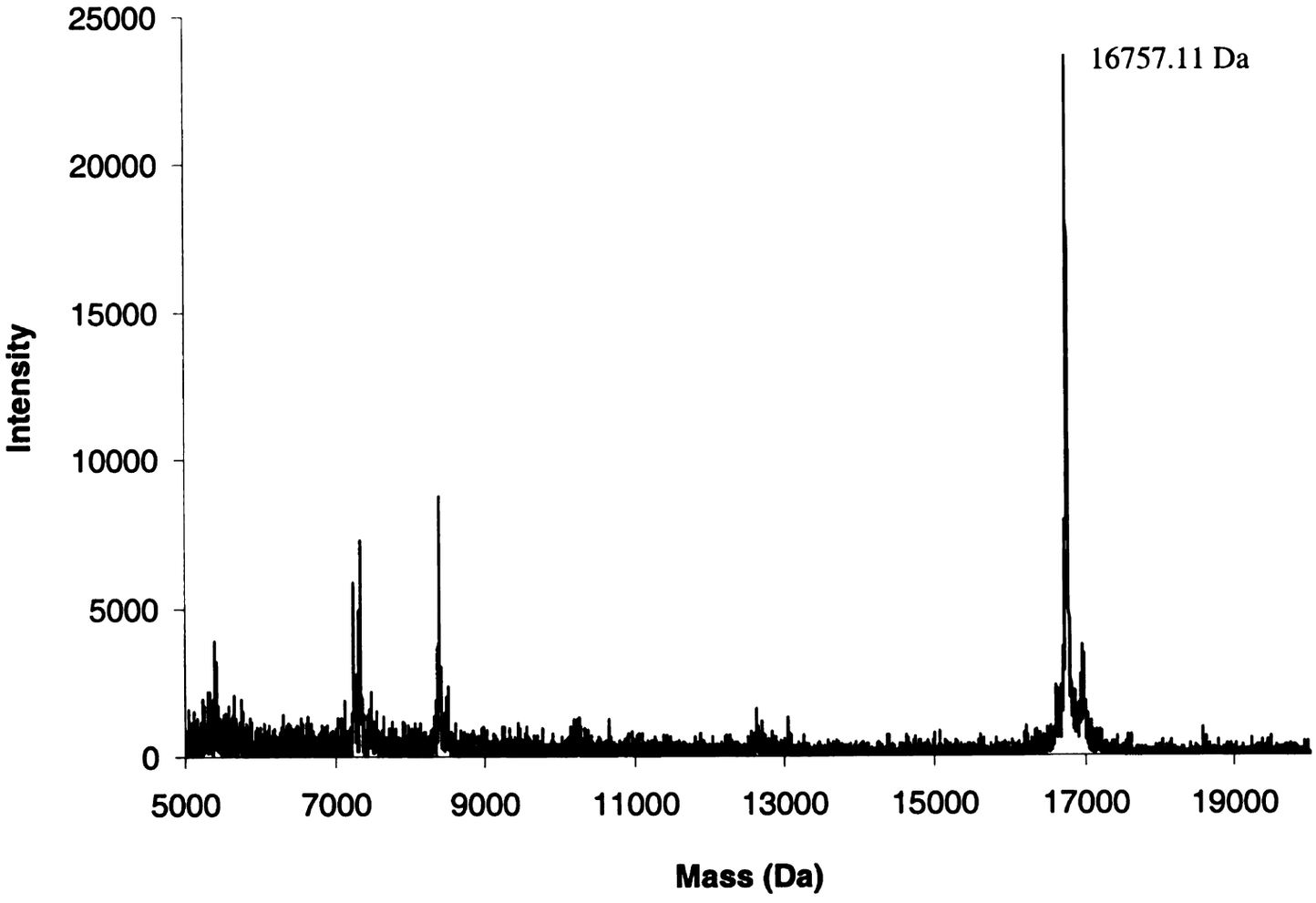

CRABPII Y134K::R132F::R111L::L121E

MALDI-TOF, Incubation with all-*trans*-Retinal

Protein Mass = 16758.13 Da

Positive Covalent Bond Formation = Protein Mass + 268

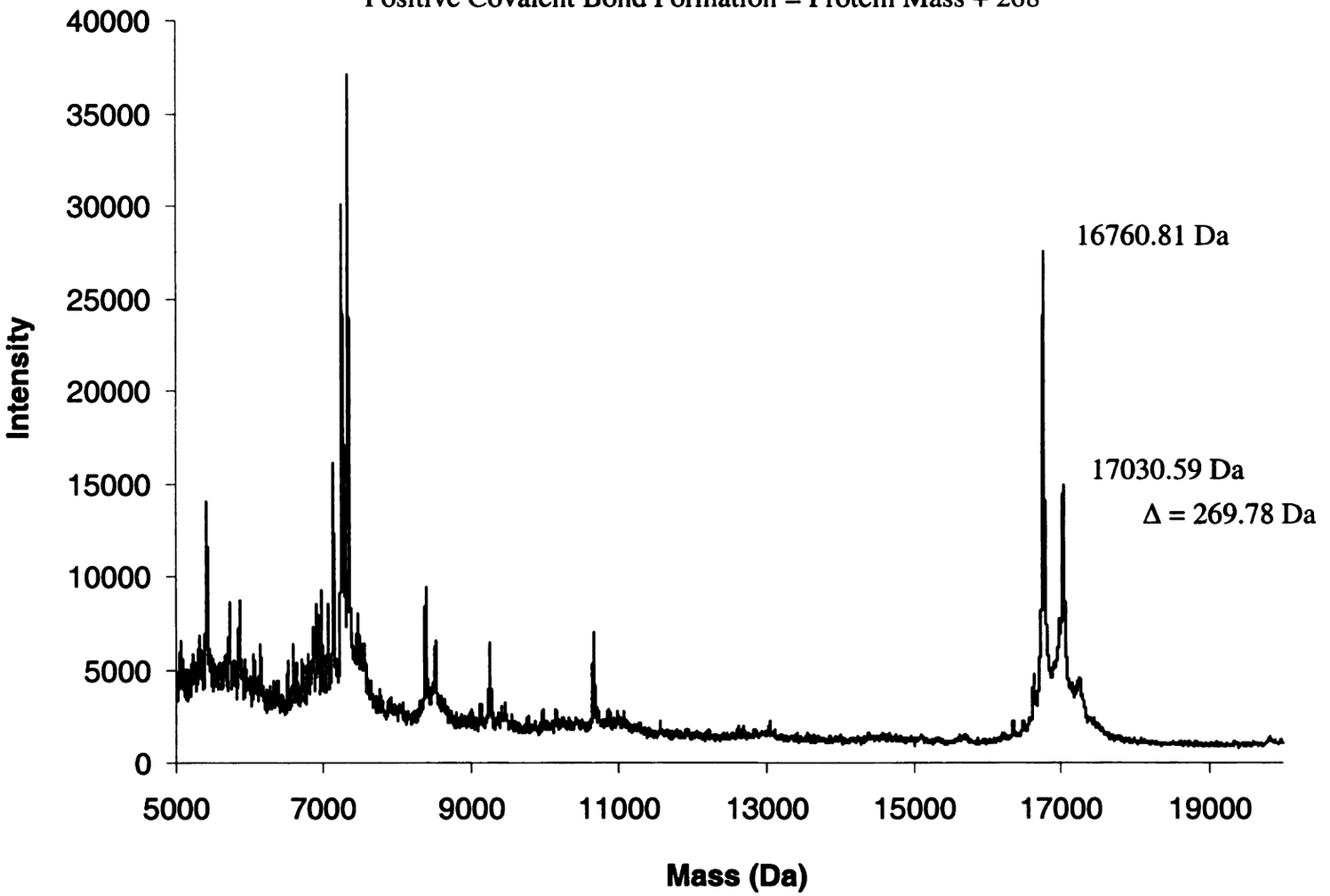

CRABPII Y134K::R132F::R111L::L121E

MALDI-TOF, Reductive Amination with all-*trans*-Retinal

Protein Mass = 16758.13 Da

Positive Reductive Amination = Protein Mass + 268

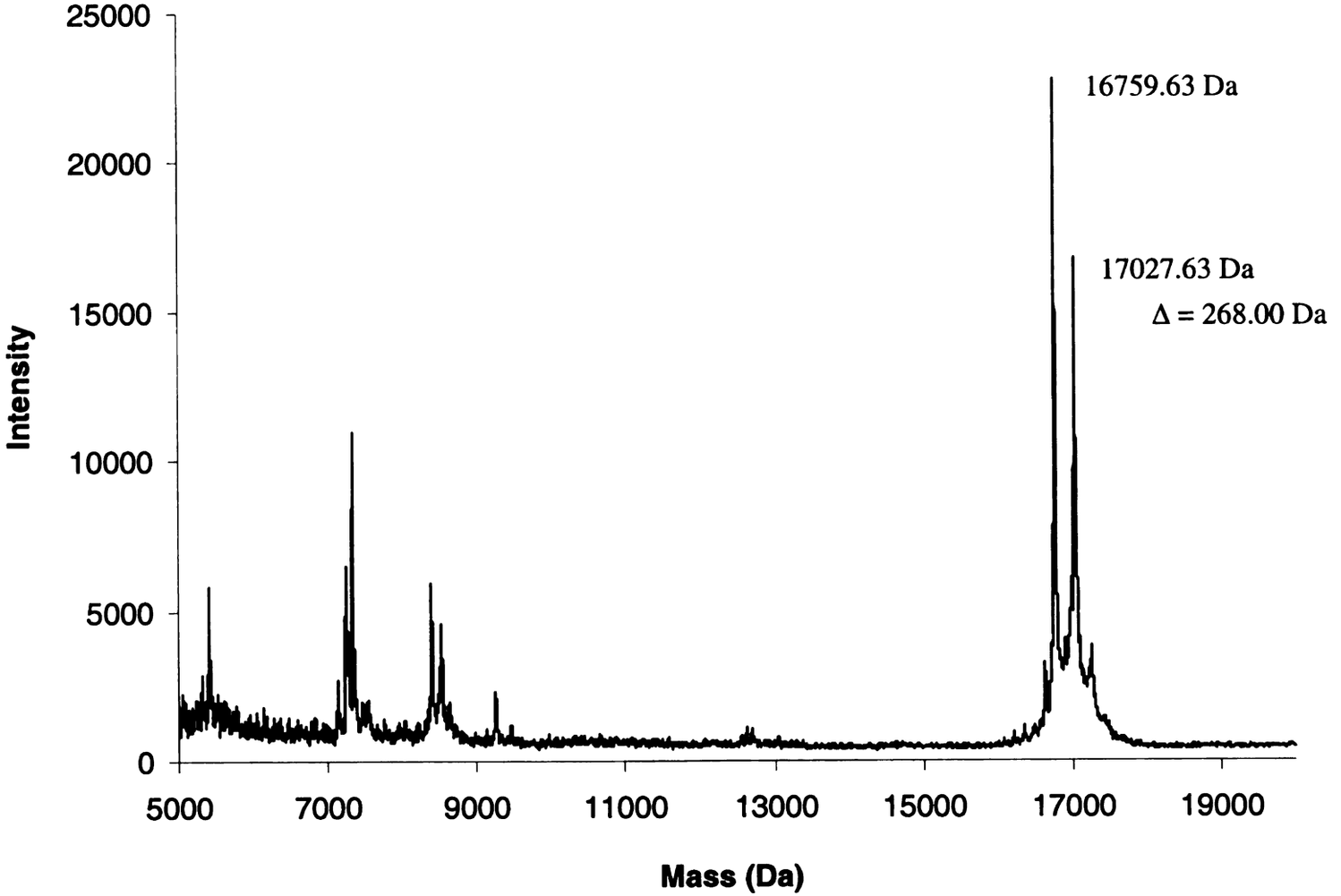

CRABPII Y134K::R132F::R111L::T54E

Molecular Weight :

16770.18 Da

Extinction Coefficient :

21,110 M^{-1} cm^{-1}

Primers :

bbb65 5' CTA CAT CAA AGA GTC CAC CAC CGT GCG

bbb66 5' CGC ACG GTG GTG GAC TCT TTG ATG TAG

CD

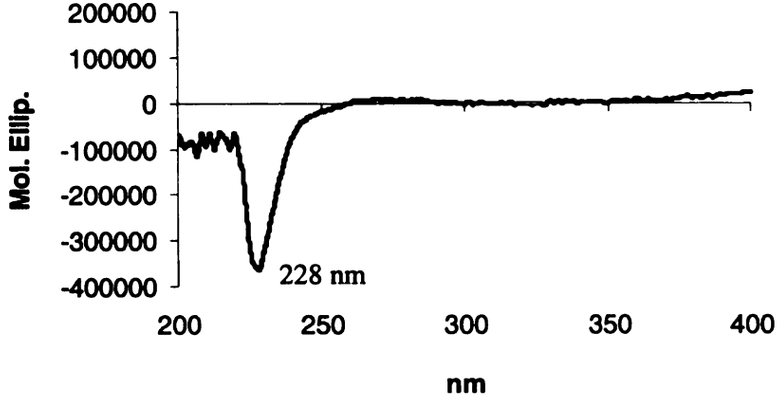

CRABPII Y134K::R132F::R111L::T54E

Sequence BB 179

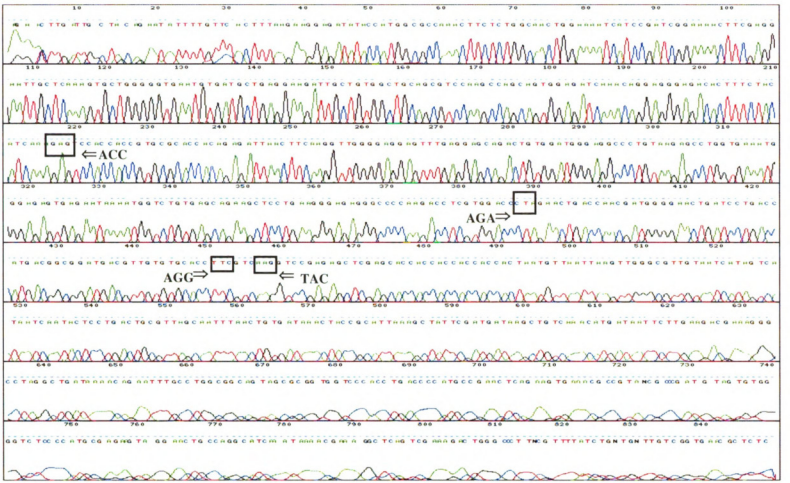

CRABPII Y134K::R132F::R111L::T54E

Fluorescence Titrations

Retinoic Acid

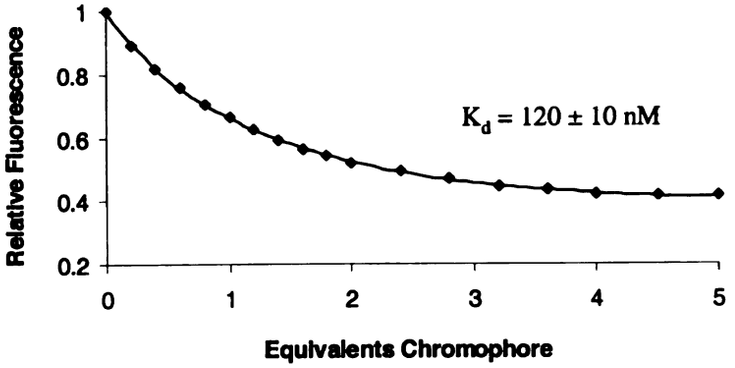

all-*trans*-Retinal

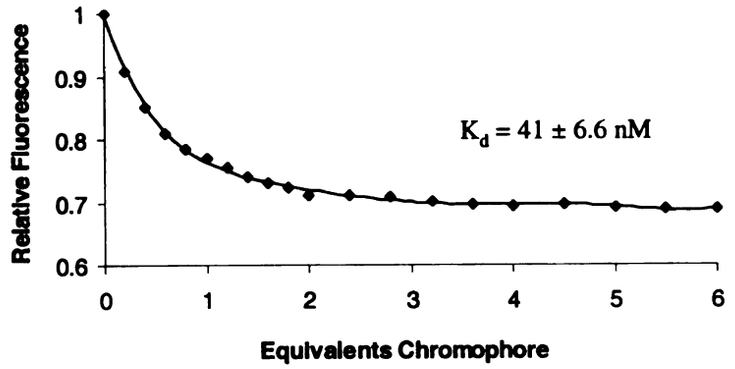

11-*cis*-Retinal

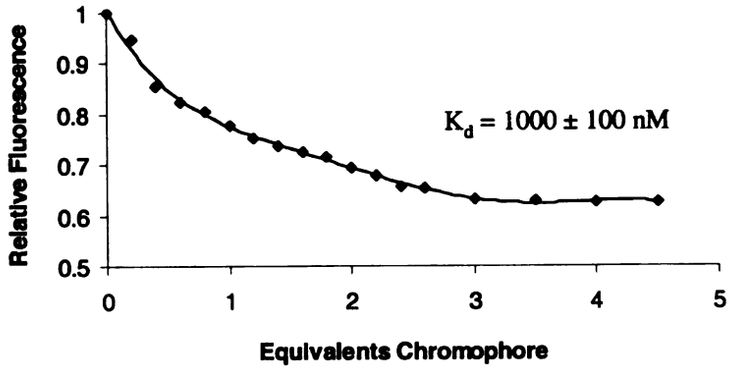

CRABPII Y134K::R132F::R111L::T54E

UV-vis Titrations, all-*trans*-Retinal

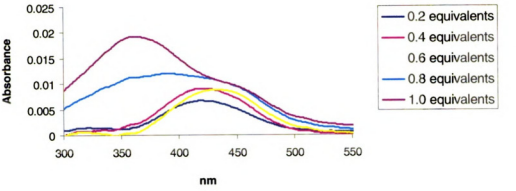

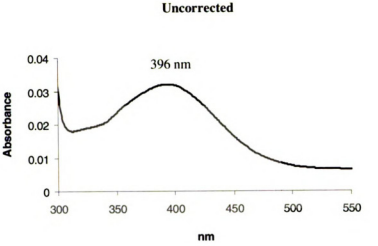

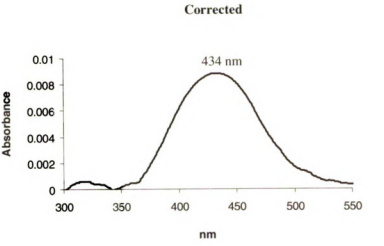

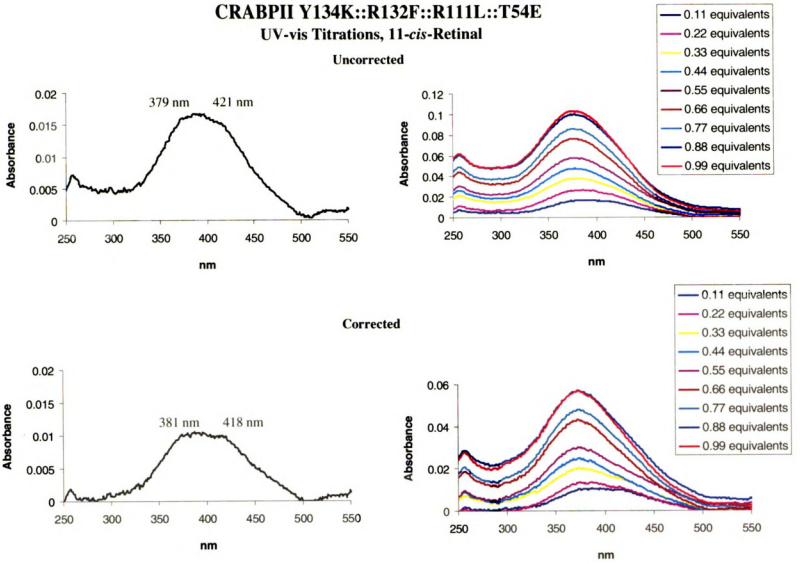
CRABPII Y134K::R132F::R111L::T54E
UV-vis Titrations, 11-cis-Retinal
Uncorrected
379 nm
421 nm
Absorbance
nm
0.11 equivalents
0.22 equivalents
0.33 equivalents
0.44 equivalents
0.55 equivalents
0.66 equivalents
0.77 equivalents
0.88 equivalents
0.99 equivalents
Corrected
381 nm
418 nm

CRABPII Y134K::R132F::R111L::T54E

MALDI-TOF, Reductive Amination with all-*trans*-Retinal

Protein Mass = 16770.18 Da

Positive Reductive Amination = Protein Mass + 268

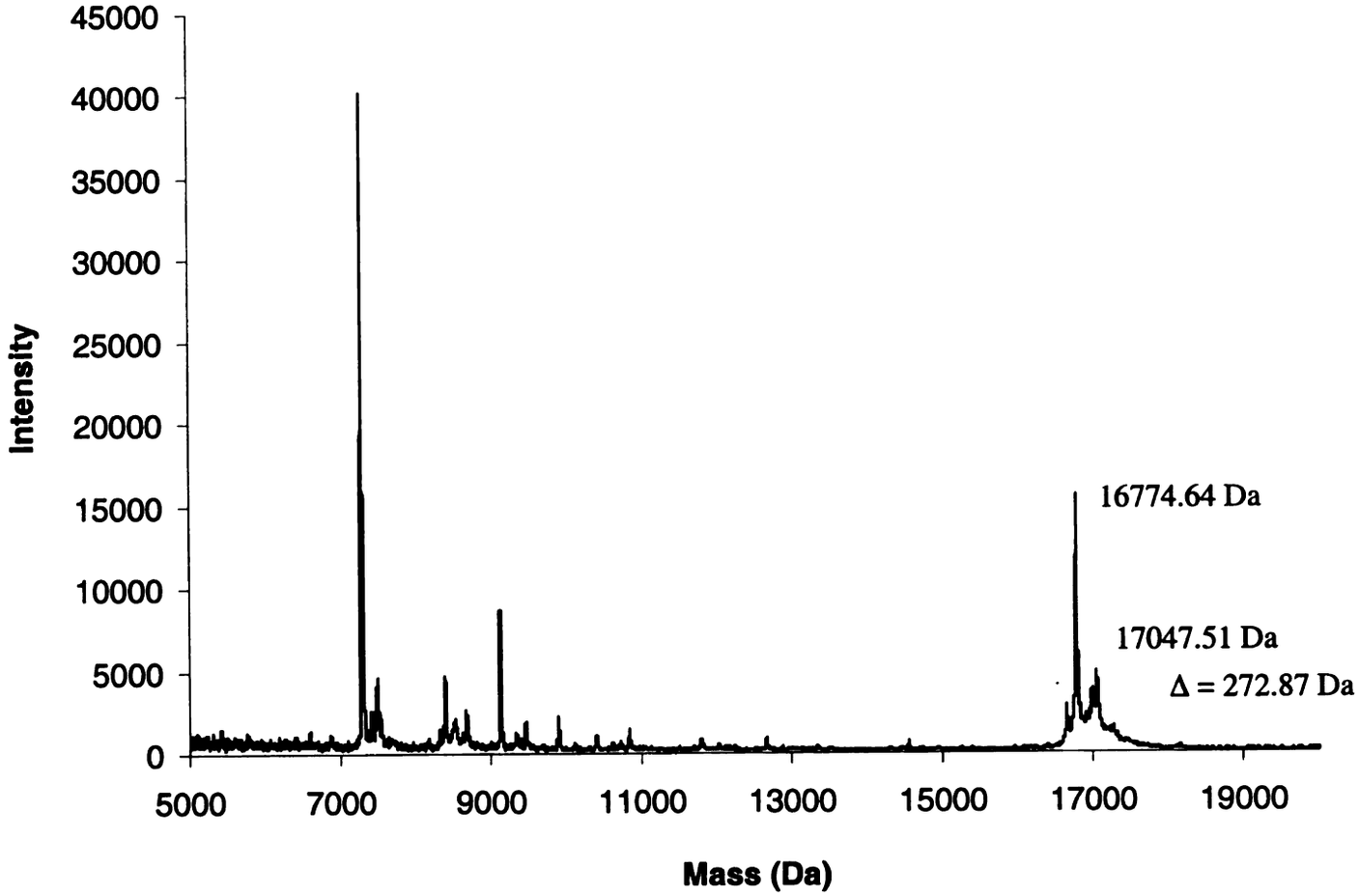

CRABPII Y134K::R132L::R111L

Molecular Weight :

16708.15 Da

Extinction Coefficient :

19,931 M^{-1} cm^{-1}

Primers :

bbb39 5' CCC AAG ACC TCG TGG ACC CTG GAA CTG ACC AAC GAT GGG

bbb40 5' CCC ATC GTT GGT CAG TTG CAG GGT CCA CGA GGT CTT GGG

CD

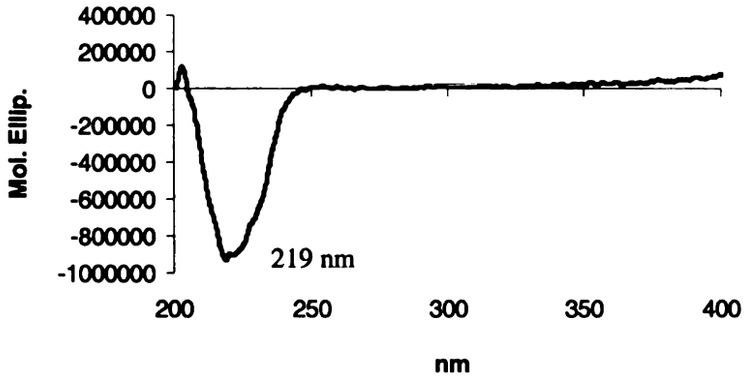

CRABPII Y134K::R132L::R111L

Sequence BB 106

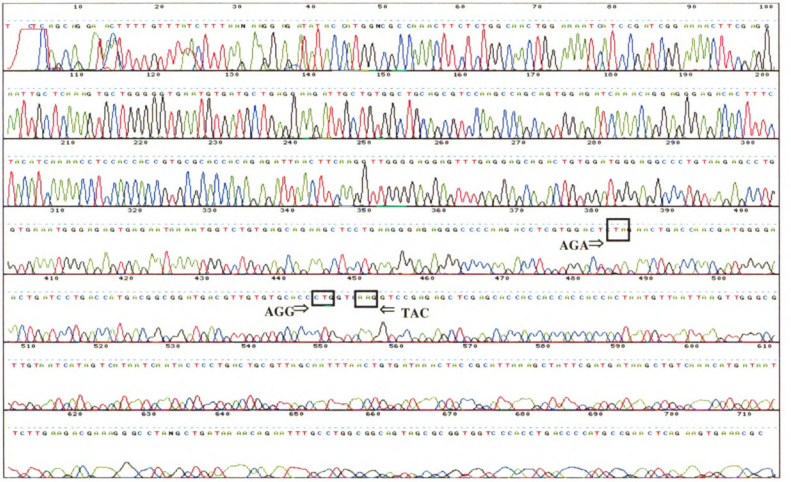

CRABPII Y134K::R132L::R111L

Fluorescence Titrations

Retinoic Acid

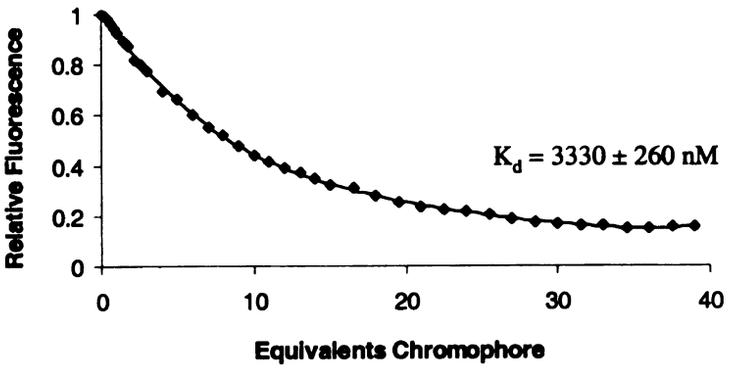

all-*trans*-Retinal

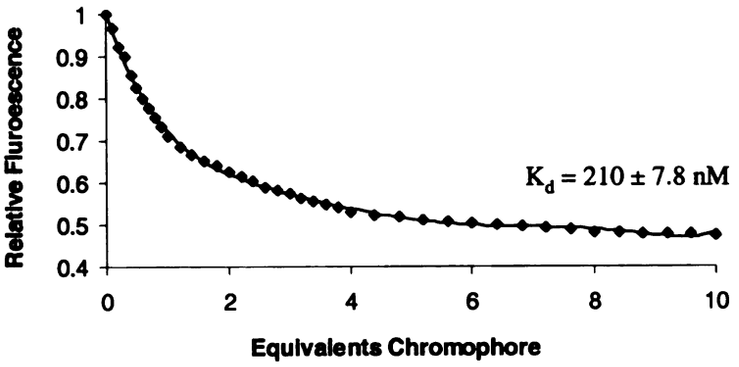

CRABPII Y134K::R132L::R111L

UV-vis Titrations, all-*trans*-Retinal

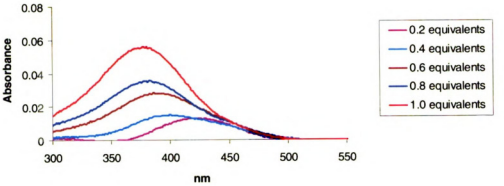

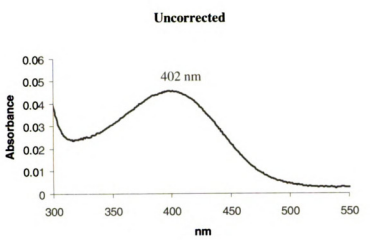

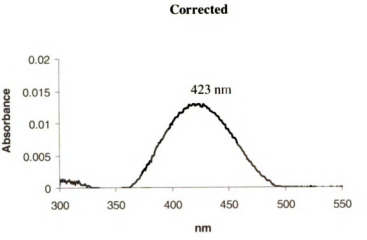

CRABPII Y134K::R132L::R111L

MALDI-TOF, Protein

Calculated Mass = 16708.15 Da

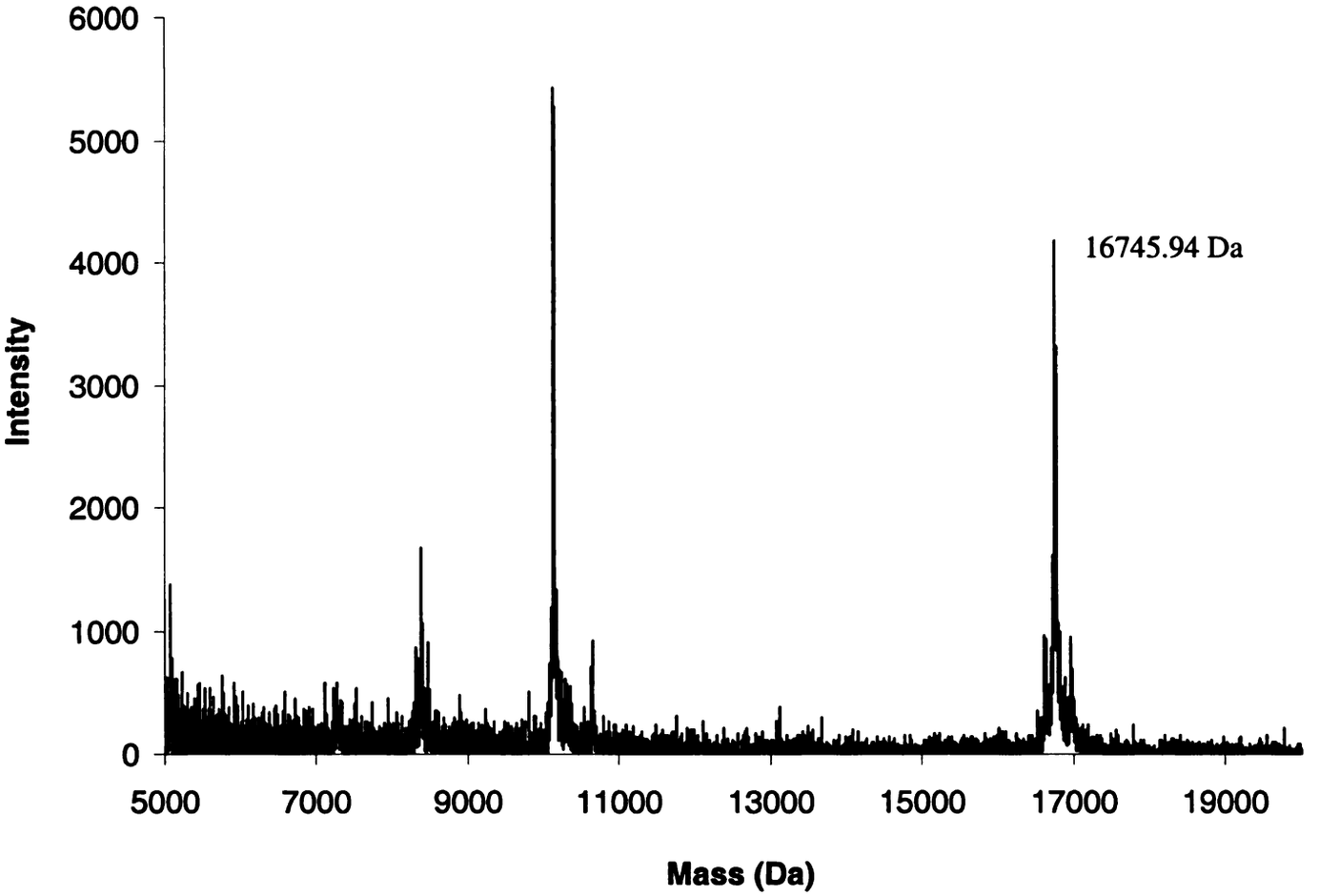

CRABPII Y134K::R132L::R111L

MALDI-TOF, Incubation with all-*trans*-Retinal

Protein Mass = 16708.15 Da

Positive Covalent Bond Formation = Protein Mass + 268

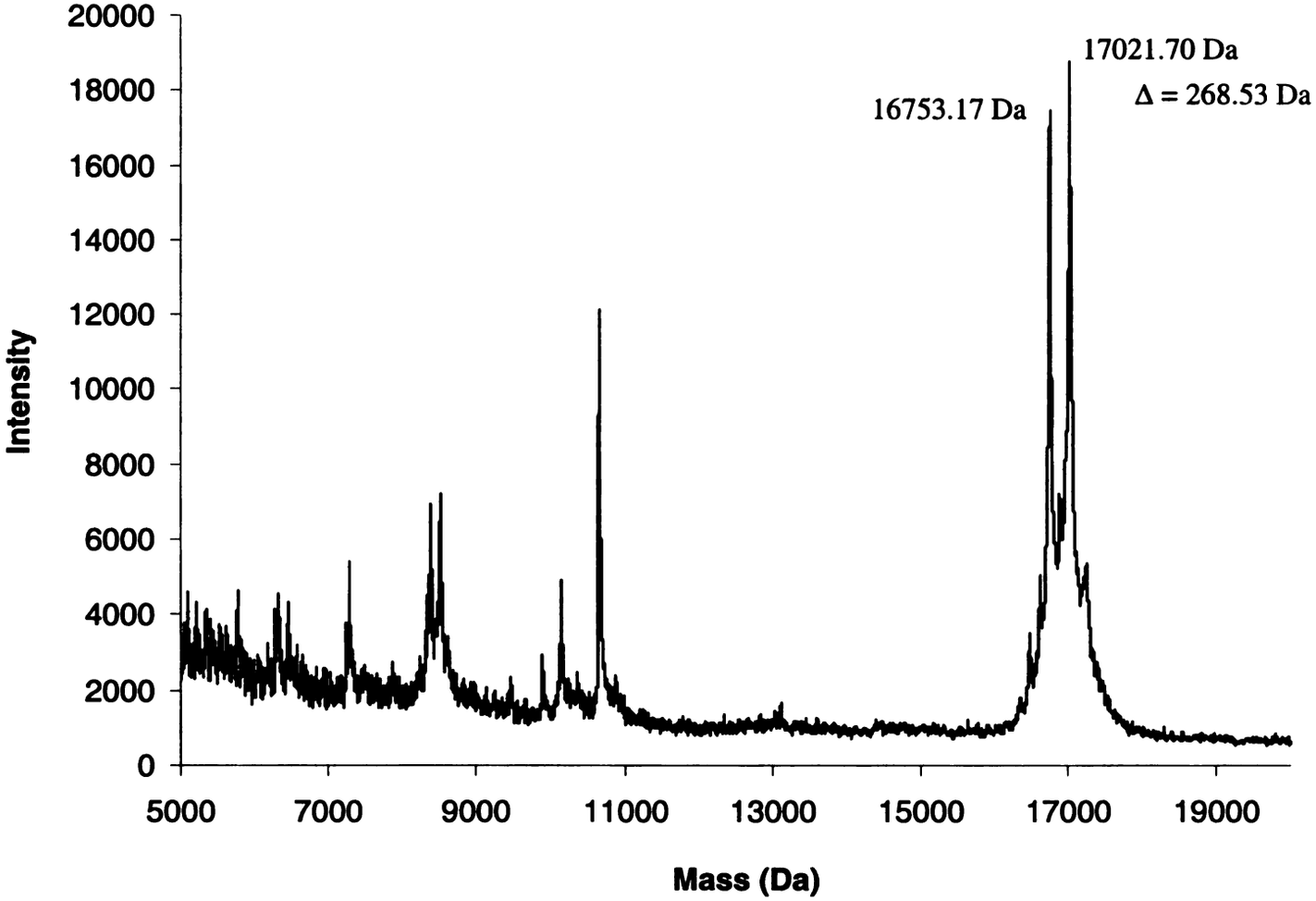

CRABPII Y134K::R132L::R111L

MALDI-TOF, Reductive Amination with all-*trans*-Retinal

Protein Mass = 16708.15 Da

Positive Reductive Amination = Protein Mass + 268

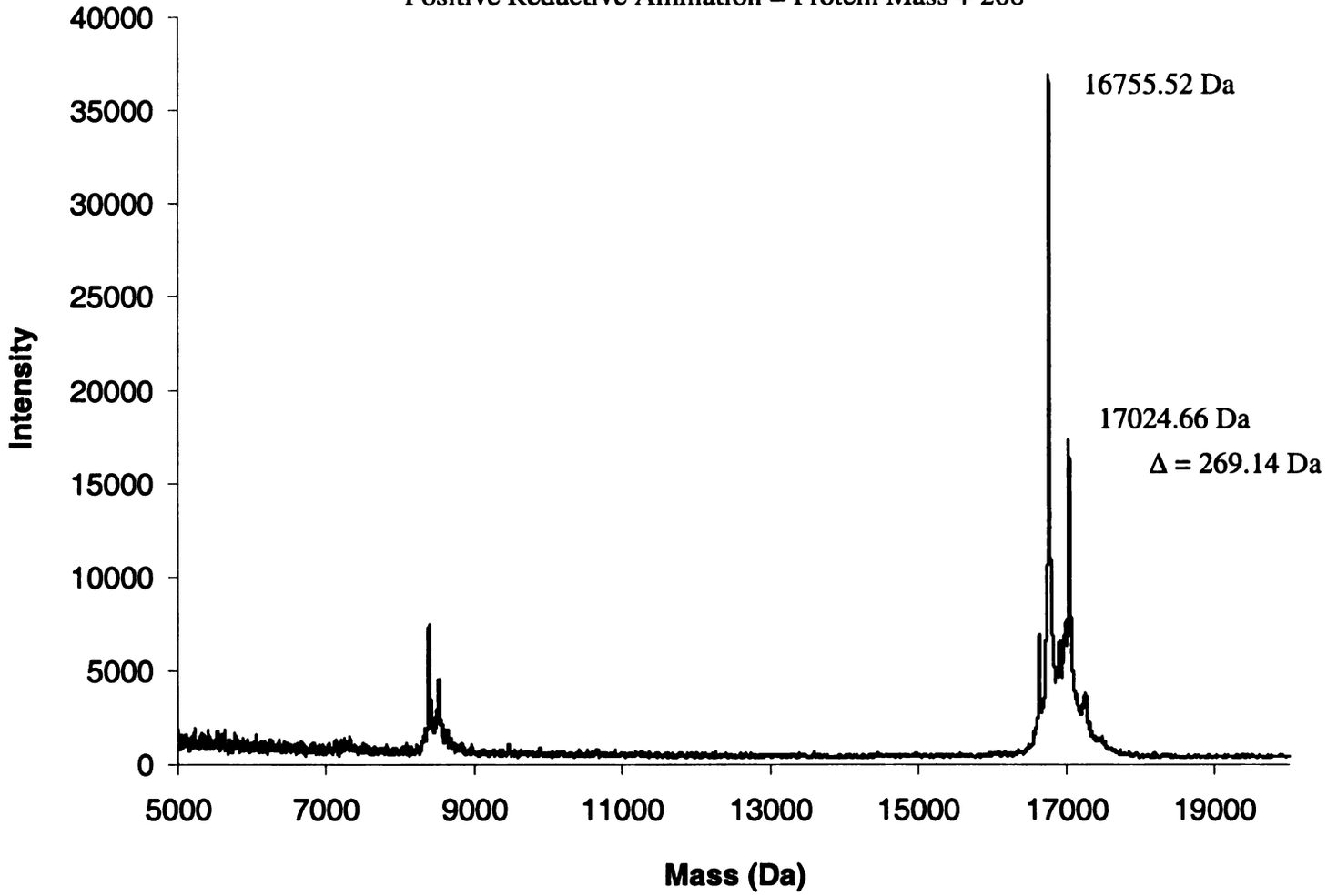

CRABPII Y134K::R132L::L121E

Molecular Weight :

16767.14 Da

Extinction Coefficient :

19,315 M^{-1} cm^{-1}

Primers :

bbb37 5' CGT TGT GTG CAC CCT GGT CTT CGT CCG
bbb38 5' CGG ACG AAG ACC AGG GTG CAC ACA ACG

CD

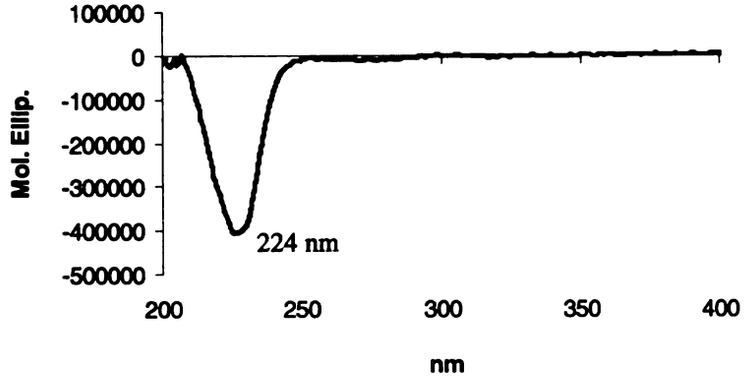

CRABPII Y134K::R132L::L121E

Sequence BB 111

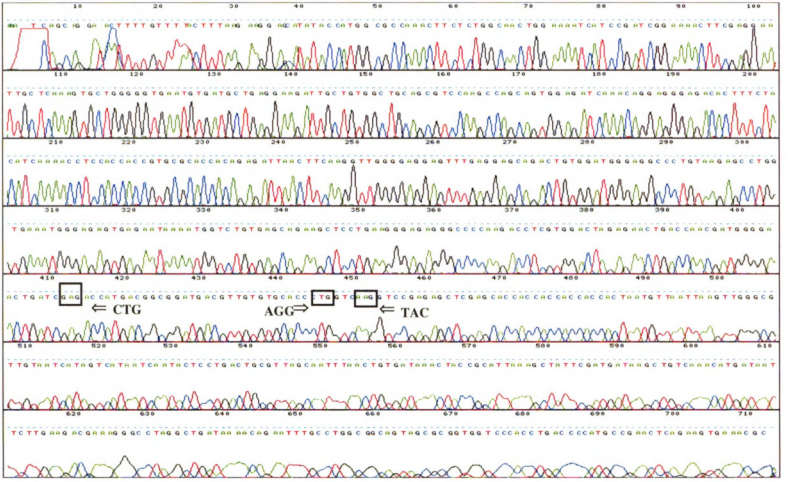

CRABPII Y134K::R132L::L121E

Fluorescence Titrations

Retinoic Acid

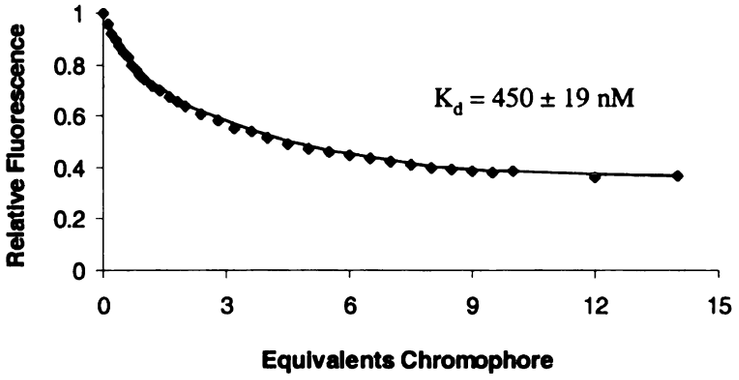

all-*trans*-Retinal

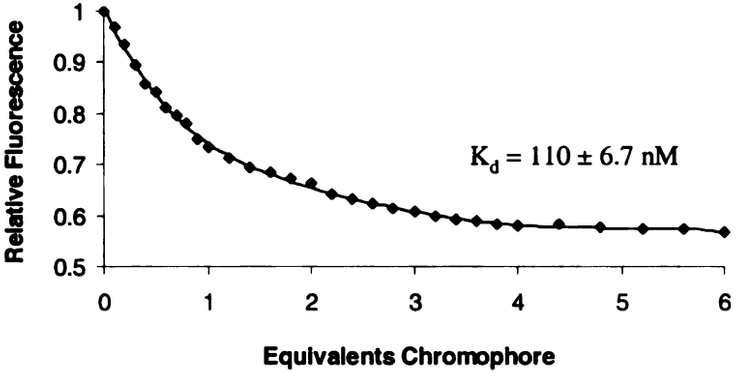

CRABPII Y134K::R132L::L121E

UV-vis Titrations, all-*trans*-Retinal

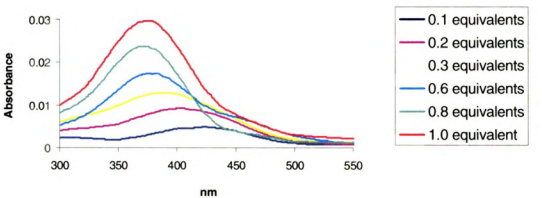

Uncorrected

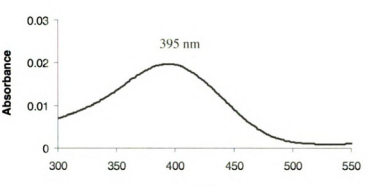

Corrected

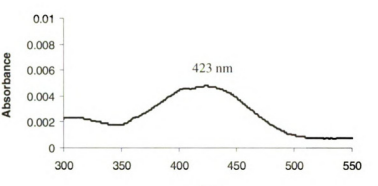

CRABPII Y134K::R132L::L121E

MALDI-TOF, Protein

Calculated Mass = 16767.14 Da

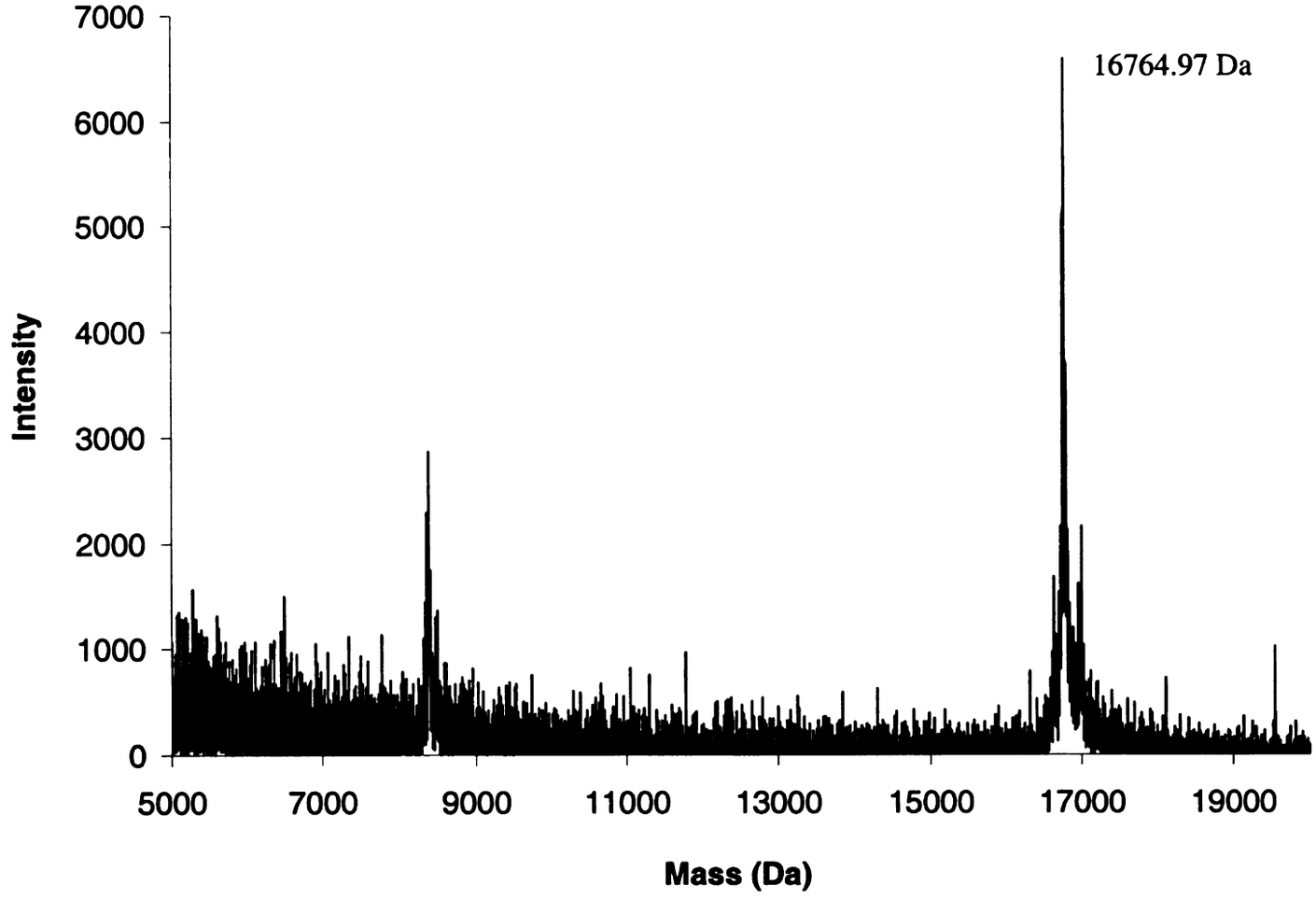

CRABPII Y134K::R132L::L121E

MALDI-TOF, Incubation with all-*trans*-Retinal

Protein Mass = 16767.14 Da

Positive Covalent Bond Formation = Protein Mass + 268

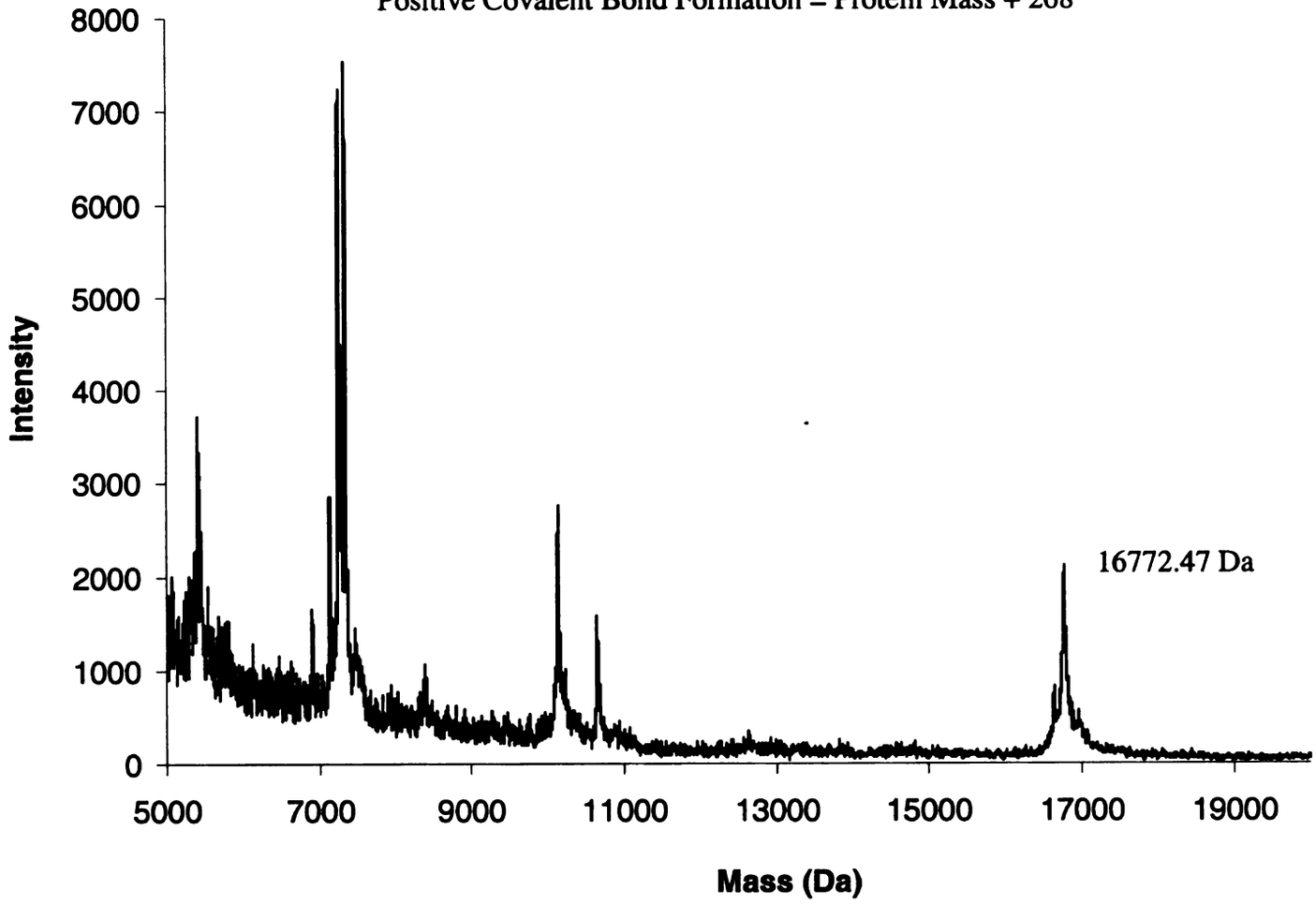

CRABPII Y134K::R132L::L121E

MALDI-TOF, Reductive Amination with all-*trans*-Retinal

Protein Mass = 16767.14 Da

Positive Reductive Amination = Protein Mass + 268

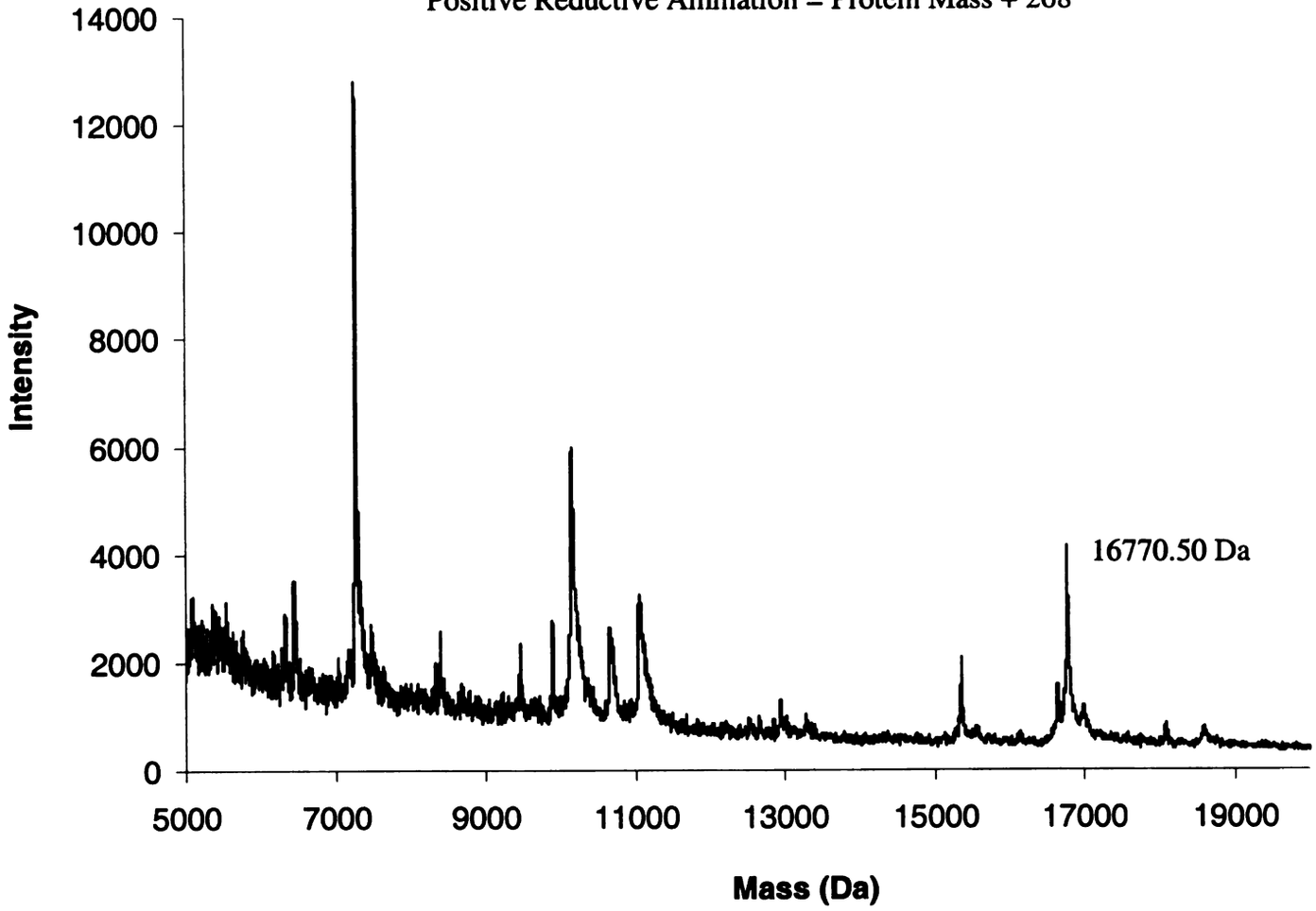

CRABPII Y134K::R132L::R111L::L121E

Molecular Weight :
16724.11 Da

Extinction Coefficient :
19,152 M^{-1} cm^{-1}

Primers :
bbb37 5' CGT TGT GTG CAC CCT GGT CTT CGT CCG
bbb38 5' CGG ACG AAG ACC AGG GTG CAC ACA ACG

CD

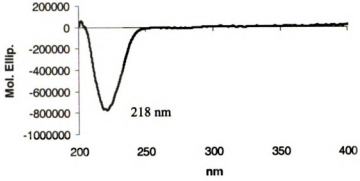

CRABPII Y134K::R132L::R111L::L121E

Sequence BB 178

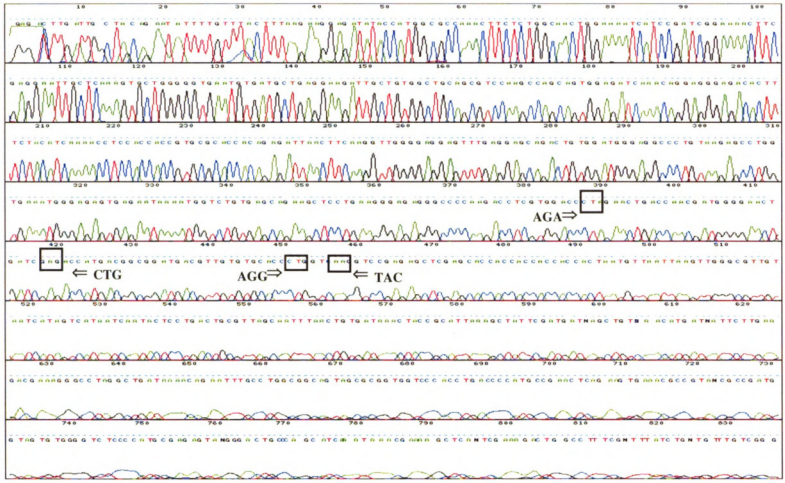

CRABPII Y134K::R132L::R111L::L121E

Fluorescence Titrations

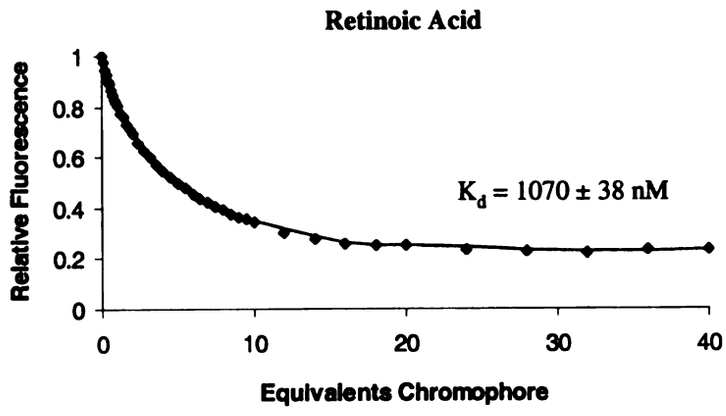

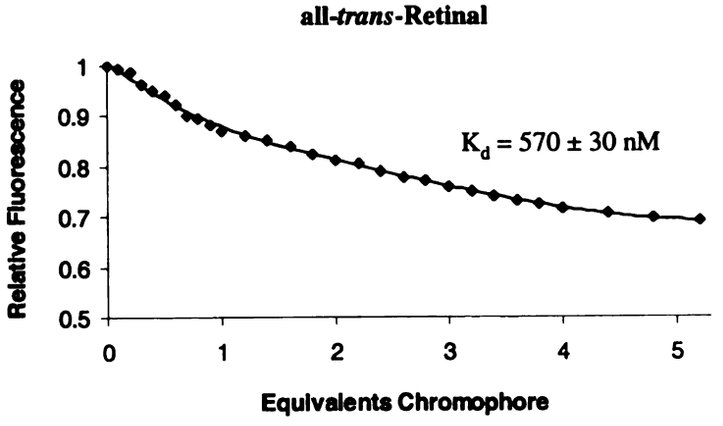

CRABPII Y134K::R132L::R111L::L121E

UV-vis Titrations, all-*trans*-Retinal

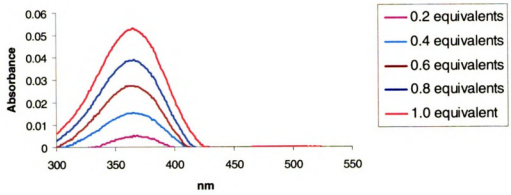

Uncorrected

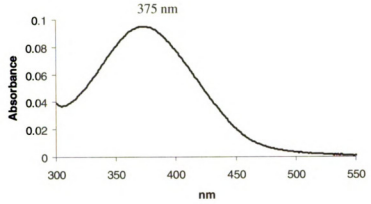

Corrected

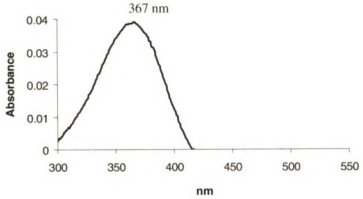

CRABPII Y134K::R132L::R111L::L121E

MALDI-TOF, Protein

Calculated Mass = 16724.11 Da

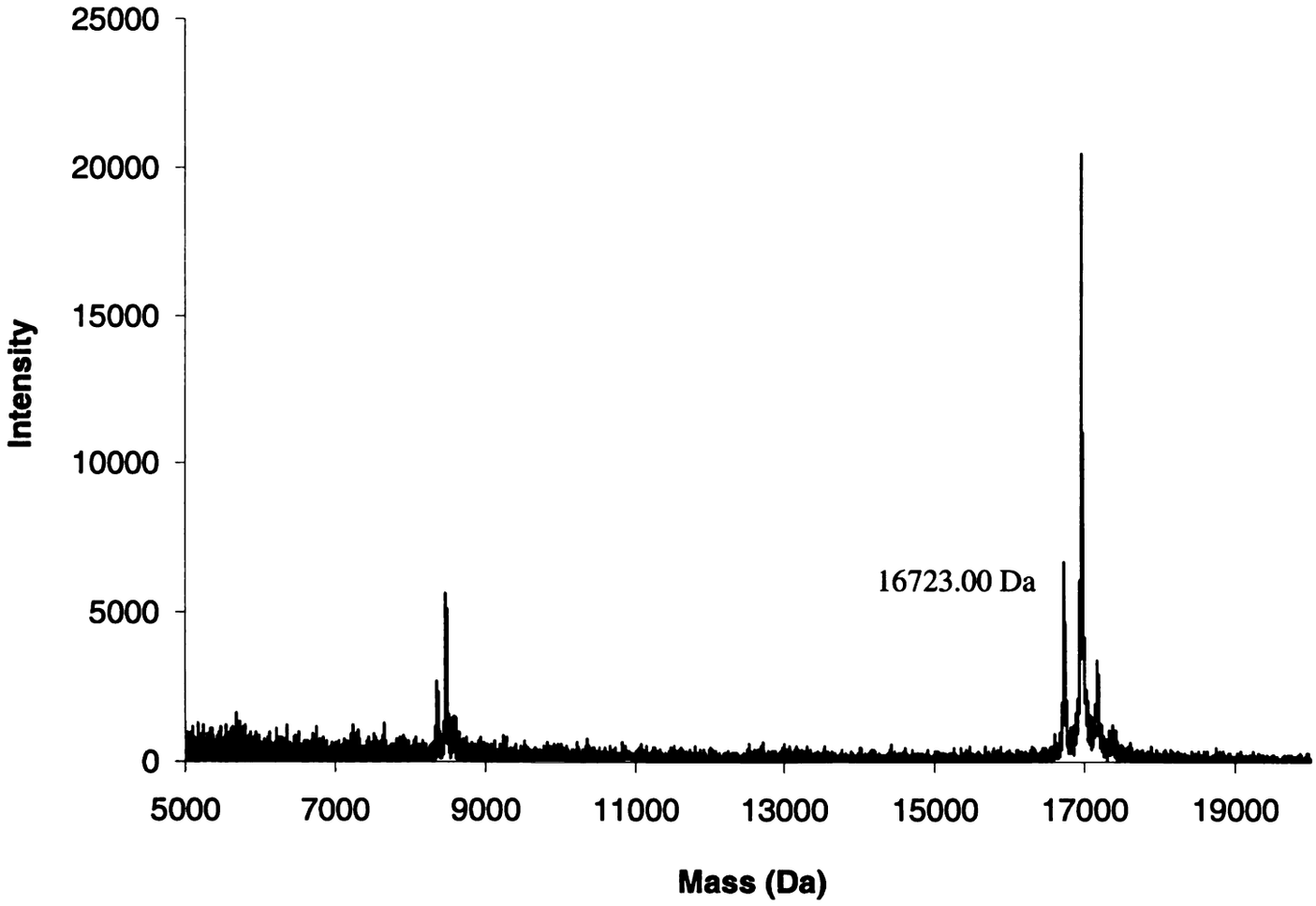

CRABPII Y134K::R132L::R111L::L121E

MALDI-TOF, Incubation with all-*trans*-Retinal

Protein Mass = 16724.11 Da

Positive Covalent Bond Formation = Protein Mass + 268

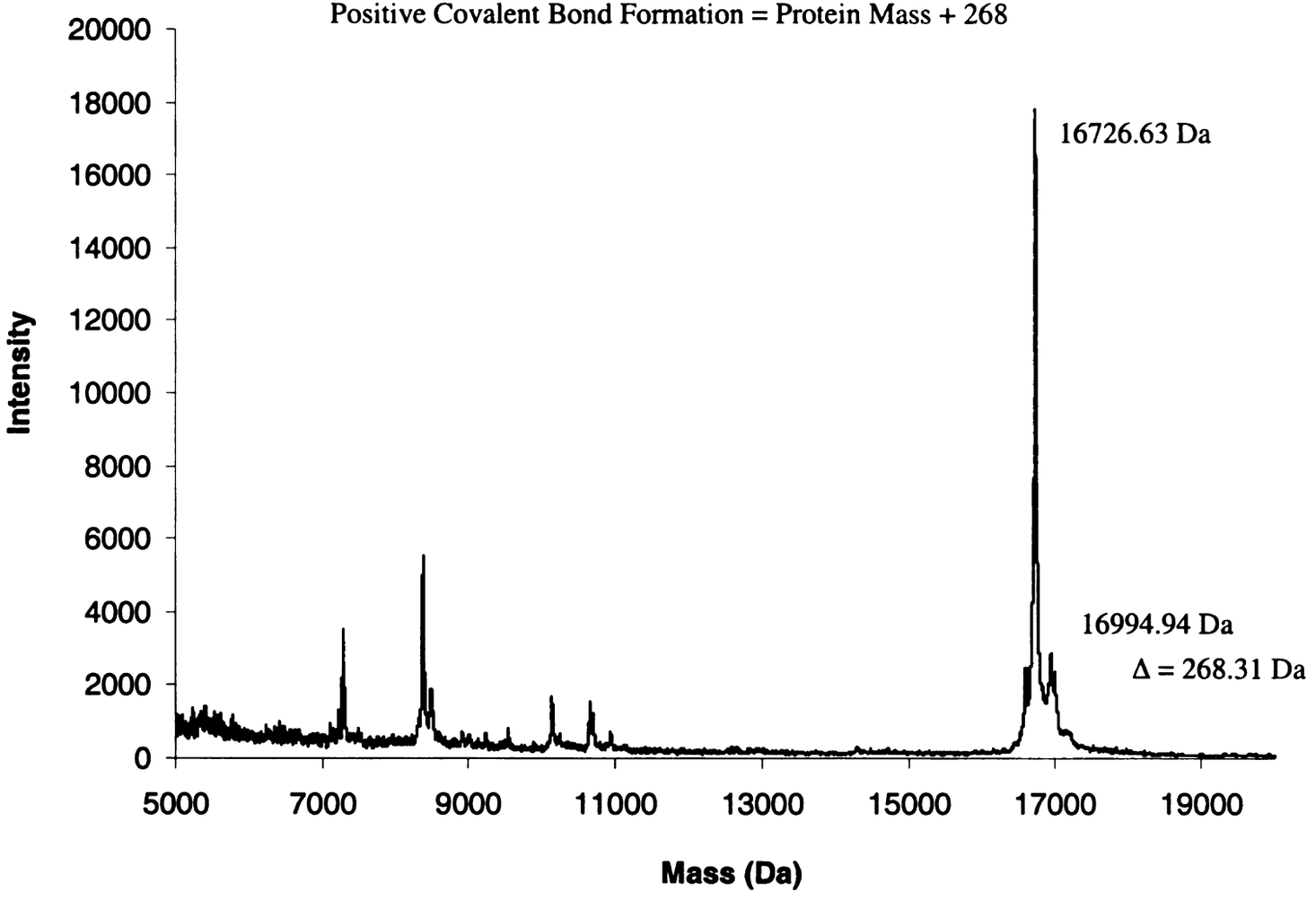

CRABPII Y134K::R132L::R111L::L121E

MALDI-TOF, Reductive Amination with all-*trans*-Retinal

Protein Mass = 16724.11 Da

Positive Reductive Amination = Protein Mass + 268

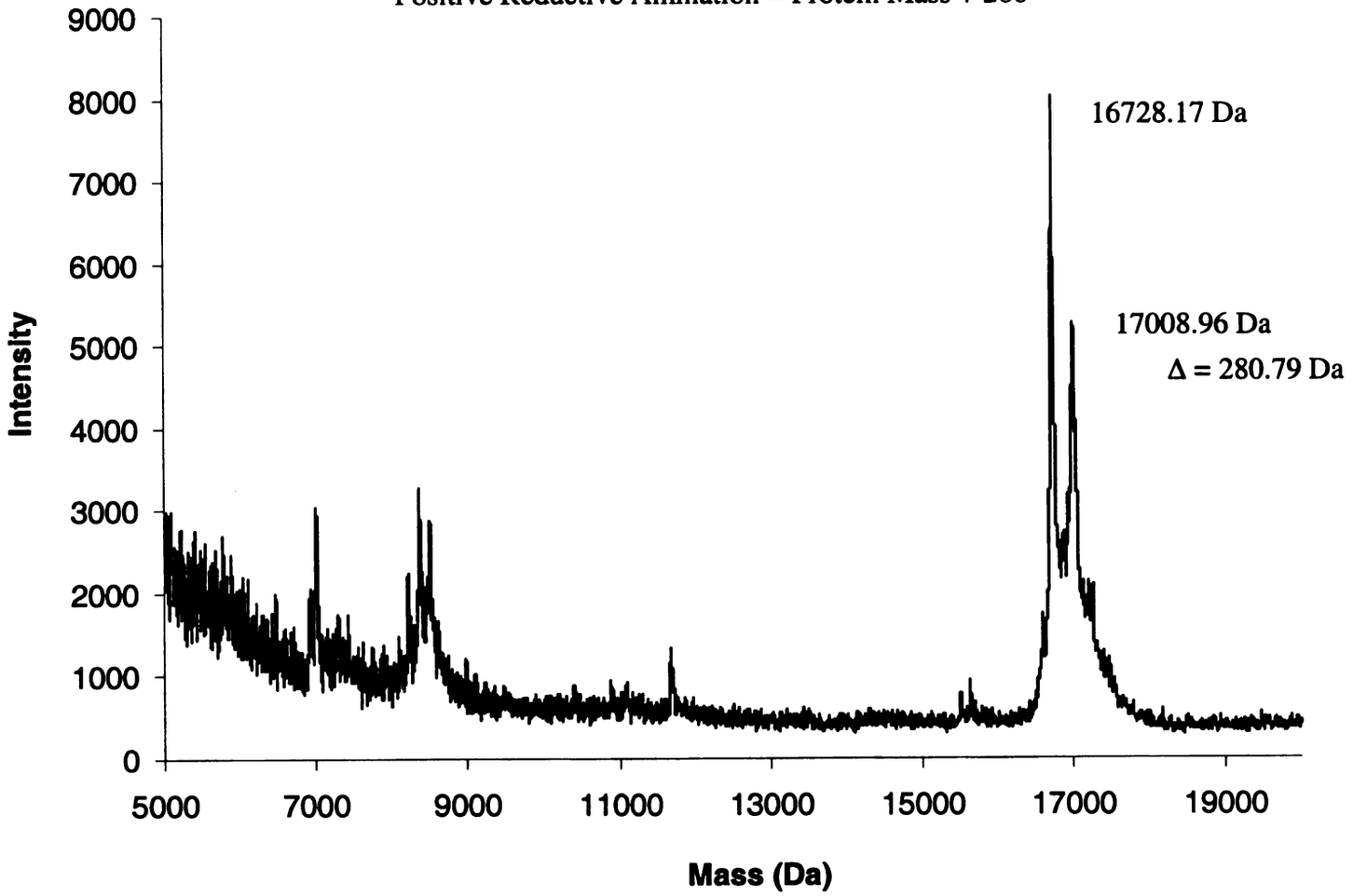

CRABPII F15W

Molecular Weight :
16868.25 Da

Extinction Coefficient :
28,022 M^{-1} cm^{-1}

Primers :
bbb49 5' CGA TCG GAA AAC TGG GAG GAA TTG CTC
bbb50 5' GAG CAA TTC CTC CCA GTT TTC CGA TCG

CD

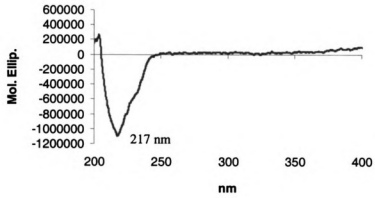

CRABPII F15W

Sequence BB 12

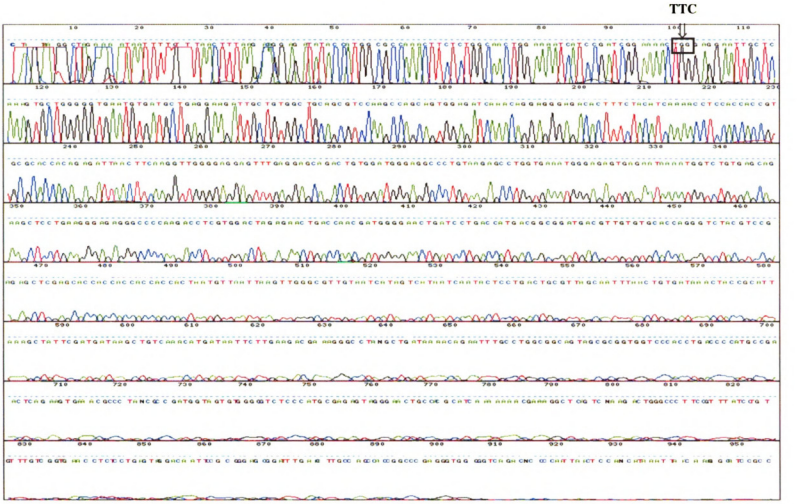

CRABPII F15W
Fluorescence Titrations

Retinoic Acid

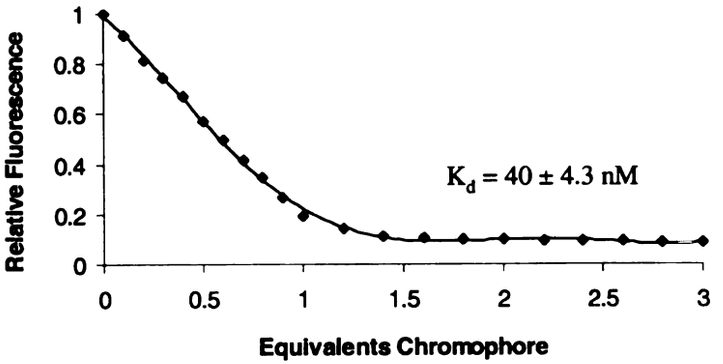

all-*trans*-Retinal

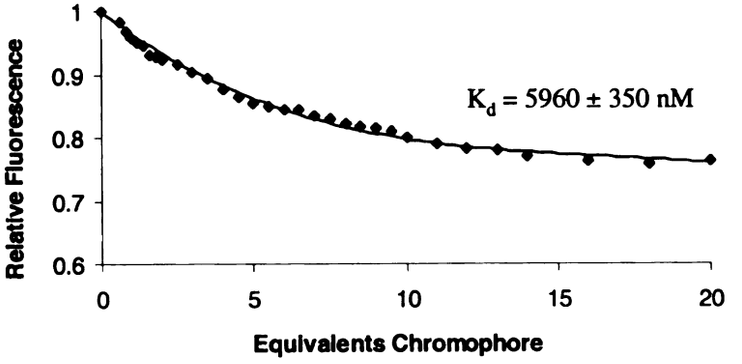

CRABPII F15W

UV-vis Titrations, all-*trans*-Retinal

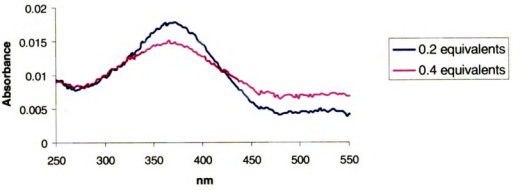

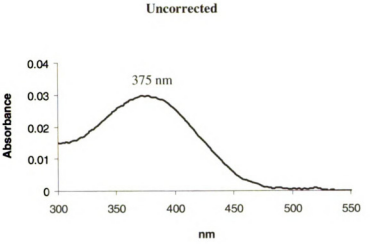

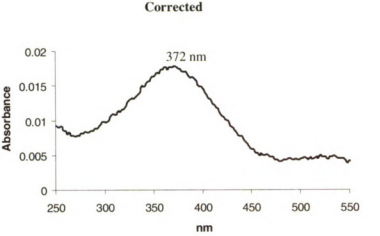

CRABPII F15W

MALDI-TOF, Protein

Calculated Mass = 16868.25 Da

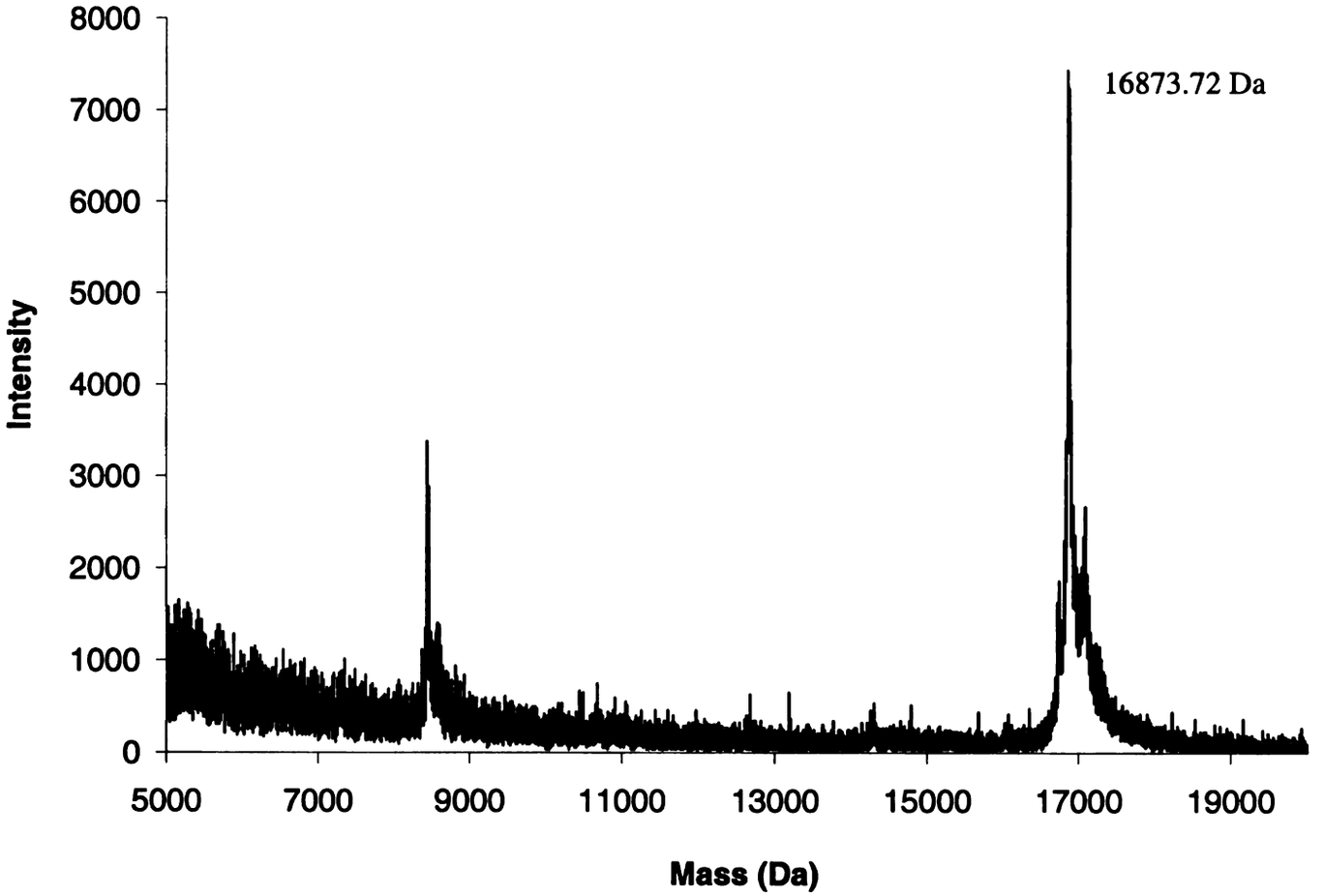

CRABPII F15W

MALDI-TOF, Incubation with all-*trans*-Retinal

Protein Mass = 16868.25 Da

Positive Covalent Bond Formation = Protein Mass + 268

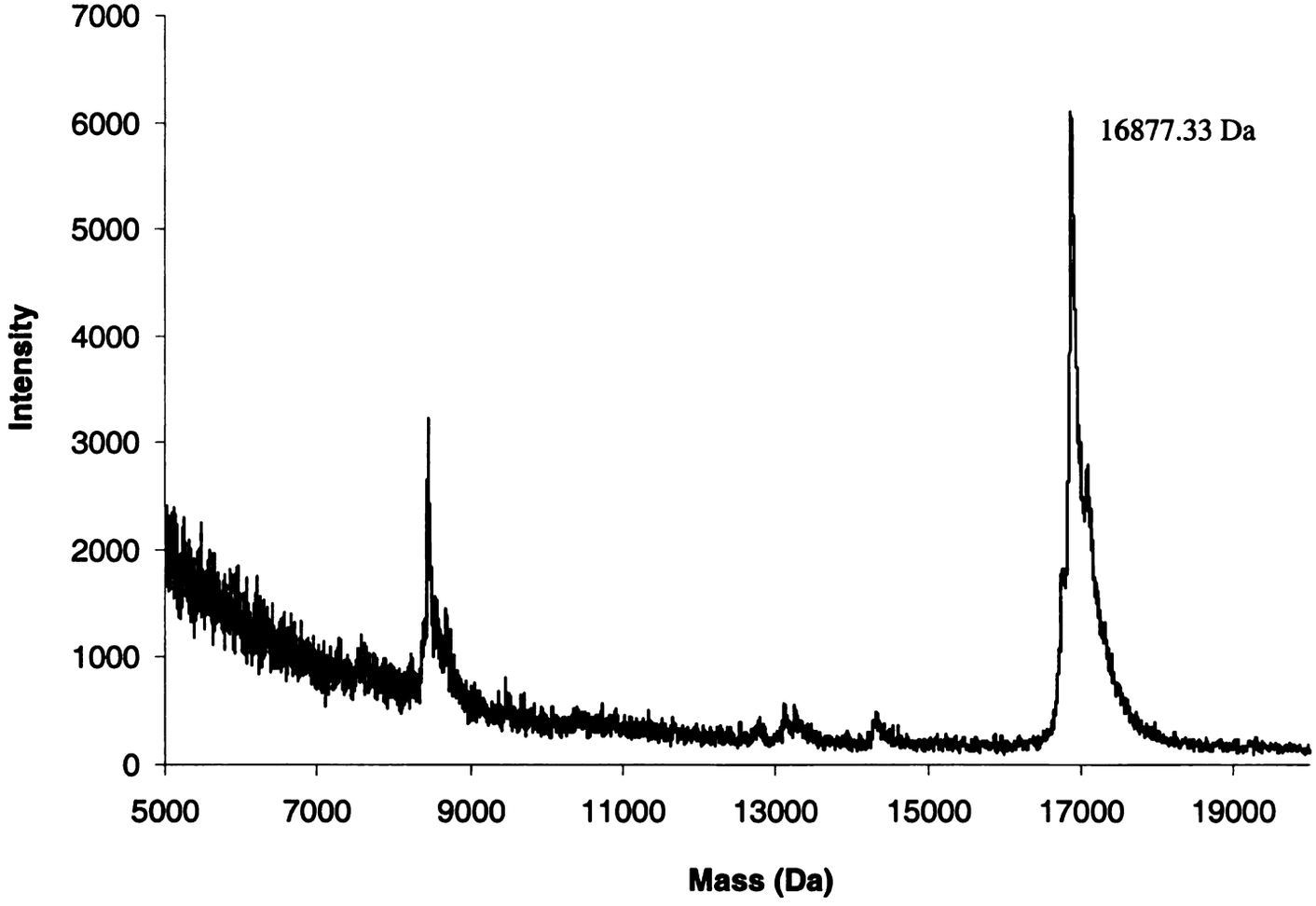

CRABPII F15W

MALDI-TOF, Reductive Amination with all-*trans*-Retinal

Protein Mass = 16868.25 Da

Positive Reductive Amination = Protein Mass + 268

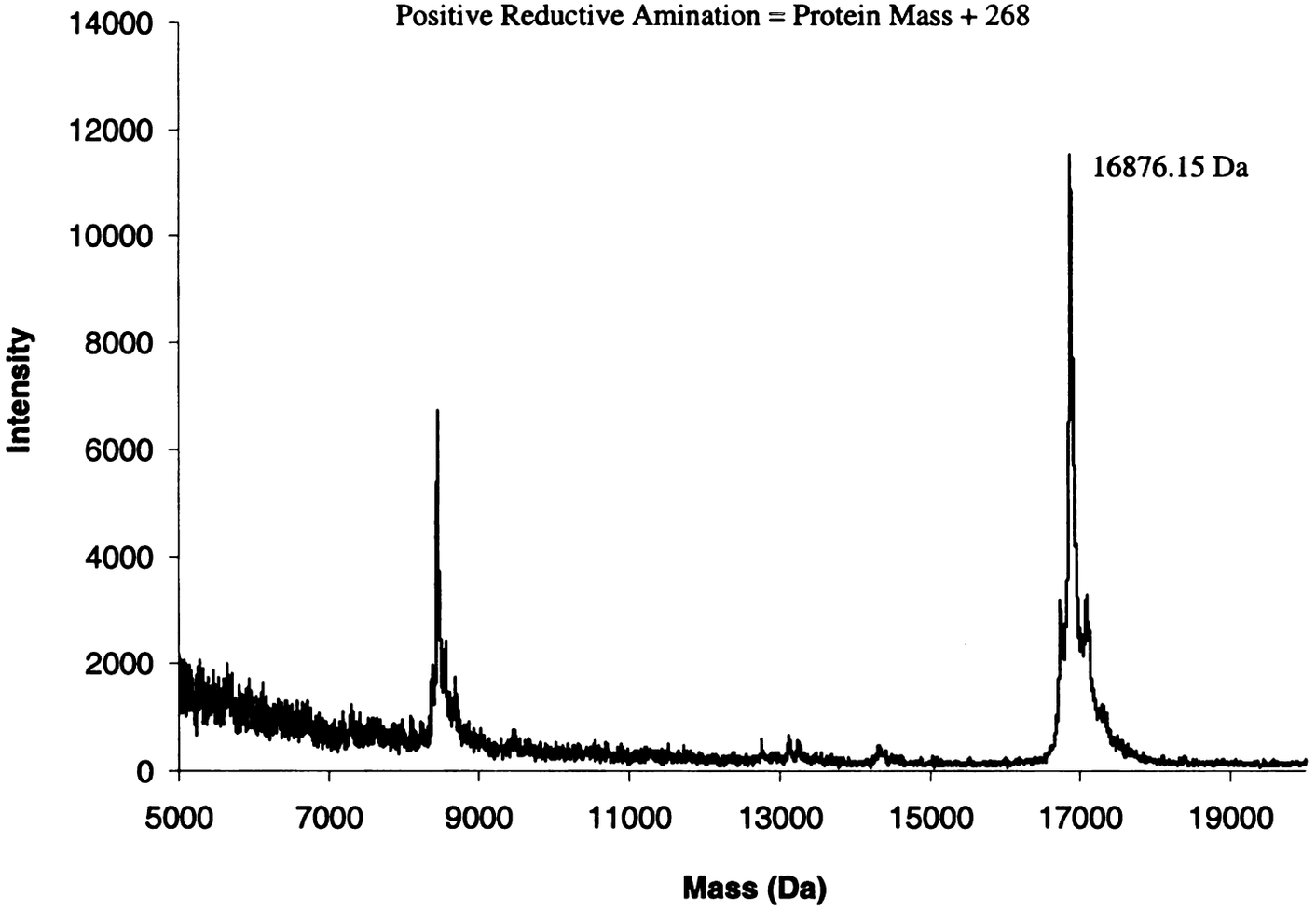

CRABPII R132K::Y134F::F15W

Molecular Weight :
16824.24 Da

Extinction Coefficient :
37,716 M^{-1} cm^{-1}

Primers :
bbb49 5' CGA TCG GAA AAC TGG GAG GAA TTG CTC
bbb50 5' GAG CAA TTC CTC CCA GTT TTC CGA TCG

CD

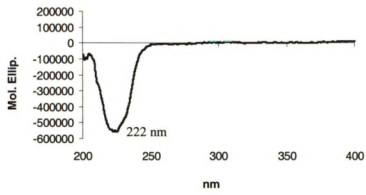

CRABPII R132K::Y134F::F15W

Sequence BB 17R

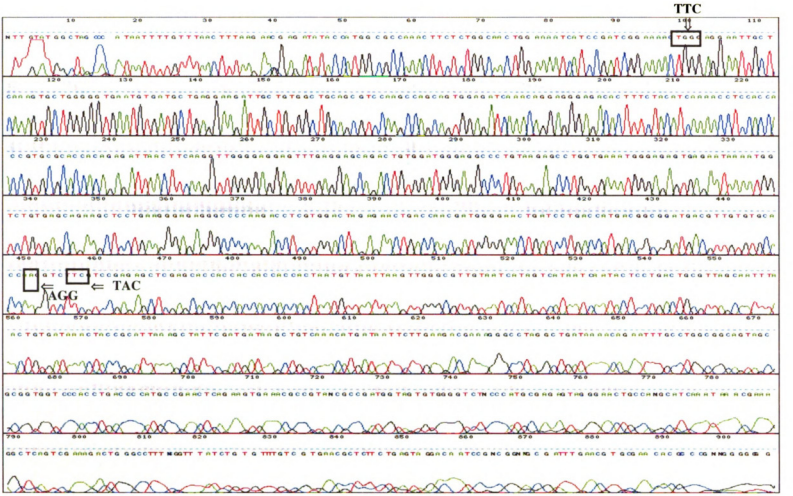

CRABPII R132K::Y134F::F15W

Fluorescence Titrations

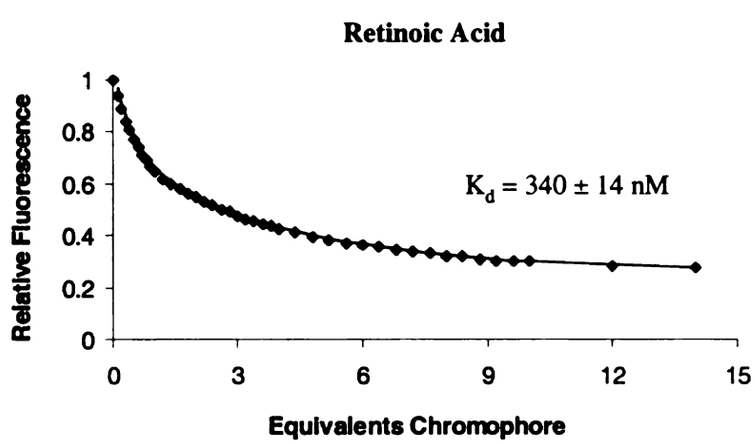

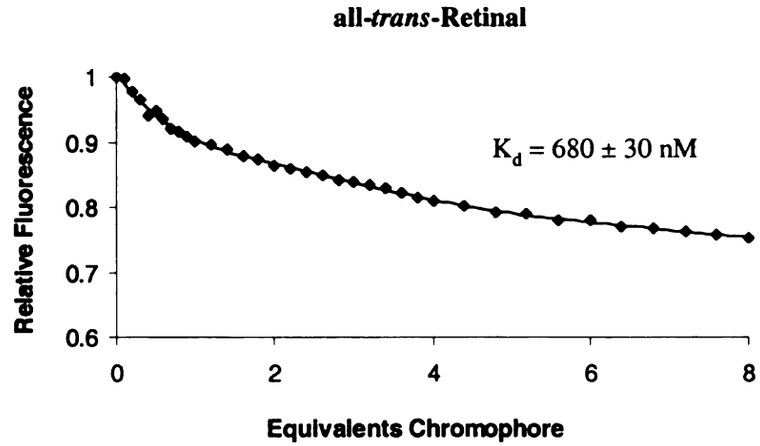

CRABPII R132K::Y134F::F15W

UV-vis Titrations, all-*trans*-Retinal

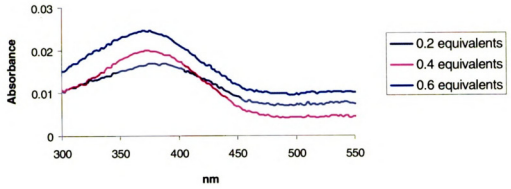

Uncorrected

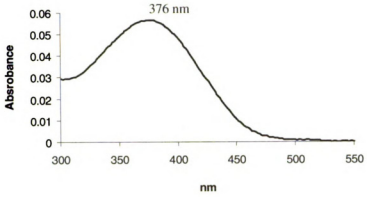

Corrected

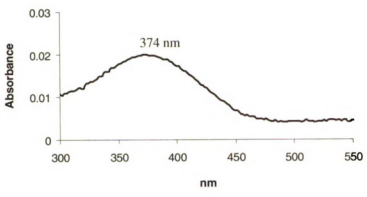

CRABPII R132K::Y134F::F15W

MALDI-TOF, Protein

Calculated Mass = 16824.24 Da

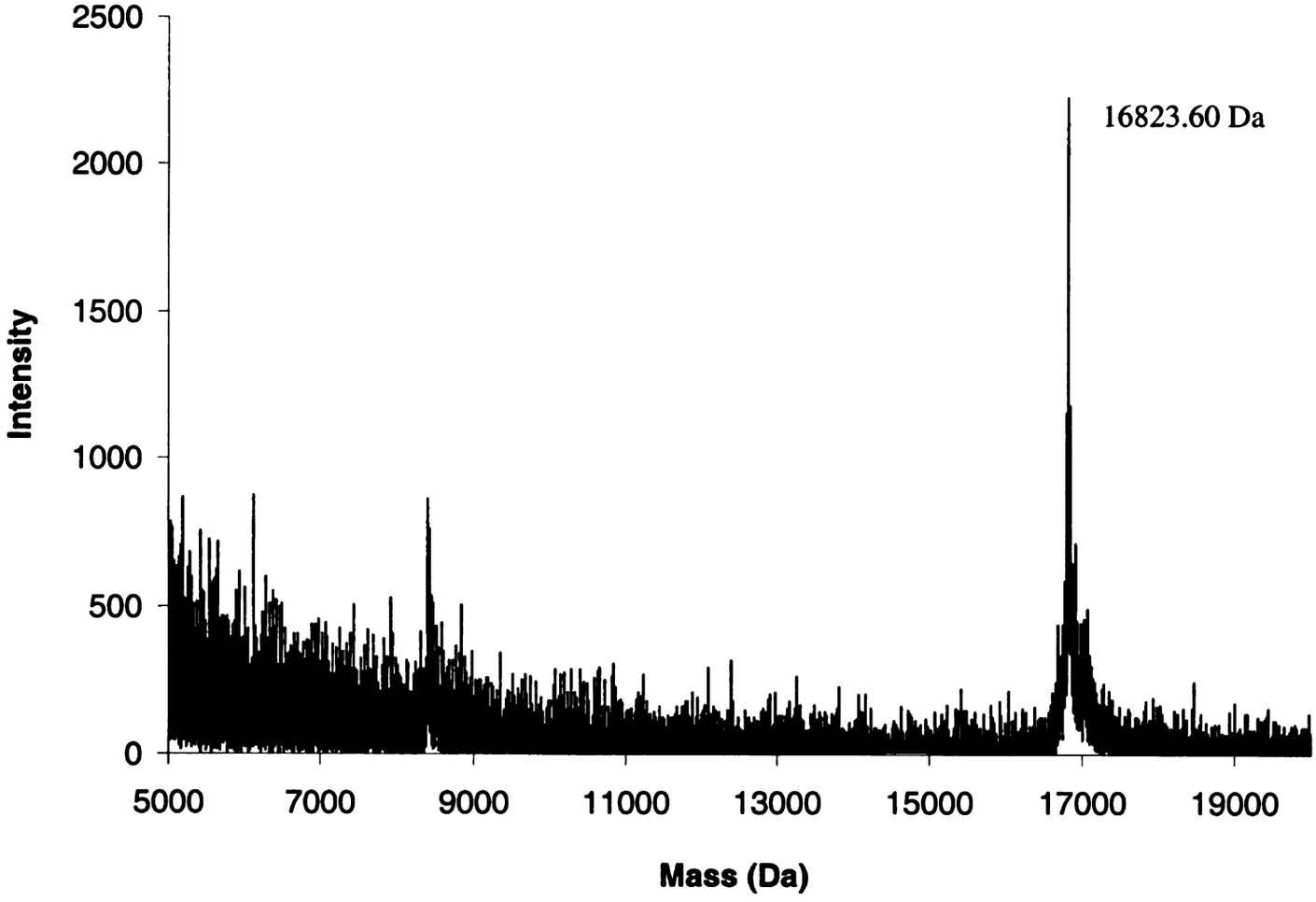

CRABPII R132K::Y134F::F15W

MALDI-TOF, Incubation with all-*trans*-Retinal

Protein Mass = 16824.24 Da

Positive Covalent Bond Formation = Protein Mass + 268

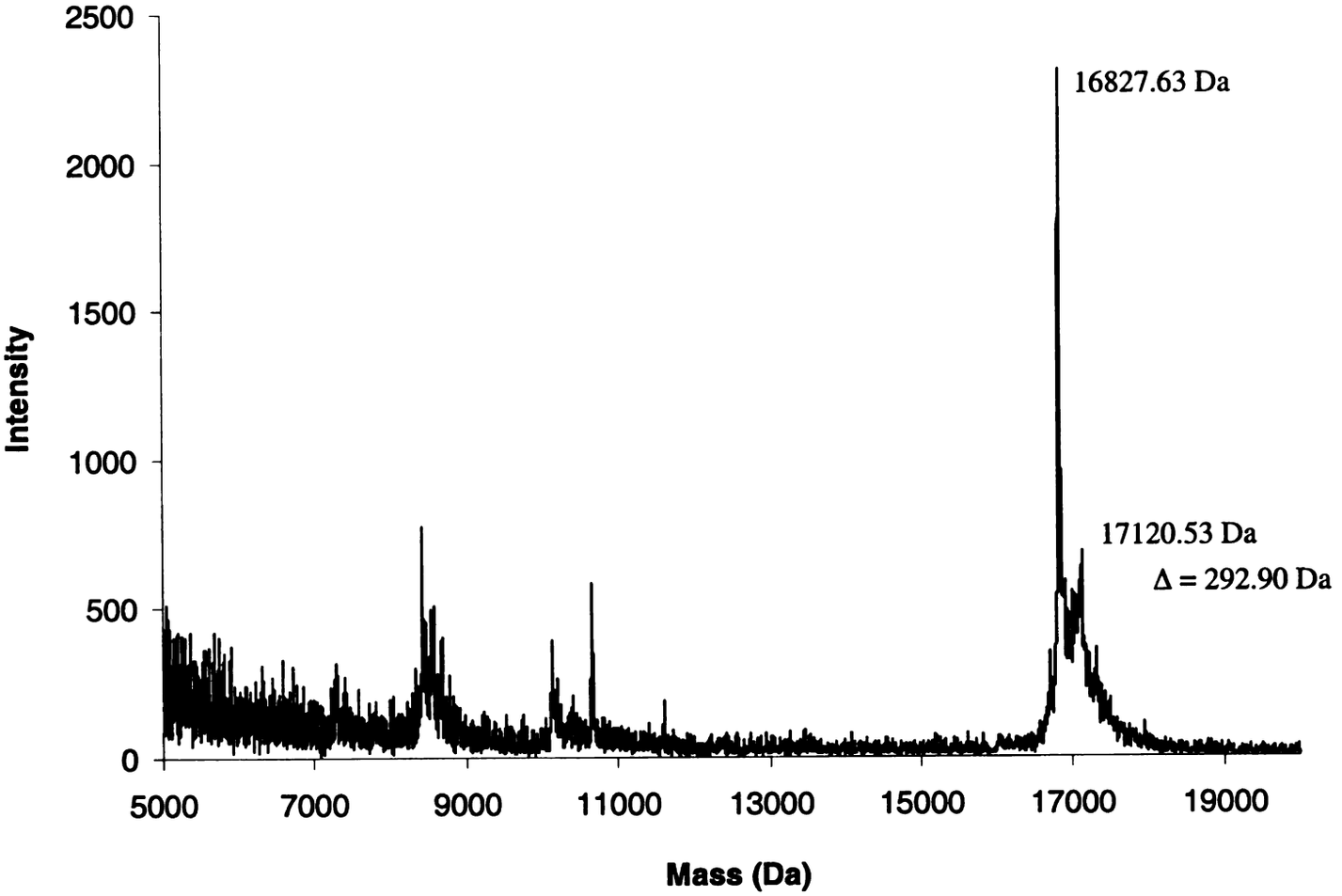

CRABPII R132K::Y134F::F15W

MALDI-TOF, Reductive Amination with all-*trans*-Retinal

Protein Mass = 16824.24 Da

Positive Reductive Amination = Protein Mass + 268

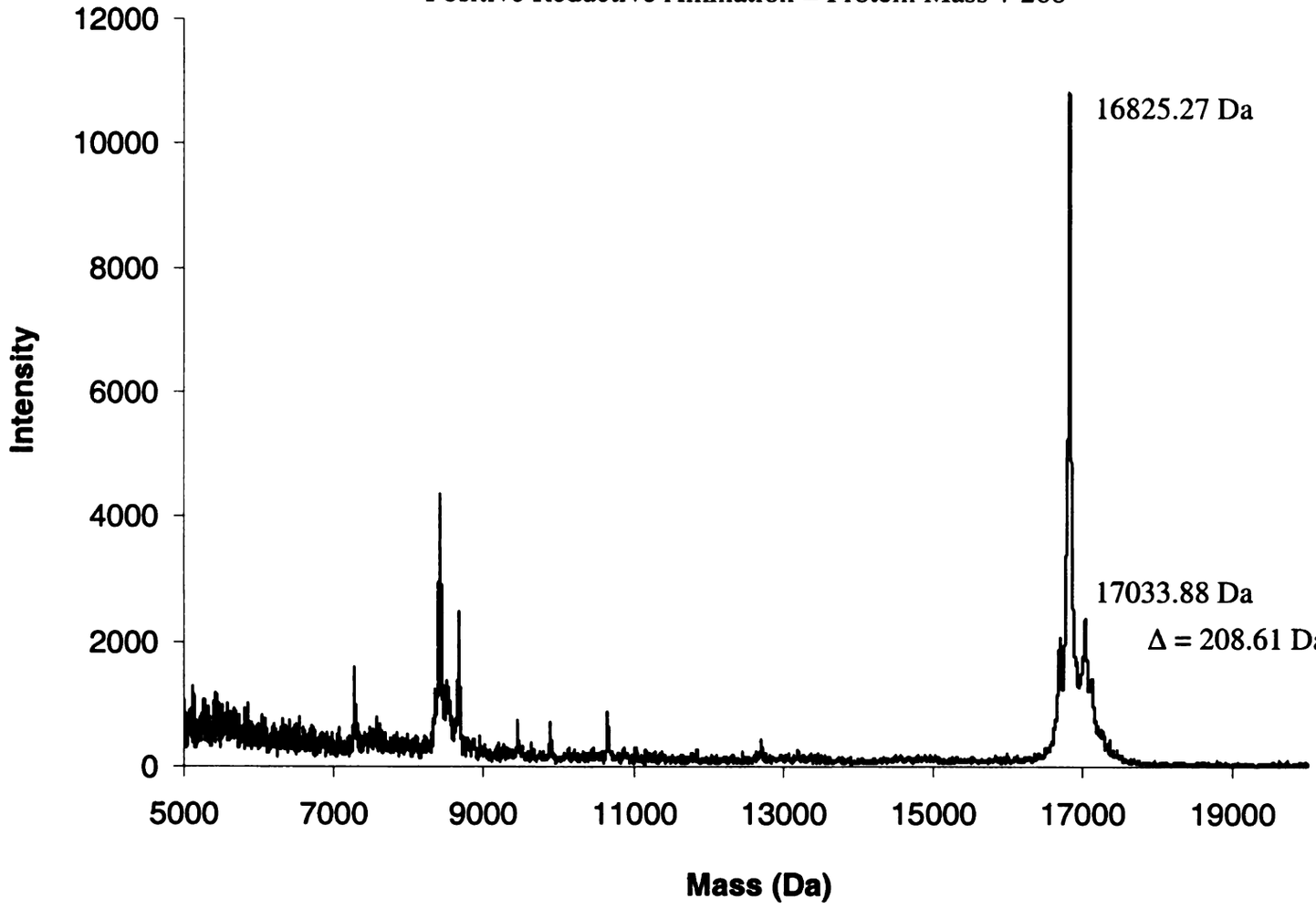

CRABPII L19W

Molecular Weight :

16902.27 Da

Extinction Coefficient :

26,639 M^{-1} cm^{-1}

Primers :

bbb47 5' CGA GGA ATT GTG GAA AGT GCT GGG G
bbb48 5' CCC CAG CAC TTT CCA CAA TTC CTC G

CD

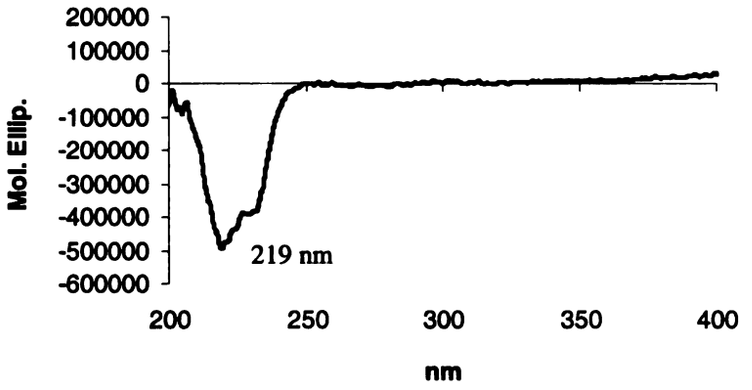

CRABPII L19W

Sequence BB 175

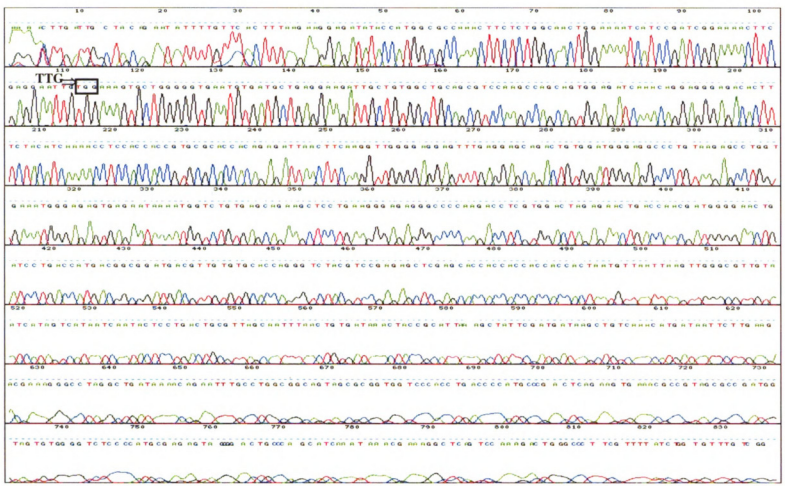

CRABPII L19W

Fluorescence Titrations

Retinoic Acid

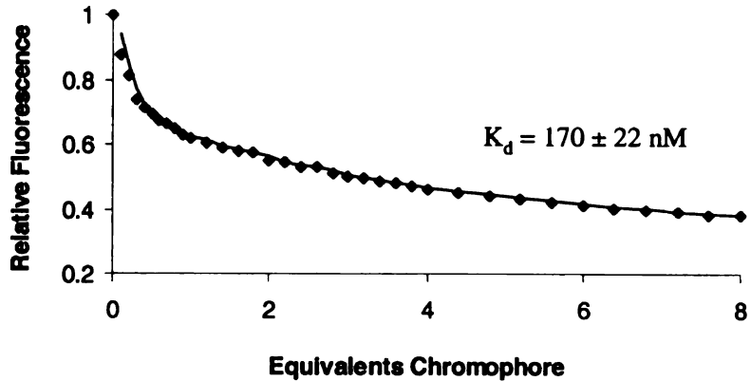

all-*trans*-Retinal

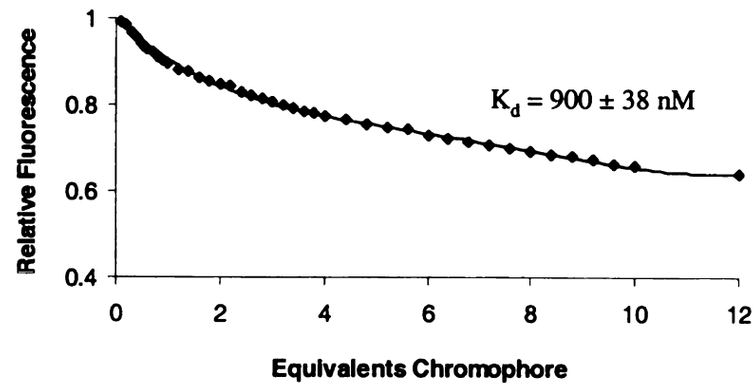

11-*cis*-Retinal

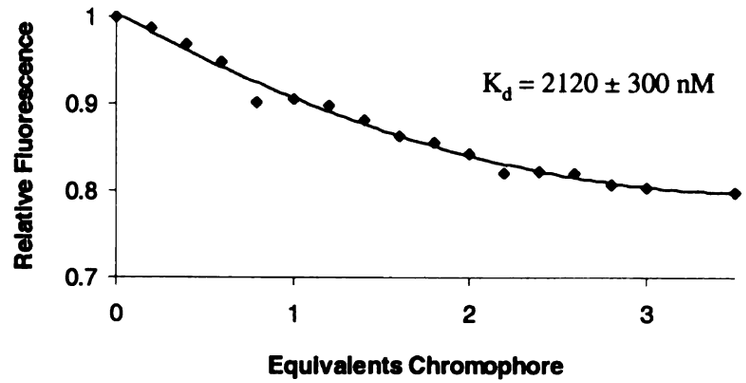

CRABPII L19W

UV-vis Titrations, all-*trans*-Retinal

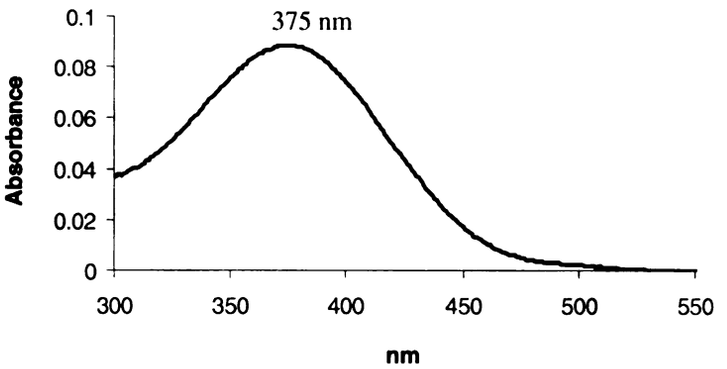

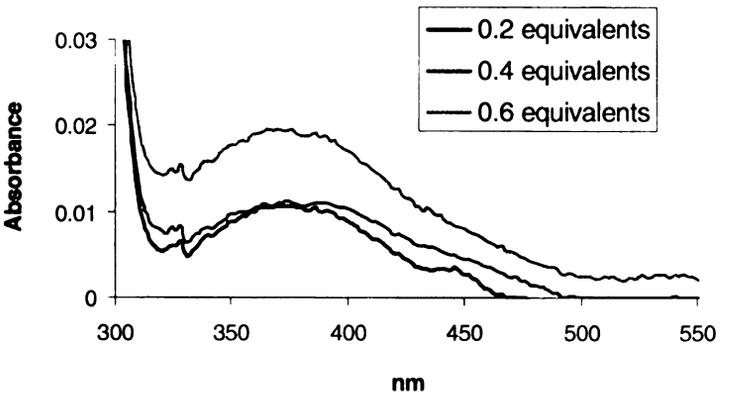

Uncorrected

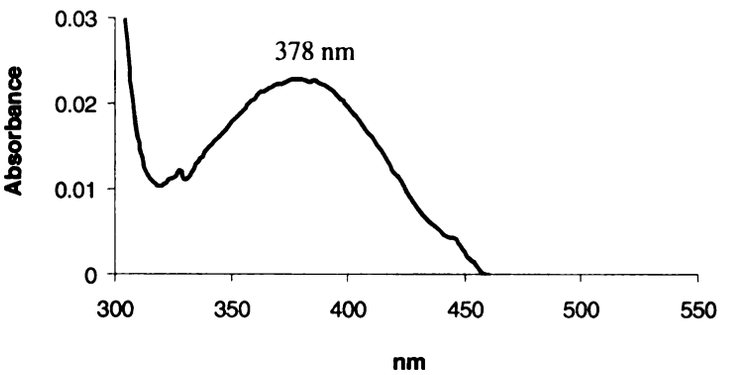

Corrected

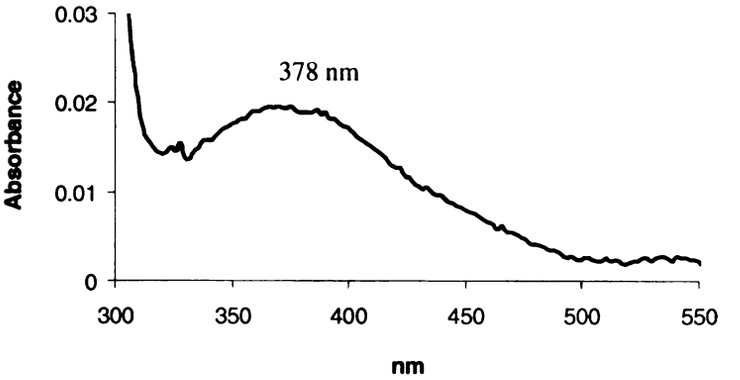

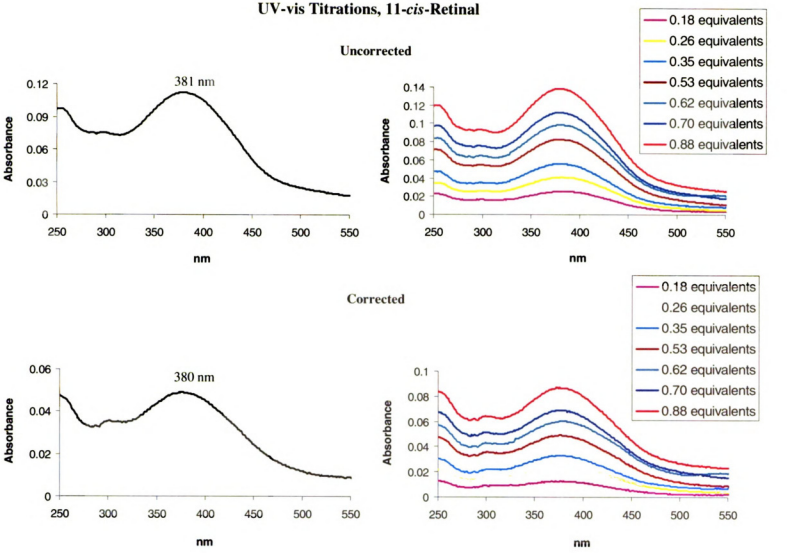
CRABPII L19W
UV-vis Titrations, 11-cis-Retinal
Uncorrected
381 nm
Absorbance
nm
0.18 equivalents
0.26 equivalents
0.35 equivalents
0.53 equivalents
0.62 equivalents
0.70 equivalents
0.88 equivalents
Corrected
380 nm

CRABPII L19W

MALDI-TOF, Protein

Calculated Mass = 16902.27 Da

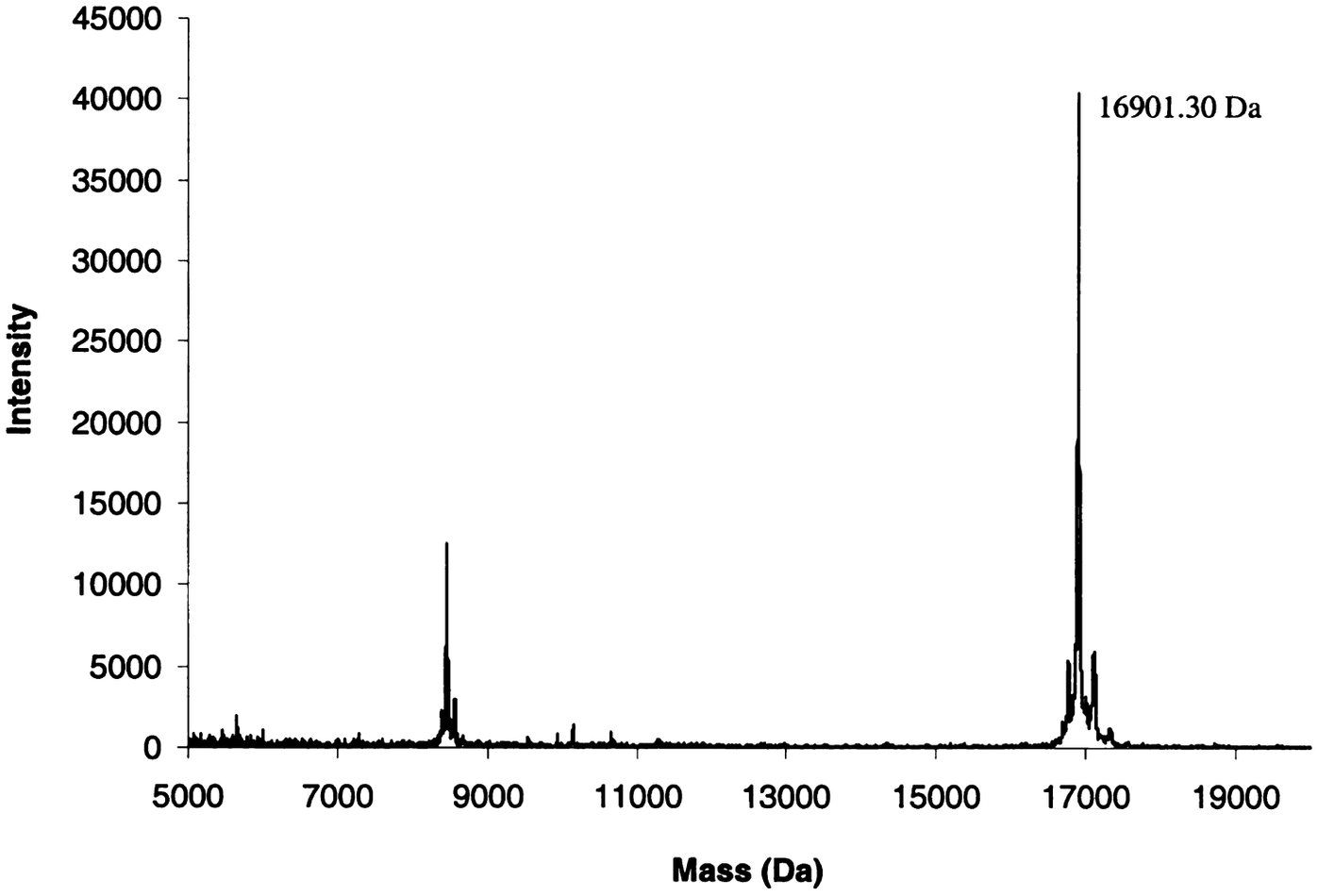

CRABPII L19W

MALDI-TOF, Incubation with all-*trans*-Retinal

Protein Mass = 16902.27 Da

Positive Covalent Bond Formation = Protein Mass + 268

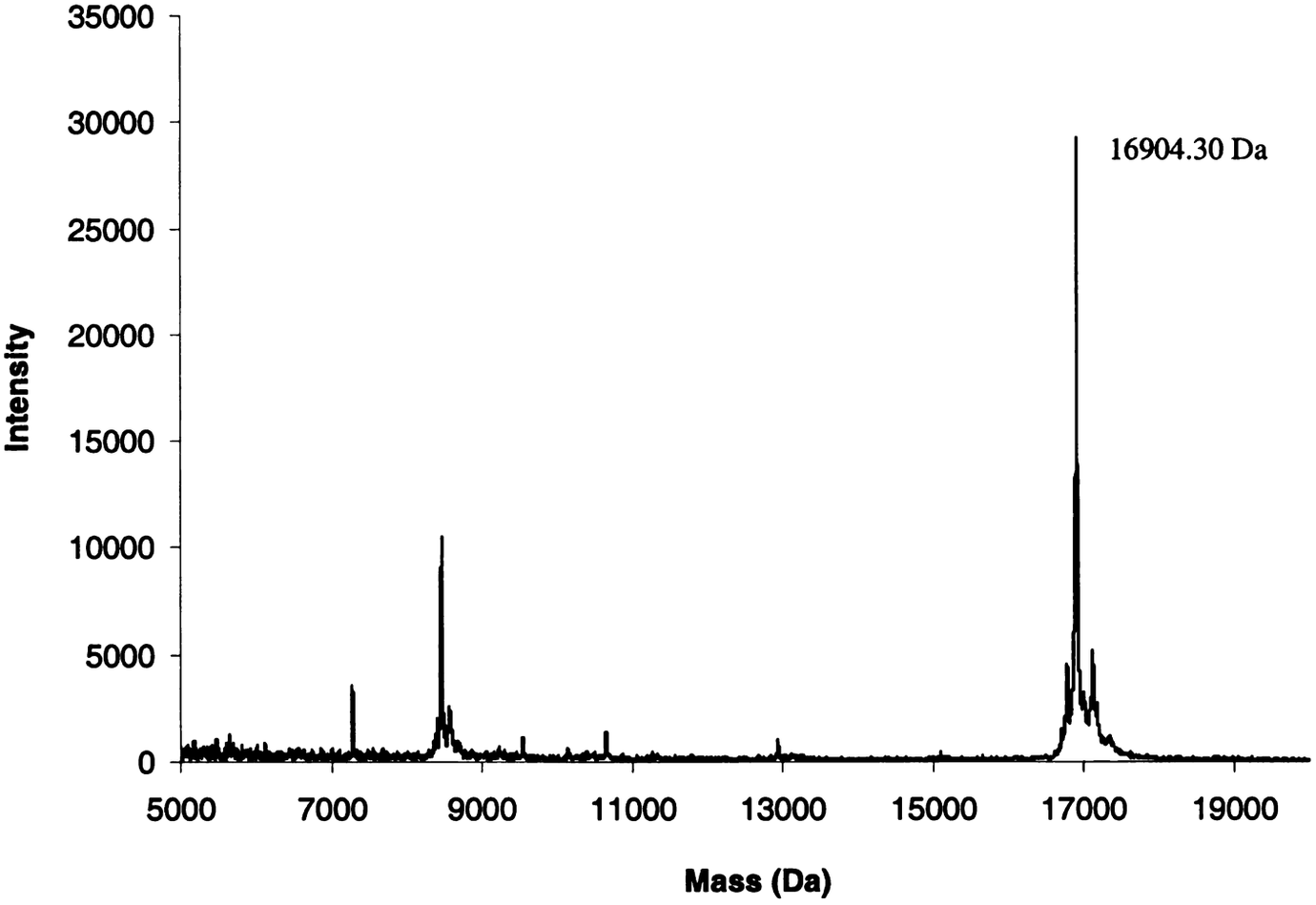

CRABPII L19W

MALDI-TOF, Reductive Amination with all-*trans*-Retinal

Protein Mass = 16902.27 Da

Positive Reductive Amination = Protein Mass + 268

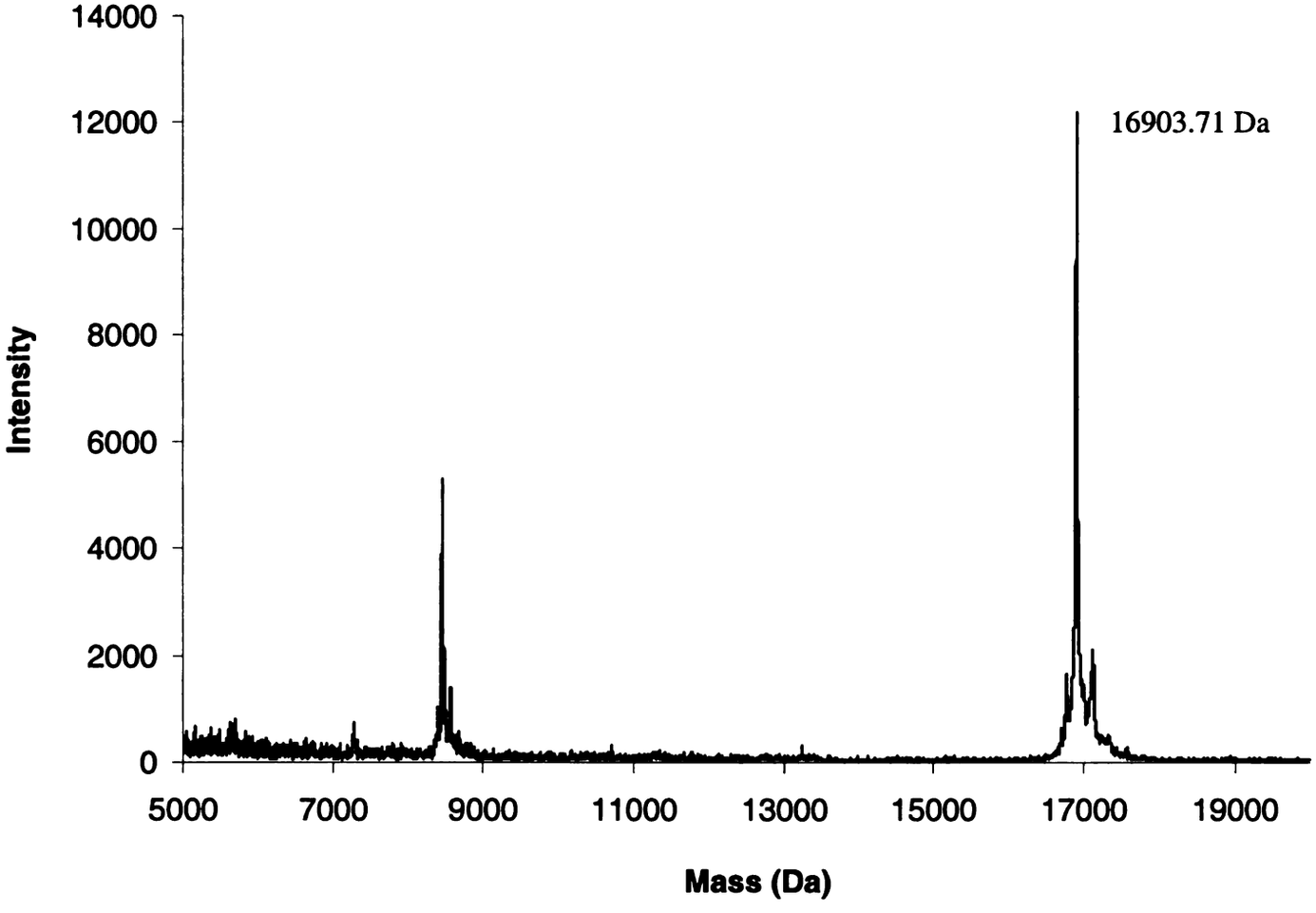

CRABPII R132K::Y134F::L19W

Molecular Weight :
16858.25 Da

Extinction Coefficient :
25,582 M^{-1} cm^{-1}

Primers :
bbb47 5' CGA GGA ATT GTG GAA AGT GCT GGG G
bbb48 5' CCC CAG CAC TTT CCA CAA TTC CTC G

CD

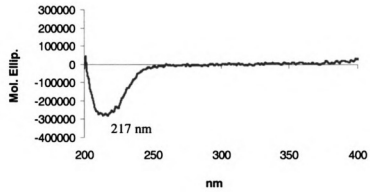

CRABPII R132K::Y134F::L19W

Sequence BB 18

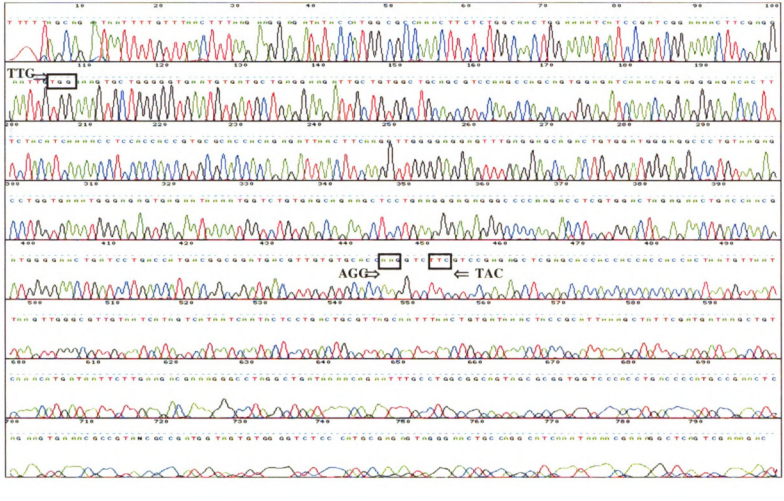

CRABPII R132K::Y134F::L19W

Fluorescence Titrations

Retinoic Acid

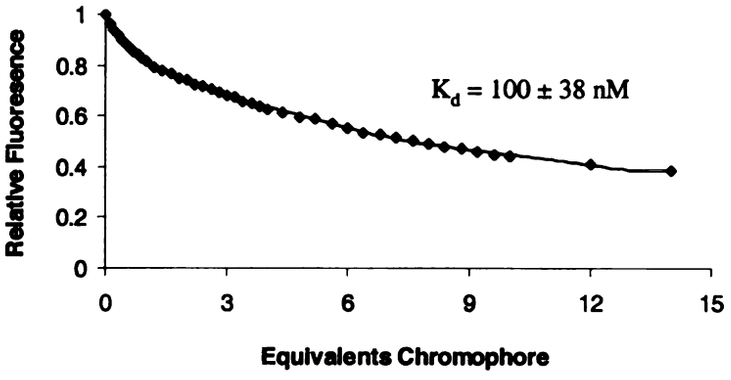

all-*trans*-Retinal

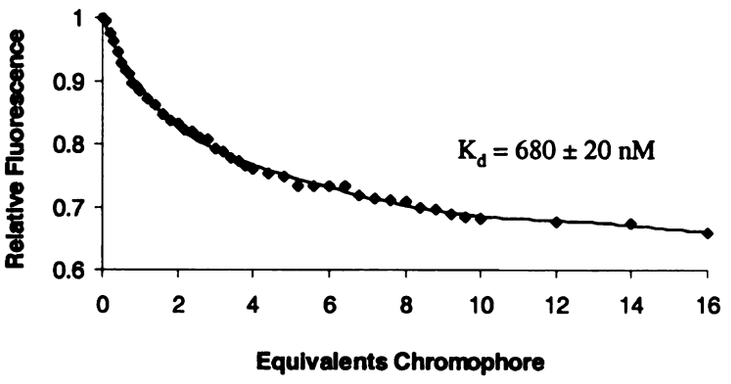

CRABPII R132K::Y134F::L19W

UV-vis Titrations, all-*trans*-Retinal

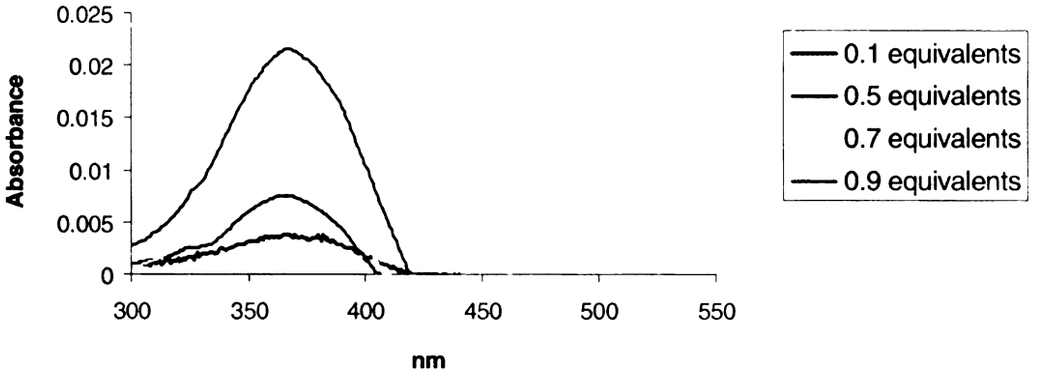

Uncorrected

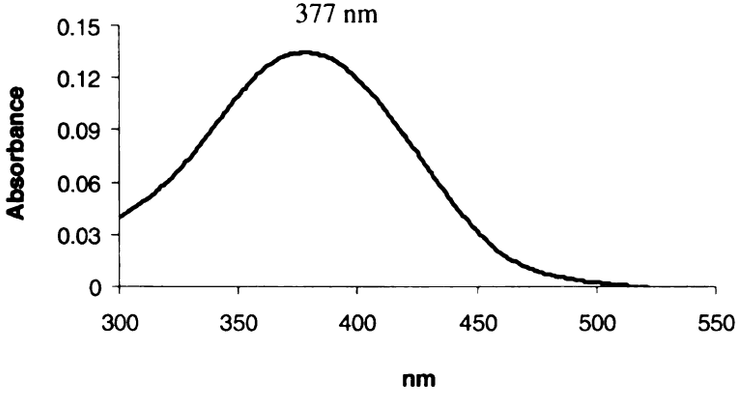

Corrected

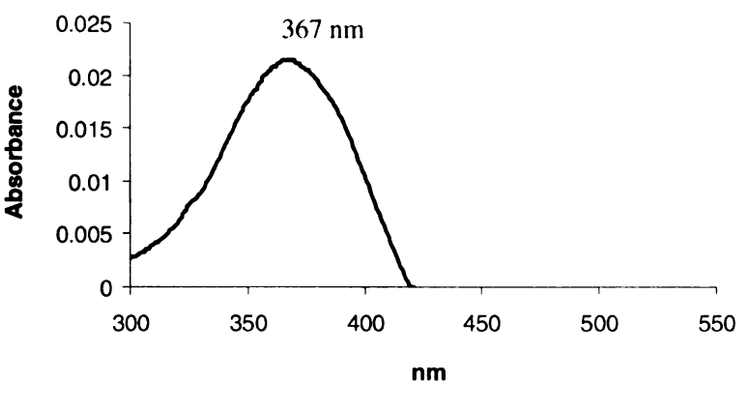

CRABPII R132K::Y134F::L19W

MALDI-TOF, Protein

Calculated Mass = 16858.25 Da

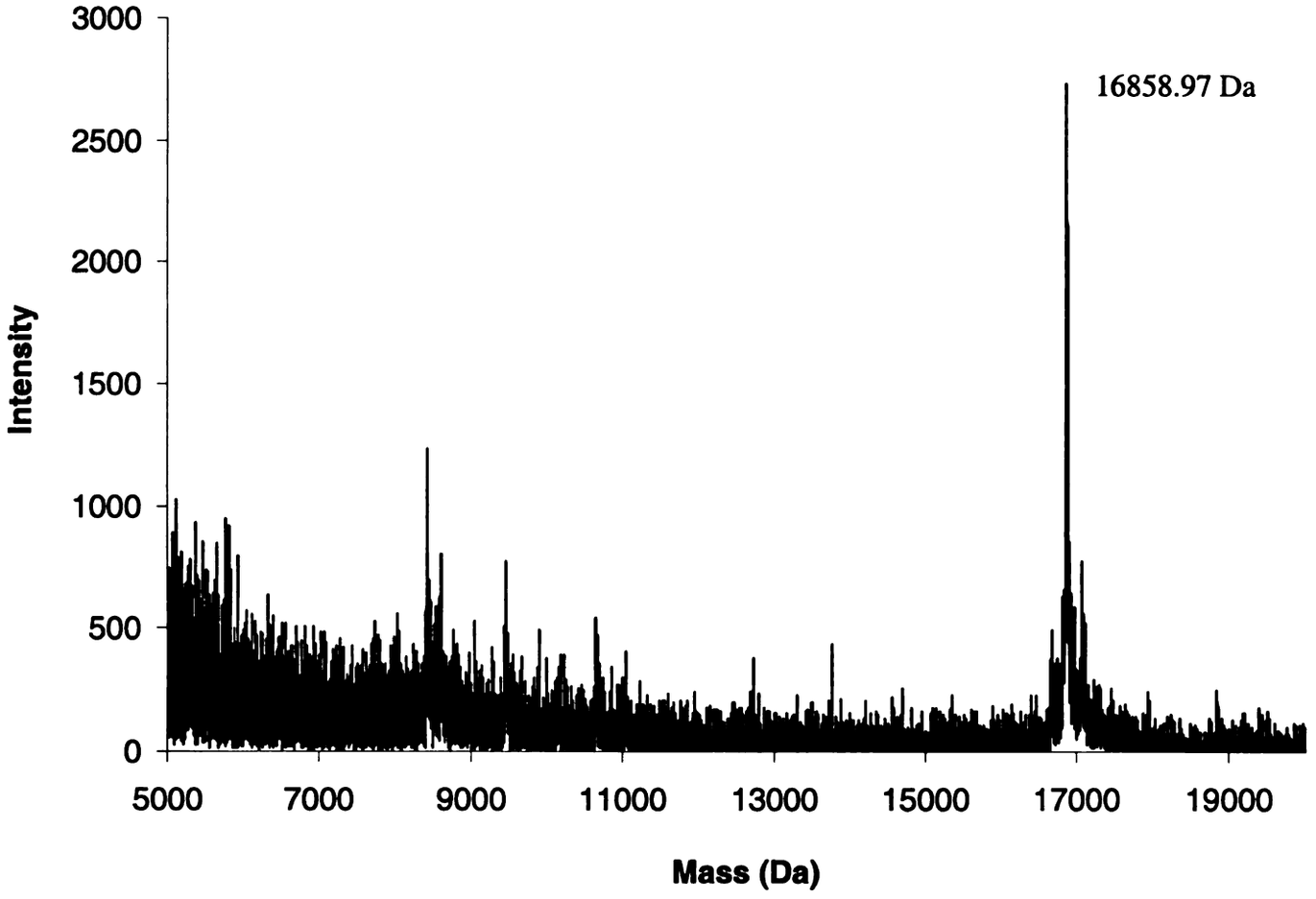

CRABPII R132K::Y134F::L19W

MALDI-TOF, Incubation with all-*trans*-Retinal

Protein Mass = 16858.25 Da

Positive Covalent Bond Formation = Protein Mass + 268

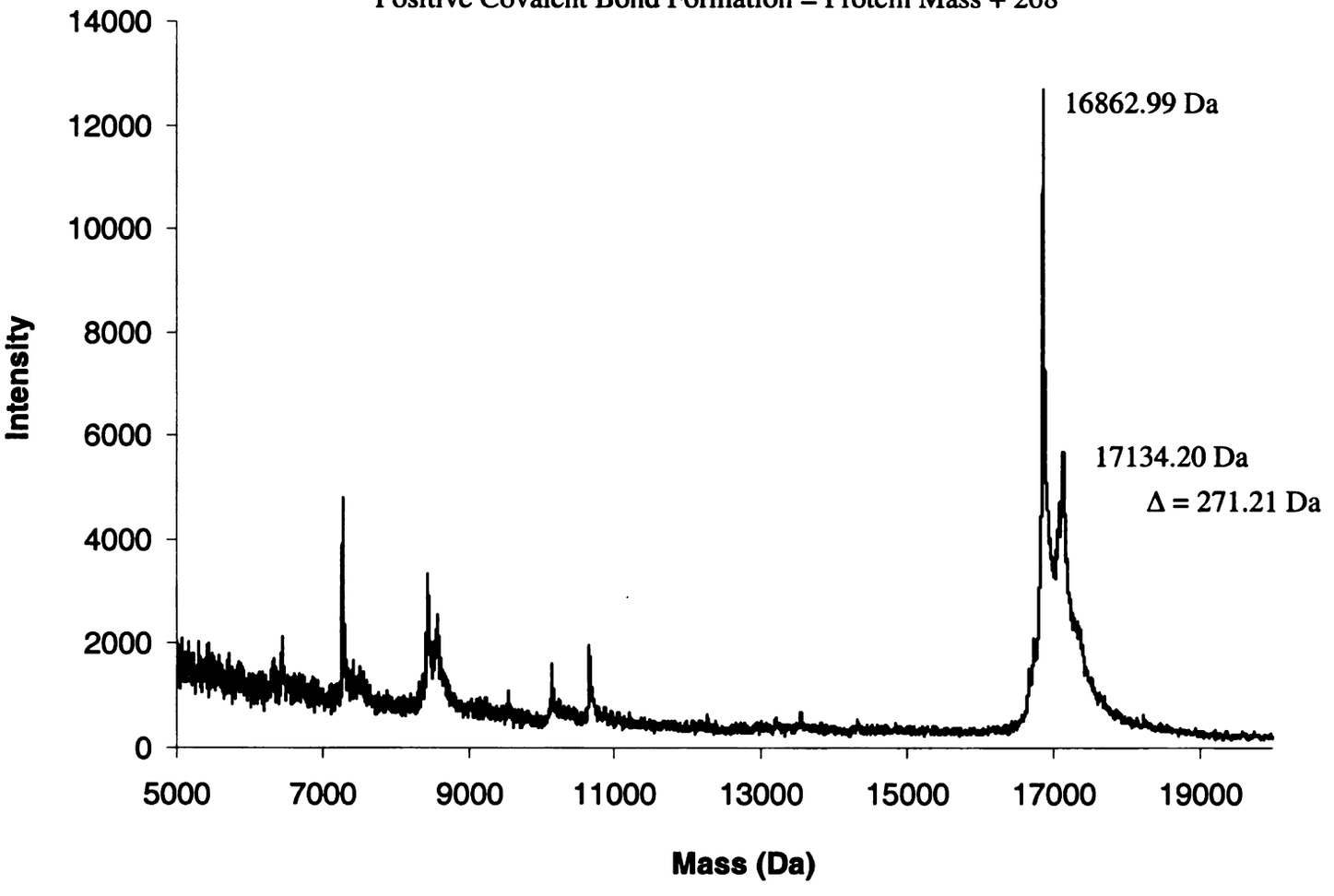

CRABPII R132K::Y134F::L19W

MALDI-TOF, Reductive Amination with all-*trans*-Retinal

Protein Mass = 16858.25 Da

Positive Reductive Amination = Protein Mass + 268